College of Instrumentation & Electrical Engineering, Jilin University

Academic Practice "Six in One" Training Project

English Proceedings

2016 (First Half)

CONTENTS

Dynamic Modeling and PID Control for Two Degrees of Freedom Helicopter

Yu Xiaoman; Chen Youcong; Ma Dongxu

(The College of Instrument Science & Electrical Engineering ,Jilin University,ChangChun,130026,China)

***Abstract*--Because of the high cost and risk in the control of the unmanned helicopter, the article is based on the designed semi-physical simulation platform of two degrees of freedom helicopter system. Firstly, according to aerodynamics theory and Euler-Lagrange equation, etc, building the mathematical model of the system. And then, by means of automatic control theory, the PID control algorithm with robustness is finished. At the same time, by presenting the model on the MATLAB/Simulink simulation environment, the comparison of output waveforms with the model without controlling algorithm on the same condition proves its effectiveness. When the algorithm is applied to the semi-physical simulation platform, the model can keep balance rapidly at the given degree and having anti-interference characteristics, which shows the feasibility.**

***Key words*--PID-controlling； mathematical modeling； 2-dof**

0 INTRODUCTION

RECENTLY, unmanned aerial vehicle has the priority of use in many fields of research.firstly,it has the characteristic of flexibility,which can reach the place that people can not.Secondly,people are not forced to drive the helicopter,but use remote control.the unmanned aerial vehicle can even work by its own attitude of adjustment,which can lower down the risk of experiment,guarantee the personal safety,and has a strong applicability.

However,because of the high risk and cost of the flight test of unmanned aerial vehicle ,researchers generally use the similarity principle to test and verify the control algorithm and then plant it into the unmanned aerial vehicle.To realize the precisely control ,at first we must build its dynamic model.Some researchers attain the input and output by a series of flight test,and then use these data to build the dynamic model based on neural network[1],which needs a mount of data to guarantee the accuracy of the model,and needs experts' data ,so,it has limitations. Some build the dynamic model based on system identification,but don't give the experiment settings or data processing methods[2].Others get the non-linear dynamic model by theoretical calculation,and unknown parameters by wind tunnel test,by which means,it is not easy to derive the equations and determine the parameters.

Many aspects considered,this article describe a practical scheme of solving mathematical modeling.Firstly design and produce a small helicopter model of semi-physical simulation.Secondly simplify it into mechanical model and build the dynamic model according to Euler-Lagrange equation and the relation between the rotating speed and the lifting force.Finally,design a control algorithm of robustness and verify it in the simulation environment in Matlab/Simulink. The test demonstrate that, the mathematical modeling and the algorithm can control the flight attitude of the the small unmanned helicopter well.

1 MATHMATICAL MODELING

The helicopter model of semi-physical simulation includes a horizontal rotor with a protection device on the head of the model,and a tail rotor in the vertical direction,as shown in the figure 1, therefore,it can realize two-degree-of-freedom motion of pitch and yaw.The helicopter model moves around the point where the model is fixed.The two propellers are separately driven by two brushless motor.A certain torsion can be produced by controlling the duty circle to change two motors' speed,which can realize the two-degree-of-freedom motion.

In the process of mathematical modeling,simplify some factors of little influence,for example,while calculate kinetic and potential energy,take two rotors as particles and ignore the holding part's width,thickness,but only mass and length.The

simplified graph is as shown in figure 2 and variables in table 1.

table 1 Explanation of variables and symbols

name		symbol
Vertical board	length	l
	mass	m_1
	moment of inertia around z axis	J_1
	velocity of body gravity	$V_{c1}=[0,0,0]^T$
	Coordinate of center of gravity	$[X_{c1},Y_{c1},Z_{c1}]^T=[0,0,\frac{1}{2}l]^T$
Horizontal board	Distance between tail rotor and the point	l_1
	Distance between main rotor and the point	l_2
	Distance between body gravity and the point	l_0
	mass	m_2
	moment of inertia around body gravity	J_2
	Coordinate of center of gravity	$[X_{c2},Y_{c2},Z_{c2}]^T$
	velocity of body gravity	V_{c2}

The velocity of body gravity is

$$V_{c2}=[-l_0\sin\theta\dot{\theta}\cos\varphi-l_0\cos\theta\sin\varphi\dot{\varphi},\ l_0\sin\theta\dot{\theta}\sin\varphi+l_0\cos\theta\cos\varphi\dot{\varphi},\ l_0\cos\theta\dot{\theta}]^T \quad (1)$$

$$V_{c2}{}^2=l_0{}^2(\varphi^2\cos^2\theta+\theta^2) \quad (2)$$

Then,the kinetic energy of the system is

$$E_k=\frac{1}{2}m_1v_{c1}^Tv_{c1}+\frac{1}{2}J_1\dot{\varphi}^2+\frac{1}{2}m_2v_{c2}^Tv_{c2}+\frac{1}{2}J_2(\dot{\varphi}^2+\dot{\theta}^2)+\frac{1}{2}m_pv_p^Tv_p+\frac{1}{2}m_qv_q^Tv_q \quad (3)$$

The potential energy of the system is

$$E_p=m_2gl_0\sin\theta+m_pgl_2\sin\theta-m_qgl_1\sin\theta \quad (4)$$

Then get the Lagrangian function $L=E_k-E_p$

Different rotating speed can attained by inputting PWM signals of different duty circles,by which the two rotors can receive different torch and lifting force to change the attitude motion.Therefore,the pitching torch is

$$\tau_\theta=k_1w_1^2l_2 \quad (6)$$

k_1 is lift coefficient of main rotor, w_1 is rotating speed of the main rotor;

The yawing torch is

$$\tau_\varphi=k_2w_2^2l_1\cos\theta(\alpha+\alpha_0) \quad (7)$$

k_2 is lift coefficient of tail rotor,， w_2 is rotating speed of the tail rotor， α is the torch-angle of the tail rotor， α_0 is the initial torch-angle of the tail rotor.

Finally,according to Lagrangian function $\frac{\partial}{\partial t}\left(\frac{\partial L}{\partial\dot{q}}\right)-\frac{\partial L}{\partial q}=\tau$,two equations taking pitch θ、and yaw φ as two variables，are derived as followed:

$$\begin{bmatrix}P_1+J_2 & 0\\ 0 & P_4+J_1+J_2\end{bmatrix}\begin{bmatrix}\ddot{\theta}\\ \ddot{\varphi}\end{bmatrix}+\begin{bmatrix}0 & P_2\dot{\varphi}\\ -P_2\dot{\varphi} & -P_2\dot{\theta}\end{bmatrix}\begin{bmatrix}\dot{\theta}\\ \dot{\varphi}\end{bmatrix}+\begin{bmatrix}P_3\\ 0\end{bmatrix}=\begin{bmatrix}\tau_\theta\\ \tau_\varphi\end{bmatrix} \quad (8)$$

In the model

$$P_1=m_2l_0^2+m_pl_2^2+m_ql_1^2$$

$$P_2=\left(m_2l_0^2+m_pl_2^2+m_ql_1^2\right)\sin\theta\cos\theta$$

$$P_3=m_2gl_0\cos\theta+m_pgl_2\cos\theta-m_qgl_1\cos\theta$$

$$P_4=\left(m_2l_0^2+m_pl_2^2+m_ql_1^2\right)\cos^2\theta$$

According to the expected effects,the model moves in a small range in the horizontal position,due to linear approximation, $\dot{\varphi}^2\approx0$, $\dot{\varphi}\times\dot{\theta}\approx0$, $\theta\approx0$, $\cos\theta\approx1$,the simplified model is as followed:

$$\begin{bmatrix}P_1+J_2 & 0\\ 0 & P_1+J_1+J_2\end{bmatrix}\begin{bmatrix}\ddot{\theta}\\ \ddot{\varphi}\end{bmatrix}+\begin{bmatrix}P_2\\ 0\end{bmatrix}=\begin{bmatrix}\tau_\theta\\ \tau_\varphi\end{bmatrix} \quad (9)$$

In the model,

$$P_1=m_2l_0^2+m_pl_2^2+m_ql_1^2$$

$$P_2 = m_2 g l_0 + m_p g l_2 - m_q g l_1$$

$$\tau_\varphi = k_2 w_2^2 l_1 (\alpha + \alpha_0)$$

What is introduced above all is the whole mathematical modeling process of the two-freedom-of-degree helicopter system.

2 SIMULATION

The system has two input signals (pitch and yaw angle)and two output signals(the rotating speed of the main and tail rotor),so it belongs to MIMO system,which can not has its transfer function model,but the state space model.Build the state space model by taking the angular velocity of pitch and yaw as the state variables,the square of the output rotating speed as the input variable,and the angular acceleration as the output variable.

The motors used in the system are the same brushless DC motors(BLDCM).DC motors can equal to a second-order linear unit $\frac{1/C_e}{T_m T_l s^2 + T_m s + 1}$, where electromechanic inertia time constant is $T_m = \frac{GD^2 R}{375 C_e C_m}$, and electromagnetic inertia time constant is $T_l = \frac{L}{R}$。According to concrete parameters of the motor,motor's transfer function is $G_m = \frac{0.1047}{0.00042s^2 + 0.042s + 1}$.

The conversion relation between the needed lifting force when the helicopter starts and the PWM duty circle that the program outputs is a question.the references[3-7]analyze the relation,which is worth referring.The reference[3] conclude that the lifting force is proportional to the square of the rotating speed using the basic method.

The software Matlab has the simulation environment-Simulink, where the simulation test can be conducted according to the system model above.the input signals of the motors is PWM impulse with a certain duty circle,and the output signals are the square of the rotating speed.Simulate the whole system consuming that two motors are of no mutual interference.the simulation diagram is as shown in figure 3.

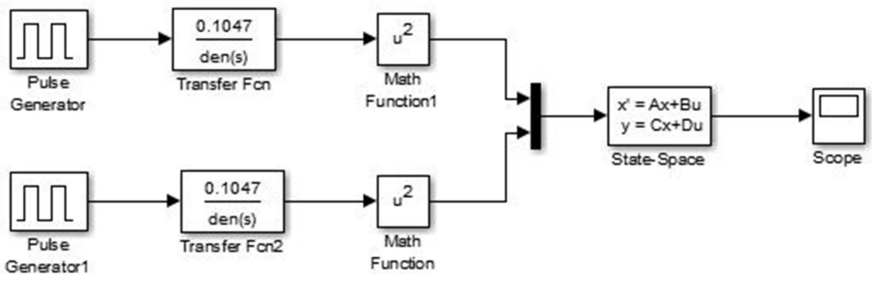

Fig.1 Simulation frame chart of system

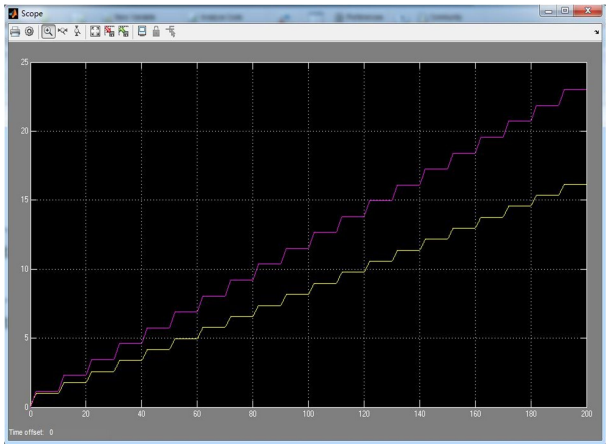

Fig.2 Output waveforms of motors

The output waveform in figure 2,in accord to the actual situation,shows that the rotating speed of the motor rises with time.However,the speed is asked to rise with the angle but not always with time.To be exact,the rotating speed of the motor is a kind of physical quantity related to the difference between the actual angle and set angle.That means an algorithm should be designed to control the speed to change with the angle difference,in order to keep the system balance at a certain degree.

3 PID CONTROLLING

PID controlling which is short for Proportion-Integration-Differentiation controlling,takes the angle difference between input signal and test signal as the controlled object,and conducts the proportion,integration,differentiation operation to reach the expected effect.PID controlling has the advantage of easy principle,easy to realize,high reliability,mature technology,and so on,which has been widely used in the field of modern industrial controlling and mechanical and electrical integration.

The article is based on semi-physical simulation platform of 2-dof helicopter motion,measuring the parameters of the 3-axis gyroscope MPU6050,comparing two methods.One is measuring directly 3-axis angle speed and angle acceleration and integrating to get yaw and pitch.The other is calculating Quaternions using DMP technology to get yaw and pitch.The comparison shows that DMP has more accurate and stable angle.The PID controller is build taking yaw θ、pitch φ as input signals and voltage as output signal.The controller modifies the output voltage using the difference of practical and expected states.Chen Qijun [8]verifies that in the condition of proportional coefficient and differential coefficient,the error can reach any expected range and also verifies the robustness of the method.But this controller design,all the three coefficients are adopted to control the rapidity and stability.The simulation diagram is as shows in figure 1.

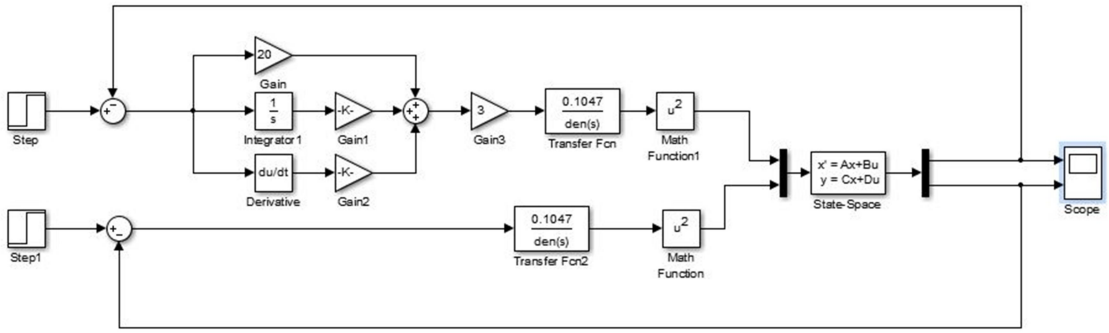

Fig.3 Simulation frame chart of control system

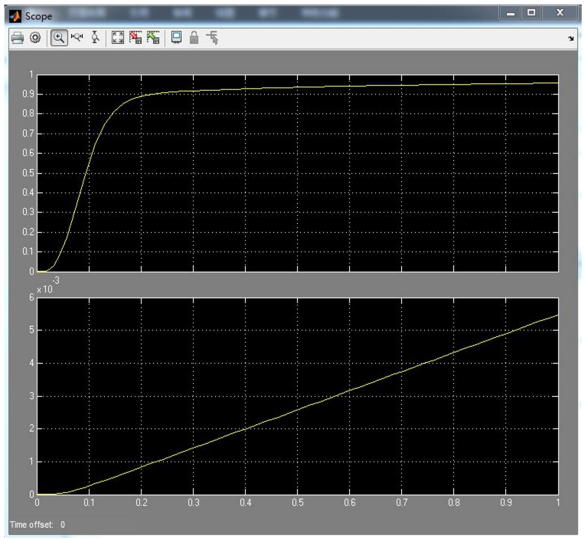

Fig.4 Speed comparison between motor with control and without control

As described in figure 3,the two degrees-of-freedom are independent ,so compare the system with PID controlling and the system without. In fact,the motions of the main rotor and the tail rotor are of mutual interference,so the feedback on the main rotor should be added.

The comparably ideal parameters are $K_p = 20$, $K_i = -0.2$, $K_d = -0.1$,by multiple tests,and the simulation is as shown in figure 4.

Concluded by the comparison in figure 4,the rotating speed of motor without PID controlling is rising all the time,resulting in the system unstable,while that with can be stable in 200ms.In summarize,these PID controlling parameters can control the rotating speed of the motors smoothly.Because of the mutual interference in practice,the parameters should be adjusted to add the feedback to cancel the influence the yaw acting on the pitch,which can help the system keep balance.

4 CONCLUDE

The article introduces how to build the mathematics model of the 2 dof motion system according to the Lagrange-Euler equation and mechanics principle.The system can be linearized around the balance position to

get the simplified model because of the small angle range of the pitch.Then PID controller according to traditional PID controlling principle is designed.Compare two motors with PID and without in the same state in the simulation environment to get the waveform starting stably and balancing fast,in order to verify the efficiency of the algorithm and keep the 2 dof helicopter balance.However,in practical controlling,the winding wire and the vibration in the joint in the movement process can effect the precision.Yaw has an angle bias of ≤1°,and pitch has an angle bias of ≤3°,which shows that the controlling method should be further optimized.

Reference

[1] Zhang Ya-ou, Lv Tian-sheng, Du Jian-fu. Yaw Predictive Model of Unmanned Helicopter Using Elman Network [J]. Journal of System Simulation,2006 ,18 (2) : 309-312.

[2] Bernard M , Takeo K, Mark B T. System Identification Modeling of a Model - Scale Helicopter[C]Proceedings of the 55th Annual Forum of the American Helicopter Society. Montreal: American Helicopter Soc.,1999 :1706-1717.

[3] Wang Donglai, Lu Qiang, Liu Feng. Determination of Quadrotor Dynamic Parameters [J]. Science and Technology Review, 2011, 29(36): 42-45.

[4] Yao Yuanpeng. Research of Four-rotor Helicopter Control[D]. Harbin: Institute of Technology, 2007.

[5] Jiang Zhe ,Zhao Xin Gang ,Han Jianda. Design and Implementation of Experimental testbed for Small Unmanned helicoPter [J].2006.6（Supplement）:1858-1860.

[6] Zeng Wei. Control of Quadrotor Unmanned AerialVehicles's Actuators via Digital Signal Processor[D].TIANJIN University, 2012.

[7] Zhai Kun,Chen Ping,Ge Wenzhe.etc. BLDCM Drive System Design for Small Tilt Rotor Aircraft [J]. 2013. 1-6.

[8] Chen Qijun, Wang Yuejuan, Chen Huitang. Comparative Research of Trajectory Tracking Performance of Robotic Manipulator Based On PD Control Scheme [J]. Control and Decision,2003 , 18(1) : 53-57.

Based on the Pulse Wave Conduction Time Sleeveless Blood Pressure Measurement Instrument Design

Liushuainan; Zhangqilin; Xuchuanbin

（jilin university instrument science and electrical engineering ,changchun,130021）

***Abstract*--Blood pressure is one of the important physiological parameters of human body, can reflect the function of human body heart and blood vessels, is disease, observe clinical medical effect, such as the important basis.In this paper, we design a sleeveless with blood pressure measuring instrument, it is mainly composed of pulse wave measurement, data processing, feature point extraction and mathematical modeling of four units.Single pulse wave data processing the data of the measuring results output in an asynchronous serial communication to PC, PC potter character extraction pulse points, calculate the pulse wave transmission time, and establish the model of the relationship between blood pressure and pulse wave transmission time, so as to realize sleeveless with blood pressure measurements.The experimental results show that the pulse wave pulse range of 20-250 times/min, pulse wave precision reached 1.4% times/min, systolic blood pressure range of 40-250 MMHG, diastolic blood pressure range of 40-250 MMHG, average pressure range of 40-250 MMHG, precision of the blood pressure plus or minus 3 MMHG, and blood pressure measurement standard deviation is less than 8 MMHG, meet AAMI the recommended standard, the standard deviation is not more than 8 MMHG can preliminary application in the medical ward.**

***Key words*--sleeveless; blood pressure measurement; feature point; pulse wave transit time**

I. INTRODUCTION

WITH the development of science and technology and people living standard rise, eating greasy, irregular life, work pressure and other factors have caused the prevalence of hypertension and other chronic diseases and sub-health population rising number of [1] traditional blood pressure measurement using his sound auscultation method, although the arterial blood pressure measurement more accurate, but was unable to track the change of blood pressure;Although with artery intubation can track change, continuous measurement of blood pressure, and the measurement result is accurate, but this method has some limitations, such as ready for long time, have a, and were easy to cause complications, such as pain, bleeding, infection, thrombosis, and air embolism, body because of ischemia and necrosis[5].

Continuous non-invasive blood pressure monitoring is through associated with blood pressure values of signal analysis and processing features of indirect, noninvasive to human body, more suitable for the research and widely used in clinical practice, clinical at present is mainly use the following four methods for continuous blood pressure measurement, they respectively are tension measurement and compensation method, pulse volume potter character parameter method, pulse wave velocity method [5].And stress measurement and compensation method, pulse volume potter character parameter method, compared the pulse wave velocity method, low requirement to the sensor positioning, measurement error is small, less discomfort, is an ideal method of noninvasive continuous measurement of blood pressure.

Based on pulse wave transmission time sleeveless with noninvasive continuous blood pressure measurement of this kind of method measuring equipment is small in size, easy to carry, and made them were thoroughly get rid of the bondage of the gasbag body [2], improves the comfort, can carry on the sleeveless with long time continuous blood pressure measurement, the prevention of high blood pressure and provides a favorable safeguard, timely diagnosis and real-time understand the change of blood pressure, to prevent sudden heart, cerebrovascular disease, also has an important meaning, at the same time, by getting the blood pressure change rule, for other important diagnosis, such as sleep quality, sleep disorder, etc. To provide the basis [3].To sum up, based on the pulse wave [4] conduction time of noninvasive

continuous blood pressure measurement for the continuous monitoring of blood pressure and heart cerebrovascular patients clinical care has important research significance and application value [8].

II. SLEEVELESS WITH BLOOD PRESSURE MEASUREMENT METHOD

A. Theoretical Basis

Blood pressure refers to the intravascular blood for blood vessels of the lateral pressure per unit area, also is the pressure, commonly referred to as blood pressure mean arterial blood pressure [7].Ventricular Systolic, aortic Pressure rise sharply, in the middle of Systolic peak, then the value of arterial Blood Pressure is called the Systolic Blood Pressure (Systolic Blood Pressure, SBP), left ventricular Diastolic, aortic Pressure drop, low heart shu late arterial Blood Pressure is called the Diastolic Blood Pressure, Diastolic Blood Pressure, DBP [4]. National authoritative organization, Systolic Blood Pressure normal value to less than 130 mmHg, Diastolic Blood Pressure normal value to less than 85 mmHg, and Systolic Blood Pressure of ideal value to less than 120 mmHg, Diastolic Blood Pressure of ideal value to less than 80 mmHg, Chinese average Blood Pressure normal reference value as shown in table 2.1 [8].

Table 2.1

the Chinese average normal blood pressure reference value

Age	Systolic blood pressure(male)/mmHg	Systolic blood pressure(female)/mmHG	Diastolic blood pressure(male)/mmHg	Diastolic blood pressure(female)/mmHg
16-20	115	110	73	70
21-25	115	110	73	71
26-30	115	112	75	73
31-35	117	114	76	74
36-40	120	116	80	77
41-45	124	122	81	78
46-50	128	128	82	79
51-55	134	134	84	80
56-60	137	139	84	82
61-65	148	145	86	83

The change of blood pressure has important clinical significance, some chronic diseases, mood swings and movement, and so on and so forth will affect the changes of blood pressure.Under normal circumstances, as long as we are not on the same day three times measured systolic blood pressure value is higher than 140 MMHG or diastolic blood pressure is higher than 90 MMHG, we can decide who have high blood pressure If the systolic blood pressure value is lower than 90 MMHG, diastolic blood pressure values less than 60 MMHG, we can decide who have low blood pressure.

Pulse wave is a result of cardiac spread along the arteries and blood flow, through a large number of experiments have confirmed that the greater the elasticity of the arteries, which is the compliance, the greater the pulse wave transmission time is longer, conversely, if the smaller the elasticity of the arteries, the shorter the pulse wave transmission time.Figure 2.1 for the standard pulse wave signal of human body.

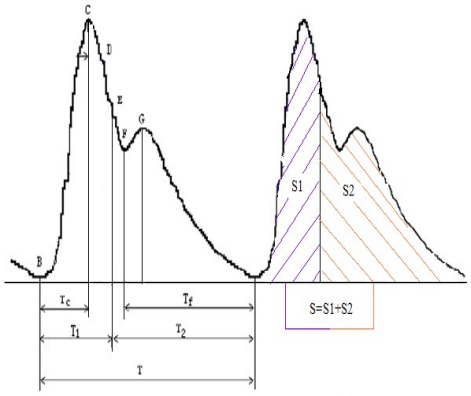

Figure 2.1. the standard pulse wave signal of human body

B. The Calculation of Pulse Wave Transmission Time

As shown in figure 2.1, the acquisition of two pulse wave signals from different parts of the human body coordinates Cx1, Cx2, calculate the difference between the two signal feature point coordinate values:

$$m = Cx1 - Cx2 \quad (1)$$

Because sampling interval is known, so you can use it to calculate the corresponding pulse wave transmission time:

$$PTT = m \times T \quad (2)$$

Type, as the pulse wave transmission time, as feature point coordinate difference, as the sampling interval.

In figure 2.2 for the two way conduction time pulse wave form, namely the pulse wave conduction time

(PTT).

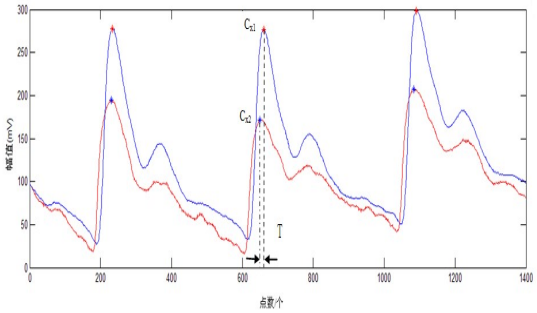

Fig. 2.2. Pulse wave transmission time diagram

C. Pulse wave transmission time and the relationship of blood pressure

On pulse wave velocity, as early as 1808 famous British physicist Thomas Yang ideal fluid elastic tube wave propagation velocity formula is as follows:

$$C_o = \sqrt{Eh/\rho d} \qquad (3)$$

Type, E for wall of young's modulus of elasticity;H as the wall thickness;D to balance the inner diameter of the elastic tube;Is the fluid density [8].

Hughes puts forward and proves that the cross wall pressure vessels and blood vessels have the following relationship between modulus of elasticity:

$$E=E_o e^{\gamma P} \qquad (4)$$

Type of E0 elastic modulus for pressure is zero, P for blood pressure, a quantity for characterization of vascular characteristics, its value from 0.016 to 0.018 (mm/Hg) [5].

In 1878 he made experiment for wave propagation velocity, wave velocity formula is as follows:

$$C=K\sqrt{Eh/\rho d} \qquad (5)$$

Type of K for moens constant, for human aortic K = 0.8.

By type (4) and (4) the pulse wave velocity is the function of blood pressure.

Pulse wave conduction time refers to the pulse wave arteries in the body in the tree spread from one point to far heart end another time, it also is often referred to as PTT, expressed by the following:

$$C = S/T \qquad (6)$$

S for pulse wave transmission in the distance, T for pulse wave transmission time.

Will type (4) type (6) into type (3), and arrange, finally get the formula:

$$P=\frac{1}{\gamma}\left[\ln\left(\frac{\rho d S^2}{aE_0}\right)-2\ln T\right] \qquad (7)$$

Derivative to get blood pressure change and the relationship between the pulse wave transmission time, formula is as follows:

$$\Delta P = -\frac{2}{\gamma T}\Delta T \qquad (8)$$

Among them, says the changes of arterial blood pressure value, represents the pulse wave transmission time, said the quantity is a characteristic of blood vessels [4].

That is, if blood vessels are elastic constant, then the change of blood pressure and the relationship between pulse wave conduction time is a direct proportion relationship, and, in fact, for vascular elasticity this parameter, in a short period of time, there is no big change the value of the same people [4].So by measuring pulse wave conduction time (PTT), the changes of arterial blood pressure can be indirectly calculated amount.

III INSTRUMENT HARDWARE DESIGN

System is mainly composed of sensors, adder pulse circuit, A/D data acquisition, the master microcontroller, data storage and display of six parts, HK - 2000 - b system based on piezoelectric pulse sensor for the measurement of the pulse wave signal, the design with the addition of multiplier circuit will be gained by the pulse signal translation up, all in the A/D signal voltage amplitude requirements within the scope of using 16 bits serial A/D chip AD7656 for two-way pulse signal synchronization sampling, the chip can 2 channel acquisition at the same time [7]. PC is the use of MATLAB software for the accurate extraction of feature points (extraction method is based on the pulse of the original signal method potter point extracting method), pulse wave conduction time calculation as well as the relationship between pulse wave conduction time and arterial blood pressure modeling, so as to realize sleeveless with blood pressure measurements.

Overall system block diagram shown in Figure 3.1.

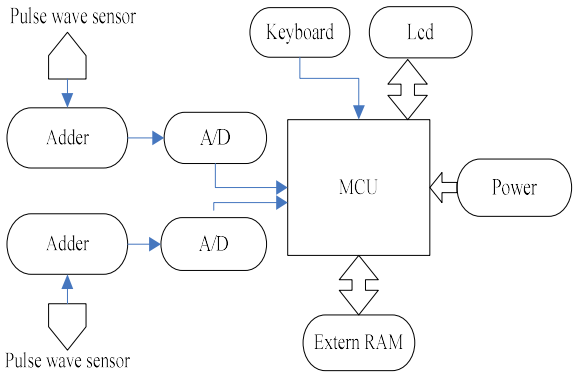

Fig.3.1 Overall block diagram of the system

IV INSTRUMENT SOFTWARE DESIGN

A.Feature Point Extraction

Using pulse wave signal feature points extraction and pulse wave transmission time calculation.Through MATLAB software to obtain the same signal waveform figure in different locations, the same time, the two lines of pulse wave signal and noise signal analysis and processing, and USES the method of original signal pulse potter collection point for the extraction and more accurate calculation of the pulse wave transmission time.

B.Modeling Of The Pulse Wave Transmission Time And The Relationship Of Arterial Blood Pressure

Polynomial fitting method is used to establish relationships with the model of the arterial blood pressure pulse wave transmission time.

An arbitrary function according to Taylor, Taylor series expansion for a polynomial, namely:

$$f(x{:}a_0,a_1,\cdots,a_m)=a_0x^0+a_1x^1+\cdots+a_mx^m \quad (9)$$

So a polynomial fitting curve between blood pressure and pulse wave transmission time, close to the original curve and can be more accurately.

Will be collected blood pressure data and calculate the coordinate difference one to one correspondence of feature points stored in TXT documents, read documents and systolic blood pressure, diastolic blood pressure, and feature point coordinate difference respectively in the three arrays, and using the pulse wave transmission time as the independent variable, with systolic pressure, diastolic blood pressure data respectively as the dependent variable, respectively, three times five polynomial fitting and polynomial fitting and calculate the coefficient, draw the fitted curve, and the fitting results compared with the actual results.

(1) The fitting formula:

Based on the relationship between systolic blood pressure and pulse wave transmission time:

$$HP=a1\times x^3+a2\times x^2+a3\times x+a4 \quad (10)$$

Fitting coefficient :

$a1=$ -2037.3002 $a2=$ 322.0839

$a3=$ -19.7838 $a4=$ 1.4934

Diastolic blood pressure and pulse wave transmission time is:

$$LP=b1\times x^5+b2\times x^4+b3\times x^3+b4\times x^2+b5\times x+b6 \quad (11)$$

Fitting coefficient :

$b1=$ -11600785.9246 $b2=$ 1982983.4213

$b3=$ -126460.3704 $b4=$ 3743.4202

$b5=$ -53.5216 $b6=$ 1.0545

(2)Curve fitting

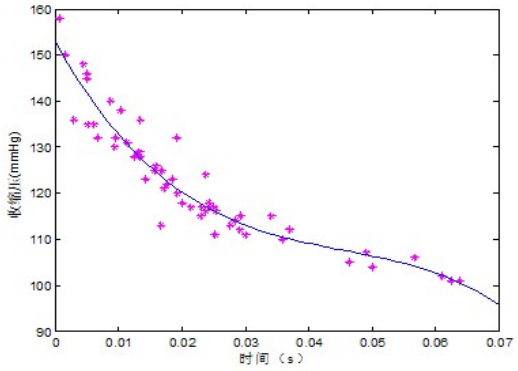

Fig.4.1 Systolic blood pressure and pulse transit time fitting Figure

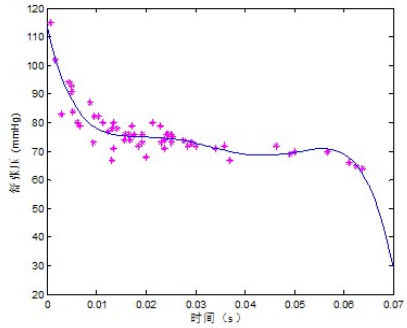

Fig.4.2 Diastolic blood pressure and pulse transit time fitting Figure

C.GUI Interface Design

MATLAB GUI interface design.To realize real-time serial communication of upper machine and lower machine, data storage, the callback data and human-computer interaction, make the system display intuitive, simple to use convenient.

V.THE EXPERIMENTAL RESULTS AND ANALYSIS

*A.*The *Experimental Results*

(1) access to information, understand the development of the noninvasive blood pressure measurement, analysis and comparison of blood pressure measurement method, design a noninvasive continuous blood pressure measurement method.

(2) explained the pulse wave transmission time, sleeveless with the principle of blood pressure measurement instrument design.

(3) to complete the operation is convenient, and the system is small in size, has a strong practical and portable pulse wave measurement system research and design of a prototype.

(4) using MATLAB software to design the algorithm of the potter character extraction pulse point, establish a more accurate relationship between pulse wave conduction time and arterial blood pressure value model, can continuous noninvasive measurement of arterial blood pressure.

(5) MATLAB GUI interface is designed.Realized the real-time serial communication of upper machine and lower machine, data storage, the callback data and human-computer interaction, make the system display intuitive, simple to use convenient.

(6) after the system test and analysis, the blood pressure measurement standard deviation is less than 8 MMHG, in accordance with the standard deviation is not more than 8 MMHG AAMI recommended standards.By the jilin institute of testing show that the system of the pulse wave pulse range has reached 20-250 times/min, pulse wave precision reached 1.42%, reached 40-250 MMHG systolic blood pressure range, diastolic blood pressure range of 40-250 MMHG, average pressure range of 40-250 MMHG, precision of the blood pressure plus or minus 3 MMHG, achieved the indicators of project requirements.

B.*The Experiment Results Analysis*

From the experiment test and analysis results showed that the system root mean square error is less than 8 MMHG, in accordance with the standard deviation is not more than 8 MMHG AAMI recommended standards.Using pulse wave transmission time and the model test of the relationship between blood pressure, the results are as follows:

(1) is proposed to fit in, mainly focused on using data of diastolic blood pressure in 65 ~ 100 MMHG interval, systolic blood pressure in 100 ~ 150 MMHG interval, so fitting results are within the area between smaller error [6].

(2) due to the relationship between pulse wave transmission time and blood pressure are individual differences, and the model used by fitting the data contains only part of the human body health, so the test (in case of high blood pressure, the error results in [3].

VI . EXPECTATION

In future work, the modeling results for the purpose of this article and artery intubation presently used a large number of clinical control experiment, and focus on establishing hypertensive patients or hardening of the arteries of the patient's pulse wave transmission time and the relationship between arterial blood pressure model, so as to correct the parameters of the mathematical model built by, reduce the error.Suggestions can model respectively for different ages, different age paragraph the formula, so that more targeted, the result more accurate.

References

[1] Martina, Jerson R, Westerhof, Berend E, Van Goudoever, Jeroen, De Jonge Nicolaas, et al. Noninvasive Blood Pressure Measurement by the Nexfin Monitor During Reduced Arterial Pulsatility: A Feasibility Study[J]. ASAIO Journal.2010,56(3):221-227.

[2] CHEN W, KOBAYASHI T, ICHIKAWA S, et al. Continuous estimation of systolic blood pressure using the pulse arrival time and intermittent calibration[J]. Medical and Biological Engineering and Computing, 2000,38(5):569-574.

[3] Youngsung Kim; Jeunwoo Lee; Cuffless and Non-Invasive Estimation of a Continuous Blood Pressure Based on PTT[C]. Information Technology Convergence and Services(ITCS), 2010 2nd International Conference on.2010:1-4.

[4] Sai Kolluri，Lawrence Hersh，Richard Medero(Greneral Electric Company).System and Method for a Non-invasive Blood Pressure Measurement[P].US:12/415575,09/30/2010.

[5] TAEWOON, JONGMAN C, JU NHO P, et al. A coronary pulse wave velocity measurement system[C]. Lyon: Proceeding of the 29th Annual International Conference of the IEEE EM BS,2007:975-977.

[6] Y. Chen, C Wen, G C Tao, et al. Continuous and noninvasive blood pressure measurement: a novel modeling methodology of the relationship between blood pressure and pulse wave velocity[J]. Annals of Biomedical Engineering, 2009, 37(11): 2222-2233.

[7] Rachel E.D. Climie, Martin G. Schultz, Sonja B. Nikolic, Kiran D.K.Ahuja, James W. Fell and James E. Sharman. Validity and Reliability of Central Blood Pressure Estimated by Upper Arm Oscillometric Cuff Pressure[J]. American Journal of Hypertension, 2012.

[8] N. A. Zakaria, N. B. Sharifmuddin, W. M. F. Wan Mohd, et al. Pulse Wave Transit Time and Its Relationship with Systolic Blood Pressure[C]. 6th World Congress of Biomechanics(WCB 2010). August 1-6, 2010 Singapore IFMBE Proceedings,2010,31(6):1354-1357.

The research of speaker recognition technology based on MFCC

HeYing; XuLijiao; ChenShaokang

(College of Instrument Science and Electrical Engineering, Jilin University, Changchun, 130061, China)

***Abstract*--Speaker recognition is through the speaker's voice feature to automatically identify the speaker's identity, which in many areas have a very unique advantages and good prospects for development. Due to the development needs of the application and digital signal processing technology, the speaker recognition technology research has been extensive and in-depth development. Although the study of speaker recognition technology has gradually entered the practical applications, but in the effective integration of the existing characteristic parameter extraction and new voice features and parameters for the selection of the reference model is still hot and difficult research. This design simulation using MATLAB software implements a speaker recognition system. Feature extraction, chose Mel cepstral coefficients (MFCC) and the first difference as speaker recognition feature parameters collectively describe the speaker's personality traits. Aspects of recognition algorithms, dynamic time warping (DTW) recognition algorithm, the algorithm uses the data used in the process continue to amend the original template, so the template successive perfecting. Experimental results show that the characteristic parameter extraction method proposed in this paper and its binding to its first difference can significantly improve system performance with fast speed, small amount of calculation, the error rate is low.**

***Key words*--Speaker Recognition Mel Cepstral DTW**

I.INTRODUCTION

SPESKER recognition[1] is a technique that can identify the speaker's identity by analyzing the speech signal. The key is to accurately distinguish the characteristics of different voice and its information content[2]. In the 1930s, Bell Labs proposed speaker recognition method based on pattern matching and statistical analysis of variance, mainly for the various identification parameter extraction, choice, and the cepstrum and linear prediction analysis method is applied to speaker recognition[3]. Since the sixties of the 20th century so far, with the digital filter, fast Fourier transform, homomorphic signal processing, linear prediction coding, vector quantization algorithm appear constantly improvement, coupled with the popularity of the development of microelectronics technology and computer, research in this field has made rapid progress in[4]. Speaker recognition research focus to enhancement of speaker characteristic extraction and separation, personality characteristics, to reflect the speaker characteristics of acoustic parameters and the new speaker recognition mode matching method, such as dynamic time warping (DTW), principal component analysis (PCA), vector quantization (VQ), hidden Markov model (HMM), artificial neural network method (ANN) and the method of the combination technology first-class.

The development of speaker recognition technology today has decades of history, has made many outstanding achievements, but there are still a lot of difficulties, mainly as follows:

(1) there is no good way to put the speaker characteristic from the speaker's voice characteristics in isolated[5].

(2) with the speaker's characteristic length change characteristic, will change with time and age changes.

(3) the sound recording is easy to imitate.

Based on the previous research, the key part of speaker recognition, feature extraction and pattern are discussed. Feature extraction using Mel frequency cepstral coefficients (MFCC). In terms of pattern matching, dynamic time warping algorithm (DTW). Finally, the system simulation software[6] in MATLAB.

II. THE PRINCIPLE OF SPEAKER RECOGNITION

Speaker recognition is divided into two stages: speech training and speech recognition[7]. In the training phase by using a microphone input voice

command, and then the analog voice signal pretreatment, to the digital signal processing of speech feature extraction, after income characteristic parameters to establish a corresponding speech feature model library. After the completion of the training, to enter the stage of speech recognition, through a microphone input to be the recognition of voice commands and to the speech signal pretreatment, extracted speech feature parameters of the obtained after processing the digital signal, followed by redeployment of speech feature model library matching detection. If the distance between the characteristic parameters of the speech and the recorded parameters in the model base is not more than the threshold value, then the original speaker is judged, and vice versa. Its principle block diagram is shown in figure 1:

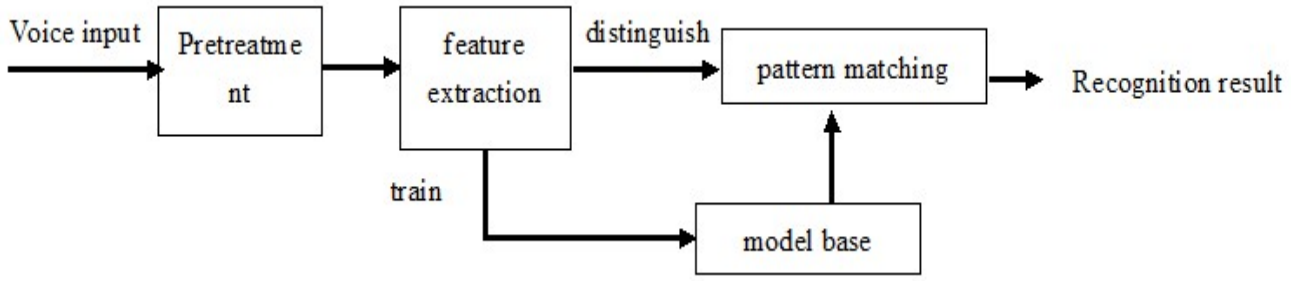

Fig. 1. Principle of speaker recognition system

III. IMPLEMENTATION OF SPEAKER RECOGNITION

A.Extraction of characteristic parameters

Feature extraction is to extract the basic features of the speech signal, which can be divided into different speakers, and the change of the same speaker is relatively stable.

a.Mel extraction (MFCC)

Feature parameters extracted from the speaker shall meet the corresponding conditions: to outside variables is not sensitive, such as the impact of the speaker's emotional, stable for a prolonged period of time, often shown; easy to measure, and other features. Among all the parameters, the characteristic of the spectrum is much more than other parameters, which can be used to characterize the speech signal. Experiments show that, in most cases, MFCC is better than that of other cepstrum, the extraction process is divided into preprocessing (sampling / quantization, pre emphasis processing, feature extraction and windowing).

Mel frequency can be expressed by the following formula：

$$\text{Mel}\ (f) = 2595 * \lg(1 + \frac{f}{700})$$

Type in the F for the frequency, the unit is Hz.

The specific extraction process of MFCC parameters is as follows：

(1)Pre emphasis, Framing, Plus window:

Preconditioning is actually the voice signal through a high pass filter:

$$H(z) = 1 - \mu z^{-1}$$

The purpose of pre emphasis is to enhance the high frequency part, so that the spectrum of the signal becomes flat, to maintain the whole band in the low frequency to high frequency, can use the same signal to noise ratio of the spectrum. At the same time, in order to eliminate the effect of the vocal fold and lips, to compensate for the high-frequency part of the speech signal is suppressed by the pronunciation system, highlighting the high frequency resonance peak[8].

The pre emphasis signal is processed by the frame and the window, and the time domain signal X (n) of each speech frame is obtained.

(2)Fast Fourier transform:

Because only through the signal in the time domain transform is usually very difficult to find that the signal characteristics, so usually it converts the frequency domain energy distribution to observe, different energy distribution, can represent different speech characteristics[9]. Therefore, in the Hamming window, each frame must also go through the fast Fourier transform to get the energy distribution on the spectrum. Each frame signal on the window frame after the fast Fourier transform spectrum of each frame. The power spectrum of the speech signal is obtained by the spectrum of the speech signal. DFT for voice

signal:

$$X_a(k)=\sum_{n=0}^{N-1}x(n)e^{-j2\pi k/N},0\le k\le N$$

Type X (n) for the input of the voice signal, N, said the number of Fourier transform.

(3)Triangular bandpass filter:

The energy spectrum through a set of mel scale triangular filterbank, a M filter filter (filter number and critical with a number of similar), using the filter for triangular filter, the center frequency f (m), M = 1,2,..., M is defined. M usually takes 22-26 (this system takes 24). The interval between the f (m) decreases with the decrease of m value, and increases with the increase of m value, as shown in figure 2:

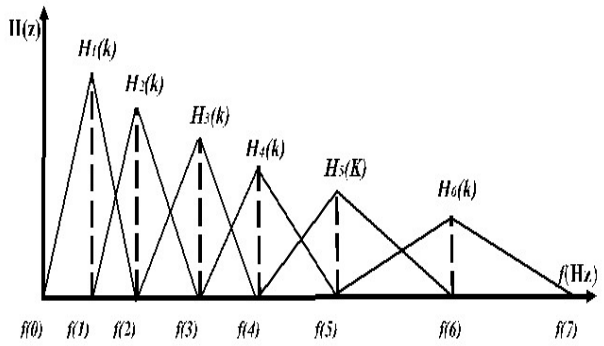

Fig. 2. filter bank

Triangular band-pass filter has two main objectives: one is to smooth the spectrum and eliminate harmonics, highlight the original speech formants, so a voice tone or pitch is won't appear in the MFCC parameters, in other words, the MFCC as feature of speech recognition system, and not by the tone of the speech input different; second, can reduce the amount of computation[10].

(4)The logarithm of the output of each filter bank is calculated:

$$s(m)=\ln\left(\sum_{k=0}^{N-1}|X_a(k)|^2H_m(k)\right),0\le m\le M$$

(5)obtained by the discrete cosine transform (DCT) MFCC

$$C(n)=\sum_{m=0}^{N-1}s(m)\cos\left(\frac{\pi n(m-0.5)}{M}\right),n=1,2,\ldots,M$$

b. Differential MFCC

The standard[11] parameter MFCC only reflects the static characteristics of the speech parameters, and the dynamic characteristics of the speech can be described by the differential spectrum of these static features. Experiments show that the combination of dynamic and static features can effectively improve the recognition performance of the system. The calculation of differential parameters can be used in the following formula:

$$D_t=\begin{cases}C_{t+1}-C_t, t<Q\\ \dfrac{\sum_{k=1}^{K}k(C_{t+k}-C_{t-k})}{\sqrt{2\sum_{k=1}^{K}k^2}}, \text{other}\\ C_t-C_{t-1}, t\ge Q-K\end{cases}$$

Formula, said the first t of the first order difference, that the first t of the coefficient of the Q, coefficient of the coefficient of the order of the coefficient, K said the first derivative of the time difference, it is desirable 1 or 2,. The results will be the type and then you can get the parameters of two order difference.

B.Dynamic time warping algorithm DTW

DTW is a nonlinear regularization technique which combines time warping and distance measure computation[12]. This technique is to find a time warping function j= (I), the time axis of the test vector is mapped to the time axis of the template J, and to meet the function:

$$D=\min\sum_{i=1}^{M}d[T(i),R(\omega(i))]$$

Where $d[T(i),R(\omega(i))]$is the first i test vector T（i） and the first j frame template vector R(j) distance between the test, D is in the optimal time of the regular pattern of the matching path between the two vectors [13].

Due to the DTW continuously computing the distance between two vectors to find the optimal matching path, so obtained is two vector matching the cumulative distance minimum corresponding to a warping function. This ensures that the similarity between them, there are the maximum acoustic. The essence of the DTW algorithm is the use of the idea of dynamic programming, using local optimization processing to automatically find a path, along this path, between two feature vectors accumulated distortion minimum, so as to avoid because of different length and may introduce error.

IV. EXPERIMENTAL RESULTS AND ANALYSIS

In accordance with the above method for feature extraction and pattern recognition, the use of MATLAB software programming, the use of computer sound card recording, analysis of different thresholds in the recognition of the effect. Recording environment for the common room, recording sampling frequency 16bit, wav 44100Hz voice file for system testing. A total of 3 men and women of the speaker, speech to "open the door", each speaker recorded 30 times, 5 times for training, 25 times for recognition. Get the following experimental results table under different threshold:

TABLE I

Correct rate under different thresholds

threshold	1.00	1.05	1.10	1.15	1.20	1.25	1.30	1.35
False rejection rate (%)	80.0	63.3	53.3	40.0	26.7	6.7	6.7	6.7
False positive rate (%)	4.0	6.0	8.7	10.7	14.0	18.0	22.0	24.7
Correct rate (%)	58.0	65.4	69.0	74.7	79.7	87.7	85.7	84.3

From the test results, the recognition method is very effective, the improved system has a high recognition rate.

V. CONCLUSION

Based on the previous studies, this paper studies the key technologies of the speaker recognition system. In the feature extraction of speech signal, the Mel frequency spectrum coefficient (MFCC) and its first order difference. In the recognition algorithm, dynamic time warping algorithm is adopted and implemented. Finally, a speaker recognition system is built by using MATLAB software simulation and GUI function, which includes speaker training module and speaker recognition module. The program has friendly interface and convenient operation. Through testing and adjusting the recognition threshold, the system achieves the ideal recognition accuracy.

The function of the system has strong portability, if the further perfection and improvement, widely used in the financial system, computer information and network security, especially in the field of intelligent building and identity authentication and access control management aspects.

Reference

[1] Zhao Li, Zou Cairong, Wu Zhen Yang.HMM in speaker recognition application [J]. Journal of circuits and systems.2009,8（8）：32-35.

[2] Jin Xuecheng. Research on Speaker Recognition Based on speech signal. Master thesis. University of Science and Technology of China.2007.

[3] Wang Yi. Research and implementation of adaptive speech recognition technology. Master thesis. Tsinghua University.2003.

[4] Zhang Junying. Modern methods and techniques of speaker recognition. Northwestern University press.1994.

[5] Yang Hangjun, late wellSome. Digital processing of speech signal. Beijing: Electronic Industry Press.1995:129-161,412-428.

[6] Chen Yining, Zhou Jingfang. Robust text independent speaker recognition based on Gauss speech filtering [J]. computer engineering.2013（4）：68-69.

[7] Wang Biao. Research on the speech recognition system based on [J]. Matlab computer and digital engineering.2011（12）：85-87.

[8] Wang Yunhong, Tan Tieniu. New technology of modern identification: biometric identification technology [M]. Chinese basic science. 2005（12）：55-63.

[9] Furui S.An overview of speaker recognition technology[C].ESCA Workshop on Automatic Speaker Reconnition,Identification and Verification.1994:1-9.

[10] Nicholson J,Takahash K Nakatsu R . Recognition in Speech Using Neural Networks . Neural Computing and Applictious,2000, 24(11):435-438.

[11] Wasserman . ED . Advanced Methods in Neural Computing,NewYork,VanNostrandReinhold . 1993,18(3) :43-45.

[12] Ms. Vimala C.V. Radha,et al.Speaker Independent Isolated Speech Recognition System for Tamil Language using HMM[J].Procedia Engineering,2012,30:1097-1102.

[13] Gaurav Gaurav, Devanesamoni Shakina Deiv,Gopal Krishna Sharma,Mahua Bhattacharya,et al.Development of Application Specific Continuous Speech Recognition System in Hindi[J].Journal of Signal and Information Processing, 2012,(03):394-401.

Study on Automatic berthing model based on fuzzy control

Qiu chun-ling; Bai yu-xin;Wang kai; Gu jia-yue
（College of Instrumentation & Electrical Engineering Jilin University，chang chun,130022,china）

***Abstract*--Automatic berthing system is a kind of environment through the information collection around to find suitable berthing vessels, automatically enter the position control system..According to the automatic berthing method time-consuming problem in foreign and domestic ,there is an urgent need to develop a can effectively realize independent berthing, good system stability system. Combined with the actual of berthing motion model analysis, design of vertical, parallel, oblique three berthing fuzzy controller whose the simulation and verification were performed in the Matlab/Simulink. According to the proportion of each component of ships, design a model to make a automatic berthing test by using ultrasonic distance measurement to obtain the surrounding environment data technology and converting to C code. finally, the test results show: the system can effectively realize independent berthing, and provide a theoretical reference value for the further research and development.**

***Key words*--Automatic berthing system; fuzzy control; ultrasonic**

I. INTRODUCTION

AT present, the small vessels in the docking is generally more than manual operation, control of the ship, others use the rope will be fixed on the shore of ship, this way is very time-consuming. For middle and small boats, most tourists themselves unable to fix in the mooring rope pole, so the bank should have a fixed responsible person[1]. In recent years, domestic and foreign existing related automatic docking solution, one of them to ship automatic berthing terminal magnetic mooring device, ships berthing, when the suction cups on the ship and the wharf steel plate after absorption, start the hoist, steel cable tension magnetic chuck make the ship on to the wharf. Although this way solve the problem of the specialist unattended, but magnetic distance of demanding problems, so the ship should have very precise positioning system, not only need to aim at hull magnetic device, but also to the driver's technical requirements is very high, and the device need to consume a lot of energy, currently only be put into use on a large ship[2]. Through the analysis of present situation, level of technology at home and abroad while part can realize automatic docking, however, is very tall to the requirement of technology of human and crew. The author in view of the existing technology time-consuming deficiency, such as research and design a oblique lines and vertical lines, parallel three docking fuzzy controller, and through the ultrasonic distance measurement, image processing technology to obtain the environment data, effective and stable to realize the automatic docking, provides a theoretical reference value for further research and development.

II. THE SYSTEM OVERALL DESIGN

System consists of signal acquisition, data analysis, result output three main parts[3-4]. System design is shown in figure 1.

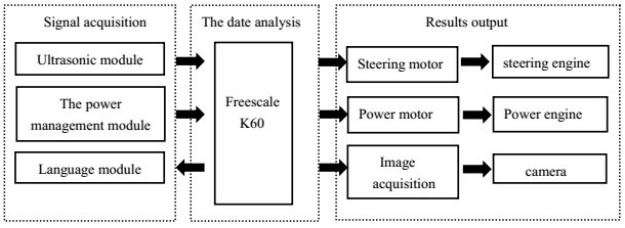

Fig.1system diagram

Ships passing docking position, ultrasonic module receives the environment information, so as to identify and storage information of the scale of the position, establishing docking area map and automatic docking way choice. K60 control steering motor driver module output PWM wave to dc motor to control the boat. Motor driver module through the output PWM wave to drive dc motor control the boat forward and backward. Ultrasonic module to collect environment information input to K60 controller, forming PID closed-loop

control, precise control of ships to completed into the position. Docking process, camera to collect the stern surface image information, and displayed on the monitor screen of a ship or wirelessly transmitted to the ground. When found the suitable position and at the end of the docking, voice modules for voice remind; When the ship and obstacle distance is too close, voice modules for alarm to remind, and with the minimum distance of obstacles of ship and more and more close, alarm frequency will be more and more high, make the system more intelligent.

III. THE SYSTEM HARDWARE DESIGN

A. Ultrasonic ranging sensor module

System USES eight ultrasonic device are all placed in the model ship environment measuring device, position in the environment can be precise positioning, ensure the reliability of the system. Ultrasonic module and the hardware structure of the ultrasonic module hull distribution as shown in figure 2, 3:

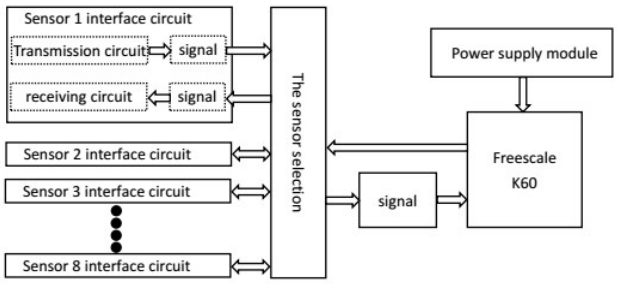

Fig. 2 Ultrasonic module hardware structure chart

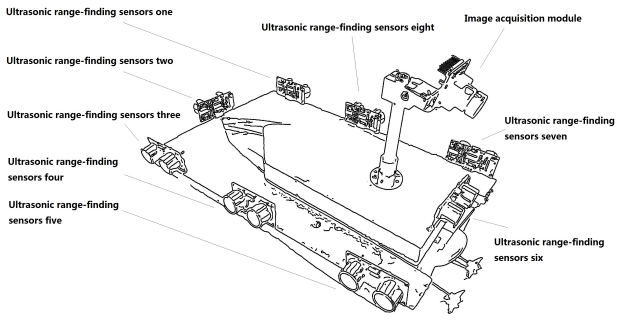

Fig. 3 the boat distribution of ultrasonic ranging system

B.Power motor and steering motor drive control circuit

Dc motor drive circuit is mainly used to control the motor and steering motor steering and speed. By changing the voltage polarity at the ends of the dc motor to control the motor to[5]; And control the speed of the dc motor has a different approach, the general method is by changing the PWM duty ratio control. L298N motor driver circuit completely meets the requirements. Motor drive control principle diagram as shown in figure 4.

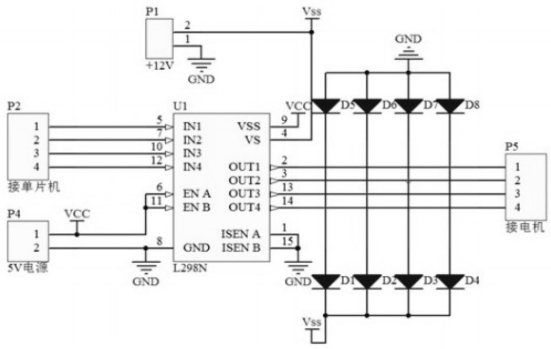

Fig. 4 Schematic control diagram of motor drive

IV. THE KINEMATICS MODEL OF MODELING

A.Steering principle modeling

In order to study the law of ship motion trajectory, the boat kinematics model is established, the model in order to effectively solve the automatic docking process. Is the ship into a rectangular rigid body can be turned to, boat on the basis of the principle of steering trapezoid kinematics model is set up[6]. For the boat model in this paper, we study, it can be simplified to "bike" model, after ignore water resistance, midpoint between front axle and the boat model for reference to describe the movement of the ship. For the purpose of this article research the ship steering model as shown in figure 5:

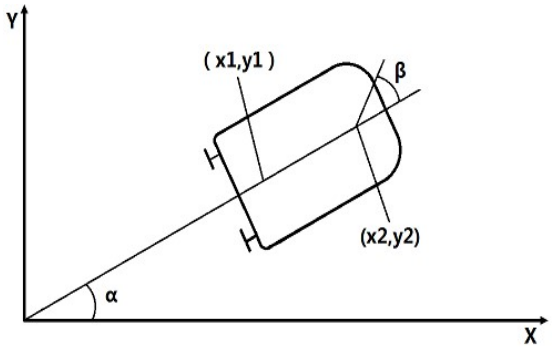

Fig.5 steering model

In the x, y in the two-dimensional plane, (x2, y2), (x1, y1), respectively model of ship rudder, rear axle midpoint coordinates; Beta model ships sailing directions and angles; Alpha said model ship hull course Angle (hull and x axis Angle); L said model ship "axis" from; V model ship speed. Ignore the natural environment such as water influence on ship

motion model, simplified model of the ship motion equations as follows:

$$x1 = v\cos\alpha\cos\beta$$
$$y1 = v\sin\alpha\cos\beta$$
$$\alpha = v\sin\alpha / l$$

Analysis equations available: speed is slow, model ship of rear axle center trajectory for a circle (in the actual process due to the nonlinear effects such as water, wind and other natural factors, model ship rear axle center orbit is an ellipse). Design according to actual ship parts scale model ship and its experimental environment, and the boat kinematics model is established in the Matlab/Simulink, for the following automatic docking provides the necessary theory basis for fuzzy controller design.

B. The Fuzzy Controller Design

Fuzzy control is using the theory of fuzzy mathematics basic thoughts and methods of control.In the field of traditional control, the accuracy of the control system dynamic model is the most important factor affect the performance of control, system dynamic information is more detailed, the more able to achieve the purpose of precise control[7]。But for too complicated or difficult to accurately describe the system, the control is not ideal.So try the method of fuzzy mathematics to solve these complex problems,Automatic docking fuzzy controller design including the oblique line, vertical and parallel three docking model design,Due to the principle of three kinds of design schemes is roughly same, docking with the vertical line as an example to explore the design of fuzzy controller.The fuzzy control principle diagram of model ship is shown in figure 6.

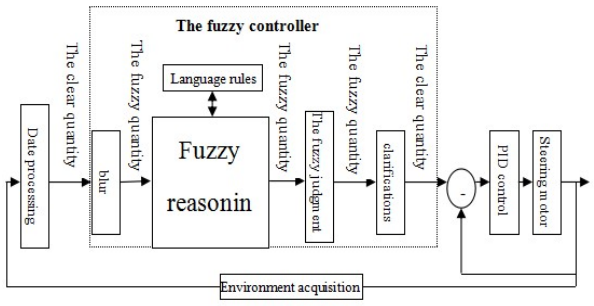

Fig. 6 Fuzzy control principle diagram

Including fuzzification, fuzzy reasoning, fuzzy judgment, motivation and language rule five parts of fuzzy controller[8-10].Freescale controller through the following three processes to achieve fuzzy control.

(1) By ultrasonic ranging sensor module for model ship distance barrier, the calculating model of ship position and Angle, sampling to data preprocessing, blurred.

(2) According to the fuzzy control rules of language, combined with the crew daily docking experience every fuzzy quantity calculated.

(3) To analyze the fuzzy quantity, after the motivation to give a good indication of the output dc motor driver module, the control model of ship steering, forward and backward.

V. CONTROL PROGRAM DESIGN

Download the fuzzy controller to form c code to freescale microcontroller, the automatic docking system, choose appropriate docking way, according to the actual surface ultrasonic ranging sensor measured data will be input into the freescale microcontroller, control model of ship steering, retreat, automatic docking.The flow chart of control program are shown in figure 7.

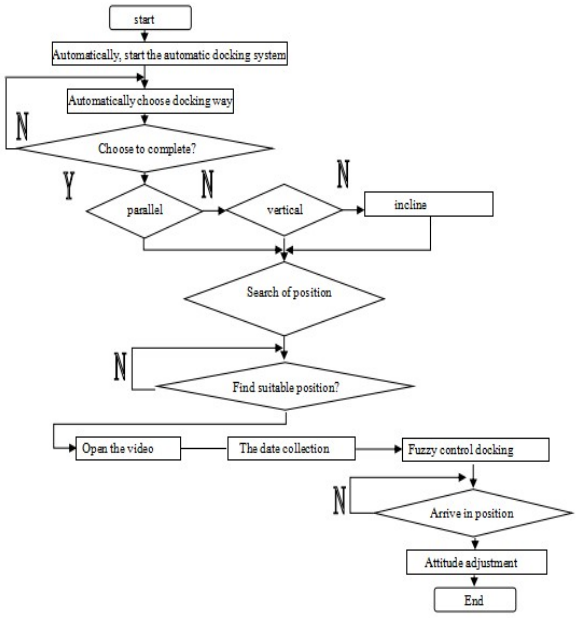

Fig.7 control program flow chart

VI. TEST AND ANALYSIS

This design docking system based on fuzzy control model is established, the crew with the actual operation experience, according to the ultrasonic sensor to determine the model ship back axle center coordinates and the boat heading Angle, initial

position and under the environment of matlab/Simulink simulation.The model car conductor l = 420 cm, car l1 = 160 cm wide, wheelbase l2 = 240 cm, position = 200 cm wide, position = 500 cm long, figure 8 is vertical the docking process simulation in matlab.Ships in the process of simulation, on the basis of the above algorithm to pour ship proved the rationality and accuracy of fuzzy controller design.

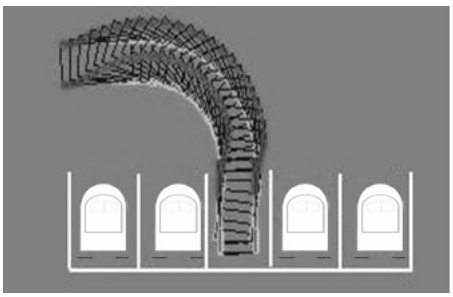

Fig.8 automatic docking Matlab simulation results

At the same time to five models of the same size as a reference for ships, according to the actual dock size proportion design of position, the reserved empty position between the two reference ships in the middle.Test, model ship is perpendicular to the position straight from right to left, found an empty position after a distance to stop down, back into position. Change model ship and the position of vertical distance, observe whether the model ship into a success, and in time.Test results are shown in table 1.

Table 1 docking test table

Test times	1	2	3	4	5	6
In a time t/s			29.2	27.3	30.4	33.2
The vertical distance	10cm	20cm	30cm	40cm	50cm	60cm
Whether or not complete	No	No	Yes	Yes	Yes	yes

By the test results can be seen that model ship hull after an automatic docking system with the position of the vertical distance of 30 cm is the best (ships 30 cm in length), lower than this distance is the boat does not have enough space to realize the large Angle turning back into position, higher than this distance model ship all can realize automatic docking, high precision and good stability.But as the horizontal distance increases, the docking time longer, lower efficiency.

VII.CONCLUSION

Design of the automatic docking system, not only can complete the model ship automatically search for the minimum empty position, and USES the fuzzy control method to complete three different docking way of docking, also USES the voice module implements voice remind, and with the minimum distance of obstacles of ships and getting closer and closer to remind the sound frequency is higher and higher, and displayed on the onboard display ship back at the stern of the surface condition, make the laboratory docking system model design more human, intelligent. For ordinary ships r&d automatic docking system to provide more theoretical basis.

References

[1] Miao Hong-song.The design of fuzzy control parking system model of ultrasonic distance measurement 2014,9(2)：1-8.

[2] Jin Ying-lian,Wang Bin-rui.A large angle in small ship automatic berthing device[P] . china:CN201971145U，2011.09.14[2015.04.26].

[3] Guo Wei-ming,Guo Xiao-xiao,Ding Yi-fan .The realization of automatic ship berthing and mooring terminal magnetic device[J].Chinese Journal of Ship Research,2006,31(2):20-32.

[4] Li Ting,Zhu Kang-fu,Fang Hong-wei. the "Freescale" creative competition of college student's smart cars[J].Value Engineering,2012，31(3):1-9.

[5] Liu De-ying, Jiang Bing,Cheng Kun-jie. The research and development of intelligent vehicle highway line drawing of ultrasonic ranging and positioning system[J],Mechanical electrical Engineering, 2010,21(6):1-6

[6] Li xudong,Liao zhonghao,Meng jiao.Intelligent vehicle control system design and realization based on CMOS camera[J].Journal of Jilin University (Information Science Edition), 2013,31(4): 414-418.

[7] Chang Jiang, Fuzzy Controller Based on Genetic Algorithm Design and Application [D] . Xi'an : Northwestern Polytechnical University, 2006.

[8] Li Qing, etal. Application of fuzzy control in bed temperature control system of circulating fluidized bed boiler[J],Journal of Ordnance Engineering College, 2009，21(5)：13-16.

[9] Kang Bing,Liang Yan-lei,Yan Dong-mei.Design of intelligent embed based parking assist system[J]. Journal of Jilin University (Information Science Edition), 2012,30(3): 223-227.

[10] Sun Bo-xun. Ultrasonic ranging automatic parking assist system based on [D].Changchun:Changchun University of Science and Technology School of Electronic and Information Engineering, 2011.

Design and implementation of intelligent voltmeter variety of detection method

Qian Chenghui; Bin Kangcheng; Zhang Hanliang; Song Jibin

(College of Instrumentation and Electrical Engineering，Jilin University，Changchun 130026，China)

***Abstract*--This article is designed voltmeter to type ARM 32-bit RISC processor for the control of the core, using the hardware circuit detection means, to achieve the AC signal peak, RMS and any periodic measurement of the average, and to achieve measurement automation. Join in the software to Extreme average filtering algorithm, filter out the obvious glitches and minor random noise is suppressed. The table can be measured signal frequency range: 1Hz ~ 1MHz, amplitude range: 0.1V ~ 10V, the measurement results of the relative error is less than±1%. This voltmeter small size, light weight, easy to carry, the voltage signal measurement greatly expanded market multimeter functions.**

***Key words*--Voltmeter; detection methods; detection waveform; band; digital filtering algorithm**

0 INTRODUCTION

AT present, the market of digital multimeter AC voltage profile using the average detection principle, can only measure the distortion sine wave signal and a narrow band of operation[1-4].Waveform detection, detection limits and working bands, affecting the use of digital multimeter. In order to obtain more comprehensive information voltage signal, AC voltage measurement should achieve peak, average and RMS detection function[4-8].

This article is designed voltmeter using a variety of detection methods to achieve any measure of cyclical AC signal the peak, average and RMS. System operating band of 1 Hz ~ 1 MHz, the measurable signal amplitude range: 0.1 V ~ 10 V, fully automated measurement process, the measurement results of the relative error is less than ±1%.

1 OVERALL DESIGN FOR SYSTEM

The overall design scheme of the system shown in Figure 1, which consists of the protection circuit, signal conditioning modules, the peak detection circuit, RMS detector circuit, the average detection circuit, A / D, ARM processor, LCD and power modules and other components .Figure 1 Overall system block diagram.

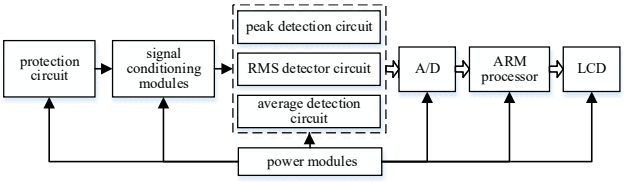

Fig.1 Systematic block diagram

To prevent damage to the system input signal is too large, the first test signal through the protection circuit; signal conditioning module comprises a voltage follower, programmable low-pass filter and amplifier circuit, amplification or attenuation of the signal peak value is determined by the multiples to achieve the measurement process automation; signal conditioning after the peak detector circuit, and average RMS detector circuit detecting circuit into a corresponding analog signals, analog signal by the A / D conversion is stored in system memory, CPU voltage signal is converted to digital was digital filtering and peak RMS average value of the measured signal and filtered on the LCD; the machine uses a battery-powered, with the use of portability.

2 HARDWARE DESIGN

2.1 Peak detector circuit

Figure 2 is a schematic diagram of the peak detector circuit. When the input voltage has not reached the peak, the diode D1 is turned off, D2 is turned on, before the signal passes through the operational amplifier A1 charging the holding capacitor C1, D1 due to the shutdown, after the op amp A2, D2 and

resistor R1 constitute a feedback path, so that the front maintained between the input of op amp A1 "Virtual Short", and because "Virtual Break" so that no current flows through the (voltage of 0 V), can be regarded as a short circuit on the R1. A1, A2 composed of a voltage follower, so that the output terminal voltage tracks the input terminal voltage A2 of A1.

When the input signal from the peak fall, before the output voltage of the operational amplifier A1 becomes smaller. When the voltage drops to a voltage holding ratio h capacitor C1, D1 conduction, D2 off [12]. Since no holding capacitor C1 discharge circuit, so Uc1 remained at the peak of the input signal, and because after the op amp A2 "Virtual Short", Uout = Uc1, enabling signal peak detection.

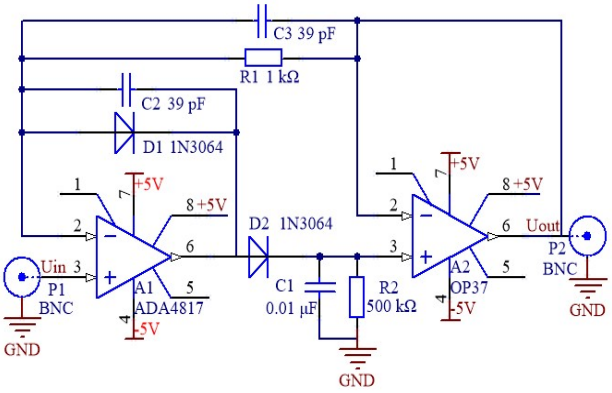

Figure 2 Peak detector circuit schematics

In order to eliminate the input offset current and maintain stable operational amplifier A1 of the front, in the D1 and R1 in parallel with a capacitance of 39 pF. After the first op amp feedback op amp access path A1 and A2 diode D2, eliminating the error by the voltage drop after the op amp's input offset voltage A2 and D2 on arising. Because the signal frequency range of 1 Hz ~ 1 MHz, the former peak detector circuit operational amplifier A1 must be large enough and strong enough slew rate of capacitance drive capability, in order to play the role of trapping voltage peaks. In order to avoid pre-amplifier A1 in the nonlinear area, select ADI produced low noise, 1 GHz FastFET ADA4817 operational amplifier as a pre-amplifier A1. ADA4817 the -3 dB bandwidth of 1050 MHz, slew rate of 870 V / us, fully meet the needs of the circuit design.

After the operational amplifier A2 must have high input impedance, acting as a buffer between the holding capacitor C1 and output, prevented by R1 and the load caused by the discharge, as the selection OP37 op amp A2.

Junction capacitance diodes use less than 1 pF, reverse recovery time of 4 ns fast recovery diode 1N3064, thus ensuring the high-frequency signal peak detection.

2.2 RMS detector circuit

According to the definition of RMS voltage equation:

$$U_{\text{rms}} = \sqrt{\frac{1}{T}\int_0^T u^2(t)dt} \tag{1}$$

RMS voltage detection principle is shown in Fig3. It is mainly composed squarer, integrator and prescribing composed, it can be realized using analog operation circuit detection voltage rms, and specific detection circuit shown in Figure 4.

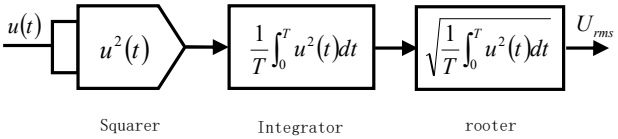

Figure 3 RMS measurement block diagram

First, the use of analog multipliers squaring the two inputs of the signal multipliers access to output u2 (t). Then use the op amp integrator circuit implementation average of time. Finally prescribing circuit consists of op amp and a multiplier for the output of the integrator root operation, to obtain the square root, the final output of the op amp voltage value of the measured signal is the RMS[4].

ADI's analog multiplier select produce low noise, four-quadrant voltage output analog multiplier AD835, it is only the product of noise (50 nV / √Hz), - 3 dB output bandwidth of 250 MHz, 0.1% of full scale settling time of only 20 ns, suitable for high speed multiplication, division, squaring, meets the design requirements of the system broadband, small signals.

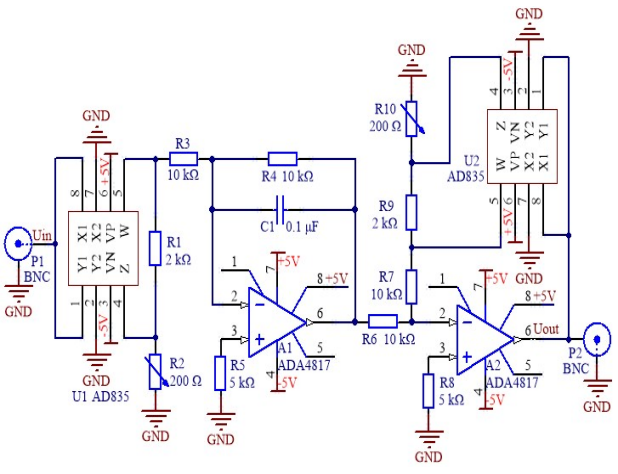

Figure 4 RMS measurement block diagram

2.3 Average detector circuit

In electronic measurement, the average voltage is an average post-detection, that is full-wave average. Therefore, the signal must first go through the full-wave rectification circuit converting an absolute value, and then filter to elect its DC component, enabling the detection voltage average [5]. The specific circuit shown in Figure 5.

Operational amplifier A1 constitute a half-wave rectifier circuit, for a positive polarity signal, the diode D1 off, D2 conduction, the output voltage half-wave rectifier circuit is -2Uin; for negative signals, the diode D1 is turned on, D2 off, half-wave rectifier circuit the output voltage is zero [14].

Constitute a reverse amplifier A2 summing circuit so Uout = - (Uin + UA1), namely Uout = | Uin |, to achieve full-wave rectification. A2 op amp feedback resistor R5 in parallel with a 330 uF end and a 100 pF capacitor constituting mean filter, and make Uout | Uin | proportional to the average value, in order to achieve the detection signal average.

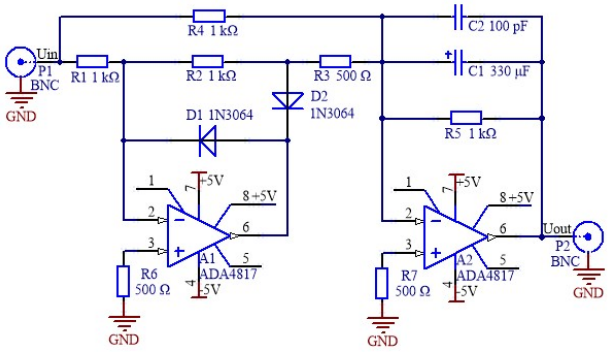

Figure 5 The average value of a measuring circuit

3 SOFTWARE ALGORITHMS

Measured AC voltage signal by the detection circuit after the conditioning module and converted into a DC voltage signal, a DC voltage signal is converted to digital by analog-voltage signal. To avoid measurement errors and interference from external amplitude pulse train into the instrument caused by random interference, the need for analog-digital conversion after the data for effective data processing, but also the design of instrumentation essential part [15]. As used herein, nonlinear filtering algorithm to Extreme average filtering algorithm designed to overcome the small-amplitude high-frequency electronic noise and interference A mutation due to external factors caused by A / D quantization noise. Extreme to the average filtering algorithm flow chart shown in Figure 6.

Extreme to average filtering algorithm: continuous sampling N times, removing its maximum and minimum of the last strike arithmetic average remaining N-2 sample data. Wherein Si is the i-th sample value, A valid data filtering algorithm for the final after.

In frequency Instek AFG-2225 signal generator company output is 1 kHz, the amplitude range 0.1 V ~ 10 V sine wave signal as a reference source, the measurement accuracy were tested before and after the filtering algorithm was added, the accuracy reflected by the relative error . The test results shown in Figure 7, wherein the dotted line represents a measurement is added before filtering algorithm relative error, a solid line indicates the measurement was added after filtering algorithm relative error.

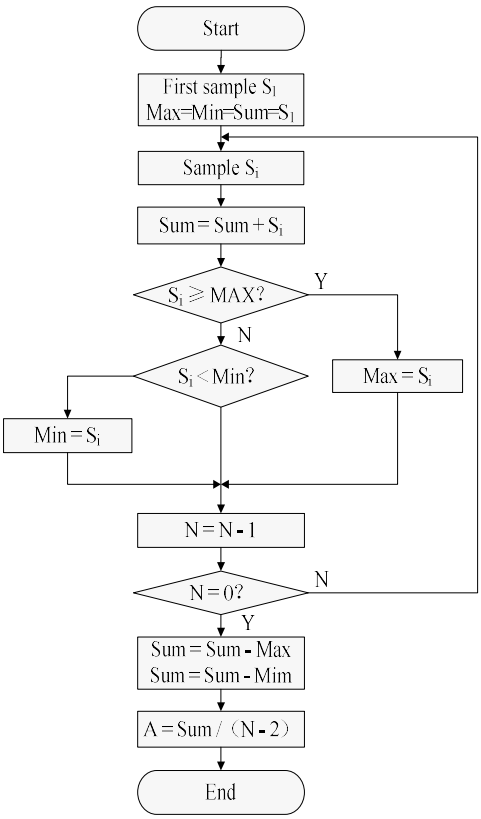

Figure 6 Extreme program flow to the average filtering

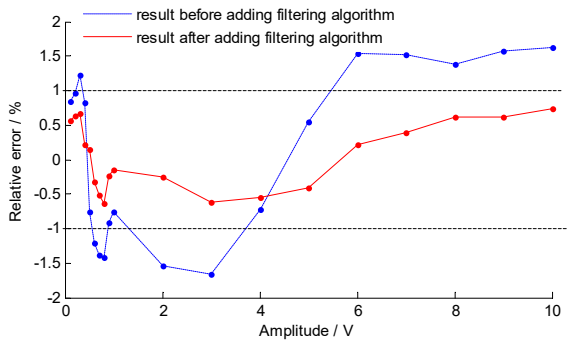

Figure 7 Before and after the filtering algorithm was added to the average relative error extreme value contrast curve

As can be seen from Figure 7: Relative error filtering algorithm was added before the test results is less than ± 2%, after adding filtering algorithm test results relative error is less than ± 1%. The test results can be obtained: Extreme average filtering algorithm to filter out the obvious glitches and minor random noise is suppressed, thereby reducing the random measurement error and improve the accuracy of measurement results.

4 THE OVERALL SYSTEM TESTING

System testing using Instek AFG-2225 company measurement reference signal generator, the measurement results and AC voltage profile measurements market DMM comparing the test results by the relative error representation.

Comparative test curve shown in Figure 8, (a), (b) and (c) are a frequency of 1 kHz, the amplitude range 0.1 V ~ 10 V sine, triangle and square wave signal to make the test curve , it can be seen from the figure: a digital multimeter AC voltage sine wave profile can only make accurate detection, and can only be measured RMS signal. The article is designed to be the peak voltage meter, RMS and average value of any periodic signals to make accurate detection and measurement of the relative error is less than ±1%.

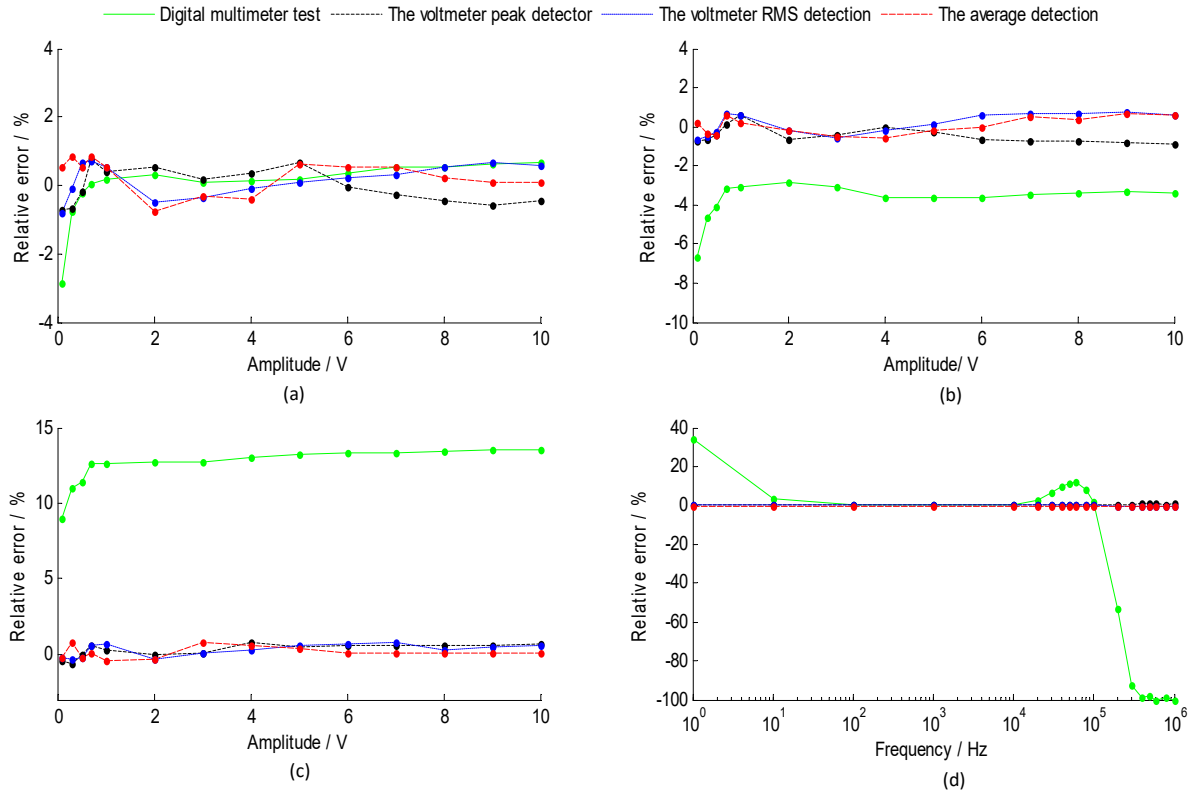

Figure 8 (a): 1KHz sine wave signal test data comparing the curve, (b): 1KHz test data comparing the triangular wave signal curve, (c): 1KHz square wave test signal contrast curve data, (d): the frequency characteristic curve data comparison test

Figure. 8 (d) is the amplitude of 1 V, a frequency of 1 Hz ~ 1 MHz sine wave signal to make test curve, it can be seen from the figure: AC voltage profile detection narrow band digital multimeter, can only relative error of 40 Hz ~ 10 kHz signals to make accurate detection, and this article is designed voltmeter has good frequency characteristics, which may be of 1 Hz ~ 1 MHz signals to make accurate detection and measurement results were less than ± 1 %.

5 CONCLUSION

This article is designed to measure the peak voltage meter intelligent arbitrary periodic AC signal, RMS and average operating frequency band of 1 Hz ~ 1 MHz, the measurable signal amplitude range: 0.1 V ~ 10 V, fully automated measurement process, measurement relative error is less than ±1%. Compared with the digital multimeter, which significantly improves the detection frequency band, increasing the detection mode extends the detection waveform can be more fully reflect the characteristics of the voltage signal, and having a stable, practical, small size, light weight, easy carry.

References

[1] SONG F J,SUN J,LI G ZH. Designing of 89c51 SC Computer-based Digital Voltmeter[J]. Manufacturing Automation,2007,02:89-90+93.

[2] XIONG J J,HUANG H,GUO K Q,et al. Study on measurement device for transfer overvoltage of GIS transformer[J].Chinese Journal of Scientific Instru -ment ,2013,S1:121-125.

[3] M.Maruyama, A. Iwasa, H. Yamamori, et al., “Develop -ment of zener calibration system using 10 V programmable Josephson voltage standard at NMIJ,” in Proc. CPEM, Aug. 2014, pp. 260–261.

[4] C. J. Burroughs et al., “NIST 10 V programmable Josephson voltage standard system,” IEEE Trans. Instrum. Meas., vol. 60, no. 7, pp. 2482–2488, Jul. 2011.

[5] LIANG Q. Design of True RMS Value DVM with High Precision Based on Chip AD637 [J]. China Instrumentation,2008,11:57-60.

[6] RONG F,MIAO CH Y,Xu W. Development of ILS signal monitor [J]. Journal of Electronic Measurement and Instrument,2010,09:872-877.

[7] A. Rüfenacht et al., “Cryocooled 10 V programmable Josephson voltage standard,” IEEE Early Access Article, vol. PP, no. 99, pp. 1-6, 2014.

[8] LIN ZH J. Electronic Measurement Technology(Second Edi-tion)[M].Beijing:Electronic industry press 2007, 82-100.

[9] LU Y F,ZHAO J T,HE Q,ZHANG ZH H. Low current precision measurement technique based on cryogenic current comparator [J]. Chinese Journal of Scientific Instrument,2013, 12:2812-2817.

[10] F. Müller et al., “NbSi barrier junctions tuned for metrological applications up to 70 GHz: 20 V arrays for programmable Josephson voltage standards,” IEEE Trans. Appl. Supercond., vol. 23, no. 3, pp. 1-5, Jun. 2013, Art. ID 1101005.

[11] S.-F. Chen, Y. Amagai, M. Maruyama, and N. Kaneko, “Uncertainty evaluation of sampling measurement system using AC-programmable Josephson voltage standard,” in Proc. CPEM, Aug. 2014, pp. 258-259.

[12] XU L L. Non-sinusoidal test signal peaks on the Realiza-Tion of simulation testing machine[J].IC application,2003,04:38+33.

[13] WANG B S. AC voltage and current RMS Transmitter [J]. Measurement Technique,1990,10:16-17.

[14] WEI X P. Measurement and Analysis of Voltage Fluctuation and Flicker [D]. Electric Power University of North China (Beijing),2010.

[15] CHENG D F. Intelligent instruments (Second Edition) [M].Beijing:Machinery Industry Press,2009,113-119.

Multi-Input DC/DC Topology Model for Complementary Clean Energy Generation System

Zhao Zibo; Ding Sibao; Zheng Bowen
（jilin university instrument science and engineering institute,changchun,130021）

***Abstract*--This paper proposed a voltage stabilized topology model of multi-input DC/DC based on buck circuits in terms that the prevalent multi-input DC control algorithm had been relatively complicated ， because the complementary clean energy generation systems have characteristics of intermittent and random. The model can steady voltage in any value of input voltage, providing relatively simple control methods, to ensure stable load and improved the efficiency of generating electricity of clean energy. This paper analysed the theory of the model, simulating the three-input circuits of model validation in Matlab software and carried out the experiments by using an input of solar and wind energy. It proved that the topology model not only had plenty of advantages of buck circuits, but also achieved a better use of complementary energy in complementary clean Energy generation systems with multi-Input DC/DC circuit and improved the stability and feasibility of the output of systems.**

***Key words*--Complementary clean energy; topology model; DC/DC; buck circuit**

I. INTRODUCTION

NOWADAYS, as the dwindling of fossil fuels, compared with the traditional thermal power, there are shortcomings , such as low efficiency and serious pollution .Wind power, solar power, and other forms of renewable energy power generation have become more and more favored by people, it is the main subject of global research. Solar and wind energy and other forms of clean energy generation due to the wide variety of sources, stability is relatively high, has become the development of better forms of electricity generation [1]. Single clean energy generation by natural factors greatly constrained, so people put forward a Multiple-Input Converter（MIC), instead of a plurality of single-input DC converter [3], to achieve energy conversion.

Depending on the variety of ways to connect the energy source, MIC is generally divided into two types: (1) sharing power supply type: any time are only one input power source to the load. (2) simultaneously powered: more energy input simultaneously, when the power supply to the load can be combined to be a separate power supply. With the recent development of the MIC, MIC greater variety of circuit topologies have been proposed [3-9]. The paper[3] proposed a dual input Buck topology, this topology is simple, not only to enter a separate power to the load, you can also power to the load. In the paper [4] ,Luo Quanming proposed a multi-input high boost topology, the topology of simple control, low voltage stress of the switching device. The paper [5] introduces a two-input flyback DC / DC converter, the use of conventional electrical isolation transformer to resolve the issue, but also enter either work individually or simultaneously. The paper [6] describes a suitable low voltage source input topology.

The MIC mentioned above , their circuit voltage have more complex relationship between the input and output voltage. So to absolve this problem, this paper proposes a multi-clock input DC / DC regulator topology model. The topological model is applicable to replace the DC transmission bus in wind and solar power generation system, not only achieving Buck circuit operated an energy input of electrical energy, but also for a variety of clean energy generation series regulator under way to facilitate the output voltage amplitude controlled energy storage more conveniently.

II. THE BASIC PRINCIPLE BUCK TOPOLOGY

Traditional single input Buck chopper circuit principle of the circuit shown in Figure 1.

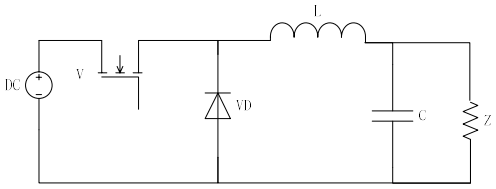

Figure 1 Single - input Buck step-down chopper circuit

On the basis of the ideal circuit analysis, assumptions: (1) provided in the inductor current iL is the continuous transformation; (2) the capacitance is large enough to do, in order to ensure that the output voltage of the text of the wavelet zero; (3) Suppose circuit switch capacitor and inductor is used as the ideal device, ignore the effects of parasitic elements; increased conduction (4) assume the switch and turn-off waveform and fall time is zero. Suppose when t = 0, V switch is turned on, UGE represents the voltage between the drain and gate switch, ie a driving voltage switching tube. When the switch is turned on, the power flows through the switch, inductor and capacitor to supply the load, the power supply current flows shown in Figure 2, flowing through the load current io exponentially rising trend. When each component parameters match, io final output will reach the input voltage, that is, at a time t = t1 before, Uo = Uin.

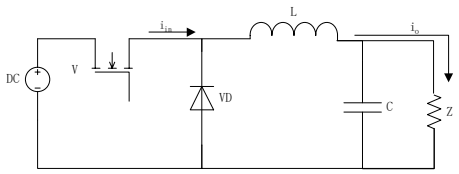

Figure 2 Circuit current flows when the switch conduction

When t = t1, UGE from high to low voltage, V control switch is turned off, this time due to the effect of having a freewheeling inductance, the load current will continue to circulate along the diode VD, while continuing to ensure that the output voltage of the storage capacitor load current exponential curve trend down until the next V switch is turned on. Figure 3 (a) is a waveform UGE conducting switch V; Figure 3 io waveform (b) flowing through the load

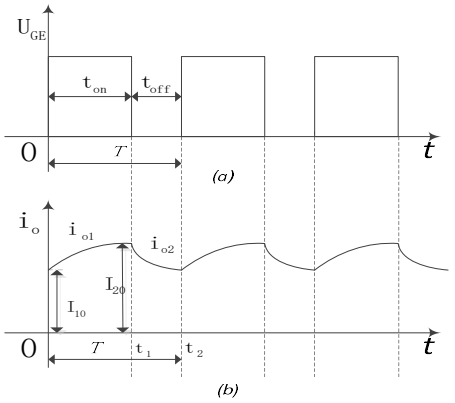

Figure 3(a) The waveform of voltage between Gate and Drain

(b) Output current waveform

According to FIG. 3 io output waveform, the average within a period of the output voltage is:

$$U_o = \frac{1}{T}\int_0^T U(t)dt \qquad (1\text{-}1)$$

$$U_o = \frac{1}{T}[\int_0^{\alpha T}(U_{in} - L\frac{di_L}{dt}) + \int_{\alpha T}^{T}\frac{di_L}{dt}L] \qquad (1\text{-}2)$$

Wherein in the formula (1-2) α is duty ratio of the drive signal switch, namely:

$$\alpha = \frac{t_{on}}{T} = \frac{t_{on}}{t_{on}+t_{off}} \qquad (1\text{-}3)$$

Since the device is an ideal model of the circuit element, the output voltage reduces to:

$$U_o = \frac{1}{T}t_{on}U_{in} = \frac{t_{on}}{t_{on}+t_{off}}U_{in} = \alpha U_{in} \qquad (1\text{-}4)$$

Clean Energy Generation System Multi added storage batteries, either store excess energy, but also to ensure that when the power is limited to the load to provide power [10]. When the voltage at the load contains energy storage components, energy storage element is equivalent to a back electromotive force, then the equivalent circuit shown in Figure 4:

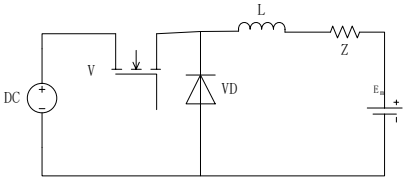

Figure 4 The equivalent circuit comprising the counter electromotive force when loading

When the switch is turned on in the period V, load current is set io=1, you can list the following equation:

$$L\frac{di_o}{dt} + Ri_o + E_m = U_{in} \qquad (1\text{-}5)$$

Wherein the formula (1-5) Em is the equivalent voltage of the energy storage element. When the set

switch is turned on t = 0, the initial value of the load current is I10, the time τ = L / R, into the formula (1-5), formula (1-6):

$$i_{o1} = I_{10}e^{-\frac{t}{\tau}} + \frac{U_{in}-E_m}{R}(1-e^{-\frac{t}{\tau}}) \quad (1\text{-}6)$$

When the switch is turned off, the load current is set at this time io2, at this time are listed according to the following equation KVL:

$$L\frac{di_{o2}}{dt} + Ri_{o2} + E_m = 0 \quad (1\text{-}7)$$

Let the initial shut-off switch value I20, into the above equation, can be obtained at this time is the load current io2 is:

$$i_{o2} = I_{20}e^{-\frac{t-t_{on}}{\tau}} - \frac{E_m}{R}(1-e^{-\frac{t-t_{on}}{\tau}}) \quad (1\text{-}8)$$

Since the inductance effect, so in this case the load current is continuous, according to FIG. 3, the relationship can be obtained:

$$I_{10} = i_{o2}(T) \quad (1\text{-}9)$$

$$I_{20} = i_{o1}(t_1) \quad (1\text{-}10)$$

That switch V into a conducting state and the initial value of the switch current value V in the off state of the initial value. According to the formula (6), equation (8), the equation (9) and Equation (10) can be introduced I10 and I20: [11]

$$I_{10} = \left(\frac{e^{\frac{t1}{\tau}}-1}{e^{\frac{T}{\tau}}-1}\right)\frac{U_{in}}{R} - \frac{E_m}{R}$$

$$= \left(\frac{e^{\alpha\rho}-1}{e^{\rho}-1} - m\right)\frac{U_{in}}{R} \quad (1\text{-}11)$$

$$I_{20} = \left(\frac{1-e^{-\frac{t1}{\tau}}}{1-e^{-\frac{T}{\tau}}}\right)\frac{U_{in}}{R} - \frac{E_m}{R}$$

$$= \left(\frac{1-e^{-\alpha\rho}}{1-e^{-\rho}} - m\right)\frac{U_{in}}{R} \quad (1\text{-}12)$$

In the above formula, φ = T / τ, m = Em / Uin.

According to Figure 3 (b) known in I10 and I20, respectively, for the minimum and maximum load current, based on the formula (1-11) and Equation (1-12) Taylor series expansion analysis, you can get:

$$I_{10} \approx I_{20} \approx \frac{(\alpha-1)U_{in}}{R} = I_o \quad (1\text{-}13)$$

It can be concluded that the inductance L infinity, the maximum and minimum load current is approximately equal to the average of the load current Io.

Ⅲ. MULTI-INPUT DC / DC BOOST TOPOLOGY MODEL

Since the multi-input complementarity between power generation system to produce clean energy is isolated from each other, so the voltage of each power generated by the system can be connected in series or parallel with each other. FIG. 5 is a multi-input DC / DC regulator topology model, model In_DC1, In_DC2, In_DCn represent the input voltage, V1-Vn represents each input corresponding to the MOS transistor, VD1-VDn is corresponding to each input circuit of the diode.

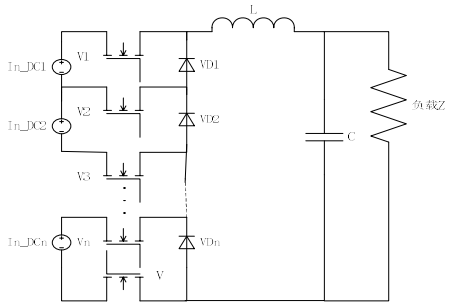

Figure 5 Multi-input DC / DC boost circuit topology

As shown in figure 5, when any input, through the opening of the input MOS transistor and diode in series constitute the input voltage, input as a whole Buck circuit, relying Buck circuit form, a plurality of input voltages whole buck.

For n input j has any input voltage condition is met, the output voltage Uo size:

$$U_o = \alpha\sum_{i=1}^{j} In\_DCn(i) \quad (2\text{-}1)$$

Where α = ton / T.

Which can be constructed input relationship, the only way for the first series in the load drive voltage MOS transistors, open the corresponding separate input circuit of the MOS transistor, each input rely freewheeling diode. Figure 6 is In_DC1, when MOS is a schematic view of the current loop In_DC2, In_DCn three transmission depressed.

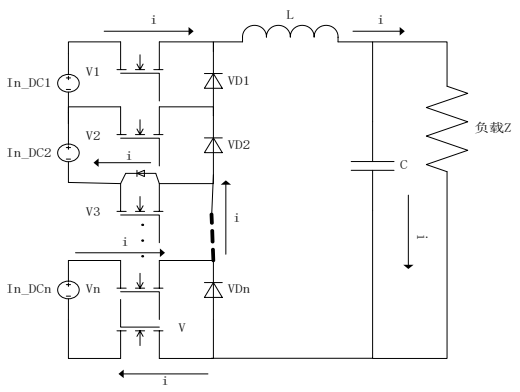

Figure 6 The current loop of three-input

In the control circuit, as long as the input voltage detection and analysis of the input voltage, the input voltage is determined voltage in series form the corresponding single or multiple synchronous drive voltage MOS tube loading. By adjusting the duty ratio of the driving voltage waveform to adjust the size of the output voltage, the output voltage stability.

Ⅳ. EXPERIMENTAL DATA

Since the current widespread use of clean energy power generation will be limited by natural conditions, DC proposed / DC regulator topology model for the use of a variety of clean energy generation or more clean energy generation systems, in order to verify this design MIC circuit, using the MATLAB simulink simulation circuit MIC and produced a small three-input power, the use of solar panels as the three three-input voltage. FIG. 8 is a three-input DC / DC regulator circuit simulation simulink the topology model.

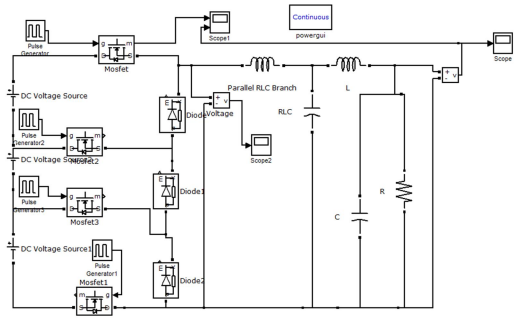

Figure 7 Three-input DC / DC buck topology model simulation Figure

FIG. 9 is a simulation results. Wherein (a) is a driving waveform; (b) simulation of the input and output voltage.

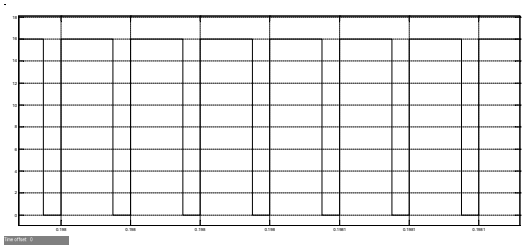

(a)

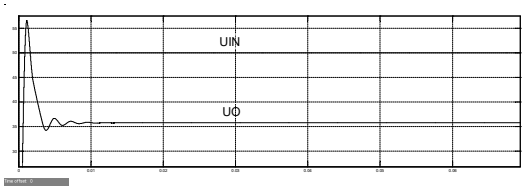

(b)

Figure 8 (a) The voltage waveform of input and output (b) The trigger waveform of MOSFET

Experimental set up a three-input low-power DC / DC boost topology model, inductance is 120μH, use 2200μf capacitive,51Ω load resistor and DC power supply as input voltage. Figure 10 (a) are MOS tube drive voltage waveform; (b) the voltage waveform between the drain and source of the MOS tube; (c) for the output voltage waveform.

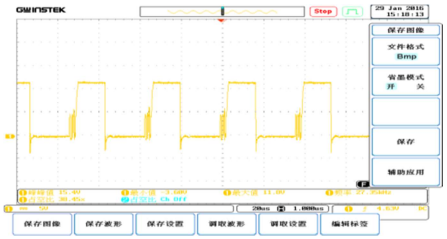

(a)

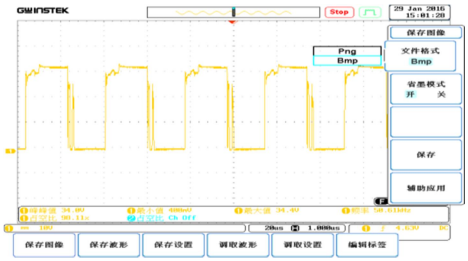

(b)

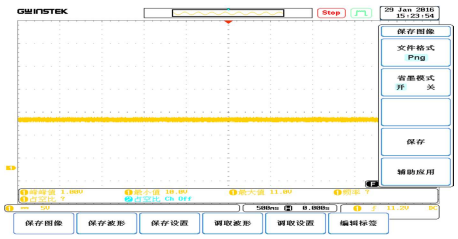

(c)

Figure 9 (a) The output voltage (b) The trigger waveform of MOSFET (c) The voltage between the drain and the source of MOSFET

Ⅴ. CONCLUSION

Multi-input DC / DC boost topology model in practical applications, not only to ensure complementary clean energy generation system stability of output voltage but also power generation efficiency can be improved. At the same time, the topology model in any input enables can stable voltage output, and the system control algorithm is simple for output voltage and input voltage relationship clear. This model will ensure efficient work in the clean energy power generation system.

References

[1] Zahedi A . Solar photovoltaic (PV) energy : latest developments in the building integrated and hybrid PV systems[J].Renewable Energy,2006,31:711-718 .

[2] Liu Longfei,Jia Kejin,Du Taihang .Low-power wind-solar hybrid power control system[J]. Power Supply Technology and Its Application , 2014(02):59-67

[3] Li Yan,Ruan Xinbo,Yang Dongsheng. A New Double . Input DC-DC Converter[J].TRANSACTIONS OF CHINA ELECTROTECHNICAL SOCIETY, 2008 , 23 (6) : 77-82.

[4] Luo Quanming, Zhu Binxin,Wang Yang. High Step-up Boost Converter With Multiple-input[J]. Proceedings of the CSEE, 2012 , 32 (3) : 9-14.

[5] Wang Qin,Zhang Jie,Ruan Xinbo. A New Double-Input Flyback DC/DC Converter[J]. TRANSACTIONS OF CHINA ELECTROTECHNICAL SOCIETY , 2011 , 26 (2) : 115-122.

[6] Chen Y M ,Liu YC ,Lin S H ,et a1 .Double—input PWM DC / DC converter for high / low voltage sources[J] . IEEE Trans . Ind . Electron . , 2006,53(5) : 1538-1544

[7] NICHOLAS D B , PATRICK L C. Power budgeting of a multiple-input Buck-Boostconverter [J]. IEEE Transactions on Power Electronics , 2005 , 20 (6) : 1303-1309.

[8] LIU Y C , CHEN Y M. A systematic approach to synthesizing multi-input DC-DC converters [J] . IEEE Transactions on Power Electronics ,2009 ,24(1):116-127.

[9] Lu Zhiguo,Liu Jiefeng,Zheng Luyao. Double-input Boost converter[J]. Electric Power Automation Equipment ,2010 , 30 (9) : 42-45.

[10] WANG Zhaoan,HUANG Jun.Power Electronies[M].Beijing:Mechanieal Industrial Publishing House,2008:119-121.

Workpiece Dimension Measurement Based on digital Image Processing Technology

Ling Zhenyou; Ling Chenyu; Deng Shengzhong

（jilin university instrument science and engineering institute,changchun,130021）

***Abstract*--With the popularity of computers in various fields and technology continues to improve, the intelligent level of metal workpieces manufactured in China is also growing. For the shortcomings of the current workpiece dimension measurement, were studied by means of digital image processing technique to measure the dimensions of the workpiece. Using MATLAB to design an intelligent measurement system of workpiece size, the device consists of camera systems, data transmission device, image processing system and other system components. Applying the principle of indirect measurements, calibration using standard reference material, and then to measure the actual size of the workpiece.**

***Key words*--Digital image processing Industrial camera MATLAB Workpiece measurement**

I. OBJECTIVE

WOKPIECE dimension measurement is an essential step in the production process of workpiece,workpiece dimension measurement in many places still use mechanical measuring, precision has some errors and inconvenient, especially unable to automate the measurement process, needed someone in custody. Therefore,given a workpiece dimension measurement system based on digital image processing technology. The system through the industrial camera images and automatically measuring of workpiece and can record off size of the workpiece. This system is convenient for monitoring the production quality of the workpiece, and saves the human and material cost.

II. RESEARCH SIGNIFICANCE

Digital image processing is to use digital computers and other digital technologies, image processing, to achieve the desired objective. With the development of computer image processing technology has been widely applied in many fields, digital image processing has become electronic, information, communication, computer, automation, signal processing and other important lessons. Digital image processing and measurement technology is based on the measuring method of digital image processing, with the traditional measurement method has advantages[1,2].
Traditional workpiece dimensions tools include scales, calipers, also based on optical, micro-measuring instruments.

Disadvantages:

1. Based on the traditional contact measurement due to measure the environmental impact of large, most of the time restrictions on conditions of use. For complex artifacts, irregular, often can not be measured directly. Traditional contact measurement, accuracy is not high, the measurement of time.

2. Conventional optics, microscopy measuring instruments, although accuracy is high, but tend to design more complex to use, need to be able to use certain knowledge, complex operation, and the equipment is expensive.

Measurement method using digital image processing is a very reliable method of high speed, high precision, high speed, low cost and easy, provided a new way for object measurement and ideas[3,4].

III. THE OVERALL DESIGN

A. Research Ideas

Through a large number of digital image processing literature information in this regard, after discussion and summary, we propose a measurement of workpiece length of design ideas[5]. Use MATLAB, workpiece image in a camera that arrived at the computer. Using digital image processing software for processing, are parameters such as the length of the workpiece, the interface displays the measurement result.

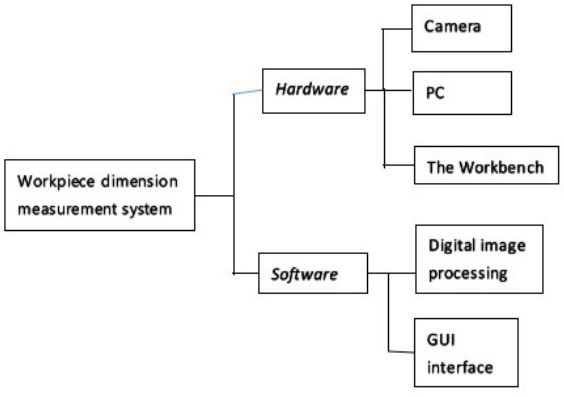

Fig.1 general architecture of system

B. The Main Module and Design

a. Part of Hardware

Workpiece by using high resolution industrial camera shot and designed an adjustable bracket for fixing the camera and adjust the camera and the distance between the workpiece[6,7].

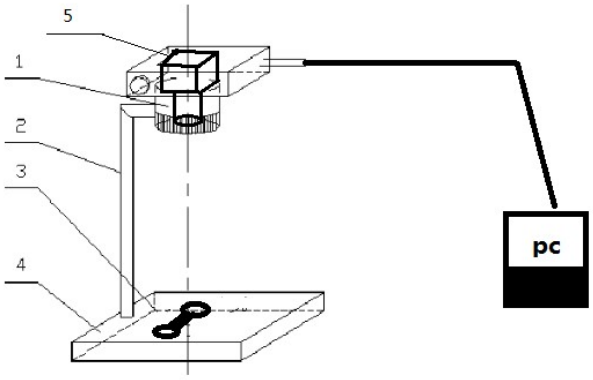

Fig.2 Hardware structure diagram

(1.Light. 2.Bracket 3.Workpieces 4.Base 5.Camera)

b. Software system

Software includes algorithms programmed in programming and interface design, programming, algorithm programming, including aspects of binarization and edge detection, according to the pixel with the proportion of the actual size and workpiece parameters are obtained by indirect measurement method. Interface programming allows people to simple operation and workpiece parameters were observed.

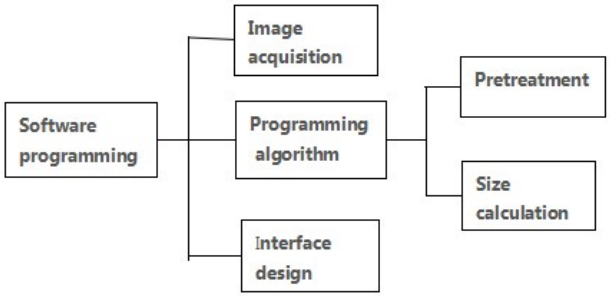

Fig.3 Software structure diagram

IV. Each Module Implementation

A. Hardware Parts

Hardware platform consists of industrial cameras, lighting equipment, frame, chassis, PC components.

Industrial cameras are Basler camera with 2592x1944 resolution, the camera uses GigE Vision transmission through the network cable connected to the PC, with low noise and high resolution, fast transfer speeds, with little distortion and so on. Industrial cameras are an important part of the image acquisition process.

Fig.4 Industrial Camera

Lighting tool is adjustable ring-shaped LED lights, adjustable brightness, low power consumption, lighting more efficient features installed on the camera lens, but can reduce the light dead ends, provide important protection for camera image capture.

By cameras and table structures, providing work environment for object measurement. The hardware part is the function of image acquisition, camera control based on the PC industry photos

B. Software

a. Image Collection

Image acquisition part is controlling the camera took pictures, and image transfer to PC, waiting for further processing.

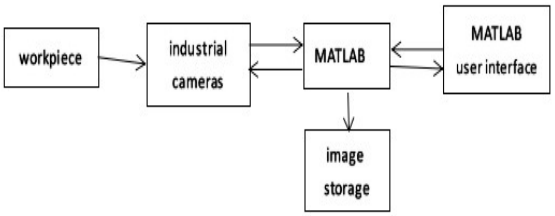

Fig.5 Schematic of image acquisition

1. The monitor interface

By videoinput function, here we use the default video capture format, to monitor the cameras took pictures of the interface, and displays the video camera in the GUI interface.

```
obj=videoinput('winvideo',2,'YUY2_2592x1944');
axes(handles.axes1);
vidRes = get(obj, 'VideoResolution');
        nBands = get(obj, 'NumberOfBands');
        hImage = image( zeros(vidRes(2), vidRes(1),
nBands) );
        preview(obj, hImage);                    (1)
```

2. Resolution settings

Resolution settings using the interpolation method, image resampling, bicubic cubic interpolation takes into account not only the direct effect of adjacent to it, also taking into account the pity Dorado, around 16 effect of adjacent to it. Because the sampled values using interpolation function s (x) =Sin (pi*X)/(PI*x) interpolation, then restoring the original functions of the precision and, of course, any of which can be accurately sampled point values, this method calculates the volume but high accuracy, can keep a good image.

```
frame=imresize(frame,fbl,'bicubic')              (2)
```

3. Photo storage

In order to secure the workpiece image processing, so to get the images from the camera and stored in the PC, so that we can later image processing. Function:

getsnapshot(obj) (3)

Captured images can be provided, but this function is YCBR captured image format, image is displayed red, to display this image if you want to convert to RGB format:

frame=ycbcr2rgb(frame) (4)

But in our image, we don't need to color the image, in order to facilitate the handling of late, convert a color image to grayscale images:

frame=rgb2gray(frame); (5)

b. Image Preprocessing

1. Greyscale Distribution

Histogram is reflected in an image gray-level graphics with the probability of this gray, which is a function of gray level. Reflected image in the histogram of the image intensity distribution property. From the histogram, you can see an image of quality. One image is good, bright and dark clear images of the histogram for a bimodal curve. If the histogram of an image has only one peak, and at the high gray levels, means that the image is overexposed and vice versa, lower peak is located in the gray, it means that the image is underexposed. Above problem appears if the image histogram, histogram modification methods can be used to enhance images.

Workpiece image and its histogram as shown in the figure. Graph abscissa v is the gray value, and ordinate is the number of pixels of this gray value. Based digital image pixel gray value of V0, V1, Vi-1, the grayscale values of probability p (Vi) (digital image f (i,j))

$$P(Vi)=\frac{\text{Vi number of pixel}}{\text{Total pixel values on the image}} \quad (5)$$

And

$$C=\frac{U_o*(1-D)}{8*U_o*L*f^2} \quad (6)$$

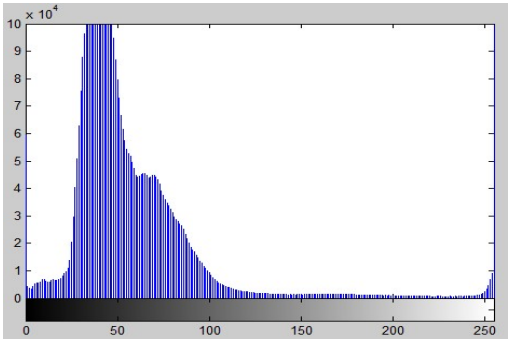

Fig.6 The image gray level distribution

2. Binarization

Image binarization aimed images as targets and backgrounds of two parts.Result of binary decides the result of image edge extraction. Determines the accuracy of detection.According to the image histogram to select suitable threshold values, and achieve better binary image.

Binarization divided into two parts, automatic and selected values binarization.

Automatic binarization:

level=graythresh(M);
M1=im2bw(M,level); (7)

Use graythresh function automatically get pictures threshold for image segmentation.

Set value and binarization:

Adjust the slider, threshold from small to big, change level, binary image, by observing the change of image binarization image, obtain the best binary images for later image processing provide an important guarantee for the work.

3. Edge Recognition[8]

Hough function to detect circular.Hough transform is one of the basic methods of image recognition in image processing.Hough transform is the principle of duality of use of point and line, the original image space of a given curve by curve expression parameter space of a point.Detection of the curve given in the original image into looking for peaks in the parameter space problems. Detection detection parameters into properties. Such as lines, ellipses, circles, arcs, etc[9,10].

In short, Hough transform thought: a point in the coordinate system of the original image corresponding to the parameters of a straight line in the coordinate system, the same straight line parameters corresponding to the coordinate system of the original coordinates of a point, and then the original coordinates By presenting all points straight lines, their slope and intercept are the same, they correspond to the same point in the coordinate system parameters.After each point of the original coordinate system projected coordinate system to the next parameter,Have gathered point of view coordinate system parameters, such aggregation point corresponding to the straight line of the original coordinate system.

In practical applications, y=k*x+b linear equations have no way to express a straight line in x=c form (at this time, the slope of the line is infinite). So in practice,is the use of parametric equations：

p=x*cos(theta)+y*sin(theta). (8)

In this way, a point on the image plane corresponding to the parameter p---Theta on a curve in the plane, the other is still the same[11,12].

c. Calibration and Measurement

Because the actual object exists with the image size

derived from a scaling factor k, to measure the actual size of the workpiece, you must first get the scaling factor k. So it is necessary to calibrate the system.

Using a calibration plate, under the premise of not changing themeasurement parameters, to calibrate the measuring system K=L/L0.Computer image size where L0 is the calibration plate, L is the facto standard for the calibration plate size. L is known, the unit is mm[13].

After calibration the values for k. Fig.7 is a workpiece image.

Fig.7 image of Workpiece

Measuring section including the manual measurement and automatic measurement

1. Utomatic Measurement

Due to the application of the Hough transform for circle detection, Hough transformation detection principle in the above description[14], so this is not repeated.By Hough transform, O' Access Center coordinates (x, y) and radius R ', and the circle is displayed on the image.Two holes in the workpiece's Center distance L is:

$$L = k * \sqrt{(x1 - x0)^2 + (y1 - y0)^2} \tag{9}$$

K is the scaling factor. x, y as the Center coordinates. Actual workpiece hole radius r is:

$$R = k * R' \tag{10}$$

2. Manual Measurement

In order to secure workpieces of irregular, difficult to automatically identify the dimensions of a shape parameter, manually measured as a supplement of automatic measurement of workpiece size parameters. Use the ginput function manual measuring.

Ginput provides a cross hair so we can choose what we need to more accurately position and returns the coordinate values. Function call in the form of:

$$[x,y] = \text{ginput}(n)$$
$$[x,y] = \text{ginput}$$
$$[x,y,\text{button}] = \text{ginput}(...) \tag{11}$$

[x,y] =ginput (n), will enable you to read from the current coordinate system of n points, and returns n x, y coordinates of a point are nX1 vector.You can press ENTER to end early readings.

In this article uses the ginput function, use the mouse to move the cross cursor on the image, select two points on the image pixel coordinates for the location of A1 (x1,y1), A0 (x0,y0), D is the distance between these two points on the actual work:

$$D = k * \sqrt{(x1 - x0)^2 + (y1 - y0)^2} \tag{12}$$

k is a scaling factor.

V. Performance Tests and Results

After the completion of system software, a MATLAB GUI interface, through the interface can be a simple operation, setting parameters and measuring of parameters of the parts of the image.

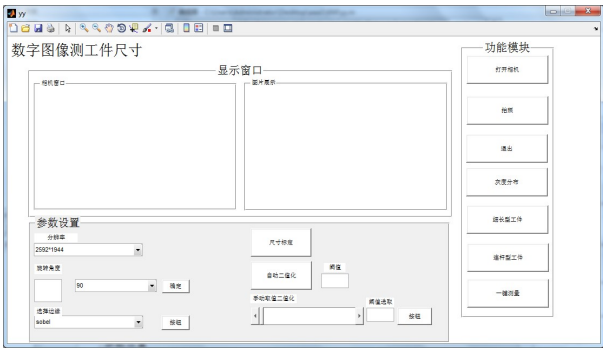

Fig.8 GUI interfac

Through the MATLAB GUI interface of workpiece image acquisition and image processing, can automatically identify the workpiece hole and inner and outer diameters of the circular hole is the center distance between the two holes, can use manual measurement to measure the distance between any two points on the image. The following Fig. 9.

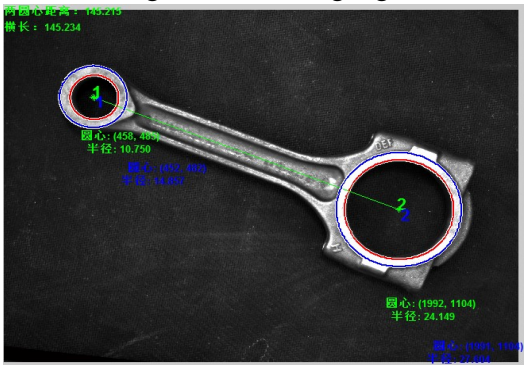

Fig.9 image of Measurement result

We have to measure the same workpiece, reflected inTable.1

Table.1 **The measured results**

Order	Inner radius of the small hole （mm）	outer radius of the small hole （mm）	Inner radius of the large hole （mm）	Outer radius of the large hole （mm）	The two hole center distance （mm）
1	10.722	14.706	23.948	27.551	145.063
2	10.633	14.621	24.168	27.632	145.102
3	10.556	14.762	24.623	27.684	145.120
4	10.852	14.920	24.765	27.362	145.058
5	10.610	14.870	24.544	27.822	145.032
Actual size	10.50	15.0	25.00	28.00	145.00

As can be seen from the table, the system can automatically identify and measure of the workpiece for two-hole distance of the inside and outside diameter have two holes. Meet expectations as a whole.

VI. ERROR ANALYSIS

Measurement results can be seen in the table of measured data and actual values for errors still exist, after summarizing, the error can be caused by the following.

1.Tailed to level the camera, between the camera and the base are not parallel, is the camera base where there is a certain angle with the workpiece, it may cause error .

2.There is a distortion of the lens of the camera, so that a tiny gap between the workpiece on the image

3.The work piece is not placed directly below the camera, can also make the camera and workpiece have certain inclination. Causing errors.

4.The algorithm is not perfect, the workpiece edges smooth enough, edge detection, resulting in big diameter, outer circle is small.

VII. CONCLUSION

This measuring system for fast, automatic, non-contact the workpiecedimensions are measured. Different from the traditional way, it is a newway of measuring.By using MATLAB GUI interface to intuitively and simply measure.With automatic, manual and key measurements for three kinds of measuring methods. For applications in industry and production, such as production on the parts of the plant or production line.The systemHas good scalability , be able to meet a variety of needs, to design different measuring algorithm.But there are still some problems, such as accuracy, background and color of the workpiece to be raised further separation.There are high requirements for light, and so can still be further improved.

References

[1] Yangyi. Geometric Size Detection Method Based on Image Processing [D]. Xihua University, 2011

[2] GaoXiuzheng. Course Design of Digital Image Processing Report-Image Measurement of Workpiece Dimensions [D]. Electronic and Information Engineering . 2012.

[3] ZhiYan. Dental Root Canal Length Measurement Based on DigitalImage Processing [D]. Xi`an Technological University. Computer Software and Theory .2009.

[4] Ye Guiru, Zhou Qingsong, Lin Xiaowei. Measurement of Surface Cracking Width Based on Image Processing [J]. Road Traffic Technology. 2010

[5] Sun Kemei. Development of Real-Time Workpiece Length Measuring System [D]. Journal of Shenyang Institute of Aeronautical Engineering. 2014

[6] Hou Xuezhi. Digital Image Measuring Machine for Tool[D]. University of Electronic Science and technology. 2004

[7] Zhou Yonglin. Automatic Measurement System for Turning Center[D]. Tool Technology. 1999, Vol 3.

[8] Hou Yu. Rapid Method for Detection of Circle and Ellipse Edge. Journal of China Institute of Metrology, 2000,11:140-1443, No 7-353

[9] Zhang, Lu Zhimin. A Quick ROUGH Algorithm for Circle Detection[J]. Micro Computer System. 2000

[10] Zhang Yu. Application of Image Measurement Technology to the Theelset Profile Measurement [D]. Southwest Jiaotong University . 2003

[11] Sugata Ghosal, Rajiv Mehrotra. Detection of Composite Edges. IEEE Transactions on Image Processing, 1994, Vo1. 3, No. 1114252 1:970-973

[12] D. J. Kerbyson, T. J. Atherton. Circle detection using Hough transform filters. Fifth

[13] International Conference on Image Processing and its Applications,1995, 370-374

[14] J.Sklansky .On the Hough Technique for Curve Detection. IEEE Transactions Computers,1978, 10:923-926

Design of A Near-Infrared Spectra Anti-Disturbance Cerebral Oxygen Analyzer

CAO Ze-yuan; ZHOU Ge; ZHOU Xiao-yu

（College of Instrument Science and Electrical Engineering, Jilin University., Changchun 130061, China）

***Abstract*--For that conventional test methods of cerebral oximetry are complex, test probe often need have special shading treatments and testees have to remain stationary and other issues, In this paper, a sort of anti-disturbance cerebral oxygen analyzer based on the near-infrared spectroscopy was researched. By selecting the suitable three-wavelength near-infrared detection light source (735nm/805nm/850nm) and using the absorptivity of HbO2 and HbR in the near- infrared spectra, the variation of the two substance's concentration was received, and source interference expression resulted from the impact of oxygen detection accuracy was calculated . Detecting ambient light in the detection terminal simultaneously to eliminate the interference from leaked light. Finally, the original data from the upper computer and the interference data were processed to realize the real-time monitoring of the blood-oxygen fluctuation in the prefrontal lobe of the brain. The correctness of instrument was proved by breathlessness experiment and source interference experiment. The experimental results showed that the cerebral oxygen analyzer designed in this paper can detect the changes of hemoglobin and eliminate the interference of the source effectively, and the anti-disturbance algorithm can correct the source interference error about 70% or more. This instrument can be used to monitor the changes of blood oxygen parameters in the prefrontal lobe of the brain.**

***Key words*--NIRS; Cerebral oxygen; Anti disturbance ; Interference model; Breathlessness experiment**

I. INTRODUCTION

THE brain is the nerve organ of the human body, which is responsible for the daily physiological activities of the human body. Brain organizations are of high oxygen consumption in normal physiological activities, and are very sensitive to hypoxia . Short time of hypoxia will cause the central nervous system damage. Near- infrared spectroscopy (NIRS) as a non- intrusive optical monitoring mean, the scope of application of it is becoming more and more common. It is mainly used to observe the cortical regions containing HbR oxygen hemoglobin (HBO2) and deoxygenated hemoglobin concentration、Changes in blood flow cerebral (CBF) and Changes in blood volume cerebral (CBV).

In 1977, Jobsis NIRS was firstly used to measure the animal's head, opened up the application of optical technology in noninvasive oximetry precedent [1]. However due to the interference of the skin, skull ,muscle and other tissue on the near infrared spectrum of blood is serious, resulting in near infrared cerebral oxygen saturation detection technology hasn't been used in clinical. Although Somanetics Corp launched the commercialized cerebral oxygen [2], but due to the large individual differences in using, poor reproducibility and the questioned measuring accuracy and many other factors ,it needs continuous improvement. So far, the effect is not ideal. In 1995, the Japanese Omron Corporation developed a portable blood oxygen detection system [3]. In 2002, the University of Pennsylvania B.Chance team developed a set of three wavelength light sources and 8 detectors from the FNIR detection system [4]. In 2003, the Delpy research group at the University of London developed a blood oxygen detection probe for the prefrontal cortex [6]. In 2006, a new method of simultaneous detection of blood oxygen content in bilateral brain tissue was proposed by the brain blood oxygen detection device developed by Li Liangcheng, [7]. Luo Qing-ming, Huazhong University of Science and Technology, developed a portable fNIRS instrument for the study of brain functions related to cognitive learning [9]. However, the designs of the above test methods are complex, the test personnel must remain stationary and appropriate measures are taken to ensure the accuracy of the test, so the actual effect is not ideal.

In this paper, the design of the brain blood oxygen analyzer, creates a disturbance model aiming at the source interference and environmental light leakage interference,by comprehensiveiy analysising and discussing the factors influencing on the accuracy of cerebral blood oxygen measure. Select the three wavelength (735nm/805nm/850nm) detection light source combined with the following derivation of the source of interference expression to revise the test data, in order to achieve a reasonable and accurate detection of cerebral oxygen.This design reflect the activities of the prefrontal lobe of the brain, through the detection of changes in the brain prefrontal lobe of the blood oxygen parameters. This design is characterized with a safe non-invasive, small size, wearable, continuous monitoring.

II. BASIC PRINCIPLE

2.1. The basic principle of cerebral blood oxygen detection

Routine cerebral oxygen saturation detection are based on the Lambert Beer's law [10], according to the near infrared bsorption spectra characteristic of HBO2 and HbR in biological tissue, using absorbance in the near infrared region of the spectrum on both sides of the two substances' equal absorb spot (805 nm), the concentration changes of HBO2 and HbR can be effectively detect.

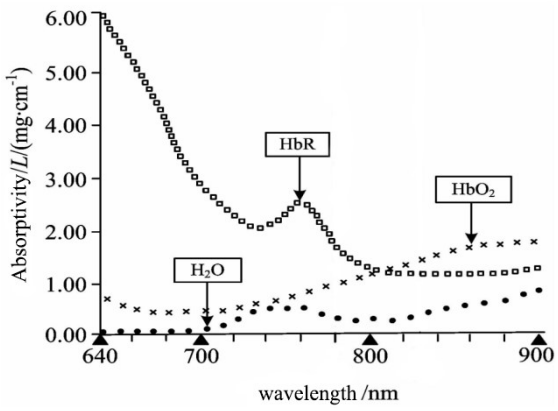

Fig.1. The absorption spectra of HbR and HbO2

According to Lambert- Beer' s law ,we can get:

$$OD = \ln\frac{I_0}{I} = \varepsilon cL \qquad (1)$$

In formula: I0, I shows the incident intensity and received light intensity respectively, c shows the concentration to be tested of non homogeneous scattering medium, the media on behalf of epsilon absorbance, L said the path length of light passes through the medium, OD optical density.

2.2 Cerebral blood oxygen detection model

Near infrared lights enter the prefrontal brain and then go through layers of different thickness of brain tissue, spreading in intracranial banana type optical path. The lights undergone absorption and scattering ,and exited through the scalp at a certain distance. The penetration depth is equal to1/4 of the distance between the light source and detector [11-13].

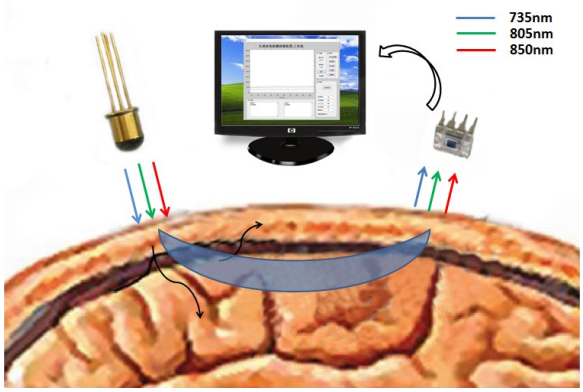

Fig.2. The principle of system detection

For biological tissue, the photons spread in the organization regularly and randomly. According to the modified Lambert-Beer's law, when the incident intensity is I0, and the thickness is D ,which the wavelength λ parallel lights go through,the concentration of uniform medium is C, and the emission intensity is ***I***. Optical density

$$OD^{\lambda} = ln\frac{I_0^{\lambda}}{I^{\lambda}} = DPF^{\lambda} \cdot D \cdot \sum \varepsilon_i^{\lambda} \cdot c_i + G^{\lambda} \qquad (2)$$

In formula: OD^{λ} is the absorbance of the wavelength λlight,ε^{λ} is absorption coefficient of the medium，DPF^{λ} is the path difference factor of the wavelength λlight, G^{λ} is the optical loss caused by background .

The design selects two different wavelength lights on both sides of the two substances' equal absorb spot .The variation of optical density was measured to reflect the changes in prefrontal cortex of oxygenated hemoglobin and reduced hemoglobin content .

$$\Delta c(HbO_2) = \frac{\frac{\varepsilon_{HbR}^{850} \cdot \Delta OD^{735}}{DPF^{735}} - \frac{\varepsilon_{HbR}^{735} \cdot \Delta OD^{850}}{DPF^{850}}}{D \cdot (\varepsilon_{HbO_2}^{735} \cdot \varepsilon_{HbR}^{850} - \varepsilon_{HbR}^{735} \cdot \varepsilon_{HbO_2}^{850})} \quad (5)$$

$$\Delta c(HbR) = \frac{\frac{\varepsilon_{HbO_2}^{735} \cdot \Delta OD^{850}}{DPF^{850}} - \frac{\varepsilon_{HbO_2}^{850} \cdot \Delta OD^{735}}{DPF^{735}}}{D \cdot (\varepsilon_{HbO_2}^{735} \cdot \varepsilon_{HbR}^{850} - \varepsilon_{HbR}^{735} \cdot \varepsilon_{HbO_2}^{850})} \quad (6)$$

Using the Clem- rule to solve linear equations and reach the following formulas [14]:

$$\Delta c(HbO_2) = \frac{\frac{\varepsilon_{HbR}^{850} \cdot \Delta OD^{735}}{DPF^{735}} - \frac{\varepsilon_{HbR}^{735} \cdot \Delta OD^{850}}{DPF^{850}}}{D \cdot (\varepsilon_{HbO_2}^{735} \cdot \varepsilon_{HbR}^{850} - \varepsilon_{HbR}^{735} \cdot \varepsilon_{HbO_2}^{850})} \quad (5)$$

$$\Delta c(HbR) = \frac{\frac{\varepsilon_{HbO_2}^{735} \cdot \Delta OD^{850}}{DPF^{850}} - \frac{\varepsilon_{HbO_2}^{850} \cdot \Delta OD^{735}}{DPF^{735}}}{D \cdot (\varepsilon_{HbO_2}^{735} \cdot \varepsilon_{HbR}^{850} - \varepsilon_{HbR}^{735} \cdot \varepsilon_{HbO_2}^{850})} \quad (6)$$

In formula: $\varepsilon_{HbO_2}^{735}$, ε_{Hb}^{735}, $\varepsilon_{HbO_2}^{850}$, ε_{Hb}^{850} ,each represents absorbance of HbO_2, HbR to corresponding wavelengths as 735nm and 850nm;ΔOD^{735}, $\Delta OD^{850}$are changes of absorbance to corresponding wavelengths as735nm and 850nm.

2.3 The establishment of interference detection model

In the process of measuring Cerebral blood oxygen will have unstable contact, leakage etc. and cause affect the accuracy and precision of detection.

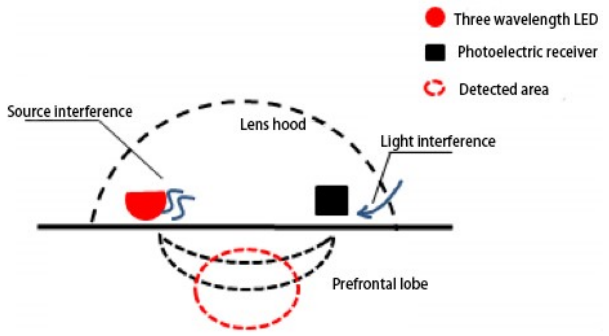

Fig.3. The schematic diagram of interference model

Fig3 is the schematic diagram of interference model. Interference comes mainly from two aspects, one is that receiver receives the extraneous environmental light interferences, second the contact between transmitter and skin changes with the breath ,and results of source drift interference, which is mainly reflected as the changes of incident light intensity I0.

Here is the method of eliminating interference source:

According to(2) formula,we can reach:

$$OD^{735} = \left(\varepsilon_{HbO_2}^{735} \cdot c_{HbO_2} + \varepsilon_{HbR}^{735} \cdot c_{HbR}\right) DPF^{735} \cdot D + G^{735} \quad (7)$$

$$OD^{850} = \left(\varepsilon_{HbO_2}^{850} \cdot c_{HbO_2} + \varepsilon_{HbR}^{850} \cdot c_{HbR}\right) DPF^{850} \cdot D + G^{850} \quad (8)$$

$$OD^{805} = \left(\varepsilon_{HbR/HbO_2}^{805} \cdot (c_{HbO_2} + c_{HbR})\right) \cdot DPF^{805} \cdot D + G^{805} \quad (9)$$

Make: $A^{735} = \mathrm{OD}^{735} - G^{735}$,

$A^{850} = \mathrm{OD}^{850} - G^{850}$,

$A^{805} = \mathrm{OD}^{805} - G^{805}$,

Then from (7)(8) formula, we get:

$$c_{HbO_2} + c_{HbR} = \frac{\frac{A^{735}(\varepsilon_{HbR}^{850} - \varepsilon_{HbO_2}^{850})}{DPF^{735}} + \frac{A^{850}(\varepsilon_{HbO_2}^{735} - \varepsilon_{HbR}^{735})}{DPF^{850}}}{D \cdot \left(\varepsilon_{HbO_2}^{735} \cdot \varepsilon_{HbR}^{850} - \varepsilon_{HbR}^{735} \cdot \varepsilon_{HbO_2}^{850}\right)} \quad (10)$$

Then from (9) formula, we get:

$$c_{HbO_2} + c_{HbR} = \frac{A^{805}}{D \cdot DPF^{805} \cdot \varepsilon_{HbR/HbO_2}^{805}} \quad (11)$$

from (10)(11) Equal, and order

$$m = \frac{\varepsilon_{HbR/HbO_2}^{805} \cdot (\varepsilon_{HbO_2}^{735} - \varepsilon_{HbR}^{735})}{\left(\varepsilon_{HbO_2}^{735} \cdot \varepsilon_{HbR}^{850} - \varepsilon_{HbR}^{735} \cdot \varepsilon_{HbO_2}^{850}\right)}$$

$$n = \frac{\varepsilon_{HbR/HbO_2}^{805} \cdot (\varepsilon_{HbR}^{850} - \varepsilon_{HbO_2}^{850})}{\left(\varepsilon_{HbO_2}^{735} \cdot \varepsilon_{HbR}^{850} - \varepsilon_{HbR}^{735} \cdot \varepsilon_{HbO_2}^{850}\right)}$$

we get:

$$A^{805} = \frac{A^{850} \cdot DPF^{805}}{DPF^{850}} \cdot m + \frac{A^{735} \cdot DPF^{805}}{DPF^{735}} \cdot n \quad (12)$$

Will be launched on the type can be obtained

$$m \cdot lnI^{850} + n \cdot lnI^{735} - lnI^{805} = c \quad (13)$$

In formula c depends on the intensity of the incident to the frontal lobe of the cerebral. G is the Optical loss of prefrontal lobe,we can get

$$C = mlnI_0^{850} + nlnI_0^{735} - lnI_0^{805} - (\mathrm{m}G^{850} + \mathrm{n}G^{735} - G^{805}) \quad (14)$$

If $I_0^{850} = \mathrm{p} \cdot I_0^{805}, I_0^{735} = \mathrm{q} \cdot I_0^{805}$

$$\Delta C = m\frac{\Delta I_0^{850}}{I_0^{850}} + n\frac{\Delta I_0^{735}}{I_0^{735}} - \frac{\Delta I_0^{805}}{I_0^{805}} = (m + n - 1)\frac{\Delta I_0^{805}}{I_0^{805}} \quad (15)$$

Then

$$\frac{\Delta C}{(m+n\text{-}1)} = \frac{\Delta I_0^{805}}{I_0^{805}} = \frac{\Delta I_0^{735}}{I_0^{735}} = \frac{\Delta I_0^{850}}{I_0^{850}} \quad (16)$$

In a differential manner

$$\frac{\mathrm{C}(\mathrm{t}_i)\text{-}\mathrm{C}(\mathrm{t}_{i\text{-}1})}{m+n\text{-}1} = \frac{I_0(t_i)\text{-}I_0(t_{i\text{-}1})}{I_0(t_{i\text{-}1})} \quad (17)$$

order $\Delta \mathrm{I}(t_i) = \frac{\mathrm{C}(\mathrm{t}_i)\text{-}\mathrm{C}(\mathrm{t}_{i\text{-}1})}{m+n\text{-}1}$ we get

$$\frac{I_0^{\lambda}(t_i)}{I_0^{\lambda}(t_0)} = \prod_{i=1}^{k}(1+\Delta I(t_i)) \quad (18)$$

In formula，λ express the Arbitrary wavelength of 735nm,805nm,850nm.Using (18) can correct the mistakes come from Source Interference，Variation of correcting light density is：

$$\begin{aligned} \Delta OD^{\lambda} &= OD^{\lambda}(t_i) - OD^{\lambda}(t_0) \\ &= \ln\frac{I_0^{\lambda}(t_i)}{I^{\lambda}(t_i)} - \ln\frac{I_0^{\lambda}(t_0)}{I^{\lambda}(t_0)} \\ &= \ln\frac{I_0^{\lambda}(t_0)}{I^{\lambda}(t_i)} + \ln\frac{I_0^{\lambda}(t_i)}{I_0^{\lambda}(t_0)} \end{aligned} \quad (19)$$

III. SYSTEM DESIGN

The system shown in Figure 4, contains the light source driving circuit, three wavelength light source detector, photoelectric receiver, amplifier and filter circuit, main controller and PC.

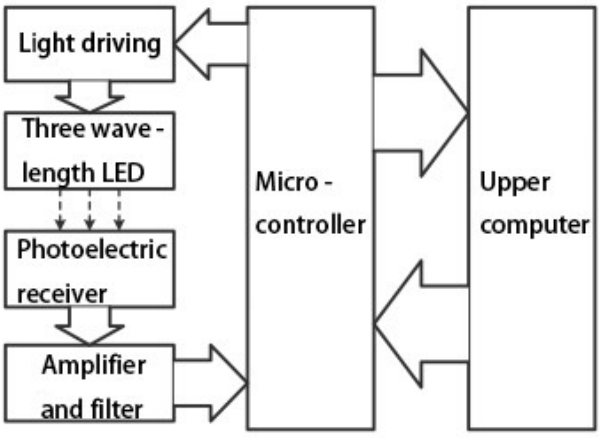

Fig.4. The hardware function block diagram

The micro controller can control the time-sharing driver of the three wavelength light source by controlling the light source driving circuit, and control the three wavelength light source to illuminate the brain's prefrontal lobe. After been absorbed and scattered by the frontal lobe of the brain ,light is received by the photoelectric receiver. The output signal of the photoelectric receiver is amplified and filtered by the AD to upload the collected data to the host computer through the micro controller.The host computer is responsible for the filtering of the original data and the calculation of the change of the concentration of hemoglobin.

The non-stationary NIRS signal is with white noise, heart rate (~1.1Hz), respiration (~0.25Hz),Mayer wave (~0.1Hz) and other ingredients. In the experimental design to study of brain function , hemodynamic response signal induced by the task is concerned with, whose frequency is usually less than 0.1Hz. Therefore, the application of high order digital filter (Butterworth) was used to eliminate the physiological signal components [15].

IV. EXPERIMENT

4.1 Breath holding experiment

In order to verify the correctness of the analyzer on hemoglobin concentration response, breath holding experiment was carried out to testing personnel and we analyses of the C (HBO2) and C (HbR) changes in the situation.

Experiment 1 the testee was a 21 year old adult female college students, physical health, without cardiovascular disease, diabetes and neurological history. Methods: Firstly, the testee keeps normal breath for1min, then hold her breath for 1min, finally , recover normal breath after finishing operation. Before the experiment, the self-made double channels blood oxygen probe was fixed to the forehead of the testee, and the probe was taken the necessary shading measures. During the whole test process, the testee is in the upright sitting position and no mood swings.

Figure 5 shows the changes of the hemoglobin concentration in the two channels in one test at a time. It is seen clearly in that 1min before C (HBO2) and C HbR changes in the stability; 1 min after the start of breath, prefrontal original oxygenation hemoglobin

content by consumption has not been timely supplement resulting in C (HBO2) decreased, prefrontal reduced hemoglobin C HbR content increase, experiments were performed to 2 min after the measured recovery

Complex normal breathing, C (HbO2) and C (HbR) quickly recovered to the original level.

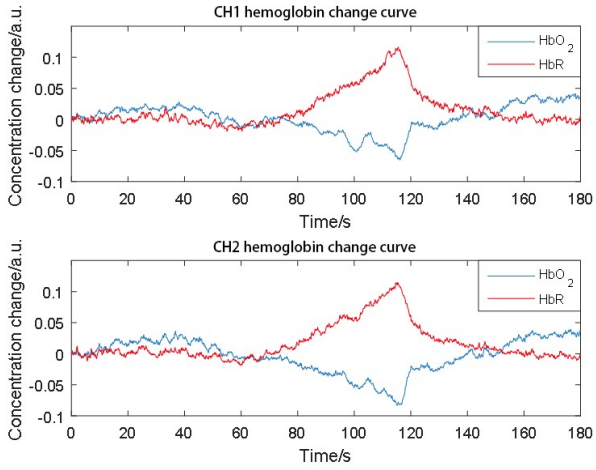

Fig.5. The concentration curves measured by the breathlessness experiment

4.2 Source interference cancellation

In order to verify the source anti interference algorithm correctness and evaluate the quality of source anti-jamming algorithm , the brain blood oxygen detecting probe was fixed on one point.Source end interference was simulated, by means of adjusting the potentiometer adjustment in the observability probe to control the luminous intensity of three wavelength light source .Now the oxygen probe is not fixed for oxygen detection. Therefore, theory of experimental results have demonstrated for that C (HBO2) and C (HbR) had no change.

Experiment 2, the brain blood oxygen probe is fixed at a point, between 5s-20s and 45s-60s to adjust potentiometer to reduce the output light intensity of the brain blood oxygen probe respectively, and then return to the initial light intensity. Fig. 6 showed the change trend of C (HbR) and C (HbO2) before and after the correction of anti interference algorithm. it is thus evident that,before the correction, the experimental results are affected greatly by the variation of the incident light intensity for that the change of the incident light intensity is considered as the change of tested materials. The anti interference algorithm can effectively identify the change of the source interference and the changes of C (HbR) and C (HbO2) have stabilized after correction.

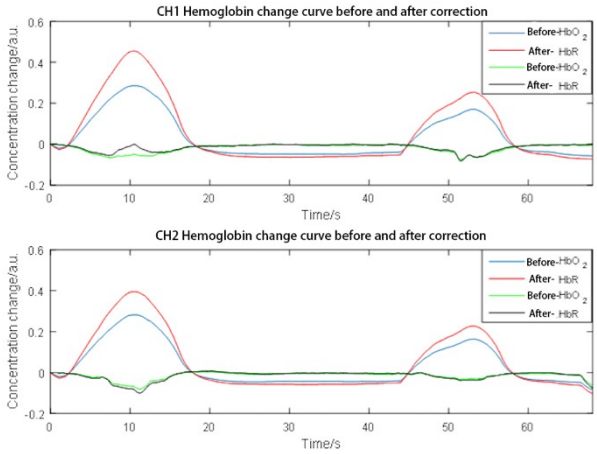

Fig.6. The concentration curves before and after correcting the source interference of experiment

Using the absolute error (AE)between the consentration of oxyhemoglobin and deoxyhemoglobin and theoretical value before and after correction ,and corrected relative error(CRE) to make quantitative description of the quality of the source interference correction algorithm。

$$AE = x'-x \tag{20}$$

$$CRE = \frac{AE^{**}-AE^{*}}{AE^{*}} \times 100\% \tag{21}$$

In the formula , x' indicates measured changes in hemoglobin , x indicates theoretical changes in hemoglobin. AE^{**} indicates absolute error after correction of source correction algorithm , AE^{*} indicates the absolute error without the source correction algorithm .

The result is in the table 1：

TABLE I

THE EFFECT OF SOURCE INTERFERENCE CANCELLATION

	CH1				CH2			
	HbO2		HbR		HbO2		HbR	
Time/s	10	53	10	53	10	53	10	53
AE*	0.26	0.18	0.45	0.25	0.26	0.15	0.38	0.22
AE**	0.05	0.05	0.02	0.07	0.06	0.04	0.07	0.04
CRE	80.8%	72.3%	95.6%	72%	76%	73.3%	81.6%	81.9%

The experimental results show that the anti interference algorithm can correct at least 70% of the source interference, and effectively eliminate the error caused by the change of the incident light intensity I0 at the source.

V. CONCLUSION

In this paper, the present situation of complex and anti disturbance measures is set out from the traditional method of blood oxygen detection. The interference model of source side interference and ambient light interference is established. Then the basic principle of the brain blood oxygen detection system and the method of eliminating the interference of the source are introduced in detail。Results show that the cerebral blood oxygen analyzer could achieve real-time monitoring of changes in hemoglobin concentration in the prefrontal lobe of the brain，And can be achieved through the source side correction algorithm to achieve the source of interference suppression，Interference suppression ratio of up to 70%. The experimental results are in agreement with the theoretical values. It basically achieves the goal of non-invasive, real-time and accurate monitoring of the human body. Can help doctors more intuitive, specific grasp of the basic situation of the patient, has a certain use value and social benefits.

References

[1] Jobsis F F, etal..Science ,1977,198:1264 .

[2] Madsen PL, Secher NH.Near infrared oximetry of the brain[J]. Prog Neurobiol,1999,58:541-560

[3] Valerie Pollard ,Donald S.Prough,Eric DeMelo A, et al.. Validation in volunteer of a near –infrared spectroscope for monitoring brain oxygenation in vivo[J]. Anesth Analg ,1996,82:269-277.

[4] Yuanqng L , Lech G , Nioka S, et al.. Noninvasive , low-noise, fast imaging of blood volume and deoxygenation changes in muscles using light-emitting diode continuous-wave imager[J]. Rev. Sci. Instrum., 2002, 73 (8): 3065-3074

[5] Vaithianathan T., Tullis I. D. S., Everdell N., et al.. Functional imaging of the brain using a portable NIR instrument[J]. Proc. SPIE., 2003, 4955:96-102

[6] Vaithianathan T., Tullis system for topographic (10): 32763283 LD.S imaging Everdell N., et al. Design of a portable near infrared of the brain in babies. Rev. Sci. Instrum., 2004, 75(10):3276-3283

[7] LI Liang -Cheng, ZHANG Yong-shun, LI J i-Gang. Design of Brain Blood-oxygen Monitor with Dual Light Sources and Dual Detectors[J]. Laser&Inrared,2007,37(7):653-655.(in Chinese).

[8] ZHENG Yi,LUO Qing-Ming ,et al.. A Portable Instrument for Brain Activity Detection Based on Near-infrared Spectroscopy[J].Chinese Journal of Biomedical Engineering,2007, 12(6): 898- 902.

[9] GONG-Hui ,LI Cheng-Jun,et al.. Science in China(Series G),2007,37(B10):110-117.

[10] Van de Ven MJ,Colier WNJM,Van der Sluijs MC,et al..Can cerebral blood volume be measured reproducible with an improved near infrared spectroscopy system[J].K Cer Blood Flow Metab,2001,21:110-113.

[11] LI Liang-Cheng , LI Kai-Yang ,Qin Zhao. Development of New-type Near-infrared Brain Blood-oxygen

Monitor[J] . Laser&Inrared , 2007 , 36(8):661-664.(in Chinese).

[12] Cratton E ,Fantini S , Franceschini MA , et al.. Measurements of scattering and absorption changes in muscle and brain[J]. Philosophical transactins of the Royal Society of London.Biological Series B,1997,352(1354)：727-735.

[13] Martin W , von Siebenthal K . Comparison of three methods to measure absolute cerebral hemoglobin concentration in neonates by near-infrared spectrophotometry [J].Journal of Biomedical Optics,2002,7(2):221-227.

[14] ZHA Yu-tong ,LIU Guang-da ,et al.. EEMD-ICA Applied in Signal Extraction in Functional Near-Infrared Spectroscopy[J]. Spectroscopy and Spectral Analysis. 2015, 35(10): 2746-2751. (in Chinese).

[15] XU Gang ,LI Xiao-li ,et al.. A Simple Design of Functional Near-Infrared Spectroscopy System[J]. Spectroscopy and Spectral Analysis.2015,35(2):552-556. (in Chinese).

High-power wireless charger design

Xiao Changchen, Guo Qun, Hao Renpu
（*Jilin university instrument science and engineering institute,Changchun,130021*）

***Abstract*—Based on the principle of electromagnetic induction and the analysis of wireless charging technology as well as basic structure , to design the wireless charging circuit's main circuit, resonant circuit and the transmitter and receiver coils, and make wireless charging device. The device's core parts are transmitting and receiving coils, PMW wave signals generated by chip SG3525 are transmitted through the push-pull driver to chip KD301, and then signals in KD301 drive the Infineon's chip IPW6OR041C6 to convert the DC to high-frequency AC, which can be transmitted wirelessly. When the primary and secondary coils are mutually touching, the practical test of the device shows that the efficiency can reach 75%.**

***Key words*: Wireless charging Resonant coupling**

I. FOREWORD

DEVELOPMENT of electric vehicles is the future direction, convenient e-car battery charging stations has become an urgent problem. The project is intended for wireless charging device, which is efficient and easy to use.

II. CIRCUIT DESIGN

The high-power magnetically coupled resonance wireless charging circuit can be divided into transmitting and receiving parts. Wherein the transmission section is divided into the inverter circuit, the resonant circuit and transmitting coil; receiving section is divided into receiving coil, the resonant circuit, rectifier and filter and voltage regulator modules. The overall topology of the circuit is shown in Figure 1.

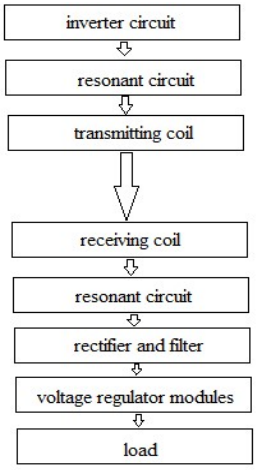

Fig.1 The overall circuit topology

A. Inverter circuit

Single-phase inverter circuit has two forms: half-bridge inverter circuit and full-bridge inverter circuit, respectively, both are shown in Figures 2 and 3.

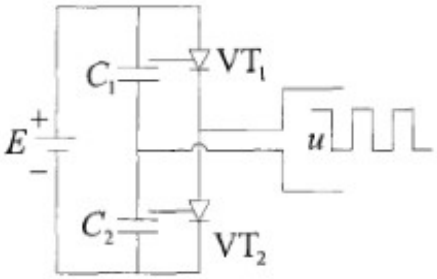

Fig.2 Half-bridge inverter circuit

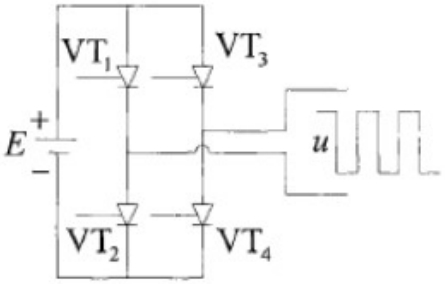

Fig.3 Full-bridge inverter circuit

In the half-bridge inverter circuit, take turns conducting VT1 and VT2, output AC square wave, and the off-switching-tube affords the reverse voltage E. Due to the presence of voltage dividing capacitor, the output AC voltage contains no DC component. In the full-bridge inverter circuit, VT1 and VT2 form one bridge arm, VT3 and VT4 forming another. When VT1, VT4 on, VT2, VT3 off; and when VT1, VT4 off, VT2, VT3 on , the output is AC square wave and its amplitude is E, and the off-switching-tube affords the reverse voltage E. When the output square wave's duty cycle is not 50%, the output AC current contains a DC

component. Typically, in order to avoid two switches of the same arm are simultaneously turned on, causing a straight short of arm , dead time is set in a set of switches , so that the duty cycle of the output square wave is no longer 50%, namely DC component in the output AC current appears to be inevitable.

B．Rectifier circuit

According to the composition of the device, rectifier circuit can be divided into three kinds: uncontrollable, half-controlled and fully controlled. According to the circuit configuration, rectifier circuit can be divided into a bridge circuit and zero circuits, etc. There are various classifications.

Single-phase bridge uncontrolled rectifier circuit is shown in Figure 4, single-phase bridge controlled rectifier circuit is shown in Figure 5, only taking purely resistive load case into consideration.

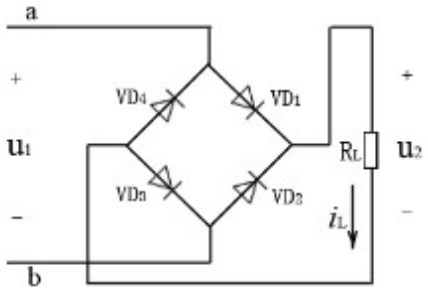

Fig.4 Single-phase bridge rectifier circuit uncontrollable

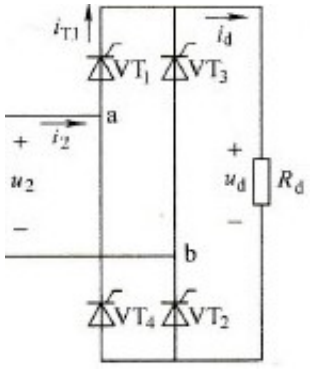

Fig.5 Single-phase bridge full-controlled rectifier circuit

Control circuit of Single-phase bridge controlled rectifier circuit is more complex, it also brings the extra power loss, so the paper chose the single-phase uncontrolled rectifier circuit.

C．Resonant circuit

Inductors and capacitors have different connections, so the coupling coil has series - series, series - parallel and parallel - serial, parallel - parallel these four different topologies. In this paper, input of the system is DC voltage, the transmitting part's inductors and capacitors are in series, so only the series - series and series - parallel two structures were analyzed.

In tandem structure, transmission efficiency is very low when corresponding load resistance is large, but transmission efficiency of parallel structures is high in the same load resistance , nearly 90%[1], so chosen topology is: the transmitter coil inductors and capacitors in series, receiving coil inductors and capacitors in parallel. Hereinafter analysis are based on this topology .

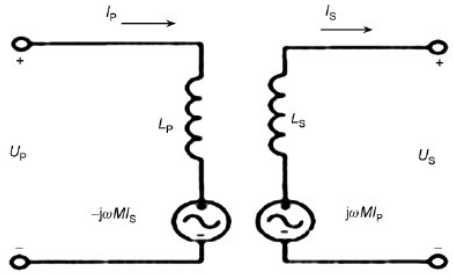

Fig.6 Primary and secondary coils of equivalent circuit

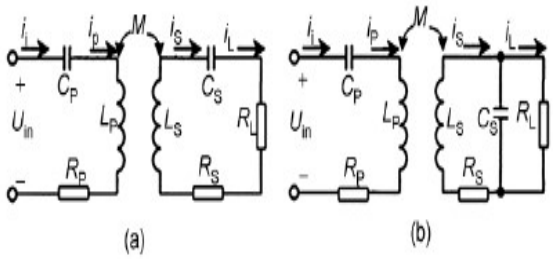

Fig.7 Two basic circuit topology structure coupling coil

（a）SS (b)SP

Assuming that the system angular frequency is ω, primary,and secondary loop voltage KVL equation can be obtained from Figure 7 :

$$\begin{cases} Z_p I_P - j\omega M I_S = U_P \\ -j\omega M I_P + Z_S I_S = 0 \end{cases} \quad (1)$$

Wherein, Zp and Zs represent impedance of primary circuit and the secondary circuit respectively. Solving equation (1), we can get two equivalent current of these two loops:

$$I_P = \frac{U_P}{Z_P + \frac{(\omega M)^2}{Z_S}} \quad (2)$$

$$I_S = \frac{j\omega M \frac{U_{in}}{Z_p}}{Z_s + \frac{(\omega M)^2}{Z_P}} \quad (3)$$

Equation(2) describes that after the forming of coupling loops, the value of primary current is not only related to ZP, but also (ωM) 2 / ZS. (ωM) 2 / ZS

is called secondary circuit's reflecting impedance to primary circuit, indicating secondary circuit's effect on the primary circuit, marked as ZPS. Similarly, (ωM) 2 / ZP is called primary circuit's reflecting impedance to secondary circuit, marked as ZSP.

Power transmitted from the primary coil to the secondary coil of the System can be expressed as:

$$p = \mathrm{Re}[Z_{ps}]I_P^2 \qquad (4)$$

Theoretically when the resonance frequency of the operating frequency and secondary systems are same, the secondary coil receives the largest energy, and transmission efficiency of the system reach its maximum, namely:

$$\omega_0 = \frac{1}{\sqrt{L_S C_S}} \qquad (5)$$

III. Parameter Design

A. Inverter circuit

According to the selected resistance of primary and secondary coils, electromagnetic wave frequency of the primary emission is 43kHz[2], so the frequency of the drive signal of MOS is the same. PWM wave is generated by chip SG3525[3]. The circuit is shown in Figure 8. Full-bridge inverter main circuit is shown in Figure 9.

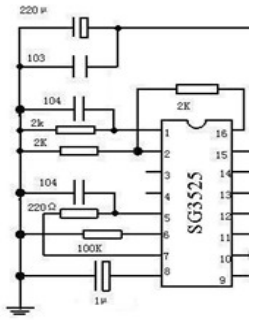

Fig.8 SG3525 PWM wave generating circuit

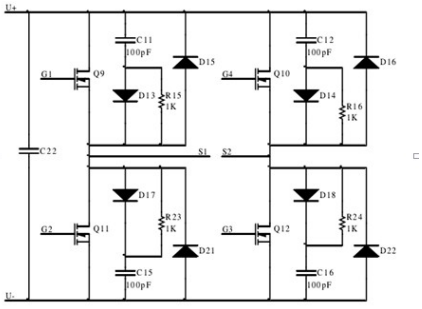

Fig.9 Full-bridge inverter circuit

In the full-bridge inverter circuit, we chose Infineon MOSFET chip IPW6OR041C6, which has small on-resistance, little switching loss, barely heats, reduces the loss of the inverter, and improve the efficiency of wireless charging [4] The core data are in the following table:

Table 1: IPW6OR041C6 core data

Maximum drain-source voltage *VDSS*	650V
Continuous drain current *ID*	77.5A/25℃
	49A/100℃
On-resistance *RDS(on)*	41mΩ
Rise Time *tr*	10ns
Fall Time *tf*	7ns

Frequency formula of SG3525:

$$f_{OSC} = \frac{1}{C_T(0.67R_T + 1.3R_D)} \qquad (6)$$

CT is capacitor , RT is resistance connected to feet 6, RD connected resistors 5 and 7 feet. To make the output frequency is 43kHZ, select the CT value 1500PF, RT 22000Ω, RD, 200Ω.

Select LuoMuYuan's chip KD301 as the driving chip of IPW6OR041C6. KD301's front circuit requires a greater output capability, which normal PWM IC can hardly meet, so we need to add current buffer stage and add push-pull circuit. Typical application circuit of KD301 is shown in Figure 10.

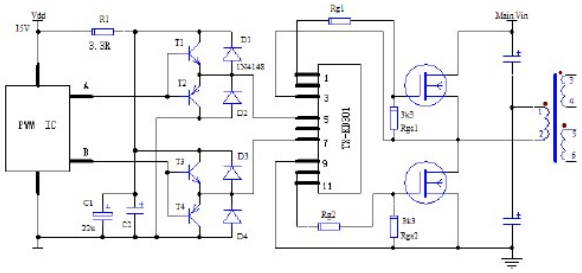

Fig.10 Typical applications of KD301

B. Coil design

1).Wire selection

The presence of skin effect will make the equivalent cross-sectional area smaller and the resistance larger, even obvious at higher frequency. In fact the coil resistance will cause a considerable impact on transmission efficiency of the system. The greater coil resistance are, the lower transmission efficiency will be [6]. The design uses a parallel multi-strand copper wire to produce coupling coils, each wire's

cross-sectional area is 2.513mm2. Required transmission maximum power is 40W, input voltage is 220V. Provided that transmission efficiency is 75% , input current will not exceed 1A. But in fact sinusoidal current flowing through the coil is much larger than the input current, considering that bigger cross-sectional area of the conductor has smaller resistance, so we chose wire of the larger effective cross-sectional area. Coils in the design are composed of 80 fine enameled wire, and each wire is insulated from other, thus the effective conductor cross-section [7] increases greatly.

2).Coil winding

Increasing the number of turns of the coil can increase inductance value, help to improve the transmission efficiency, but considering the size of the charging device, we wound primary ring-type coil as 24.5cm outer diameter, 15cm inner diameter, totally 19 laps, the resistance value is 2Ω. Secondary ring-type coil as 19.2cm outer diameter, 12cm inner diameter, the resistance value is 1.4Ω.

C．AC-DC secondary design

Induced AC voltage coupled by secondary coil of receiving circuit is transmitted by the rectifier bridge into DC power for the load. In order to reduce the interference by the AC component to the load, the filter circuit should be added. Rectifier circuit is shown in Figure 4. Load parallel filter capacitor.

Selection filter capacitor[8]:

Due to the induction voltage of the secondary coil is V1=20V, and frequency f=43kHz, Output Power P=40W, DC voltage after rectification can be obtained:VL=1.2V1=24V. Load Resistance RL = $\frac{P}{VL}$ =1.67Ω, and RLC=4×$\frac{T}{2}$ =2T=2×$\frac{1}{43000}$ =4.6×10-5s, so filter capacitor C=$\frac{4.6\times10\text{-}5s}{RL}$ ≈3.2μF, Considering the voltage fluctuates around ± 10%, the maximum withstand voltage of the capacitor:VCM=√2V1×1.1=30.8V, So the selection of a nominal value of electrolytic capacitor is 100μF / 100V.

IV．TEST RESULTS

A．Experimental Conditions

Experimental temperature:25℃

Laboratory equipment: GDS-2202A Oscilloscope and voltage probes

DF1731SLL3A DC source

Dummy load: 40W incandescent

B．Results

Using a rated voltage 24V, power 40W incandescent as a simulation.of charging load.

Adjusting terminal voltage of primary coil to make the two terminal voltage of incandescent lamp reach 24V, the measured current through the lamp at this time was 1.67A, namely Poutput = 24V × 1.67A = 40W. At the same time the measured DC output voltage was 28.1V, current was 1.88A, namely Pinput = 28.1V × 1.88A = 52.83W, efficiency of transmission device can be calculated : η=$\frac{Pinput}{Poutput}$ =75.7%. Normal light of incandescent is shown in Figure 11.

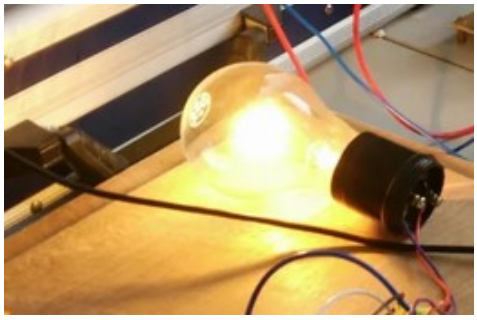

Fig.11 24V 40W Normal light bulbs

V．SUMMARY AND OUTLOOK

A．Full summary

This paper is based on the technology of wireless power transmission and set in the current rapid development of electric vehicles, and study on high-power wireless charger. The study includes inverter circuit, resonant circuit, coils in the transmitting side and coil, resonant circuit in the receiving side. Wherein the L of transmitting coil and receiving coil are measured by the LCR meter, the resonant frequency control to be 43kHz. According to $f=\frac{1}{2\pi\sqrt{LC}}$, deformed into C=$\frac{1}{4\pi2Lf2}$, select the appropriate capacitor value of transmitting coil and receiving coil. Finally, at the transmitting side, chose series coupled; at the receiving side, chose parallel coupled. Finally, on the basis of these studies,complete

the design and production of high-power wireless charger and achieve the index: output voltage 24V ± 10%, output power 40W, efficiency 75%.

B. Full summary

Due to the limitations of author's effort, time and theory level, there are still disadvantages as below to be further studied.

1).Does not consider the control of the circuit, open-loop system of the charger whose receiving side has no feedback to transmitting side. When the system load changes, the load characteristics of the system will change. Therefore, further analysis of the system load characteristics is been required.

2).In the device, current flowing through the wire is larger, and as resistors, diodes, transistors are energy-consuming elements, power lose a lot in the device. Other methods can be taken to reduce energy loss of the entire system to improve system efficiency.

References

[1] Shi Song, EV pickup device wireless power feeding system design Chongqing University master's degree thesis. 2013,4.

[2] Tang Zhide, Xu Yangyang, Zhao Mao etc, LTransmission efficiency coupled resonant wireless power transmission optimal frequency. Motor and Control, 2015,3.

[3] Villa J L, Sallan J, Llombart A, et al.Design of a high frequency Inductively Coupled Power Transfer system for electric vehicle battery charge[J]. Applied Energy, 2009, 86(3): 355-363.

[4] Wu Jiahong, Research on high power wireless power transmission technology for household appliances, Harbin Institute of Technology master's degree thesis, 2013, 7.

[5] Zhang Maochun, Wang Jinhua, Shi Yawei, Summary of wireless power transmission technology[J], Chongqing Technology and Business University (Natural Science Edition), 2009,5: 018.

[6] Dou Yanjun, Design of a magnetically coupled resonance wireless charging system, Electronic scientific research papers, 2013,6.

[7] Zhang Feng, Wang Huizhen, Non-contact inductive energy transmission system loosely coupled transformer [J], Power Technology, 2007, 10 (4): 54-58.

[8] Wang Huan, Research of wireless charging system based on the coreless PCB transformer, Xi'an University of Electronic Science and Technology master's degree thesis, 2010,1.

Design of Solar Ship Model With Underwater Ultrasonic Ranging

Shuming Zhang; Cheng Zhao; Lunyuan Zhang

(College of Instrumentation and Electrical Engineering,Jilin University,Jilin Changchun 130026,China)

Abstract **--The ultrasonic sensor is a typical non-contact sensor. It's usually used to measure the distance because of the advantages of strong anti-interference. The transducer converts acoustic signals which are received after being emitted into electrical signals and collects them back to MCU by A/D. Because data collection is often accompanied by noise, so the data acquisition system needs to filter and amplify the collected signal to improve the accuracy of collected data. The innovation of the design is to put the underwater ultrasonic ranging technology onto the platform of ship model and use solar energy to provide power for the ship model. It makes science and technology more pratical.**

Key word**--ultrasonic ranging ultrasonic transducer solar energy ship model**

I. INTRODUCTION

ULTRASONIC is a kind of sound wave whose frequency is higher than 20kHz. It's the mechanical vibration state of objects or transmission form of energy. Ultrasonic has the advantages of strong directivity, slow energy consumption, and far propagation distance in the medium. Ultrasonic is usually used to measure distance because of the advantages of quick, convenient, simple calculation and easy to real-time control. In addition, ultrasonic ranging can meet the requirements of industrial and practical in terms of measurement precision[1].

Ultrasonic ranging is a non-contact measurement methods. Compared with other methods of distance measurement, it is not influenced by factors such as light, electromagnetic field, smoke, dark, the color of tested object and so on. Because of strong ability to adapt to the bad environment and being easier to get the information from close range ultrasonic ranging is widely used in reverse anti-collision system, robot navigation, ocean survey, object recognition, etc[2].

Due to the short wave lengths, ultrasonic can spread approximately as a straight line. Its energy attenuation is smaller than electromagnetic wave in the liquid. The energy of ultrasonic is easy to focus so that forming a large intensity causes intense vibration and many special effects. Thus, underwater detection using high-frequency and low-power ultrasonic ranging is effective means. Underwater ultrasonic ranging with advantages of high frequency(tens to hundreds of kHz), short wavelength, small diffraction phenomenon, good directivity and small volume launchers is easy to improve the capacity of anti-interference[3].

Because oil, coal, natural gas and other resources are dwindling and emission pollution is growing, seeking sustainable clean energy and making full use of solar energy become the inevitable trend. In recent years, with the development of science and technology, solar energy has been used on some small vessels such as tourist sightseeing boat, yacht, short ferry, etc. Firstly, it's one of the main power energy, independently or together with other energy moving ship. Secondly, it's used as auxiliary energy in ship lighting system, driving system, air conditioning system, auxiliary machinery and so on[4].

II. ULTRASONIC RANGING PRINCIPLE

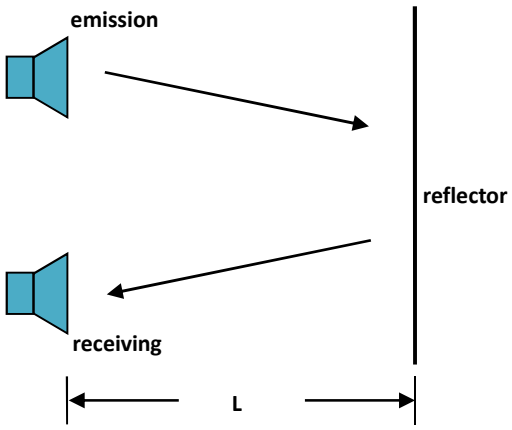

Fig.1 Schematic diagram of ultrasonic distance measurement

The basic working principle of ultrasonic distance measurement: Ultrasonic transducer emit ultrasonic to

one direction and start timing at the launching time. It return as soon as encounter obstacles in the transmission and ultrasonic receiver by reflection wave immediately stop timing. In this way, transit time t(s) is obtained. Known to the speed of ultrasonic is c(m/s), we can conclude the formula: L=c*t/2 according to the transit time t(Fig.1).

III. THE SYSTEM HARDWARE DESIGN

A. Block Diagram of the System(Fig.2)

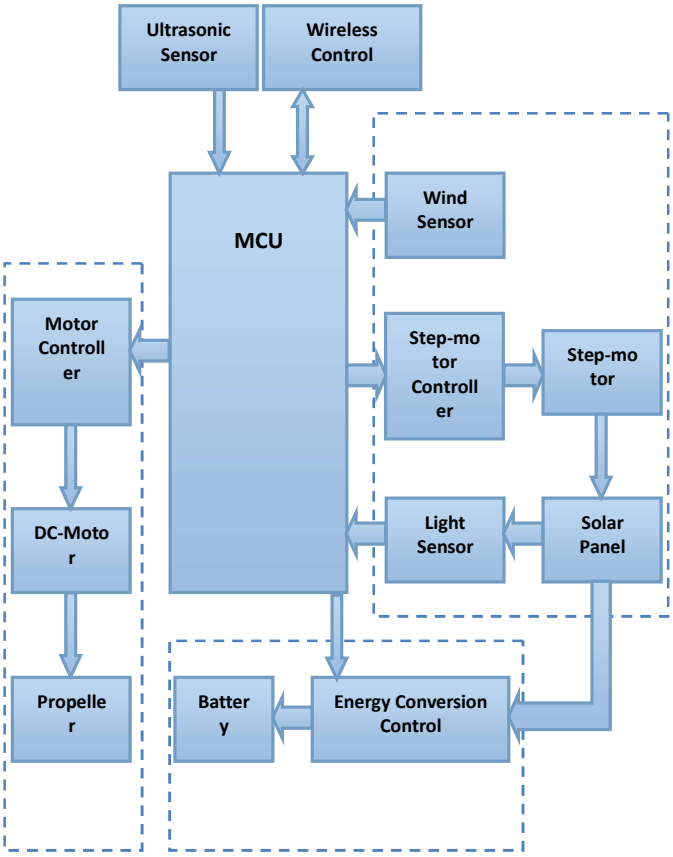

Fig.2 block diagram of the system

B. Ultrasonic Ranging Device Design

a. Ultrasonic Transmitting and Receiving Circuit Design

In ultrasonic ranging circuit, the emission circuit has two kinds, one is continuous wave emission circuit, the other is the pulse wave emission circuit. Considering that the ultrasonic transducer of system is sending and receiving together, we adopt the second emission circuit(Fig.3).

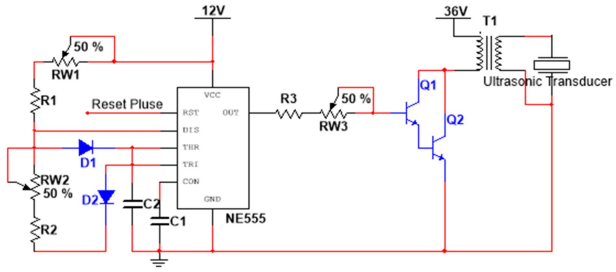

Fig.3 circuit of ultrasonic emission

b. Amplifying, Filter, Comparator, Display Circuit Design

Amplifying circuit(Fig.4) is divided into two stage amplifier whose total magnification times are 1000(60dB), first stage is 10 and second stage is 100. Signal after being amplified effectively will be send into MCU through detection and threshold adjustment circuit.

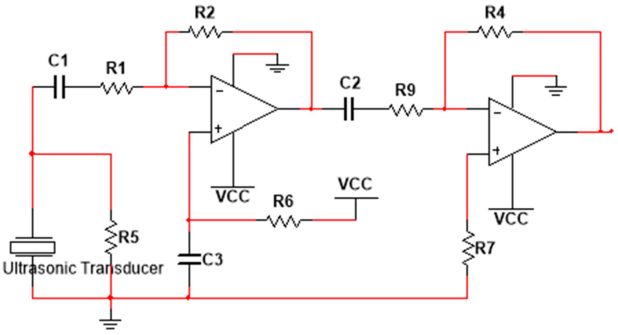

Fig.4 amplifying circuit

The main purpose of filter circuit(Fig.5) is to pass through the particular frequency of useful signal and restrain other frequency.

The signal from signal conditioning circuit will be ultimately sent into MCU, so it must be a logic signal. The voltage signal after being filtered is sent into voltage comparator(Fig.6) through being compared with the threshold level to determine the arrival of the echo or not and then sample signal correctly. Threshold level is associated with propagation distance and magnification. After lots of trials, the selected threshold level of the system is Vg=2.2V. If the peak voltage of the signal after being filtered is larger than Vg, the echo has been received. Then the external interrupt (INT1) of MCU is started, so as to stop timing and calculate from emitting to receiving time, also is the transmission time of ultrasonic.

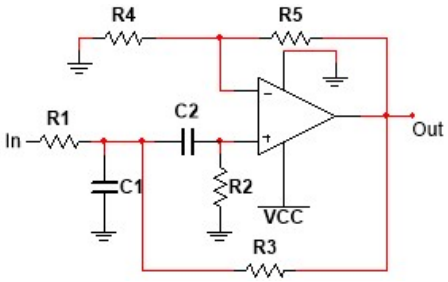

Fig.5 filter circuit

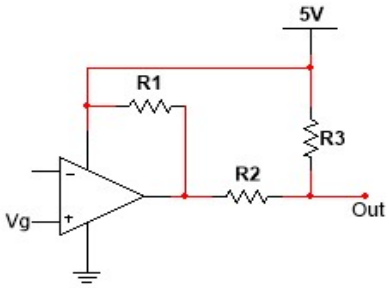

Fig.6 voltage comparator circuit

The system uses 4-LED digital tube to display the measured distance.

C. The Sun Auto-tracking Device Design

The photoelectric control of design adopts the combination of the program tracking and sensor tracking control method, which is controlled by program. Optical sensor for solar panel is used to do automatic positioning and error correction through MCU controlling stepping motor to achieve.

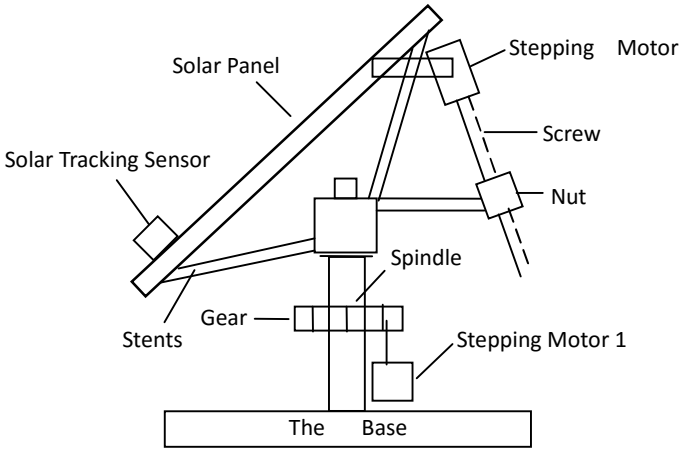

Fig.7 structural representation of sun autotracking device

The device(Fig.7) consists of fasteners such as star-bracket supporting solar panel and the base, stepping motor 1,2 and driving structure. Star-bracket has simple strucuture and good stability, especially light device weight laid a good foundation for decreasing the consumption of solar panel adjustment process. The auto-tracking operation of the control system if mainly composed of stepping motor 1 and 2. Stepping motor 1 and driving structure mainly adjust the deflection azimuth angle of tracking solar panel. Stepping motor 2 and driving structure control and adjust the height angle of solar panel. The system gets efficient photoelectric conversion through adjusting the deflection azimuth angle and height angle of solar panel timely.

IV. THE SYSTEM SOFTWARE DESIGN

Shown in Fig.10, at the beginning of the measurement, the counter is cleared and the ultrasonic is emitted. Meanwhile start the internal timer (T0) of MCU, which is used to record the launching and receiving time of ultrasonic by its counting function. When the ultrasonic transducer receive the relection wave, it will produce a negative jump on the output of receiving circuit and an interrupt request signal on the INT0. MCU responses to the external interrupt request and execute the external terminal service subroutine. Then stop counting and emitting for reading the time difference. Eventually, use the formula to calculate distance and display the result on the digital tube.

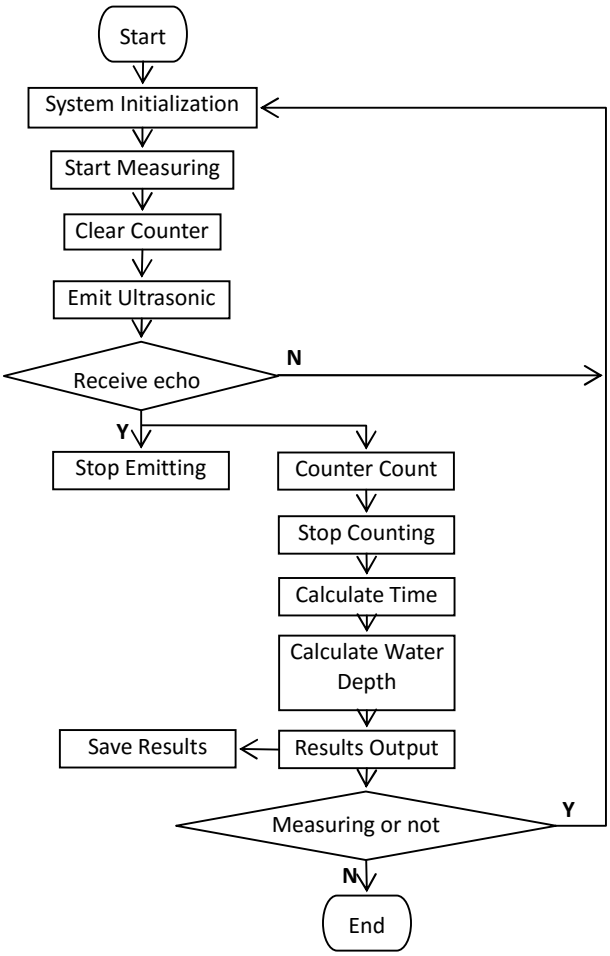

Fig.10 program flowchat

V. Measurement Test Data and Result Analysis

The type of ultrasonic transducer is DYW-1M, whose center frequency is 200kHz.

Table 1 experimental results

No.	Nominal value/cm	Measured value/cm	Absolute error/cm
1	50	51	1
2	70	73	3
3	100	102	2
4	120	122	2
5	150	149	1
6	180	184	4
7	200	207	7
8	250	256	6
9	300	308	8

From the above table, within 150cm the errors of measurement are all within 3cm , so the results are accurate. If the measuring range is too large, ultrasonic transducer with low frequency should be adopted, whose measuring range is larger than high-frequency ultrasonic transducer.

VI. Conclusion

The core concept of this design is to design a solar power unmanned ship, which can replace human working for underwater ranging. It's convenient and practical, also achieve the purpose of environmental protection. The test results are consistent with theoretical analysis. The function of measuring shallow water depth is achieved and it can be applied to small area water depth measurement without human working. Nowadays smart cars and unmanned aerial vehicle have been developed rapidly, the design is focused on underwater measurement, combining underwater ultrasonic ranging technology and platform of ship model, which applied the unmanned ship easily to life.

References

[1] Zhaoqiang Wang, Chenshu Zhang, Jianxiong Ye. "Research on High-precision Distance Measurement under Water". Journal of Xinyu University, 2011, 16(6): 71-74.

[2] Yu Lan. "Design of ultrasonic ranging system with the function of temperature compensation". Elctronic Measurement Technology, 2013, 36(2): 85-87.

[3] Jin Li. "Solar Energy Application and Prospects in Marine Power Plant". Ship and Ocean Engineering, 2010, 39(4): 70-72.

[4] Jing Wu, Yi Yang, Yingjun Pan. "Achieve the sun tracking with four quadrant-silicon photocell and MCU". Journal of Chifeng University(Natural Science Edition), 2009, 25(2): 126-128.

The research on intelligent fast charger with solar energy as the second energy source

Chunfeng Jiang; Limei Wu; Ziyi Zang

(College of Instrumentation and Electrical Engineering, Jilin University, Changchun 130061, China)

***Abstract*--In order to alleviate the contradictions between large battery power loss of electronic devices such as portable power sources and their small current chargers, based on the low- power single-chip—STC12C5A60S2 and using the voltage-type PWM controller—TL494 as the core, we design a BUCK type of intelligent fast charger. By detecting the voltage and the current of the charger, it charges by three stages, which include small current stage, constant current stage and constant voltage stage. It can reach the largest current to 4.7A when in the constant current stage. The charge can display its changing voltage, current and temperature when under the charging process. In addition, it can protect it from the destroy of high charging temperature by cutting the power. It can also prevent over-charging and backflow. Meanwhile, this charge is equipped with solar-assisted emergency charging module, which can keep a stable charging voltage of 5V and a small changing current about 0.4A to 0.8A with the changing light intensity in sunny weather. It has achieved emergency charging when no electronic supply.**

***Key words*--**TL494 Solar energy Fast Charging

I. INTRODUCTION

IN recent years, the battery capacity is increasing demand for digital products,electronic product life of mobile power consumption is large as a major selling point.Their basic capacity up 10000mA more, charger charging current is small, most only 1A, resulting in mobile power charging time required is too long.This gives the user great inconvenience.Especially when the user is outdoors for a long time (such as traveling abroad) or only a short time to the power charger,this is even more obvious drawbacks.Accordingly, the main purpose of this design is to increase the charging speed.While the new green energy solar charger used in the field of solar energy as an auxiliary charger, the charger will also have the ability to convert solar energy into electrical energy, and then the power supply electrical equipment.[1] Meanwhile phased in terms of electric charge city. By charging after the first constant-current constant-voltage mode.Since only with a smaller current charge lithium battery is completely discharged, it must first detect the battery voltage charger, if you need to fine current charge is low,when the current rose to a certain level after normal current charging.When the constant current charging, the battery voltage will rise until the voltage up to 5.0V, the charger need to transfer the constant voltage charging mode, because the voltage higher than 5.0V, then it will cause damage to the battery. In this case, current will slowly decrease naturally, when the current is less than the set value will be able to stop charging.

II. SYSTEM DESIGN

Overall system block diagram shown in Figure 1, including solar modules, mains charger main circuit, sampling circuit, protection circuits, human-computer interaction.Mains charger main circuit including the AC / DC converter circuit section, BUCK DC / DC step-down circuit section.The sampling circuit includes sampling voltage and current temperature, small signal amplification, A / D conversion, voltage and current control.[2]Voltage protection circuit includes a current limit overshoot protection, high temperature protection, anti-reflux and the like.

The system can realize intelligent control of the charging voltage and current, temperature, voltage monitoring shows, as well as solar energy, mains charging two ways.

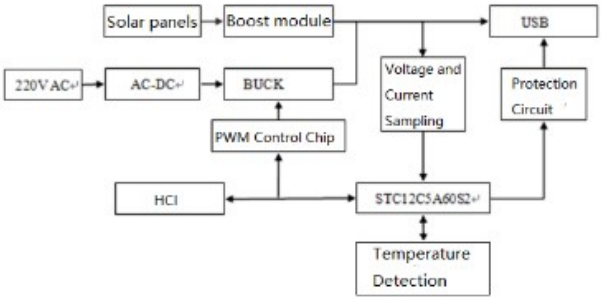

Fig1.General architecture of the system

III. SOLAR CHARGING SECTION

This part of the auxiliary charging circuit for emergency charging purposes. Hardware circuit mainly to solar panels and integrated chip 34063 as the core, the main work is to build a booster circuit, and filtering to obtain a more stable charging voltage.

A. Solar Panel

Common single crystal silicon solar panels, poly-crystalline silicon, amorphous silicon, compound of four, of which the first species is more commonly used. High photoelectric conversion efficiency of mono-crystalline silicon solar panels, about 15%, up to 24%, but higher prices. Photoelectric conversion efficiency of poly-crystalline silicon solar panels than single crystal silicon reduce the number, about 12% of the total production costs lower than single crystal silicon. Further life than mono-crystalline silicon solar panels poly-crystalline solar panels long, considering the above factors, the choice of low cost, poly-crystalline silicon solar panels suitable for mass production as a photoelectric conversion element.[3]

B. Booster Circuit

Figure 2 is a circuit diagram of a boost module.The 34063 chip will use part of the unstable voltage solar panel output rose to a stable 5V (open circuit voltage), the device itself contains the main function of DC / DC converter is required monolithic control circuit and inexpensive.

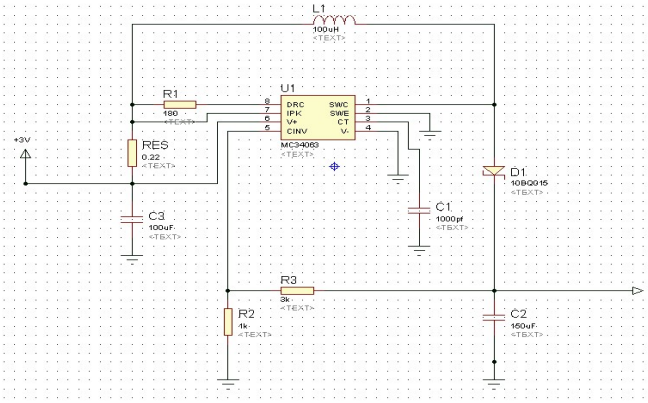

Fig.2 Boost Converter Circuit Diagram

C. Performance Testing

Independently of mobile phone batteries and mobile power charge. Can be measured with load voltage of 4.7-4.9V, meet the requirements of standard charger.

The charging current with the intensity of sunlight changes. Emergency charging function can be achieved when no electricity. Figure 3 is a single test result panels sunny.

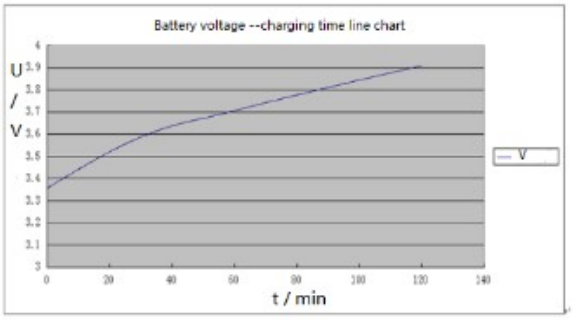

Fig3.The relationship between the battery voltage and the charging time of the single solar panel charging

Ⅳ.SECTION OF ELECTRONIC SUPPLY

The main part of this section is hardware circuit. Through AC-DC module and buck converter circuit, we can transform the electronic supply to continuous current, which can charge for mobile devices. According to the Optimal charging curve, we divide the process of charging into three stages: small current stage, constant voltage stage. Meanwhile, we add feedback signals to control a stable charging.

A. Design of the Step-down Circuit

Buck circuit（Fig.4）is a buck converter circuit, which has lots of virtue such as high efficiency, large output current and small quiescent current. Thus, it is always used into the design of switched-mode power

supply. This design adopts the BUCK circuit as well.

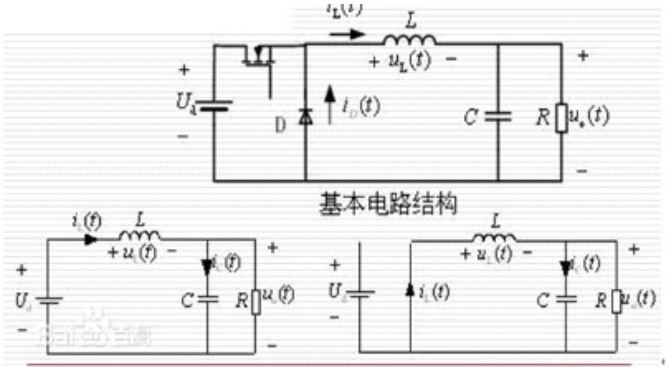

Fig4.Buck converter circuit diagram

B. Selection of Controlling Chip

TL494 device is a fixed-frequency pulse-width-modulation control circuit, whose internal structure diagram is shown in Figure 5. This chip is mainly designed for switching power supply controller.

Its oscillator can work in active mode and passivemode, you can control the frequency of the oscillator by a resistor and a capacitor. It contains two error amplifiers, an on-chip adjustable oscillator. The dead-time control has a fixed offset that provides approximately 5% dead time. And its output transistor sink current is up to 500 mA.[4]

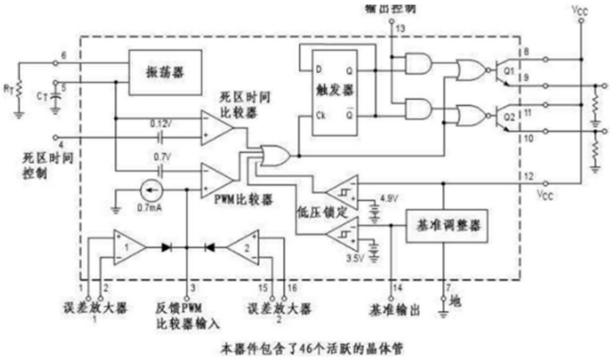

Fig5.Internal structure diagram of TL494

C. Section of Constant Voltage and Constant Current

Fluctuations in voltage and current will cause varies degrees of damage to the charging devices, so it is required to provide a constant voltage or a constant current while charging. This section controls the output to be stable by using the PWM chip and BUCK circuit.

D.Performance Testing

This section almost achieves functions as expected: it can control the charging models through different voltages of battery (Fig. 6).

It can control the output being 200 mA when the voltage of battery is under 2.7 V;

It can control the output being 2000 mA when the voltage of battery is above 2.7 V but under 5.0 V;

It can control the output being 5.0 V when the voltage of battery is above 5.0 V;

Electricity charge results is shown in Figure 6. The voltage of battery grows 1.5 V every 30 minutes. Table1shows the comparison of normal charger and the prototype, from which you can see this prototype charges more quickly than normal chargers.

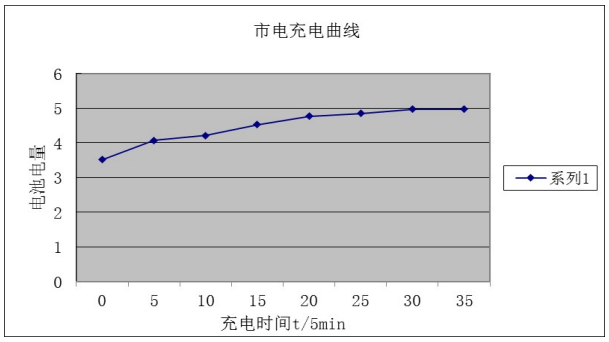

Fig.6 The charge curve diagram of 220V

Tab.1 Charging contrast diagram

Charge timet/min	Battery level/V	
	Normal charger	Homemade charger
0	3.52	3.52
5	3.91	4.07
10	4.1	4.21
15	4.16	4.53
20	4.28	4.77
25	4.54	4.85
30	4.8	4.97
35	4.9	4.97
40	4.95	4.97

Ⅴ.THE CHARGE STATE DETECTION AND DISPLAY

This part is used to detect the temperature by controlling the charging voltage and current, the testing results of the working state of the charger,At the same time, the monitoring results are displayed.The voltage current detection of electric charge play a supporting role,to determine the state of charge, the temperature sensor detects the temperature of the chip chip high temperature power to prevent burning.

A.Principle block diagram

Temperature detection using digital sensor DS18B20.It is a kind of digital temperature sensor,is a single bus digital thermometer programmable resolution,the programming can be achieved 1/2 ~ 1/16

four grade precision conversion.It only need one line connected with the CPU without peripheral circuit,Support one multi-point temperature measurement model.

Voltage detection using STC12C5A60S2 MCU internal A/D.The A/D is a 10 bit successive than high speed A/D converter has the advantages of high speed, low power consumption.Detection system diagram as shown in Figure 7.

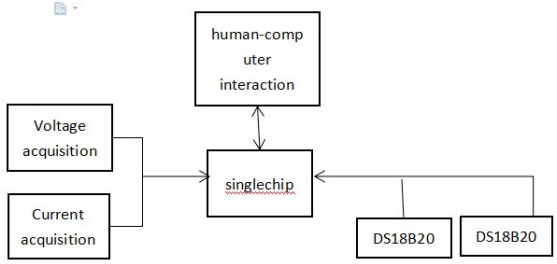

Fig.7 Principle diagram of detection syst

18B20 single multi-point temperature measurement model.The number of 18B20 received a single chip a I/O port, which uses a single bus control number from the machine, through the serial number, time, read all the data from the machine.To issue the command from the machine, according to the need for programming and control or time control.It only use a I/O microcontroller port, greatly saves the resource of MCU.

B.Performance Testing

The test results of absolute error can be maintained at 0.7 DEG C, and has high measurement precision, which can meet the requirements of the chip temperature test.A separate test voltage detection module, were detected by lift and drop, the measurement results of absolute error is less than 0.1V.

Ⅵ.The Overall Performance Index

According to the above the performance test shows that this design can realize the charging, solar charging double charging mode.The charging by fast charging characteristics, can be divided into intelligent charging stage,According to the situation of battery trickle, constant current, constant voltage charging, stable output voltage and current, charging speed is better than the ordinary charger.As an auxiliary solar charging module, emergency charging can be achieved without electricity, provide a wider use of the environment for the charger.Tt can the state of charge to achieve real-time display.And it has high power, anti backflow protection module, high safety performance.

Summary of the charger performance as shown below.

A.Solar Charging Part

The conversion efficiency of solar panels: 10%

No-load output voltage: 5V;

Load voltage: 4.7-4.9;

B.Charging Part

The maximum charge current: 4.7A;

Constant voltage charging: no-load 5V, load 4.8-5.0V;

Ripple: about 50mV (without noise)

Ⅶ.Conclusion

Using STC12C5A60S2 microcontroller with BUCK intelligent fast charger TK7500B chip design,using high-power original heat dissipation design reasonable, can achieve the maximum charging current of 4.7A.Stage charging mode to further enhance the charging speed, charging 1 hours faster than the common charger.No power can meet the requirements of the temporary charging solar charging mode.

References

[1] Wang Honglin. Intelligent Fast Charger Design and Production [M]. Beijing: Science Press, 2002.

[2] Li Ye, Chen He, Wang Dongyang, et al. Lithium Battery Charger Intelligent Design [J]. Jilin University, 2012,30(3): 256-259.

[3] Yang Bangwen. Practical Battery Charger and Protection Circuits Collection [M]. Beijing: Electronic Industry Press, 2000.

[4] Tan Faming. Intelligent Lithium Battery Charger Based on KA7500B [J]. Jiangsu Insititude of Techonology, April 2014 20(2).

Optimization of the control for charging lithium battery using in energy storage of clean energy

YUE Qian-hui; ZHANG Chen-xu; ZHANG Xin

(College of Instrumentation and Electrical Engineering，Jilin University，Changchun 130026，China)

***Abstract*--In this paper, a set of buck circuit and boost circuit is developed. In addition, a sampling circuit and a MOSFET driver circuit are designed. The mathematical model and the transfer function of buck are studied,in the meantime. The parameters of PI controller are set up based on the amplitude frequency characteristics of the system. Simulation and experimental results verify the validity of the control method.**

***Keywords*--clean energy generation; Lithium battery energy storage; MSP430F149 MCU; PI controller**

I. INTRODUCTION

IN recent years,environmental situation is not optimistic with the rapid development of economy and the increasing depletion of fossil fuels. Therefore, the demand for energy is growing which caused the emphasis on environmental protection has been strengthened and the use of clean energy has become an inevitable trend. In addition，because clean energy generate energy instability and the rate of storage utilization is not high, optimizing the control of clean energy generation is perfectly significant[1].

The system of lithium battery energy storage can be used as a buffer between a variety of electric energy and the stable needs of electricity generation capacity. Lithium battery can optimize the unstable power supply,such as wind and solar. If the power supply is too much, energy storage system will be used to store the excess energy in battery.Otherwise if the power supply is insufficient,energy storage system can will quickly respond, timely release energy from the battery. At the same time, the energy storage system can adjust the voltage and control frequency in off-grid power system.

Therefore, lithium is applied to the yield of clean energy storage which will greatly improve the present situation,and save resources. Moreover it will make efficient use of clean energy, to make up for some shortcomings of lead-acid batteries.

II. SYSTEM DESIGN OVERVIEW

The control system takes optimizing the control of lithium battery for energy storage in the case of clean energy generation as the core. The overall diagram is as follows.

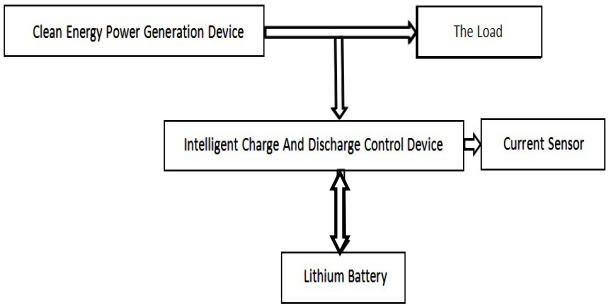

Fig. 1. Overall Diagram

Firstly, when abundant energy is generated from the clean energy generation,the generation provide power directly to the load. At the same time, the excess energy is stored in the lithium battery through the charging circuit of the intelligent charging and discharging device. However when the energy generated from the generation device is insufficient , promptly cut off the charging circuit, so lithium battery stop charging. The discharge circuit of the intelligent charging and discharging device immediately response to discharge to the load, so that the load can be maintained for a while.

In general,the system can be divided into two parts--hardware and software. Hardware part includes BUCK circuit,BOOST circuit,drive circuit, current sampling circuit, MSP430F149 minimum system and some power supply modules. Software part is based on the lithium battery charging process using the PID as the core, to achieve to charge with constant current , over-current protection, overcharge protection, and automatic switching the power supply to the load

between the clean energy and lithium battery. The two parts of hardware and software are in close contact with each other, working together to achieve the basic functions. of optimal control of charging and discharging.

III. HARDWARE DESIGN

A.BUCK Charging Circuit

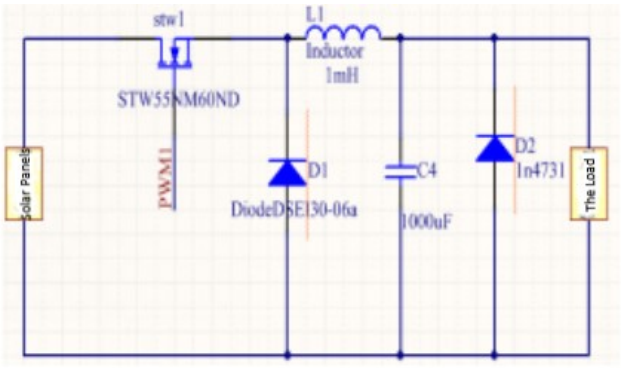

Fig. 2. BUCK Charging Circuit

BUCK circuit is used as a charging circuit, and its total power supply is three parallel solar panels (12V, 3W).The switching element is a fast recovery MOSFET transistor--STW55NM60ND, and the diode is a fast recovery diode--DSEI30-06A, in order to reduce power consumption and enhance the reaction rate. In the circuit, C=1000uF and L=1mH. Calculated by the following formula.

$$C = \frac{U_o(1-U_o/U_{in})}{8Lf^2\Delta U_o} \tag{1}$$

$$L = \frac{U_o(1-U_o/U_{in})}{2fI_o} \tag{2}$$

The lithium batteries--18650 are manufactured by Sony Corporation in Japan.The charge voltage when full power is 4.2V, and the discharge voltage is 3.7V. The charge current is in the range of 1A to 2A.

There is a 4.2V regulator between BUCK circuit and lithium batteries, which is used because of lithium battery charging characteristics and capacities. Lithium batteries should be charged under 1.5A constant current, and in the meantime, the voltage will gradually increasing. When the voltage rises to 4.2V, the limit voltage of regulator will not rise ,and lithium battery will be charged under 4.2V constant voltage. Because of power constraints, in the process of constant voltage charging,the current will gradually reduce.Until the current is lower than the lower limit of 0.2A, the lithium batteries stop charging.

B.BOOST Discharge Circuit

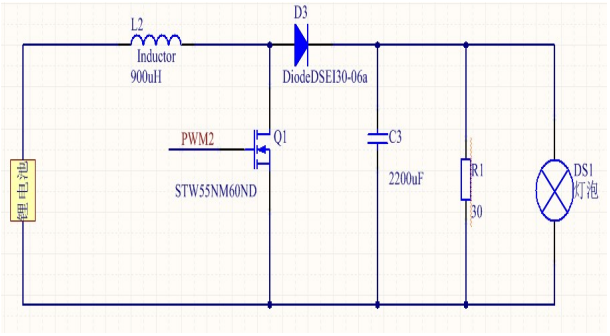

Fig. 3. BOOST Discharge Circuit

BOOST circuit used a discharge circuit ,its switching element uses a fast recovery MOSFET transistor products STW55NM60ND, and diodes use fast recovery diodes DSEI30-06A. In the circuit, the capacitance parameter is 2200uF, and inductance parameter is 900uH.Incandescent lamp(12V，5W) is used as the load.Calculated by the following formula.

$$C = \frac{D_{\max}T_s}{\Delta U_o} I_o \tag{3}$$

$$L = \frac{U_o T_s}{2I_{ol}} D_{\min}(1-D_{\min})^2 \tag{4}$$

C.MOSFET Driver Circuit

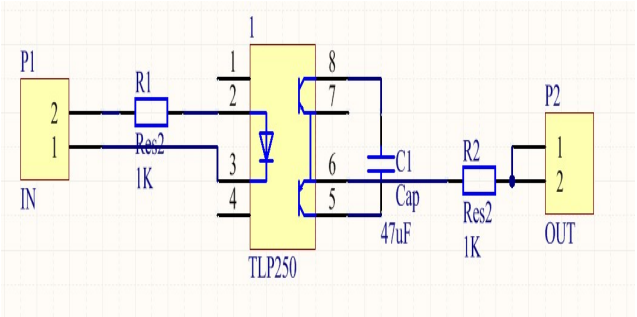

Fig. 4. Driving Circuit

Drive circuit is made up of an optical coupler and peripheral circuit.It is used to amplify the PWM signal from the micro-controller output and drive the MOSFET transistors. TLP250 has a one-way channel,and DC inputs. Its isolation voltage of transmission delay is 2500Vrms, and forward current is 20mA.

D.Sampling Circuit

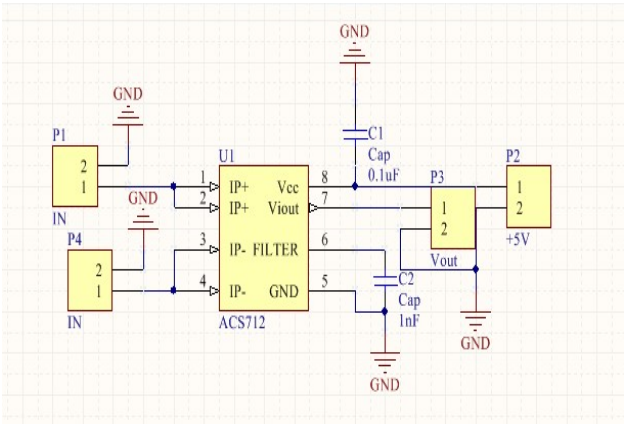

Fig. 5. Sampling Circuit

ACS712 sensors are produced by the Allegro are used in the sampling circuit. ACS712 sensors is a linear current sensor and sampling BUCK circuit current. The device has a built-in precise low-offset linear Hall sensor circuit that can accurately measure the current.

E.MSP430F149 micro-controller

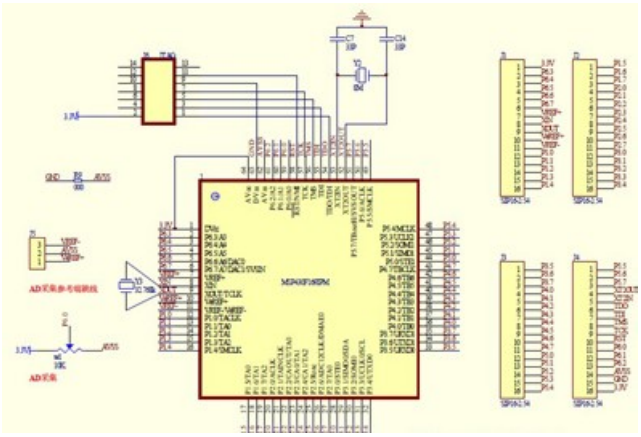

Fig. 6. Circuit Diagram of Single Chip

MSP430F149 is a 16-bit micro-controller, which has advantages of high integration, rich peripherals，and low power consumption. It has been widely used in industry. Integrated 8 channel and 2 AD converter, watchdog timer, a hardware multiplier and 48 IO pins. In operation ,the device enters the low-power mode to reduce system power consumption.

F. Auxiliary Power Module

1.QAW01 Power Modules

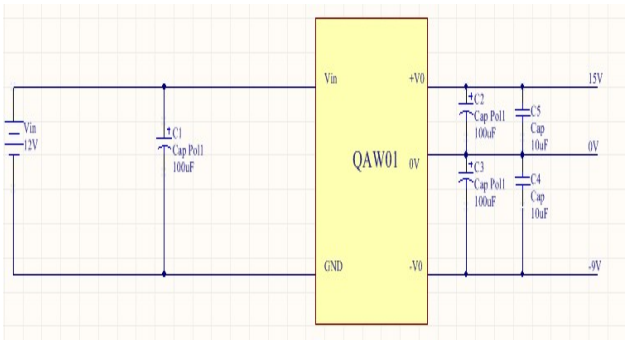

Fig. 7. The circuit schematic diagram of Power supply for driving circuit in buck circuit

QAW01 is isolated dc-dc power modules produced by MORNSUN company. Its input is 12V, output is + 15V and -9V, and supply to TLP250.

2.B0305xt-1wr2 Power Modules

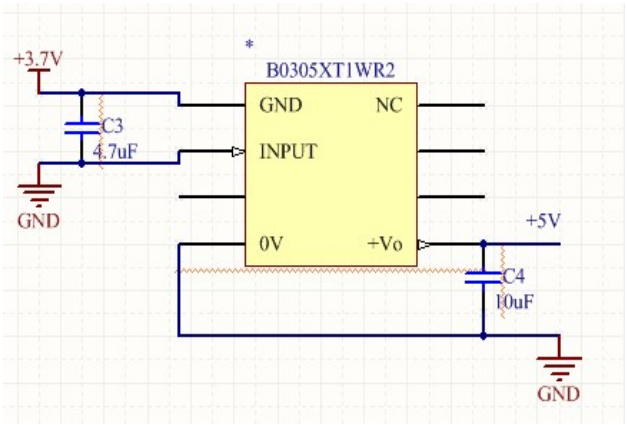

Fig.8. The circuit schematic diagram of Power supply for Sampling Circuit and single chip in boost circuit

B0305xt-1wr2 is 3V or 5V input of dc-dc constant voltage, and single-output isolation of non-regulated power supply module .Its power is 1W, and supply to the micro-controller in the discharge circuit .It has characteristics of sustainable short circuit protection and 1500VDC isolation.

3.f1205xt-1wr2Power Modules

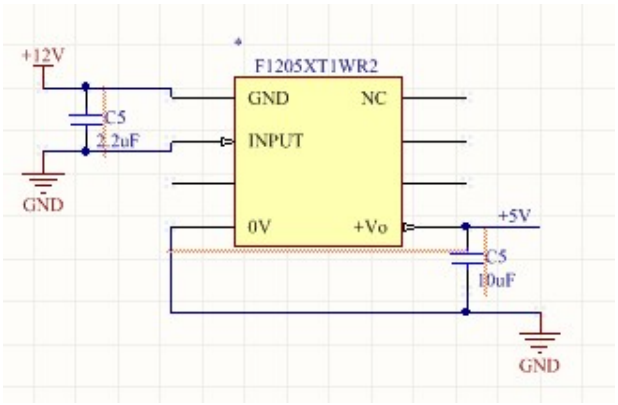

Fig9. The Circuit Schematic Diagram of Power Supply for Sampling Circuit and Single Chip in Buck Circuit

F1205XT-1WR2 is 5v or 12v input of dc-dc constant voltage, and single-output isolation unsteady power supply module. Its power is 1W, and supply to the micro-controller in the discharge circuit. It has characteristics of sustainable short circuit protection, low ripple noise, 3000VDC isolation, and efficiency up to 80%.

4.XC9119 Boost Power Module

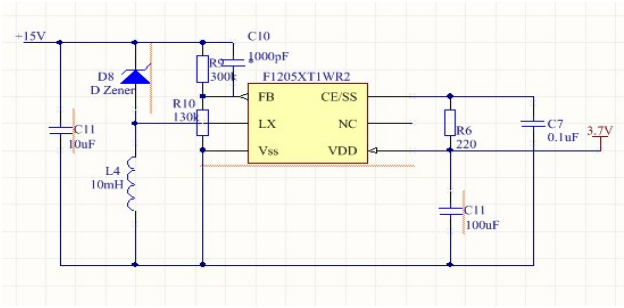

Fig. 10. The Circuit Schematic Diagram of Power Supply for Driving Circuit in Boost Circuit

XC9119 is adjustable boost chip input and output. It can be used for general-purpose high-voltage power supply and efficiency up to 86%. Here is a 3v / 15v boost circuit, in the discharge circuit to provide input for the QAW01 power module.

IV. Software Design

A.Fundamental Principles

Constant current charging is controlled by the digital PI controller.

PI regulator is a linear controller, which according to the given value--r(t) constitute the actual output--c(t) the value of the control deviation.

$$e(t) = r(t) - c(t) \tag{5}$$

The deviation of the ratio (P) and integral (I) by forming a linear combination of a controlled amount of the controlled object, its control law is as follows.

$$u(t) = K_p[e(t) + \frac{1}{T_I}\int_0^t e(t)dt] \tag{6}$$

Where u(t) is the output of the PI controller, y (t) for the PI regulator input, K_p is a proportionality factor, TI is the integration time constant[4].

The proportion of links: timely response proportional control system deviation signal e(t), deviation, once produced, the controller generates control action immediately in order to reduce bias.

Integral part: mainly used to eliminate static error and improve the system's no difference degree.

PI control using incremental, feedback control diagram is as follows.

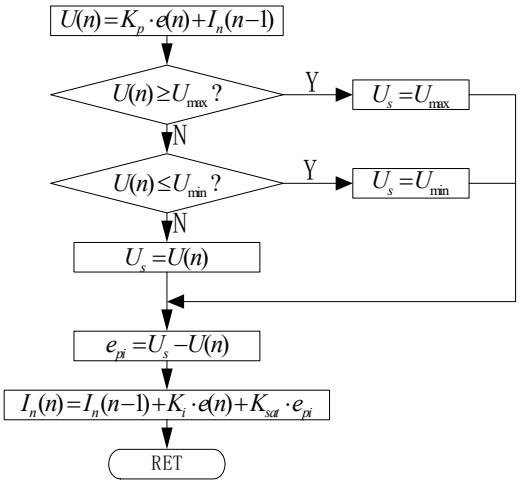

Fig. 11. Program Flow Diagram of PI Regulator

B.PI Parameter Selection

According to the transfer function (7) and BUCK circuit capacitance and inductance parameters to get the transfer function, and the use of PI correction, so that the function reaches a steady state. I_g = 1.5A, L = 1mH, C = 1000uF, R = 50Ω, K_p = 0.008, K_i = 0.02.

$$G_{vd}(s) = \frac{I_g}{1 + \frac{L}{R}s + LCs^2} \tag{7}$$

The transfer function Bode diagram and the Bode diagram after correction are as follows.

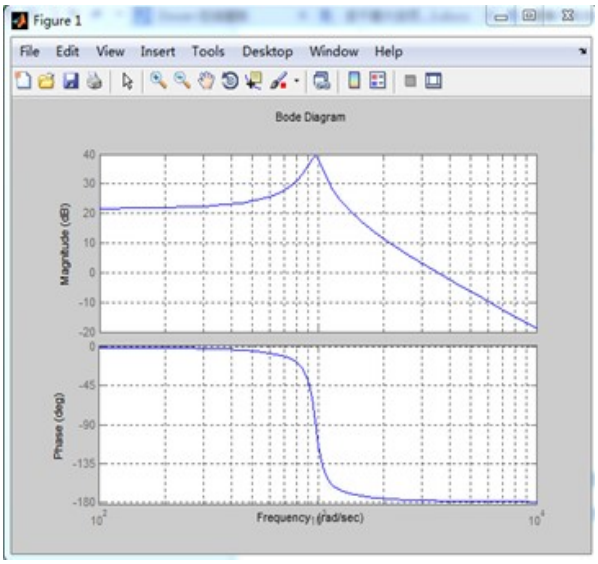

Fig. 12. The Transfer Function Bode Diagram

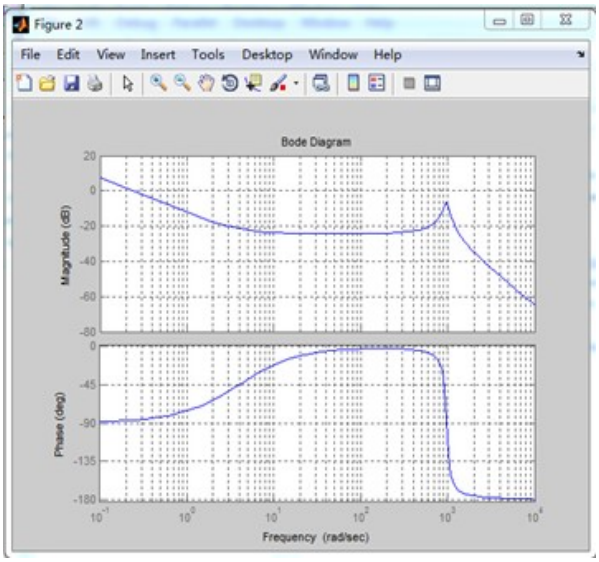

Fig. 13. The Bode Diagram After Correction

C.Practical Application

Since the current sensor output voltage signal, it should be by the relation I = (U-2.5) /0.185 to convert the data into a current value, and then use the digital PI controller for each sampling value and the set value to obtain three error by K_p, K_i is calculated to maintain constant current output 1.5A PWM wave duty cycle required, in order to control the MOSFET is turned on and off time, and then play a regulatory role buck circuit output current, output reached 1.5 a constant current to charge the lithium battery effect.

V. The Progress of The System

A. The Progress Of Charging And Over-current, Over Charge Protection

When the sunlight is sufficient, with solar panels working, its output voltage is higher than that of discharge circuit,reverse switching diode between solar panels and the output of discharge circuit,the load is directly supplied by the solar energy power. On one hand,solar panels give power to the load.On the other hand,solar panels charge lithium battery through the buck circuit with current sensor real-time sampling and monitoring the current value and translating the collected data to MSP430F149 MCU,which adopt PI algorithm and calculate the PWM duty ratio to maintain a constant current ,as well as always keep stable current value of the charging circuit at 1.5A. In order to averting the fluctuation of solar energy, which makes the current of charging circuit is too large, the upper limit value is set in the charging procedure, to play the role of over current protection. During this period, the voltage gradually rises until 4.2V is reached.Due to the effect of the voltage regulator tube, the voltage is maintained at 4.2V. Lithium battery become charged with a content value of voltage,during this period, the current decrease gradually until 0.2A is reached. If the value of current is below the low limit （0.2A)，adjust the duty ratio of the electric circuit of DC-DC buck to 0,to stop charging, so as to avoid the damage to lithium battery due to that the current of charging circuit is too low.

B. Discharge Process

When solar energy is not enough,voltage of the the solar panel is lower than that of the discharge. The load is switched to the state of supplied by lithium battery because of switching diode conduction. Lithium battery power give power to the load through the Boost Circuit, so that the load can continue to be supplied for a period of time. Switching time is for the nanosecond, so as to achieve continuous working of the load.

VI. Actual Situation

A.Experimental Waveform

1.The open-loop output current waveform of BUCK circuit is as follows.

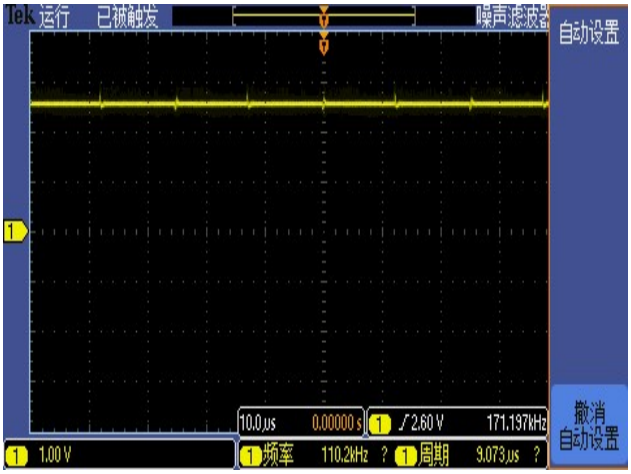

Fig. 14. The Open-loop Output Current Waveform Of BUCK Circuit

2.The open-loop output voltage waveform of BOOST circuit is as follows.

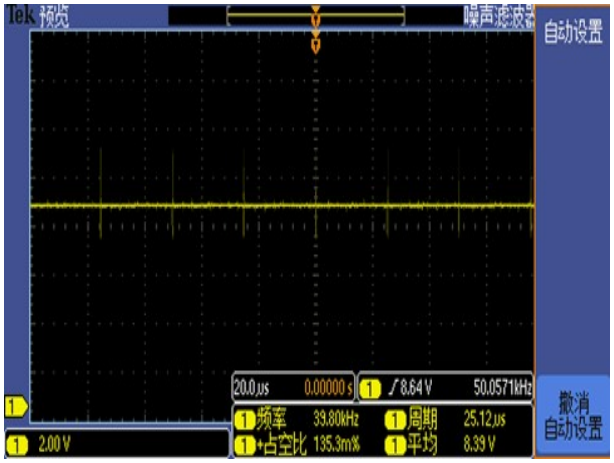

Fig. 15. The Open-loop Output Voltage Waveform Of Boost Circuit

In Fig. 15 and Fig. 16, the load is a resistance, and The crane overload protection system is a open-loop control system, so the error of the test waveform is relatively large.

3.The closed-loop output current waveform of BUCK circuit is as follows.

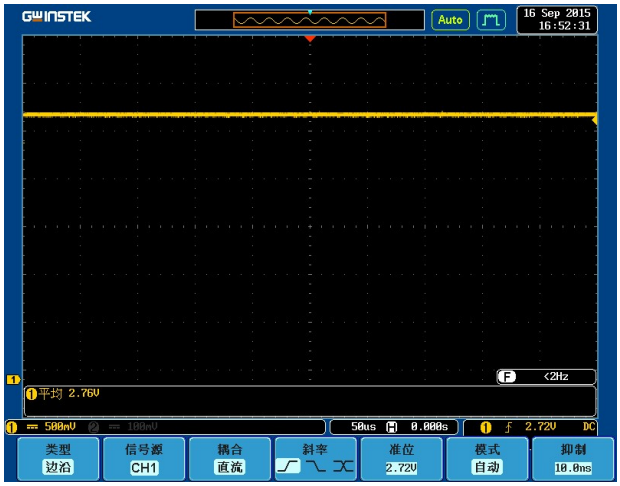

Fig. 16. The Closed-loop Output Current Waveform Of Buck Circuit

In contrast, the effect of the closed-loop control of the output waveform is better.

B.Physical Work

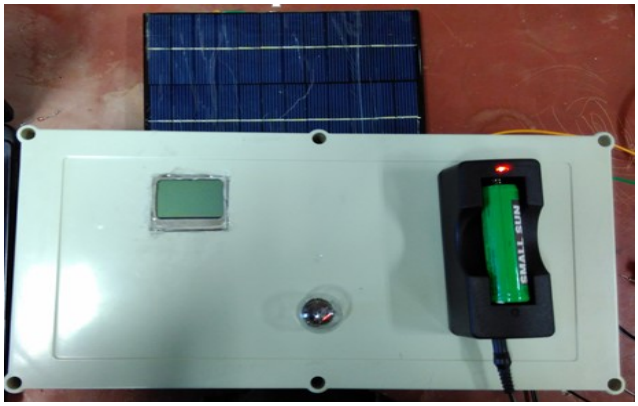

Fig. 17. Physical Work

C.Outdoor Measuring Case

The experiment is conducted in fine weather where the measured ambient temperature is 27ºC .Solar panels is selected as the clean energy and an incandescent lamp is selected as the load.

When solar panels are expanded and lighting is adequate,the output voltage of solar panels is measured as 12.6V. The current value of the duty cycle can be seen in the 5110 screen which gradually rise，stabilize at 40% and 1.5V in a short period of time and the incandescent light can bulb normally.

When a half of solar panels is covered,the output voltage of the solar panels is 5V,while the incandescent light is made glow. The switching time between the two power supply-solar panels and lithium battery is less than distinguish time of human eye so it achieves the desired effect.

VII. Practical Significance

Due to the increasing depletion of fossil fuels, clean energy applications is also augmenting. However the stability of clean energy supply is disturbed by weather, temperature and other factors. Clean energy fluctuation is an important reason why clean energy development is limited. For example, if a sudden power outage,but there is not enough time to save the important data in some devices , it may result in Immeasurable losses. In this system,a lithium battery is used to store excess energy firstly. It not only maximizes the use of clean energy but also supply the devices for a while when clean energy can not generate enough energy. If the capacity of lithium battery is large enough, it can ensure that there is enough time to complete the remaining work or save important data, so that the supply of clean energy is greatly improved to be more stable, meanwhile the energy utilization ratio of clean energy is higher. In addition, lithium battery is a new type of energy storage device which embraces features of environmental protection,small volume and light weight，the advantages that lead-acid batteries have not,so that it have a very prospective development prospect.

VIII. Conclusion

Through the experiments can explain that

optimizing the control of clean energy generation to lithium battery for energy storage system can be applied in the case when the clean energy is abundant or not,so that the load can work normally in both two cases because of the control of charging and discharging of the lithium battery, and the switching time between the two power modes is less than the time distinguished by human eyes so as to achieve the desired effect. The system has an effect of improving the energy utilization ratio of clean energy and enhancing the stability of clean energy generation,so there is a certain practical significance.

References

[1] Fan Wen.Charger circuit [M]. Electronic world, 2005,4

[2] Feng Chang, Xu Jin-ming.Ultra-high brightness LED applications in solar lighting system in the city of [N]. Wuhan University of Science and Technology, 2003

[3] Kang Hua-guang.Electronic technology foundation [M]. Higher Education Press, 2005

[4] Liu Jin-kun. Advanced PID control and MATLAB [M]. Electronic Industry Press, 2003

[5] Huang Zhonglin, Zhou Xiang-ming. Control system MATLAB computing and simulation training [M]. National Defense Industry Press, 2006

[6] Chen Li-lan. Electronic automatic control theory [M]. Industry Press, 2006

Design and Implementation of Intelligent Garbage Collection Car

QIN Peng-fei; CHEN Chuan-qi; WEI An-wen
(College of instrumentation and Electrical Engineering, Jilin University,Changchun 130022,China)

***Abstract*--The main content of this article is to the research and development of a smart car which is based on the stm32F103 micro controller. The design aims to design and implement a preset trajectory of the smart car travel and garbage collection main functions. The design of the car consists of four modules. They are called power system design, control system design, image recognition system design, wireless communication system design. Power system with four-wheel design architecture uses DC motor. Control system uses stm32f103 chip as the core, by changing the duty cycle of the output PWM wave Implementation of the trolley travel control. Image recognition system is to use the camera to identify the road ahead, which can automatically avoid obstacles. The electrical design of trash implements wireless communications between trash and car. Those make the car complete to the design requirements.**

***Keywords*--Smart Car Garbage collection STM32F103 Wireless communication**

I. INTRODUCTION

ECONOMIC development accelerates the improvement of people's living standards and urbanization process, at the same time ,the emission of waste is increasing rapidly. For reality of garbage swamping, the sight of the world not only stays in how to control and destroy the garbage, we need take a positive attitude and effective measures to deal with the waste,and put the garbage as "the second resource"of maintaining sustainable economic development, ask the garbage for resources and energy.

According to the present needs of the community, to be garbage intelligent car research project [1]. The project design smart car to the STM32f103 micro controller core, using the camera to achieve recognition and avoidance of road use NRF2401 2.4G wireless communication module and communication between the trash, 12,864 pairs of the car with LCD display real-time status, low cost, feature-rich, stable performance, easy maintenance, etc., at the same time without changing the hardware of the premise, to upgrade a large space, practicality.

In this study, the smart car is bold apply to people's daily life, it is possible to reduce the waste of human resources and economic resources, reduce the burden on commercial streets or living quarters sanitation cleaners make up for the domestic market in this area.

II. SYSTEM DESIGN

The trolley system, including the two most intelligent cars and stations, control stations using wireless communication to achieve the main set mode of operation of the car, deployment and real-time status of each trash display. Car section with minimum system micro controller to control the core, through the completion of a number of peripheral drive has been set garbage disposal. The car has a camera tracking, speed measurement, wireless control, sound and light tips and other functions.

Car with automatic and manual modes of operation. Automatic mode by the camera to detect traffic and trash to find the target, the camera tracking can achieve obstacle avoidance function [2], to enhance the car's road adaptability. After the trash after electrical design, can be alarm, when carrying trash to a certain extent, it will trigger the sensor sends a signal overflowing and buzzer alarm, the car after detecting the signal, signal source analysis, arrived at the designated location simulation of the garbage collection process. After the recovery is completed, the alarm is released, the car returned to the specified location and continue to stand [3].

Car manual mode consists of 4 * 4 keyboard switch, designated trash man selected by the automatic car search to locate and simulate the

garbage collection process. The manual mode is good to avoid the appearance of interference in a wireless communication after garbage collection problems[4].

III. GARBAGE COLLECTION CAR HARDWARE DESIGN

Smart car with a sound sensor system [5] motion control algorithms, real-time communications capability and reliable actuators. Overall system configuration diagram shown in Figure 1 with specific functions:

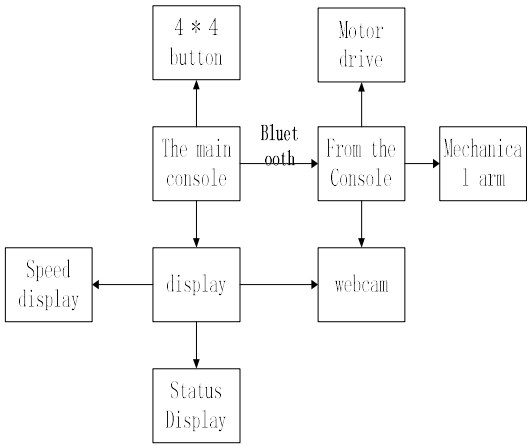

Fig .1.Structure and function diagram

Trolley hardware from the power system,control system,wireless communication systems,image recognition system.

A. Dynamic Design System

Firstly power DC motors, DC motors can achieve a smooth and effective governor. And you do not need with other devices, just change the input or excitation voltage and current can achieve speed [6]. Linearity of the DC motor mechanical characteristics good, fast, responsive, rotation torque, small size, light weight, low cost, in addition, with a load capacity DC motor, speed smooth, wide PWM adjustment range. Realize the car steering, steering is achieved by the power difference by changing the speed of the wheels on both sides, resulting in a speed difference. This program does not require steering, the program is simple, easy to control. Car driven by PWM pulse generated by the controller, use L298 module for power amplifier, and then drive a DC motor driven trolley. PWM pulse drive pulse car use, improve the accuracy of the DC motor.

B. Control System Design

Selection STM32F103 series low-power single-chip [7]. The devices based on the ARM Cortex-M3 core, fast processing speed, clock frequency up to 72MHz, while rich peripheral resources, low prices. Compared with 51 single-chip, more prominent advantages, including the obvious advantages on processing speed, ample space and on-chip memory address space, as well as development tools UV4 STM32F103 with a complete library functions and standard C compiler.

C. Wireless Communication System Design

Use, the module has a transmission speed, low power consumption and low cost advantages based NRF2401 2.4G wireless communication module [8]. This design is to achieve trash and trolley links. Module on the dustbin of signals, control the car forward or backward, to achieve intelligent effect. Implement instructions via wireless communication technology to receive and transmit [9], and can display the current job status of each case and trolley bins in real time.

D. Image Recognition System

Plane array camera using CMOS sensor [10], the information collected throughout an image of the road ahead, get traffic information in front of the car, in Figure 2, then collected images through software "binary" (Camera when collecting gray image is larger than the preset threshold value be set to 1, the contrary is set to 0), the use of PID algorithm based on the binary image of the servo and motor control [11]. In the automatic control system, PID controller is a control method has been widely applied. Since the size of the motor speed and armature substantially proportional to the applied voltage, which forms the basis of PID regulation. PID operation process parameters and calculated values are all multistage byte floating-point representations, in the control process changing control parameters. System run by the timer interrupt once every interval T seconds, to complete a PID control calculation, so as to continuously adjust the controlled parameter, the main program of PWM drive module is changed according to the control parameters P0 port output value to adjust the PWM output waveform, complete Real-time control tasks, and finally to the car can advance along a predetermined path. This method can not only identify the center position of the road, but also the direction of the road can be obtained, the curvature of the road information and the like. This

can effectively exercise control of the car, improving Cars path tracking speed and running speed.

Fig.2 .The car in front of the road image

Secondly, the two stations as the core part of the trolley car, the master station can display the name and status of the car, when the car forward or backward, the display will have a corresponding status display, it is easy to adjust the car ready state. Car speed through speed encoder on the display, so you can according to the actual situation of the car speed subtraction. Master control station and from a control station connected by Bluetooth module communications, the keyboard connected to the main control station. Initially, the keyboard a starting signal to the car, the car began to move, the camera on the road conditions were collected and determine, camera will capture the image binarization process, so that the car can move forward along a predetermined path. Trash in the specified location next to the road, camera capture into the trash, if the trash does not reach a certain level alarm, the car will not be processed trash. When the garbage to a certain extent, an alarm signal, after the car receives this signal to determine the signal source, and travel to the specified location, simulation garbage collection. When processing is complete return to the specified location [12].

E. Manipulator System Design

Manipulator using six degrees of freedom servo, can freely grab any direction. When the car reaches the specified position, the micro controller will send a trigger signal to the robot,the robot motion instructions execute stored grab handle to complete work on the garbage.The smart car [13], a micro controller to control the core, with a low cost, feature-rich, stable performance, easy maintenance, etc., but without changing the hardware of the premise, to upgrade a large space, practicality.

IV.SOFTWARE DESIGN CRUISER

System used keil uvision4 and the stm32 micro controller for data processing, using C language development software part, so the software has good readability, portability is good. The entire system uses modular design program subroutine call each subroutine block design is relatively independent, easy to modify and adjust late. Program flow shown in Figure 3.

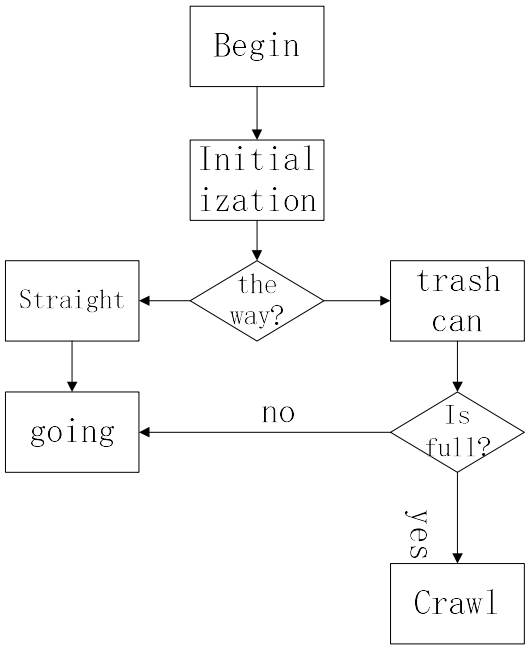

Fig.3 .Program flow chart

V.TESTING AND ANALYSIS

A. The camera parameters set

Camera with OV7670 module, which works for the master system to FPGA platform, set the image sensor output format RGB565, work clock is 72MHZ, acquisition speed up to 30 frames per second, 300,000 effective pixels. We know that high-level width equal HREF our line of pixels to display data [14] number: VSTART VSTOP these two registers determines the number of rows collection is highly VSTART = HEIGHT * 2 + VSTOP; as long as the input image starting line, field starting, width, height calculated value of the corresponding register. We need to spread the camera frame image width and a height of 320 pixels and 240 pixels, register values can be obtained according to the above method.

Fixed threshold image used. 110,0-110 to a threshold, greater than 110 representatives of the white areas is 0, 1, 0 represents black areas. Figure 4.

Fig.4 . Camera captured images

For accuracy with the camera tracking also made the corresponding test, only around ten laps the car tracking will be deviations from the runway, so the camera tracking with high accuracy.

B. Robot parameter settings

Robots six servos, requires six timer channels, we used different channels to control timers six servos are the following timer: 4 channels 1 and timer 3 channel 2 and 3. The specific parameters CCR41_Val = 800; CCR42_Val = 1350; CCR43_Val = 1500; CCR44_Val = 400; CCR32_Val = 1500; CCR33_Val = 1000; through different duty cycles to control the rotation of different angles, the total length is 400 to 1600 on behalf of the angle from 0 to 180 °. From top to bottom to open the corresponding timing channels, the gradual completion of the mechanical arm to rotate at different angles. Every movement of the arm about a second delay. Kind shown in Figure 5:

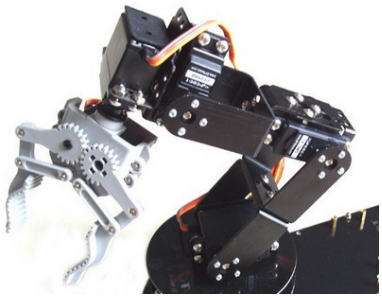

Fig. 5. Robot physical map

VI.CONCLUSION

Intelligent garbage collection car designs based on application requirements to stm32F103 control core, combined with DC motor drive module, camera driver module, sound and light tips modules and photoelectric tachometer module, automatic tracking trolley walk, automatic obstacle avoidance function , and through wireless communication between the hopper and the precise positioning of trash and garbage points eliminate the analog signal emitted. It implements intelligent and practical car.

The overall function of the car's design is divided into manual and automatic modes. In automatic mode, the car after receiving a signal emitted by garbage overflowing point, the self-designated garbage starts to complete the elimination of the analog signal at the point of the task and return to continue to stand. In the manual mode of operation can be selected at random garbage bins, the car according to the selected task. The manual mode is good at avoiding the emergence of interference in a wireless communication after garbage collection problems.

Joining in the garbage disposal robot, experimental requirement in this regard is well done. Trash electrical design also reflects intelligence. So we achieve the aim to automatic manage the garbage.

References

[1] CHEN Zhi-hua, XIE Cun-xi, ZENG Huai-de. Patrol robot research status and application prospect [A]. Mechanical engineering technology.2003,32(6):19-21.

[2] JIANG Yue-yue,WANG Hong-hua. Intelligent security based on multi sensor information fusion patrol car [B].Electric technology and automation.2012,41(6): 203-205.

[3] YING Xiang, LEI Peng-fei. Analysis and implementation of the system of intelligent patrol car. Fujian computer, 2012 (1):203-205.

[4] GAI Zi-xing. Robotics Trends and Development Strategy[J]. Robot Technique and Application,2001(4):188-216.

[5] ZHU Hong,ZENG Xiang-jin. Multi-sensorInformation Fusion Research[J]. Computer and Digital Engineering.2007(12)：46-48.

[6] HU Run-feng. NTC thermistor temperature sensor [J].Technology and applications, 2001 (7): 26-29.

[7] HE An-ke.Based on the STM32 and light intensity sensor BH1750 wireless street lamp control

system[A].Development of science and technology enterprises. 2011（20）:15-17.

[8] SHA Ai-jun. Research and design of ultrasonic ranging system based on single chip microcomputer[A].Electronic technology. 2009:57-61.

[9] Wang Sheng-yuan, Zhang Hong-wu, zhao kai, et al. Design and Realization of Wireless Transceiver Module in Communication of Many Machines[J]. Journal of Jilin university (science edition), 2006, 44 (3): 470-472.

[10] LI Xu-dong,LIAO Zhong-hao,MENG Jiao. Intelligent Vehicle Control System Design Realization Based on CMOS Camera[A]. Journal of Jilin University: Information Science Edition. 2013,31(4):414-418.

[11] YUN Zhuo,CHEN Long-dong,LIU Fu. Design of Intelligent Electric Vehicle Based on Freescale Microcontroller[A].Journal of Jilin University: Information Science Edition.2013,31(3):272-278.

[12] LI Xing-ze,WANG Fu-ping. Automatic tracking the parking system cell based on CCDcamera[A].Computer application,2013,33(S1):321-323.

[13] JIANG Xue-run,LI Zhong-hua,MAO Zong-yuan. Realization of Serial Communication Between Intelligent Module and Host Computer in VB Environment[J]. Automation and Instrumentation. 2003(6)：61-63.

[14] ZHAN Xin-sheng, ZHANG Jiang-wei. Design of wireless data acquisition system based on AT89S51 [J]. Research and exploration in laboratory. 2011,30(4)： 199—202.

The measurement of cores' young's modulus and Poisson's ratio based on electrical measuring method

Xiong Yonghui; Chen Ying

(College of Instrument Science and Electrical Engineering, Jilin University, Changchun, 130061, China)

***Abstract*--Research on mechanical properties of rocks has great role in promoting seismic exploration, underground mining and Carbon Dioxide and pollutand Sequestration . We can calculate the young's modulus and Poisson's ratio of the core by measuring the stress and strain with the geophysics knowledge. These two physical quantity reflects the corresponding vertical (horizontal) changes of the core when it's in the transverse (longitudinal) force, this corresponding relationship of single variable can be applied to the detection of underground. We have three modules to complete this work, they are sensor design, data acquisition system design, program design of data analysis. This article first descriptions the research background, then explains the design ideas and innovations, the feasibility of the experiment, focuses on how to carry out the design of sensor and other information on the data collection and data etc.Finally, standard aluminum and rock core samples are measured through experiment. At last, we draw some conlusions and disscuss the result.**

***Key words*--Electric measuring method Young's modulus Poisson's ratio high-precision real-time detection**

Ⅰ OBJECTIVE

WITH the function of force F, a metal wire will extend ΔL,whose length being L and cross-sectional area S. F/S stress and its physical meaning is the force on the wire cross-sectional area; δ L/L strain and its physical meaning of elongation for wire per unit length. Stress and strain than modulus: δ l is a tiny change.

Young's modulus, which is along the longitudinal modulus of, but also in terms of mechanics of materials. In 1807 for United Kingdom doctor and physicist Thomas young (Thomas Young, 1773-1829) the result name. According to Hooke's law, objects within the elastic limit, proportional to the stress and strain, the ratio is called the modulus of the material, it is the characterization of material properties of a physical quantity, depending on the physical properties of the material itself. Marks the rigidity of the material size of young's modulus, young's modulus, and less prone to deformation.

One of young's modulus of elasticity is the basis for selected parts materials, is commonly used in engineering design parameter. Study on the determination of young's modulus of metal materials, fiber materials, semiconductors, nanomaterials, polymers, ceramics, rubber, and other mechanical properties of materials is important, can also be used for machine parts design, bio-mechanics, geology, and other fields.

Poisson's ratio, elastic strain in the stress direction contraction of objects (stretching) is also often accompanied by perpendicular to the direction of the horizontal strain ratio of lateral strain and strain known as Poisson's ratio.

This physical volume indicates that the core force of physical characteristics on underground exploration and utilization of materials has been a big help.

Ⅱ SYSTEM DESIGN

A Principle analysis

The project obtained by measurement of stress-strain young's modulus and Poisson's ratio to measure the mechanical properties of rocks.

Due to the nature of the material, by a force the strain produced when very small. As a deformation of a test is very difficult.

Solutions：Changes in deformation resistance strain gages, resistance is proportional to strain relations, strain converts the measurement of strain gage measurement of resistance. Due to the small strain, resistance values corresponding to the little, you want to test is not easy to achieve, but through different bridge circuits can be small changes in resistance to big changes in the voltage change. Measurement of

strain measurement of resistance into the bridge voltage. Through the conversion of the final calculated by measuring the voltage after external structure of strain[1].

Were used to measure the electrical measuring method, measurement is easy to zoom in, operations such as filtering, facilitates high-precision dynamic measurement of transient measurements. Young's modulus and Poisson's ratio of these non-electric use corresponds to the ratio of stress and strain analysis. Sensor using strain gage Wheatstone bridge made for conversion will be converted into voltage signals corresponds to the direction of stress in order to collect and process. In the zero-point correction in bridge measurement processes by adding high precision digital potentiometer for automatic compensation for temperature effects, 18B20 chip is used. For voltage measurement conversion 24-bit AD converter chip for sample collection, and then into the computer to the last step in processing the data operation.

B System design

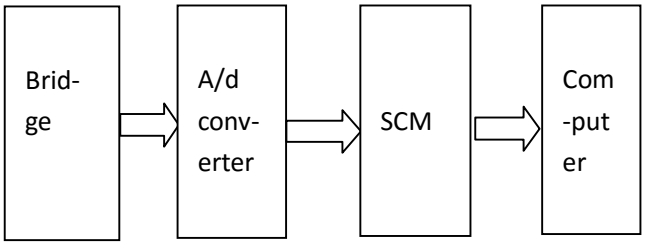

Fig.1 System block diagram

A/d converter, microcontroller, stress and strain measurement device and computer, composed of bridge and strain gauge sensors.

III HARDWARE DESIGN

A Measurement circuits

Measuring circuit in Figure 2, circuit sensors for pressure Gages, using high precision resistors with sensitivity coefficients for Hui Sitong arm made of 155 of the strain-gauge bridge circuit Rg1,Rg2 for strain gauge, Rg1=Rg2=R, leg equal to the initial resistance, the error is less than 1 ‰, two strain gage force uniform and the same character.

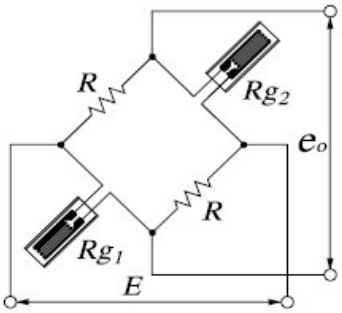

Fig.2 Schematic diagram of bridge

Eo output voltage is derived as follows:

$$\mathrm{Eo} = \mathrm{E}\left(\frac{Rg2+\Delta R}{R+Rg2+\Delta R}-\frac{R}{R+Rg1+\Delta R}\right)$$

$$\mathrm{Eo} = \mathrm{E}\frac{\Delta R}{2R+\Delta R}$$

$$\mathrm{Eo} = \mathrm{E}\frac{\Delta R/R}{2+\Delta R/R}$$

On resistance strain gage are as follows:

$$\frac{\Delta R}{R} = K\varepsilon$$

K strain sensitivity coefficient in the formula, to strain;

So there are:

$$\mathrm{Eo} = \mathrm{E}\frac{K\varepsilon}{2+K\varepsilon}$$

$$\frac{Eo}{E} = \frac{K\varepsilon}{2+K\varepsilon}$$

Solution:

$$\varepsilon = \frac{2\,Eo/E}{K(1-Eo/E)}$$

From the results, the bridge output voltage values for the two strain gauges the stress of single-valued functions, and in the application process, simply measure the horizontal and vertical stress of the same section. For accurate data, measured by average decreases in the form of random error.

Young's modulus is based on isotropic linear elastic theory, assuming that imposing uniform distribution, there are, as the standard aluminum axial stress. Young's modulus and Poisson's ratio of rock samples as follows:

$$\sigma_{11} = E_{rx}\varepsilon_{11}^{rx} = \sigma_{al} = E_{al}\varepsilon_{11}^{al}$$

$$E_{rx} = E_{al}\frac{\varepsilon_{11}^{al}}{\varepsilon_{11}^{rx}}$$

$$\mu = -\frac{\varepsilon_{22}^{rx}}{\varepsilon_{11}^{rx}}$$

rx representing rock, al represents the aluminum standard sample, ε_{11} represents the axial strain, ε_{22} stands for transverse strain. Standard samples of aluminum is a known constant young's modulus 69GPa.

B Data processing circuit

This part is divided into A/D two parts: reading and computer processing, the amplifier directly amplified by software, rolling up the data is magnified into the computer through the MATLAB program for calculation and mapping.

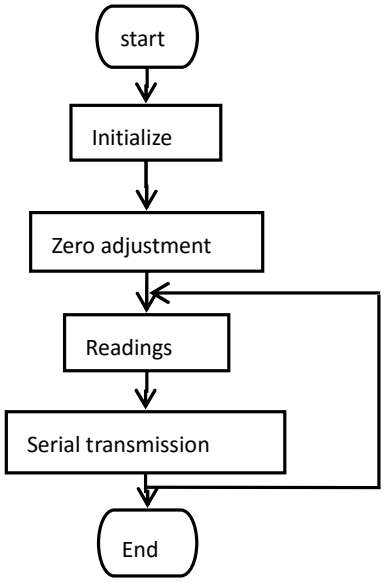

Fig.3 Program flowchart (SCM)

When bridges is working, zero balance bridge outputs are necessary, the traditional method is in constant pressure water supply increased on the bridge of a resistance larger of zero adjustment potentiometer, manual adjustments. But here we are using digital potentiometers in parallel in the form of automatic zero, auto-zero circuit as shown in Figure 4. It is mainly composed of R1~R4 strain resistance, resistance RP w, instrument amplifiers, Digital Potentiometers as well as microcontroller components. Bridge potential differences transmitted signal Digital Potentiometers to MCU, microcontroller determines whether the output voltage is zero voltage range specified, if there are deviations, through single-chip digital potentiometer for adjusting the output to meet the requirements[2]. Program flow chart as shown in Figure 6.

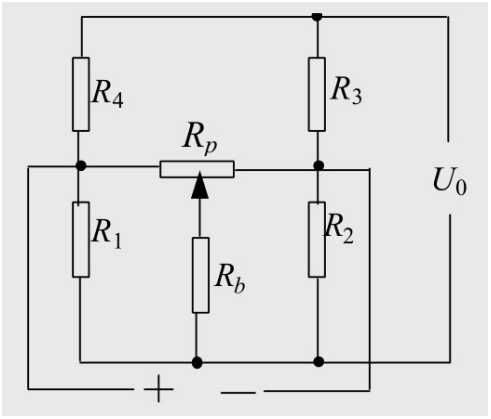

Fig.4 Zeroing circuit schematic diagram

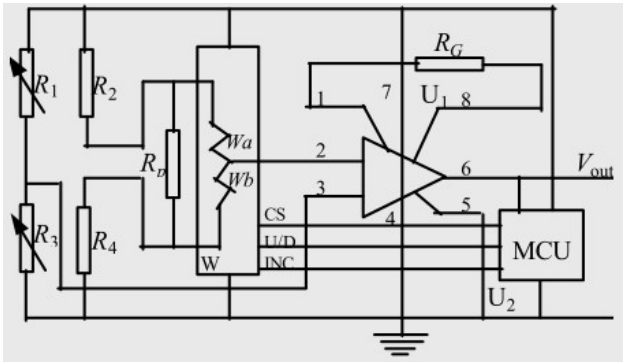

Fig.5 Zeroing circuit diagram[3]

Because of the special strain gauges work environment, bridge output that is orders of magnitude smaller, vulnerable to interference, and the change in temperature is another important factor. 18B20 we use electronic chips to compensate.

Using resistance strain gages consisting of small signal measurement circuits, the temperature when the temperature drift of interference factors that cannot be ignored. In order to minimize distortion caused by temperature measurement, 18B20 can be used to detect the ambient temperature after the measurement results for a certain amount of compensation. Advance on the resistance strain gage calibration; Strain gauges placed in incubators, incubator temperature balance, each record pressure and temperature signals. Adjust the temperature in the incubator can be measured throughout the temperature range under all selected points of pressure and temperature signals. Then prepare a temperature, linear error compensation procedures, by measuring the temperature, calculate the temperature area, and calculate the linear coefficient of pressure signal area. Calculate actual data point where the signal through the system. By computer calculations and processing, temperature compensated pressure signal error, zero temperature error[4].

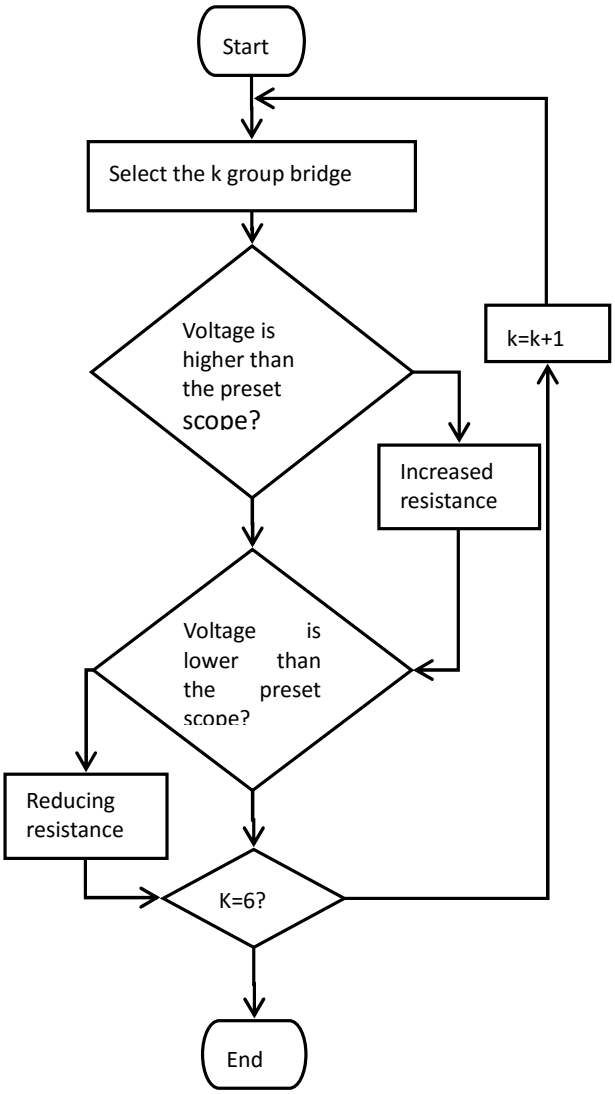

Fig.6 Zeroing procedure chart

Ⅳ DATA ANALYSIS

Table 1 output of the bridge

Times	1	2	3	4	5	6
output（mv）	1.415	1.416	1.415	1.449	1.442	1.439

Without zero before setting and temperature compensation, percussion having strain-gauge aluminum, the data as shown in the table 1. Available indicators of HX711 qualified for the requirements, can test out the materials due to the low frequency vibration and strain. But because of the strain gauges are use Scotch tape to paste, force transmission is not stable, So bridge output hysteresis exists.

In addition,In order to collect more accurate data,We set a shorter collection cycles,Therefore more data.Which valid data accounted for a small part, so late in the join filter in MATLAB may produce better results

Ⅴ CONCLUSION

Measurement of mechanical properties of rocks, bridges can input micro-strain amplifier and converted into electrical signals for us to use the computer for real-time analysis. This measuring device using temperature-compensated chips and Digital Potentiometers to eliminate errors and disturbances in the process, makes the process more stable and reliable. Of course, there will be more in the practical use of interfering factors, measurement accuracy and chip parameters, but practice shows that this device is more convenient, fast, intuitive, able to do real-time detection, we have produced a finished product and validate them with good results.

References

[1] Hou Deting. Wheatstone bridge to measure method and error analysis of resistance [j]. Experiment of College physics, 1996,03:45-48

[2] Ju Wenbin, Yu Hongfeng, Wu Yalin. Wide temperatur-e Piezoresistive sensor compensation of thermal sensitivity shift [j]. Sensor technology, 2002,05:43-45.

[3] Liu Guozhong, cardiology. Strain measurement circuit design of automatic zero setting [j]. Sensor world, 2003,09:15-17.

[4] Yin Fuyan. Temperature compensation of strain gauges and other [j]. Scales, 2009,09:40-44+53.

High Efficiency Portable Photovoltaic Solar Cell Phone Charger

Shuchao Song; Zhang Xue; Shenzhen Yang
（ *Instrumentation & Electrical Engineering Institute,Jilin University,Changchun,130021*）

Abstract: **In this paper, a high efficient solar charger for mobile phone is implemented, which can transform light energy into electricity by photovoltaic cells, and use the BUCK circuit to drop voltage amplitude to around 4.7 V. The electrical energy transformed by solar energy is alternated into stable dc voltage to charge the mobile phone. The value of input voltage, input current and output voltage are sampled by MSP430 microcomputer. The output voltage is controlled at the largest mobile phone charging voltage through the MPPT algorithm and PI algorithm. In addition, the maximum output power of the photovoltaic cell is tracked and the charging is more fast and efficient. The simulation and experimental results verify the feasibility of the charger and algorithms.**

Key words**: Solar mobile power supply Digital analog converter PI controller BUCK converter MPPT algorithm**

I.DIRECTION

WITH China's rapid economic development, population increase, rising living standards, people demand for energy is growing. Traditional energy sources such as oil, natural gas and coal, etc, with the steady growth of the future world energy consumption, one day will reach the limit. Therefore the development and use of renewable energy and green energy is important in order to achieve sustainable development. And solar energy is undoubtedly conform to the ideal of the strategy of sustainable development of green energy, the application of solar power has become the focus of world attention.[1] In this paper, A MPPT algorithm was used to optimize the monocrystalline silicon solar energy as energy input, the additional charges and related protection circuit and single-chip microcomputer control circuit of photovoltaic charger. Circuit has the advantages of 121 simple structure, overcurrent, overvoltage protection and charging efficiency higher characteristic can effectively prevent the battery because of sunshine duration of not are in the process of charging and discharging due to overcharge and deep discharge according to the cell loss.

II.SYSTEM DESIGN AND WORKING PRINCIPLE

System is divided into two parts: hardware design and software design. Hardware, MSP430 MCU minimum system module, power module, buck circuit, driving circuit module and sampling module five parts together to form a step-down voltage regulator circuit; software on the maximum power point tracking count method and digital PID control algorithm, the solar output power is transferred to the maximum and the output voltage is stable in the range of mobile phone rechargeable.

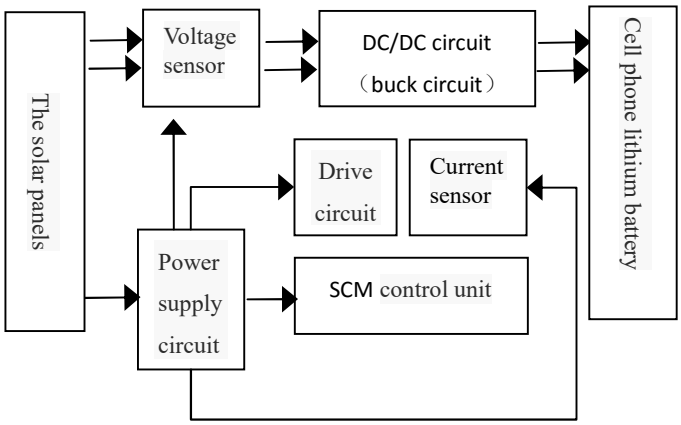

Fig.1. Block diagram of solar cell phone charger

III. HARDWARE DESIGN

A. MSP430 profile

MSP430 is TI company launched a series of ultra low power consumption microprocessor. Its remarkable characteristic is with ultra-low power consumption, there are five low power modes to choose from, wake up time is very short, just 6 US, also has powerful processing ability, high integration, embedded module rich (12 bit A/D conversion, the 16

bit timer, flash, etc)[2]. The charger adopts MSP430 series of MSP430F149 microcontroller as the main control chip, through the sampling circuit real-time acquisition of solar panels to the output voltage and current, and the battery charge state, by calculating the will In order to find the maximum output power of the battery plate and determine the state of charge of the rechargeable battery, it can also make the MCU enter the low power consumption mode, effectively reduce the system power consumption and enhance its efficiency.

B. Power Module

This module uses 16 pin LLP or etssop package single, dual output, buck regulator with fixed frequency 500kHzwide input range as the power chip, with 3-20V input voltage range, dual 2A output, the output voltage could be as low as 0.6V, with over current protection, thermal shutdown characteristics, used for set-top boxes, automobile, computer peripherals and industrial control field.[3] This module the LM26400Y and its peripheral circuit, was designed, which can output 5V and 3.3V voltage power supply circuit module at the same time, 430 and amplifier power supply and power circuit transmission The input voltage can be obtained directly from the solar panel, so that the single circuit can be characterized by a single power supply, as shown in Figure 2.

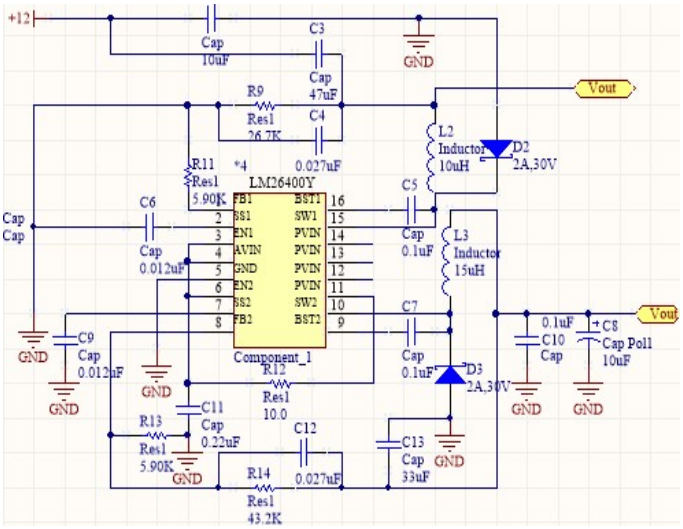

Fig.2. Power supply circuit

C. Buck Circuit Module

The figure 3 shows the buck circuit as the main charging circuit. The ST company launched a new fast recovery MOSFET transistor STW55NM60ND and Eiseth company launched a fast recovery epitaxial diode DSEI30-06A as a switch and fast recovery diode. Were taken and 150uF 15uH electric and capacitor composed a LC filter, inductance [6] capacitance calculation formula is as follows:

Filter inductance: $$L=\frac{(1-D)*U_O}{2*f_s*I_o}$$

Filter capacitor: $$C=\frac{U_o*(1\text{-}D)}{8*U_o*L*f^2}$$

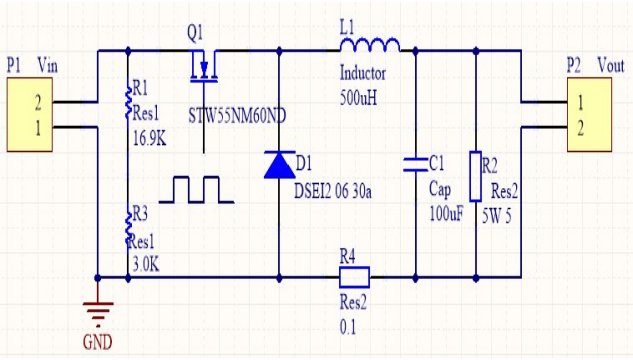

Fig.3. BUCK main circuit

D. Drive circuit module

This module uses the optocoupler isolation chip (tlp250) and its peripheral circuits constitute. Driving circuit and output voltage characteristic curve as shown in Figure 4,5 and tlp250 is Japan's largest semiconductor maker Toshiba launched, with isolation voltage: 2500Vrms, one-way channel, output current: 1.5A and DC input characteristics.BUCK main circuit using pulse width modulation (PWM) control the charging current, the drive pulse width of the PWM signal amplifying circuit after the increase or decrease to change the size of the charge current.[4]

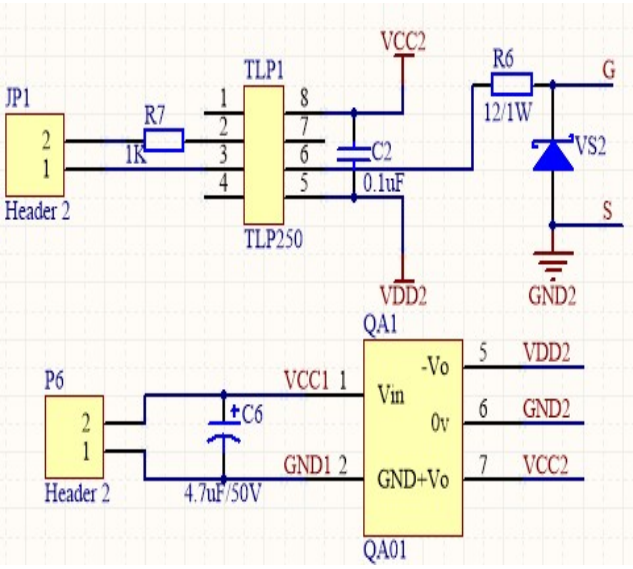

Fig.4. The driving circuit of TLP250

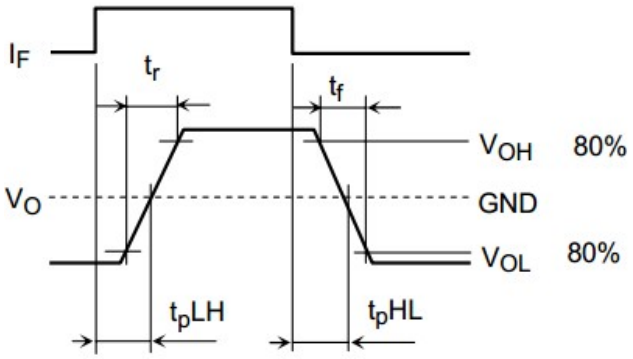

Fig.5. Output voltage characteristic curve of TLP250

E.Sampling module

This module uses the acs712 current sensor module and its peripheral circuit, to detect the current in the system. By converting the current signal into a voltage signal, access the MSP430 and realize A/D conversion. Specific conversion formula for

Sampling of the voltage signal is based on the voltage on both sides of the series sampling resistance, and according to the proportion of acquisition voltage through the following circuit to the microcontroller to collect.

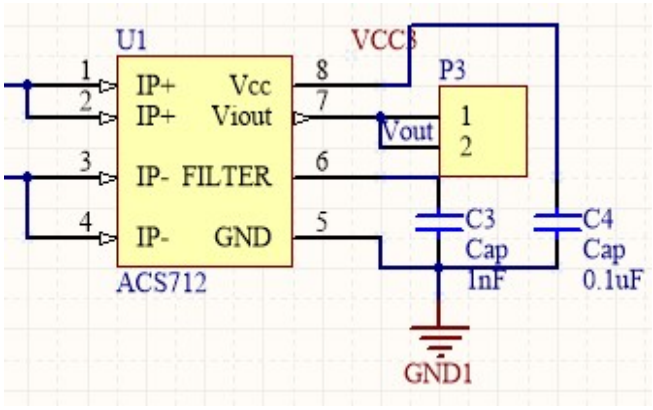

Fig.6. Sampling module circuit

IV. SOFTWARE DESIGN

A. MPPT: maximum power point tracking

Output characteristics of 3.1.1 solar cellsThe output characteristics of the solar cell is a nonlinear, but also by the light intensity and temperature effects, such as shown in Figure 7, solar battery at any time there are a maximum power output, and with the light intensity and temperature changes and changes. In order to make solar battery in the power supply system give full play to its photoelectric conversion ability, on the need to control the operating point of the solar cells to obtain maximum power output.

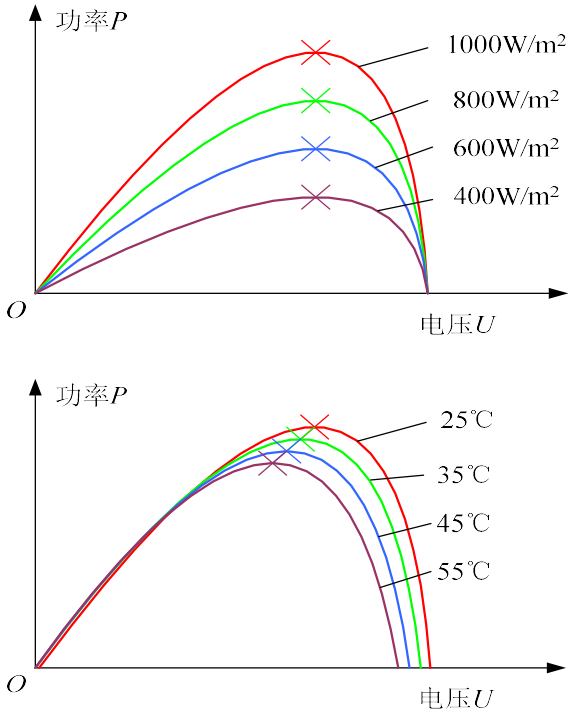

Fig. 7. Power output curve

At present, there are three kinds of MPPT control methods: fixed voltage method (CV), perturb and observe (PO) method, incremental conductance method (IC) and fuzzy logic control method etc. Is the most commonly used method of Po. Every certain time through changing the PWM wave accounted for empty than disturbance voltage output or PWM+blank PWM-blank and in real time sampling the output voltage and current of the solar panels calculated corresponding to an output power PI and then compared with the pre disturbance power (PB), according to the power variation is decided after the disturbance direction when Pi>Pb to adjusted according to PWM+blank; when Pi<Pb is adjusted according to the direction of the PWM-Pb. Step is according to the direction of the maximum power point gradually narrow. This will ensure the output power of the solar panels to increase in the direction of change, so repeated disturbance, measurement and comparison, as to realize the maximum power point tracking.[5]

Because of the disturbance observation method of the MPPT algorithm in the actual operation may be due to the disturbance frequency is too large to large power oscillation, so in the MPPT system, voltage and current sampling precision is very important. Hardware we first use the MSP430 series of 149 microcontroller based on voltage and current sampling, the software we use statistical methods to realize sampling

interference. The flow chart of the algorithm as shown in Figure 8.

Before reading the current value of the voltage, the following processing: the average value of the collected data, excluding the difference between the average value of the data, and then the average value.

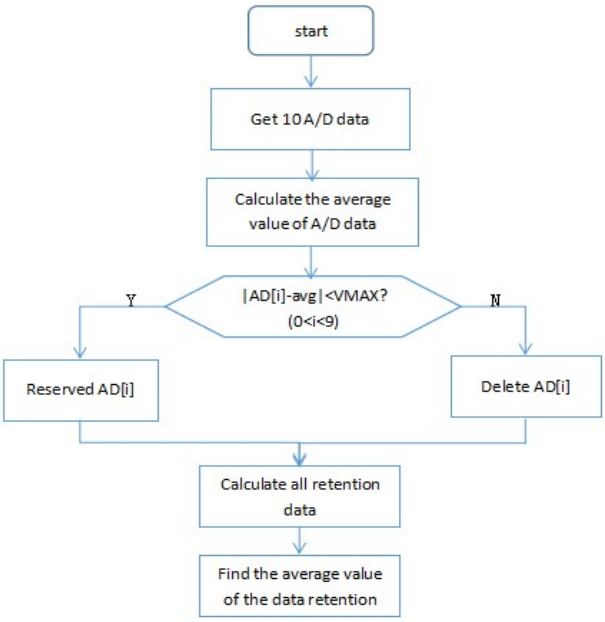

Fig.8. The data acquisition flow chart of MPPT

B. Digital PI control Basic principles of PI

1) The basic principle

PI regulator is a linear controller, it is based on a given value R (T) and the actual output value C (T) constitute the control deviation

$$e(t) = r(t) - c(t)$$

The deviation ratio (P) and integral (I) are controlled by the linear combination of the control object.

$$u(t) = K_p[e(t) + \frac{1}{T_I}\int_0^t e(t)dt]$$

Among them U (T) for the output of the PI controller, e (T) for the input of the PI regulator, Kp for the ratio coefficient, Ti for the integral time constant.

2) Discretization

Due to the control of the microcontroller is a sampling control, it can only according to the sampling time error value calculation amount control. Therefore, it is necessary to of type is discretized by a series of sampling time point K represents the continuous time t, discrete PI control algorithm expression is:

$$\Delta u(k) = u(k) - u(k-1) = K_p[e(k) - e(k-1)] + K_i e(k)$$

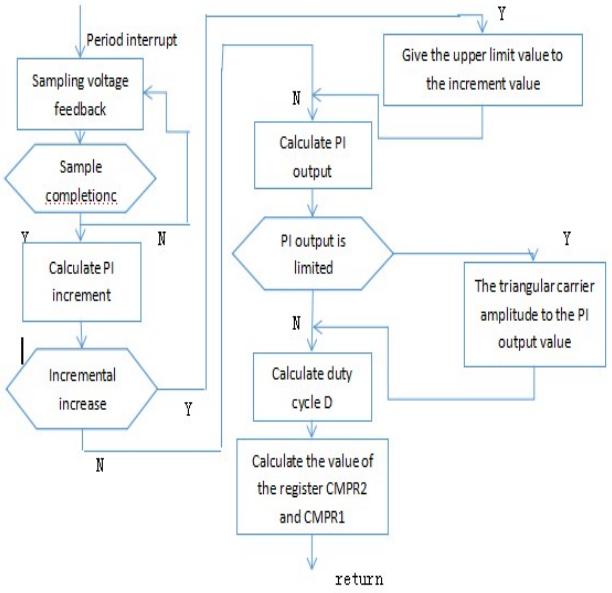

Fig. 9. Flow chart of PI control

C. Practical application of PI algorithm

In this paper, the digital PI regulator, to adjust the buck circuit output voltage. Uses PI regulator for real time and measuring the current in the circuit. Specific ways for: from the main circuit, the current sampling, conversion voltage and magnified and transported to 430 singlechip, and the ad program transforms analog quantity into digital quantity data, and carries on the judgment, at this time if the current is too large, the PI regulator off; if in the normal range will be the current default values are compared. The error of PI algorithm adjusted, output voltage leaping out of the maximum limit, the output duty ratio equal to 90%, namely cmpr2=u0 =cmpr1*90%; if the output voltage leaping out of the minimum limit, the output duty ratio is equal to 10%, that is cmpr2=u0=cmpr1*10%.PI output voltage value as the duty ratio adjustment to 430 SCM outputs are accounted for empty than to the switch tube, thus changing the circuit voltage. Schematic diagram as follows:

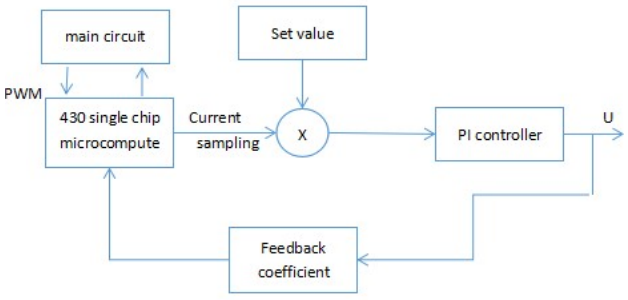

Fig.10. PI algorithm implementation principle diagram

D.Simulation on Line

To the charging system modeling and a series of simulation using Matlab/Simulink components, circuit diagram is as shown in the following image, shown in the discrete sampling time, combined with POWERGUI to simulation of the model, optimized the parameters of the PI controller, in several tests obtained under ideal waveform.

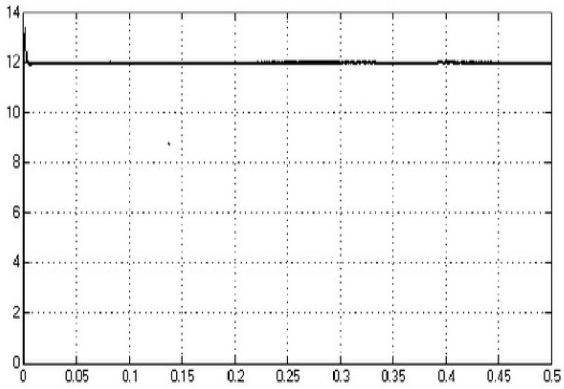

Fig11. Output voltage waveform under PI control controlling

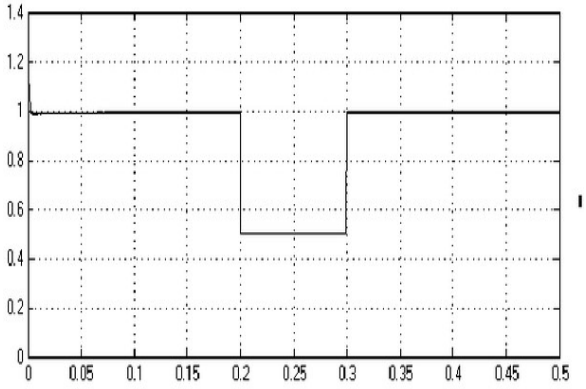

Fig. 12. Output current waveform under PI controlFig

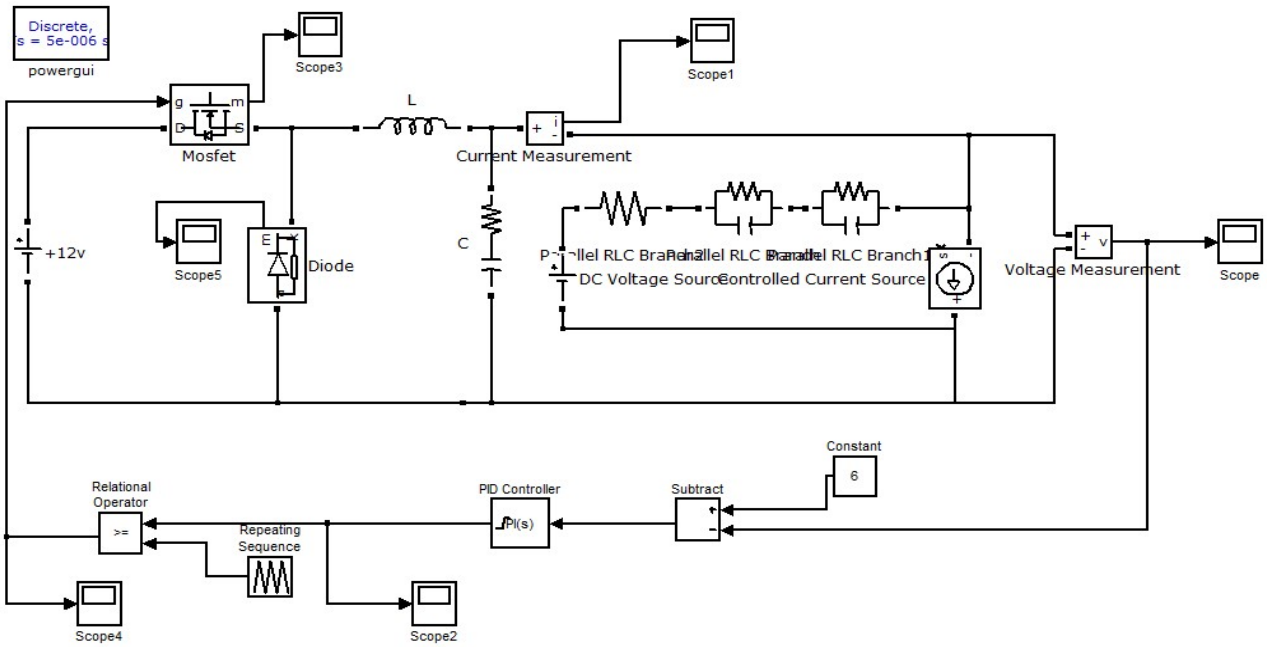

Fig.13. System simulation model

V. COMPARISON AND ANALYSIS OF EXPERIMENTAL RESULTS

A.Implementation of digital PI control

In each specific light illumination conditions, board testing system to stabilize the charging voltage of the maximum value, and the output voltage stable near the set point, without static error adjustment. (best picture)

Artificially given output voltage setting value, and in accordance with the step increase or decrease set, after measuring, using 10 lamp 220V, 60W incandescent lamp to illuminate the solar battery board, to achieve the maximum stable voltage 5.2v. At this time, the PWM air ratio is about 33%; if off two lamps with incandescent lamp, the maximum voltage stability will be dropped to 4.4V.

B.Implementation of MPPT algorithm

In the test methods mentioned above, each light illumination conditions, the maximum power point tracking algorithm can achieve solar panels under specific conditions output maximum power. Using the perturbation and observation method, depending on the direction of the maximum power point determines the output voltage change, change the output voltage setting, followed by the use of PI regulator output voltage follow to set the value. In the measurement process, the specific light illumination conditions, the MPPT algorithm to realize the system automatically adjusts the output voltage maximum to achieve maximum power output.

Cc. To achieve the charging of mobile phone charger

The system output voltage is maintained in the range of 4.5V~5.2V, the charge current is maintained at about 0.4~0.7A, can realize the specification is 4.2V, 5Wh mobile phone lithium battery fast charge.

D. On the problem of charging efficiency

The charge efficiency is the ratio of the output power of the system and the output power of the solar panels, the LCD screen is used to display the input power of the solar panel, and the output power of the output is displayed.

The following is the two test data and conclusions:

Test time: September 5, 2015 afternoon 2:00 tester: Zhang Xue Song Shuchao test instrument: oscilloscope, MSP430F149 (AD12 sampling).

Data 1:

TABLE 1

TEST DATA 1

	Vin (V)	Iin (A)	Vout (V)	Iout (A)	Pin (W)	Pout (W)	η (%)
Oscilloscope1	12.38	0.538	5.145	1.129	6.66	5.81	87.34%
sampling1	12.4	0.53	5.2	1.1	6.57	5.72	87.3%
Oscilloscope2	12.87	0.542	5.205	1.158	6.98	6.03	86.44%
sampling2	12.8	0.54	5.2	1.15	6.92	5.98	86.5%
Oscilloscope3	11.99	0.563	4.955	1.209	6.75	5.99	88.81%
sampling3	12	0.55	4.9	1.2	6.6	5.88	88.8%
Oscilloscope4	12.05	0.587	5.01	1.257	7.07	6.3	89.04%
sampling4	12	0.58	5	1.25	6.96	6.25	89%
Oscilloscope5	12.46	0.512	4.88	1.113	6.38	5.43	85.03%
sampling5	12.5	0.51	4.9	1.1	6.37	5.39	85%

Test time: September 6, 2015 morning 11:00 tester: Zhang Xue Yang Shenzhen Song Shuchao test instrument: oscilloscope, MSP430F149 (AD12 sampling)

Data 2:

TABLE 2

TEST DATA 2

	Vin (V)	Iin(A)	Vout (V)	Iout (A)	Pin (W)	Pout (W)	η(%)
Oscilloscope1	11.28	0.512	4.83	0.985	5.78	4.76	82.28%
sampling1	11.3	0.52	4.8	1.02	5.87	4.89	83%
Oscilloscope2	11.04	0.576	4.72	1.106	6.36	5.22	82.04%
sampling2	11	0.57	4.7	1.1	6.3	5.17	82%
Oscilloscope3	10.96	0.567	4.58	1.109	6.22	5.08	81.67%
sampling3	11	0.56	4.6	1.11	6.23	5.1	81.7%
Oscilloscope4	10.56	0.58	4.32	1.1	6.125	4.75	77.55%
sampling4	10.6	0.57	4.3	1.1	6.06	4.73	77.6%
Oscilloscope5	11.58	0.553	4.95	1.078	6.4	5.34	83.42%
sampling5	11.6	0.56	5	1.1	6.55	5.5	83.4%

Comparison of two experimental data:

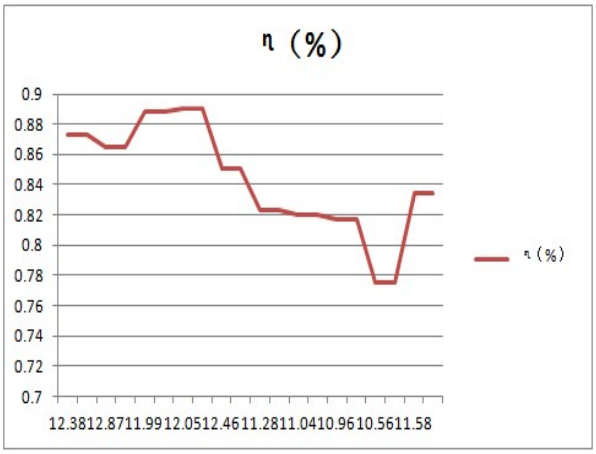

Fig.14. Test data comparison chart

The following conclusions can be drawn from the above data: When the input voltage is about 12V, the conversion efficiency of the main circuit can reach 90%, the average efficiency is 84.4%, the input voltage is 10-13V, the output voltage is 4.5-5.2V, the output current 0.8-1.2A, can give the phone fast charge.

VI .CONCLUSION

Using MSP430F149 microcontroller as the main

control unit, combined with other chips and circuit is composed of a solar cell phone charger, the PWM output voltage, which has the advantages of flexible control, strong carrying capacity, stability, with characteristics of self adjustment ability, can automatically find the maximum power point of solar panels, to improve the conversion efficiency of the charger.

References

[1] Liu Wenji, Dong Ruiqing, Liang Mengzhuo. Global solar photovoltaic industry development and China's Countermeasures [J]. global scientific and technological economic outlook, 2011,26 (12)2

[2] Shi Wenhua. Research on high efficiency solar cells [J]. Journal of Chongqing Academy of Arts and Sciences (NATURAL SCIENCE), Vol.30, No.06, Dec., 2011

[3] Li Ming Huang, even Yong Sheng, Chen Biaolong. Based on perturbation method was used to observe MPPT control optimization strategy. Modern electronic technique, Vol.34, No.24, 2011, 12 (15)

[4] Zhu Xianzhong, Xu Bin, Yang Qi, Zhang Zhou I, Joan. The circuit design of [J]. electronic world solar mobile phone charger, 2012,11

[5] Zhang Xing, Zhang Chongwei, Sun Benxin. Research on the grid connected inverter based on the MPPT PV array with current optimization [J]. Journal of solar energy, Vol.122, No.13, July, 2001

[6] Kang Huaguang. Foundation of electronic technology [M]. Beijing: Higher Education Press, 2005

Research and Manufacture of Remote Control Intelligent Power Supply

Qiao Donghao; Wang Nan; Chu Shiying
(College of Instrumentation and Electrical Engineering, Jilin University,Changchun 130026,China)

***Abstract*--This design is based on the MSP430 microcontroller remote control intelligent power supply. The hardware design of the system includes a battery charge / discharge module, a voltage conversion module, an overcurrent protection module, an alarm module, a LCD liquid crystal display module and a keyboard control module. The output voltage value of the system can be continuously adjusted from 0V to 20V and the step value is 0.1V. In software design, the MCU program is written in C language and the upper computer program is developed in Visual Basic 6.0. The experimental results showed that the system can not only well realize serial communication between the upper computer and the MCU, but also achieve the purpose of accurate data exchange. We transmit data by using an USB data line to connect the hardware circuit and the upper computer. The advantages of this system are low cost, high reliability, simple and convenient operation. We connected the upper computer with the MCU and as a result, the system was able to supply power in a remote and intelligent way.**

***Key words*--long-distance intelligence storage battery man-machine interaction**

I. INTRODUCTION

NOWADAYS people greatly enjoy the convenience of electronics, but all electronic devices have a common power supply circuit. With the development of science and technology, electronics are now widely used in various daily routines, scientific research as well as fields of academics. Power is an essential energy supply when it comes to electronic components, research and development on power has made indisputable contributions to the development and promotion of new technologies and equipment. Today, an increasing number of people have more than one electronic device, and companies keep come out with more and more devices in all shapes and sizes. Each device has its own method of power supply, therefore significant problems have arisen when we charge our devices. Furthermore, battery life and its safety is no longer guaranteed[1].

II. MEANING OF REASERCH

With the rapid development of electronic sector, supplying power and charging devices has penetrated into all walks of life, bringing mankind great market opportunities while at the same time imposing challenges to the power market. High market opportunities lead to high demand, as a result, new requirements for the power supply have been requested and companies have no choice but to implement them. Equipment that provide power to electronic devices should be highly reliable and easy to control. Now, along with the rapid development of the DC power supply technique, the rectification system has broken away from its previous discrete components and integrate circuit control to evolve into microcomputer control. The result of its evolution succeed in making the DC power intelligent, capable of remote monitoring and alarm functions, so as DC power could function without human attendance.

Generally, the voltage source is either at a fixed or a limited number of voltage values, making it hard to achieve universality. Common DC power supplies adjust the output voltage by first adjusting the output sampling resistor branch in the potentiometer. The resistance of the potentiometer changes in a nonlinear matter with a narrow range of adjustment, stopping the common DC power supplies from gaining a precise output voltage adjustment. In addition, most DC power supplies have a knob switch that enables voltage adjustment, yet these switches not only have low accuracy, they are also very complicated to use.

We've integrated two different technologies: the digital control technology of single chip microcomputers and the remote control technology of the host computer, designing a cost-effective remote control and intelligent power supply. The circuit can be

adjusted simply by clicking a button, and the step value of the adjustment increases by an increment of 0.1V, eliminating possible inaccurate voltage adjustment for different electronic devices. In addition, the host computer can set the output voltage, simplifying the process of voltage adjustment. There is an LCD screen on the power supply that enables users to observe the output voltage and current simultaneously, ensuring users that the output voltage is safe and stable. The device is also intelligently managed and able to effectively overcome the disadvantages of that traditional power supplies possess. It can also charge electronics such as cellphones, computers and other small devices that require power. We've made a machine that has multiple uses: the device has a safety monitoring function that can be observed real-time through a computer. When the numbers do not meet the safety regulations, an automatic alarm system will sound and cut off power supply immediately. The device can bring much convenience to users while at the same time reducing emission, protecting the environment and ultimately contributing to the advancement of science and technology in our era[1].

As we advance forward in time we have seen social progress, science and technological development as well as an advancement and improvement of people's living standards and quality of life[2]. Therefore, researching and designing a high performance, efficient and intelligent power supply device is more than essential, so as to meet the needs of the people of the 21st century.

III. IMPLEMENTATION PLAN

A. The research ideas and methods

The hardware design of the system includes a battery charge / discharge module, a voltage conversion module, an overcurrent protection module, an alarm module, a LCD liquid crystal display module and a keyboard control module. The output voltage value of the system can be continuously adjusted from 0V to 20V, with the step value at 0.1V. The battery posses the function to prevent overcharge, and it can be charged with a 220V charger. When the battery discharges, its output voltage is at 24V, which then converts into 0-20V after passing through the voltage conversion module. By clicking the buttons on the device we can adjust the output voltage that has a step value of 0.1V. precisely so that it can adapt to the electronic device in use. The liquid crystal display module's function is to display the output voltage and current. If the output current is too large, if the power consumption is less than 15% or if the circuit is malfunctioning, an alarm will sound automatically.

This circuit uses the MSP430 single chip microcomputer as the motherboard that controls every part of the device while maintaining the normal operation of the system[3],[4]. The MSP430 single chip has strong processing abilities, a fast computing speed, low power consumption and as well as other advantages[5]. This design also has a remote monitoring module, which can connect the battery to a computer using an USB data line or wireless internet. We use VB to design an upper computer interface on the computer so as to to display battery output voltage, current, charge / discharge time and cell loss. The interface can also control the battery output voltage and operation of the charge / discharge and system. The block diagram of the system is shown in figure 1.

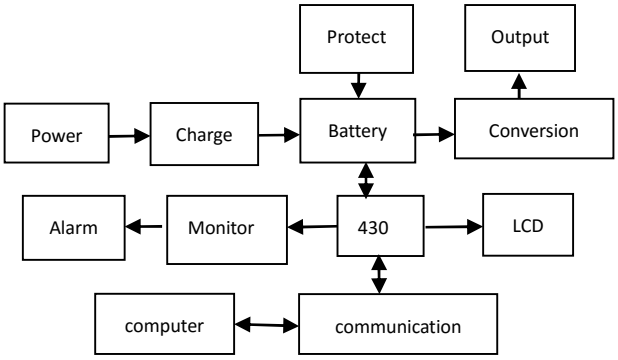

Figure1 System Block Diagram

B. The main module, implementation plans and technology roadmap

The battery charge/discharge module charges using a 220V battery, and if the battery is being charge with a high current and the voltage reaches its supper limit, a silicon tube will conduct and offset the battery so that it will emit a smaller and more allowable charge. The data communication module transmits data back and forth the MCU and the upper computer using a USB date line.

The computer monitoring module first receives the information transmitted by the USB, then displays and saves the relevant data onto the computer, finally processing the data and analyzing it. The computer can

also control battery charge/discharge, the battery's system of operation as well as its output voltage.

The voltage conversion module converts the initial battery output voltage of 24V into a continuous voltage that adjusts between 0-20V so as to meet the needs of different charging devices. The power supply module uses a 24V regulator as a 7824 chip, and if the preceding output power supply shows fluctuations, it will have no negative effects on the latter half of the output because there is a self-regulating chip. When battery is less than 15%, or the battery is faulty, the alarm module will sound. The alarm function is locked when device is charging.

The MSP430 basic circuit module connects a MCU to a crystal oscillator and reset circuit, finally connecting the whole thing to a power supply and the ground. The monitoring module will reset the system when it breaks down, and it will also monitor whether or not the microprocessor is functioning normally. If there are problems such as a system crash, the monitoring module will generate a reset pulse that will effectively reset the system so it restores to normal operation. The LCD module receives and displays data sent by the MCU, and the circuit protection module prevents the battery from overvoltage, over-current and short circuits[2],[6]. The MSP430 peripheral circuit is shown in figure 2.

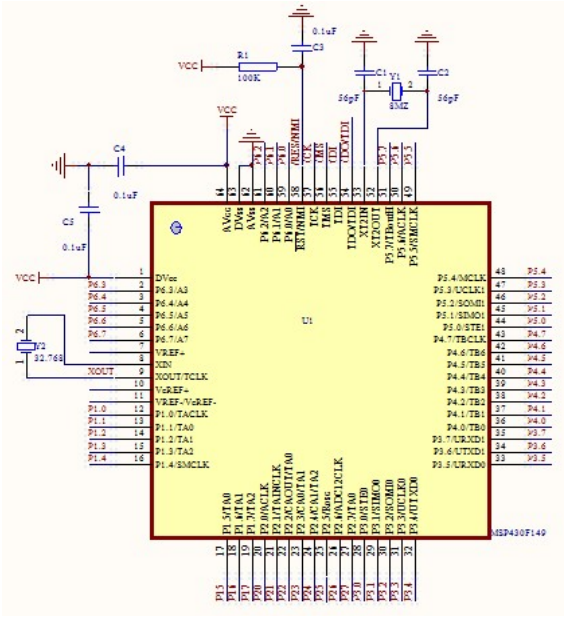

Figure2 MSP430 Peripheral Circuit

IV. CIRCUIT COMPARES

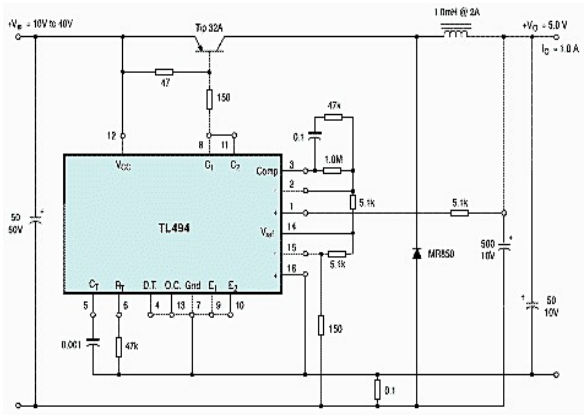

Figure3 Switch Power Supply Circuit Diagram

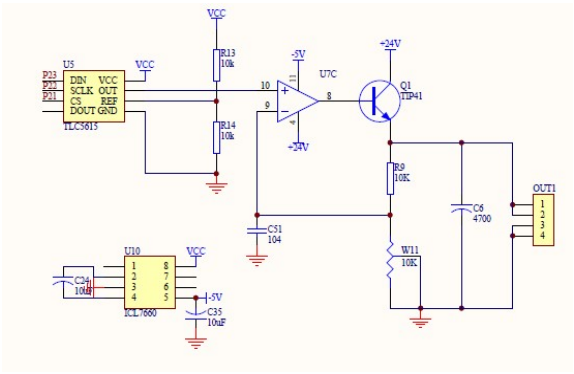

Figure4 Linear Power Supply Circuit Diagram

Figure 3 is a TL494 with a built-in reference voltage source of 5V, it uses pulse regulation to control output voltage[1]. The device is highly efficient, yet in reality difficult for it to be adjusted to 0V. However, as shown in figure 3, TLC5615 can convert digital signals into analog. After comparing the analog signal output using a comparator an output voltage is produced. The circuit is simple and easily achieved. The ripples are small and within controllable range. Thus shown in figure 4, selection of the DA model resulted in the active control of the circuit's output voltage[7].

V. FUNCTIONS IMPLEMENTED

A. Basic Functions

The output voltage value of the system can be continuously adjusted from 0V to 20V with the step value at 0.1V. We can adjust the output voltage by the pressing the keys on the device, making usage more convenient and data more accurate for various types of electronics. The output voltage and current will display on the LCD screen. As shown in figure 5, the device can also charge cellphones, computers and other small electronics, ultimately achieving multifunction. The device also has alarm function that detects over-current, making the system safer and more reliable. The use of

serial data lines connects the hardware circuit to the upper computer, which displays the output voltage and power supply[8]. The output voltage can be conveniently set on the upper computer. This system can also be controlled remotely, so as to bring convenience to people' lives

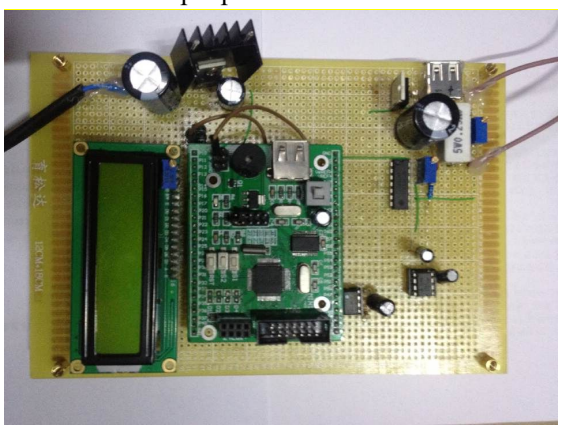

Figure 5 Hardware Circuit

B. Project innovation

-- alarm sounds when overvoltage and overcurrent occurs

-- an upper computer that displays and controls the output voltage and current.

-- use of a USB data line to connect the hardware circuit and the upper computer in order to achieve remote control

--Fourth, continuously adjustable voltage with a step value of 0.1V. This facilitates the accurate matching of various small electronics.

Ⅵ. Software Function of Remote Measurement

Comparing to other similar products in the market this product has it own characteristics, it has the function of remote upper computer control. The maintenance and adjustment of other similar products require staff to the power supply. If a larger range measurement in the field, when the output voltage value needs to be adjusted, back and forth measuring will increase staff's workload and waste them a lot of time. The power supply can provide voltage of 0-20V to the experimental equipments from a long distance and remote setting of the output voltage, greatly reducing the power user's workload, improve work efficiency. This product can also be used as a backup power supply for cars. For the vehicles which will travel for a long-distance, the power supply can not only provide 12V as the vehicle power, but also for people's mobile phones, computers and other electronic communications equipment to charge, so that it provide convenience for travel. Upper computer interface displays the current output current and voltage, users can set the output voltage on the upper computer, it is very convenient and quick. The upper computer interface is shown in figure 6[9].

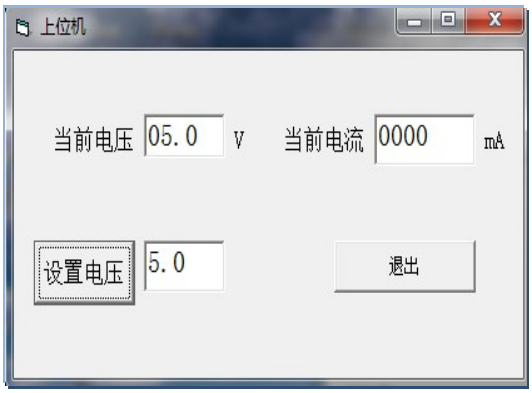

Figure6 Upper Computer Interface

```
void PutString(uchar *ptr)
{
        uchar i;
        for(i=0;i<9;i++)
        {
                while (!(IFG1 & UTXIFG0));
// TX buffer empty?
                TXBUF0 = *ptr++;
 // send data
        }
}
 ptr[1]=vout/100+'0';
          ptr[2]=vout%100/10+'0';
          ptr[3]='.';
          ptr[4]=vout%10+'0';
          ptr[5]=Curr_Volt/1000+'0';
          ptr[6]=Curr_Volt%1000/100+'0';
          ptr[7]=Curr_Volt%100/10+'0';
          ptr[8]=Curr_Volt%10+'0';
ck++;if(ck>5){ck=0;PutString(ptr);}
                    //send data to pc
```

Table1 Data Format

Start	D0	D1	… …	D6	D7	Stop

Start—Start bit

D0 ～ D7—8 bit data

Stop—Stop bit

A. Transport Protocol

--First, baud rate: the microcontroller need tocalculate the value of the UART register according to the use of

the system clock frequency Rate (fosc), combined with the selected communication baud rate, the result is 9600.In order to ensure the accuracy of data transmission, the communication band rate of upper computer COM port must also be set the same value as the rate of microcontroller.

--Second, data format: data format consists of 1 start bit, 8 data bits, no parity, 1 stop bit, as shown in table 1.

The standard values of the data bits are 5, 7, and 8 bits, depending on the information that is required to be delivered when the system is designed. For example, the standard ASCII code is 0 to 127 (7 bits), the extension of the ASCII code is 0 ~ 255 (8 bit). The stop bit is used to indicate the last bit of a single package, typically 1, 1.5, and 2 bits. Since the data is timed on the transmission line, and each device has its own clock, it is possible in the communication between the two devices appeared a little bit of synchronization. So stop bits are not just the end of the transmission, but also provide the opportunity for the system to correct the clock synchronization. Parity bits in the serial communication is only a simple way of checking, can not be considered[8],[10].

B. Software Flow Chart(As shown in diagram1)

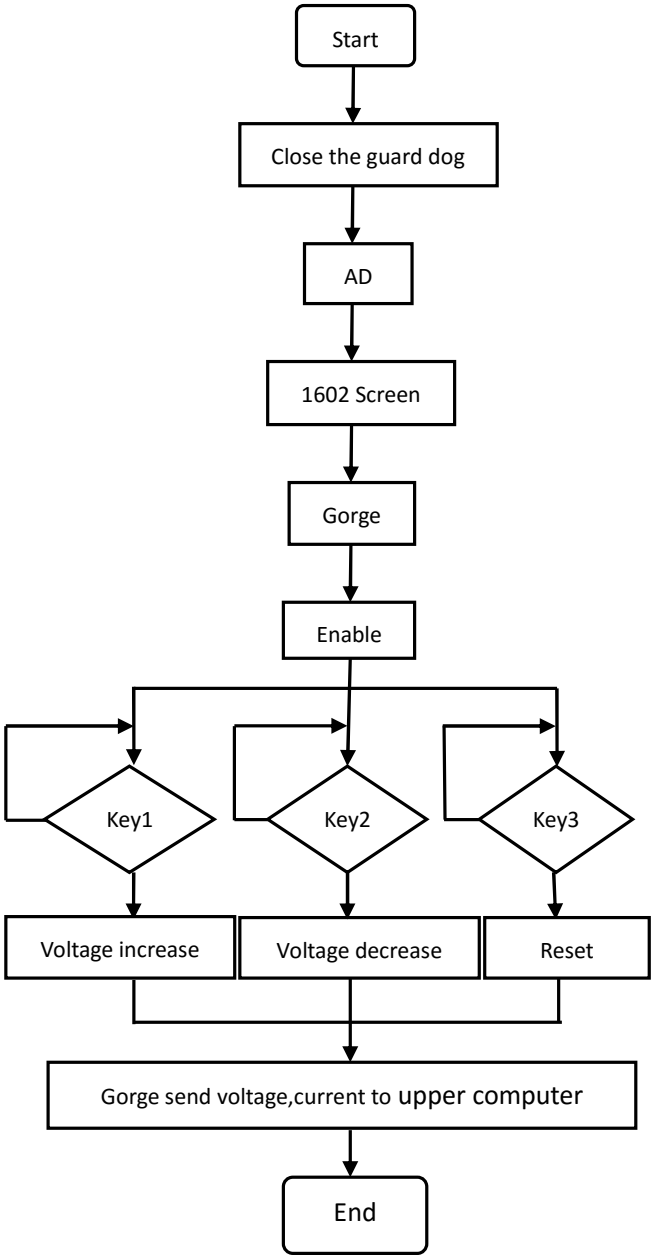

Figure 7 Software Flow Chart

Figure 8 is a curve diagram indicating the calculated test results of voltage error. We can see from this diagram that within 0-20V, error is small with no load, output errors are more stable than no load and when the load is small the overall results are better than that of a big load.

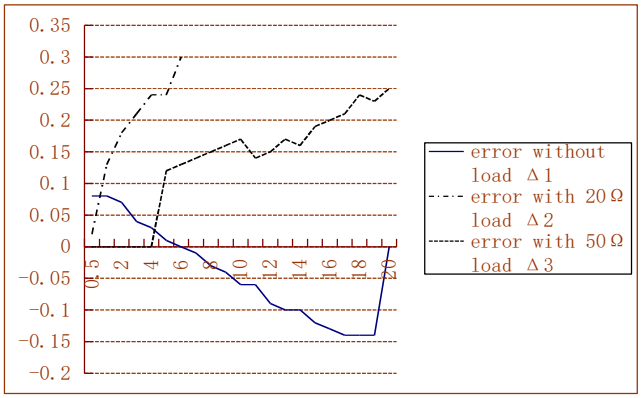

Figure8 Output-voltage Error

Ⅶ.Test Result

Data in table 2 is the technical index of the remote control power supply acquired through tests

Table2 Technical Indicators

Maximum current	500mA
Ripple wave（output voltage=5V，load=20Ω、5W）	5mV
Maximum power	6859.8mW
Maximum efficiency(20Ω)	76%
Maximum efficiency(50Ω)	77.6%
Range of ouput voltage	0~21v
Voltage regulation factor（20Ω）	Sv=89.7%
Current regulation factor（20Ω）	SI=83.3%

Ⅷ. Conclusion

This design has met the desired standards and requirements of design. We have invented a device that can regulate voltage between 0-20V, a device that has a maximum current of 50mA and a maximum efficient greater that 75%. The device is a handy charging machine that is convenient for both indoors and outdoors. The battery has found solutions to the problems that cellphones, tablets, laptops, chargeable lamps as well as other electronics have when charging. Compared to similar devices on the market, ours have an additional remote control capacity, making it more reliable and easily accessed. Users of the device are able to observe output voltage and current, control the battery, as a result greatly facilitating users themselves. We have also taken a stride in the aspect of power control. However, among other defects, the range of control is limited by the length of the USB cord. In the future, we can add Bluetooth to the power supply and computer so as to make communication simpler and more convenient while increasing range of communication.

References

[1] Xianxing Liu.New Type of Intelligent Switch Power Technology.China Machine Press,Sep,2012.

[2] Daqian Fang,Qiaowei Bao.Practical Power Supply And Protection Circuit.People Post Press,Feb,2003.

[3] Hailong Jin,Cong Li.C Language and Program Design. Beijing Science and Technology Press,1st,Aug,2012.

[4] Dake,Hu.Principle And Application of MSP430 Series Ultra Low Power 16-bit Singlechip Microcomputer.Beijing University of Aeronautics and Astronautics Press,Jun,2000.

[5] Qiao He,Qiangming Duan,Chunling Qiu.Principe And Applications of Singlechip.China Railway Publishing House,1st,Jan,2008.

[6] Linxing Zhang,Huaizhu Zhang.The Experiment Instruction Assembly.Jilin University Press,2011.

[7] Numerical control dc current source design based on MSP430 single chip Microcomputer. http://wenku.baidu.com/view/cd0bb304e87101f69e319554.html

[8] Yanbin Yang. Technical of Data Communications. Beijing University of Posts And Telecommun- -ications,2009.

[9] Zhuoran Lin.VB Language Program Design.Electronic Industry Press,Jan,2009.

[10] Huizhong Wang,Qiang Wang.Microcomputer Principle and Interface Technology.China Machine Press,Aug,2010.

Portable air humidifier based on the two-wheel self-balanced vehicle

Wang Hao; Guo Ying jie; Li Jia
(Jilin university instrument science and engineering institute,changchun,130021)

***Abstract*--The ordinary air humidifier humidification scope is limited, and it can't adjust the indoor humidity. Portable air humidifier of the two-wheel self-balanced vehicle can move to indoor humidifying. It uses single-chip microcomputer control technology and PID control for the entire indoor humidity balance, and it can monitor the indoor humidity.**

***Key words*--Two-wheel self-balanced vehicle Air humidifier**

I. INTRODUCTION

THE climate is very dry, and the air humidity is small. It not only made people uncomfortable, also had some bacteria and germs multiply and spread. Test showed that it should be controlled in45% ~ 60%. And the current commercially available air humidifier can't achieve this range accurately. It also can not reach uniform indoor humidifying. Two-wheel self-balanced vehicle has flexible, intelligent control and the advantages of simple operation. It applies to run within the narrow space, and it has good prospects for development. It support the development and utilization of later. Therefore, this project is portable air humidifier based on the two-wheel self-balanced vehicle[1-3]. It can be movably uniform on indoor humidifying, and realize the balance of the indoor temperature. In the office without air conditioning, especially the bedroom environment, mobile air humidifier is very practical.

II. PROJECT INTRODUCTION

The project design of the portable air humidifier with the single chip processor as the master control chip. Installed on the body of the gyroscope (gyro output value is relatively sensitive shaft angular rate, the angular rate of time integral can get around the sensitive axis rotation Angle values) and acceleration sensor real-time acquisition data, and transmit to the master controller main controller for kalman filtering and balancing algorithm processing. Then it attitudes adjustment needed for the wheel acceleration value, conversion for motor control. Through a serial port sent to the servo controller, and two routing control servo drive of servo motor encoder of posture adjustment is installed on the wheel to get the actual speed [4] and run distance. It feedbacks back to the main controller, through the PID algorithm[5] adjusted again for error control quantity is sent to the servo controller, forming a closed loop feedback constant adjustment and the whole system can maintain the balance of the car, through the acquisition of temperature and humidity, air temperature and humidity information to humidity information transmission to master control chip, humidifier for fuzzy control and PID control to adjust the humidity to specify humidity; Master control chip by ultrasonic sensor control motor, returned to the car in indoor automatic obstacle avoidance, and use the humidity information collection back to make cars tend to be low humidity area.

III. THE SYSTEM STRUCTURE

The circuit design of the whole system includes MCU module, automatic humidification module, temperature module, obstacle avoidance module, balancing module, voltage regulator module. System structure diagram is shown in Figure 1.

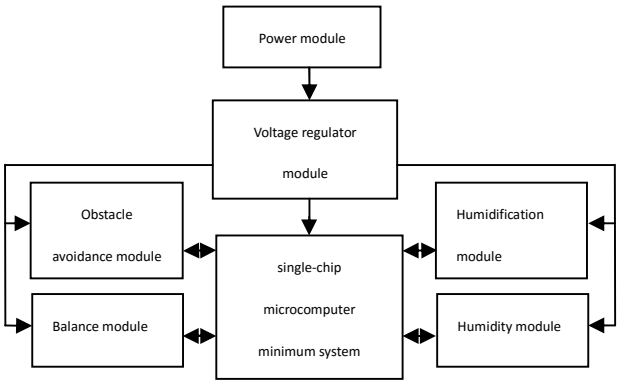

Fig.1 System structure block diagram

IV. STRUCTURE MODULE

A. Voltage Regulator Module

Use 3 section 3.7 V lithium batteries. For single chip microcomputer minimum system, need to provide the stability of the 5 V power supply, as the linearity LM2940 voltage stability is very good, so choose LM2940-5 single on the power supply. LM2596-5 conversion efficiency is high, the load capacity is big, but the disadvantage is that the ripple voltage is big, not suitable for single chip power supply, while other modules need by large current, to other modules to make sure that the power charging power supply.

B. MCU Module

Use STM32F103C8T6 single-chip microcomputer[6] as main control chip. the microcontroller architecture includes Cortex-M3 CPU, 20 KB RAM, 12 road PWM output, working voltage is 2.0 ~ 3.6V, 64KB storage space, seven timer, 16-way external interrupt I/O port, nine communication interface. By including Vision4 IDE program burning software of single chip microcomputer burn. The corresponding circuit Figure 2.

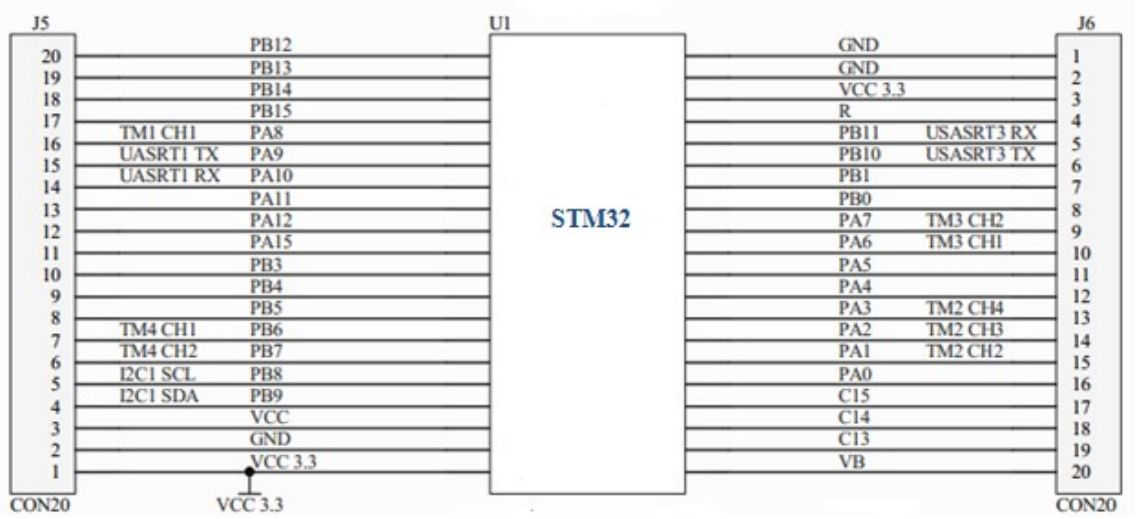

Fig.2 Single chip microcomputer minimum system circuit diagram

C. Balance Module

Choosing MPU - 6050 as measuring car Angle sensor. The measured data into master control chip, through the main control chip kalman filtering and balancing algorithm processing, attitude adjustment needed for the wheel acceleration value, conversion for motor control, through a serial port sent to the motor drive, two routing motor driven dc motor control posture adjustment is installed on the wheels of the encoder to get the actual speed and distance, feedback back to the main controller, adjusted by PID algorithm error will be sent to the motor driver control quantity again, forming a closed loop feedback constantly adjust the whole system can maintain the balance of the car[7]. MPU - 6050 gyroscope[8] circuit diagram as shown in figure 3, motor drive circuit diagram as shown in figure 4.

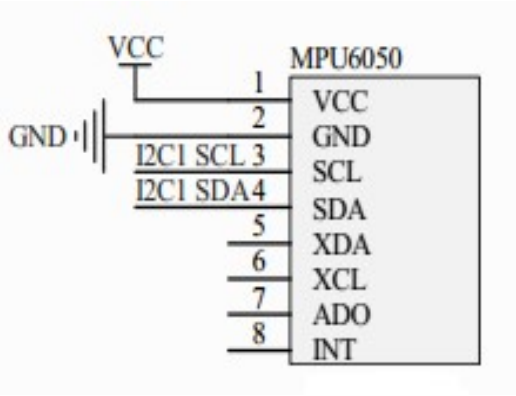

Fig.3 MPU - 6050 circuit diagram

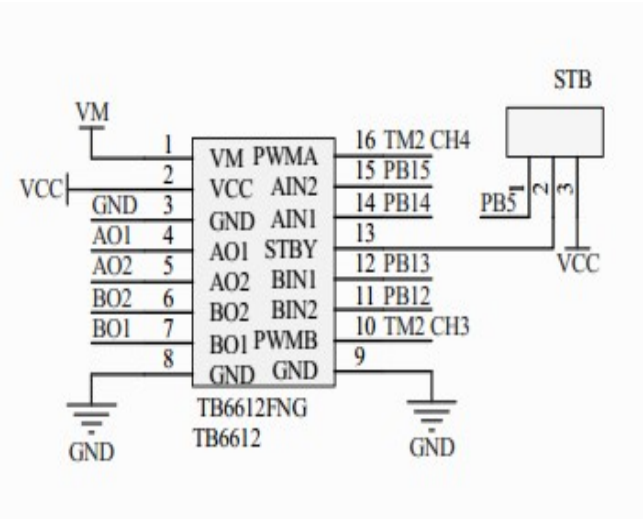

Fig.4 Motor drive circuit diagram

D. Obstacle Avoidance Module

Obstacle avoidance module mainly through the HC - SR04 ultrasonic sensors to collect information. It determines the car around the obstacle position, and makes the car in a timely manner to avoid. Moving towards the direction of the relative humidity is low. HC - SR04 ultrasonic ranging module can provide 2 cm to 400 cm non-contact distance measurement function, measuring Angle is 15°, high ranging accuracy can reach to 3 mm. The input trigger signal for the 10μs TTL pulses.

E. Humidity Module

DHT22 digital temperature and humidity sensor is a containing compound sensor has been calibrated digital signal output temperature and humidity. It uses a dedicated digital acquisition technology and the temperature and humidity sensor technology. Includes a capacitive moisture sensor element and a NTC temperature measuring element. It is connected with a high-performance 8-bit microcontroller, so it is super fast response, strong anti-interference ability and extremely high performance-price ratio. Every DHT22 sensor in extremely precise humidity calibration laboratory calibration, the calibration coefficient in the form of a program stored in the OTP memory, sensor inside in the process of detecting signal processing to invoke the calibration coefficient. DHT22 sensor signal transmission distance can reach more than 20 m and its measuring conditions for -20℃~80℃, humidity accuracy of ± 5% RH, temperature accuracy is less than the plus or minus ±0.5℃; Single bus interface, communication time is 5 ms.

F. Humidification Module

Ultrasonic humidifier adopt high-frequency oscillation (oscillation frequency is 1.7 MHz, more than hearing range). By atomizing chip high frequency resonance, leaving the water and produce natural flowing water mist on the water surface. It produces atomized particles even in 5 microns, the index of energy consumption per unit of humidification quantity to a minimum. Power consumption of the ultrasonic humidifier is much lower than other humidifier, and its noise is smaller than other humidifier. Using other humidifier is big two rounds of the car can't balance problem, and the ultrasonic humidifier is small in size. So the ultrasonic humidifier is more suitable for this design.

V. SOFTWARE PROGRAM

System software flow is shown in figure 5.

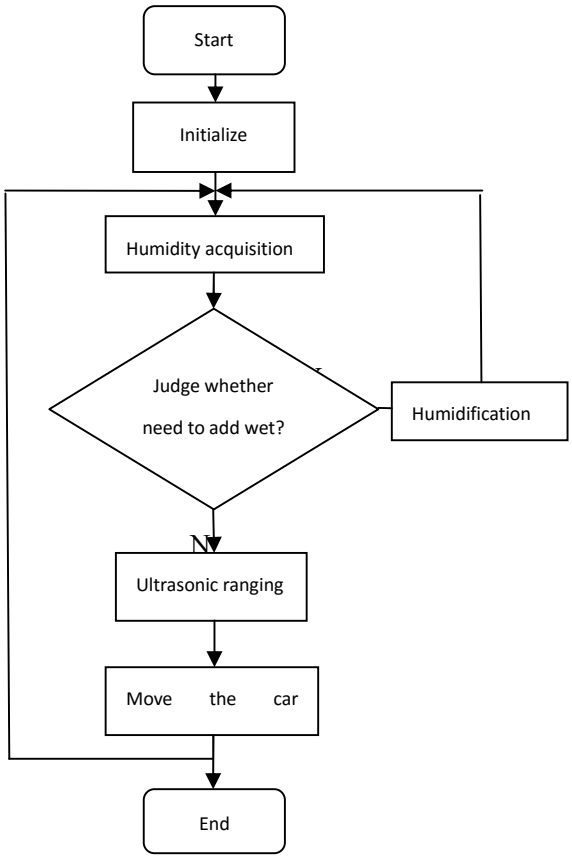

Fig.5 The flow chart of system software

After turn on the switch, System start into initialization, mainly completing soft reset, model set, clock frequency setting and tube Angle setting. Then balance module measure all the data which is transmitted to the single chip microcomputer minimum system module to control the two rounds of car balance, after acquisition of humidity, distance of the

transferred to SCM smallest system, notify the PWM control the motor rotation and humidifier humidification accurately. Two rounds of car since the balance of PID control[9-10] flow chart as shown in figure 6.

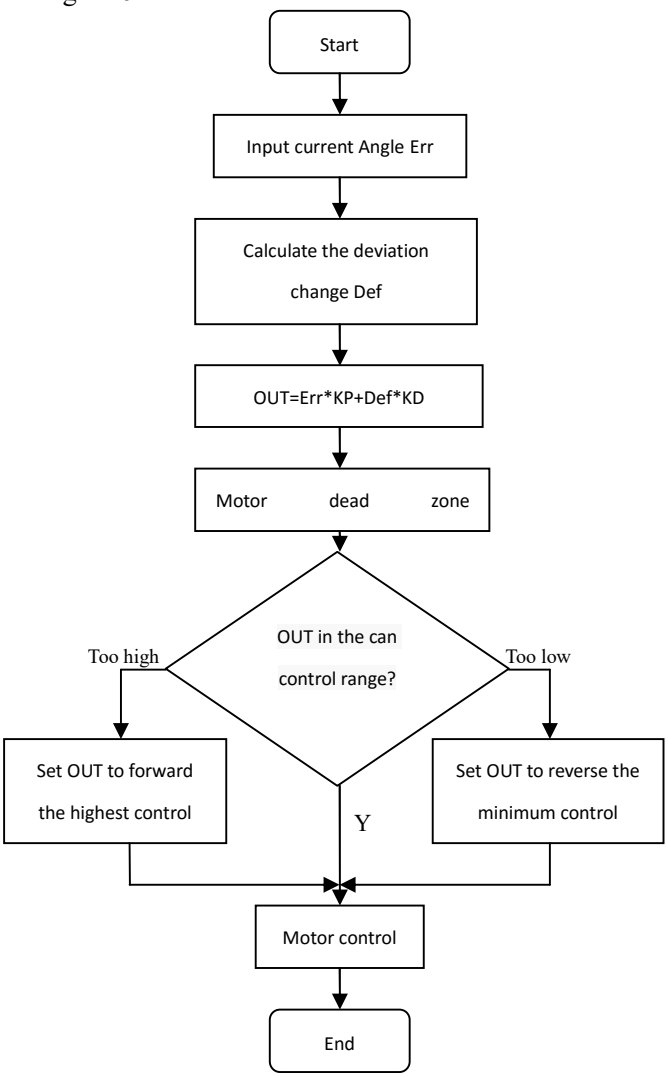

Fig.6 Since the balance of PID control flow chart

VI. FUNCTIONAL TESTING AND APPLICATION

The design of the system is used to let the city wetter. To test the effect of humidification, choosing the weather (average humidity) in the experiments and indoor different place (in indoor take five points) begin humidification test. Test results such as table 1 and table 2.

Table 1 Different weather humidity test table

The serial number	Weather	Initial humidity	Final humidity	Time
1	Sunny	31%	42%	2h
2	Rain	38%	46%	1h
3	Cloudy	35%	45%	1.5h
4	Cloudy	36%	43%	1.3h

Table 2 Different locations humidity test table

Location	Initial humidity	Final humidity
1	35%	45%
2	35%	44%
3	34%	42%
4	33%	44%
5	32%	43%

Table 1 and table 2 show that our basic design can reach above specified humidity in any weather. But the time required are greatly influenced by the weather changes. In a rainy day humidifier or humidity, it is easier to reach their goals. Measured indoor humidity of the maximum in different parts deviation is also less than 5%. It achieves uniform humidification basically.

VII. CONCLUSION

This paper presents a design scheme of movable humidifier. The combination of the two-wheel self-balancing dolly and humidifier realize in an indoor mobile humidifying, and it realizes the uniform humidification. The car can be under the control of unmanned air humidification, through ultrasonic obstacle avoidance function successfully to avoid obstacles. Experimental results show that the design of indoor humidifying in any weather can reach the goal. The humidity indoor humidity biggest difference (the largest indoor humidity and the difference of minimum humidity) can also be controlled in 5%, and it achieves good experimental effect, this basic design meets the requirement. This design has the characteristics such as small volume, low power consumption, and action address. Thus, it has a broad application prospect.

References

[1] Li Hong mei, Li Zhi, Gao Fer. Balanced masterpiece, segway FIT two rounds of platform for electric vehicle [J]. Electrical equipment industry. 2002, [6] : 19-21.

[2] Zhang Pei ren. 16/32 of a DSP based robot control system design and implementation [M]. Beijing: tsinghua university press, 2006:911.

[3] Huo Liang. Two rounds of the key technology of self-balancing electric vehicle research [D]. Harbin: Harbin engineering university, 2010.

[4] Yu Qing guang Liu Kui, Wang Chong etc. Selection of photoelectric encoder and synchronous motor speed and rotor position measurement [J]. Electric drive, 2006 4 [4] : 17 ~ 20.

[5] Xie Ke ming. Automatic control principle [M]. Beijing: electronic industry press, 2009.

[6] Xue Tao. Microcontroller and embedded systems development methods [M]. Beijing: tsinghua university press, 2009.10.

[7] Ren Yafie,Ke Xizheng,Liu Yijie.MEMS Gyroscope Performance Estimate Based on Allan Variance[A].In Proceedings of 2007 8th International Conference on Electronic Measurement & Instruments, Xi'an China.1, 260-263.

[8] N. Yazdi, F. AyaZi, andK. Najafi. MICROMACHINED INERTIAL SENSORS[J]. Proceedings of the IEEE, Aug. 1998. 86[8], 1640 ─ 1659.

[9] Hongxia Guo,Jinming Yang,Wengang Liu, PID neural network control of brushless doubly-fed machine[J].Control Theory & Applications. 2008,25[1],53-56.

[10] He Kezhong,Sun Haihang,Guo Mtthe ed all.Research of intelligent mobile robot key techniques[J].IEEE International Conference on IndusIrial Technology.1996:503 ~ 507.

Design and implementation of multifunction distributed environmental monitoring system

Gang Chen; Jiaxin Zhang;Ning Guo
(Instrument Science and Electrical Engineering, Jilin University, Changchun 130012)

***Abstract*--This paper introduces a design that STC89C52 high-performance single chip micro controller as the core, using temperature and humidity sensor DHT11, smoke detectors MQ - 2 and sensor DSM501 air data, and pass by GPRS module to send first place machine distributed environmental monitoring system. The system can quickly and real-time monitoring of the key data index system environment, and the wireless signal coverage through general packet radio service (GPRS) technology will monitor the data sent to the specified upper machine, overcome before enough relevant data monitoring system in real time, shortcomings and so on instrument bulk is not convenient to carry, is the future focus direction of the field.**

***Key words*--Environmental Monitoring STC89C52 GPRS**

INTRODUCTION

IN recent years, with the continuous development of social economy, environmental problems increasingly serious, the environment problem is very serious. In environmental protection work, environmental monitoring as a important link, can to people around the living environment for effective monitoring, and to warn of sudden environmental problems, at the same time better problem handling measures are put forward combining with actual situation, and thus the establishment of environmental monitoring system more and more get the attention of people[1][2]. This design main research question is how to more effective and more rapid monitoring atmospheric environmental data, and real-time measurement results will feedback to monitor host, thus to further data analysis, put forward the solution of the current environmental problems.

I.OVERALL DESIGN

This design mainly consists of the following six modules, respectively is a single-chip microcomputer control module, the temperature and humidity monitoring module, smoke monitoring module, air quality monitoring module, LCD display module and the data transmission module. Of single-chip microcomputer control module is the core part of the whole system, by the process data, and transmit to the data transmission module to send data, control the coordination of various modules work. System begins to work, the temperature and humidity detection module, smoke monitoring module, air quality monitoring module first carried out on the system's environment air quality data collection, data processing, after and transmit to MCU, MCU to various detection module to process incoming data, and then to transmit data to the LCD display module; Through the GPRS module at the same time, to the monitor host computer (PC), the PC software of monitoring host the index data real-time display the current air quality.

II. THE SPECIFIC DESIGN SCHEME

2.1 Hardware Design

The system structure is shown in figure 1:

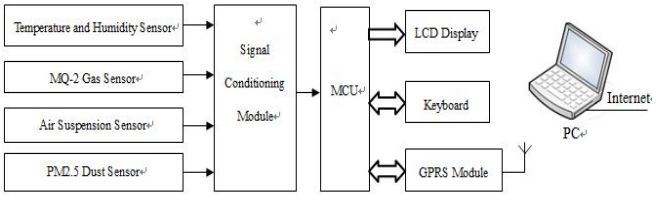

Fig.1 The diagram of system's module

2.1.1 Detection module circuit

The design of the temperature and humidity measuring temperature and humidity sensor to measure the DHT-11. DHT-11 temperature and humidity sensor is a containing compound sensor has been calibrated digital signal output temperature and humidity, it dedicated digital module acquisition

technology and the temperature and humidity sensor technology, ensure that the product has a very high reliability and excellent long-term stability. Sensor consists of a resistance type moisture element and a NTC temperature measuring element, and connected to a high-performance 8-bit microcontroller. So the product has small volume, super fast response, strong anti-interference ability, high cost performance, etc[3].

Smoke detection module uses is MQ - 2 smoke sensor, MQ - 2 gas sensor used by the gas sensitive material is in clean air conductivity low tin oxide (SnO2). When sensor exist combustible gas in the environment, the sensor of electrical conductivity increases with the increased concentration of combustible gas in the air. Using a simple circuit can converts the change of the conductivity and the gas concentration corresponding to the output signal[6].

Our air quality monitoring circuit of the high precision measurement by the DSM - 501 dust sensors. We choose is South Korea SYHITECH patent product, its features are: using pulse width modulation PWM output, on the principle of particle counting, sensitive test particle diameter in more than 1 um suspended in the air, and one of the built-in heater, can be automatically in ambient air monitoring, and the size is small, weight is light, easy to install and use[4].

Each sensor module circuit is shown in figure 2.

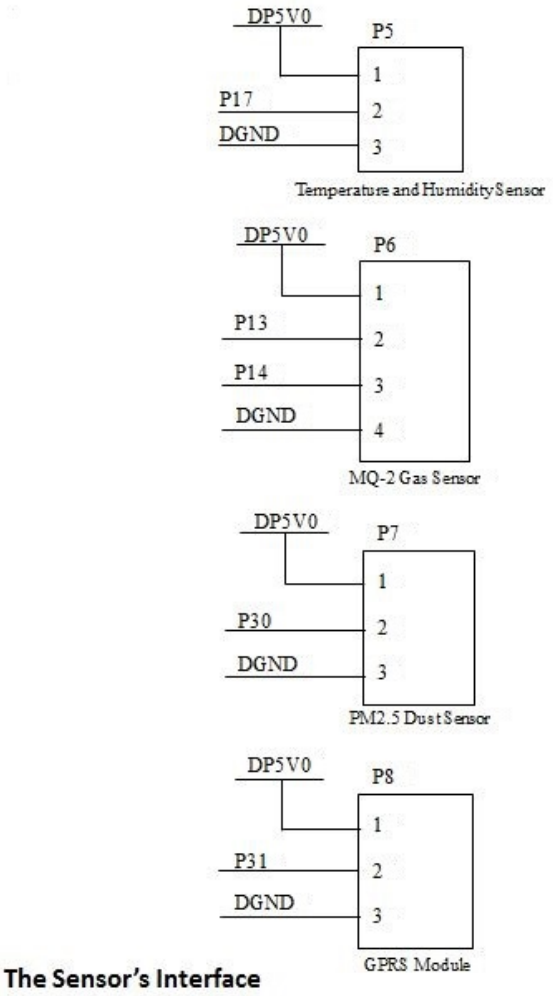

Fig.2 The diagram of sensor module circuit

2.1.2 Data transmission module circuit

GPRS,which is also called general packet radio service, is one of the GSM mobile phone users can use mobile data services, with high transmission rate, transmission distance and low rates, etc[5]. The Data acquisition system based on GPRS wireless communication mainly include Data acquisition Terminal with homemade (Data Terminal) and the server side of management software. Data acquisition terminal with analog and digital I / 0 interface, can be connected data acquisition device[8]. Data acquisition terminal and a wireless communication interface, can through the GPRS wireless network and TCP connection to the server management software, the data acquisition equipment collected data sent to the server. Server management software to analyze the collected data, processing and storage, so as to realize the monitoring of the terminal or associated equipment.

Module communication principle [7]and the connection with MCU as shown in the figure below.

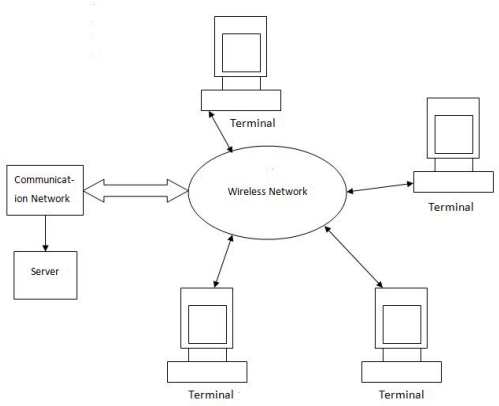

Fig.3 The principle diagram of the GPRS module communication

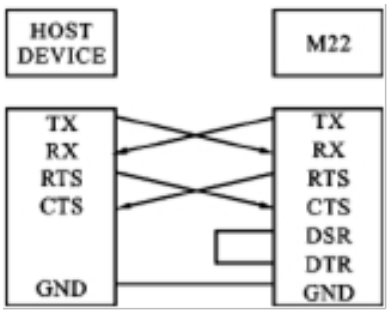

Fig.4 The diagram of MCU and GPRS module connection

2.1.3 LCD display circuit

Using industrial character type LCD display LCD1602 to display the measurement data of monitoring, facilitate timely observation and record at the scene.

The LCD display circuit connection diagram as shown in figure 5.

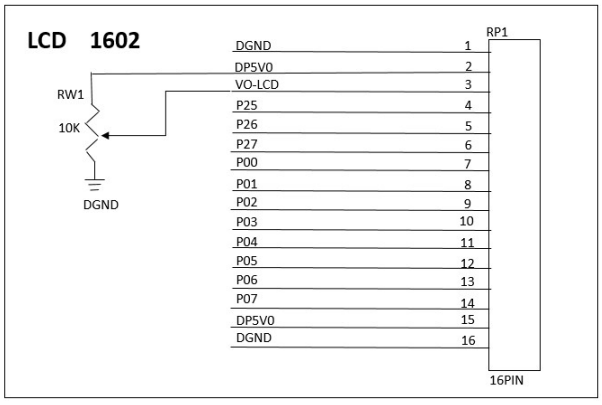

Fig.5 The diagram of the LCD display circuit connection

2.2 Software design

Give full play to the design of the main program modularity and reusability characteristics of C language, according to the characteristics of the single-chip computer program writing. Initialized main program after enter an infinite loop, barring any interruption, microcontroller will always run in the loop.

The flash reading program is as the main branch to draw near, when flash data read operation of the main program was in an irregular pattern. Usually doubt the data of the terminal to send the check to use, then the rest of the main program is not running. The other did not reflect any interrupt handlers in the main program.

PC software using the graphical LabVIEW complete design and development, don't need to write the complex computer program code, the construction of monitoring system can be realized, and friendly interface, and beautiful. Main functions are: to monitor TCP port, the connection is established, receives the GPRS module of data; The data processing, display the data, and save to the database; View the historical data, and so on.

PC LabVIEW design block diagram is shown in figure 6.

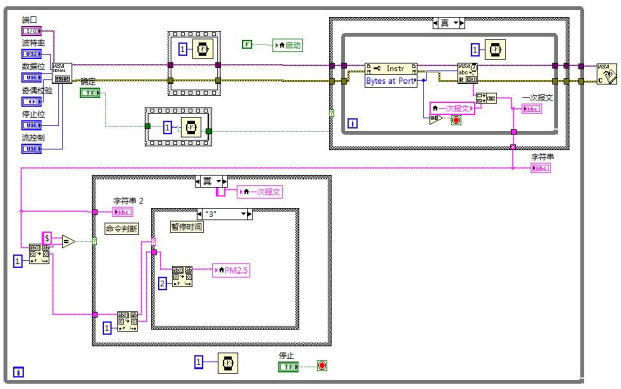

Fig.6 Monitoring programming block diagram

III. THE TEST RESULTS ANALYSIS

Upon the completion of the design, we have a complete set of product technical test was carried out. System is running in good condition, the temperature of the measuring range of 0 ℃ to 50 ℃, the error is within plus or minus 2 ℃. Humidity measurement range from 20% to 95%, the error is within +/- 5%. We also tested for smoke detection module, environment, when the module in the smoke alarm system, shows that the smoke concentration is too high; Can work properly under normal air environment. PM2.5 detection module is working properly, the measured error is less than 0.1 ug/m3. GPRS data transmission module can accurately transmit data, but due to reasons such as network transmission speed, the measurements of the upper machine to receive a little slower than system real-time monitoring data.

Physical figure of the whole monitoring system and PC interface as shown in the figure below.

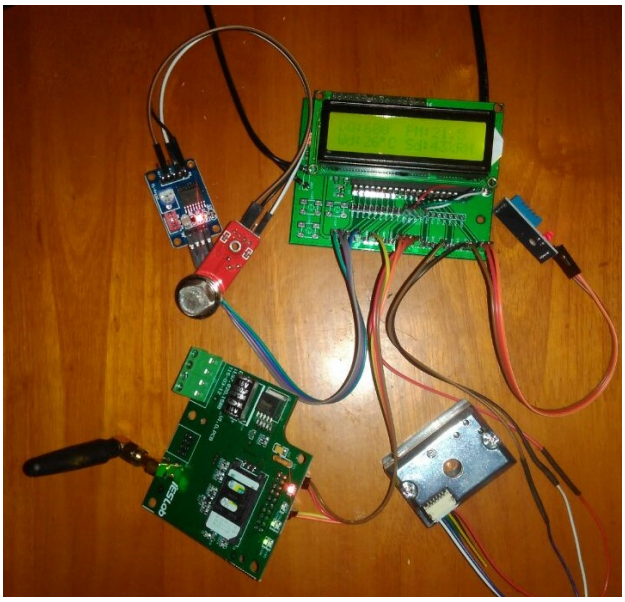

Fig.6 System's real figure

Fig.7 Moitoring program interface

IV.CONCLUSION

This paper designs a multi-function environmental monitoring system based on microcontroller STC89C52, through multiple modules to cooperate, can real-time monitor the scene of the temperature and humidity, smoke concentration, PM2.5 data, such as air and transmission through GPRS module to the distant monitoring host, facilitate monitoring and further analysis of the data. Through further perfect, the system can be applied to various conditions of environment monitoring, and small volume, easy to carry, can be effectively applied in a variety of complex environment.

References

[1] Yang Gengfeng. Talk about the Application of Environmental Monitoring and Emergency System Development [J]. Journal of Environmental and Life. 2014,22 : 426-428.

[2] Xue-song Zheng. Indoor Air Pollution and Environmental Detection Strategy Research [J]. Science and Technology and Business. 2015, 6: 85.

[3] Ni Tianlong. Single Bus Sensor DHT11 Temperature and Humidity Measurement and Control Application [J]. Journal of Microcontroller and Embedded Systems Applications. 2010,6:60-62

[4] He Qiang, Wen Hui. Based on Single-chip Microcomputer and PM2.5 DSM501 Measurement [J]. Journal of Electronics World. 2014,16:27-28.

[5] Tang Qiangyi, Tang Chengkai. GPRS Technology Application in the field of Environmental Monitoring [J]. Journal of Xi 'an Aviation Technology College. 2011,29 (5) : 72-74.

[6] Li Wenchen. Wireless Environment Monitoring System Based on Multi-sensor Data Fusion [D]. Nanjing:Nanjing University of Science and Technology, 2014.

[7] Wang Dongqing. Wireless Sensor Network in the Environmental Monitoring System of Research and Application [D]. Wuhan: Wuhan University of Technology, 2008.

[8] Cui Zhouhua. Environmental Monitoring System Based on GPRS and the ARM of the Study and Implementation [D]. Wuhan: Central China Normal University, 2010

Design of baby sleep monitoring system based on STM32

Zewen Zhou; Dawei Yan; TianHui Wang

(College of Instrumentation and Electrical Engineering, Jilin University, Changchun 130000, China)

***Abstract*--With the development of science and technology, in order to better take care of the baby, we propose a microcontroller based STM32F103 infant sleep monitoring system. The system has kicked quilt detection, use the temperature and humidity sensors which is placed under the mattress to detect the baby's quilt cover state. When placed under the mattress temperature and humidity sensors to monitor the baby's sleep area no quilt cover when playing music arouse the attention of parents. There are precise temperature detection, use AD590 current output temperature sensor for measuring the body temperature, the LCD5110 LCD display various information. After testing, the system is reliable, low-cost, practical.**

***Key words*-- STM32F103 microcontroller sleep monitor**

I. INTRODUCTION

IN today's society, as the pace of life and work increasingly tense, women usually have to deal with their work and families, not only do they have to take care of their babies, but also have to do the housework. At this condition, mothers are often in a rush and a muddle. Baby are in sleep most of the time in a day, how to do the sleep monitoring, which is reminding parents timely when the baby kick or wake up to prevent the baby from having a cold, is particularly important. Nowadays, foreign baby sleep monitoring system only video the baby and transmit it to the receiver, which need for parents to judge by themselves. This kind of monitor without intelligence requires the parents with babysitting experience. And eventually it did not play a part in further reducing the pressure. The baby sleep monitoring system designed in this paper can solve this problem effectively. The use of the temperature and humidity sensor placed under the mattress DHT90 to detect whether the baby's sleeping area covered with a quilt, if no quilt cover, will play music to send an alarm. Making use of the temperature and humidity sensor DHT90 placed under the mattress to detect whether the baby's sleeping area covered with a quilt or not. If it is covered without quilt, the monitor will play music to send an alarm to remind parents to observe the baby's sleep [1].

II. THE DESIGN OF THE TOTAL SYSTEM

Based on the investigation of the current systems of baby's sleeping monitoring, we will integrate several practical functions, and design a smart baby sleep monitoring system [2]. The system contains the detection module, the music player module, the temperature precision detection module, the data processing and control module, and the display module. The structure diagram of baby sleep monitoring system is shown as Fig. 1.

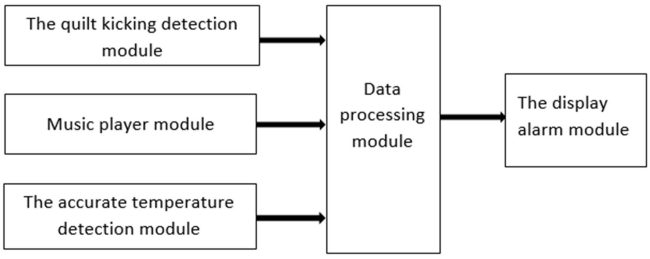

Fig.1. The structure diagram of baby sleep monitoring system.

III. THE HARDWARE DESIGN OF THE SYSTEM

Considering the power consumption of the system,

because of the use of battery power, this design make use of STM32F103 MCU with high performance, low power for data processing and the control of each module's operation. The resources that STM32F103 process including: 48KB of SRAM, 256 KB of flash, 2 basic timer, 4 general purpose timer, 2 senior timer, 2 DMA controller (the total of 12 channels), three SPI, IIC, five serial port, a USB, a CAN, three 12-bit ADC, a 12-bit DAC, a SDIO port and 51 general IO port. The MCU is small size, and with perfect interface, has a strong computing power. So it is a good value for us using this chip.

A.The Kick Detection Module

This module uses four temperature and humidity sensor DHT90 embedded to the baby sleep pads, measuring the temperature and humidity values of the region covered by quilts. These values are considered the temperature and humidity inside the quilt [3]. And then measure the temperature and humidity of the surrounding environment by another temperature and humidity sensor. This module determines whether the baby kicked the quilt or not by comparing the bed temperature and humidity inside and outside. The diagram of kicked quilt detection module is shown as Fig. 2.

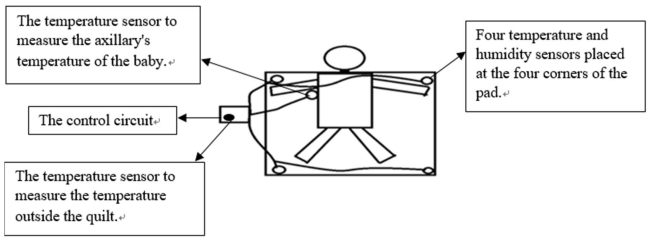

Fig.2. The diagram of kicked quilt detection module.

The kick detection module adopts DHT90, a temperature and humidity sensor with the calibrated digital signal output. The sensor includes a capacitive polymer humidity sensitive element, a temperature measurer made from energy gap material. Besides, it can achieve a seamless connection with a 14-bit analog-to-digital converter and the serial line interface circuit on the same chip. Therefore, the sensor has the advantages of small volume, low power consumption, fast response, strong anti-interference ability, good value etc. Each sensor chip is calibrated in a highly accurate humidity chamber, and the calibration coefficient is stored in the OTP memory in the form of the program, and will be used in the calibration process. Sensors will recall these calibration coefficients in the processing of detection signal. Two wire serial interface and internal voltage adjustment make the integration of periphery system easier and faster. DHT90 applies the 2.4~5.5V DC power supply, the range of humidity measurement is 20~90%RH, the precision of humidity measurement is ±4.5%RH, the resolution of humidity is 0.05%RH, the precision of temperature measurement is ±0.5℃, it can be completely interchangeable, long-term stability is less than 0.5%RH/year.

The connection between the temperature and humidity sensor DHT90 and the microcontroller STM32F103 is as shown in Fig. 3. The power supply terminal of the microcontroller is connected with the power supply. The ground terminal of microcontroller is connected with the ground, and the power supply uses +3.3V. The DATA terminal and SCLK terminal are respectively connected with the I/O port PA5 and PA6 of the MCU.

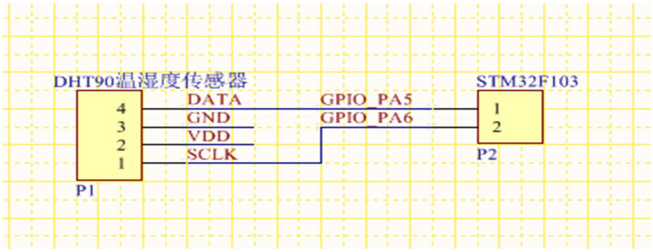

Fig.3 The interface circuit of the temperature and humidity sensor

B. Body Temperature Accurate Detection Module

The temperature precision detection module applies a high precision current-output type temperature sensor AD590 to detect the temperature of the baby's armpit, to determine whether the baby's temperature is normal, the accuracy of temperature measurement can

reach $\pm 0.1℃$[4].

The core of how AD590 works is the output current follows the temperature change at the same time for the same amount to absolute zero $(-273℃)$ as the base, each additional $1℃$, the output current will increase $1\,\mu A$. The output current of AD590 is $I = (273 + T)\mu A$ (T is the temperature in degrees Celsius). So at the condition of the room temperature is $25℃(273K + 25K = 298K)$, it's output current $I_0 = 298\mu A$. The temperature range of management is $-55℃ \sim +150℃$, the nonlinear error is only $\pm 0.3℃$. The conditioning circuit of AD590 temperature sensor is using a single ended calibration circuit as shown in Fig. 4.

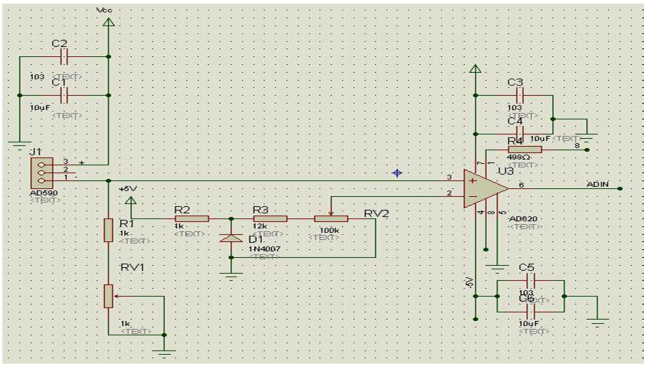

Fig.4 The conditioning circuit of AD590

Pre-differential amplifier applies AD620 instrumentation amplifier, anti-aliasing low-pass filter using the first-order active low-pass filter constituted by the operational amplifier OP07, resistors and capacitors. The A/D module using TI's TLC2543, which is with 12-bit serial A/D converter, using switched-capacitor successive approximation technique to complete A/D conversion process. As it is serial input structure, you can save the I/O resources of STM32F103 microcontroller, and it is inexpensive. Its characteristics are: (1) 12-bit resolution A / D converter; (2) 10μs conversion time in the operating temperature range (3) 11 analog input channels; (4) 3-way built-in self-test mode; (5) sampling rate of 66kbps; (6) linearity error +1 LSB (max) (7) have the end of conversion (EOC) output; (8) with a single, bipolar output; (9) programmable MSB or LSB preamble; (10) programmable output data length. The whole circuit of accurate temperature detection module is shown as Fig. 5. The current signal that the temperature sensor AD590 obtains change to a voltage signal over a 1K resistor, the voltage signal amplifies through the instrumentation amplifier AD620 100 times, and then is filtered by the operational amplifier OP07, which is a first-order low-pass active filter with an 1Hz cut-off frequency. After that he signal is input to the 12-bit A/D TLC2543. Eventually, the value of A/D is read by the microcontroller, and obtain the converted Celsius temperature through the digital filter and numeric conversion. The entire module of the accurate temperature detection circuit is shown as Fig.5.

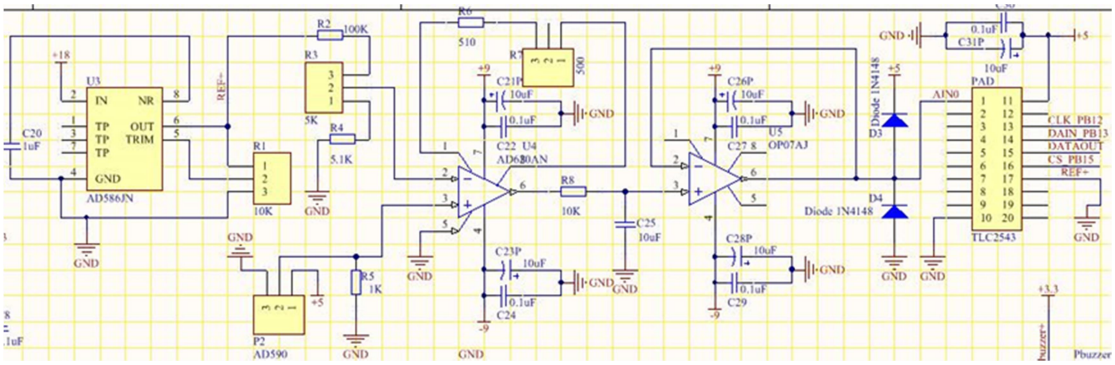

Fig.5 The total circuit of accurate temperature detection module

C. Music Player Module

Music player module can play quiet music, make the baby to get in sleep. And you can play a specific song, remind parents timely care about when the baby kicked quilt or a relatively large change in temperature occurs.

Music player module use domestic music Manifold HS-088, only need to add a transistor 8050, a ceramic capacitor, a small speaker can constitute a music player module. The music is beautiful, and the price is cheap.

D. Display Alarm Module

Display alarm module applies LCD5110 LCD monitor. LCD5110 can display 15 characters, 30 characters, connecting with a simple microcontroller interface requires only four I/O lines can, it is low-power, low price. When detecting the occurrence of baby kicking the quilt, the liquid crystal displays "baby kick the quilt" four words. If the baby not, it will display "The baby sleep well" .

IV. THE DESIGN OF SYSTEM SOFTWARE

A. System Flow

The flow of the system is programmed after the system initialization. First of all, it determines whether the temperature measurement key is on, if so, then measure the baby body's tempreture and after that detect the key again and again. Not until the key is off, can the system stop detect this key, jump out of the loop, and keep going on. When the key is off, you could determin wether the baby kick the quilt or not. If so, play the music and then return to initialization. If not, it also return to the initialization. The system flow chart is shown as Fig.6.

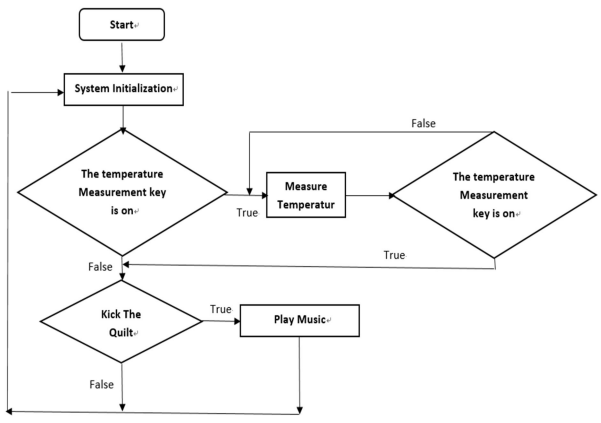

Fig.6 The system flow chart

V. PERFORMANCE TESTING

In order to achieve standard each system's performance of infant sleep monitoring system. As shown in Table 1 and Table 2, respectively, are the test temperature data measured by AD590 and the temperature and humidity values meatured by sensor DHT90. The measuring instrument testing AD590 is a fine mercury thermometer with ±0.1℃ and 0~50℃ management range. The test equipment of the temperature and humidity sensors DHT90 is AS837 air temperature and humidity measuring instrument. AS837's temperature accuracy is ±1.5℃, and its humidity accuracy is±3%RH.

Table 1 The test data of AD590

The standard temperature (℃)	The measured temperature of AD590 （℃）	The errors （℃）
2.61	2.6	-0.01
5.42	5.4	-0.02
8.43	8.4	-0.03
14.34	14.3	-0.04
20.98	21.0	-0.02
26.59	26.6	-0.01
30.35	30.3	-0.05
35.43	35.4	-0.03
37.58	37.6	-0.02
39.54	39.5	-0.04
40.93	41.0	-0.07
42.02	42.1	-0.08

Table 2 The test data of DHT90

The temperat-ure of DHT90 (℃)	The tempera-ture of AS83 (℃)	The tempera-ture error (℃)	The humid-ity of DHT90 （%RH）	The humi-dity of AS837 （%RH）	The humi-dity error （%RH）
26.6	26.3	+0.3	52.3	50.6	+1.7
19.2	20.1	-0.9	36.0	33.0	+3.0
22.2	22.7	-0.5	33.8	30.2	+3.6
19.6	19.1	+0.5	23.0	19.0	+4.0
28.1	28.0	+0.1	44.9	43.7	+1.2

Summary: AD590 temperature measurement accuracy is ±0.1℃. DHT90 temprature measurement accuracy is ±1.5℃, the humidity measuring precision is ±0.5%RH. It can achieve the target that thesystem requires.

VI. CONCLUSION

For the real difficulties on babysitting, we designed a infant sleep monitoring system with low-power based on the STM32 ,which can achieve quilt-kick detection, temperature detection, music playing etc. And improved the disadvantages of the products on the market. Using this device ,parents could take care of the babies easily and timely. The test proved the high reliability and the strong practical of this infant sleep monitoring system. And it could be for long-term use, otherwise it is easy to maintain and expand more functions.

References

[1] Yong Yuan, More Kinetic Energy Design Baby Monitoring System. [Papers] Electronic World 2014 (9)

[2] Tingting Wang, Yuan Yuan, Pan Xiaohui. MSP430-based Infant Sleep Monitoring System, Electronic Design Engineering, 2014.5,22 (9): 65-68.

[3] Hui Tu, Minghui Cheng, Zouxue Yu, Design and Implementation of ZigBee Technology Baby Monitor System TV Technology, 2013.7,37 (21): 71-74

[4] Hui Tu, Detection And Monitoring System To Achieve Yang Infant Baby Crying Module, Digital Technology And Application, 2014,4: 172-173

Development of magnetic electrode in high density resistivity method

Qiu Zhuo; Wang Qi; Song Xinhua
(College of instrumentation &Electrical Engineering, Jilin University,Changchun 130061,China)

***Abstract*--High density resistivity method is one of the effective tools for geophysical exploration, which is widely used in the detection of underground mineral resources and the prevention of debris flow disasters. High density electrical equipment used in the electrode is often the metal electrodes or non polarizable electrode, in using process needs to be buried deeply in the ground, and then through the lead wire is connected to the host, it is difficult and unable to break into the electrodein in some high density electrical prospecting[1] . This topic researchs magnetic electrode in a high density electrical equipment, which can overcome the traditional metal electrode or non polarizable electrode in the use of the lack and increase the range and practicality of high-density electrical prospecting apparatus, preventing electrode is driven into the ground and causing electrode wear, and at the same time, it can improve the work efficiency, realize the data of rapid measurement.**

***Key words*--Physical exploration High density electrical instrument Magnetic electrode**

I. INTRODUCTION

HIGH density resistivity method is widely used in the exploration of underground mineral resources and the prevention of debris flow, as one of the effective tools for geophysical exploration. The data has the advantages of high accuracy, large amount of data, abundant information, fast measurement speed and so on[2].High density electrical equipment used in the electrode is often the metal electrodes or non polarizable electrode,but in use process, it needs to be buried deeply in the ground, and then which is connected to the host through the lead wire, in some high density electrical prospecting, it is difficult to break into the electrode. This topic research magnetic electrode in a high density electrical equipment, which can overcome the disadvantages of traditional metal electrode or non polarizable electrode,it can increase the usage range and practicality of high-density electrical prospecting apparatus, prevent electrode was driven into the ground and cause electrode wear, and at the same time, it can improve the work efficiency and realize the data of rapid measurement[3].

Ⅱ. SYSTEM DESIGN

The purpose of this project is to design a magnetic electrode high-density electrical prospecting apparatus, which can measure DC electric field signal transfer to high-density electrical prospecting apparatus in the subsurface flow using magnetic electrodes, so it can overcome the shortcomings of the traditional electrode and improves the work efficiency.

2.1 Design of magnetic electrode measurement

2 to n-1 metal electrodes or non polarizable electrode in the original high density resistivity method replaced magnetic electrode of the invention, the high density electrical instrument, the current signal of high density electrical instrument through high density line by 1 metal electrode and metal electrode n to the underground supply by electrical prospecting method the requirements, the current signal flows in the underground space and generates a magnetic field signal corresponding to the power supply current signal, the magnetic signal corresponds to the distribution 2 to n-1 on the ground magnetic electrode measurement and power supply current signal, then it can be converted to digital signal through the communication path of high density electric line and transmitted to the high density electrical instrument. Magnetoelectric signal is be processing,then calculating the magnetic potential at the electrode position of 2 to n-1.

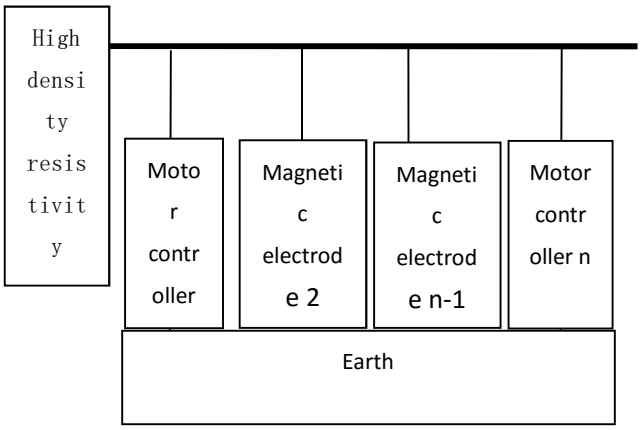

Figure 2.1 schematic diagram of magnetic electrode and the high density electrical instrument connection

2.2Composition of magnetic electrode system

The magnetic electrode system comprises a magnetic resistance sensor module, a signal amplifying circuit module, a A/D data acquisition module, a single chip microcomputer module and a liquid crystal display module.

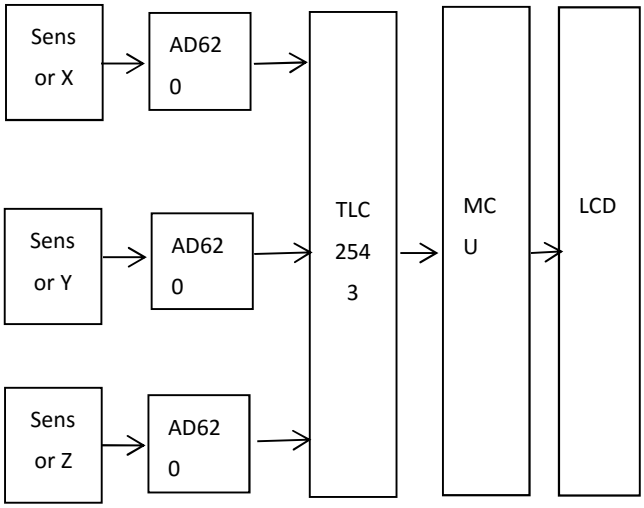

Figure 2.2 diagram of magnetic electrode system

Reluctance sensor module: collecting the magnetic field signal generated by DC current in underground flow.

Signal amplifying circuit module: the signal to be amplified by the sensor.

A/D data acquisition module: the collected analog signal is converted to digital signal, the transmission to the microcontroller.

Single chip microcomputer module: as the main control unit, mainly responsible for the acquisition and conversion of magnetic field signal.

Liquid crystal display module: display the received magnetic field information.

III. SYSTEM HARDWARE DESIGN

The design is to be STC89C52 as control core,HMC1001/2 Honeywell Honeywell company production of one axis and two axis sensor chip as a sensor to collect the underground magnetic field data acquisition, it uses AD620 as amplifier signal amplifier , a / D with 12 bit resolution TLC2543 and uses as LCD1602 display data.

3.1 Main controller STC89C52

The main control module uses STC89C52, STC89C52 is a kind of low power, high performance CMOS8 bit microcontroller, which is produced by STC. It has 8K in system programmable Flash memory. STC89C52 uses the classic MCS-51 kernel, and makes a lot of improvements that makes the chip better,it has advantage thana traditional 51 chip. In a single chip, with 8 CPU smart and in system programmable Flash, the STC89C52 provides a highly flexible and cost-effective solution to many embedded control applications.

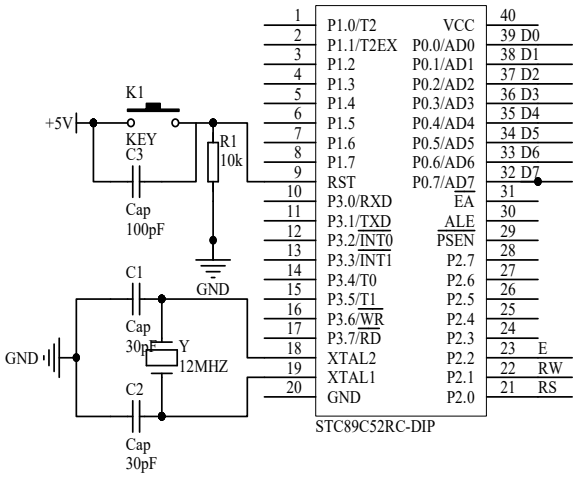

Figure 3.1the smallest single-chip system

3.2 Sensor

The Honeywell Honeywell company productes HMC1001/2 axis sensor core .working principle of the sensor is using anisotropic magnetoresistance effect, magnetoresistive sensor uses silicon as a substrate in the production and four identical iron nickel alloy as Wheatstone bridge. Three magnetoresistive sensor is composed of three magnetic resistance, the magnetic direction of three magnetic resistance is perpendicular each other, in actual use, each internal magnetic resistance with four permalloy strips is to form a core

part of Wheastone bridge.the magnetoresistive sensor is mainly bridge. Due to permalloy,magnetoresistance effect is anisotropic, the resistance change of bridge resistance leads to changes in the output voltage of the sensor, sensor has two ring current aluminum belt, including a set and reset current,which can be used to modify the sensitivity of the sensor, also be used to set and reset output polarity.another a compensation current, it is used to offset the external magnetic field environment.

When the electromagnetic film is placed in an external magnetic field, the resistance of the film will change. When the magnetic field is zero, four pieces of thin film resistor R, bridge power supply drives current in the films. When an external magnetic field m is applied, the magnetic state of the film changes, magnetization directes along the direction of the current, the relative placement of two thin film resistance decreases R1, also two thin film resistor magnetization direction and current are in the opposite direction,R1 resistance increases, within the linear range, output and magnetic field and the bridge output voltage are proportional to the:

$$\Delta V_{OUT} = (\frac{R1}{R})V_b$$

$$\Delta V_{out} = V_b \times M \times S$$

R is for semiconductor thin film resistor , R1 is resistance variation, S is for magnetoresistive sensor sensitivity and M is the magnetic field, the output voltage signal is proportional to the magnetic field, the equation above:

$$M = \Delta V_{out} / (V_b \times S) .$$

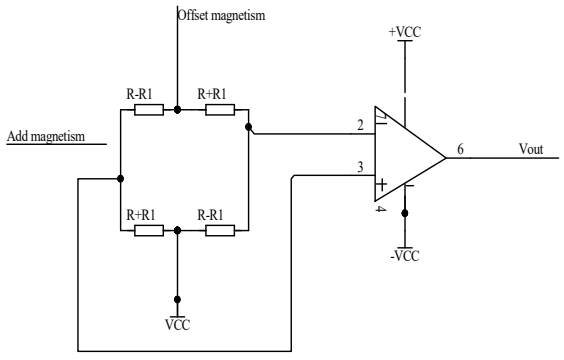

Figure 3.2 schematic diagram of working principle of magnetoresistive sensor

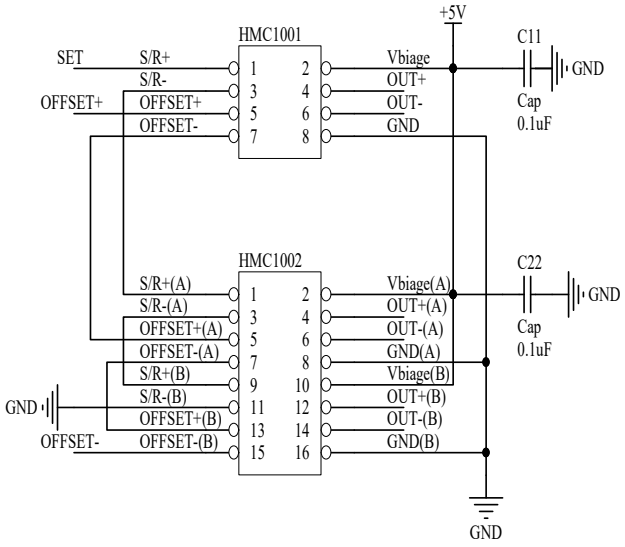

Figure 3.3 magnetoresistive sensor connection circuit

3.3 Amplifier

The system uses AD620 to amplify the signal of the reluctance sensor. AD620 is a low cost, high precision instrumentation amplifier and easy to use,using an external resistor to set the gain. Its magnification is 1-1000, considering the accuracy, the amplification is 500,which is most accurate. The output voltage signal of magnetoresistive sensor is about tens of millivolts, in order to meet the need of AD converter, the signal amplification is 100 times.

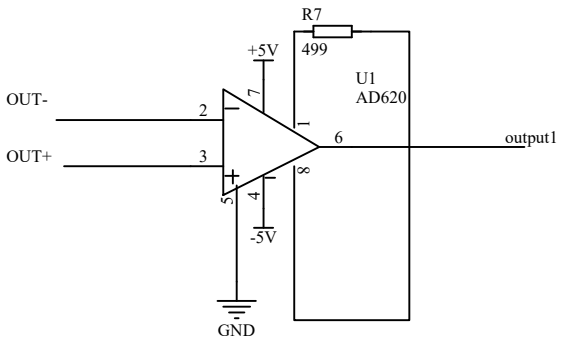

Figure 3.4 AD620 amplification circuit

3.4 A/D module

According to the measurement precision,outputing range signal amplification and the analog signal inputing channel, the converter chooses TLC2543,which can convert analog signal to digital signal . TLC2543 is using CMOS 12 bits successive approximation analog-to-digital converter, it has eleven analog inputing channels, each channel conversion time is 10us. Three component magnetic measurement uses the three analog inputing channels, the remaining channel is for orientation, temperature signal acquiring, it can simplify the circuit structure.

TLC2543 works in + 5V voltage conditions, analog channel inputing voltage range n is for -0.3V-5.3V and is compatible with amplifying circuit output signal voltage range , TLC2543 with three control inputs: chip select (CS), A / D conversion mark the end of (EOC), data input line (data input).

DATA INPUT port and 8 bits serial inputing address control register is connected through the register definition AD conversion inputing channels, output bits and output data format. Analog digital converts through two different cycles to achieve continuous (I/O cycle and conversion cycle), I/O cycle achieves the TLC2543 control byte writing, and reads the results of the last A/D conversion. Conversion cycle achieves A/D conversion.

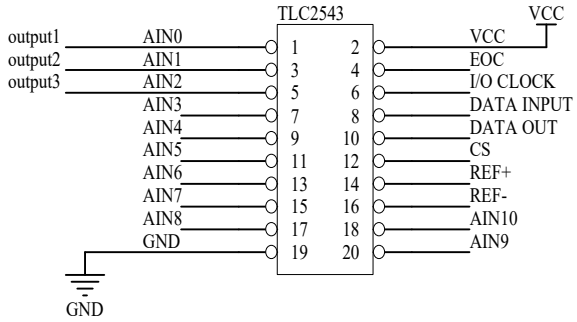

Figure 3.5 A/D module

3.5 LCD module

The LCD module adopts LCD1602, it display sletters and numbers more convenient, easy to control, and low cost.

3.6 System integrated circuit diagram.

The whole system includes sensor module, amplifier module, A/D data conversion module, MCU control module and displaying module.

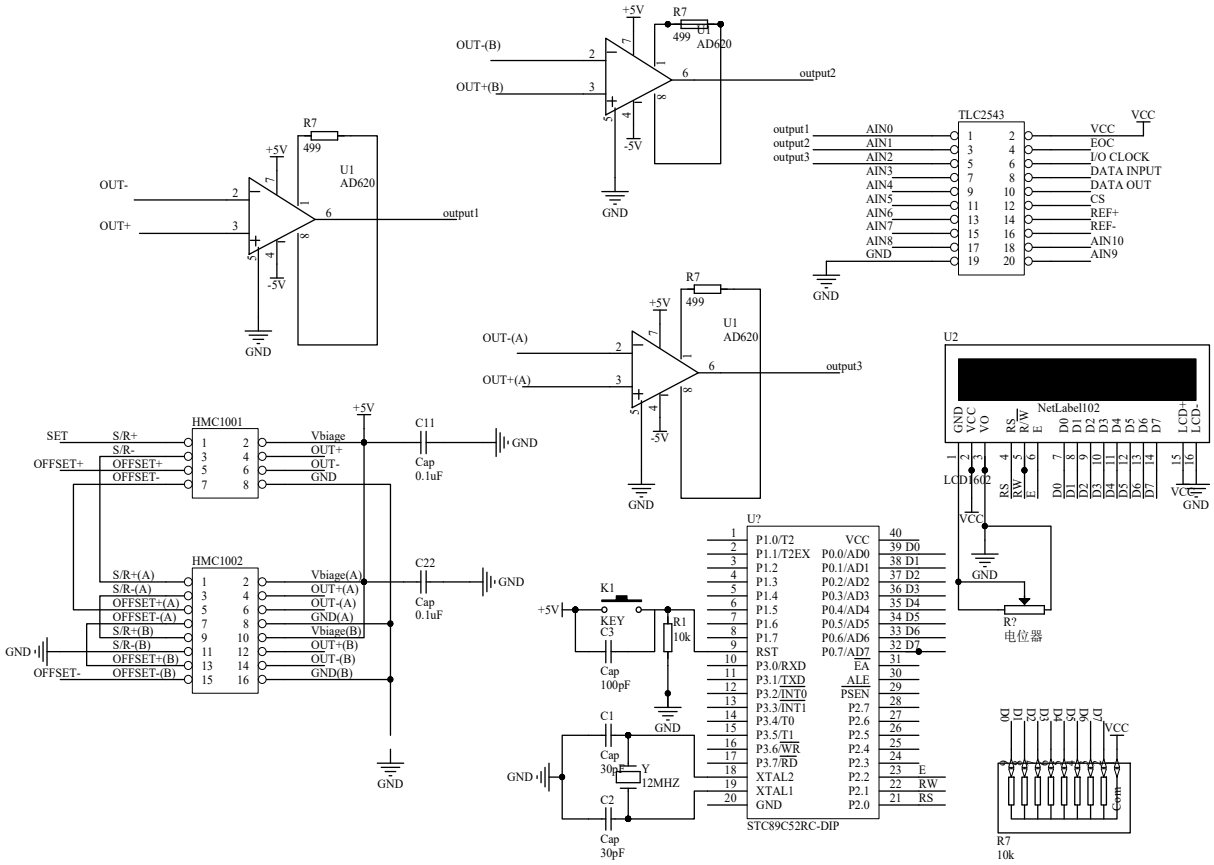

Figure 3.6The whole circuit system diagram

Ⅳ. MATHEMATICAL MODELING

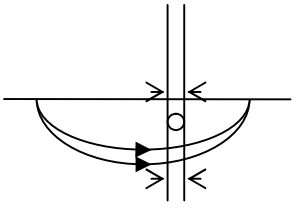

Figure 4.1 schematic diagram of magnetic electrode simulation

In air,he magnetic induction intensity is B_0， The length of magnetic sensor is L。The three component measured by the magnetic sensor is B_x B_y B_z

$\therefore B_{t0}=\sqrt{B_x^2+B_y^2}$ ， $B_{n0}=B_z$ ， B_1 Underground magnetic induction strength，

$$\therefore B_{n1}=B_{n0}$$

$$\because H_{t1}=H_{t0}$$

$$\therefore H_{t1}=\frac{1}{\mu_0}B_{t0} \qquad H_{n1}=\frac{1}{\mu_1}B_{n0}$$

$$\therefore H_1=\sqrt{\left(\frac{B_{t0}}{\mu_0}\right)_x^2+\left(\frac{B_{n0}}{\mu_1}\right)_y^2}\longrightarrow$$

$$H_1^2=\left(\frac{B_{t0}}{\mu_0}\right)_x^2+\left(\frac{B_{n0}}{\mu_1}\right)_y^2 \qquad (1)$$

The current distribution in the magnetic electrode is arranged on a circle with a radius of a.

$$\therefore \oint_l \overrightarrow{H_1}d\vec{l_1}=I\longrightarrow 2\pi aH_1=I$$

$$\frac{U}{R}=I\longrightarrow\frac{\gamma\pi a^2U}{L}=I$$

γ for electrical conductivity

$$\therefore \gamma UI=4\pi LH_1^2 \qquad (2)$$

Make a ball with a radius of 0.5L in the cylinder:

$$\oint_S \vec{D}d\vec{S}=q$$

$$D\cdot 4\pi\left(\frac{L}{2}\right)^2=\frac{4}{3}\pi\left(\frac{L}{2}\right)^3\rho$$

$$\varepsilon E=\frac{\rho L}{6}$$

$$E=\frac{\rho L}{6\varepsilon}$$

$$\because E=\frac{\rho L}{6\varepsilon} \qquad \therefore U=\frac{\rho L^2}{6\varepsilon} \qquad (3)$$

（1）（2）（3）：

$$\begin{cases}\gamma UI=4\pi LH_1^2\\ U=\dfrac{\rho L^2}{6\varepsilon}\\ H_1^2=\left(\dfrac{B_{t0}}{\mu_0}\right)_x^2+\left(\dfrac{B_{n0}}{\mu_1}\right)_y^2\end{cases}$$

$$\therefore \frac{LI}{24\pi}=\frac{\varepsilon}{\gamma\rho}\left[\left(\frac{B_{t0}}{\mu_0}\right)_x^2+\left(\frac{B_{n0}}{\mu_1}\right)_y^2\right]$$

L I B_{n0} B_{t0} Known ε γ ρ μ_0 unKnown 。

The four current can be obtained from the ground to, and a set of equations are obtained to solve the above parameters.

Ⅴ. SYSTEM TEST

5.1 System test

By using the independent design of magnetic electrode,it is connected to the high density resistivity instrument. Doing a survey before the geological palace in a certain distance of the magnetic electrode and the use of traditional metal electrode.by comparing the two datas. The experiment is carried out by measuring the 5 points in the distance of 1m before the geological palace, Comparing the data of the magnetic electrode and the data of the traditional metal electrode.

Table4.1 magnetic electrode measurement data

Distance（m）	Potential（mV）
0	5000
0.2	4009
0.4	3017
0.6	2006
0.8	1002
1.0	0

Table 4.2 metal electrode measurement data

Distance（m）	Potential（mV）
0	5000
0.2	4018
0.4	3007
0.6	1996
0.8	1004
1.0	0

By comparing the data of 5 points in the same distance between the magnetic electrode and the traditional metal electrode, we can know that the data error of the magnetic electrode is small.

Ⅵ. CONCLUSION

In this paper, a kind of magnetic electrodes is designed to replace the traditional metal electrodes , we can solve the problems that the electrode is hard to penetrate into the ground, and improves the efficiency of field exploration.

References

[1] Saizhen. Chinese prospecting development [J]. Chinese Journal of Geophysics, 1994,37 (1): 409-423

[2] Xue Guoqiang transient progress of the research on the theory and application of electromagnetic method [J] geophysics, 2007,22 (4): 1195-1200

[3] Pei Kexuan. The principle and application of electrical prospecting technology used for [J] science and Technology Innovation Herald, 2010 (19): 70

Research of droplet velocity, speed control and alarm devices

Liu Guangcai; Tian Yu; Shi Hanyao
（jilin university instrument science and engineering institute,changchun,130026）

***Abstract*--With the popularization and application of computer technology in various fields and continuously improving, China's medical equipment industry intelligence level also is growing.For the defects in the current medical liquid monitoring,This paper studies the liquid drip monitoring program.Using single-chip microcomputer to design a liquid drop speed of intelligentmonitor and control device,with droplet velocity system,drip rate control system,the display device,keyboard,alarm system and so on.with the principle of drinking water as the height difference between the pressure variation and change,by controlling the stepping motor to control the drip rate lift.Droplet velocity can be used to set the keyboard.The range is from 30 to 140 (drops / min),control error in the range of about 10% ± 1 drop.Change the setting from the play bit rate basically stable adjustment time of the whole process less than 3 minutes.At the same time the water reaches below the warning line can send an alarm signal.**

***Key words*--Drop speed Alarm device Infrared sensor 51 Microcontroller Stepper motor**

I. OBJECTIVE

INFUSION equipment is essential for the hospital, and infusion equipment droplet velocity is generally patient or doctor manual control. Control range limitations and inconvenient, especially unable to automatically monitor the infusion bottle capacity, needed someone in custody. Therefore, there is an automatic alarm system for liquid drop. The system keyboard setting the stepper motor controlling of the infusion speed and automatically alarm when the liquid level below the set value. The system is convenient for doctors, nurses, care for the sick and make patients feel at ease in the treatment, without fear of infusion bottle drop shed, causing blood flowing back.

II. RESEARCH SIGNIFICANCE

At present, medical monitoring in China are basically artificial method. Patients in the infusion process, you must always pay attention to the remaining liquid in the bottle, and when the liquid is about conveying finished, must inform the medical staff to deal with keys. Because the medical staff busy and didn't have the energy to take into account each patient's transfusion, therefore, patients usually need, accompanied by family members. While the fatigue of long term monitoring of infusion and medical accidents caused by negligence. Especially for bed inpatient, assisted the infusion method of management there is always a potential security risk. So far, most hospitals still rely on manual monitoring of infusion, used only in the ICU ward of intelligent infusion monitoring system, and imported products. Due to imports of intelligent monitoring and control products are expensive, general hospitals cannot afford to bear the costs of big spending, which hospitals had clinical medical monitoring intelligent system management more difficult. Home monitoring devices have been marketed, the price is relatively cheap, but basically monitored independence, cannot form network systems management, and a common domestic pump prices nearly million, the price is not affordable. Therefore urgently need a cheap set of medical application of the intelligent monitoring and control network system in hospital management, thus excluding clinical safety and savings in manpower resources, improve the efficiency of management.

III. IMPLEMENTATION AND DEMONSTRATION

A. Research Ideas

Speed control system by dropping speed testing system, display device, SCM system, keyboard, and alarm systems. Using single chip computer to do

simple math, signal processing and control functions, a bit closed-loop speed control. Speed range of the device is 30--140 drops/min, 10% ± 1 drops of errors, from changing the set value until the drip rate basically stable throughout the process of adjustment of less than 3 minutes, and below water line can give an alarm signal[1].

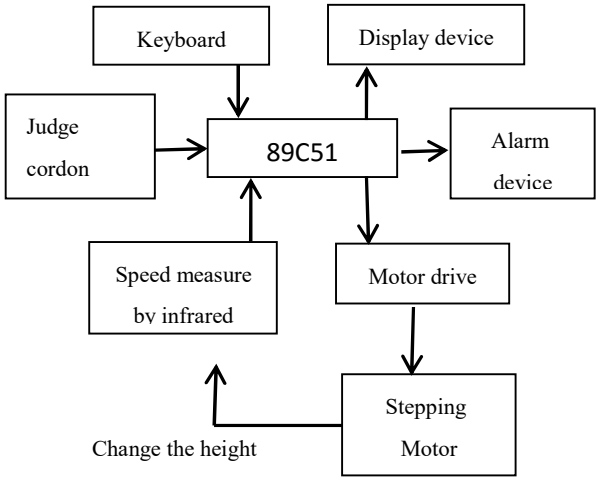

Fig.1 Device structure

B. Main Modules and Design

a. Speed Measure Methods

Infrared sensor in the modern practice is playing its important role with detection equipment and other parts and technology, infrared sensors can have more performance and better sensitivity. It is better to use infrared sensors to measure the bottom of the speed.

Using reflective infrared sensor is difficult to judge the water and using correlation infrared sensor can use water refraction, refraction that when water dropping makes the infrared signal receiver receives no signal, so better to correlation infrared sensor used.

Using correlation infrared sensor to detect the speed of water droplet at the funnel, and by measuring the time interval between two droplets to calculate speed. The infrared emission control and the receiver are relative, infrared light-emitting diodes emit infrared light, light through bucket drops shine on the photoelectric triode, optical transistor receives the optical signal into an electric signal output.The receiver receives the infrared signal and output low when no liquid drops;The receiver output pulse when liquid drops down.Due to sensor generates a irregular pulse signal,in order to let the microcontroller changes into the regular pulse signal,use LM339 design shaping circuits and use potentiometers to adjust a comparator threshold voltage to output regular waveform[2].

b. Liquid Level Monitoring Method

Liquid level detection with speed measuring principle is similar to using radiation infrared sensor to measure liquid level alarm level. Install correlation infrared sensor on liquid bottle neck,using full reflection principle can launches tube issued of signal full reflection to received tube,using received tube can accept to launches tube issued of signal, change its in circuit in the of level,using LM339 will change the signal to voltage jump,will its entered single tablets machine, according to corresponds to port of level changes to judge liquid bit whether below set of location to achieved alarm[3].

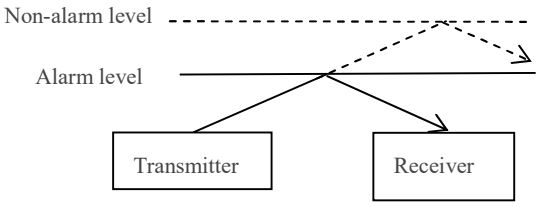

Fig.2 Level Monitoring Schematic

C. Stepper Motor Parts

Using the principle of stepping motor and pressure to control liquid drop speed.By the formular:

$$P=\rho*g*h \quad (1)$$

We can know because of different liquid height, the pressure is different, thus changing the liquid drop speed. Such a system better control than control the tightness of the hose, relatively easy to achieve,2-meter-high enough to achieve speeds from 30--140 (drops/min) Regulation[4].

First experiment about measure the height corresponding to the drop corresponding speed and saved in a microcontrollers and wait for calling. When you press enter on the keyboard a little speed, redeployed from the microcontroller corresponds to the height, and then coarse control stepper motor, with infrared feedback to fine-tune the system, until the infrared feedback match to the speed[5].

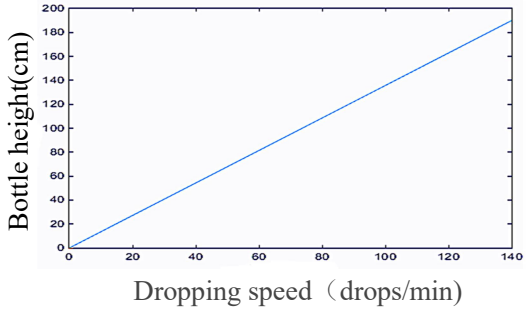

Fig.3 Bottle height and drop speed diagram

d. Mechanical Structure Parts

Mechanical parts by 4-8 stepper motor driven, motor driven by LM298N. Pulleys reduce the friction to reduce the out of step. Number of circles by a stepper motor can calculate the height of bottle variation.

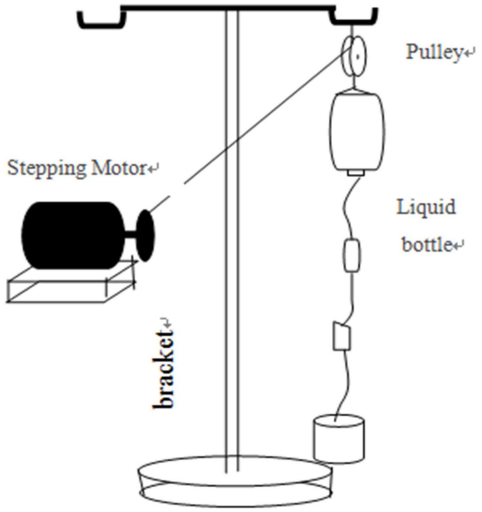

Fig.4 Mechanical structure diagram

Ⅳ. CIRCUIT DESIGN

A. MCU Part

Microcontroller control consists of a 80C51 single-chip, using serial works. 80C51 the main measurement of droplet velocity and control the stepping motor to call drop rate and judge the water level and the police.Microcontroller core and control centre of the whole system, all system data is sent to the SCM process, and all commands are issued by the SCM, so is the core part of the hardware and software[6].

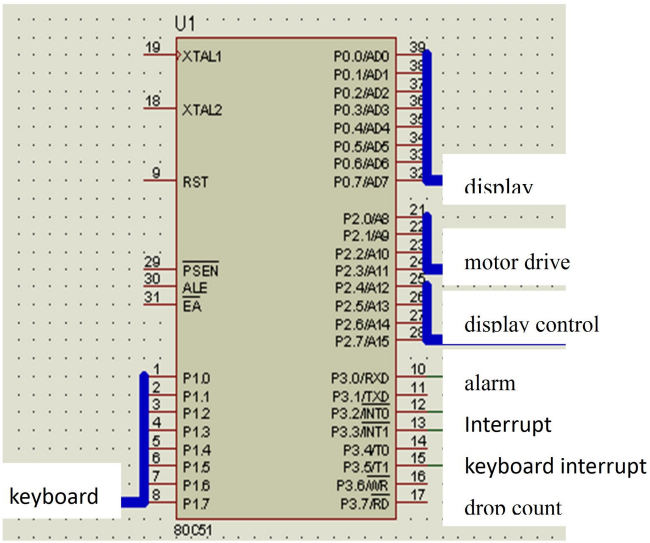

Fig.5 Microcontroller circuit

B. Signal Processing Part

Comparison of the infrared sensor and circuit, comparer LM339. LM339 voltage comparator chip with four independent voltage comparator, LM339 is a common integrated circuit. The small voltage comparators feature is the offset voltage, supply voltage range, restrictions on the internal resistance of the source a wide common-mode range is very large, the differential input voltage range, output voltage can be selected flexibly and easily.

Survey was to drop part of the sensor's output is about 2V--4V per cent jump, use a comparator with hysteresis, the door limiting voltage is set to 3.6V, the threshold voltage is set to 2.8V, signal shaping for the square wave. Measuring liquid level sensor output about is a 1V--3V jumping, door with comparator voltage limit is set to 2V, signal plastic SCM can jump[7].

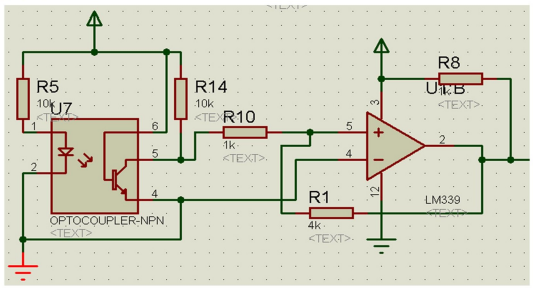

Fig.6 Signal processing circuit

C. Alarm Part

The alarm circuit using a buzzer, usually working current is large, TTL driver on the circuit not the buzzer, you need to add a current amplifier circuit can, the microcontroller pin hard drive the buzzer sounds, so adding a transistor to increase the current through the buzzer.

Join the positive end of the buzzer to 5V power supply, and received the transistor's collector on the other end, the base of the transistor from the P3.0 pins to control when P3.0 PIN to low, transistor break over, current loop of the buzzer, sound. P1.5 pin high, the transistor up, buzzer does not produce sound[8].

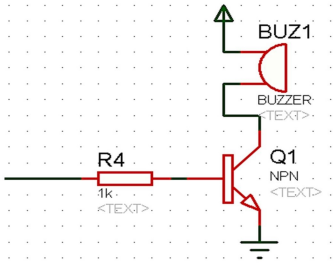

Fig.7 Alarm circuit

D. Motor Drive Part

In this circuit, we have chosen LM298N as a driver,

LM298N can provide bi-directional current for the load. Suitable for driving 2 or 4-phase stepper motors and DC motors, especially when driving motor direction when you want to change, just reverse motor direction of the position. LM298N drive motor 2A above for us to design the system, need to drive some heavier dropping bottle, LM298 motor driver module meets the requirements[9].

The system uses a stepper motor, can control precisely the height liquid, liquid drop speed is more accurate.

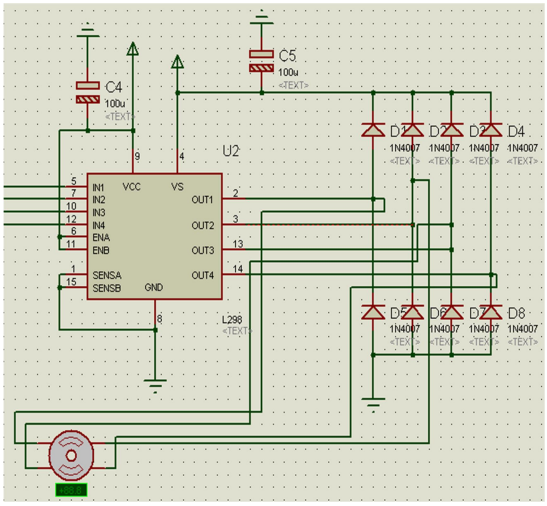

Fig.8 The motor drive circuit

E. Display Part

Use LCD1602 to display.It is a specifically designed to display letters,numbers, symbols, such as the dot-matrix LCD modules.It is made up of several dot-matrix characters such as 5*6,each a character dot-matrix characters can be displayed.Because P0 port no internal pullup resistor,you need an external pull-up resistor to display properly[10].

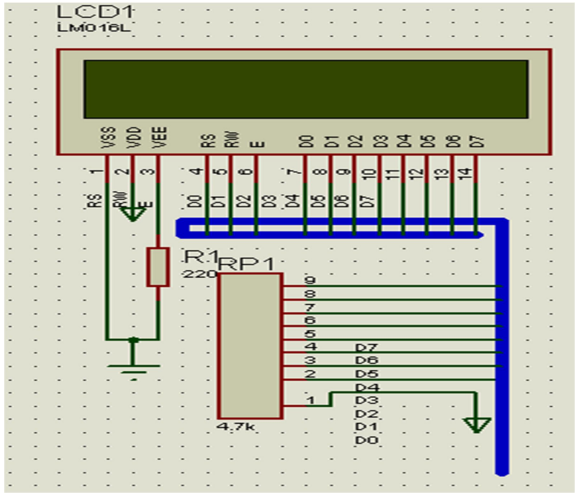

Fig.9 Display circuit

Ⅴ. SYSTEM SOFTWARE DESIGN

A. The Main Program

The main program includes interrupt to initialize and display initialization, speed and display will show the measured speed.

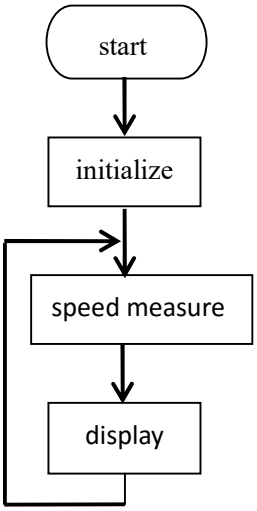

Fig.10 The main program flow chart

B. External Interrupt 0

This part is used to test the keyboard, once someone pressed a keyboard input when a droplet velocity, SCM will be compared with the current speed, faster than its small step motor controlled by SCM will pull up, faster than it stepping motor controlled by single-chip will go down[11].

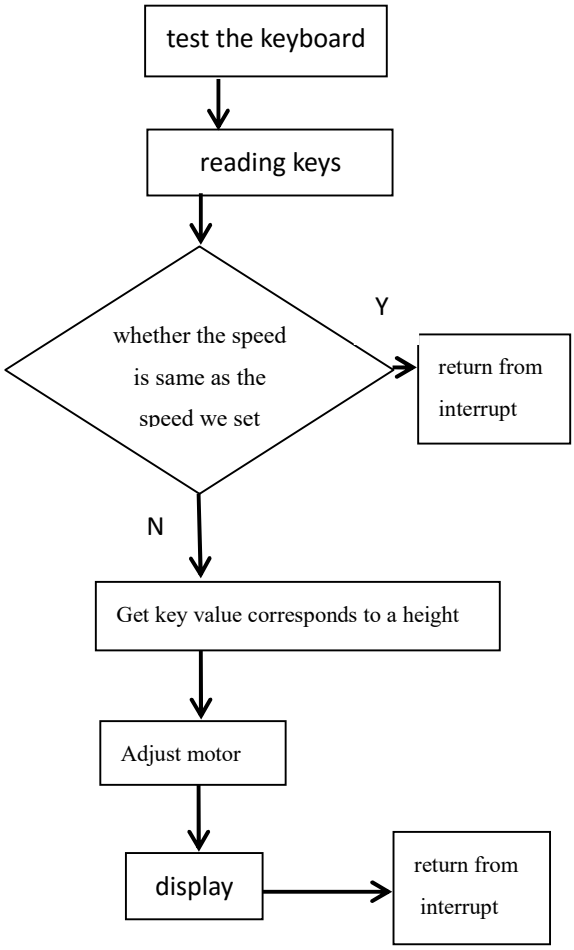

Fig.11 External Interrupt 0 flow chart

C. *External Interrupt 1*

External interrupt 1 used to monitor water levels, once the water level drops to a certain level, the sensor sends signal to the MCU, microcontroller Alarm buzzer program is executed[12].

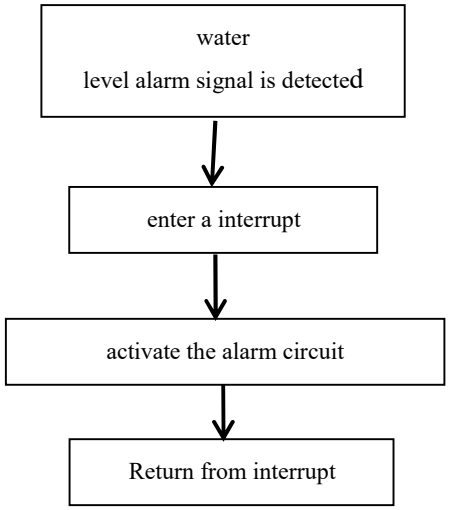

Fig.12 External Interrupt 1 flow chart

VI. Test Results

After the installation of the appliance, we used tape and stopwatch on the liquid heights and droplets to measure the speed, supported by several sets of data from data to draw the figure below.

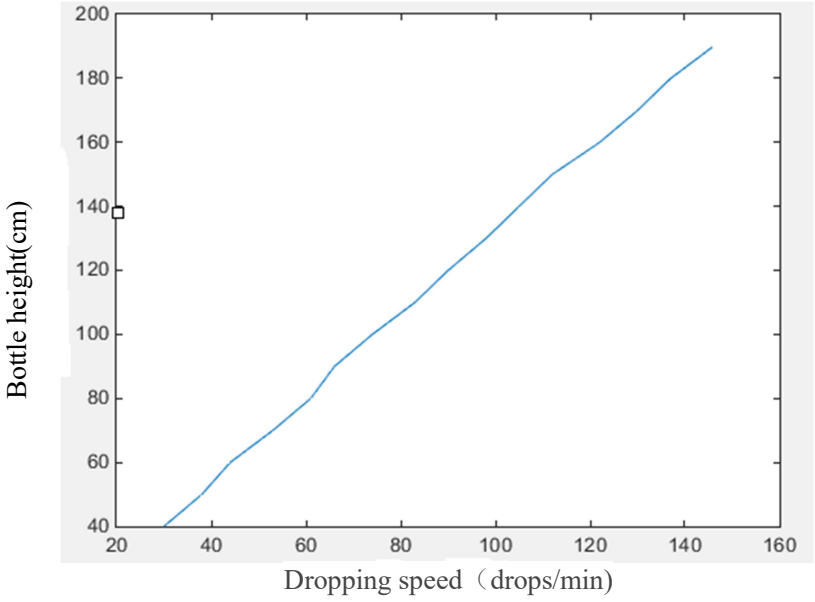

Fig.13 Bottle height and drop speed measurement diagram

From here you can see that, liquid speed is essentially proportional to the heights and droplets, agreement on a formula to calculate data, called coarse data of step motor, this error is very small and the bottle height adjustment according to speed.

When system runs,testing our speed parts,LCD screen displays data collected per second,choose a different bottle,collection for a minute, to error analysis to determine their accuracy.

And we have to adjust the time to do a test, adjusting

from a drop location to another location to see whether it meets the requirements of speed.

TABLE I

The results of the analysis speed

Actual speed （drops/min）	60	102	137
Measured speed （drops/min）	27 drops/min 1 times 39 drops/min 2 times 41 drops/min 3 times 57 drops/min 7 times 58 drops/min 7 times 59 drops/min 12 times 60 drops/min 10 times 61 drops/min 10 times 62 drops/min 5 times 75 drops/min 2 times 105 drops/min 1 times	41 drops/min 2 times 74 drops/min 3 times 99 drops/min 5 times 100 drops/min 5 times 101 drops/min 9 times 102 drops/min 8 times 103 drops/min 9 times 104 drops/min 10 times 105 drops/min 4 times 107 drops/min 3 times 138 drops/min 2 times	75 drops/min 1 times 76 drops/min 1 times 107 drops/min 2 times 132 drops/min 3 times 134 drops/min 9 times 135 drops/min 8 times 136 drops/min 8 times 137 drops/min 9 times 138 drops/min 7 times 139 drops/min 5 times 141 drops/min 6 times 150 drops/min 1 times

TABLE II

The test results of adjust time

Initial speed （drops/min）	140	30	60	110	140	90	40	30
Set speed （drops/min）	30	60	110	140	90	40	30	140
Actual speed （drops/min）	32	60	113	145	94	42	31	146
Time to adjust （second）	146	59	87	64	91	93	42	152

As can be seen in table I speed measurement function of the system is very accurate and fast drop height error will be larger, falling more slowly, the design speed is measured more accurately.

Table II shows that the appliance's adjust time and velocity error is accord with expected results.

Ⅶ. CONCLUSION

This thesis developed a new infusion to measure and control speed, alarm automatically system. The advantage of using infrared tube circuits and automatic alarm infusion drip rate measurement and control, and automatic alarm, to overcome the existing control speed warning device complex structure, high cost, bulky problem. Proven that the alarm system in a timely manner, easy to install, can effectively reduce the intensity of the work of the medical staff, while improving the level of hospital care, it has some practical value. However, there is so much hardware in the system , and applied to two infrared sensors. Although the system on the stability has some defects, it will not affect the normal work.

References

[1] He Qiao.Fundamentals of Mono-chip computers and applications.BeiJing:China railway Publishing House.2008

[2] Cheng Defu,Wang Jun,Ling Zhenbao,Wang Yanzhang. Sensor principle and application.BeiJing:Machinery Industry Press.2007.12.

[3] Yang Xinyu,Liu Zhengliang.Design and implementation of a liquid droplet velocity AT89C51 Based Monitoring

System[J].Journal of Qiqihar University.2005.21.（01）：55～57

[4] Dai Xinyu.Based photoelectric sensors accurately measure the concentration of the solution transparent research. Computer Measurement and Control.2005.03, 28-30.

[5] Yan Huailong. Microcontroller-based data acquisition system.Guangxi light industry.2006.06.82-83

[6] Song Xueli,Wang Hulin,Wan Jinling.Monitoring devices based on liquid droplet velocity SCM System[J].Computer Development & Applications.2007.20.(05).：43～44.46.

[7] Li Jianjun. Based stepping motor drive control system of the microcontroller[D]. South China University of Technology.2012

[8] Gu Zhijian. Single-chip stepper motor control system based on. outh China University of Technology.2013

[9] Meng Huiling,Luo Haitao.Liquid drip intelligent speed control system of fuzzy control algorithm[J].Xi'an International College.2007.03(02)：99～102.

[10] Ureten,O.Serinken,N.Wireless Security through RF Fingerprinting [J]. Electrical and Computer Engineering, Canadian Journal of, 2007, 23(1):27-33.

[11] Schroeder,ME Wolman,RL Wetterneck,TB Carayon,P. Tubing misload allows free flow event with smart intravenous infusion pump[J].Anesthesiology,2006, vol.105 no.2: 434~435

[12] Thiang. Implementation of Speech Recognition on MCS51 Microcontroller for Controlling Wheelchair [A] International Conference on Intelligent and Advanced Systems[C], 2007, 9:1193-1198.

Research of Virtual Seismograph Data Preprocessing

Guo Haozhe; Wang Danyang; Wang Yang
(College of Instrumentation and Electrical Engineering, Jilin University,Changchun 130026,China)

***Abstract*--In the course of geophysical, collected signals due to interference by Geophones, and complex construction site, making acquisition system the data corrupted by noise, inconsistent or incomplete, lead acquisition to seismic waves are not satisfactory, errors or errors are brought to subsequent analysis. To solve this problem, proposed virtual seismic data processing based on Matlab simulation research. By eliminating waste road, vertical stacking, automatic gain and filtering methods, removed some noise in seismic data and available information, improve the seismic data in the signal strength. Simulation results show that virtual seismograph data pre-processing can improve the signal to noise ratio of seismic signals, and through its processing of seismic data of 24 results, virtual seismograph data pre-processing is a certain practical and meaningful.**

***Key words*--Virtual seismograph seismic wave signal to noise ratio preprocessing**

I. INTRODUCTION

IN recent years, with the rapid development of geophysical instruments, we are increasingly using seismic waves, electromagnetic waves, such as geological exploration, energy and mineral extraction, water structure, or even used in defense, disaster warning and other fields. Geophysical instruments before processing an important part, is for signal preprocessing. Thanks to computer technology matures, signal preprocessing has been intelligent development, how to use computer software for automatic processing of the signals is the current research trends. Signal preprocessing can be weakened to filter out noise and retain or even strengthen the desired target reflection and improve signal to noise ratio, helps to improve the accuracy of the final results, reducing unnecessary labor and environmental interference, reduce the ultimate signal processing required to cycle. Signal preprocessing, can be said to make geophysical instrument outputs reliable basic protection[1-3].

II. THE SIGNIFICANCE

With the development of geophysical instruments, signal preprocessing and more important, in the course of geophysical, there are various disturbances, collected signals due to interference by Geophones, and complex construction site, making acquisition system the data corrupted by noise, inconsistent or incomplete, lead acquisition to seismic waves are not satisfactory, errors or errors are brought to subsequent analysis. As possible exclusion of manual and instrument error, weakening disturbance of the surrounding environment, get as close as possible to real, accurate signals required, on the latter part of efficiency of signal processing and instrumentation has a large performance impact. Signal preprocessing can filter the interference to a certain extent, improving the signal to noise ratio, signal preconditioning is very important in the process of signal analysis and processing[3].

III. IMPLEMENTATION

A. Research Thought and Methods

Simulation of seismic signals using Matlab software to simulate linear FM Chirp signal vibroseis (frequency of the frequency at the beginning and end frequency between uniform changes over time). To adding noise and attenuation, then the received signal pre-processing of simulation.

B. Implementation Plan

Simulation of linear frequency modulated Chirp signals (original) level targets (different media) onto the ground detectors, first eliminate the waste of road, thus obtaining the desired seismic signal simulations. And analog acquisition to seismic

signals associated with the excitation signal detection. Because of the seismic source signal is weak, so the vertical stacking technology needed to enhance the signal, facilitate the acquisition of seismic wave[4]. In the process, because of the deeper strata to greater attenuation of the signal, in order to get the different depth strata of signal strength close to automatic gain control of target reflection signal amplification and processing. Because of the resulting signal contains simulations of ambient noise interference and noise within the device itself, so need to filter the collected signals, through mathematical operations on collection of discrete signal filtering is performed. Filter out noise in the signal or false contents, improving the signal to noise ratio, interference signals. Figure 1 shows the data pre-processing steps and content[5]:

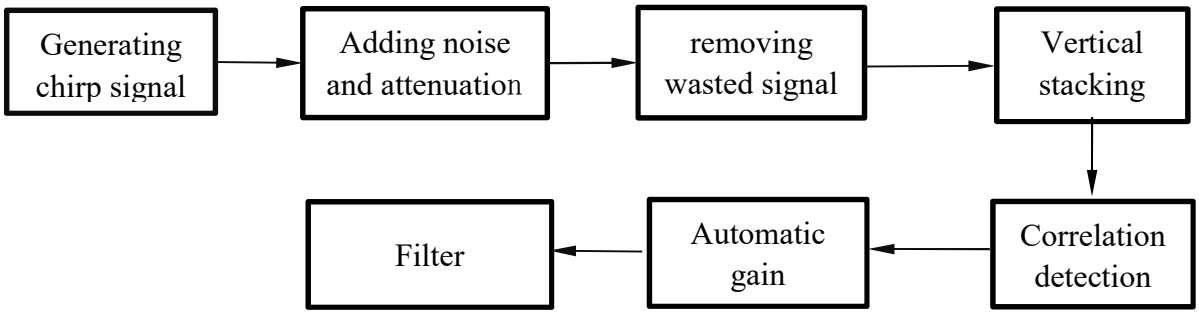

Fig.1 Data preprocessing steps and content

Ⅳ. FUNCTION

GUI interface consists of parameter settings, display Select button display in three parts. Parameter set can on inspired signal source of entered site value, starting frequency, terminated frequency, offset from, scan time for set; also can through on target layer of depth and geological components or earthquake wave spread speed of set, simulation multiple target layer situation of single signal pretreatment process; and can through sampling frequency, overlay times and filter way of adjustment, to for different situation of pretreatment simulation, through get of letter noise than to made better of select. Show selection button area when direct display option is used, each processing step can also be the graphics displayed, as shown in Figure 2:

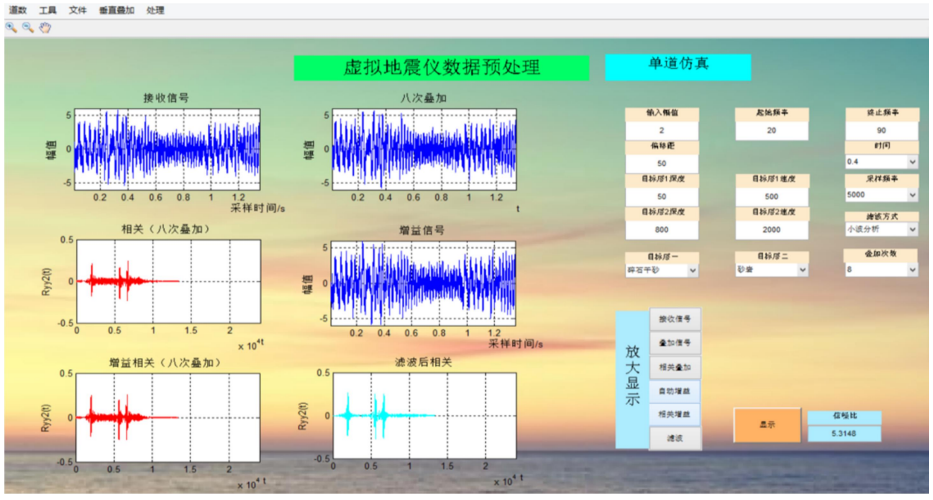

Fig.2 Single channel simulation interface

When using the left hand every step of the execution button, you can display each step corresponds to the graphic to enlarge,You can also use the tool bar above to enlarge it. For example, when using received signal button, as shown in Figure 3:

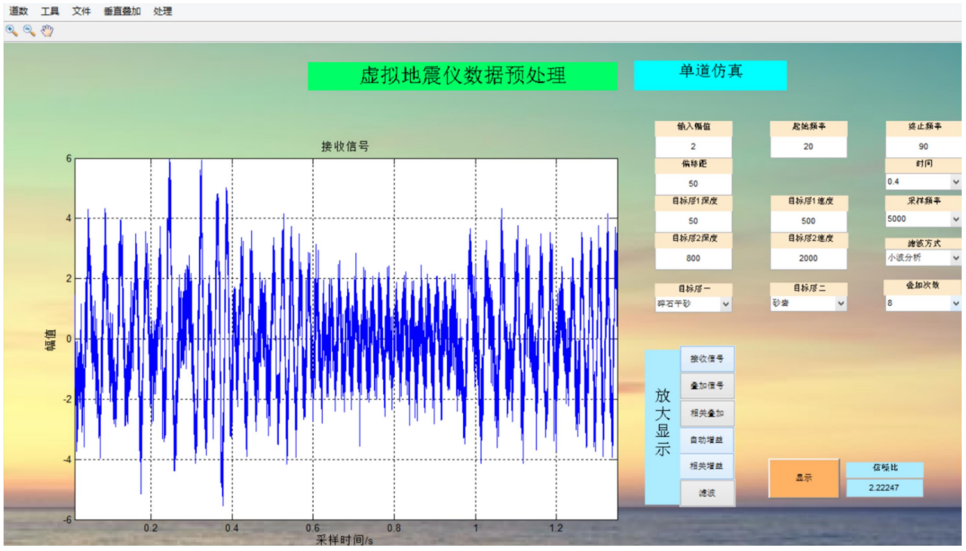

Fig.3 Receive signal display

Ⅴ.KEY TECHNOLOGY

A. Vertical Stacking

Using direct vertical stacking technology, by simulating the same source several times shooting, the collected signal vertical stacking, inhibiting random noise, improving the signal to noise ratio. Located i receive the signal of the detector as follows:

$$X_i(n) = S(n) + N_i(n) \qquad (1)$$

$S(n)$ is the reflected signal without noise, $N_i(n)$ is random noise as I recorded, without loss of generality, it is assumed that the expected value is 0,variance is σ_i^2, as well as assumptions $S(n)$ and $N_i(n)$ are unrelated, random noise in different records are not related.Set $\overline{X}_i(n)$ as output for direct vertical stack, then:

$$\overline{X}_i(n) = \frac{1}{M}\sum_{i=1}^{M} X_i(n) = \frac{1}{M}\sum_{i=1}^{M}[S(n)+N_i(n)]$$

$$= S(n) + \frac{1}{M}\sum_{i=1}^{M} N_i(n) = S(n) + \overline{N}(n) \qquad (2)$$

Visible,Useful signals is still $S(n)$ in Arithmetic average,Noise becomes:

$$\overline{N}(n) = \frac{1}{M}\sum_{i=1}^{M} N_i(n) \qquad (3)$$

Therefore, the use of vertical stack technique can reduce the power density uniform noise Gaussian white noise, can to a great extent weaken the effect of random noise for seismic signals.

B. Automatic Gain

Auto-gain technology, refers to the gain by choosing the appropriate value, reflected deep stratum with weak signal enhancement. To determine the gain value, first determine the attenuation of seismic trend and curve. Generally speaking, as the formation depth and geological composition, seismic wave propagation speed, the greater degree of attenuation of seismic signal, and with a frequency sweep signal, high frequency parts relative to the low frequency part more likely to decay. It can be seen that on a single target, sweep signal decay exponentially; for multiple targets, deep reflection for the shallow greater attenuation.

First of all, the known absorption parameters is $Q = 1.4 * V^{2.2}$, then the formula can be obtained by the following formula:

$$\frac{A_n}{A_0} = \exp(-Q^{-1}\pi f t_0) \qquad (4)$$

Including A_n is target reflected wave amplitude, A_0 for the initial amplitude, f for the seismic wave

frequency， t_0 is seismic waves two-way travel time。Through the acquisition to gain value corresponding to the signal is multiplied by A_0 / A_n， the received signal automatic gain can be realized.

C. Filter

Collect seismic signals often contain a lot of noise, like power noise, random noise caused by wind or cars, Gaussian white noise and so on, select the appropriate filter to filter noise, is a very important virtual seismograph data preprocessing step. First, we set a 49 to 51Hz band, band-stop filter frequency noise filter and reuse digital lowpass filtering to Gaussian white noise. To design the ideal frequency response of the filter was $\mathrm{H}_d(e^{j\omega})$， unit impulse response is $\mathrm{h}_\mathrm{d}(n)$， they are a pair of Fu-transform, it is:

$$\mathrm{H}_d(e^{j\omega}) = \sum_{n\to-\infty}^{\infty} h_d(n)e^{-jn\omega} \qquad (5)$$

$$\mathrm{h}_d(n) = \frac{1}{2\pi}\int_{-\pi}^{\pi} H_d(e^{j\omega})e^{jn\omega}d\omega \qquad (6)$$

In order to have a cause and effect and finite filter $h(n)$， the most straightforward way is to use the Windows function $\omega(n)$ to add its window handle. That is:

$$h(n) = h_d(n)\omega(n) \qquad (7)$$

Its frequency response is:

$$H(e^{j\omega}) = \sum_{n=0}^{N-1} h(n)e^{j\omega} \qquad (8)$$

Therefore, the digital low-pass filter using kaiser window, and Wavelet analysis in two ways[6][7], the seismic signal is filtered. Filter as shown in Figure 4, Figure 5, Figure 6:

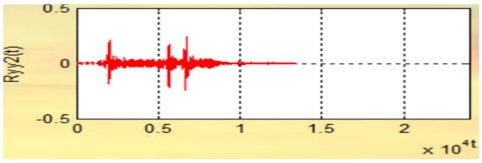

Fig.4 The signal before filtering

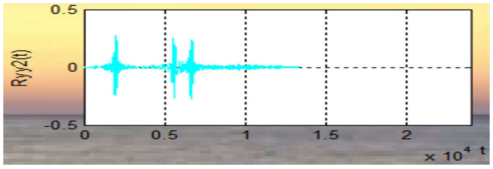

Fig.5 The signal after wavelet analysis

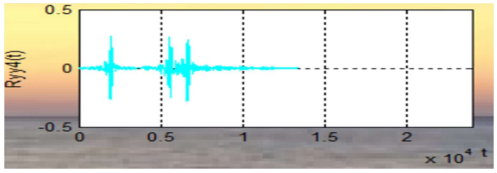

Fig.6 The signal after Kaiser window low pass filters

D removing wasted signal

Signal acquisition process, because of poor geophone coupling or due to the interference problem and circuit over, may be collecting obvious errors or not available signal, the signal needs to eliminate waste signal, for example, in Figure 7 below the 15th and 19 signal is the obvious waste of signal. Waste removal need to judge each one along with its former degree of correlation, two signals of $x(t)$ and $y(t)$, then the correlation function:

$$R_{xy}(\tau) = \lim_{\mathrm{T}\to\infty}\frac{1}{\mathrm{T}}\int_0^{\mathrm{T}} x(t)y(t+\tau)dt \qquad (9)$$

If its normalized is less than the set threshold, the judge to scrap signal, with the closest before the signal normal signal it replaced. Threshold selection is to reference statistics generally agreed that micro-related thresholds 0.3, can also be based on the entire set of data each and preceding cross-correlation of average of the normalized values for proper adjustment. Through the waste out of the seismic data as shown in Figure 8:

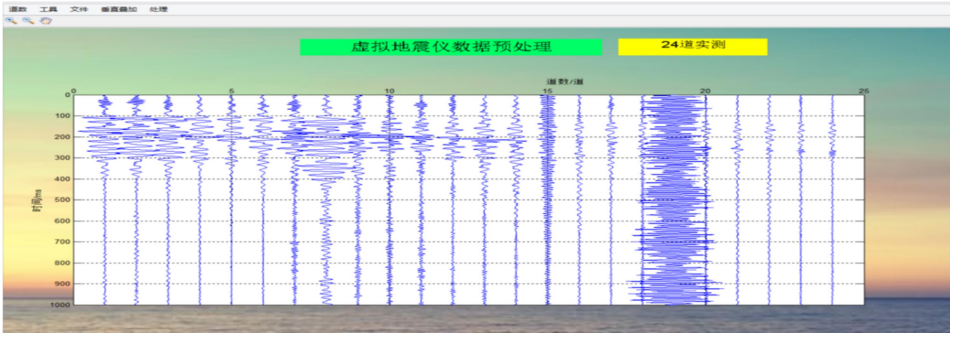

Fig.7 Before removing wasted signal

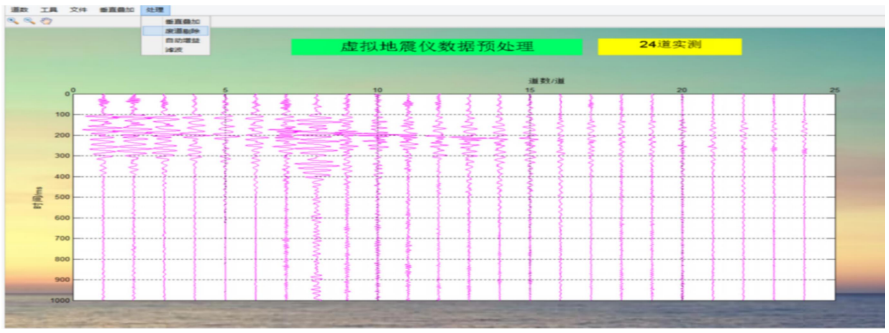

Fig.8 After removing wasted signal

Ⅵ. Results

Importing 24-ways data through the preprocessing of data than the original data changes, noise reduction, and more useful information, signal to noise ratio improves nearly 8dB, so virtual seismograph data preprocessing is a certain practical value.

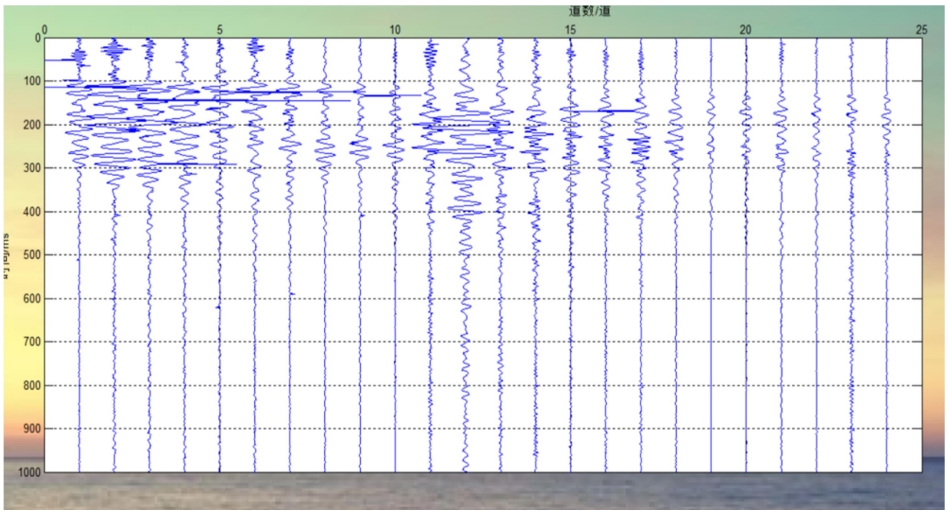

Fig.9 Data before preprocessing

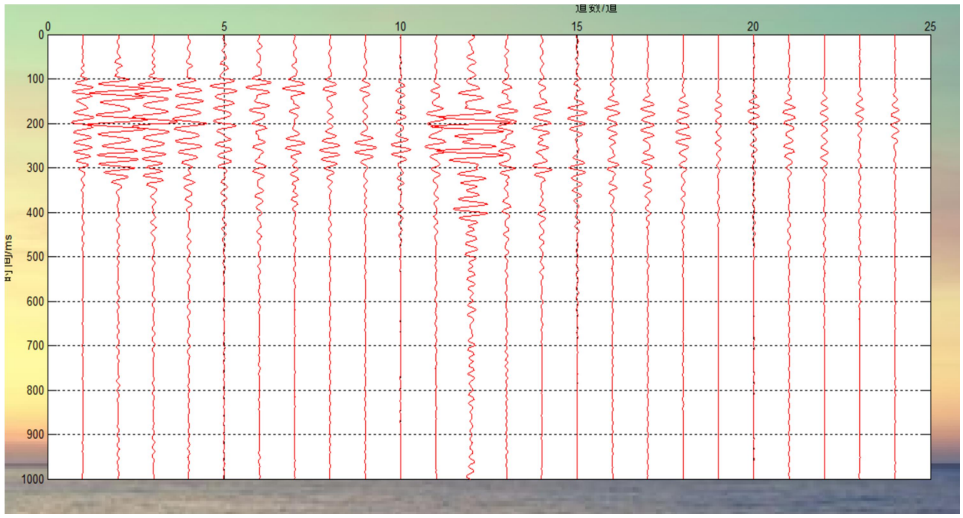

Fig.10 Data after preprocessing

Ⅶ. Conclusion

This innovative project has basically completed the expectations, realize Single channel Multiple Target layer signal pretreatment process and 24-ways simulation signal and 24-ways signal processing of measured data, waste can be carried out, after dealing with an increase in the signal to noise ratio, embodies the meaning of signal processing.

References

[1] Jiang Tao, Lin Jun. Vibroseis seismic correlation detection technology of phased [J]. Instrumentation Reported 2005,26 (4): 336-339.

[2] Zhang Zisan, Lin Jun. Analysis of vibroseis scanning techniques [J]. Petroleum Equipment, 1997,11 (6): 10-14+60.

[3] Wang Junqiu. Vibroseis metal ore and key technique of seismic exploration Test [D]. Changchun: Jilin University, 2013.06.

[4] Jiang Zhongjin. Elastic wave chirp signal detection and time delay estimation research [D]. Changchun: Jilin University, 2004,02.

[5] Deng Qiaolin. Seismic wave reflection and transmission of energy in the worst affected Analysis of reduction [D]. Changsha: Hunan University, 2013,05.

[6] Zhang Defeng. Matlab Wavelet analysis and its engineering application [M].Beijing: national defense industry press, 2008-2.

[7] Jiang Shubo. Chromatographic signal filtering based on wavelet transform application development [J]. Micro-computer, 2007,23 (8): 150-152.

Virtual seismic design based on LabVIEW

Xiaolong Lu; Yanhui Liu; Meiqi qin
（jilin university instrument science and engineering institute,changchun,130012）

***Abstract*--Field seismic exploration need to spend a lot of manpower and resources, it is difficult to achieve teach. The essay designs a virtual earthquake instrument that is based on the software of LabVIEW and simulating of the whole process of field seismic exploration. Let we can learn knowledge of seismic exploration in the interior and mastering the basics of operation. Designing exploration process is divided into multiple modules. It is to programming by the LabVIEW. Filter consists of the LMS algorithm that is making use of the MATLAB to programming. Be based on a single signal to build multichannel signal by the way of building array. Through reading and comparison of the actual measurement signal, Verifying the correctness of the virtual earthquake instrument and proving the feasibility study field seismic exploration in the Interior.**

***Key words*--Virtual instrument Seismograph LabVIEW**

I. INTRODUCTION

GEOLOGICAL survey seismic survey techniques are an important source of technology, using advanced seismic survey techniques, we can find many resources, such as oil and natural gas. In surveying technology in the seismic survey is the most frequently used and most effective technology.[1]The further development of seismic surveys are part of the solution to the energy crisis problem. Seismic survey and experimental needs in the field of environment, but also related to the need to carry equipment. The process brought great inconvenience to Trier, and the experiment will also need to consider the wild involves risk.

Today, the rapid development of computer technology, and because the virtual instrument is different from the traditional instrument is simple, the advantages of convenient use, virtual instrument technology has been continuously used. Virtual seismograph used in computer software, there is no real instruments in data processing, display and transmission constraints to simulate the seismic exploration process.[2]Virtual seismographs designed so that people can clearly understand the process of field seismic survey and user convenience, there's no need to experiment in the field, avoiding the risk of seismic surveys are likely to occur in the wild.

This study mainly using MATLAB and LabVIEW software for seismic signal to the whole virtual data acquisition process, first of all, to understand the actual exploration seismograph working processes and working principle, use of MATLAB and LabVIEW to this process and simulation instrument system design. Design is modular in design, the overall system is divided into different functional modules, modules one by one after achieving complete simulation of actual seismograph. And then designed a good visualization, adjustable parameters, simple virtual seismographs.[3] Graphical language LabVIEW instrument system with good visual and adjustable features, is easy to operate for the public. MATLAB is used for algorithm development, data visualization, data analysis and numerical calculation of high-level technical computing language and interactive environment, with powerful features. Use of MATLAB and LabVIEW software, two powerful software functions into full play and learn from each other, to improve the system design of the instrument.

II. THE SIGNEFICANCE

This study is the whole process of seismic exploration instruments for field work simulations and simulation of the seismograph basic composition. By simulation to show part of the seismic exploration equipment for field work, to Trier has brought great convenience, but also to avoid uncertainty of the field survey.[4]Virtual seismograph made familiar a seismograph of structures and functions of each part, and make it easier to understand the basic principles of seismographs. Through the design of a low cost, visualization, virtual seismographs with adjustable parameters, you can make it more convenient for

operation. Therefore, by making virtual seismograph seismic to simulation process is of great significance.

III .OVERALL DESIGN PLAN

This design is the whole process simulation of field seismic exploration. Figure 1 diagram of the process of seismic exploration as a whole. Signal source is system of signal occurred part, to produced test signal and simulation source signal; more road simulation switch is on signal source produced of signal for select; earthquake wave spread simulation part is simulation earthquake wave in underground spread and was detector received process; zoom device to will received of signal for Zoom; filter part is on received signal for drop noise processing, then get effective signal, storage displayed part is will processing Hou of signal for storage and will get of results displayed out.[5]

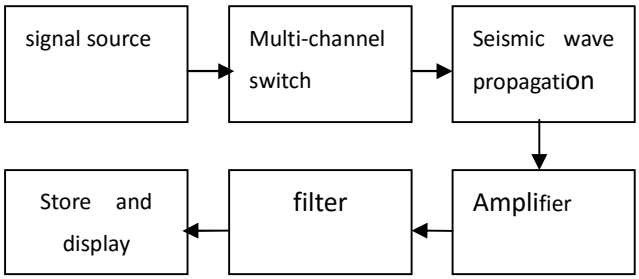

Fig.1: Overall design diagram

For the convenience of users of the operating system and study seismic exploration related knowledge, this design is divided into four modules, namely the source module, the Seismometer modules and parameters to set some module, displaying the result. This design is based on LabVIEW virtual instrument design for software platform, and through the design of complex signal simulation with MATLAB filter.

IV. VIRTUAL SOURCE MODULE BUILD

Virtual source mainly used in simulation of seismic exploration source section. In the actual field seismic exploration, commonly used excitation wave hammer, explosives and seismic vibrations. Here is the simulation of vibroseis vehicle-generated earthquake wave and vibroseis vehicle produces a linear changed continuous frequency sweep signal, this is an example of time-varying signals, are widely used in communications, radar, sonar, medical as well as seismic and other signal processing areas.[6] Virtual source include test signal simulation, seismic signal simulations, formation simulation in three parts.

A. Seismic signal simulations

Artificial stimulation of seismic waves using vibrator, is now a commonly used method of seismic exploration. This method of seismic waveform is known, is during the scan frequency chirp linear increasing or decreasing over time (chirp) signal[7]. Figure 2 is a linear frequency-modulated signal waveforms.

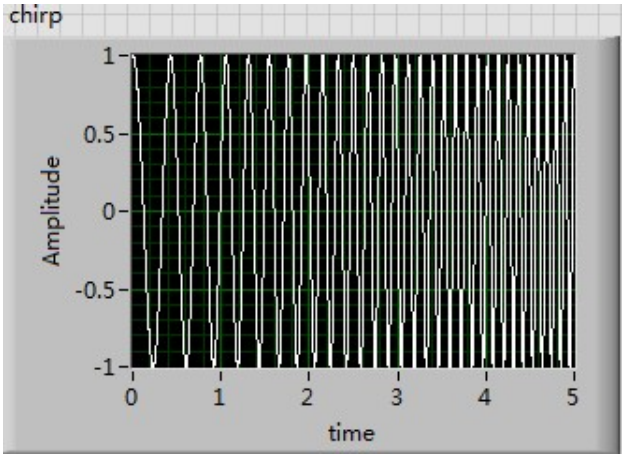

Fig.2: Linear frequency-modulated signal

This design of chirp signal call MATLAB nodes to LabVIEW Simulation. In LabVIEW, you can write a MATLAB program by calling the node. Has a specific function in MATLAB to chirp signal adjustable parameters. The main parameters are signaling the start time, signals an end time, signal instantaneous frequency, signal the instantaneous frequency of the end times. Program source signals as shown in Figure 3.

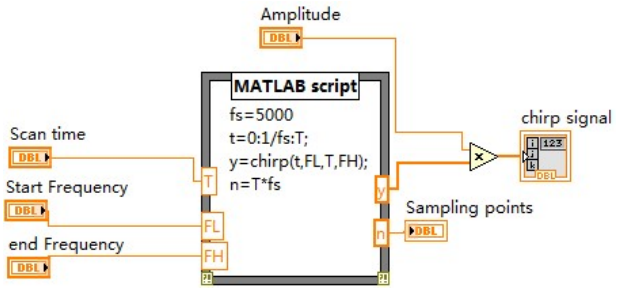

Fig.3: The source signal program

Sources also produce three test signals: random noise, sine wave and pulse. Simulation source in order to facilitate these types of signals and signals for the choice, we need to design a multi-channel analog switch. Conditions of this design will take advantage of LabVIEW structure to achieve this function,

specific procedures, such as in Figure 4.

Seismographs can receive a variety of signals: three test signal with the signal. In order to facilitate these kinds of signals are selected, you need to design a multi-channel analog switch. Conditions of this design will take advantage of LabVIEW structure to achieve this function, specific procedures, such as in Figure 4.

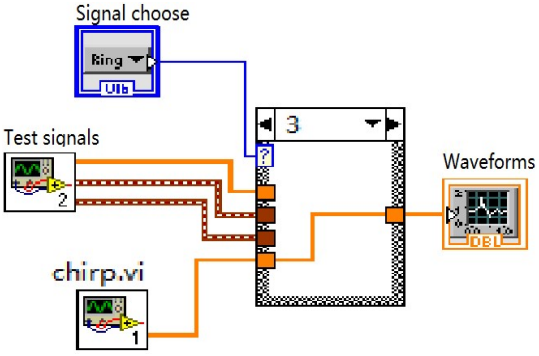

Fig.4: Multi-channel analog switch

B The Underground Simulation Of Seismic Wave Propagation

When the source after the seismic wave, in part through the detector directly on the ground receiving, this part is called the direct wave, after reflection, the others into underground detectors to receive, this part is called the reflected wave. Seismic wave propagation in the ground, when two interface interfaces are encountered, formed a portion of the energy is reflected back to the original media reflections and then received by the detector, another part of the energy through the interface into the next medium. [8]In this design, only assumptions of seismic waves through a single interface.

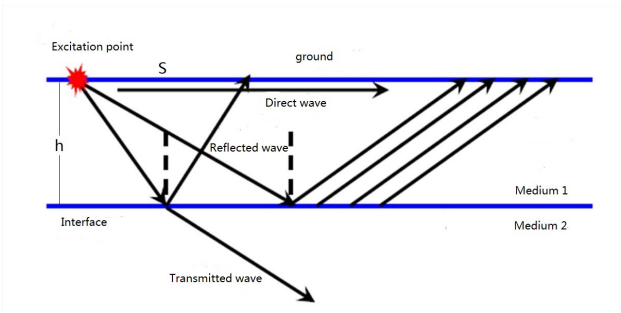

Fig.5: Seismic wave propagation

Assuming the shot point distance of the first detector to S, distance to the surface of the ground for h, seismic wave velocity to be V, you can get source seismic wave reflection reaches the first detector after time T.

$$T = 2\frac{\sqrt{\frac{S^2}{4} + h^2}}{V} \quad (1)$$

Happened due to seismic waves excited by ground reflection, transmission, loss of energy, and underground media will absorb seismic energy, so the detector is a significant decay in amplitude of the received signal, need to enlarge it for further processing. Due to shooting and receiving conditions, the natural environment and the effects of surface conditions, geophone seismic signals received by the also contains a lot of noise, the variety of things and more difficult to deal with, the design only three typical noise simulation: frequency noise, Gaussian white noise, random noise.

By equation (1) can be obtained by the LabVIEW detector receives the reflected wave does not contain noise.

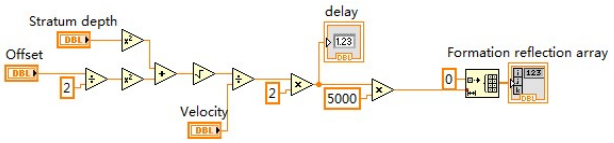

Fig.6: Without noise reflection wave program

Simulation noise added to the reflected wave, and can be called noise waveform control in LabVIEW to simulation. In order to make the program more concise, this design of chirp signal formation process of reflection, noise simulation VI. Module program is implemented.

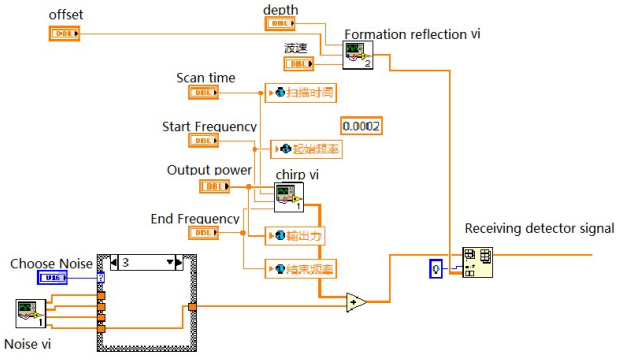

Fig.7: The reflected wave simulation

V. SEISMORGRAPH IN MODULE CONSTRUCTION

Seismic exploration instruments General recorded

by seismometers, amplifying and filtering processes, the system consists of 3 parts. Seismic vibration detector parts can be picked up directly, and convert the vibration energy instruments record form. Magnification filter part of the role is to filter the faint signal detector output noise and gain control. Recording system to record signals in different ways. Detectors, amplifying and filtering processes, composed of 3 basic parts of records a trace. Seismographs are usually multiple, followed by road will be constructed through a signal signal.

A. Filter part

Seismograph module receives the signal contains a lot of noise, and will seriously interfere with signal detection, noise processing need to design filters. This design using LMS Adaptive Filter combined with band-pass filter design algorithm. Since the chirp signal is frequency range, frequency in linear change between the initial frequency F0 and the end frequency F1, so using a band-pass filter with F0 and F1, respectively, as a low-pass filter, high pass cutoff frequency. Overlap in the frequency, this design using adaptive filtering LMS algorithm for noise reduction. Adaptive Filter is a filtering method developed in recent years. It is in the Wiener and Kalman filtering of linear filter developed on the basis of a filter. And it is more adaptable and better filtering capability.

LMS algorithm is a linear adaptive filtering algorithm, generally consists of two basic processes:

(1) the filtering process: calculating linear response of output to input signals by comparing the output with the expected response estimation error.

(2) adaptive processes: automatically adjusts the filter parameters according to estimation error.

Their specific program in Figure 8:

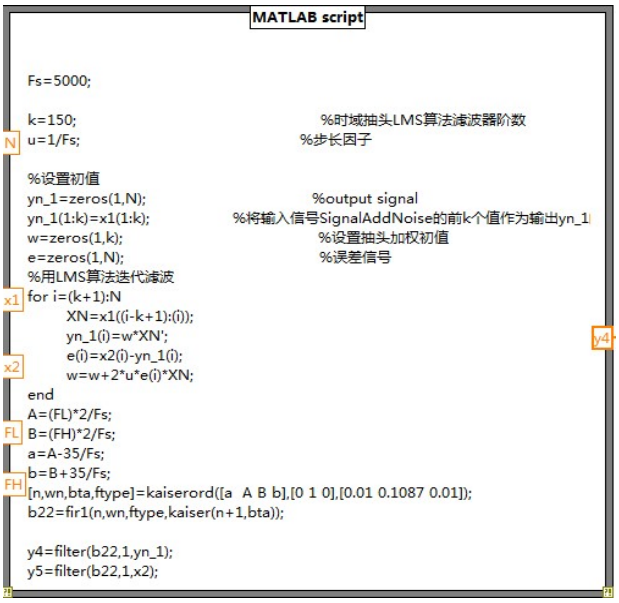

Fig.8: Filtering algorithm program

In order to verify that the filter effect is good or bad, must be filtered before and after the signal to noise ratio, its get procedure as in Figure 9:

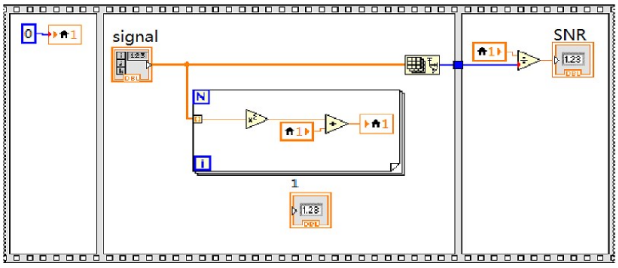

Fig.9: Calculating a signal to noise ratio

B. Recording system

Data storage module of this design is the result of filtering with a. txt format file to your computer. In LabVIEW, write spreadsheet VI is called a filtered signal as an input, as a string data type, enter the address of the computer you want, enabling data storage this function. Waveform data stored procedure as shown in Figure 10:

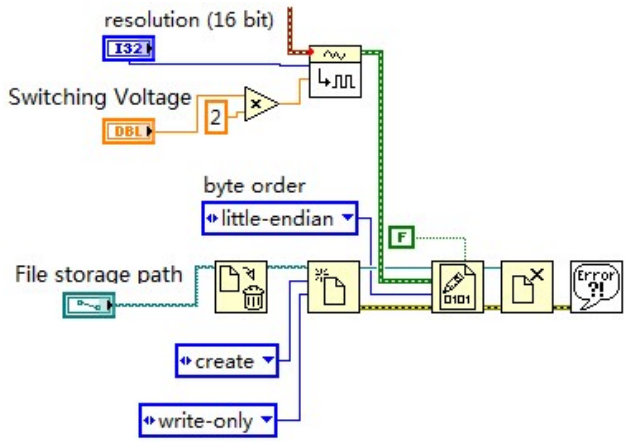

Fig.10: Waveform stored program

VI. PARAMETER SETS THE MODULE CONSTURCTION

Set up in the module, you can select and set parameters of the input signal, you can choose to join the noise signal, and can also set the wave velocity, offset, channel space, depth and other environmental parameters and amplification, stores paths, AD Seismometer parameters such as resolution. This module is designed to allow users to operate the entire system, no need to jump between each interface operation.

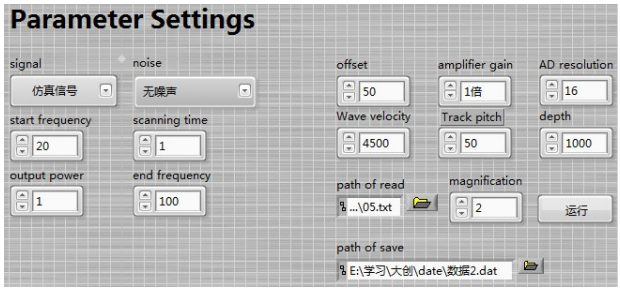

Fig.11: Parameter settings on the front panel

The front part back panel program is the virtual source and Seismograph of the part VI, then called VI to finish each part. Due to this design simulation shows 24 seismic signals, so need to write 24 waveform construction program.

Analog 24 signals in this design is implemented as array operations in LabVIEW, analog 24-detector receives seismic signals, 24 Avenue signal spacing, offsets can be adjusted. Each detector receives signals transmitted by ground direct reflection reflection and formation, and mixed with the noise in the communication process. And then to follow up on adding 24 signal amplification, filtering, and ultimately stored in the computer.

Construction method of the array consists of a single simulation 24 signal road signal, a single channel signal as an input, use an array initialization control to determine the length of the array, and then create an array using controls to create an array of 24 of the same. While structure to delay processing the array of 24, a total of 24 cycles. In while structure in the, using delete array elements controls followed by out 24 a array, using a dimension array cycle displacement controls on out of array for two times translation, first times of translation is direct wave spread of time, second times only need translation reflection wave and direct wave spread of time, 24 a array are after such of processing, then using array insert controls followed by will 24 a array plug back original array. While offering after each processing input and output shift register to save the results. After 24 loop, for 24 signal simulation is complete.

Original part VI called noise, choose Gao Sibai, random noise and frequency interference and other noises.

Delay time formulae:

$$t_{直} = \frac{s + id}{u_1} \qquad (2)$$

$$t_{反} = \frac{2\sqrt{\left(\frac{s+id}{2}\right)^2 + h^2}}{u_2} \qquad (3)$$

S spacing is user adjustable offset and d road, h-depth, i cycle, u1 is the propagation velocity of seismic waves in the Earth's surface (3200m/s), the u2 for seismic wave propagation speed for user input in the formation.

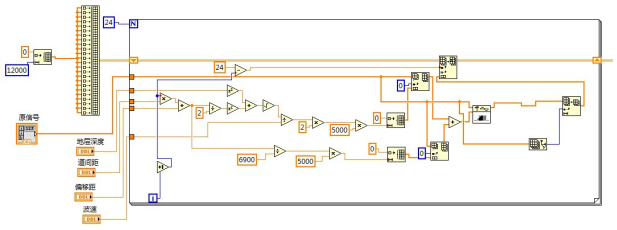

Fig.12: 24 Channel signal building

VII. DISPLAYING THE RESULT

Results display module can display source signal, the detectors receive signal, the filtered signal, filter before and after the relevant signal and simulation signal and measured 24 24 signals. By visualizing the results of each part, and allow users to clearly understand the entire process of seismic exploration. This design is to achieve this by means of a global function, to output the results of the preceding sections as a global variable, then calls the global variable to display the results of each part.

In LabVIEW, if you need to use a global variable, it is necessary to establish a separate global variable VI, the VI has one input and one output, and cached when

the data input in the global variables in the VI can be called at any time. Establishing global variable data format must be set when the variables, global variables corresponding to the entry must be a data format.

Fig .13: Global variable settings

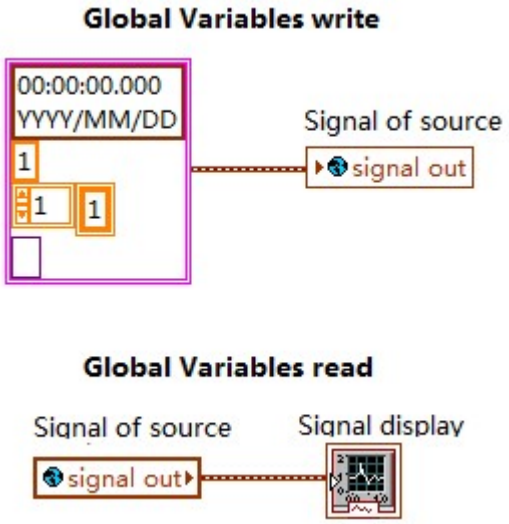

Fig. 14: Global variables written calls

VIII. CONCLUSION

Based on the LabVIEW software platform designed a virtual seismograph, simulation of field seismic exploration of the whole process and displays the results of each part of the process, more intuitive display seismic exploration process, making it easier for teaching. LMS Adaptive Filter algorithm in the design of filters designed to increase SNR 20dB, allowing earthquakes to be effectively extracted. This virtual instrument used in teaching provides an example, present virtual instrument technology is booming, but now teaching of many instruments is difficult to implement. Virtual instrument is widely used in instrument teaching.

References

[1] Junhua Liu. Design Of Virtual Instrument Based On LabVIEW. electronic publishing house in Beijing, 2013.

[2] Yuan Yuan, Jun Gu. Virtual Instrument Based Tutorial [m]. Chengdu: University Press, 2010.

[3] Shanbang Li. Early Development Of Seismic Survey In China [j]. Journal of Northwest earthquake, 2000.2 (1): 1-5.

[4] Leping Yang, Haitao Li,. LabVIEW Programming And Application [m]. Beijing: Beijing Publishing House of electronics industry, 2002.

[5] Junhua Liu, Huiqin Jia. Virtual Instrument And LabVIEW Graphical Programming Language Tutorial [m]. Xian: Xidian University Press, 2011.

[6] Kai Zhang. LabVIEW Virtual Instruments Engineering Design And Development [m]. Beijing: national defense industry press, 2012.

[7] Xiaoquan Han. Status And Development Trends In Seismic Exploration Instrument [j]. geophysical equipment, 2011,3-181.

[8] Ling Cheng, Dongdong Xu. Application of MATLAB In Simulation In Communication Principle Teaching [j]. laboratory research and exploration, 2010,29 (02).

MRS parameter extraction method based on BP neural network

Jinming Jiang; Zhenyu Zhou; Ying Yang; Chuandong Jiang
(Instrument Science and Electrical Engineering, Jilin University, Changchun 130000)

***Abstract*--In order to realize the four key parameters extraction, the initial amplitude, mean relaxation time, frequency deviation and initial phase of the magnetic resonance sounding (MRS) signal for the groundwater detection, a nonlinear fitting method based on BP neural network is proposed in this paper. The modeling method of nonlinear fitting of BP neural network is studied. The four key parameters extraction and the design of graphical user interface are realized. Using linear fitting , nonlinear filling and BP neural network are used to extract the four parameters of MRS signals with different signal-to-nosie ratio, by comparison, the MRS parameter extraction method based on BP neural network has the highest accuracy and stability.**

***Keywords*--MRS signal,BP neural network,key parameters extraction**

I. INTRODUCTION

THROUGH extracting the initial amplitude, mean relaxation time, frequency deviation and initial phase of MRS signal, the hydrogeological parameters is calculated, therefore, we can obtain the distribution of underground aquifer and the size of water content , and estimate the permeability ,hydraulic conductivity and the size of the water inflow , which provide quantitative reference for groundwater wells and water capacity. When the SNR is high , linear fitting and nonlinear fitting method are used to achieve better extraction effect, but the problem is still in the low SNR [1].So it is necessary to seek more accurate methods to extract nuclear magnetic resonance signal parameters.

As a typical algorithm of artificial intelligence network, the BP neural network has the advantages of simple structure, high precision, easy to use programming, etc. and has strong nonlinear mapping ability, the BP neural network is one of the most important algorithms to solve some nonlinear problems, and one of the most important algorithms in the field of intelligent . Based on these advantages, based on the BP neural network fitting method is used to extract the MRS signal parameters in this paper .We can build a suitable neural network model, initialize input data for training the neural network, and then input test data to extract parameters, in order to get more accurate parameters.

II.RESEARCH FOUNDATION

In order to facilitate the extraction of parameters, first of all, the two orthogonal signal of the MRS signal envelope signal is simulated[2].

$$E(t) = x(t) + i \cdot y(t) \quad (1)$$

$$x(t) = E_0 e^{-t/T_2^*} \cos(\delta\omega t + \varphi_0) + \varepsilon_x(t) \quad (2)$$

$$y(t) = E_0 e^{-t/T_2^*} \cos(\delta\omega t + \varphi_0) + \varepsilon_y(t) \quad (3)$$

Among them, $E(t)$ is a time domain signal of MRS, δω is the difference between receiving angular frequency and Larmor angular frequency ω0, and εx(t) and εy(t) is the combined effect of various noises. Taking

t = 0~1s,E0=200nV, T_2^* = 0.4s, δf = 0.5Hz,

φ_0 =0, SNR=10 to obtain the ideal X component, Y component signals MRS FIG 1 (a), 1 (b) in Fig.

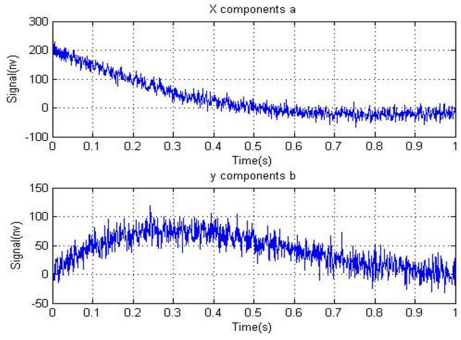

Fig. 1 .MRS signals X, Y component

A. linear fit

In order to extract the initial amplitude E_0 and mean relaxation time T_2^*,Linearization of Formula 1,obtaining:

$$L(t) = \log(|x(t) + i \cdot y(t)|)$$
$$= \log(E_0) - \frac{t}{T_2^*} + \varepsilon_L(t) \quad (4)$$

Among them, ε_L is the transformed mold noise of x and y components . Visible, the curve after transformation is linear with respect to time variable , and can use the least squares straight line fitting to obtain E_0 and T_2^*. Similarly, in order to extract the initial phase ϕ_0 and receive frequencies δf , following conversion of the Formula 1:

$$\mathrm{A}(t) = \arg(x(t) + i \cdot y(t))$$
$$= 2\pi \cdot \delta f \cdot t + \phi_0 + \varepsilon_A(t) \quad (5)$$

Among them, ε_A is transformed Phase noise. Available obtained by least squares linear fitting ϕ_0 and δf ,Receiving frequency $f = f_0 + \delta f$. Apparently due ε_L and ε_A , the four key parameters are extracted an error, it should be possible to improve the SNR [3].Based on the above principle, linear fitting, inthe case of SNR=10, the amplitude and phase of the fitted curve are shown in Figure 2 (a) 2 (b) below. We can see a higher SNR, the better the effect of linear fit.

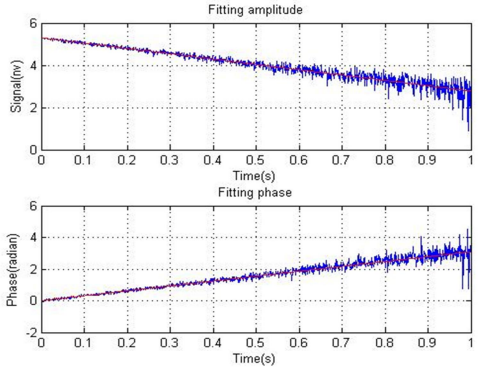

Fig. 2.Linear fitting curve

B. nonlinear fitting

In order to reduce $\varepsilon_x(t)$ and $\varepsilon_y(t)$, It can be based on the minimum mean square nonlinear fitting methods, definitions function

$$\min[\sum_k (x(t_k) - x_c(t_k))^2 + \sum_k (y(t_k) - y_c(t_k))^2] \quad (6)$$

Among them

$$x_c(t) = E_0 \cdot \cos(2\pi \cdot \delta f \cdot t + \phi) \cdot \exp[-t / T_2^*] \quad (7)$$
$$y_c(t) = E_0 \cdot \sin(2\pi \cdot \delta f \cdot t + \phi) \cdot \exp[-t / T_2^*] \quad (8)$$

δf is representative of the frequency deviation, E0 is represents of the initial amplitude, ϕ is Representative of the phase, the above principle, based on nonlinear fitting method minimum mean variance of x, y component extracted by fitting the four parameters [4] .In the case of SNR=10, the fitting curve in Figure 3. It can be seen lower SNR, the better the effect of nonlinear fitting.

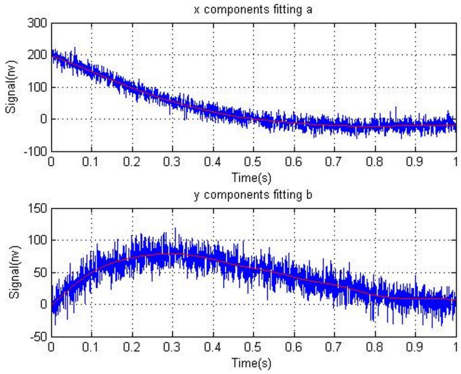

Fig. 3 .Nonlinear curve fitting

III.BP NEURAL NETWORK NONLINEAR FITTING

A. Principle scheme

BP network construction, the first to determine the nonlinear function of the input, the number of output.BP neural network to determine the structure and input layer, hidden layer, the number of nodes in the output layer, input and output data with nonlinear function of neural network training, so that the network can predict the output of nonlinear function .Firstly, the input and output data of the N group are obtained from the nonlinear function, and the most training data are used to train the network in the M group. The rest of the N-M group as the test data for testing the

performance of the network fitting. The fitting process as shown in Figure 4 [5].

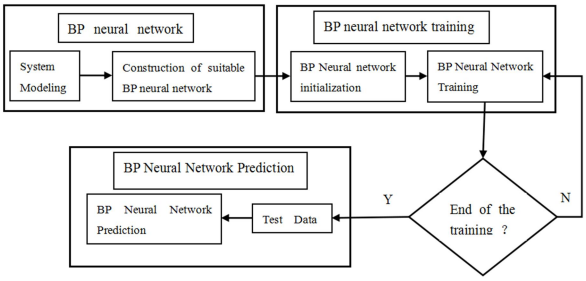

Fig.4. BP fitting process block diagra

B. Design

The simulation data were randomly selected in the 2000 groups, the data were normalized mapminmax, and the BP neural network with single input and double output was constructed.In order to make the data fitting effect better, and select the single hidden layer node number is 6, the number of iterations for 100, the learning rate is 0.1 and target error 0.00004 of BP neural network for training and the X, Y component of predictive output and reduce the error and then fitting the nonlinear parameter extraction [6] .The BP neural network model is shown in Figure 5.

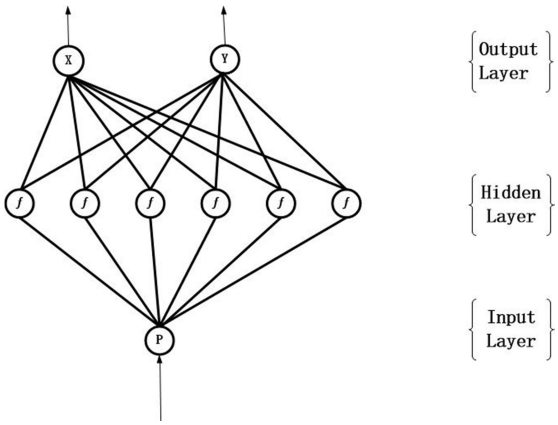

Fig.5. BP artificial neural network model

IV. User Interface Design

Design idea is to create a new graphical interface, and then add a button on the GUIDE interface, and finally add the button to the program code to achieve the function of the display[7].Guide interface, there are three buttons, respectively, on behalf of the linear fitting amplitude fitting and phase fitting drawing, drawing the nonlinear fitting of the x component fitting and Y component of the fitted, BP neural network is used to fit the x component fitting and Y component of the fitted and 20 times the initial amplitude, the average decay time, frequency deviation and the initial phase is a state density curves of histogram[8]. The user interface is shown in figure6:

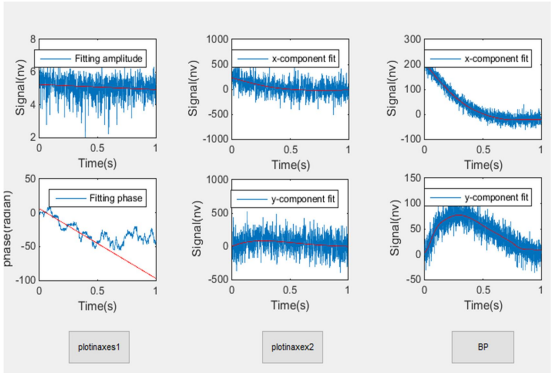

Fig.6 .User interface

V. Comparison of the Results

Selecting the initial amplitude for 200 NV, the average decay time is 0.4 s, frequency deviation for 0.5 Hz, the initial phase is 0 DEG, substitute it into formula (1) calculated by MRS Signal in time domain.And add 5%, 10%, 20%, 100%, 1000%, of the Gauss noise.

The accuracy of the key parameters of the initial phase is extracted by comparing the different methods to extract the initial amplitude, mean time to decay, frequency deviation. four key parameters are extracted by using linear fitting, nonlinear fitting and BP neural network nonlinear fitting method.Results are shown in Table 1, table 2, table 3, table4, table 5.

From the table, when the SNR is 20, the four key parameters are obtained by using the linear fitting method. The key parameters of nonlinear fitting method and BP neural network are used to obtain the key parameter error. When the signal to noise ratio is 10, the four key parameters are obtained by using the linear fitting method.The key parameters of nonlinear fitting method and BP neural network are less error. When the signal to noise ratio is 5, the four key parameters are obtained by using the linear fitting method.The key parameters of nonlinear fitting method and BP neural network are less error. When the signal to noise ratio is0.1, the four key parameters are obtained by using the linear fitting method.The key parameters of nonlinear fitting method and BP neural network are less error. But the same data, linear fitting, nonlinear fitting can only be extracted once

parameters.But BP neural network can be used for the same data samples randomly selected data fitting, selection of 20 times. Although the fitting effect of BP neural network and nonlinear approach, but the same time for each signal to noise ratio of the same data fitting 20 data statistics, compared with the previous fitting method to improve the reliability of the extraction of four parameters.

TABLE I

SNR =20 PARAMETER EXTRACTION RESULT OF THE COMPARISON

SNR = 20	Initial Amplitude (nV)	Error%	The average decay time (s)	Error%	Frequency Deviation (Hz)	Error%	Initial Phase (rad)	Error%
Linear fit	200.139	0.070	0.320	20.050	0.498	0.480	0.004	0.410
Nonlinear fitting	200.294	0.147	0.400	0.100	0.500	0.020	5.721 e-004	0.005
BP neural network nonlinear fitting	200.023	0.012	0.400	0.025	0.500	0.020	0.001	0.010

TABLE II

SNR =10 PARAMETER EXTRACTION RESULT OF THE COMPARISON

SNR = 10	Initial amplitude (NV)	Error%	The average decay time (s)	Error%	Frequency deviation (Hz)	Error%	Initial Phase (rad)	Error%
Linear fit	193.631	3.184	0.321	19.725	0.496	0.880	0.008	0.750
Nonlinear fitting	200.588	0.294	0.399	0.200	0.500	0.040	0.001	0.110
BP neural network nonlinear fitting	199.630	0.185	0.400	0.025	0.498	0.320	0.000	0.020

TABLE III

SNR =5 PARAMETER EXTRACTION RESULT OF THE COMPARISON

SNR = 5	Initial amplitude (NV)	Error%	The average decay time (s)	Error%	Frequency deviation (Hz)	Error%	Initial Phase (rad)	Error%
Linear fit	173.320	13.340	0.322	19.400	0.494	1.260	0.011	1.060
Nonlinear fitting	201.176	0.588	0.398	0.400	0.500	0.060	0.002	0.230
BP neural network nonlinear fitting	199.819	0.091	0.401	0.125	0.502	0.340	0.001	0.100

TABLE IV

SNR =1PARAMETER EXTRACTION RESULT OF THE COMPARISON

SNR = 1	Initial amplitude (NV)	Error%	The average decay time (s)	Error%	Frequency deviation (Hz)	Error%	Initial Phase (rad)	Error%
Linear fit	197.444	1.278	-0.014	error is too big	-11.695	error is too big	16.261	error is too big
Nonlinear fitting	205.891	2.945	0.392	1.975	0.500	0.180	0.011	1.050
BP neural network nonlinear fitting	196.660	-1.667	0.482	-3.645	0.411	2.825	0.011	1.074

TABLE V

SNR =0.1 PARAMETER EXTRACTION RESULT OF THE COMPARISON

SNR = 0.1	Initial amplitude (NV)	Error%	The average decay time (s)	Error%	Frequency deviation (Hz)	Error%	Initial Phase (rad)	Error%
Linear fit	-	error is too big	-0.015	error is too big	-10.824	error is too big	4.829	error is too big
Nonlinear fitting	308.227	54.113	0.279	30.300	1.870	274.020	-0.927	92.710
BP neural network nonlinear fitting	194.380	-2.810	0.436	8.943	0.456	-8.786	0.101	10.102

VI. CONCLUSION

We use linear fitting, nonlinear fitting, BP neural network nonlinear fitting methods are three ways to MRS initial signal amplitude, the average decay time, frequency deviation, the initial phase parameter extraction, and the extraction results were compared. Whether seen from the comparison result of BP neural network nonlinear fitting the extracted data has a higher reliability in the case in which SNR [9], you can more accurately study the distribution of underground aquifers and water content the size of the nuclear magnetic resonance to detect groundwater extraction efforts [10], to lay the foundation for future work.

References

[1] Panyu Ling, Chang-ground nuclear magnetic resonance of the theory and methods of Beijing: Press, 2000

[2] ACTUATORS Lizhou Bo, Wang Xueqiu layered conductive medium surface NMR response characteristic theory Journal of Geophysics, 2004, 47 (1): 156 - 163

[3] ACTUATORS Wangxue Qiu, Liu Guoxing, etc. conductive MoviesSound ground NMR inversion in Geophysics Newspaper, 2007,50 (3): 890 ~ 896.

[4] Wang Peng. Uniform ground conditions three-dimensional magnetic resonance ground c forward [D]. Wuhan, China University of Geosciences. 2007

[5] Jiangchuan Dong magnetic resonance detection system groundwater data processing software design and application of [D]. Jilin University. In 2009

[6] Wang Zhongxing, bright Rong, Lin Jun, Shangxin Lei, Duan clear, Jiangchuan Dong Based 4x digital quadrature FID signal detection technique. Data acquisition and processing, 2010 5

[7] Liu Tong Su nuclear magnetic resonance instrument research prototype data preprocessing software design [D] Changchun: Jilin University .2007 years

[8] Cao Xiange. Neural network based on GPS Elevation Abnormal Fitting methods [D]. Wuhan, China University of Geosciences. In 2008

[9] Li Jun. Qingyi River water quality forecast based on BP neural network model of Anhui Science and Technology. Engineering .2008.02

[10] Anatoly Legchenko, Pierre Valla. Processing of surface proton magnetic resonance signals using non-linear fitting. Journal of Applied Geophysics 39 1998. 77-83.

Intelligent Cruise robot Based on Multi-sensor Detection

FU Bo; GAO Song; SONG Chunyu; YANG Guang

(College of insrumentation and Electrical Engineering, Jilin University,Changchun 130022,China)

***Abstract*--Alone at home for the elderly to design a set of security issues on the tube infrared sensors, smoke sensors, infrared obstacle avoidance sensors and other multi-sensor in one of the intelligent cruise robots. Coordinated by the main controller, complete tracking, obstacle avoidance, smoke alarms, video transmission and other functions. Trolley through the host computer for remote control, real-time transmission of images collected on-site environment. Smart Cruise effects of the present device can meet the current development requirements, its small body, full-featured, practical, with a wide range of market applications, reducing the possibility of accidents.**

***Key words*--sensor system remote monitoring and control real-time communication**

I.INTRODUCTION

WITH the development of society the aging society is coming, most of young people are working outside and unable to take care of the elderly, so elderly care is becoming more and more important. Some people choose to hire a nanny at home to take care of their parents, others decide to send elderly to nursing homes, both two ways cost much money, and young people can not be in direct contact with their relatives, so these methods can not solve the problem well. In order to solve this problem effectively, the electronic devices of the elderly care have been paid more and more attention. So we try to design a robot with intelligent cruise function to solve these problems[1]. Through the monitoring functions of the device the robot we design can make the young people be know health and lifestyle information of their parents at home, in the event of accidents or emergency situations they can got the news and deal with it at the first time , which greatly reduces the possibility of accidents[2].

At the same time, with the further development of material life, people pay more attention to the enjoyment of family material life and ignore the safety problem. For example, the gas leak, because the gas is easy to transport and storage and It has a wealth of resources, etc. So the gas occupies an important position in the country's development and our daily life. With the wide use of gas, the types of gas accidents are also diversified, the frequency of accidents also increased year by year. Because gas is flammable, explosive, easy flow and easy diffusion, once leakage, the leakage gas and air become explosive mixtures, if it meet the heat or fire the explosion and fire dangerous easily occurs, if the leakage gas is inhaled human body, still can make people poisoning and even death. Therefore, how to accurately determine whether the gas leak at home and take appropriate measures to control the occurrence of accidents in time, has been a subject of research. Our project is designed to produce smart home robot with a gas leak detection function, to avoid the occurrence of major accidents.

II.THE SYSTEM DESIGN

Intelligent cruise control system using 89C51 MCU plus Arduino chip coordinated to control the entire system stably operate. The main controller 89C51 chip mainly control the car's normal running, autonomous tracking, autonomous obstacle avoidance, smoke detection, auxiliary controller Arduino chip mainly perform the function of video acquisition and wireless transmission[3～4].

During the cruise, the robot detect the road ahead through the camera, and the scene video uploaded to the host computer software. Its variety of sensors can be aware of environmental changes, once the detection of smoke, the robot will send alarm signals. Robot uses the infrared sensor for dynamic monitoring of the field environment, and avoid the encountered obstacles. The robot has a self tracking function, can be in accordance with the provisions of autonomous cruise line. Based on these features, it can be intelligent cruise at home

and improve the security.

III.THE HARDWARE DESIGN OF THE ROBOT

The cruise robot has perfect sensor system, the ability of real-time communication and a reliable execution mechanism[5]. The overall structure of the system and the specific functions shown in figure 1:

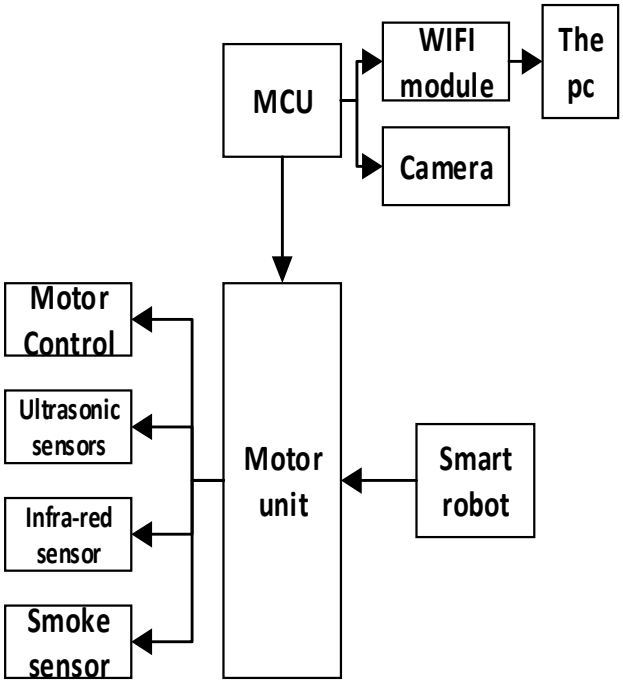

Fig.1 The system's overall diagram

The specific work of each module is as follows:

(1) Motor drive module: using L298N as the motor driver chip. L298N with a high voltage, high current, high frequency response of the full bridge driver chip, a L298N can control two DC motors. The motor driving chip has the advantages of strong driving ability, convenient operation, good stability and excellent performance. The L298N enable terminal can be connected to the level control, it can also be used to control the MCU software to meet the needs of a variety of complex circuits. In addition, the drive power of L298N is large, the different voltage and power can be output according to the size of the input voltage, which can solve the problem that the load capacity is not enough.

(2) Tracking module: using pulse modulation reflection type infrared emitter and receiver as a tracking sensor, signal modulation with AC component, can reduce the external interference. Signal acquisition part is equivalent to the eyes of the intelligent tracking car, by which complete black line recognition and high production, flat signals are transmitted to the control unit and microcontroller to generate the instruction to control the driving module and to control the working state of the two DC motors to complete automatic tracking. JY043W type photoelectric tube and voltage comparator LM393 as the core part, plus the necessary peripheral circuit[6].

(3) The ultrasonic module and the two way pulse modulated reflection type infrared emission receiver. Ultrasound can realize ranging, using ultrasonic return signal changes make the MCU interrupt, realizing the judgment, when the distance is larger than a value it can continue to move forward, when the distance is less than a certain value, the SCM processing to achieve obstacle avoidance[7].

(4) Gas detection module: the gas leak detection device uses MQ-5 gas sensor, the sensor is used in the gas sensor material in the clean air conductivity of the lower two tin oxide (SnO2). The electrical conductivity of the sensor increases with the increase of the gas concentration in the air when there is a gas leak in the sensor. With simple circuit, the change of conductivity can be converted to the output signal corresponding to the gas concentration. MQ-5 sensor has high sensitivity to methane. This kind of sensor is a low cost sensor suitable for this product. When the gas concentration exceeds a certain concentration, the gas detection device will alarm to remind people caution.

(5) Based on HD camera and WiFi module, which is developed for on-site environmental monitoring function[8], it has video capture, coding, and transmission function: intelligent robot can identify the environment according to the input image recognition in front of the camera[9～10]. By optimizing the software and hardware of the intelligent robot, to ensure the completeness and accuracy of the gathered under different environmental information.

IV.THE SOFTWARE DESIGN OF THE ROBOT

The system uses 89C51 single chip microcomputer to carry on the data processing[11], uses the C language to carry on the development to the software part, makes the software readability, The program of the whole system uses the modular design method of the subroutine call, the design of each module is relatively independent, which is easy to modify and

adjust. The flow of the program is shown in Figure 2.

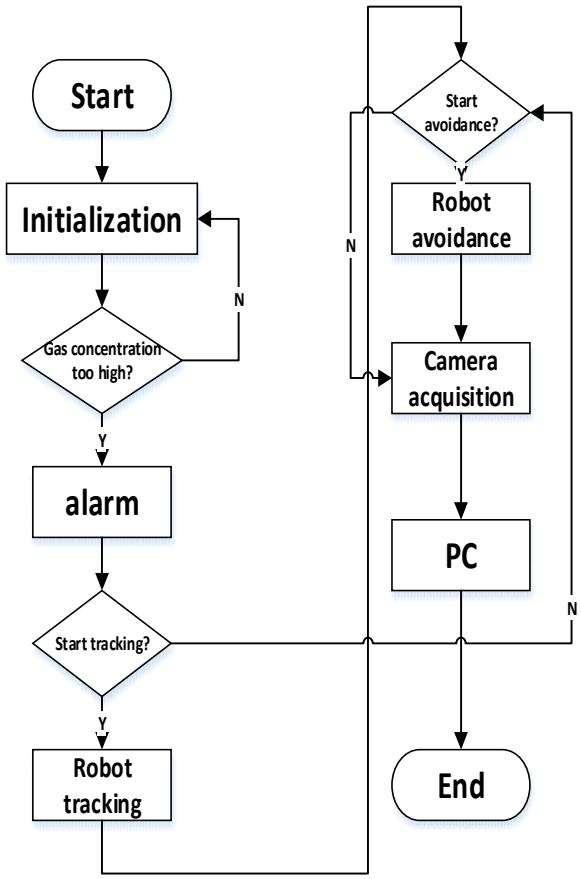

Fig. 2 program flow chart

V.THE TEST AND ANALYSIS

Tracking test results: black tape affixed in the blank of foam board, which is S type, open robot tracking function. The specific phenomenon are as follows: the left sensor to detect black line, robot left; right sensors detect black line, robot turn right; left and right sensor together to detect black line robot straight line. After repeated testing, reached the requirements of target tracking.

Function test results: the test is mainly to test the ultrasonic detection obstacle distance and make obstacle avoidance reflect accuracilly. The test results shown in table 1:

TABLE 1

MEASURING DISTANCE AND AVOIDANCE FUNCTION TEST RESULTS

Test times	1	2	3	4	5	6	7
Test distance （cm）	2	4	6	8	10	12	14
Make the right movement or not	Y	Y	Y	Y	Y	Y	N

Smoke detection function test results: due to the certain effect of the sensor caused by temperature, so the robot is tested under different temperature conditions, which is used to simulate when the room temperature is different, how the temperature and smoke sensors work. Test results are shown in table 2:

TABLE 2

TEMPERATURE CHANGE ON SMOKE DETECTOR TEST RESULTS

Test times	1	2	3	4	5	6
Test temperature （℃）	5	10	15	20	25	30
Working properly or not	Y	Y	Y	Y	Y	Y

As shown in Table2 5 ~30 ℃ is the normal temperature of the home, the test temperature in this range of smoke detection device can work to meet the design needs.

Real time image acquisition results: wireless image transmission image acquisition module movement process[12 ～ 13], and displayed by PC software (Figure 3) screen effect visible, video acquisition system can clearly and truly reflect the environment of the robot, the effect is good, in line with expectations[14].

Fig.3 PC software interface

The whole works as shown in figure 4.

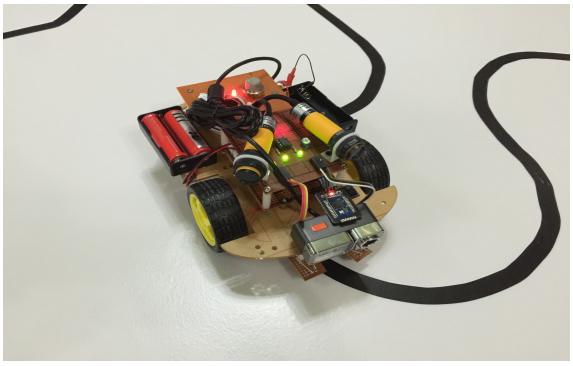

Fig.4 Intelligent cruise robot physical map

VI.CONCLUSION

After the smart cruise robot completing, on the one hand its autonomous patrol function will replace humans cruise work completely, reducing the people's burden. On the other hand, intelligent security patrol car with a variety of sensor detection function, real-time detection to the environment and the indoor gas concentration can be detected and alert, thus promptly eliminate hidden chamber, effectively guarantee the safety of residents in the state. Smart Cruise as a new era of human using robot technology to solve their problems, it is flexible and efficient, convenient and practical, easy to popularize. It can be widely promoted.

Reference

[1] CHEN Zhihua, XIE Cunxi, ZENG Huaide. Patrol robot research status and application prospect [J]. Mechanical engineering technology.2003,32(6):19-21.

[2] CAI Zixing. Robotics Trends and Development Strategy[J]. Robot Technique and Application,2001(4):188-216.

[3] JIANG Yueyue, WANG Honghua. Intelligent security based on multi sensor information fusion patrol car [J].Electric technology and automation.2012,41(6): 203-205.

[4] YING Xiang, LEI Pengfei. Analysis and implementation of the system of intelligent patrol car[J]. Fujian computer, 2012 (1):203-205.

[5] ZHU Hong, ZENG Xiangjin. Multi-sensor Information Fusion Research[J]. Computer and Digital Engineering.2007(12)：46-48.

[6] WU Chuangui, LIU Xingzhao, ZHANG Wanli, et al. Application of [J].pyroelectric thin films in infrared detector infrared. 2004(3):5-10.

[7] SHA Aijun. Research and design of ultrasonic ranging system based on single chip microcomputer[J].Electronic technology. 2009(11):57-61.

[8] Wang Shengyuan, Zhang Hongwu, zhao kai, et al. Design and Realization of Wireless Transceiver Module in Communication of Many Machines[J]. Journal of Jilin university (science edition), 2006, 44 (3): 470-472.

[9] SUN Baofa, ZHANG Xiaoling. Use camera tracking the hardware design of a smart car system [J]. Value Engineering.2012(30):201-202.

[10] LI Xudong, LIAO Zhonghao, MENG Jiao. Intelligent Vehicle Control System Design Realization Based on CMOS Camera[J]. Journal of Jilin University:Information Science Edition. 2013,31(4):414-418.

[11] YUN Zhuo, CHEN Longdong,LIU Fu. Design of Intelligent Electric Vehicle Based on Freescale Microcontroller[J]. Journal of Jilin University:Information Science Edition.2013,31(3):272-278.

[12] LI Xingze,WANG Fuping. Automatic tracking the parking system cell based on CCD camera[J].Computer application,2013,33(S1):321-323.

[13] ZHAN Xinsheng, ZHANG Jiangwei. Design of wireless data acquisition system based on AT89S51 [J]. Research and exploration in laboratory. 2011,30(4)：199—202.

[14] JIANG Xuerun, LI Zhonghua, MAO Zongyuan. Realization of Serial Communication Between Intelligent Module and Host Computer in VB Environment[J]. Automation and Instrumentation.2003(6)：61-63.

Design and implementation of the portable UV detector based on Android system

Liu Jie; Zheng Ruyi; Jiang Bo; Zhao Wei

(Jilin university instrument science and engineering institute,changchun,130021)

***Abstract*--It introduces an ultraviolet detector design. The design includes upper and lower machine two parts. The lower machine's task is UV measurement and simple data processing. The stm32 microcontroller is chosen as controller, combined with UVM-30 UV sensor module, CA3140AMZ operational amplifier-based signal conditioning modules, 5110 LCD module, button module and SH-HC-05 Bluetooth module. Upper machine's task is further processing and display of data, including Bluetooth data reception and Android app. Bluetooth module receives transmitted data through the phone's Bluetooth feature, app's task is data processing, drawing a line chart and display. It can achieve real-time monitoring of UV intensity field.**

***Key words*--UV measurement; Microcontroller; Android app; Bluetooth**

I. INTRODUCTION

UV has a bactericidal effect, but also has to adjust and improve the nervous, endocrine, digestive, circulatory, respiratory, blood, immune system and promote vitamin D generation function, so for medical and chemical industry [1]. However, in recent years because stratospheric ozone has been increasingly serious damage, the amount of UV radiation received ground gradually increased. Excess UV is one of main causes of skin cancer, cataracts, immune system decline[2], particularly in the area of strong ultraviolet radiation, ultraviolet radiation on human harm is particularly significant.

II. LOWER MACHINE

A. Hardware Design

Hardware circuit mainly includes MCU module, an ultraviolet sensor module, signal conditioning module, the mode switching module, LCD display module and data transmission module. UV ultraviolet sensor module collects data and converts it to an electrical signal and then enlarge the signal by the signal conditioning circuit , A/D converter module is to convert analog signals to digital signals, and then by the microcontroller to convert it to the UV intensity with displaying on the LCD and data transfer by the Bluetooth module. Lower machine kind is shown in Figure 1. Lower machine structure diagram is shown in Figure 2.

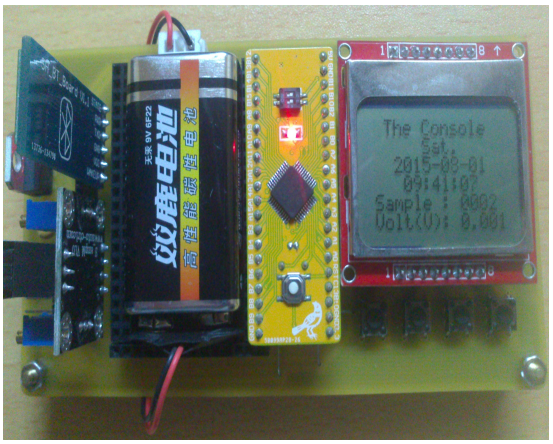

Fig.1 Lower machine physical map

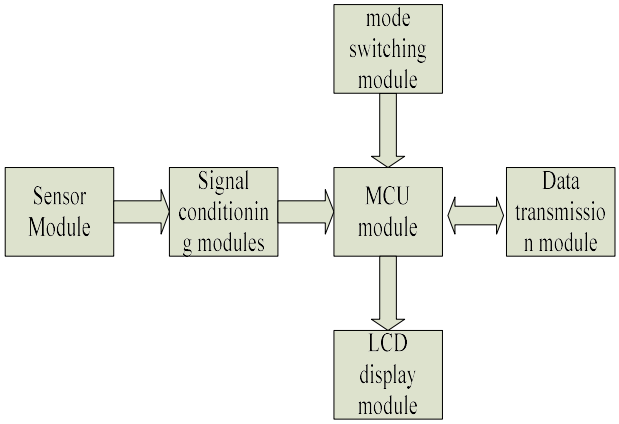

Fig.2 Lower machine structure diagram

MCU module: MCU module is stm32 SCM as a controller to control data acquisition and processing. stm32 STMicroelectronics company's high-performance 32-bit microcontrollers for embedded control systems, with a wealth of internal resources, high-performance, low-power, low-cost features. The design of A/D acquisition using stm32 is internal integrated 12-bit successive approximation

type A/D to reduce hardware costs.

UV sensor module: UV sensor module is UV sensor module UVM-30 based on GUVA-S12SD . UVM-30 UV sensor module can detect 200 ~ 370nm UV wavelength range , suitable for measuring the total amount of solar ultraviolet radiation intensity. Output voltage of UVM-30 corresponds to the WHO UV Index classification index, and has high sensitivity [3],[4]. Features ofUVM-30 UV sensor module are fast response, interchangeable, linear voltage signal output, small footprint, suitable for portable applications, can be used for UV tester, outdoor sun UV monitoring, fire detection and so on. Figure 3 is a typical UVM-30 response curve. The ordinate is the output voltage, the abscissa is the UV index level [3].

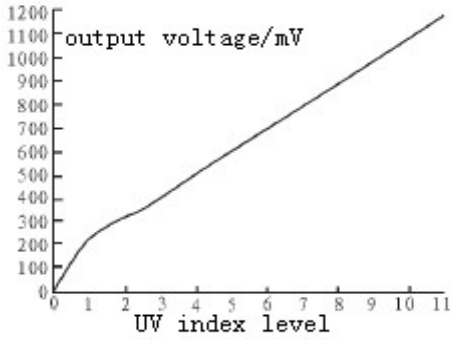

Fig.3 UVM-30a typical response curves

Signal conditioning module: signal conditioning module is CA3140AMZ amplifier. CA3140AMZ is general-purpose op amp. UVM-30 output voltage is 0-1V. CA3140AMZ enlarge the range of the A/D to reduce the error.

Mode switching module: mode switching module is set module by the key control module , to change the measurement interval. LCD display module is 5110 LCD screen to display data related to measurements. 5110 LCD is developed by the NOKIA company that it can be used for liquid crystal display modules. 5110 LCD has 84x48 dot matrix LCD, to display 4 lines of Chinese characters; using a serial interface to communicate with the main processor; only nine signal cables including power and ground. A printed version of the module can be connected by a conductive adhesive, instead of connecting cables. 5110 LCD module is small, and its power supply voltage is low.

Data transmission module: SH-HC-05 Bluetooth module is used as data transmission module .It can communicate with mobile phone to achieve real-time transmission of measurement data, and enables end-to-PC mode data measurement system control, and facilitates timely adjustment of the measuring system parameters. SH-HC-05 Bluetooth module Shenzhen City Year of Science and Technology Co., Ltd. is designed for intelligent wireless data transmission and the development of a Bluetooth module, which the British CSR's BlueCore4-Ext chip, followed Bluetooth V2.0 + EDR Bluetooth specification, the highest transfer rate up to 2.1M, transmission distance of more than 20 meters.

B. Software design

Software part includes initialization, key scan, LCD display, A / D, filtering, and data transfer routines. MCU power to achieve initialized by the key scan mode settings. Data collected by sensor will be amplified and then achieve A / D converter ,with filtering to reduce the error. Then the processed data is displayed by the LCD 5110, and through Bluetooth uploaded to the host machine. Microcontroller program flow chart is shown in Figure 4.

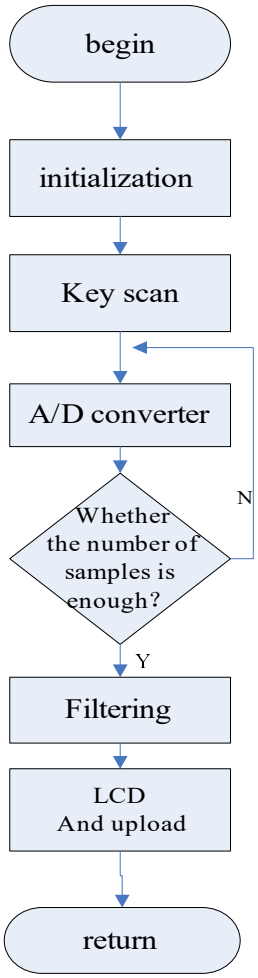

Fig.4 Microcontroller program flow chart

Filtering Algorithm: number: Because a single measurement has some chance, the measurement data with uncertainties produce more variations, with taking into account the higher bandwidth of the measurement channel itself and the signal amplitude changing small in a short time, so the software used mean filter the way to eliminate measurement errors caused by accidental factors. It is not only simple operation, but also can effectively reduce the measurement noise power density distribution. So it is appropriate for the processing of the present system involved in the slow-varying signal [5].

Average filter is the N consecutive samples (respectively X1 ~ XN) are added and then the arithmetic mean X as a filter value for this measurement [5], namely:

$$X = \frac{1}{N}\sum_{i=1}^{N} X \tag{1}$$

Assume $X_i = s_i + n_i$ (2)

n is the sample value signal; ni random errors. Then

$$X = \frac{1}{N}\sum_{i=1}^{N}\left(s_i + n_i\right) = \frac{1}{N}\sum_{i=1}^{N} s_i + \frac{1}{N}\sum_{i=1}^{N} n_i \tag{3}$$

And according to the law of statistics，statistical mean random noise is zero, so there:

$$X = \frac{1}{N}\sum_{i-1}^{N} s_i \tag{4}$$

As can be seen from the above mean filter can effectively eliminate random noise.

Changes the operation mode of realization: In view of the process of change of the measured signal is extremely slow, Signal acquisition doesn't need a high frequency signal acquisition, only the trigger several times to the data acquisition and processing at a certain time. But on the other hand, if it desires to ultraviolet radiation situation in a short time when sudden there is a need for continuous monitoring another mode to choose from, so in this system design use Internal microcontroller RTC clock for clock function, and realize Operation mode selection under different working conditions mode by controlling the acquisition time.

III. UPPER MACHINE

Upper computer design includes Bluetooth communication and Android app design.

A．Bluetooth communication

Bluetooth wireless technology work in the industrial, scientific and medical Public Utilities 2.4GHz ISM band, this band worldwide and without authorization. Bluetooth system[6] uses full-duplex transmission of information sharing technology, information in the manner of a packet structure for data exchange. During transmission, each packet of information to transmit information uses different frequency hopping algorithm. "Hopping" technology is the band into a plurality of channel hopping. In a single connection, the radio transceiver according to a certain code sequence "jump" continuously from one channel to another channel. Only the sender and receiver communicate according to the law, other noise is impossible interference by the same law of interference. Hopping the instantaneous bandwidth is very narrow[7], which makes the possibility of household appliances from the same work in the 2.4GHz ISM band brings interference becomes small, such as microwave ovens. In the same band wireless system compared to other work, Bluetooth hopping is up to 1600 times per second, speed faster and shorter packets, so that Bluetooth is more stable than other systems.

Android platform supports Bluetooth network protocol stack, which allows a Bluetooth device with other Bluetooth devices for wireless data exchange. Application provides access to Bluetooth functionality through Android Bluetooth API. These API will connect applications to other Bluetooth devices with point to point and multi-point wireless feature [8]. Android platform includes Bluetooth support network protocol stack, which allows a Bluetooth device with other Bluetooth devices for wireless data exchange. Application provides access to Bluetooth functionality through Android Bluetooth API. These API applications will connect to other wireless Bluetooth devices wireless with point to point and multi-point wireless feature [8].

When using the Bluetooth API, Android applications can perform the following functions:

① scanning other Bluetooth devices;

② inquiry local paired Bluetooth adapter ;

③ establishing RFCOMM channel;

④ to connect to other devices via service discovery;

⑤ transfer ring data between devices;

⑥ to manage multiple Bluetooth connections [10].

Bluetooth communication data transfer process is shown in Figure 5.

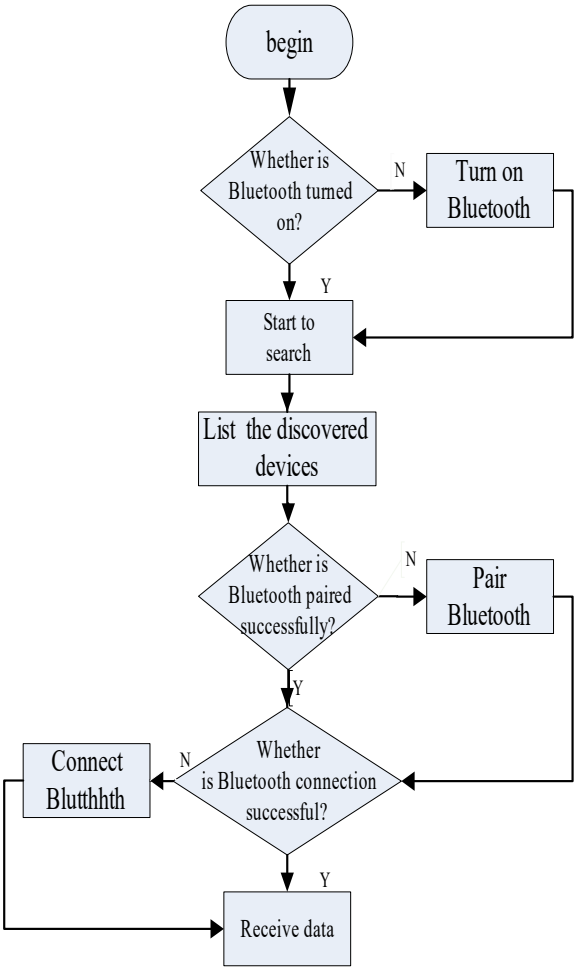

Fig.5 Bluetooth data transmission process

B. Android app design

Android system from bottom to top consists of five parts: Linux kernel, Android Runtime, libraries, application frameworks, applications [9]. Android app is mainly used to process lower computer data transmission, and ultraviolet plotted versus time line chart. Design process is shown in Figure 6 [10].

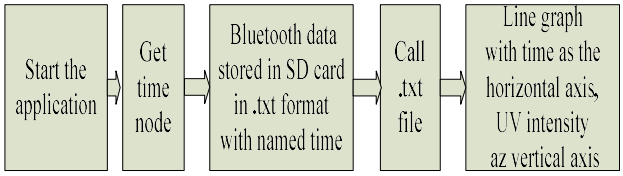

Fig.6 Design Flow

Draw a line chart of realization: SurfaceView is derived class of View, this view embedded Surface a dedicated drawing. It can control the surface's format and size. SurfaceView Control Surface rendering this position [11]. Implementation involves the following steps:

① Inheritance SurfaceView and implement SurfaceHolder.Callback interfaces;

② SurfaceView.getHolder () gets SurfaceHolder objects;

③ SurfaceHolder.addCallback (callback) adds a callback function;

④ surfaceHolder.lockCanvas () obtains Canvas object and lock the canvas;

⑤ Canvas painting;

⑥ SurfaceHolder.unlockCanvasAndPost (Canvas canvas) ends the lockout drawing, and submits changes to the graphic display.

Android phone app interface is shown in Figure 7.

Fig.7 Android app interface

IV. CONCLUSION

Figure 8 is actual measurement UV data FIG in case of UV lamp simulation the sun's ultraviolet

We designed a UV monitor combination of Android app. The monitor monitors UV intensity real-time field, and upload the data to your Android phone. So it can a timely reminds of People outdoor activities take certain protective measures, and help to reduce excessive ultraviolet radiation on human health hazards. The design compared to most current UV monitor, it has some advantages .such as :low cost, more portable, more humane, easy to implement. It provides a new design ideas for the development of UV detector.

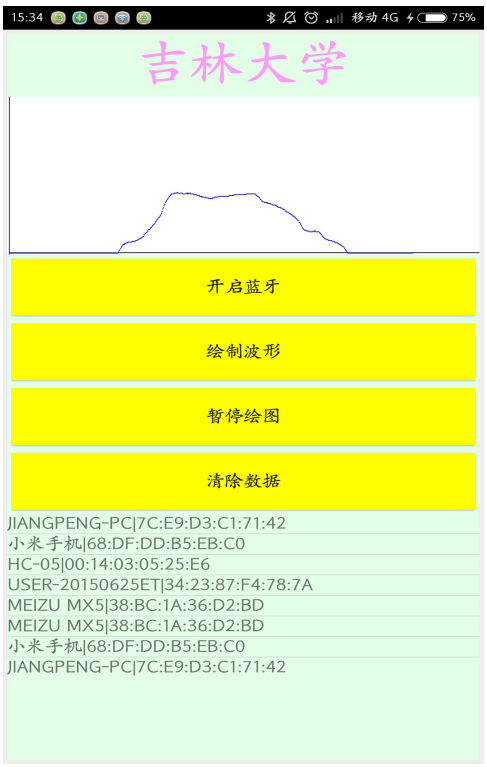

Fig.8 actual measurement UV data fig

References

[1] Cao Yu, Shi Weiduo etc. UV intensity monitoring system based SUV-C of [J]. Shanxi Electronic Technology ,2012,(4):17-19.

[2] Zhao Xiaolan , Nie Fei etc. Testing Technology of solar ultraviolet intensity [J]. Test Systems and Components, 2008, 31(1):112-115.

[3] Hu Liqun , Chen Dunjun etc. Visible and ultraviolet light intensity detection system based on Microcontroller [J] . Electronic Design Engineering, 2013,21 (24): 81-84.

[4] Liu Chiyang, Yang Jingbo etc. MSP430-based portable ultraviolet detector [J]. Modern electronic technology, 2012,35 (8): 132-134.

[5] Cheng Defu, Lin Jun. Intelligent instruments [M] . Changchun Machinery Industry Press: 2005.113-119.

[6] Pu Dongbing, Zhao Donglai, Zhang Xue. Smart Home Gateway based on Bluetooth [J]. Information Technology, 2010 (2): 11-12.

[7] Li Liguo, Zhang Hui,Cheng Hao. The Design and Implementation of Bluetooth Software Based on Android Health Service Terminal [J] . Electronic Science and Technology, 2012,25 (2): 115-118.

[8] Luo Fucai. Research and Implementation of the Bluetooth Communication System based on Android system [D]. Beijing: China Electric Power University, 2012.

[9] E2ECloud studio. Dive Google Android [M]. Beijing: People's Posts and Telecommunications Press, 2009.

[10] Ding Shan. Android programming tutorial [M] Changsha Machinery Industry Press: 2015: 243-251.

[11] Wu Jianxia. Remote video monitoring system based on Android mobile phone design [D]. Beijing: North China University, 2015.

The rapid analysis and technical research of DECG

Yu Zining; Chao Yunfeng; Zhou Haijian
（jilin university instrument science and engineering institute,changchun,130021）

***Abstract*--It is particularly necessary for heart disease patients to have the real-time dynamic monitoring system, it can be achieved on a patient for a long time to monitor and record the patient's ECG data[1]. Traditional ECG data is large, the staff need to observe the problem waveform by eyes,which takes a long time and is easy to lose information as well[2]. For these shortcomings of traditional diagnostic methods, we use the computer software named MATLAB, by the use of one-dimensional continuous wavelet transform algorithm to detect QRS complex on ECG[3][4], after repeated testing, we designed a reasonable threshold, we can quickly find the location of R-wave and calculate the heart rate . This will not only shorten the time of ECG interpretation, but also simplify the workload of medical staff, besides lay the foundation for the next step.**

***Key words*--ECG data MATLAB wavelet transform locate R-wave**

0.INTRODUCTION

IN modern medical diagnosis, when it comes to heart disease, electrocardiogram is the most intuitive, the most widely used cardiac clinical examination techniques. Although today's ECG monitoring technology has matured, but in the state of motion ECG monitoring process, there is always kind of problem, so to some extent distorted ECG, so the unreliable results bring thediagnosis trouble to doctors. At present there are two main methods to detect heart disease, the first patient intentions electric meter real-time detection in the case of lying, but the process is very short, it is prone to miss arrhythmia characteristic signal, which often occur hospital patients diagnosed as healthy but they feel obviously conscious reaction; the second is what we call the 'Holter', leads patients through their daily behavior does not affect the situation, monitoring ECG 24 hours, the time to go to the hospital to collect the Electrocardiograph for playback through our extensive visits to the hospital[5], the doctor found that most still see with your eyes, which makes the doctor a lot of work, there will be a high turnover rate. The hospital now has this one instrument, but it is huge and expensive. There is an urgent need to the use of computer and digital processing. Based on this background, we would like to use computersoftware for data processingECG signal,which can quickly and accurately calculate important ECG characteristic parameter associated with heart disease in order to achieve the functional analysis and secondary diagnosis.

1.ECG SIGNAL DE-NOISING THEORY AND METHODS

1.1 ECG signal theory and noise analysis

During learning the ECG polarization and electrocardiogram (ecg) ,we understandsome knowledge related to biological parameters. We put forward to a judge of ecg characteristic points location, by finding the feature points on the heart whether there is abnormal for analysis. In the data processing part we mainly detect R wave, as R wave amplitude value is the largest,its frequencythe highestin figure 1 .

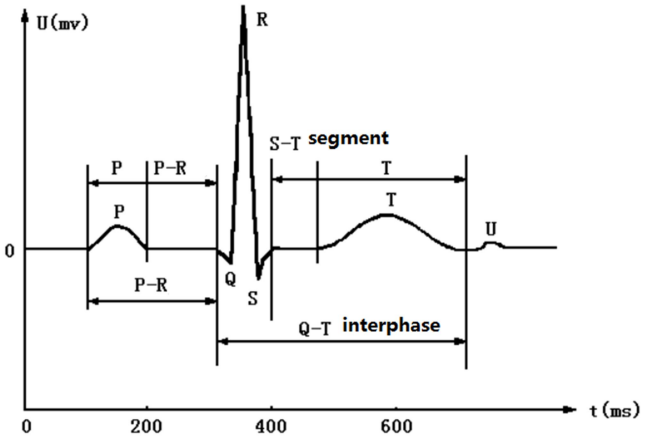

Fig.1. A typical ECG waveform

1.2 The original ECG signal filtering

ECG is a physiological signal, the spectrum in the range of 0.03 ~ 110Hz, and most of the ECG concentrated in 14 ~ 75Hz, the proportion of more than

100 Hz signal in total accounted for a small part, signal amplitude of 5uV (fetus)-5mV (adults). The original ECG include frequency interference, EMG interference, baseline drift, electrode contact noise and motion artifacts, etc., through a lot of analysis of existing data, including baseline drift 2Hz below the main source of interference.

Baseline drift is changed by the body movement caused by breathing or the electrodes, the amplitude and frequency of the time, frequency 2Hz or less, it belongs to the low-frequency noise. Because of the overlap with the frequency of ECG ST segment, baseline drift is more difficult to filter out. ECG baseline drift by signal interference characteristics as shown in fig 2.

ECG baseline drift of the interference has the following characteristics:

(1) Lower frequency, typically between 0.05-1.5Hz, belongs to the low-frequency interference, usually presents slowly changing curve.

(2) Baseline drift frequency and ECG ST-segment baseline drift have overlapped, so the baseline will seriously affect the detection of the ST segment.

Based on the baseline drift noise is low frequency noise, we use FIR high pass filter. After filtering, baseline drift significantly removed, as shown in fig 2. Its advantage is faster, algorithm is simple,saving time for subsequent positioning R wave .

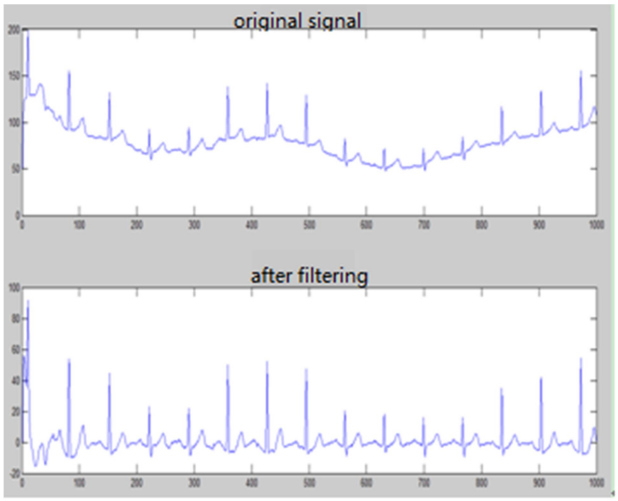

Fig.2. Original ECG and filtered ECG

2. WAVELET TRANSFORM ANALYSIS

2.1 Wavelet transform and one-dimensional continuous wavelet transform principle

Wavelet analysis is a window size (window area) fixed but its shapecan change , which isa kind of time-frequency localization analysis that the time window and frequency window can change. For example, in the low-frequency part having a higher frequency resolution and lower temporal resolution, with a high time resolution and frequency resolution in the lower frequency portion, it is called mathematical microscope. Because of this characteristic, there is a signal of the wavelet transform adaptive.

Let $\psi(t) \in L^2(R)$ denote the number of square integrable real space, namely energy limited signal space, its Fourier transformψ(ω). When ψ(ω) satisfied permit conditions[6]:

$$C_\psi = \int_R \frac{|\hat{\psi}(\omega)|^2}{|\omega|_{\hat{\psi}}} d\omega < \infty$$

We called $\psi(t)$ as a basic wavelet or mother wavelet. The generating function $\psi(t)$ after scaling and translation, you can get a wavelet sequence.

For the case of continuous wavelet sequence

$$\psi_{a,b}(t) = \frac{1}{\sqrt{|a|}}\psi\left(\frac{t-b}{a}\right)_{a,b \in R;\ a \neq 0}$$

Wherein, a is the factor for the stretch; b is the translation factor[7].

For any of the functions $f(t) \in L^2(R)$ of continuous wavelet transform

$$W_f(a,b) = \left\langle f, \psi_{a,b} \right\rangle = |a|^{-1/2} \int_R f(t) \overline{\psi\left(\frac{t-b}{a}\right)} dt$$

Its inverse transformation is

$$f(t) = \frac{1}{C_\psi} \int_{R^+} \int_R \frac{1}{a^2} W_f(a,b) \psi\left(\frac{t-b}{a}\right) da db$$

Base on the wavelet transform, wavelet $\psi_{a,b}(t)$ generated because the basis wavelet $\psi(t)$ in the wavelet transform for signal analysis plays a role in the observation window, therefore $\psi(t)$ should also satisfy the constraints of the general function

$$\int_{-\infty}^{\infty} |\psi(t)| dt < \infty$$

It is a continuous function. This means that in order to meet the perfect reconstruction condition (the condition), the origin must be equal to 0, that is

$$\hat{\psi}(0) = \int_{-\infty}^{\infty} \psi(t)dt = 0$$

In order to achieve the reconstructed signal values are stable, except perfect reconstruction condition, but also requires the Fourier transform of the wavelet $\psi(t)$ satisfy the following stability condition:

$$A \le \sum_{-\infty}^{\infty} |\hat{\psi}(2^{-i}\omega)|^2 \le B$$

Wherein, $0 < AB < \infty$.

Continuous wavelet transform the one-dimensional signal to a two-dimensional space, so there is redundancy information expressed in continuous wavelet transform. Wavelet transform in different (a, b) increased correlation between wavelet transform to analyze and interpret the results difficult, therefore, redundancy wavelet transform should be reduced as far as possible, it is a major problem in wavelet analysis[8]. In MATLAB, the functioncwt can be used to realize the continuous signalwavelet transform.

2.2 R-wave detection algorithm analysis

2.2.1 Software flow of positioning R-wave

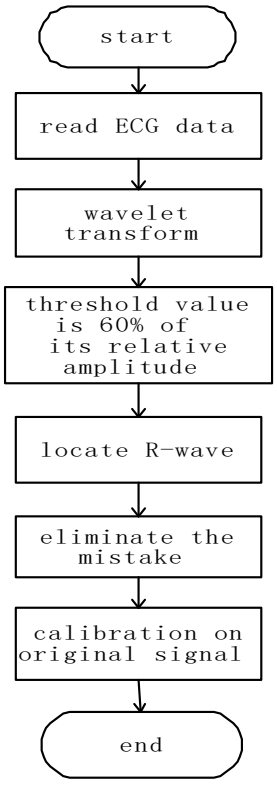

Fig.3. Positioning R-wave flowchart

2.2.2 Algorithm steps

(1) For a given ECG for continuous wavelet transform, select mexh wavelet as wavelet base.

(2)ECG cardiac cycle segmented[9], segmentation algorithm is the first step to measure a time-scale chart according to a direction to accumulate, resulting in integral value in the direction of the scale wavelet change over time curve, for mexh wavelet concerned, there will be a crest before the R-wave, then a trough after R-wave. Re-election were 60% of its maximum value as a sign of positive and negative threshold, the integral value over time curve thresholding process, and to make a point greater than the positive threshold is + l, smaller than the negative threshold point -1, between the two points is equal to 0, so that before each R wave position there is a + l, then there is a -1, the area between the two is zero. The midpoint of a some -1 and the first position of +1 subsequent of this piece of data is set at the dividing point of the cardiac cycle, in order to achieve the sub-signals, each section comprises one cardiac cycle, and wherein R wave is in the middle of this paragraph.

(3) For the time-scale chart for each cardiac cycle segment signals, respectively, to identify positive and negative maxima maxima at every scale, which is connected into the line to give positive and negative modulus maxima value line, the slope of each of the positive and negative modulus maxima lines obtained Lee index corresponding to the point and then exclude the value of modulus maxima lines which less than 0 and more than 1.

(4) Since the modulus maxima line of continuous wavelet transform signal may interrupt, so we need to fit a straight linefor each of the positive and negative modulus maxima line , in order to determine their position whentheir respective time scale a = 0 . If the positive and negative modulus maxima when a = 0does not converge to the same point, then take the average of the two initial positions as R-waves.

Inthe preliminary determination, location corresponding to the R-wave cost 10ms.It can detect of extreme points of the original signal, and ultimately determine the R-wave position.

3.DESIGN AND DEVELOPMENT OF 3 ECG HMI USER INTERFACE

Using MATLAB graphical user interface to display the ECG signal processing. Graphical User Interface(abbreviated GUI) is a kind of user interface displayusing computer graphical operations[10].

There are 8-lead ECG data read control, single-lead zoom control, forward and backward controls and other control data and the corresponding dialog box is displayed in MATLAB program in accordance with the function respectively. Namely, we do the interface initialization by OpeningFcn function, and add the appropriate function control in fig, then we write the appropriate callback function to achieve the corresponding functions. When you create a graphic object in each fig , MATLAB is assigned a unique value for the object, called the graphical object handle. The handle is a unique identifier for the graphic object. When making button design, input and output functions to make the button now, we should call some function file by its handle value, the method is to provide a unique 'Tag' property string through to the desired graphic object; and when the handle is unknown, It provides a unique 'Tag' property string through to the desired graphic objects, using findobj function to find the handle with the desired identification label.

The interface design controls and features of the ECG data analysis is in the following table.

Tab.1. interface design menu table

Contral name	function
Open a file	Open the patient's ECG data
start	Read the patient's ECG 8-leads data
Save the picture	Save the ECG signal instantly
One lead	Choose one laed signal and magnify it
Single page move forward or back up	8-lead ECG figure read 2000 points forward or back up togrther
Slowly move forward or back up	8-lead ECG figure read 20 points forward or back up togrther
slider	8-lead ECG figure move togrther
Locate R-wave	Show the R-wave with red points
Heart rate	Show the patient's heart rate
end	Close the window

Interface displays is shown in the fig 4:

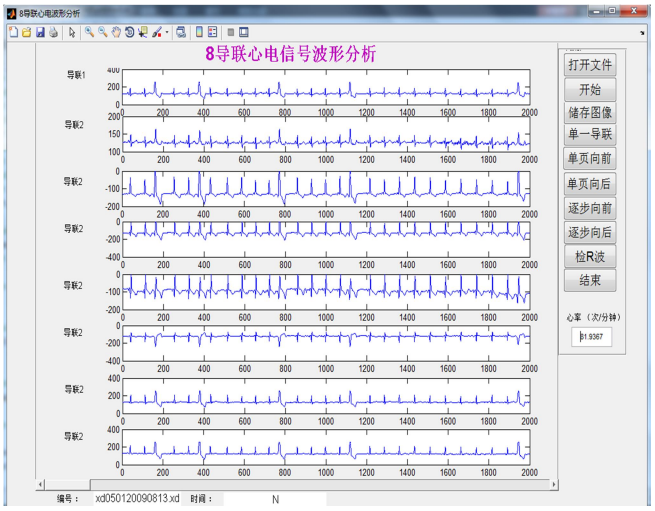

Fig.4. interface display

4. ANALYSIS

The original ECGsaved as .sd file format. Open this file in MATLAB with fopen function, and read it with imread draw.

After high-pass filtering, the wavelet transform can detect R-wave, a logo with a red dot, the test results is shown in Fig 5.

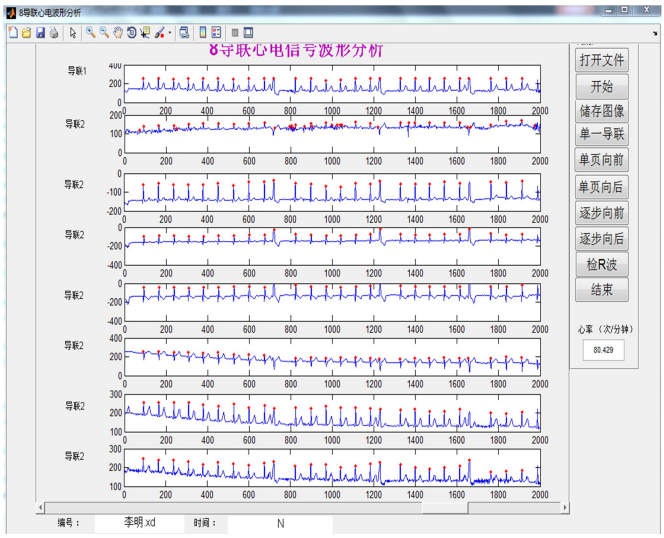

Fig.5.Positioning R wave renderings

This algorithm uses wavelet transform to detect R-wave of ECG, through plotting the collection of data, validated this algorithm can achieve the location of R-wave rapidly and accurately, in addition to calculate the heart rate.The algorithm written for a variety of abnormal ECG can detect 100,000 pointsin 20 seconds.

5. RESULT

Rapid detection of R-wave plays an important role in the medical equipment industry. This paper describes the theory and QRS wave of ECG detection significance, focusing on the principle of the algorithm using wavelet transform method for detecting R waves, and in the design of the foundation of the ECG on the man-machine interface, completing with MATLAB filter out heart baseline electrical signal drift and fast positioning R wave. Compared with traditional techniques, the algorithm designed saving time, improving efficiency,will be a deep foundation. for the further analysis.

Reference

[1] Li Shu-yuan,Wu Shui-cai,Bin Guang-yu,et al.Design and Implementation of a Wearable Wireless Low-Power ECG Recorder[J].China Medical Devices,2015(03):21-23.

[2] He Ling-li,Wang Yu-feng,He Wen-jing,et al.Design of Detection Amplifier Circuit for Electrocardiogram Monitor[J].Journal of Biomedical Engineering Research, 2013(01): 31-34.

[3] Shang Yu;Lei Sha-sha.QRS waves detection algorithm based on positive-negative adaptive threshold method[J].Journal of Beijing Institute of Technology , 2014(01):63-66.

[4] Yao Cheng,Si Yu-juang,Lang Liu-qi,et al.Modified Algorithm of QRS Wave Detection Based on Wavelet Transform[J].Journal of Jilin University(Information Science Edition),2011(05):1-7.

[5] Yuan Hai-bo,Dai Shuang,Xiao Bu-wen,et al.Design of Portable Wireless ECG Monitoring System Using SOC Chip[J].Journal of Jilin University(Information Science Edition),2015(03):1-8.

[6] Jin Xin,Zhen Zhao-rui,Han Yan.X-ray Image edge detection based on Wavelet Transform[J]. Journal of Taiyuan University of Technology, 2003,1[1]:3-4.

[7] Chen Dong-yang,Gao meng,Hao Rong-hua,et al.Electrical Load Wavelet Analysis in Centralized Supply System[J].Industrial Measurement,2006,1(5):4-7.

[8] Sun Yan.Image edge detection based on Wavelet Transform[D].Xi'an : Northwestern Polytechnical University, 2006.

[9] Zhao Yi-ou,Liu Yang.Improved Differential Threshold ECG Detection Algorithm[J].Computer Engineering.2011(S1):347-348.

[10] Che Zi-Ping.A Virtual Signal Cenerator Based on Matlab[J].Computer Study,2010,1(1):1-7.

Improvement of electronic measuring instrument platform based on Virtual Instrument Technology

HUANG En-hao; LI Yan; ZHOU Ri-zhang

(College of Instrumentation and Electrical Engineering，Jilin University，Changchun 130026，China)

***Abstract*--In this paper ,a virtual platform was built which possesses the function of electronic measurement system in software and hardware,according to the basic principle of the traditional instrument within the field of electronic measurement technology in time-frequency domain. LabVIEW software program was used to control and simulate traditional electronic measuring technology. The platform optimals the performance of electronic integrated measurement system,which increases the functions of existing electronic measurement platform.**

***Keywords*--Virtual Measurement LabVIEW Electronic Measurement Platform**

I. INTRODUCTION

SINCE the 90s of the 20th century, with the constant progress and development of the economy, the rapid development of computer science,humanity has entered the Internet era, which resulted in the virtual instrument as the symbol of intelligent and template measuring instruments and the control system has been developed rapidly, more and more people will focus on data acquisition system and electronic measuring instruments, thus creating the virtual instrument system, LabVIEW is a powerful graphical programming language, is one of the most popular virtual instrument software.The virtual electronic measuring platform is used LabVIEW to the measurement parameters design, can make the signal generator to achieve more perfect FM / AM signal function, but also can achieve universal meter measuring current, power, DB and a number of functions, virtual instrument can also auto power spectrum density, phase spectrum, spectral purity, degree of distortion, distortion stability and frequency ratio, the interval of time, phase, phase difference parameters.

II. ABOUT LABVIEW PROGRAM

A. About LabVIEW

The LabVIEW is by the NT company developed a software, it is a graphical programming language development environment, design and application of research and development of virtual instrument, it is the use of established and link icon constitute virtual instrument program, omit writing steps of dense source code. It can also communicate with a variety of testing instruments.

B. The advantages of LabVIEW in time domain electronic measurement

LabVIEW has four advantages in the time frequency domain electronic measurement: data flow programming, modular method, graphical language, user defined[1].

Data flow programming is a big advantage of LabVIEW program, and traditional programming language is different, the traditional programming language implementation depends on the text sequence of program code, LabVIEW program is the segmentation procedures for all program node and all the nodes of the program is completely correct can run the program. In this way, the program is compiled and convenient testing, software development efficiency is greatly improved. Modular approach is the most significant feature of LabVIEW program, program design, according to the different division of the system are mutually independent and have contact plate, such as the virtual measurement in the virtual spectrum analyzer by the division of the sub modules, thus the program were plate, more conducive to the use, at the same time, if the a plate can be a problem for its maintenance than traditional instrument maintenance saves time and effort. Graphical programming language LabVIEW program control very common numeric button and switch device and used to display graphics, icons, etc., make such language programming interface intuitive, programming is more conducive to memory. To achieve the preparation of.

User custom, under the support of the general module and the software environment, the user can according to design their own measurement scheme, more humane, avoid to data, the measurement is more convenient, efficiency, and reduce the cost of unnecessary waste.Part of the program display:

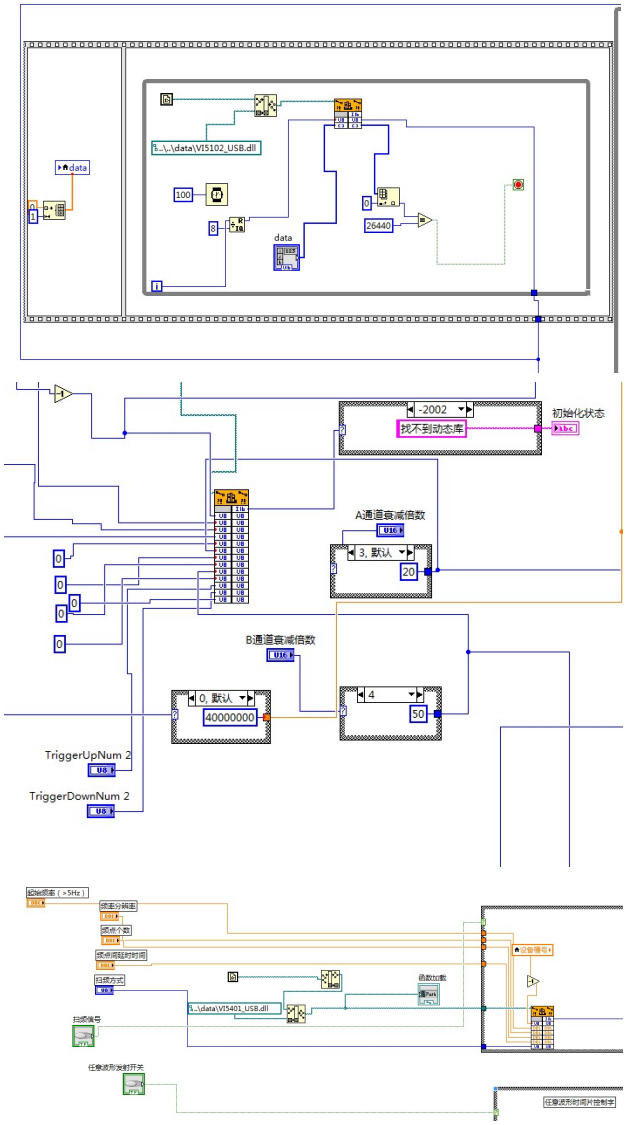

Fig.1 Partial subroutine diagram

III .VIRTUAL INTEGRATION BASED ON LABVIEW PROGRAMMING ENVIRONMENT

System design ideas

The experimental design of the virtual instrument, in general can be divided into two parts, one is using the LabVIEW data analysis software, a is used for collecting the realization of data acquisition card, and the overall structure is as follows:

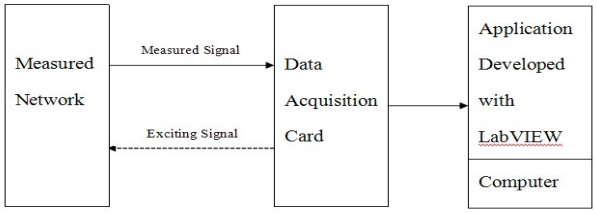

Fig.2 Data acquisition process

First conducive includes two analog output function data acquisition card is used to achieve functional virtual testing platform, for generating an excitation signal, two data acquisition card can be added to the test excitation signal network, and then the two analog input signals, collected to a computer, analyze and process, will produce a corresponding amplitude and phase frequency characteristic curves, the final output to the computer can result in the Virtual Instrument display on the computer screen. Optimization and improvement objectives virtual instrument test platform, there are four virtual instruments: Signal generators, multimeters, spectrum analyzers, frequency counters.

IV: VIRTUAL INSTRUMENT TESTING PLATFORM SPECIFIC OPTIMIZATION SOFTWARE

Contents and results Gallery

The virtual test platform designed for the analysis is the use of traditional electronic measuring instruments, its basic function as a guide, in LabVIEW software method, which creates a virtual test platform includes not only traditional electronic measuring basic functions, also added some more using the measurement and analysis of accessibility, better help users complete the test[2].

The virtual test platform designed for the experiment is the use of fixed-point method dynamically loaded way to achieve multi-panel design process, so-called multi-instrument control panel is more virtual page, the user needs to choose according to their own use virtual instrument for testing.

The first virtual instrument is signal generator, signal generator, also known as the signal source, it is possible for the user to set various parameters, such as waveform, frequency setting parameters set by the user at the core of the signal generator generates, and then

after a certain conditioning instrument to an external output signal, which can be based on user needs to use. Virtual Signal Generator is a computer hardware and I / O interface device composition, transmission and is responsible for signal conditioning, software functionality includes generating (sine, square, triangle) simulation signal, parameter setting, data acquisition card drive. Compared with the conventional signal generators, signal generator virtual sufficient to reduce the traditional instrument signal generator high cost, bulky, and other shortcomings are not s mart, more convenient and easy to use on upgrades and maintenance. Virtual Signal Generator specific display as shown below[3]:

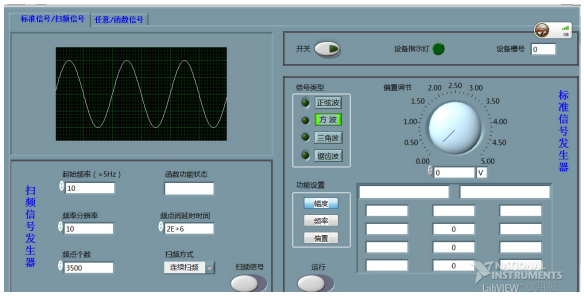

Fig.3 Virtual instrument signal generator interface

The second virtual instrument multimeter, Multimeters are essential field of electronic measurement instruments, primarily by measuring current, voltage, resistance, and other various corresponding electrical parameters. Virtual multimeter is the use of computer hardware for data acquisition, analysis, processing and display virtual instrument data measuring function, The main principle is to be realized using the conversion circuit converts the signal to a DC voltage signal, Re-use converter digital signal in the form of the show, and finally through the electronic counter of calculation results directly show in display [4]. This virtual virtual multimeter measurement platform designed with the following seven functions : Basic measurement function, range selection function, math functions, digit display , readings deliberately amplification and offset function, auto-zero function, filtering function. Specific virtual multimeter display as shown below:

Fig.4 Universal data interface

The third virtual instrument is spectrum analyzer, Spectrum analyzer's front panel is composed of spectral analysis, spectral analysis of amplitude and phase and power spectrum page of the composition, Users can c ustomize various parameters to achieve the defined signal generates various wave signal, such as frequency and phase parameters set, users can control various parameters by adjusting the input value of the specific parameter, in addition. Users do not havee to write too cumbersome code and configuration files. Waveform generated is very convenient and easy to operate, greatly reducing the difficulty of using the spectrum analyzer[5]. Virtual spectrum analyzer rear panel of the waveform generated by the module, the control range of the X-axis sub-module, waveform analysis sub-module, filter / frequency / phase frequency characteristics of the sub-module , data storage sub-module five sub-modules. Specific virtual spectrum analyzer display as shown below:

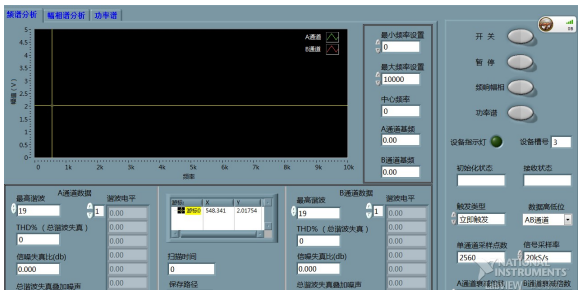

Fig.5 Spectrum sensing data interface

The fourth virtual instrument is frequency counter, the frequency counter is a signal frequency measuring instruments specially. Virtual frequency counter is mainly composed of six parts : Limiter circuit, switching circuit, a frequency dividing circuit, shaping circuit. Pc machine with 51 single-chip system. The working principle of the virtual frequency counter: Standard square wave converter use the measured signal is converted to a square wave, square wave and then adjustments are the main mode of limiting, shaping, dividing, and finally the input signal into a

single-chip set for corresponding to the received amplitude wave, and sends it to the microcontroller, the microcontroller will be measured, the measurement instruction has issued the PC, microcontroller upon receiving the standard square wave signal sent by the PC, it will be measured, measuring the low-frequency signal Zhou measured using a method to measure frequency to meet the needs of PC, high-frequency signal directly measured using the method of counting measurements to complete. LabVIEW software for PC-programming play a crucial role. Virtual frequency counter with respect to the traditional conventional frequency counter for lower cost, more practical. Specific virtual frequency counter is shown below:

Fig.6 Virtual frequency counter measurement data interface

V.ADVANTAGES AND SIGNIFICANCE OF VIRTUAL TEST PLATFORM

The traditional electronic measuring instruments in the field of electronic measurement plays an important role, but with the development of society, slowly can not meet market demand. Mainly due to the traditional electronic measuring instruments flexibility is not high, low precision, the old instruments can only achieve electronic measuring one or both, virtual testing platform based on traditional analyzers meet the flexibility, higher accuracy, but also provides the user with four electronic detection equipment to achieve the feature set, many traditional electronic measuring instruments can not provid these functions. Virtual test platform is also more and more people pay attention to the key of the virtual electronic measurement platform.

Another using LabVIEW virtual test platform as the development of software, compared with the traditional electronic measuring instrument need to write tedious code, only need a simple software programming can be achieved, much easier. Thus caused the development cost and the difficulty of the virtual test platform is greatly reduced, effectively improve the efficiency of the virtual test platform development, LabVIEW has friendly man - machine interface, the collected data is more conducive to the user, this is one of the traditional electroni c measuring instrument to reach the effect[6].

VI CONCLUSION

Introduced above, is based on the LabVIEW progr-amming environment perfect the process of virtual test platform, the virtual test platform to make full use of the electronic computer data analysis ability, realize the goal of the basic function of four kinds of electronic equipment, effectively reduce the cost, provides the analysis efficiency and flexible, abounded the function of the integrated system, the innovation project have a certain practical significance. Thanks to the help of the teachers and students here.

Reference

[1] Sun Chunlong. Based on the LabVIEW multi-channel data collection and analysis system development [D]. Wuhan university, 2012.

[2] BiHu, law of ejection, Li Yanqing, he-ming li.LabVIE-W in several different ways to access the database [J]. Microcomputer information, 2013,01:131-134.

[3] hanley, xiao-hui qiu, zhao, YanWei MiaoFei. Based on the LabVIEW data acquisition and signal processing system design [J]. Journal of nanjing normal university (engineering and technology edition), 2010 01:7-10.

[4] Chen li digital test platform based on virtual instrument [D]. University of electronic science and technology, 2014.

[5] lun- fa wang. Multifunctional irtual test platform research [D]. University of electronic science and technology, 2012.

[6] zhong-li ma, hong-da liu, Zhang Jingna. The development of virtual experiment and virtual test platform [A]. National university in electrical engineering and its automation major teaching guidance committee. The first national conference on electrical engineering and its automation major t eaching reform [C]. National

university in electrical engineering and its automation major teaching guidance committee, 2012.

Fast charger designed for high-capacity smart-phones batteries

Wang Wenbo; Zhu Yongxing; Cai Kailong

(College of Instrumentation and Electrical Engineering，Jilin University，Changchun 130026，China)

***Abstract*--In this paper, a set of buck circuit is developed，use MCU as the core of smart-phones lithium batteries charger. The sampling circuit , MOSFET driver circuit and Phone battery charging measurement and control circuit and display circuit are designed. The mathematical model and the transfer function of buck are studied. Through the BUCK circuit for lithium battery charging, sampling and monitoring the charging current in real time and after using the PI algorithm, adjusting the MOSFET turn-on and off in order to control the charging current in stable range, and intelligent modules will prevent hazard factors such as over current, over voltage and over temperature. Simulation and experimental results verify the validity of the control method.**

***Keywords*--The smart fast charging Lithium battery energy storage MSP430F149 MCU PI controller**

I. INTRODUCTION

IN recent years, with the development of science and technology, the function of the smart phone is becoming more and more ,and people are also getting more and more dependent on smart phones, but also makes the power of smart phone is more and more big, the power dissipation only grow but the charging time, charging accidents also happen from time to time. Therefore, how to realize the intelligent mobile phone battery quick charging and intelligent charging[1] was imminent, and it also has great practical significance.

And this smart quick charger design can not only effectively reduce charging time but also improve the quality of the charging, real-time monitoring of mobile phone battery at the time of the current state of voltage and temperature, and make the corresponding protective measures in a timely manner[2-3], effectively guarantee the safety charging. Therefore, this design effectively optimize the function of cell phone battery charger and ensure the security of the charging[4], make people have a better phone using experience.

II. SYSTEM DESIGN AN OVERVIEW

System is divided into hardware design and software design of two parts. The hardware is divided into MSP430 minimum system module, power module, buck circuit module, driver circuit module and sampling module etc. All of them constitute a step-down voltage stabilizing circuit; Software design is mainly based on PI principle[5] as the core of lithium battery program, realized the constant current charging, over-current protection, overcharge protection. Two parts of hardware and software closely linked, mutual cooperation, common realize the rapid charging basic functions.

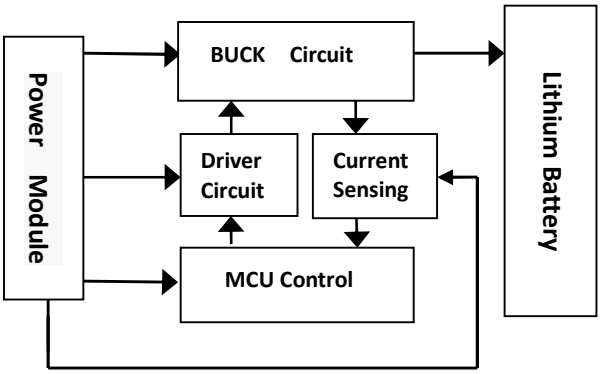

Fig 1 Basic diagram

III. HARDWARE DESIGN

A. Introduction of MSP430

MSP430 is a series of low power consumption microprocessor which is launched by TI company. Its remarkable feature is ultra-low power consumption from which contains five low-power modes to choose. It takes very short time to wake up, only 6μs. At the same time, MSP430 has strong processing capacity, high integration and abundant embedded modules(12 bit A/D conversion, 16-bit timer, FLASH, etc.). The

charger that we designed adopts MSP430F149 single chip microcomputer as main controller. The SCM changes to low power mode, effectively reduces the power consumption of the system, and enhances itself efficiency through the output voltage and current of the battery charging status which are sampled by sampling circuit in real-time .

B. Power module

a. QAW01 power module

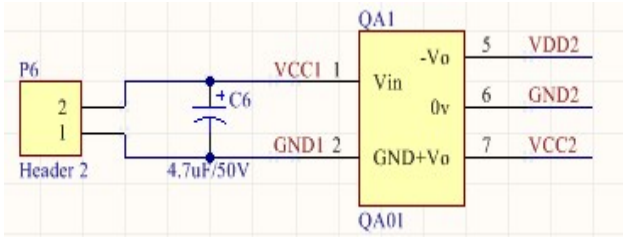

Fig 2 QAW01 power module

QAW01 is a DC/DC power supply module that is produced by Jin Shengyang company. Its input is +12v and output is +15v or -9 v. It will not only be used to provide power for TLP250 but also have the function of isolation.

b. F1205xt-1wr2 power module

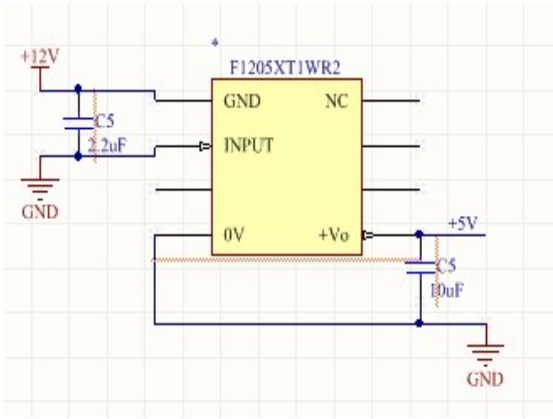

Fig 3 F1205xt-1wr2 power module

F1205xt-1wr2 is a single output isolation unsteady power module which is produced by Jin Shengyang company. It can change +12v to +5v(DC),and its power is 1w, used to offer power for single chip microcomputer in the charging circuit. It has lots of features such as sustainable short circuit protection, low ripple noise, high isolation voltage(+3000v) and high efficiency(80 percents), etc.

C. BUCK circuit module

Using the BUCK circuit[6] shown in figure 4 as the main charging circuit. Among them, the ST company has produced a new fast recovery of the MOSFET transistor STW55NM60ND and ai Seth's fast recovery epitaxial diode DSEI30 - 06 as the switch and fast recovery diode. Respectively take 220 μF and 470μF the inductance and capacitance of the LC filter part, the formula of capacitance and inductance computation is as follows:

$$C=\frac{U_o(1-U_o/U_{in})}{8Lf^2\Delta U_o} \quad L=\frac{U_o(1-U_o/U_{in})}{2fI_o}$$

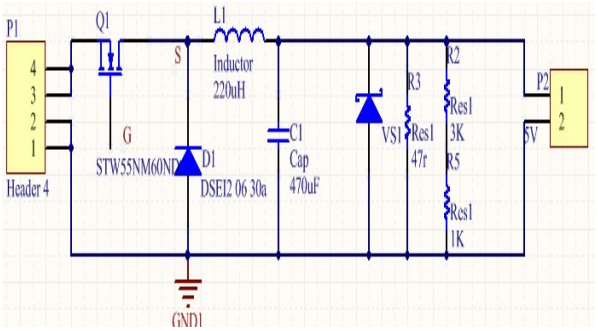

Fig 4 BUCK main circuit

D. Driver circuit module

This module uses the optical coupling isolation chip (TLP250) and its peripheral circuit. TLP250 is produced by Japan's largest semiconductor maker Toshiba corp with isolation voltage: 2500 VRMS, one-way channel, output current: 1.5A, DC input, etc. BUCK main circuit adopts the pulse width modulation (PWM) method to control charging current, through the drive circuit of PWM signal pulse width enlarge the size of the increase/decrease to change the charging electric current.

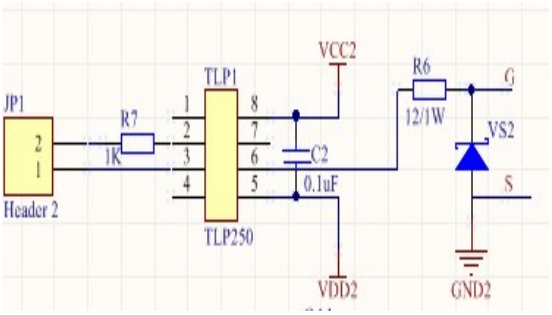

Fig 5 TLP250 driver circuit

E. Sampling module

This module uses the current sensor ACS712 module and its peripheral circuit to test the current in the system. Converted into the current signal into voltage signal, then send the signal to MSP430, realize A/D conversion. Specific conversion formula is:

$$V_{out} = 2.5V + I_{in}(A) * 0.185 \quad (1)$$

The voltage signal sampling is through the series on each side of the voltage sampling resistance, and according to the proportion sampling voltage sent to

MCU through the following circuit.

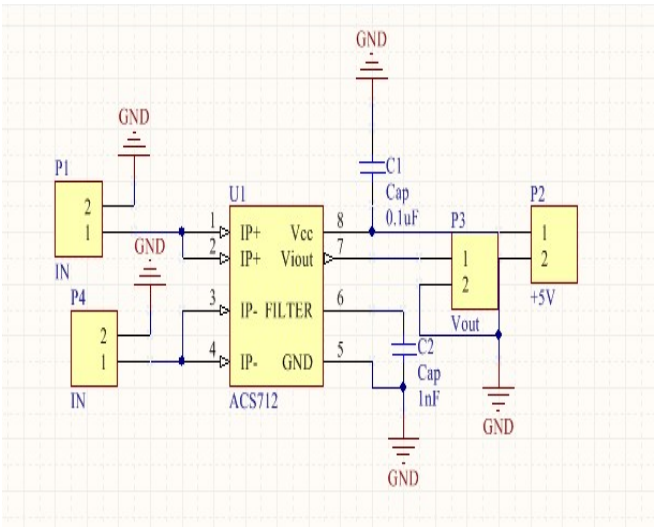

Fig 6 Sampling module circuit

IV. THE SOFTWARE DESIGN

A. Basic principle

Constant current charging control performed by digital PI regulator[7].

PI controller is a linear controller, it according to the given value r(t) and the actual output value c(t) to control deviation

$$e(t) = r(t) - c(t) \tag{2}$$

Will be in proportion to the deviation (P) and integral (I) by linear combination of control volume, to control the controlled object, the control law for

$$u(t) = K_p[e(t) + \frac{1}{T_I}\int_0^t e(t)dt] \tag{3}$$

The u(t) as the output of the PI controller, $e(t)$ as the input of the PI controller. Kp is the proportional coefficient .TI is the integral time constant.

Proportion link: instant is proportional to reflect the deviation of the signal control system, once produced, deviation controller immediately control effect, to reduce the deviation.

Integral part: mainly used to eliminate static error, and improve the system of no deviation.

Here using incremental PI control, feedback control block diagram is as follows:

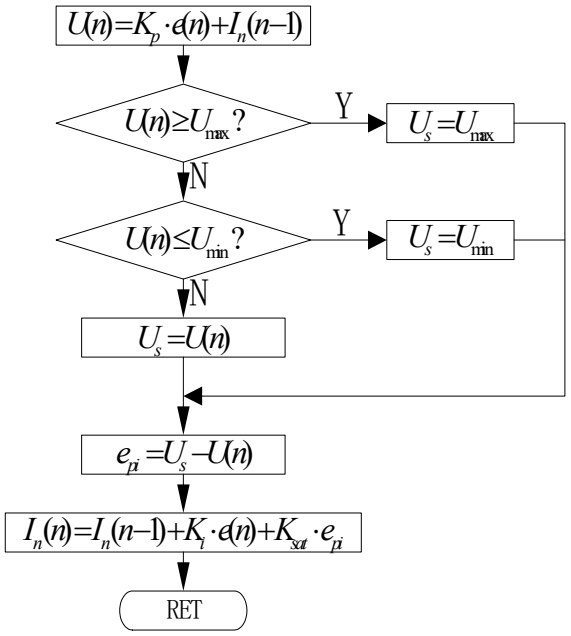

Fig 7 Feedback control diagram

B. The discretization of PI algorithm

As a result of the single chip microcomputer control is a kind of sampling control, it can only be the amount of control is calculated according to the deviation of the sampling times, so must be conducted for the discretization process, with a series of sampling time point k represents a continuous time t, PI control algorithm based on discrete expression is:

$$\Delta u(k) = u(k) - u(k-1) = K_p[e(k) - e(k-1)] + K_i e(k)$$

C. The actual application

This article uses the digital PI regulator, to adjust the output voltage of buck circuit. PI controller in real time to measure the current in the circuit. Specific way is: sampling current of the main circuit, , and converted into voltage enlarged to 430 single chip microcomputer, and uses the AD program convert analog to digital data, and carries on the judgment, if the current is too large, will be PI regulator close; If it is in the normal range will be compared with the current default values, to adjust the PI algorithm, error to control the MOSFET turn-on, and by the time, in turn, have the effect of adjusting the BUCK circuit output current, output reached 1.5 A constant current to the effect of lithium batteries.

V. WORKING PROCESS AND THE RESULTS

Through the BUCK circuit for lithium battery charging. In the process of lithium battery, charging

current value by current sensor real-time sampling monitoring, and the sampling data to the MSP430F149 MCU, using PI algorithm, and calculate the maintain constant current needed for the PWM duty cycle, always adjust the charging current value, make its stability in 1.5 A, keep the lithium battery in the constant current charging status. To prevent because of voltage fluctuation and make the charging current is too large, so the upper limit set in the charging process, the over-current protection. During this time, the voltage rise gradually, when 4.2 V, due to the effect of voltage regulator tube, no longer increases, voltage at 4.2 V lithium battery entered into A state of constant voltage charging, during this period, current gradually reduce, when less than charging program set the lower limit of 0.2 A, make the duty cycle of 0 BUCK circuit, stop charging, prevent due to the charging current is too low harm the lithium battery.

Table 1 The test result of the battery to be charged

Charging time （min）	Voltage（V）	Current (A)
10	3.6	1.47
20	3.78	1.41
30	4.02	1.43
40	4.16	1.46
50	4.17	1.28
60	4.17	0.75
70	4.18	0.22

VI. CONCLUSION

Using MSP430F149 MCU as the main control unit and in combination with other chips and circuit structure phone quick smart charger, using PWM voltage output, flexible control, the characteristics of the load ability, self-adjustment, can greatly improve the charging efficiency and to protect the battery during the charging process, meet the demand of intelligent era, has certain practical significance.

Reference

[1] Wang Shanyin, Wang Jiake. The design of portable mobile charger study [J]. Journal of mechanical design and manufacturing and automation. 2011.2.158-159

[2] Zhao Pu. Based on the design and implementation of MCU multi-functional charger [J]. Microcomputer information. 2012.5.75-76

[3] Lin Jianchun. Based on single chip microcomputer intelligent charger [J]. Journal of modern electronic technology. 2012.12.30-31 * 38

[4] Wu Wei, Wang Ruifeng. Based on single chip microcomputer intelligent charger design [J]. Science and technology information. 2011.12.137-138

[5] Liu Jinkun. Advanced PD control and MATLAB simulation [M]. Electronic industry press, 2003

[6] Yan Yanxia, Jiang Liying, Jiang, Suxia. Based on single chip microcomputer intelligent charger hardware design [J]. Microcomputer information. 2012.10.211-212

[7] Xie Qiaojia, Pan Chujia. Theory of smart phone quick charge design [J]. Journal of digital technology and application. 2012.04.163-164

Intelligent lamp control system based on infrared positioning

Duan Chongli; Tan Shixiong; Jie Haohan
（*Jilin university instrument science and engineering institute,Changchun,130021*）

***Abstract*—With the development of electronic technology, people have put forward higher and higher request to the car's automation and intelligence. The project is to measure the distance of two cars traveling in opposite direction by infrared distance measurement and to adjust the lighting brightness and the angle of the main light of the vehicle according to the distance change. The hardware model of the intelligent control system based on infrared positioning is established.**

***Keyword*--Infrared distance measurement Intelligent control Lighting change**

Ⅰ PREFACE

TRAFFIC safety is a core issue in the automotive industry. It is obvious that, to get traffic information, 80% from the driver's visual capture, including traffic information, signal lights, traffic conditions, etc.. And these are particularly important at night. The improvement of the lighting system can not only provide timely and accurate information for the driver, at the same time, it can effectively reduce the driving fatigue, reducing accident hidden danger. Nowadays, the number of cars in our country is increasing year by year, and the application of the self adjusting optical system is more important. It is of great significance to improve traffic safety and reduce economic losses. For this reason, we hope to make the lights more automated and intelligent, For this reason, we hope to make the lights more automated and intelligent. When there is a vehicle coming across the road, so that the car lights to make intelligent regulation, such as changing the brightness and angle of light, lighting control area etc. In order to reduce the probability of accident and improve the safety of traffic.

Ⅱ PRINCIPLE

A. Infrared distance measurement principle

This is the process of infrared distance measurement: The infrared ray emitted by the distance measuring instrument is reflected by the measured object and received by the distance measuring instrument. Distance measuring instrument and record the time of infrared ray. The half of the product of the speed of light and the round-trip time, the distance between the range finder and the object being measured[1]. If the speed of light in the air in the spread of A, B between the time required for a round-trip time is t, Then A, B distance between the two points D can be expressed as follows:D=ct/2.

B. PWM control voltage principle

PWM (Width Modulation Pulse) control technology is the width of the pulse modulation technology. By modulating the width of a series of pulses, the desired waveform (including the shape and amplitude) can be obtained. Area equivalence principle is an important basic theory of PWM technology. A typical PWM control waveform SPWM: The width of the pulse is changed by the sine law and the PWM wave is called the SPWM wave.

Ⅲ OVERALL STRUCTURE

When the car in the evening or at night when driving (usually cases are used in light), in the event of a two car trains, receiver detection to the signal distance, feedback a signal to the control circuit, STM32 control circuit through the PWM Buck modules enable small lighting voltage gradually decreased from the 12V, at the same time, STM32 control circuit servo control resulting in small lighting angle by 90 degrees decreased, simulation of such car is by the high beam light switch into headlight. When after the car crossing, the receiver does not receive the signal distance, will also be the feedback signal to the control circuit, control circuit of STM32 control steering gear and small lighting voltage, so as to restore the high beam lamp circuit. If applied to an automobile can be in the

middle of the front of the car to install an infrared transmitter, for transmitting a infrared signal to the other side of the vehicle, and on both sides of the front of the installation of an infrared signal receiver, for receiving the opposite vehicle infrared signal[2]. The structure of the system is shown in Figure 1:

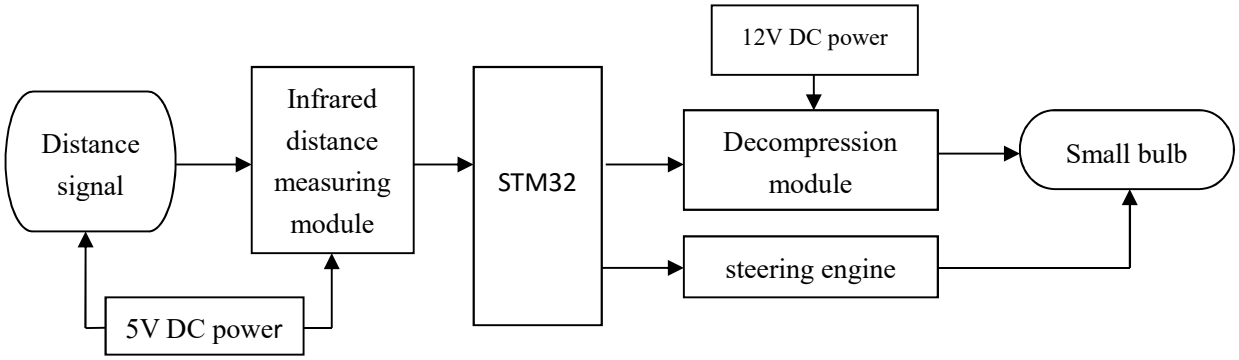

Fig.1 System structure diagram

Ⅳ DESIGN

A. Design of power supply

Step-down links is ratio is about 15.7 transformer to 220V AC sine wave voltage down to about 14V; rectifier is rectifier diodes 1N4000 (or 1N4001~1N4007 can be) barricaded bridge rectifier circuit to 14V about AC sine wave. The voltage is converted to a one - way pulse voltage with a peak value of about 18V.

Filter part is with a pressure of not less than 25V electrolytic capacitor C1 to 18V about unidirectional pulse voltage conversion with approximately 18V AC ripple DC voltage (here set aside the 7812 working voltage of 2V above, 10% of grid voltage fluctuation volume 2V and moderate amplitude ripple voltage 1V).

12V output voltage link with linear manostat 7812 to approximately 18V with AC ripple DC voltage into 12V DC voltage of a very stable quality is very good; use with the role of the output filter capacitor C2 is 7812 may occur in the work of the self-excited oscillation suppression, because the three terminal linear regulator is extremely easy to produce self oscillation, so C1 is usually not less. The pressure not less than 16V. Output 5V end will be 7805 to 7812 can be. The power circuit is shown in figure 2:

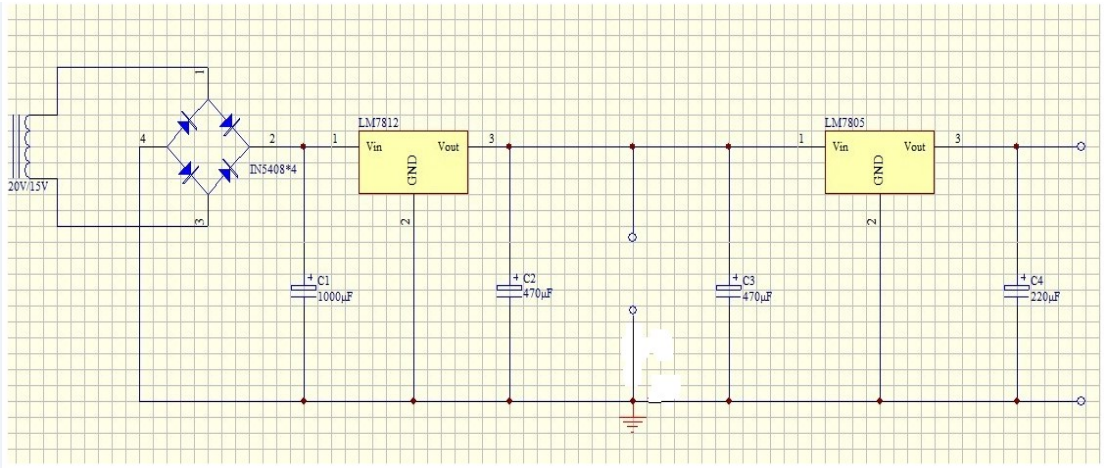

Fig.2 AC220V to DC12V and DC5V power circuit

B. Program design

The system software uses the KEIL compiler programming, chip select CortexM3 Series MCU STM32C8T6. The control part of the program consists of two parts: the control part and the peripheral part as shown in figure 3:

The Y401 module adopts the serial working mode, will enable 1 STM32 serial baud rate by 9600. According to the serial communication mode of the ultrasonic module, the 0x55 can be sent to a set of 16 bit height data in the cycle. The received data is converted to decimal, according to the size of the adjustable range and fixed range. Make corresponding data output to the corresponding

interval by using the if-elseif-else statement. When the distance data is less than 10 (simulated reality of 1m) counter CCR1, CCR2 output value 400; when data is greater than 10 less than 30 (simulated reality 1 M-10 m) output count 400-1000 adjustable; when the distance data is greater than 30 (simulated reality more than 10m) count output value of 1000. Will CCR1 PWM signal connected to the steering gear, control lamp holder of rotation angle, CCR2 PWM signal is enlarged by a triode after connecting motor drive module, output 0-12 to voltage is used to control the brightness of the incandescent lamp, so as to realize the illumination angle and illumination intensity.

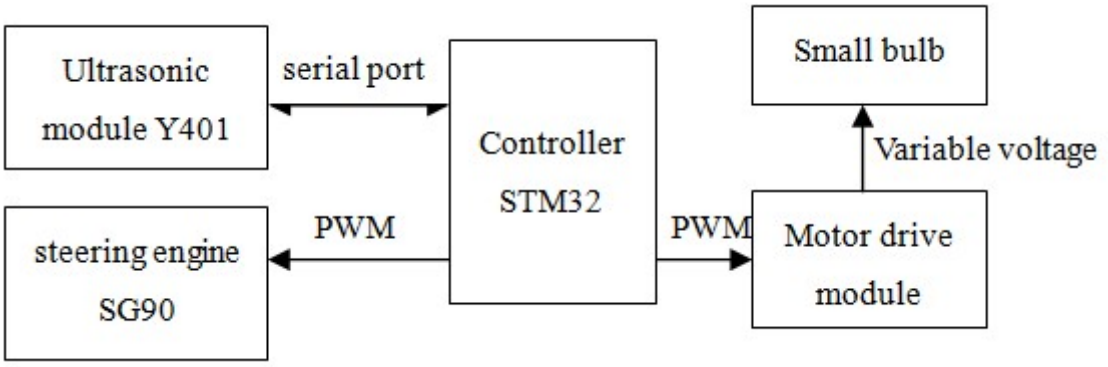

Fig.3 Block diagram of control program

C. Boost circuit

Because the STM32 microcontroller port voltage is 3.3V, and the power supply voltage is 5V, in order to ensure that the MCU can drive power supply, it is necessary to boost the ST32 microcontroller port, the structure circuit diagram is shown in figure 4:

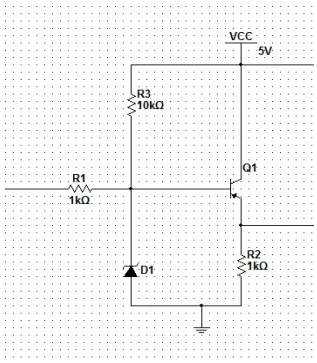

Fig.4 Boost circuit

Ⅴ TESTING DATA

A. Relationship between voltage and distance of infrared device

Due to the sharp gp2y0a21 distance sensor, the effective distance of 80cm, and between the 0-8cm is nonlinear, so we between the 10-80cm orderly eight consecutive points, the actual distance and the output voltage is measured, the compression of the data and the standard distance and the output voltage is compared, the results such as table 1 shows:

Table 1 Relationship between voltage and distance of infrared distance sensor

Distance (cm)	10	20	30	40	50	60	70	80
Output voltage theory（V）	2.27	1.32	0.91	0.75	0.63	0.51	0.45	0.40
Actual value of output voltage（V）	2.25	1.35	0.92	0.78	0.65	0.49	0.43	0.36

B. The relationship between the distance and the rotation angle of the vehicle lamp

When the obstacle is stationary, the distance between the two and the steering angle of the steering gear is recorded when the trolley is close to the obstacle, as shown in table 2:

Table 2 Relationship between distance and angle of light

Distance（cm）	10	18	26	34	42	50
Rotation angle（°）	88.4	72.1	54.7	35.2	18.6	0.0

C. Relationship between distance and light intensity (output voltage)

When the obstacle is stationary, the distance between the two distances and the light intensity (output voltage) is recorded when the vehicle is close to the obstacle:

Table 3 Relationship between distance and light intensity(voltage)

Distance（cm）	10	18	26	34	42	50
Voltage（V）	4.66	5.33	5.92	6.53	7.23	8.31

D. The overall relationship between the distance and the light intensity and the rotation angle of the steering gear

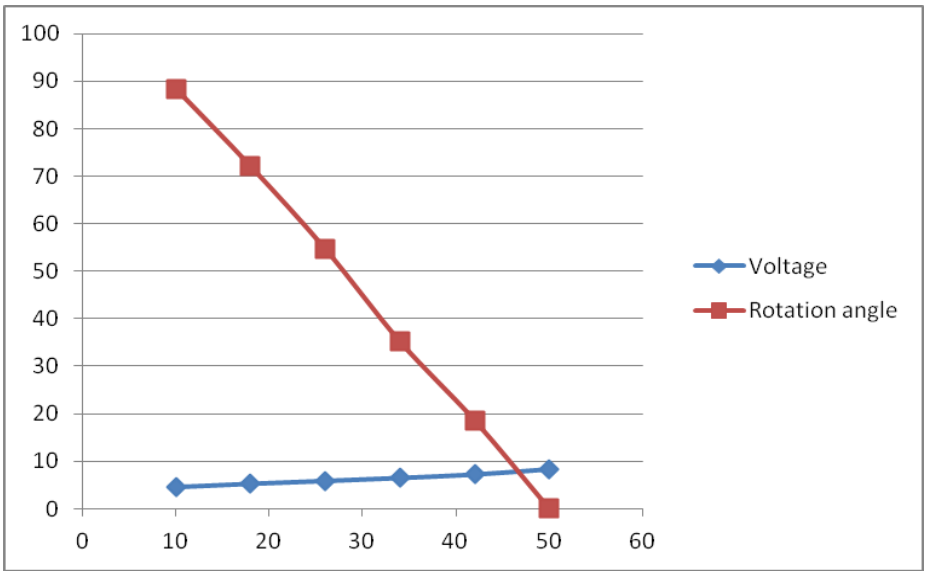

Fig.5 The relationship between distance and light intensity and electric motor

VI SUMMARY

Based on the infrared positioning of intelligent lighting control system, reduce the driver's actions in a certain extent, prevent manual switching far and near light when the attention of dispersion, reduce the anthropogenic causes other some nocturnal car safety problems. At the same time the system uses intelligent operation, can quickly make the action at the meeting of vehicles, to prevent the delay of manual operation. The design of the system is still in the primary stage, and many specific problems need to be further studied.

References

[1] Chang Rongjun. “Vehicle far and near light intelligent switching system” [J],CNKI ,2010.

[2] Jin Xiangliang , Zeng Yun , Cheng Diping. “The establishment of infrared distance measurement system and its application in automobile collision avoidance system”,J, in Infrared technology , 2001,23 (3) :43-45.

Portable PM2.5 detect transmission device

Liang Xiong-feng; Huang Shi-de; Zhang Qiang; Li Zhe
（jilin university instrument science and engineering institute,changchun,130021）

***Abstract*--In recent years, with the improvement of people's living quality, increase in the number of cars and other transportation is more, the effects of automobile exhaust pollution of urban environment is more and more obvious. Our country more and more urban air quality value extraordinary, so environmental problems got the attention of people.We aimed at the problem to develop a portable PM2.5 detect transmission device, used in the monitoring of PM2.5.The instrument with low power consumption MCU STC12C5A60S2 as the core, with GP2Y1010AU0F as sensors, and combining the TC35i GSM module and GPS ATK - NEO - 6 m - V23 module, after transformation hardware level, software filtering, data post-processing to realize real-time monitoring with PM2.5 position coordinates information display, and through the function of the SMS remote testing information extraction of PM2.5. By analyzing test data, the device has air PM2.5 levels can be within the permitted error detection.**

***Key words*--PM2.5 detection; GPS module; GSM SMS transceiver**

0 FOREWORD

PM2.5 refers to the atmosphere diameter less than or equal to 2.5 micron particles, also known as can go directly to the alveoli. Although PM2.5 is only a few components content of earth's atmospheric composition, but it has important effect on visibility and air quality etc. PM2.5 particle size is small, rich in a lot of poisonous and harmful substances and in the atmosphere for a long time, transmission distance, and to human health and the impact of atmospheric environment quality.A quarter since 2013, our country land the fog haze [1], the affected population of about 600 million people.PM, although not poisonous gas, PM due to the small diameter, carry a lot of poisonous and harmful substances, PM2.5 impact on health, in essence is PM2.5 surface adsorption of the health effects of various chemicals, such as adsorption carcinogens have carcinogenic effect, adsorption two mouth bad English have reproductive harm, if the adsorption of heavy metals is the harm of heavy metals, the key is to see what did PM2.5 adsorption [2]. PM the small diameter, the greater the damage to human body, PM2.5 can drift to the distant place, thus influence scope is bigger. PM2.5, moreover, the harm to human body health to a larger, because the smaller the diameter, the deeper into the part of the respiratory tract. 10 microns in diameter of the particles are deposited in the upper respiratory tract, under 2 microns can go deep into the bronchi and alveoli. Fine particulate matter into the human body to the alveoli, a direct impact on pulmonary ventilation function, make the body to a state of hypoxia. And this kind of fine particulate matter once in alveoli, adsorption is hard to fall in the alveoli, the adsorption is not reversible. [3] Compared with the pure "fog", "haze" is the result of the contaminated air, so haze days than fog a greater harm to human body health. In north China in recent years, influenced by global climate anomalies, lead to more severe drought, city a large number of greenhouse gases at the same time, a haze weather is on the rise in the day of [4].Research indicates that the ash haze weather caused by fine particulate matter on human health hazards even more than the sandstorm [5].So a kind of small volume, low price, easy to [6] with and which has the function of system positioning and messaging, portable PM2.5 detector was born along with the time development application [7].The instrument by STC12C5A60S2 single-chip microcomputer control GP2Y1010AU0F sensor [8], and cooperate with the TC35i GSM module and GPS ATK - NEO - 6 m - V23 module, after transformation level [9], filtering, data post-processing PM2.5 detection functions [10].

1 PM2.5 MONITORING SYSTEM DESIGN

1.1 WORKING PRINCIPLE OF THE SENSOR AND DATA PROCESSING

GP2Y1010AU0F air quality is an optical sensor, designed to induction dust particles in the air, its internal diagonal sits infrared leds and phototransistor, that it would be able to detect reflected light dust in the air, even very small particles such as tobacco smoke can be detected, usually used in air purification systems.

As shown in figure 1, the lower sensor has a heating device, can be heated, so that dust particles will be heating up. One end of the sensor is a light-emitting diodes that generated a certain intensity and frequency of light. At the other end has a receiving diode, light emitting diode light can cause reflection and refraction on the dust particles, so that will be receiving diode.

The sensor has a very low current consumption (maximum 20 ma, typical values 11 ma), can use up to 7 VDC. The sensor output voltage for simulation, its value is proportional to the dust concentration. Can smile measuring more than 0.8 micron particles, perception of tobacco produce die and pollen, house dust, etc. Small volume, light weight, easy to install.

The module is based on single chip microcomputer STC12C5A60S2. Through control, USES is GP2Y1010AU0F dust sensor, the sensor principle is through the change of output voltage to determine the size of the dust concentration, such as detection of cigarette formula is: variable range of output voltage (V) = output voltage range VoH (V) - clean when the output voltage VoC (V), the voltage conversion into detection range of dust concentration (mg/m3) = variable range of output voltage (V)/detection sensitivity: K (V / 0.1 mg/m3), the decision value = checkout concentration (mg/m3) / 10 * K (V/(0.1 mg/m3) + clean when the output voltage (V).

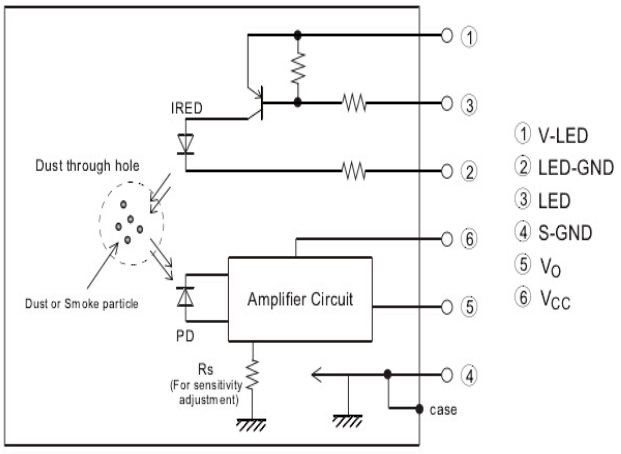

Fig.1 Working principle of the sensor diagram

1.2 CLEAN THE RENEWAL OF THE OUTPUT VOLTAGE

Clean when the output voltage is dust, smoke detection of presence of decision level of benchmark, accurate say is also the improvement of detection precision. Clean when the output voltage is based on light emitting diode output is low, in the inside of the box dust adhesion, such as ambient temperature to change.

Light output is low, clean when the output voltage drops, device in the inside of the box dust adhesion can make clean output voltage has a tendency to rise. Basically, with the passage of time, if the output voltage does not change. Will not be regarded as no detected objects, to update the standard as a clean output voltage.

Generally, light-emitting diodes (leds) under the condition of long-term electricity, the output is reduced. Light-emitting diode output to reduce dust sensor, dust-free output voltage and detection sensitivity decreases. So, need to clean the output voltage and sensitivity correction. Clean output voltage in the E2PROM chips was introduced by memories, at some point, the standard than in the case of fixed and memory will be updated when low standard, according to the clean degree of low output voltage of the corrected detection voltage

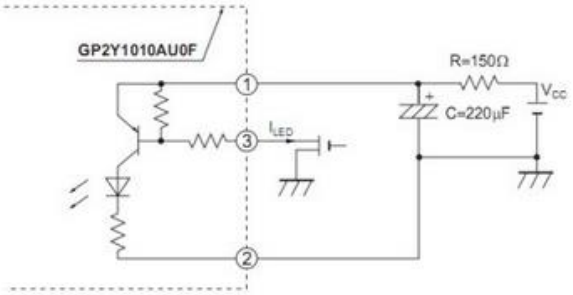

Fig.2 Input condition for LED input terminal

2 THE GPS MODULE INFORMATION ACQUISITION SYSTEM DESIGN

2.1 WORKING PRINCIPLE OF THE GPS MODULE

Positioning system using ATK - NEO - 6 m - V23 module, ALIENTEK production is a high performance GPS module, core module adopts UBLOX company NEO - 6 m module, has 50 channels, tracking

sensitivity up to 161 DBM, measuring the output frequency of up to 5 hz. ATK - NEO - 6 m - V23 small size, good performance. 20.5 dB module with ceramic antenna and MAXIM company high gain LNA chips, star search ability. Modules can be various parameters via a serial port Settings, and can block is saved in the EEPROM, easy to use. Module with IPX interface, can connect all kinds of active antenna, adaptable. Module is compatible with 3.3 V / 5 V level, convenient to connect all kinds of single chip microcomputer system. Backup module built-in rechargeable batteries, can keep the ephemeris data when power supply drop, to be able to meet the needs of real-time positioning. Chip adopts serial communication method, can obtain the coordinates of longitude and latitude, altitude and other information transmitted to the main control chip, after on the man-machine interface display.

By GPS module, access to measuring the coordinates, and to the main control chip, record the coordinate azimuth. , also added a GSM module in the system and wait for PM2.5 numerical data through the GSM network in the form of text messages sent to the mobile terminal.

2.2 NMEA-0183 INTRODUCTION OF AGREEMENT

NMEA0831 is the U.S. national Marine electronics association's standard format for sea with electronic equipment. At present has become a GPS navigation device unified RTCM standard protocol.

NMEA - 0831 protocol USES the ASCII to send GPS positioning information, we call it frame. The frame format forms such as: $aaccc, DDD, DDD,... , DDD * hh (CR) (LF)

1, "$" : frame start bit command

2, aaccc: address domain, the former two as the identifier (aa), after three for statement name (CCC)

3, DDD,... DDD: data

4, "*" : check and prefix (also may make statements marks the end of the data)

5, hh: checksum

6, (CR) (LF) : end of the frame, a carriage return and a newline character

NMEA - 0183 commonly used commands such as table 1:

Table1.Common commands of NMEA-0183

The serial number	The comm-and	instructions	The biggest frame length
1	$GPGGA	GPS positioning information	72
2	$GPGSA	The current satellite information	65
3	$GPGSV	Visible satellite information	210
4	$GPRMC	Recommended location information	70
5	$GPVTG	Information on the ground,	34
6	$GPGLL	Geodetic coordinate information	/
7	$GPZDA	The current time information	/

Here, we use the 4 $GPRMC position information (recommended)

$GPRMC statement of the basic format is as follows:

$GPRMC, (1), (2), (3), (4), (5), (6), (7), (8), (9), (10), (11), (12) * hh (CR) (LF)

We use location information

(1) UTC, HHMMSS (minutes)

(2) the positioning state, effective positioning, A = V = null and void

(3) the latitude DDMM. MMMMM (c)

(4) the latitude (northern hemisphere) or S (southern) hemisphere N

(5) precision DDDMM. MMMMM (c)

(6) precision hemisphere (east longitude) or E W (n)2.3 module connected to the microcontroller

Module is connected to the MCU minimum you just need to four lines: VCC, GND, TXD, RXD. The VCC &gnd for module power supply, TXD and RXD module respectively connect to MCU RXD and TXD, used for the transmission of information. And the module can be compatible with 5 V and 3.3V microcontroller system.

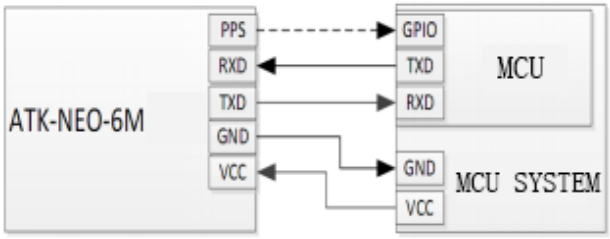

Fig.3 Connection schematic of GPS module and MCU

3 GPRS REMOTE INFORMATION TRANSCEIVER SYSTEM DESIGN

3.1 GSM SHORT INFORMATION TECHNOLOGY PRINCIPLE

TC35 is Siemeils company launched a new - generation GSM wireless communication module. With RS232 communication interface, can be easily communicates with PC machine, single chip microcomputer. Can fast, safe and reliable system to realize the data and voice transmission, Short Message Service (Short Message Service) and by fax. TC35 module of the working voltage of 3.3-5.5 V, working at 900 MHZ and 1800 MHZ two frequencies, where the spectrum respectively 2 w power consumption (900 m) and 1 w (1800 m).

Interface module has the AT command set, supports text and PDU mode of short message, a third group of 2 kinds of fax, and 2.4 k, 4.8 k, 9.6 k of transparent mode. In addition, the module also has the function of the phone book, call, roaming detection function, common work patterns have power-saving mode, IDLE, TALK, etc. Through unique 40 pin ZIF connectors, power supply connection, instructions, data, voice signal, and the two-way transmission of control signal. Through ZIF connectors and 50 antenna connector, connecting the SIM card holder and the antenna.

TC35 module is mainly composed of GSM baseband processor, the GSM radio frequency module, power supply module (ASIC), flash memory, ZIF connectors, antenna interface of six parts. As the core of TC35, baseband processor in the main processing for all analog and digital function. Under the premise of without additional hardware circuit, can support FR, HR and EFR voice channel coding C35 even machine approach:Any a TC35 module used for the first time, it must be to test whether the work is normal, because of its own RS232 interface, so we can use the PC serial debugging software debugging.

1, start the serial debugging software

There were many serial debugging software, you can use any software, can also use the "super terminal" WINDOWS. Set the baud rate 19.2 k, this is the default baud rate of TC35, even the machine can continuously from 2400 to 57.6 k for the first time test, until TC35 have response.

2, send the "AT" "

AT the enter

3, change the baud rate "AT + IPS = XXXX"

TC35 the default baud rate is 19.2 k, and the actual use, can change to 9600 or 38.4 k, as follows:

The AT + IPR = 9600, press enter

4, SMS mode Settings

There are two kinds of TEXT mode (GSM module. 1 kind is: TEXT mode; the second is: PDU mode. PDU mode can use unicode send English and Chinese. But the synthesis of PDU code is more complex, and can only send English TEXT patterns, but without coding. Actual use can use TEXT mode.

Set as follows:

The AT + CMFG = 1 enter

5, SMS mode

A SMS is formulated by Etsi standard (GSM and GSM 03.38 03.40). When using 7 - bits encode it can send up to 160 characters; 8-bit encoding (up to 140 characters). Often cannot directly through phone display; Is often used as a data message, such as: smart pictures and ringtones and OTA WAP Settings in the messaging. 16 - bit information (up to 70 characters) is used to display the Unicode text information (UCS2), can be shown most of the mobile phone. A 16 - starting with class 0 bit of text information on some mobile phone as a Flash SMS display (SMS and flashing warning SMS).

There are two ways to send and receive SMS messages: use text mode or use PDU (protocol description unit) model. Text mode (maybe some mobile phone does not support) is actually a form of a PDU encoding. The display SMS information, may use different character sets and different ways of encoding.

6, text reading method

The AT + CMGR = X return

If there is a short message, TC35 response:

The AT + CMGR = 1

+ CMGR: REC "UNREAD", "13307496548", and "04/08/17, 22:24:32 + 02

testOK

OK

Short information analysis:

"Test OK" is the message content.

Short information storage capacity associated with Ic card, the serial number from 1 - N.

REC UNREAD ": represent short messages are read.

REC READ: "has been READ.

13307496548 ": receive cell phone number.

04/08/17, 22:24:32 + 02 ": short message sending time.

No message, TC35 response:

The AT + CMGR = 3

+ CMGR: 0, 0

7, SMS deletion method

The AT + CMGD = 1 enter

8, SMS sending method

Short message sent is divided into two steps:

1: send and receive cell phone number, waiting for the reply, ">"

The AT + CMGS = "13307496548" carriage return (destination address)

TC35 response:

The AT + CMGS = "13307496548" >

2: the content of the input message (English only) : Test press enter

3.2 GPRS SYSTEM HARDWARE DESIGN

3.2.1 GPRS SYSTEM PRINCIPLE

GSM communication module the concentrations of PM2.5 data after the implementation will be treated as single chip microcomputer, and the position of the GPS module to obtain coordinate data package sent to the target phone, at the same time will receive the information real-time display on the LCD screen in 1602.

The whole system working principle is to use STC12C5A60S2 single-chip microcomputer control data collection, GSM module performs data sending. This system can realize the PM2.5 data sent to the designated a cell phone, just send module equipped with mobile phone specified format message, short message content module identification, through single chip microcomputer processing, the real-time PM2.5 data feedback in the form of a short message to the corresponding target mobile phone.

3.2.2 TC35I MODULE POWER SUPPLY

TC35i module provides all the power interface, need access to more than 5 v 2 a or 2 a dc power supply. Module is negative in the back of the board have marked: VCC access positive, GND plugged into a power supply for the cathode.TC35i pin diagram as shown in figure 6：

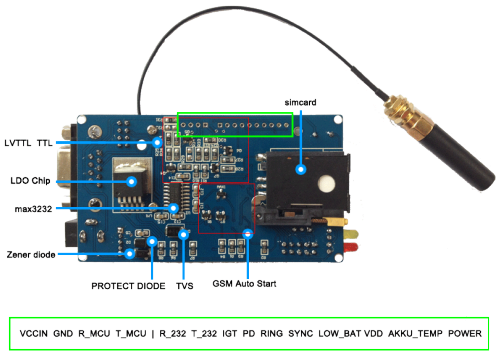

Figure 6 TC35i pin drawing

Start the TC35 way:

TC35 can be activated by the following way, begin to work

1. Through point firewire IGT trigger, into the normal working condition

2. Through the power cord, began to enter the recharge area

3. Through the RTC interrupt, start into alarm mode

3.3 GPRS SYSTEM SOFTWARE DESIGN

Software, by controlling the STC12C5A60S2, storage of PM2.5 sensor data, and through the TC35i communication module sent to the designated mobile phone. After system boot, initialized first action, open the total interruption, display the boot screen, GSM module to work properly.

GSM module is normal work, immediately to the designated mobile phone to send a contain PM2.5 data information. After that, when to accept the request message to the specified format, you can extract the phone number, then send the number of PM2.5 value at this time; Not received the message, the specified format information display shows the current PM2.5 concentrations. This feature is convenient and quick, from the design of key parts, and at the same time able to remote wireless transmission to a specified mobile phone.

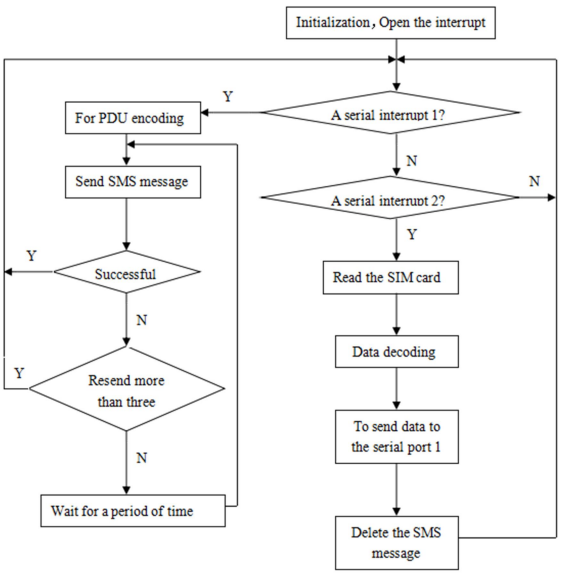

Fig.7 the main function program flowchart

4 TEST RESULTS AND CONCLUSIONS

After the experiment test, PM2.5 detector has can achieve the function of PM2.5 monitor, the screen also shows the location of measured PM2.5 levels as well as the geographic coordinates of test site. Instruments have remote message sending and receiving function, can be fixed by mobile phone on the format of the message asking, instrument through to the SMS receiving and processing, the screen information sent to the target cell phone users, so as to realize the function of remote monitoring of target location of PM2.5.

Here is in the instrument of changchun day we use the measured data of PM2.5 levels:

Table 3 Measurement data sheet

TIME	PM2.5 DATA	Website data
8:00	56ug/m³	55ug/m³
10:00	79ug/m³	77ug/m³
12:00	59.5ug/m³	56ug/m³
14:00	52ug/m³	47ug/m³
16:00	53ug/m³	60ug/m³
18:00	73.4ug/m³	70ug/m³

* measured on January 8, changchun PM2.5 numerical (micrograms per cubic meter)

Draw the following chart according to the experimental data and the observation of PM2.5 change trend in one day:

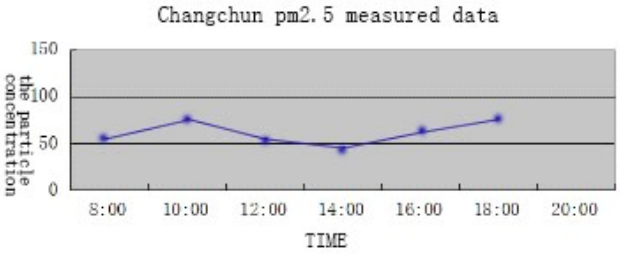

Fig.8 PM 2.5 change trend chart

Through the observation, the changchun 8:00 p.m. at eight o 'clock in the early period (winter), peaked at around this morning at eleven o 'clock PM, lowest about appeared at about three o 'clock in the afternoon. And PM2.5 floating is changed in one day.

The instrument is fully functional, novel design, have the characteristics of low cost, long service life, suitable for family use. Human-computer interaction is convenient, easy to use, simple interface style, suitable for all kinds of people. With real-time location coordinates and PM2.5 display function. To obtain the data to the GSM SMS transceiver, greatly convenient for measuring information work. Instrument as a whole is small in size, easy to use, the use of Li ion battery power supply, battery life is strong, can work continuously for several hours. Portable, real-time and accurate measurement.

References

[1] Yang Yongjie, Zhang Yusheng, Yang Saicheng, Zhang Xiaomei. The design of a kind of PM2.5 detection sensor[J].Sensor and micro system,2014,03:76-78+81

[2] Wang Ju, Li Na, Fang Chunsheng. The research of correlations of TSP、PM_(10) and PM_(2.5) in the air in Chang Chun[J].Environmental monitoring in China,2009,02:19-21+56.

[3] Wang Yan, Wang Hui.The present situation and detection technology of PM_(2.5)[J].Resource conservation and environmental protection,2014,12:139.

[4] Wang Qingyuan. The principle and application of new type of sensor [M]. Beijing: China Machine Press,2003.

[5] Zhang Wenge, Gao Sitian,Song Xiaoping, Liu Junjie, Liu Wei, Chen Zhonghui. Concentration measurement and measurement technology of fine particles PM_(2.5)[J].Powder and technology of China,2013,06:69-72.

[6] Tan Haoqiang. Program Design in C Language[M].The fourth edition.Beijing:Tsinghua University Press,2010.

[7] Guo Tianxiang. C language program of 51 single chip tutorial [M].Beijing: Publishing House of Electronics Industry,2010.

[8] Zhao Jianling, Xue Yuanyuan explanation of 51 MCU development and application technology[M].Beijing: Publishing House of Electronics Industry,2009.

[9] Zhen Feng, Wang Qiaozhi, Cheng Liping.The typical application examples of 51 single-chip microcomputer[M] Beijing: China railway industry press,2011

[10] Fan Honggang, Wei Xuehai, Ren Sijing 51 microcontroller self-study notes [M].Beijing: Beijing university of aeronautics and astronautics press,2010.

Design of solar automatic tracking system

Li Li; Wang Deyin; Xia Zhenghui

（jilin university instrument science and engineering institute,changchun,130021）

***Abstract*--Now for the development and utilization of solar energy, we basically adopt the method of fixed installation of solar panels, this way can't gain the efficient utilization of solar energy.Aiming at this problem, we adopt the method that combine trajectory tracking and photoelectric tracking method,all-day solar tracking method,based on single chip microcomputer to make full use of solar energy.Using the light sensor unit the system can analyze three different situations, sunny day, rainy day and night ,and choose effective way for tracking.Finally we achieve solar energy automatic tracking which can choose the best way of tracking according to different weather conditions, and the system can offer illumination for family yard.**

***Keywords*--solar energy solar tracking independent system**

0. INTRODUCTION

AS a clean and pollution-free energy, prospects of Solar energe for development are very broad. However, it also has the problem of low density, intermittent and spatial distribution changing,and this has put forward higher requirements for the collection and utilization of solar energy.In the solar energy heat utilization, we must make the collector from sunrise to sunset tracking in order to get high temperature heat; In solar power generation, under the same conditions, automatic tracking power generation equipment than fixed power generation equipment,generation capacity increased by 35%, the cost decreased by 25%[1], so in the use of solar energy, tracking is very necessary. According to the different situation, choose different ways of tracking to improve the accuracy, and tracking accuracy of the device significantly influenced the performance of equipment and utilization of solar energy, so it is a very meaningful work to study the control method of the tracking device.

1. THE HARDWARE DESIGN OF THE SOLAR ENERGY AUTOMATIC TRACKING SYSTEM

In some of the common solar tracking methods, photoelectric tracking and visual day tracking[2] are the most common. In order to maximize the rate of solar energy collection, we adopt a combination of photoelectric tracking and trajectory tracking, through the analysis of the different weather conditions, to determine the most appropriate follow-up to ensure maximum efficiency in the use of solar energy. The overall system tracking block diagram is shown in figure 1.

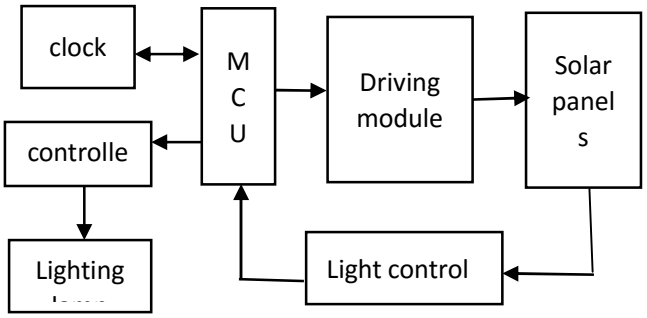

Fig. 1. overall system block diagram

1.1Photoelectric tracking design

(1)The direction of the light source is judged by comparing the light intensity of the four sensors[3], which are used as the combined sensor, by comparing the light intensity of the two relative sensors. At the same time, due to the space limitation, the distance between the photoelectric sensor is too small,so we need to add the photoelectric isolation to increase the contrast difference. The device has high stability, high reliability and high uniformity, which can be widely used.

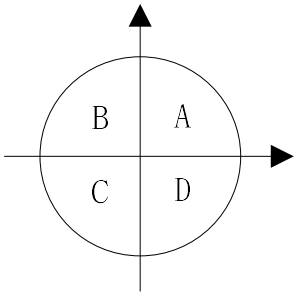

Fig. 2.schematic diagram of four symmetrical sensor

(2)Design of A/D conversion circuit

The converter uses a 8-bit successive approximation A / D converter ADC0809, which has a 8 multi-channel switches, and can be based on the address code after the lock decoding of the signal through 8 analog input signals in a A/D conversion.

1.2 Trajectory tracking design

In order to improve the collection efficiency of solar panels[4] to light energy, need to maintain the vertical solar radiation to the solar cell board as far as possible. In this paper, the description of the position of the sun is described by the elevation angle and azimuth.

Solar elevation angle α

$$\sin\alpha = \sin\phi\sin\delta + \cos\phi\cos\delta\cos\omega$$

Solar azimuth γ

$$\sin\gamma = \frac{\cos\delta\sin\omega}{\cos\alpha}$$

In the formulas: ϕ is local latitude, δ is solar declination angle, ω is solar hour angle.

Solar declination angle

$$\delta = 23.45\sin(\frac{360(284+n)}{365})$$

In the formulas:n is the cumulative number of days, January 1st is 1, January 2nd is 2, and so on ,the declination angle can be drawn.

$$\omega = 15(12-t)$$

t is the time of the year[5].

From the above formula [1],the elevation angle and azimuth angle of the sun position can be derived , in order to achieve the trajectory tracking.

1.3 Clock circuit

We select the AT89C52 as the microcontroller of the design,and the clock chip selection is DS1302. Use DS1302 do external timing, and the way of the key to the time of year, month, day, hours, minutes, seconds calibration. The clock module[6] mainly provides the time to the microcomputer, for the judgment of the night and the day and the calculation of the elevation angle and azimuth.

1.4 Drive unit

According to the moment of the whole system, the research chooses the 42-type stepper motor. The step angle of the stepper motor only has full step and half step , the whole step angle is 1.8 degrees /step, half step angle is 0.9 degrees/step. When the rotation angle is determined, the driving angle of the stepping motor is determined, and only the pulse number is converted into the pulse number. At the same time, in the photoelectric tracking, If the difference between adjacent sensors is large, then a continuous rotation;and If the difference between adjacent sensors is small, then only one rotation step, which makes the system more accurate toward the sun.

1.5 Lighting control

This paper set that the light of family courtyard is on only at night. Therefore, the system set that the intensity values of the four symmetric sensor are relatively low, and during the period of 7 pm and 6 am in the night , solar panels automatically turn to the general direction of the sun at 6 in the morning and wait for a sun rising.At the same time, MCU makes the controller connected to the working lights. But when it comes to six in the morning or there is still a strong light source, the system will keep track of the light source.

2 THE DESIGN OF SYSTEM SOFTWARE

Software flow chart as shown in Figure 3, when the system was first used, it need clock chip initialization, which need artificial time calibration and electronic quantitiy detection[7] at the same time. If the battery power is lower than a certain value, the system is to enter the sleep mode for protecting their datas, no longer work until the electronic quantity of battery was again sufficient; If the power is sufficient, then the systen is to enter the trajectory tracking mode firstly to find the general location of the sun at the moment. Thereafter comparing the pre-set time of sunrise and sunset with the time provided by the clock, if at night, adjust the solar panels to the sunrise position waiting for the sunrise, while the controller control the lights work; If after sunrise and before sunset, the sensor circuit determine that this moment is day by the light intensity, switch to photoelectric tracking mode ,then detect whether the sun is perpendicularly shining panels, if not,adjust the panels to the vertical angle constantly, at the same time ,record the number of steps of rotation of the stepping motor in order to record the current azimuth and elevation angle; if it is cloudy between sunrise and sunset, the system has been always in the trajectory tracking mode,every 15 minutes for an automatic tracking.And snow processing mode is always been in the detection, once the pressure sensor panels feel a certain pressure ,there is a certain snow needing cleaning,send disposably stepper motor multiple number and make the panels swing fast and substantially to make the snow slip off.

3 EXPERIMENTAL RESULT

The experimental system can be used to locate the position of the sun according to the azimuth and elevation angle. If the record is 0 degrees due south, west and east direction is positive and negative, system rotation angle is from negative 89 degrees to positive 89 degrees. In the changing conditions, the system is constantly in the photoelectric tracking mode and the

trajectory tracking mode,the angle error of the solar panel is calculated within 4 degrees,which is an acceptable error. The system switches smoothly between the two modes and the sleeping state.

4 CONCLUDING REMARKS

This paper studies the design of the solar tracking system based on single chip microcomputer, and it also is a double axis tracking system,can automatically detect the night and day, and judge sunny and cloudy day. The system can calculate the elevation angle and azimuth angle at a certain time, and do the trajectory tracking.According to different weather conditions, the system can choose different tracking modes, which can effectively improve the utilization of solar energy.

References

[1] Wang Linjun, Shao Lei, Zhang Dong, door Jing, Liu Wei. Research status and Prospect of solar automatic tracking system [J]. Journal of agricultural China，2014,35（1）：283-287

[2] Lishen Sheng, solar [M] Beijing: Beijing People's Education Press，1998

[3] Wangbing Zhong, et al. A comparison of several solar position calculation method [J]. Journal of Solar，2001，22（4）：413-416

[4] He You, Guan Xin, Wang Guohong Multi-Sensor Information Fusion Research Progress and Prospect [J]. Journal of Astronautics.2005.26（4）：524-530

[5] Wang Xuewen, Wang Yang, Yan Jun Feng. Automatic tracking control system design [J]. Journal of Northwestern University of solar panels，2004,34（2）：163-164

[6] Zhang Tianzhong, Jiang Baojun, Deng Xingcheng, light source tracking [J]. experimental science and technology based on MSC-51 MCU，2006，（12）：39-40

[7] Sui Bo, Deng Peng, multi channel data acquisition system based on MSP430 MCU [J]. Ship Electronic Engineering，2009,29（3）：168-170

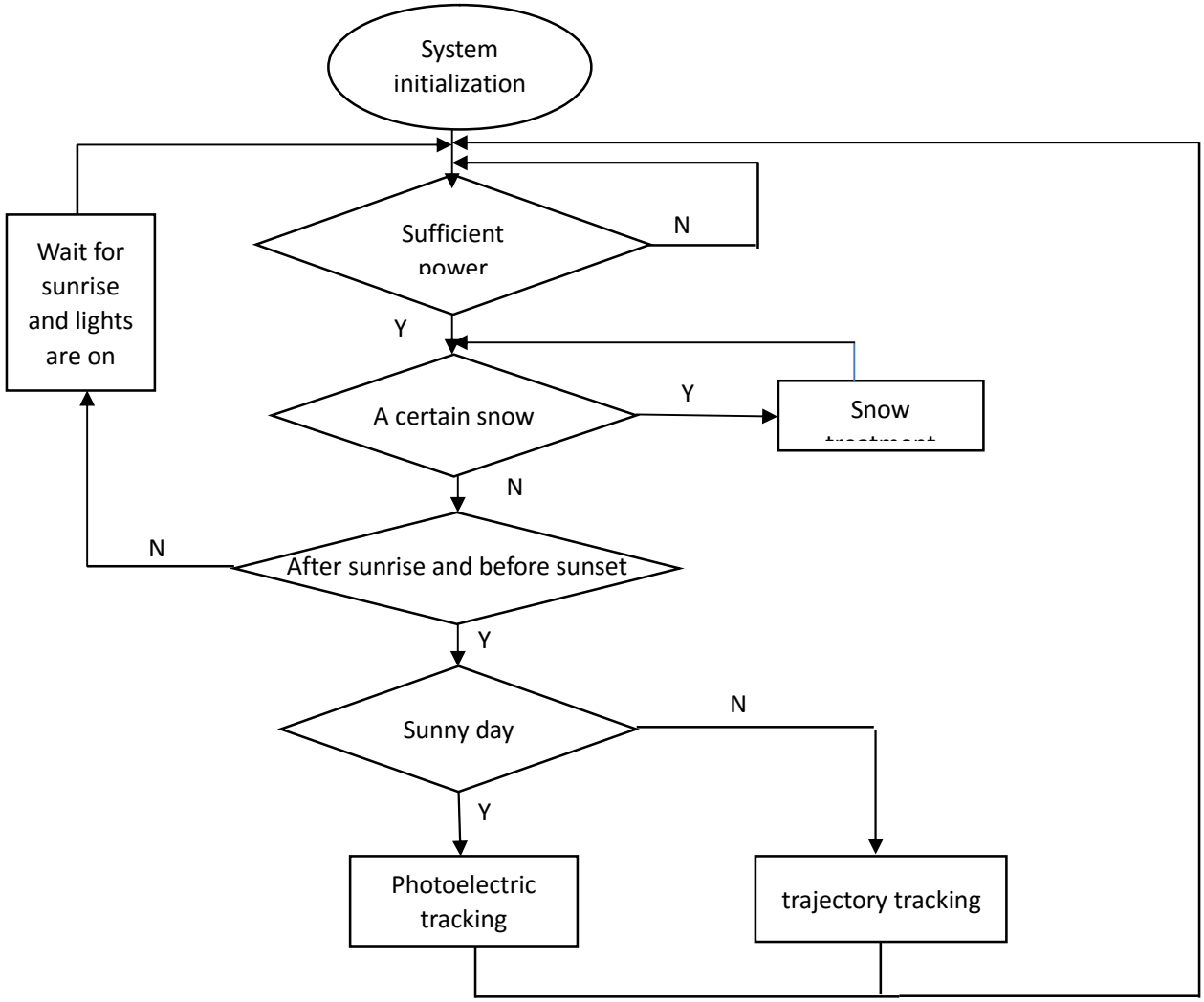

Fig. 3 general flow chart of system

The design of the shallow geothermal energy monitoring system

Sun Dan; Geng Yi-nan; Ding Jin-zhong

(College of Instrument Science and Electrical Engineering, Jilin University, Changchun 130022, China)

***Abstract*--The device of the shallow geothermal energy monitoring system based on MSP430F449 microcontroller uses the DS18B20 temperature sensor to collect temperature and use the pressure transmitter of YB - 131 type to test pressure, the 5110 LCD screen can display temperature and pressure data real-timely, the monitoring system can transmit data to principal computer via a serial port. The monitoring software is designed by the Visual Studio 2010, it is to achieve monitoring temperature and pressure data dynamically, what's more, it can choose different time intervals to collect, record and store data, complete data processing and draw the line chart.**

***Key words*--Temperature and pressure measurement; Real-time display; Data transmission; Variable time interval ; Line chart**

0. INTRODUCTION

THE shallow geothermal energy has exploitation value, which is formed by the perennial temperature difference between the rock and soil body under the surface of the earth temperature and land surface temperature, and it is a special kind of potential energy [1].It lies in certain depth below the surface (generally less than 200 meters) within the scope of rock mass and underground water and surface water, and its temperature below 25 degrees Celsius [2].The shallow geothermal energy has a high value of utilization, which is abundant and inexhaustible. As the technology matures, the development and utilization of shallow geothermal energy can have become possible [3]. In the process of the utilization of the shallow geothermal energy, it is necessary to grasp the data accurately such as temperature and pressure. The project is to design a set of cost-effective miniaturized monitoring system which can operate simply and promote greatly, finally it will play a role in the development and utilization of resources and make contributions to the country's energy conservation and emissions reduction work.

I .THE OVERALL PLAN

The design chooses PVC tube to build experimental environment and simulate the process of monitoring the utilization of the shallow geothermal energy, meanwhile, the temperature sensor and electronic thermometer are connected together by a tee coupling. Based on the mechanism of connected vessels, the model picks out a plastic hose to change water level in the PVC tube which is to simulate different water pressure; it changes water temperature poured in the PVC tube to simulate different geothermal water temperature. Pressure transmitter is on the bottom of the device. Environmental simulation device is shown in figure 1

Fig1. Environmental simulation device diagram

System is divided into hardware part and software part, and hardware part is divided into the temperature module, the pressure module, the display module and the serial port module that completes the data collecting and data transmission and data displaying. Data transmission is completed via a serial port to the PC. The design controls the software to record, store data and draw the line chart. Overall system structure

diagram is shown in figure 2.

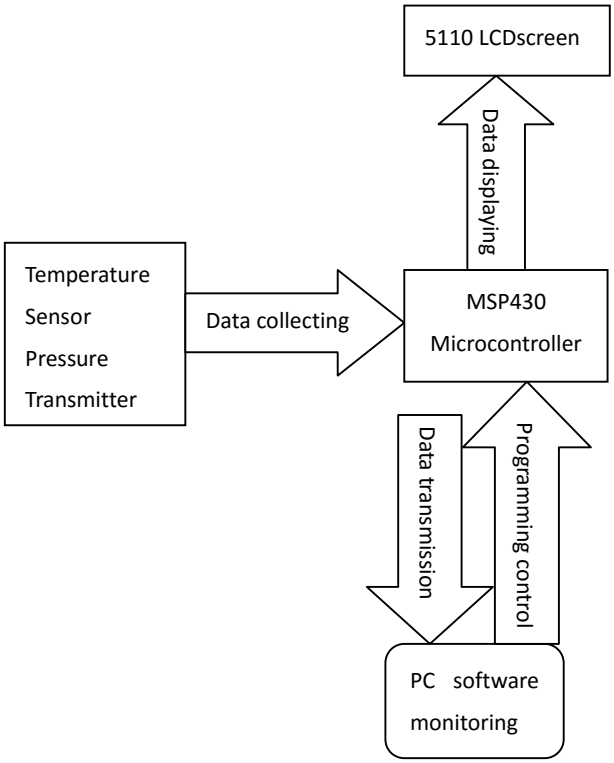

Fig2. Overall system structure diagram

Ⅱ. METHODS

A. Temperature Module

DS18B20, a common temperature sensor, has t the characteristics of small volume, low hardware overhead, strong anti-jamming capability and high precision. Its temperature measurement range is from 55 ℃ below zero to 125 ℃ above zero, and its working power supply: 3.0V to 5.5 V DC voltage signal [4].Temperature module circuit diagram is shown in figure 3.

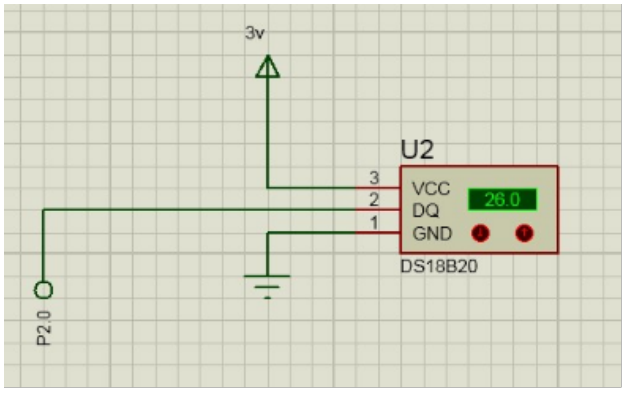

Fig3. Temperature module circuit diagram

DS18B20 temperature sensor is connected to the P2.0 pin of the microcontroller and the LM2596S step-down module provide 3V voltage for it. DS18B20 can realize the temperature automatic conversion so that it doesn't need to add external conversion components.

B. Display Module

5110 LCD screen, a high cost-benefit LCD product, can display the multi-line characters [5]. It uses 3.3V power supply, is provided by the LM2596S step-down module. Programming of the 5110 LCD screen needs LCD initialization, screen clearing and using SPI interface to write data. Because it has no their own character, it must set up an internal small Chinese character in MCU ROM. 5110 LCD screen's display circuit is shown in figure 4.

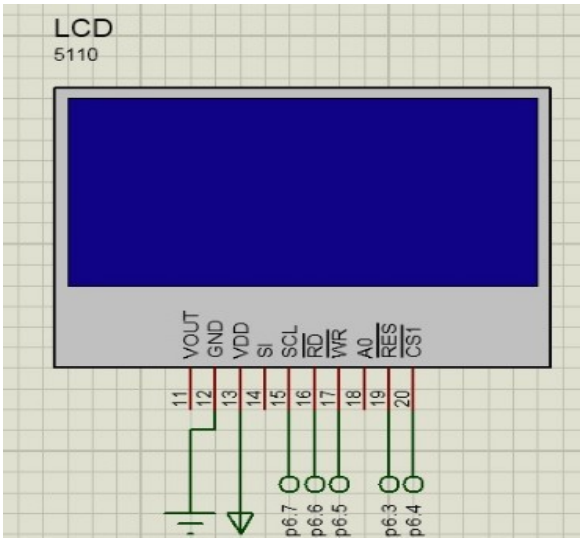

Fig4. 5110 LCD screen's display circuit diagram

C. Pressure Module

For the measurement of the pressure, the design selects the pressure transmitter of YB - 131 type, and its working voltage is 24V provided by the power adapter. Its pressure measurement range is from 0.1KPa to 100KPa, and its output signal is from 4mA to 20mA DC current signal[6].What's more, it can measure medium temperature whose range is from 40℃ below zero to 150 ℃ above zero. However, due to liquid contracts in freezing ,it will make damage to diaphragm, which causes transmitter not working, so working environment must be not below 0 ℃.

Its output signal is the current signal, but MSP430 microcomputer internal AD conversion needs the voltage signal, so using a series of 125 Ohm resistance is important so that 4mA to 2mA current signal is converted to 0.5V to 2.5V voltage signal, then the voltage signal connects MSP430 P6.0 pin,. Through internal AD conversion, analog signal is converted to digital signal, and using transformation formulas

calculates the 0 to 40KPa. The circuit diagram is shown in figure 5.The pressure calculation formula is shown as below:

$$P = 20 \times U - 10000 \quad (1)$$

Among(1), P represents the pressure; U represents the voltage.

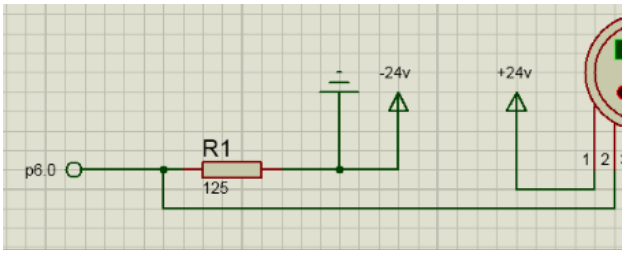

Fig5. Pressure module circuit diagram

D. PC Module

PC monitoring software uses Visual Studio 2010 as Visual development tool with c sharp programming language. PC monitoring software includes data upload, data query, data storage, line chart drawing, etc. Because of long-term monitoring and large data quantity, the monitoring software can select different time intervals to receive and store data and draw line chart. PC interface is shown in figure 6.

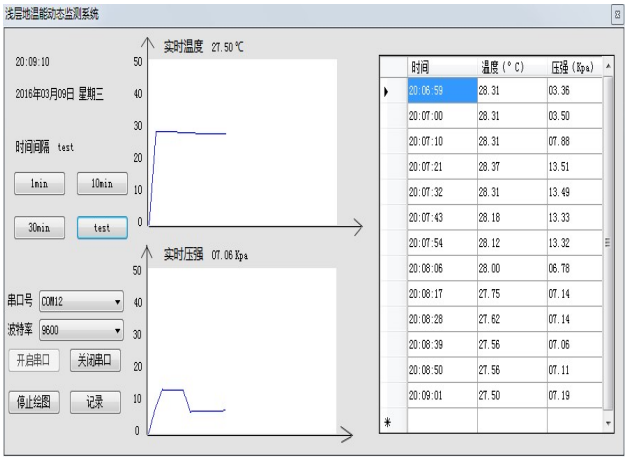

Fig6. PC interface diagram

When PC works, according to the choice of time interval, it receives the data via a serial port firstly and judges the data bits preliminarily. It receives data again when the data are not correct, it doesn't buffer data until the data are correct. At the end of data caching, the monitoring software will store data and draw the corresponding points in the drawing area.

III. THE TEST RESULTS

In order to test the accuracy and precision of the system, a lot of experiments have been done.

A. Temperature Test

An electronic thermometer is equipped in the simulation device, and ice water is added into the PVC tube, then hot water is added into the pill until the pipeline is full of water. What is more, let some water in the pipeline and keep the vertical direction getting a different temperature. The PVC tube is fixed, the water being flown in the pipe is carried out by the plastic hose, so different temperature data are measured. Through many experiments, compared with the thermometer readings, PC software readings are basically identical. The specific experimental data are drawn into a line diagram shown in figure 7.

B. Pressure Test

A plastic hose is installed at the bottom of the PVC tube to constitute a connector. The PVC tube is fixed and remains vertical. The PVC tube is filled with water, in order to change the height of the liquid level in the PVC tube, we draw off the water using the plastic hose to simulate different pressure. We can use tape to measure pipeline water level, and the theoretical pressure can be calculated by the formula (2), and the theoretical pressure and display pressure were compared. The results show the accuracy and precision of the pressure data. The specific experimental data are drawn into a line diagram shown in figure 8.

$$P = \rho \times g \times h \quad (2)$$

Among(2), P represents the pressure; ρ represents the density of water; h represents the level of the water; g represents the gravitational acceleration.

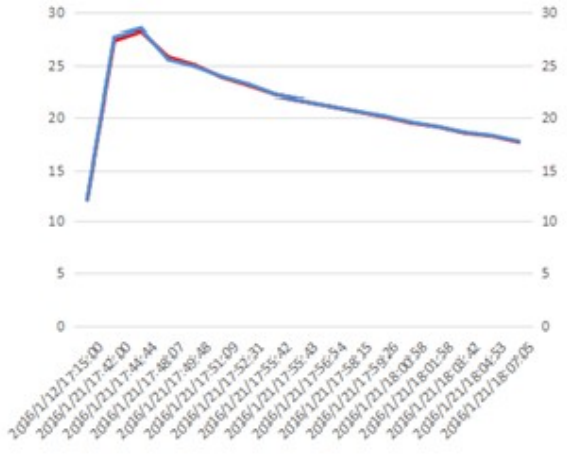

Fig7. The line chart comparing the actual temperature data and the temperature data on the screen.

In the figure7, the blue line represents the temperature data on the screen; the red line represents the actual temperature data.

Fig8. The line chart comparing the actual pressure data and the pressure data on the screen

In the figure8, the blue line represents the pressure data on the screen; the red line represents the actual pressure data.

Ⅳ. RESULTS ANALYSIS

With lots of the experiments done, we observe the drawing of the temperature curve and pressure curve, then find that two curves of the actual data and the theoretical data are coincide. It is proved that the experimental data are correct. Specific experimental data are shown in table 1.

Table1. Data of comparison test

order	h（CM）	P（KPA）	Actual Pressure（KPA）	Actual Temperature（℃）	T（℃）
1	150	14.7	15.1	27.4	27.75
2	139	13.62	13.82	28.3	28.5
3	122	11.95	12.15	12.1	12.12
4	107	10.49	10.63	25.8	25.55
5	91	8.92	8.94	23.8	23.87
6	84	8.23	8.4	23	23.12
7	75	7.35	7.35	22.1	22.12
8	64	6.27	6.44	21.6	21.62
9	58	5.68	5.68	21.1	21.12
10	45	4.41	4.5	20.6	20.62
11	36	3.53	3.57	19.5	19.56
12	28	2.75	2.99	19.1	19.12
13	26	2.55	2.56	18.5	18.56
14	15	1.47	1.47	18.2	18.25
15	11	1.08	1.12	17.6	17.68

According to the experimental data, the accuracy of the monitoring system can be obtained by comparing the two sets of data. The temperature measured by the electronic thermometer is accurate to 0.1 degrees Celsius, and the temperature data measured by the system can be accurate to 0.01 degrees Celsius, which indicates that the system precision is more than electronic thermometer precision. For the pressure data, the output of the pressure transmitter is 4~20mA current signal which is small, and the influence of the external environment is considered, the pressure data can be less than 0.5KPa. By comparing the theoretical and experimental data, it is proved that the temperature and pressure measuring by the monitoring system are so accurate.

Ⅴ. CONCLUSION

The project designs the shallow geothermal energy monitoring system. The system can display temperature and pressure data real-timely in the process of using the shallow geothermal energy; the monitoring software can choose different time intervals to collect data, transmit data, store data, and draw the line chart which can response the change tendency of the parameters visually. The temperature parameter precision can reach 0.01 degrees Celsius. The pressure parameter accuracy can reach 0.5KPa. The system has the advantages of simple structure, low cost and convenient operation which can preliminarily meet the requirement of the utilization of the shallow geothermal energy, and can be applied to the shallow geothermal energy monitoring of the miniaturized family.

References

[1] Deng Gao, Investigation and development of shallow geothermal energy resources [J]. Geological Society of China, 2011,9:67-88.

[2] E Jian, Zhou Rong-gen, Shallow geothermal energy development and utilization management research [J]. China National Land and resources economy, 2013 (3):31-35.

[3] Vaughan RG,Keszthelyi LP,Lowenstern JB et a1,2012.Use of ASTER and MODIS thermal infrared data

to quantify heat flow and hydrothermal change at Yellowstone National Park.Journal of Volcanology and Geothermal Research,233—234:72—89.

[4] Zhang Jun, Intelligent temperature sensor DS18B20 and its application, [J]instrument technology, 2010, (4):68-70.

[5] Zhang Hong-xun. Looking for cheap single chip LCD [J]. Production of heaven and earth, 2010, (11):12-15.

[6] Wang Hai-chun. Design of intelligent pressure transmitter [J]. Journal of Huaiyin Normal University, 2003, (11):300-302.

The incremental digital PID in the application of the dc motor speed control system

LIU Guang-da; ZHOU Hui; ZHAO Shu-jian; JIANG Xia-ping; CAI Jing
(college of instrumentation &electrical engineering,Jilin University,Changchun 130012,China）

***Abstract*--Selects permanent magnet dc motors as control object, and incremental PID algorithm which does not need to accumulate to control motor speed. Use computer modeling simulation platform, and set the actual circuit testing, finish the actual motor incremental PID control design. According to the permanent magnet dc motor using requirements and the simulation results reasonably adjust PID algorithm, and save the resources of the controller, realized the rapid increment of motor speed control. By actual test, compared with traditional PID algorithm, the dc motor speed regulator can achieve rapid motor speed control, meet the actual demand.**

***Key words*--Incremental PID Computer simulation Permanent magnet dc motor Motor speed contr**

I.INTRODUCTION

THE advent of more than a century, since it plays good starting performance and braking performance, speed smooth and wide, has been widely used in the field of controlled electric drive. In high precision systems, the DC motor actuators are very common. Especially small permanent magnet motor, automotive, medical equipment, electronic products often play an indispensable role. In the application, the steady-state and dynamic performance of the motor speed regulation is often the focus of attention.

PID control strategy is one of the first developed control strategies. Because of the high reliability and robustness, the algorithm is easy to implement, etc.,are widely used in PID control of industrial fields [1]. The traditional PID motor control using positional PID control algorithm, there exists a large failure or malfunction, data integration process generated huge and many other shortcomings;compared with the position PID algorithm, incremental PID algorithm has no need to do accumulate, less affected by the malfunction, etc. [2], is more suitable for use in a method based on digital PID control DC motor equipment.

In this article, select the permanent magnet DC motor as a control object, improved incremental PID algorithm is applied to the motor speed, make the modeling and simulation on a computer platform, and build the circuit measured, obtained very good accuracy and control Response rate.

II. INCREMENTAL DIGITAL PID DC MOTOR SPEED CONTROL PRINCIPLE

A Composed of DC motor speed control system

DC motor speed control system uses a 16-bit high-speed microprocessor as the main controller, the motor speed through the photoelectric sensor acquisition parameters sent to the main controller; a main controller calculates the speed deviation and generate PWM wave, and based on an incremental PID algorithm correction wave PWM output duty, the use of the motor drive circuit power amplifier to drive DC motors, complete closed-loop DC motor speed control.

The system includes four parts: a main controller section, motor drive and gun parts, liquid crystal keyboard part and PC communication section. System structure shown in Figure 1.

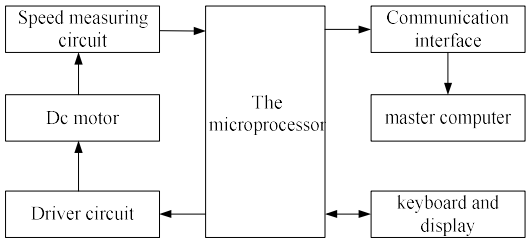

Fig.1 System structure blockdiagram

B Incremental digital PID principle

PID controller includes proportional unit(P), integral unit (I) and differential unit (D).

Traditional PID control formula is:

$$u(t) = K_p[e(t) + \frac{1}{T_i}\int_0^t e(t)dt + T_d\frac{de(t)}{dt}] \quad (1)$$

However, the controller can only deal with discrete quantity,So the formula needs to be discretized. After discrete PID equation[3]:

$$u(k) = K_p\{e(k) + \frac{T}{T_i}\sum_{j=0}^{n} e(j) + \frac{T_d}{T}[e(k) - e(k-1)]\} \quad (2)$$

Easy to see that the amount of formula (2) output is controlled quantity of added value, and every state in the past will affect the final output.

The incremental PID of the formula is:

$$\Delta u(k) = u(k) - u(k-1)$$

$$= K_p\{e(k) - e(k-1) + \frac{T}{T_i}e(k) + \frac{T_d}{T}[e(k) - 2e(k-1) + e(k-2)]\}$$

$$= K_p(1 + \frac{T}{T_i} + \frac{T_d}{T})e(k) - K_p(1 + \frac{2T_d}{T})e(k-1) + K_p\frac{T_d}{T}e(k-2) \quad (3)$$

$$= Ae(k) - Be(k-1) + Ce(k-2)$$

Compared with the traditional position type PID,Incremental PID output error only with the current beat and shot the first two related, without accumulation, small amount of calculation is easier to achieve with digital controller [4].

C DC Motor Speed Modeling and Simulation

Referring to the mechanical and electromagnetic processes of DC motor, we can list the armature voltage balance equation and torque balance equations.

Armature voltage balance equation:

$$u_a = R_a i_a + L_a\frac{di_a}{dt} + \varepsilon \quad (4)$$

$$\varepsilon = C_e\Phi i_a \quad (5)$$

torque balance equations:

$$J\frac{dn}{dt} = T - T_L \quad (6)$$

$$M = C_M\Phi i_a \quad (7)$$

There u_a is the armature voltage, ε is the armature back emf, i_a as armature current, L_a armature inductance, Φ flux per pole, n is the rotor speed, C_e to DC electromechanical potential constant, C_M torque constant, T is the electromagnetic torque, T_L load torque, J is the inertia of the rotational speed.

Finally, referring to FIG. 2, a block diagram of a DC motor transfer model, we can get the transfer function of DC motors [5-7].

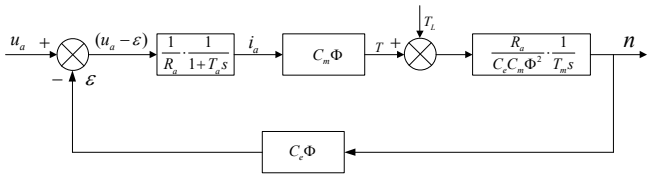

Fig.2 DC motor transfer function block diagra

DC motor speed and armature voltage transfer function is:

$$\frac{n(s)}{u_a(s)} = \frac{1/C_e\Phi}{T_m T_a s^2 + T_m s + 1} \quad (8)$$

Expansion of the use of critical ratio method [3], adjust the optimal PID parameters, select the time interval T = 0.002s, images on a computer simulation obtained as shown below.

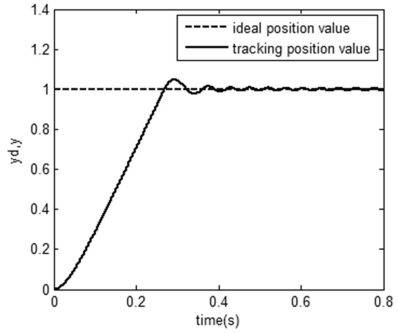

Fig.3 The computer simulation diagram

III.SOFTWARE DESIGN

Incremental digital PID algorithm is the core of the software, the optimal PID parameters obtained by the computer simulation, the curing of the program to the system controller. Flowchart software part of the system is as follows.

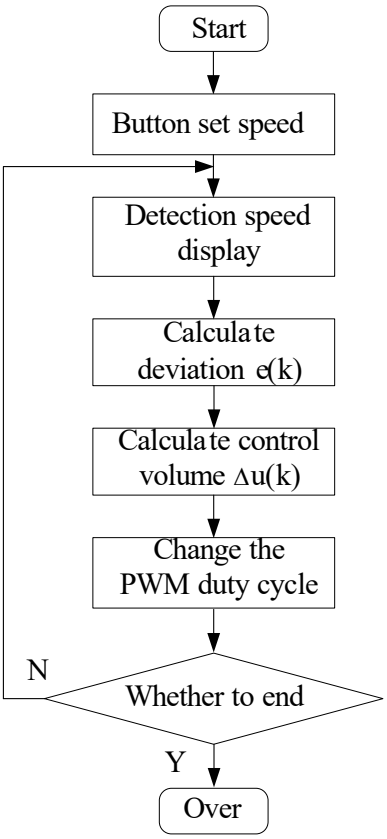

Fig.4 The flow chart ofsystem software

IV. EXPERIMENTAL TEST

The system used 16 ultra-low power consumption, with RISC MSP430 microcontroller as the main system controller, responsible for processing information, calculations and algorithms to perform [8].

Select RK370-15330-50 type permanent magnet DC motor as a control object, the motor driving portion is selected L298N chip, contains within it a full-bridge circuit can be a standard TTL level is converted into a high voltage, high current level . Level transformed can better drive DC motors.

Measuring motor speed using the photoelectric encoder speed, when the motor rotates, the corresponding circuit will produce a square wave pulse signal, and then capture the signal from the controller and measure the frequency of the signal, and finally through the calculation, you can get the motor speed. The photoelectric encoder with a precision of 37 pulses / dregee [9].

Figure 5 and figure 6 are the photoelectric encoder physical map and the measured square wave pulse waveform.

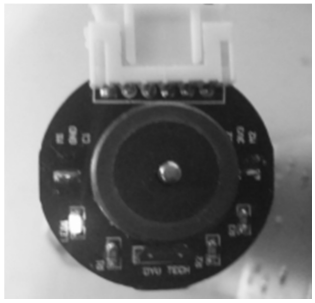

Fig.5 Encoder circuit

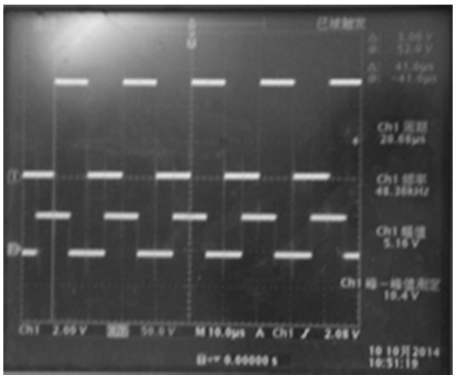

Fig.6 Square wave diagram

Figures 7 and 8 for the PWM waveform and the motor speed at 60r / min generated by the controller of the motor driving circuit outputs the drive waveform.

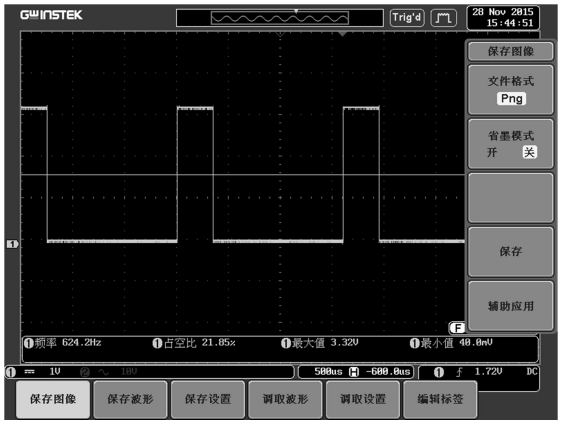

Fig.7 The controller output voltage waveform

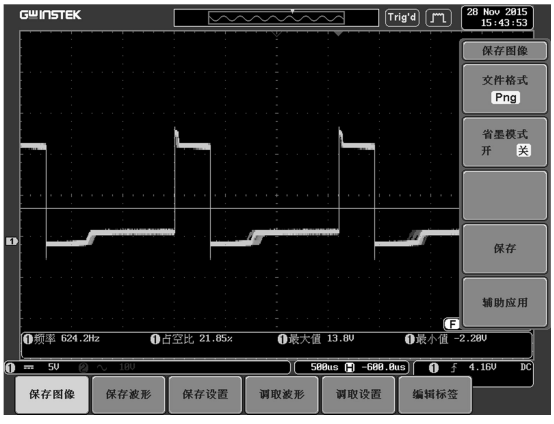

Fig.8 Motor driving voltage waveform

Figure 9 is a response curve at a given motor speed is 60r / min obtained.

Figure 9 shows that the system is no significant overshoot, rise time is about 0.5s, and the process subsequent runs basically stable.

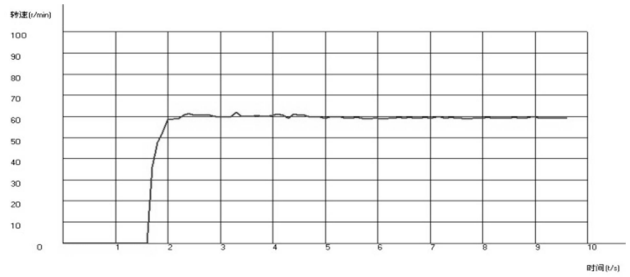

Fig.9 The measured speed rendering

V.CONCLUSION

This paper applys incremental digital PID to DC motor speed control system.The program is simple and low cost.and obtains a more satisfactory speed response and dynamic effects.

References

[1] Tao Yonghua, Yi Yixin,Ge Lusheng New PID control and its application [M] Machinery Industry Press 1997:1-18

[2] Zhao Guoshan,Qiu Xingqi Overview of the development of adaptive PID [J] Chemical Engineering 2006,33(5):1-5

[3] Zeng Haoyong, Zhou Sizhu, Yi Wenjun MATLAB-based incremental PID parameter tuning [J] Industrial control computer,2014,27(6):69-70

[4] Chen Xinyi Research and design of digital PID controller [J] mechanical engineer, 2014,05: 122-123

[5] Jin Guoqiang Mathematical model and measurement methods Brush DC Motors [J] University Physics, 2014,33 (2): 56-60

[6] Wang Yanying,Wang Zhen Experimental study on DC motor transfer function measurement [J] Experimental Technology and Management, 2008,25 (8): 38-40

[7] Zhou Ruxun DC direct identification of the model parameters [J] Computer Simulation, 2006,24 (6): 113-115

[8] Chen Mingmin,Yi Qingming,Shi Min ARMv4 embedded microprocessor instruction set design [J] Application of Electronic Technique, 2014,40 (12): 23-26

[9] Wu Qiang,Han Zhenyu,Li Cheng PWM speed control based on incremental PID algorithm brushless DC motor [J] Electrical Engineering Technology, 2013,42 (3): 63-65

The system faced to wisdom residential area intellisense and regulatory

Yue Liangguang; Liu Lei; Wang Mingchao
(College of Instrumentation and Electrical Engineering, Jilin University, Changchun 130026,China)

***Abstract*--In order to solve the traditional intelligent household system for users on the market at present the single, the product cost is high, the problem of poor scalability, based on STM32 microcontroller as the core controller, designed a set of intelligent household module and security module for the integration of active intellisense and regulatory system. System USES a WiFi communication technology has realized the control ofthe curtain; Using the infrared learning module realizes to control household appliances; Using the temperature and humidity sensor realizes to the family the real-time monitoring of temperature, humidity, Bycamera, infrared tube and the human body infrared sensing module implements the function of family security, and will be more than the information sent to the mobile phone and remote computer. So as to solve the single intelligent household system for users, the product cost is high, the problem of poor extensibility, reached the user-oriented is wide, the product cost is low, the purpose of strong extensibility.**

***Keywords*--Intelligent household module; Security module; Infrared learning module; The human body infrared sensor module; The sensor.**

I. INTRODUCTION

THE development of information technology have in-depth every field of human life，so people began to pursue combined the technology of information, security, efficient and comfortable, and have rich cultural environment of the healthy house[1]. The accelerating pace of the social life, the requirements for high efficiency intelligent household environment has been put forward by us, people need a quick and convenient system platform to us from the heavy housework work and tedious household appliances in the operation, automatic assist people's life.

On the other hand ,we analyse the current situation of urbanization, economic development and industrialization level and developing trend, Our country has entered the acceleration of urbanization development stages. Domestic most of the urban residential buildings are village form, and a sharp rise in the number of the community, size is bigger and bigger, but the current community management mode is still stay on the traditional model of safety patrol and maintenance of protection, "All pipe and all no matter[2]". For the user can't form a timely and effective emergency management, at the same time we also can't every household to realize real-time monitoring and control, to provide security, fire safety, etc.

Intelligence community security monitoring system solves this problem well, combine smart home and security monitoring, the goal is to make people have safe, comfortable, convenient, entertainment, and beautiful living environment, this is the inevitable trend of China's urban residential development in the new century. Smart home is a house as a platform, using the integrated wiring technology, network communication technology, security technology, automatic control technology, audio and video technology to integrate the equipment related to household life together, to build convenient, comfortable home facilities and management system, ascension home security, convenience, comfort, artistry, and realize environmental protection and energy saving living environment[3]. Called the safety and protection system of public security system, based on the personal property security protection, information and communication security, the purpose of loss prevention and crime prevention. Security refers to the building or buildings (including peripheral areas), or specific location, area, through the adoption of human prevention, technology prevention and physical prevention methods such as the comprehensive implementation of personnel, equipment, construction or regional security. Security System[4] (Security & Protection System, SPS) is, for the purpose of maintaining the social public safety, use security products and other related products of intrusion alarm

system, video security monitoring systems, access control system and other systems; or by these systems for the subsystem or integrated electronic system or network. Security industry in China develops very fast, also more popular,but traditional security of people's dependence is strong, very human cost,and intelligent security through the realization of intelligent machines,to realize people want to do as much as possible. Loss prevention is the industry's task, crime prevention is the responsibility of the police law enforcement.

II. THE SYSTEM OVERALL DESIGN

This system mainly divided into three aspects, namely intelligent household module, security system module and the upper software. For smart home we ARM to realize the control of temperature and humidity sensor, through the wifi module to allow the ARM to control the motor of the curtain, through infrared learning module to ARM remote control air conditioning, TV and other household appliances. For security system module, we mainly through camera, body induction module and installed in the Windows on both sides of the infrared for real-time monitoring of tube to plate a security. Finally using SIM900A module to send information to cell phones, and through the upper information sent to the remote computer software will be home, to implement intellisense and regulation. In the process of using the wifi module, we are connected to the wifi module for each module respectively to set network interface. For mobile phones and remote computers, we will develop a specific protocol, to ensure accurate regulation and control. The system composition block diagram is shown in figure 1.

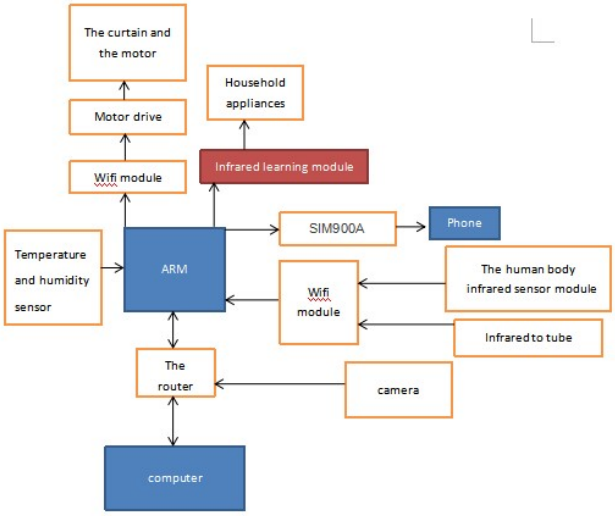

Fig.1 The curtain of intellisense and regulatory system structure diagram.

III. THE SYSTEM HARDWARE DESIGN

A. The Infrared Monitoring Module In The Pipe

Infrared monitoring module, the pipe using infrared tube as the sensor.Its working process is when there is no shade between infrared transmitting tube and receiving tube represents no invasion, infrared receiving tube can receive infrared transmitting tube lights, at this time will not start the subsequent alarm circuit.Once the infrared transmitting tube and receiving tube between block infrared transmission block, the infrared receiving tube can't normal receive infrared transmitting tube lights.Master control chip to detect the channel block, will start the subsequent alarm circuit.Red warning lights on, on behalf of the family was invaded.Infrared detection module the pipe schematic diagram is shown in figure 2.

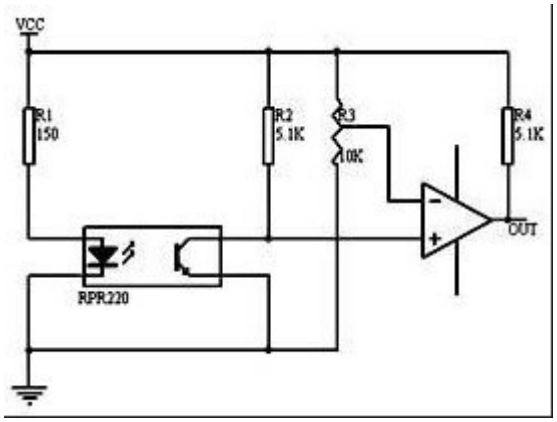

Fig.2 The principle diagram of the infrare detection module the pipe

B. Camera Video Monitoring Module

WEB CAM is the combination of traditional camera

and network video technology a new generation of products, in addition to possess all conventional camera image capture function, machines also built-in digital compression controller and the operating system based on WEB, made by compressed video data encryption, through the LAN, Internet or wireless network, to the end user[5].And the remote user can use the standard on PC web browser, according to the IP address of the network camera, on a visit to the network camera, the scene of the real-time monitoring target, and can be real-time editing and storage of image data, at the same time also can control the camera haeundae and lens, all-round monitoring.The principle diagram of the camera video monitoring module as shown in figure 3.

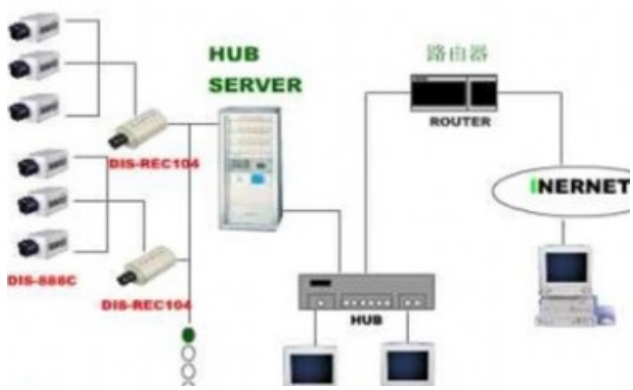

Fig.3The principle diagram of the monitoring and control system design

C .The Human Body Infrared Sensor Module

For core component HC - SR501 human body infrared sensor, the human body has a constant body temperature, generally in 37 degrees, so have a specific wavelength of about 10 um infrared, passive infrared sensor is detecting human around 10 um of ir.The human body through the thin mud around 10 um of air, filter enhanced gathered on infrared induction.Infrared induction source usually USES the pyroelectric element[6], the element in receives the infrared radiation human body temperature changes will lose charge balance, to release charge, the follow-up circuit can generate alarm signal after testing treatment.The alarm signal transmitted to the microcontroller chips, you are able to operate the follow-up of automatic lamp circuit, and start timing, in this cycle, automatic light has been lit.When one end of the cycle time, continue to detect signals from the sensors, if you still have a warning signal, then start a new timing cycle and drive subsequent automatic lamp circuit, if there is no warning signal,, no response.By unit time timing work will be efficient use of the principle of the power supply, reduced the waste of unmanned to exist "hers" phenomenon.The principle of infrared induction module diagram as shown in figure4.

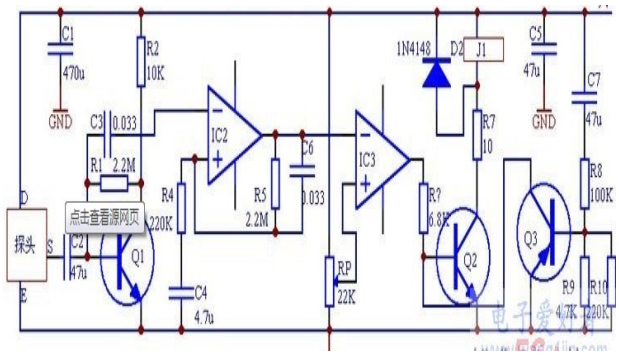

Fig.4 The principle diagram of the human body infrared sensor module

D. Intelligent Curtain Module

The curtain main engine part of the main control module for the system.Using infrared integration acquisition signal receiving, infrared remote control mode;Adopts L298 drive double step motor, adjust the attitude of the curtain;Slide the photosensitive resistance and resistance in series in the circuit, through the intermediate node gathers the voltage signal of reflected light intensity after analog-to-digital conversion to digital signal is sent to the core controller, the controller output drive signal is amplified by driving circuit, micro adjustment control stepping motor, realize the automatic electric.Curtain control module hardware schematic diagram is shown in figure 5.

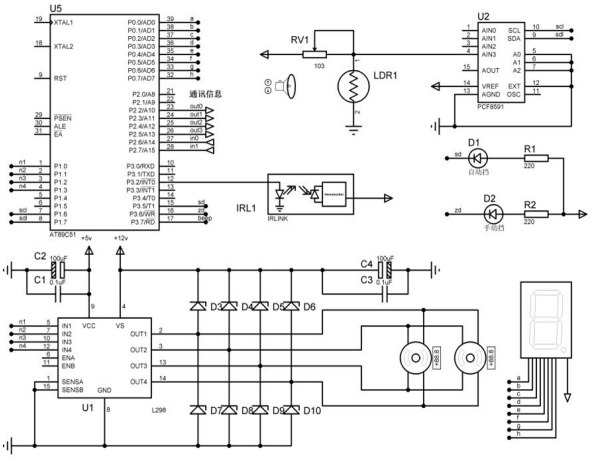

Fig.5 Curtain control module hardware principle diagram

IV. THE DESIGN OF SYSTEM SOFTWARE

System software design is divided into two parts, the

main control system and auxiliary system workflow solidified within the STM32 microcontroller using C language.

Master control system is to initialize the system, which make it into the best work state, prepare the way for subsequent correlation processing.Auxiliary system covers the infrared tube detection, video surveillance cameras, human body infrared sensor, intelligent curtain control four separate module subroutine.Interrupt mode can be used to real-time calls to each subroutine.

V. THE ANALYSIS OF EXPERIMENT RESULTS

A The Infrared Monitoring Module In The Pipe

When there is no shade between infrared transmitting tube and receiving tube, green light, on behalf of the security, as shown in figure 6 (a). Besides，when the infrared transmitting tube and receiving tube between block infrared transmission bar, the red warning lights up, on behalf of the family was invaded, as shown in figure 6 (b).

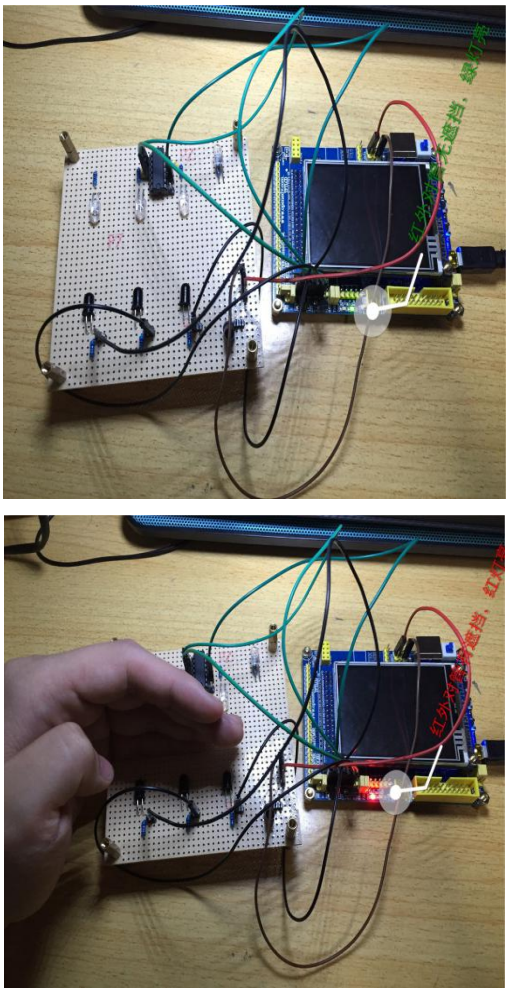

Fig.6 The experimental progress of infrared tube

B. The Human Body Infrared Sensor Module

HC-SR501 infrared sensing module pyroelectric sensing head receives the infrared radiation human body temperature, charge balance is broken, release charge outwards, and produce electrical signals, the follow-up circuit sounded the alarm[7].Figure 7 (a) represents for safety state, while figure 7 (b) represents for the risk state of alert.

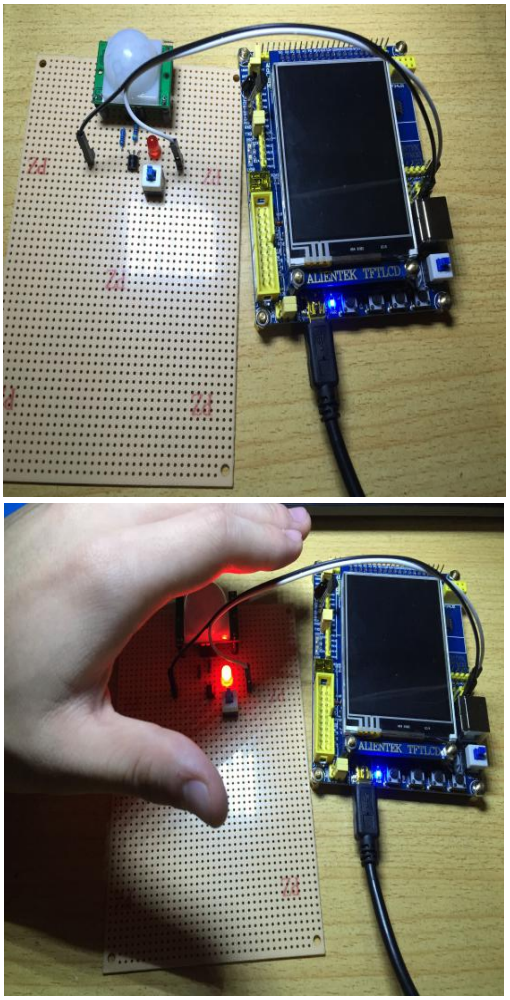

Fig.7 The experimental process of human body infrared induction

C. Camera Video Monitoring Module

Cameras connected to the wireless network, through the form of remote access can be read in real time video data taken by camera.Figure 8 (a) represents for mobile phones to read camera images data, while figure 8 (b) represents for the camera for computer data.

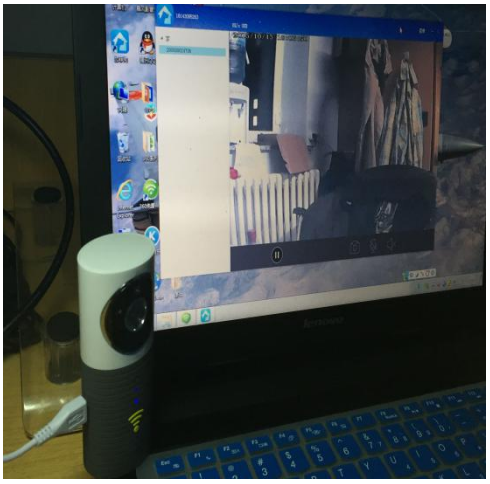

Fig.8 The display of camera video

D. Intelligent Curtain Module

Master control chip L298N motor driver module control, 5 v dc motor by controlling the motor forward, reverse and stop on behalf of the intelligent open and close of the curtain, as shown in figure 9.

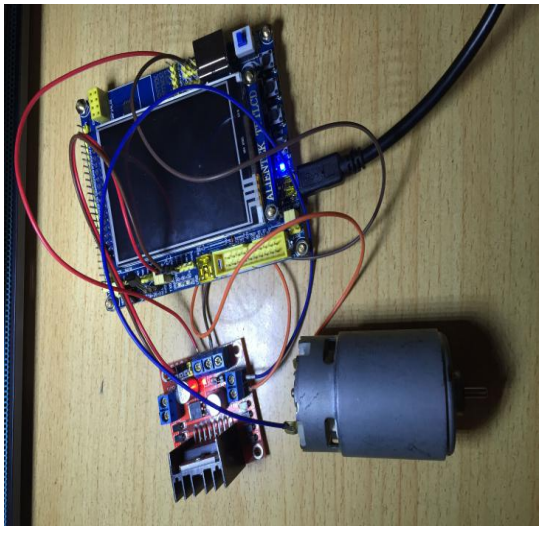

Fig.9 experimental process of driving motor

E. Temperature And Humidity Monitoring Module

Using DS18B20 temperature test environment, display process is shown in figure 10.

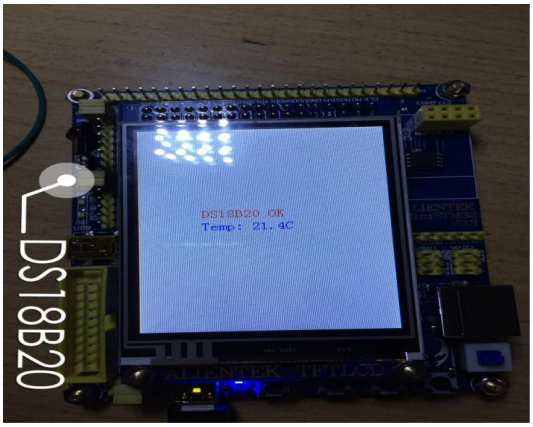

Fig.10 The environment temperature and humidity display process

VI. CONCLUSION

The design uses the STM32 as micro controller, a wi-fi network technology to realize the control of the curtain， the infrared learning module realizes to control household appliances and the sensor of temperature and humidity to realize the family the real-time monitoring of temperature. By camera, infrared tube and the human body infrared sensing module implements the function of family security, the information sent to the mobile phone and remote computer.So as to solve the single intelligent household system for users, the product cost is high, the problem of poor extensibility.Reached the purpose of wide user-oriented , low cost and strong extensibility. So the generalization get stronger.

References

[1] East China architectural design institute , Intelligent building design technology. 2nd Ed. Shanghai(Book style) , Tongji university press , 2003

[2] [EB/OL]. http://baike.so.com/doc/3950195.html

[3] Hong-guo zhang, liu yun.Foreign family network technology standard progress analysis[J],Information technology and standardization , 2005(3)：

[4] Chi hsiang Wu, Rong Hong Jan. System Integration of WAP for Home Network System[J].Computer Networks,2003,42(4):495-502

[5] Renato Jorge, Caleira Nune , Lisbon Portugal . A Web-Based Approach to the Specification and Programming of Home Automation System[C]. Proceedings of the IEEE Mediteranecan Electrotechnical Conference (MELECON),2004

[6] [EB/OL].http://www.af360.com/html/2012/12/05/201212051434019652.shtml

Stepping motors for gas micro sampling

Jiang Peng; Zhang Jianchun; Man Yi

(College of Instrumentation and Electrical Engineering, Jilin University,Changchun 130026,China)

***Abstract*--This design is based on MSP430 Stepper motor micro-gas injector, the hardware design of the system includesstepper motor control circuits, liquid crystal display and keyboard input, gas tank control circuit. In the design of software, the main problem is SCM control for each module, the realization of the stepper motor at the core of trace gas injection capabilities. Accessibility includes the gas tank temperature detection.**

***Key words*--Stepper motor gas Micro Injection Microcontroller**

I. INTRODUCTION

INJECTOR in biochemical Analyzer in today's society, chromatography instruments has a wide range of applications. Reliability and accuracy of its direct impact on results. Therefore, in research and development of biochemical analyzers, chromatography analytical instrument company first and foremost is the research and development of efficient, precision stepper motor-based gas micro-injector[1].

II. MEANING OF REASERCH

Domestic gas injector were primarily for human intake, this method is a method more waste of manpower, but also prone to human negligence, qualifying injection volume inaccurate problems. Neither intelligence, can not guarantee the accuracy. So do a stepper motor injector is very necessary. Gas detection, control and alarm means there are many, wherein the gas sensor is the best[2]. But need the gas into a gas tank for testing, we need a gas injector, so that you can better gas injected into the gas tank.

III. IMPLEMENTATION PLAN

A. The research ideas and methods

Msp430 Microcontroller core, through the drive module, control the stepper motor rotation direction, speed and the size of the amount of displacement of the stepping motor, while adding the keyboard module and a liquid crystal display module, keyboard module auxiliary setting the operating state and stepper motor numerical displacement amount of the liquid crystal display module is displaying the operating status of the stepper motor and parameter setting while msp430 control solenoid valve is turned on, the control box out of gas[3].While the auxiliary circuit is 51 microcontroller, the main function is to measure the temperature of the gas tank, but also has an alarm function to protect the safety of the system, then the measured value on the display. A system block diagram shown[4].

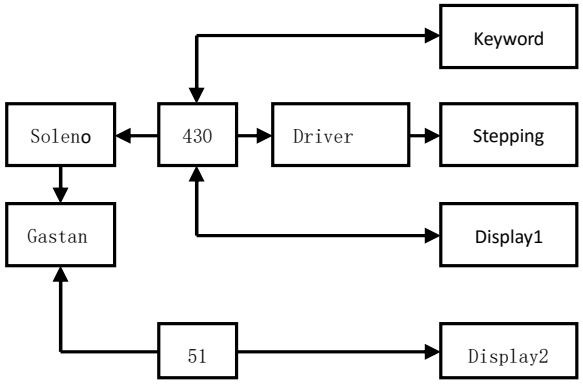

Fig.1 system block diagram

B. The main module, implementation plans and technology roadmap

Driver chip stepper motor driver module for L298N, including 4-channel internal logic driving circuit. It is a two-phase motor and four dedicated drive that contains two H-bridge high-voltage and high current queen bridge driver accepts standard TTL; logic level signals can drive 46V, 2A below the motor.

Keyboard module is used to set the start and end of the stepping motor, the rotational direction, size and amount of displacement speed setting. Keyboard module uses the key sheet 4 × 4 matrix.

The display module 1 to display the direction of rotation, speed, displacement of the stepping motor,

while the display module 2 to display the value of the air temperature inside.

Temperature measurement module uses 18B20 temperature sensor for measuring air temperature inside achieve. Both gas tank temperature alarm function, when the temperature exceeds a preset safe temperature, the buzzer will issue security alerts, security system[5].

Solenoid valve module is the control solenoid valve switches to control the gas out of the gas tank.

MSP430 basic working circuit module connected to a crystal oscillator and a reset circuit with MCU peripherals, connect the power and ground.

IV. CIRCUIT COMPARES

A. SCM Part

Msp430 microcontroller and 80C51 in part by a constitution, msp430 responsible for controlling stepper motor conduction state and the solenoid valve operation, 80C51 is used to measure the temperature of the gas tank and the high temperature alarm.

Circuit is crystal quartz oscillator. Quartz crystal oscillator has a very good frequency stability and the ability of anti-interference, therefore, quartz crystal oscillators used to generate a reference frequency. In addition, it can produce an oscillating current, sends out a clock signal to the microcontroller. On-chip and off-chip circuit device comprising a clock generation circuit, crystal frequency and more generally in select between 1.2MHz ~ 24MHz. C1, C2 is a feedback capacitance, and its value between 20pF ~ 100pF selection, usually around 30pF. Crystal frequency is 12MHz, the clock period is 1us[6]. The main function is to reset circuit microcontroller initialization, during initialization reset pin on the need to increase to a high level two machine cycles. SCM address after reset is initialized to 0000H, then the microcontroller program execution resumes from 0000H unit.

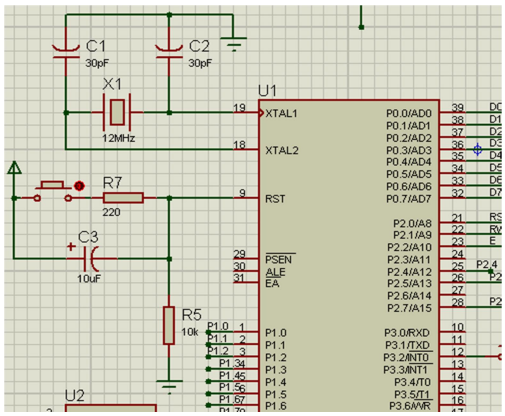

Fig.2 Microcontroller circuit1

MSP430 minimum system consists of a master MCU, power, reset circuit, clock circuit, JTAG debug circuitry, serial communications module, at the same time also designed MCU clock circuit, power circuit and JTAG debug circuitry. Clock module provides the clock source for the MCU, JTAG interfaces for microcontroller program debugging and emulation, serial 0 (USART0) through MAX232 level converter module connected to the PC for debugging embedded software, power supply module provides power to the MCU and each peripheral module . Program by P4.4, P4.5, P4.6, P4.7 pin control four motors to P2.0, P2.1, P2.2, P2.3 four pins control LED display control motor high speed and low order changes.

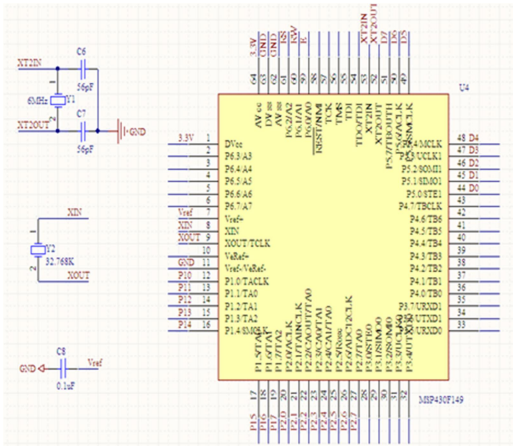

Fig.3 Microcontroller circui2

B.Motor driving section

In this circuit, we selected as a driving device LM298N, LM298N provide for bidirectional load current. Suitable for driving 2-phase or 4-phase stepper motor and DC motor, especially when the driving direction of the motor is to be changed, only the position of the original electric motor to reverse direction. LM298N can drive more than one motor 2A, LM298 motor drive module to meet the

requirements.

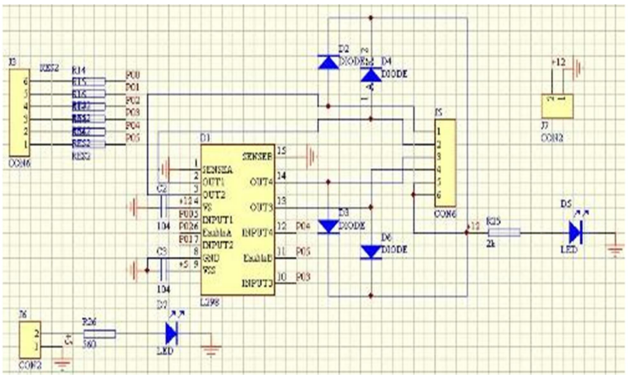

Fig.4 The motor drive circuit

C.Alarm section

When the temperature exceeds the set range, the alarm buzzer module circuit, the circuit resistance play a limiting role. Circuit works when the temperature exceeds the set range, by programming to the P2 port Chapter 7 pin Fu is low, the transistor is turned on, the buzzer sounds.

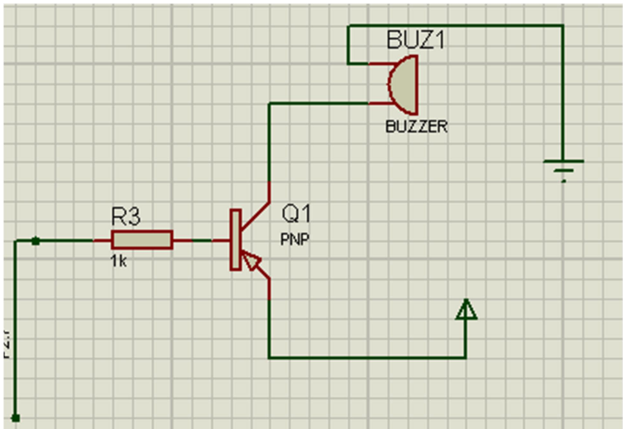

Fig.5 Alarm circuit

D.Display Part

LCD1602 display part by the composition and Nokia5110 into, LCD1602 display box air temperature, Nokia5110 display the operating status of the stepper motor.

Nokia5110 advantages are:

(1) interface is simple, only four I / O lines can drive, LCD1602 need 11, LCD12864 need 12.

(2) cost-effective, LCD1602 can display 32 characters, Nokia5110 can display 15 characters, 30 characters, only the bare screen 8.8 yuan, 15 yuan or so LCD1602 general, LCD12864 generally 50 to 70 yuan.

(3) Nokia5110 operating voltage 3.3V, operating current of 200uA normal display below the power-down mode for battery-operated portable devices.

(4) speed is 20 times LCD12864 is 40 times the LCD1602.

LCD1602 advantages are:

It is a display devoted to letters, numbers, symbols, etc. dot matrix LCD module. It consists of several 5X7 or 5X11 dot matrix character bits, each bit character dot matrix can display one character. With this module flexible interface and simple way to facilitate the operation instructions, may constitute a man-machine interface.

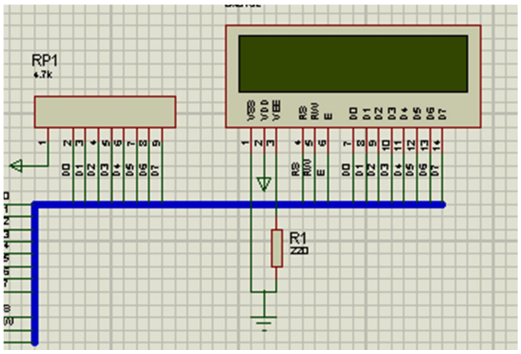

Fig.6 LCD1602display circuit

E.Temperature section

Temperature sensing circuit uses a single digital temperature sensor DS18B20. DS18B20 unique single bus interface to only one data line through the data transfer can be completed. Its supply voltage between 3V to 5.5V, temperature range between -55 degrees Celsius to +125 degrees Celsius, 9-12 adjustable resolution. DS18B20 has three output leads, respectively, then the power, the microcontroller pin, since in normal operation, the sensor is required to drive current of about 1mA, so the hardware circuits need to be connected to the power supply and two leads an indirect one about 5K resistance.

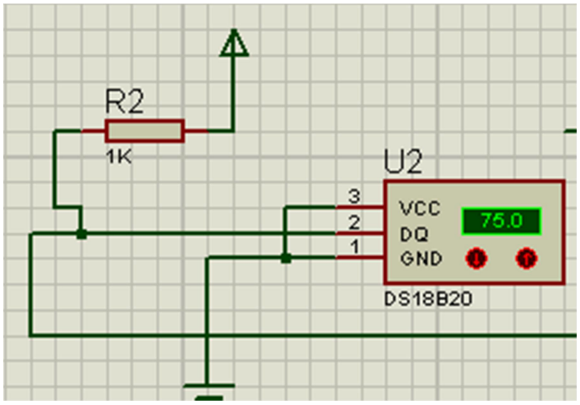

Fig.7 Temperature measuring circuit

Ⅴ. SYSTEM SOFTWARE DESIGN

A.msp430 main program flow chart 1

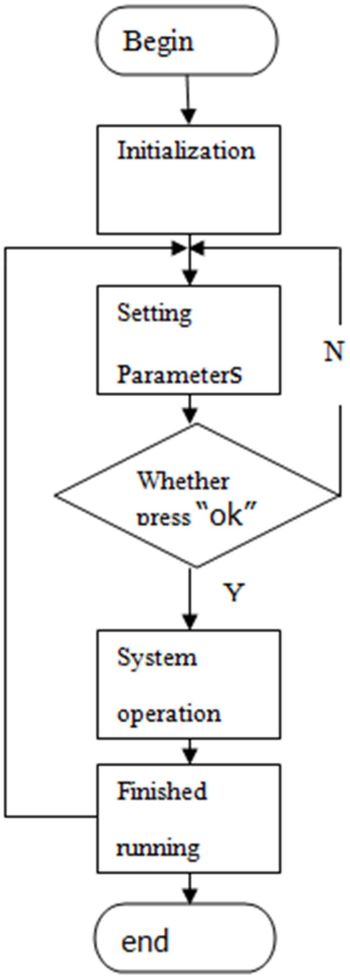

Fig.8 The main program flow chart1

42H200 linear stepper motor lead screw pitch 8mm, pulse equivalent 0.01mm, per pulse to a platform to go the distance, use the master set 430 to control the timing of each pulse in time, thus calculated speed. And then control the timing of long shift function can be realized according to the speed setting.

Buttons to set a pre-movement distance, because pulse equivalent 0.01mm, obtained after one pulse per platform go 0.01mm, and the required accuracy of 0.01mm, so the program is displayed as XX • XXmm, in order to achieve precision, the transmission of N pulse is showing movement nut N * 0.01mm, thereby to move a specified distance you can control the number of pulses sent by the realization finally achieve the purpose of precise positioning.

When the stepping motor is transferred, the solenoid valve 1 is turned on, the solenoid valve 2 is closed. When the stepping motor reversal, solenoid valve closed, the solenoid valve 2 open.

b.80c51 main program flow chart 2

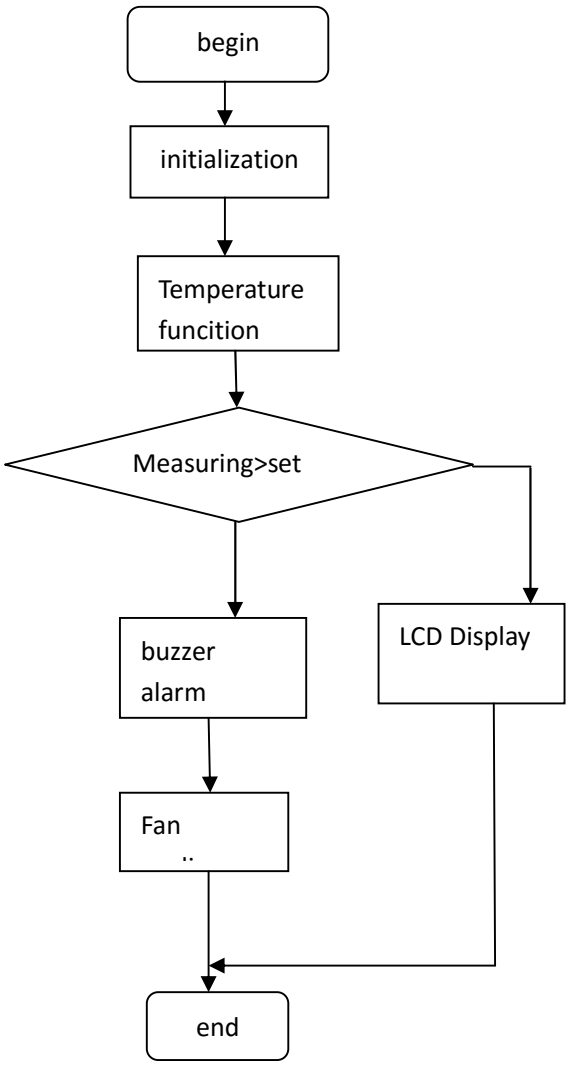

Fig.9 The main program flow chart2

Related program first macro definition, the definition of variables and arrays, the preparation needed Functions such as keyboard scan subroutine, subroutine temperature setting, temperature, etc. Functions. Then call in the main function of the

liquid crystal LCD initialization subroutine initializes and displays "wendu" in the first line of LCD display "sheding", calling on the current temperature measurement function temperature collection, call the temperature limit set in the second line of LCD Stator function set for hazardous temperature, laser diode is responsible for the heating portion, then the collected temperature values are compared with the set temperature. If the temperature is less than the danger, call the function liquid crystal display shows the current temperature; if the temperature is greater than the danger, call the function liquid crystal display shows the current temperature, the buzzer alarm, microprocessor controlled fan cooling.

Ⅵ. FUNCTIONS IMPLEMENTED

A. Basic Skills

(1) the use of SCM stepper motor control pressure into the gas tank of gas volume.

(2) using a temperature sensor so that the gas temperature is displayed in the display box.

(3) control the import and export of the gas tank switch.

(4) the length of the stepper motor motion is converted to the corresponding volume of gas tank and make it appear on the display.

B.Key issues and key and difficult project

(1) stepper motor control. How to use microcontroller programming stepper motor produces a step displacement control reversing the problem. Important part. Different products have different control waveforms need to understand the principle of stepper motor driver and master the basic knowledge to buy, in order to meet the requirements of the project.

(2) the display of the display portion. Display needs to display two parts, one is the temperature of the air box, a stepper motor displacement is converted into gas tank concentrations. So we need to know the type and model of the display, to meet the requirements, but also strive to the most economical and convenient.

(3) is connected to the computer through a serial port for remote control. Circuit overall planning and design, and software programming is the difficulty of the project.

Ⅶ.TEST RESULT

Theoretical injection volume of gas / ml	Theoretical displacement of the stepping motor / mm	The actual intake air volume / ml	error
1	3.4	1.1	10.00%
2	6.8	2.2	10.00%
3	10.2	3.2	6.67%
4	13.6	4.3	7.50%
5	17.0	5.3	6.00%
10	34.0	10.6	6.00%
15	51.0	15.8	5.33%

Fig.10 test result

From the above test results, the greater the volume of gas injection error is relatively smaller, the basic error control within 10%, in line with expectations.

Ⅷ.CONCLUSION

The project has basically completed the design specifications for realization of the stepper motor-based trace gas injections proven that the system is relatively stable, more accurate precision, can effectively save time, relatively artificial injection, saves a lot of human, has some practical value. However, the accuracy of the stepper motor application of the system is not high enough, there will the system to achieve one of the most optimization of the degree.Smaller amount of gas in future improvements, through the use of more precise steppermotor, allowing be situations when allowed precision injection cause

References

[1] Jialiang Ju, Chin Peng should, Xulin Ming, Nizi Feng, Wang Masaharu Materials Engineering, China University of Mining "Current Status and Development Trend of the gas sensor"

[2] Jia Jian, Li Jianping, high Xiaoming, Li Xiuli State Key Laboratory of Transducer Technology, Institute of

Electronics "gas sensor array Intelligent Test System"

[3] Al Kennedy, Wang Tao, Jiang Yadong University of Electronic Science and Technology "gas sensors Automatic Test System Based on Virtual Instrument"

[4] Pan Xiaoqing, Liu Qingcheng gas sensor and its development [J] Journal, 2007, (27): 89-93.

[5] Kang Chunmei, Geng Zhenya, horsepower sensor foreign market analysis and prospects [J] China Electronics News, 2004, (9):

[6] Song Ling, Shiyun Bo, virtue Bin, Hu Min, Wang right MSP430-based gas sensor batch testing system [J] Electronic Measurement Technology, 2009,10: 77-81.

The pedometer based on the power generation shoes

Sun Yong; Jiang Yuan; Suhang Li

（jilin university instrument science and engineering institute,changchun,130021）

***Abstract*--The pedometer is an electronic products which has a rise in recent years ,can exercise every day for people to provide a basic reference.Power generation shoes also is a commodity has the rise in recent years,while walking the energy needed to produce electronic products work.This article combined the two to pedometer design based on power shoes as the starting point, the piezoelectric ceramic extrusion to produce electrical energy stored, for the pedometer for PVDF sensors work, while walking, on the one hand, to achieve the production of energy, on the other hand to complete the function of the step, kill two birds with one stone.**

***key word*--Pedometer Power generation shoes Piezoelectric ceramics PVDF sensor**

1. INTRODUCTION

PEDOMETER is a relatively common form of electronic products in today's society, it can provide a simple data reference for people's daily movement. Domestic molded electronic products pedometer function xiaomi bracelet, Huawei hand ring, and other foreign products like Iwatch. But these types of electronic products have a relatively limited features, the need for particular electronic products, such as, Iwatch can only be for iPhone, and usually the high prices that most people can not afford. This makes the promotion has significant limitations. With the development of human society, less and less energy storage capacity, the search for new energy sources has become a major contemporary inescapable problem in front of us[1]. On the road to find new energy, it will focus on a series of large-scale solar energy, nuclear energy, but little attention around the existence of many small energy sources, such as vibration energy, thermal energy, etc. This makes the people in seeking new energy at the same time, undoubtedly ignore a lot of energy which are fingertips, to some extent, energy is wasted. Currently at home and abroad have made the use of mechanical energy Electric shoes, but the technology was not ripe, the main drawback is that the energy is too low , which is a problem need to overcome in front of us[2].

We propose shoe pedometer-based power generation, use piezoelectric ceramic electrical energy generated by the force of extrusion , after treatment by a specific circuit on the lithium battery charging , to a certain extent, a pedometer can be a work of power consumption supplement, pedometer signal choose PVDF piezoelectric film as a sensor, signal acquisition generated by the extrusion , counted by the controller, and sent via Bluetooth PC, the PC part select android phone system, mommunication with pedometer based on phone app via Bluetooth[3-5]. The significance of this design is that on the one hand reduces the work environment requirements, android with Bluetooth is enough , the price is cheap, so most people can use it; on the other hand, piezoelectric ceramics electric power generated by the force of extrusion of lithium rechargeable batteries, conducted a comparison of energy fully utilized.

This paper mainly consists of five parts, the overall structure of the design, hardware design, software design, the PC part of the design, analysis of the results, and at last we will make a brief summary of the project.

2.OVERALL STRUCTURAL DESIGN

Located in the foot portion of the piezoelectric ceramic, each person would have squeezed their movement to produce deformation, generates a corresponding electrical energy[6], after rectifier filter for lithium rechargeable batteries, lithium batteries as the energy storage medium on the one hand, and on the other hand，it provide the energy needed for the work of the controller and Bluetooth.

PVDF sensor is also located in the bottom of the foot, people at every step, there will be a squeeze on it，then the corresponding sensor generates a pulse to the controller[7], record the number of received pulses are counted, a pulse corresponding to step.

Controller to communicate with the host computer via Bluetooth, the number of steps to pass information to the host computer, the PC can display the information of the number of steps , send specific

commands to the controller, clear the controller for controlling the number of steps , and decided the number of steps transmission of information or not.

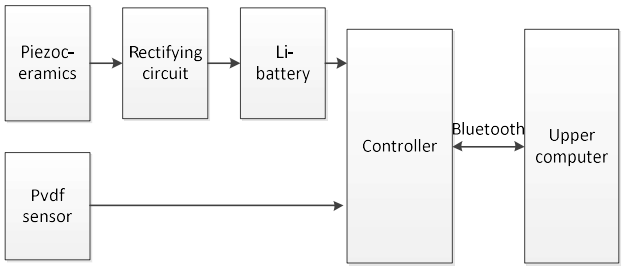

Fig.1The overall structural design

3 .HARDWARE DESIGN

3.1Power generation portion

Some dielectrics subjected to an external force in a certain direction and is deformed, it will produce internal polarization, opposite positive and negative charges appear on its two opposite surfaces[8]. When the force is removed, it will return to the uncharged state, a phenomenon known piezoelectric effect, as shown in 2 (a). When changing the direction of the force, also changed the polarity of the charge. On the contrary, when the electric field is applied in the direction of polarization of the dielectric, which dielectric deformation will occur， after the electric field is removed, the deformation disappear, a phenomenon known as the inverse piezoelectric effect[9-10], as shown in Figure 2 (b).

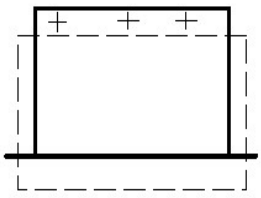

(a)Direct piezoelectric effect

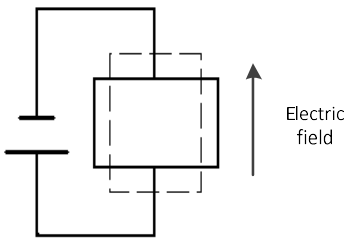

(b) inverse piezoelectric effect

Fig.2 piezoelectric effect

Theoretical basis for generating electrical energy of piezoelectric ceramics is piezoelectric effect for generating electric energy principle shown in Figure 3

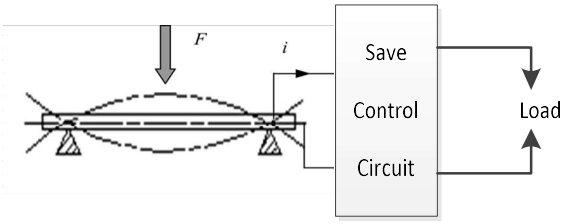

Fig.3 Principle of the electromechanical converting system

After being squeezed at both ends of the signal of the piezoelectric ceramics irregular signal[11], in order to obtain more structured signals, In the next step of the lithium battery charge is very convenient, first, the signal needs to be a simple rectifier, then filtered through a capacitor C1, to save energy, we use streamline circuit design, led5 is for fixed energy direction, allowing only after adding led5 circuit capacitor C1 to charge lithium batteries, but does not allow the recoil, it can protecting the circuit, saving energy. To save more energy, led 5 selected Schottky diodes, which have small on-voltage. Schematic in Figure 4.

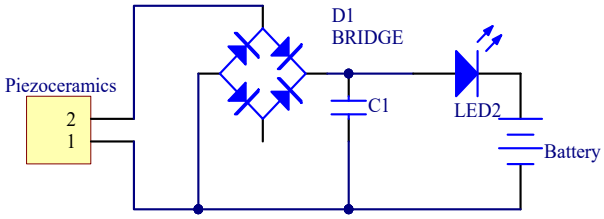

Fig.4 The principle diagram of the battery

3.2Pedometer part

Steps signal from the PVDF sensor produces a pulse every step, the number of pulses of the microcontroller statistics, the number of steps for the information.

Controller selects msp430f149 microcontroller. The model is based on single-chip RISC (Reduced Instruction Set Computer) 16-bit signal mixed-signal processors designed to meet the ultra-low-power microcontroller and well-designed, intelligent peripherals, ease of use, low cost, the industry's lowest power and other outstanding features. Pedometer which is generated by the piezoelectric ceramic electric energy as the main energy source, and therefore have a higher optional on low power consumption advantages.

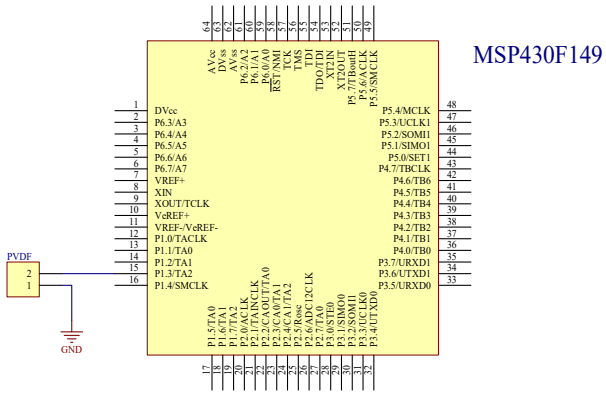

Fig.5 The principle diagram of step meter

PVDF generated interrupt signal connected to the MCU P1.3 pin. msp430f149 SCM P1, P2 pin can be used as an interrupt pin, where selected P1.3 interrupt signal, the interrupt mode selected as the rising edge. PVDF sensor when squeezed, it will produce a pulse signal, when the rising edge is detected, the microcontroller counts one, plus a number of steps. Figure 5.

2.3 The communication section

Communication between SCM and PC selection HC-05 Bluetooth as the communication medium. HC05 microcontroller is a low-power Bluetooth, the working voltage is 3.3v ~ 5v, consistent with the host microcontroller operating voltage range, no further additional access to other operating voltage. Users can set the baud rate to facilitate the transmission of data. msp430f149 microcontroller choose P3.4, P3.5 pin of the Bluetooth communication, P3.4 connected Bluetooth RXD pin, P3.5 connected Bluetooth TXD pin. Figure 6.

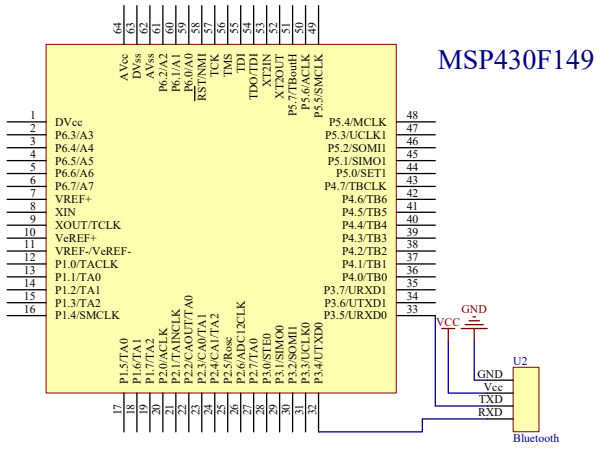

Fig.6 The principle diagram of the communication

4. SOFTWARE PART OF THE DESIGN

MCU power, first, each pin is initialized, specifically: P1.3 interrupt pin set, set the interrupt mode interrupt rising, P3.4, P3.5 pin is set to communicate. After initialization is complete, the received signal from the host computer to detect if the PC to send the number 0, the current pedometer step number is cleared, or when a signal is detected from the Pin Pvdf sensors caused the interrupt signal a record number, and then processing the data, the data is sent to the host computer via Bluetooth for display. Figure 7 is a flowchart of the software.

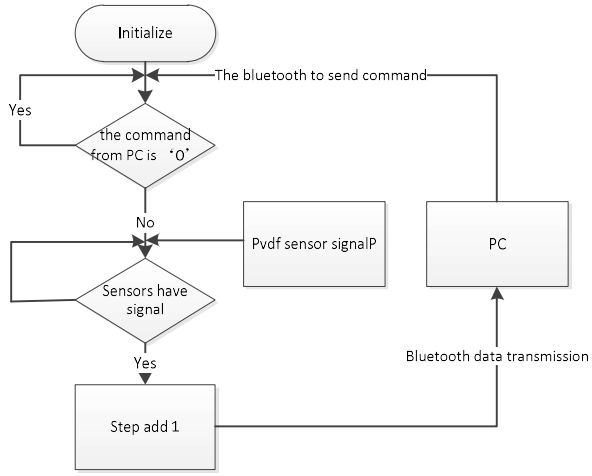

Fig.7 software flow pattern

5. PC PART OF THE DESIGN

Preparation of PC Program Based on google products Android Studio, use JAVA programming language as the basic language.

PC software steps as follows.

(1) Get Bluetooth response permissions:

Making procedures so that the local Bluetooth has the right to work or relax.

Explanation:

To use the Bluetooth function in your application, at least to declare a two Bluetooth(BLUETOOTH and BLUETOOTH_ADMIN) permissions. In order to perform any Bluetooth communication (eg connection request, receiving and transmitting data connection), you must apply for permission BLUETOOTH. To start Bluetooth device discovery or maintenance settings, you must apply for permission BLUETOOTH_ADMIN[12]. Most applications require this permission, just to be able to discover the local Bluetooth device.

(2) the configuration of the local Bluetooth module

Setting up the Bluetooth switch terminal, thereby controlling the Bluetooth discovery scan.

Explanation:

Before an application can use Bluetooth communication channel, you need to confirm whether the device supports Bluetooth communication, if supported, make sure it is available. If you do not support Bluetooth, you should disable all Bluetooth

functionality. If Bluetooth support, but is disabled, you need without leaving the application, enable the Bluetooth function.

(3) search for Bluetooth devices

Bluetooth area is scanned to obtain information and Bluetooth judge and get in line with the communication protocol Bluetooth.

Explanation:

Use BluetoothAdapter objects, a list of devices that can detect or query to find the paired remote Bluetooth device through the device.Device discovery is a scanning process, the process of the search for available Bluetooth devices within the region, and then request some of the information related to each other (this process is called "discovery", "Search" or "Scan"). However, Bluetooth devices within the region only when enabled features that can be found, will respond to discovery requests. If a device is found, it will by sharing certain information (such as device name, category, and a unique MAC address) to respond to discovery requests. Perform discovery and processing equipment uses this information to selectively initiates the connection device which is found[13-14].

(4) Socket Communications Bluetooth

Socket is a special text, socket function is for the text open, read and close operations[15].

(5) Connection Management (data communications)

Get data from the input stream

To pass data to the microcontroller from output stream

(6) data processing

Data information obtained from (5) for processing, and displayed.

Flowchart is shown in Figure. 8

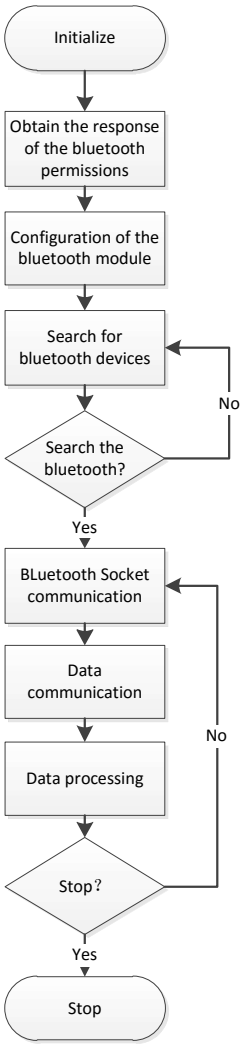

Fig.8 The flow chart of upper machine

Interface software work is shown in Figure.9.

Fig.9 Working software interface

6. Result Analysis

PVDF is used as the input signal sensor pedometer, its accuracy is relatively high, specific test data shown

in Table 1.

Table.1 A pedometer measurement accuracy

The number of experiments	Actual values	Measured values	Relative error （%）
1	10	11	10
2	50	49	2
3	100	10	2
4	150	152	1.3
5	200	202	1
6	250	249	0.4
7	300	301	0.33
8	350	349	0.28
9	400	399	0.25
10	450	451	0.22

The pedometer measurement data are plotted in Figure 10. You can clearly see by the image, with the increase in the number of steps, the accuracy of the pedometer increase as compared with the market,precise degree significantly improved.

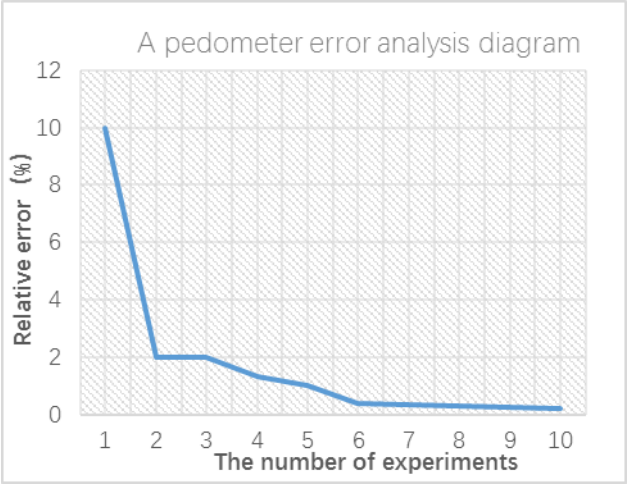

Fig.10 The error analysis diagram of pedometer

7.CONCLUSIONS

The pedometer based on the power generation shoes has basically completed the given index, even in the pedometer accuracy, its precision accuracy higher than many of the pedometer currently exists in the market. However, due to the low power generation efficiency of the piezoelectric ceramic, when used, The pedometer based on the power generation shoes can not fully meet the needs of the work, we also need to provide some external power to make the pedometer work properly. However, we believe that with further improvement of the circuit, the power generation efficiency of the piezoelectric ceramic can be further improved, The external energy needed for the work will be less , The pedometer based on the power generation shoes will take place in the future pedometer world.

References

[1] Koichi Ishida , Tsung-Ching Huang.Insole Pedometer With Piezoelectric Energy.

[2] Harvester and 2 V Organic Circuits[J].IEEE JOURNAL OF SOLID-STATE CIRCUITS,2013;255-264.

[3] Zhao Dongsheng. PVDF piezoelectric film sensors [J]. Sensors and Microsystems,2007，26(3)；51-55.

[4] Li Yan,Zhong Fangping. PVDF dynamic strain measurement applications [J]. Explosion and Shock.2003,23(3);230-234.

[5] Xi Daoying,Zheng Yonglai. PVDF piezoelectric count in dynamic stress measurement application [J]. Explosion and Shock Waves,1995,15(2):174 -179.

[6] Luo Zhizeng,He Facang. Robot made of PVDF sensor [J]. Sensor Technology,1997,16(3):1-4 .

[7] Wang Guoli, Zhao Ziying. Development PVdF piezoelectric film pulse sensor [J]. Journal of sensor technology,2012,12(4).688-692.

[8] Zhang Fuxue. Piezoelectric modern science (on) [M] Beijing: Science Press, 2002:84-101.

[9] Wang Junlong. Based on the vibration generating apparatus of piezoelectric material [D].. Jiangsu University, Jiangsu,2012.

[10] Qi Hongdong,Yang Tao, Summary of miniature piezoelectric ceramic vibration power generation technology research [J]. Sensors and Microsystems,2007,26(5);1-4.

[11] Yan Shiwei. Piezoelectric generator experiment design and application of [D]. Jilin. Jilin University,2007.

[12] Cha Sha. With Android mobile application development [J]. Special planning.2008.

[13] Wu Xianzhen. Android platform smart phone application software module design and development [D]. Heilongjiang. Harbin Institute of Technology, based,2013.

[14] Li Manling. Configuration of Android development environment [J]. Information media.

[15] Dang Licheng. Smart phone platform based Research and Application of [D]. Anhui. Anhui University,2012.

The design of the heating system leakage detection device

ZHANG Rui; GAO Ming-yu;. MA Chun-yao

(jilin university instrument science and electrical engineering college, changchun,130000)

***Abstract*--Heating pipe leakage bring huge economic losses to the country, aiming at the shortcomings of the traditional passive detection technology, uses the ultrasonic sensor, implement detection of heating pipes. Hardware design and software flow diagram are given. Using DSP technology, with 8 channel 16-bit ADS8345 chip improves the calculation precision, to optimize the human-computer interaction module, realize the data real-time processing and display functions. Experimental results show: the entire instrument error range within 0.2 m, achieve the desired requirements.**

***Key words*--Funnelled detection Sensor The human-computer interaction**

INTRODUCTION

MORE and more popular in today's society, heating system, leakage problems in heating applications, lead to serious energy consumption, operation failure occurs frequently, a serious threat to the normal operation of the heat supply network, the heating quality is difficult to guarantee. In order to make the heating system leak detection is more concise and straightforward, we have the design of the leak detection system.

1.DOMESTIC RESEARCH STATUS

Currently on the market comparison of pipeline leak detection method is rich, but usually apply to water supply, for gas and oil supply system, due to the heating pipe network heat medium temperature is high, the installation conditions, the influence of such factors as really suitable for city heat supply pipeline inspection technology is still very limited. Current heating pipeline leakage detection and location method is to learn from other network special water supply, gas pipe network, and applied in heating network existence insurmountable problems and limitations. Heating pipe network leakage occurs, can cause flow, pressure, heat medium temperature and abnormal changes in physical properties such as sound, so in the heating pipeline leak detection, can be judged according to the abnormal situation.

1.1 Artificial leak detection

At present domestic most thermal companies adopt traditional artificial leak detection methods, mainly by the engineering staff with a wealth of practical experience, according to the leakage of heating pipe network pressure and sound vibration anomaly change of physical properties such as to determine the leaking pipe section and the exact location of the leak. This method is simple and convenient, but vulnerable to human and the interference of external factors, low accuracy, poor reliability.

1.2 The acoustic emission leak detection technology

At present abroad related departments and scholars mainly study using acoustic emission technology for heating pipeline leak detection and location. Acoustic emission technique can be real-time dynamic monitoring and large coverage, is a kind of non-destructive leak detection method, the principle is: heating pipeline internal heat medium leakage occurs when a continuous and acoustic emission signal propagation in the pipe, such as the basis of the intensity of acoustic signal amplitude can reflect some of the characteristics of structure, such as the location of the leakage and leakage, etc.But according to the acoustic emission phenomenon of leak detection technology involves the influence of many factors, is a very complicated problem, such as leakage aperture size, shape and liquid pressure, turbulence and solid-liquid coupling, etc., to establish basic could not precise mathematical physical model, and by the acoustic emission signal source diversity, sudden and their characteristics such as the uncertainty and acoustic emission source to the propagation path of sensor, the accuracy of the sensor, environmental noise and acoustic emission measurement system, such as a variety of complex factors, and the acoustic emission signal waveform of the acoustic emission sensor output real signals vary widely, the diagnosis accuracy is very low.As a result, the acoustic emission leak detection technology is the key to analyze the acoustic emission signal identification, eliminating the influence of these factors on the signal, restore the real acoustic emission signal. But there is no widely accepted and can be effectively used in the heating pipeline acoustic emission test method and field application of leak detection.

1.3 Based on the mathematical model of leak detection

technology

Heating pipe network leakage occurs, can cause heat medium in the pipeline flow, the change of the parameters such as pressure, in order to be able to accurately reflect the change of the hydraulic conditions, according to the continuity equation, mass conservation equation, momentum conservation equation and energy conservation equation and so on to build the dynamic hydraulic model of heating network. Solving the mathematical model can be real-time hydraulic conditions, distribution of flow field in the pipe network, and comparing with the measured values, if the deviation is greater than the normal range, can judge pipeline leak, then according to the variation of pipe pressure gradient values to locate the leak point. In order to enhance the accuracy of mathematical model, need to fully consider when modeling the temperature, pressure, fluid density and friction factors on the influence on the hydraulic condition, according to the given boundary conditions to solve the mathematical model of hydraulic project condition. With the expansion of the heating pipe network, the system is more and more complex, it is difficult to achieve ideal conditions prescribed by the mathematical model is established, the influence of some factors must be ignored, thus solving the results and the actual value bias, affect the accuracy of the mathematical model of the leak detection technology.

2.WORKING PRINCIPLE OF THE INSTRUMENT

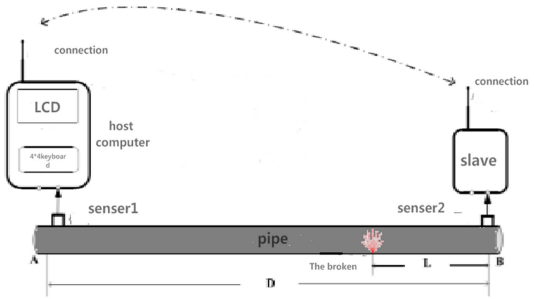

Fig.1 Working principle of the instrument

The leaking sound emitted by the use of funnelled to reach around two time and leaking sound propagation speed sensor[1][2] to calculate the leakage distance as shown in figure 1.

3.INSTRUMENT MODULE DESIGN

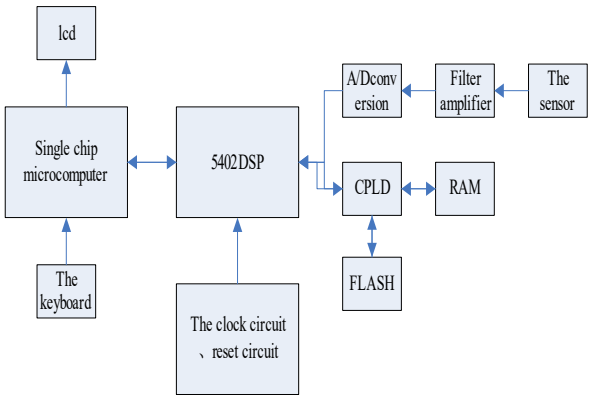

Fig.2 The principle diagram of the system

3.1 Based on single chip microcomputer module circuit design.

This system use Rabbit3000 as main control chip,Through its control LCD display and DSP for data processing.Sensor[3] collected data after pretreatment,Through DSP Mcbsp0 channel into DSP, DSP with CPLD mapping connection will Flash Flash and Ram to the application area, Ram is mapped to a data area. Detector after startup, LCD display interface design, DSP to realize parallel way to bootstrap start at the same time, the Flash program loaded into memory in fast, through the keyboard control, LCD implementation of DSP data processing step by step[4], after Rabbit3000 through the HPI of DSP to DSP processing data is read into memory, and into the LCD, it shows that in the interface[5].

3.2 A/D conversion module design

This system chooses ADS8345 A/D conversion chip, the chip is an 8 channel 16 sampling A/D conversion with synchronous serial interface[3]. When the power supply voltage of + 5 v, the frequency of 100 KHZ, the chip only 8 mw power consumption. Reference voltage of 500 mv to VCC / 2, at the same time provide a corresponding input voltage range + VRE. The chip provides closure model, can be reduced to 15 mu W power consumption. Low power consumption, high speed, multiplexing make ADS8345 choice of portable measurement equipment.

3.3 Data acquisition module design

This system through the sensors to collect data, and then through the A/D conversion, and then sent to DSP processing. Due to the sensor collected pipeline leakage signal is small, so need proper amplification of the signal, and the A/D converter ADS8345 voltage conversion range, which is 500 m V ~ VCC / 2. This system by designing the amplifier circuit voltage amplification to about 1.6 V, in order to function.

3.4 Human-computer interaction module

Human-computer interaction module mainly includes keyboard control and liquid crystal display part, the main parameters of the input, system control, information interaction, etc. The operator is designed

to easy to use and manage. Good human-computer interaction can increase the economic benefit and social benefit.

4.THE TEST RESULTS

Two sensors installed in the pipeline[6], the distance of 10 m, leaking from point b 3 m. The total dozens of sets of data,The processing results in the following table:

The serial number	L/m	Data error	The serial number	L/m	Data error
1	3.15	0.15	6	2.95	-0.05
2	3.07	0.07	7	3.11	0.011
3	3.11	0.11	8	3.05	0.05
4	2.96	-0.04	9	2.93	-0.07
5	2.83	-0.17	10	2.91	-0.09

Table 1 Collected data tables

5.CONCLUSION

Heating system leakage detection device of the actual application shows that the error of the instrument within the 0.2m, reached the expected requirements, the scheme is feasible. The instrument has high reliability, data processing is rapid, the human-computer interaction ability. Easy to promote.

Reference

[1] WANG Jun, LING Zhen-bao.Sensor Principle and Detecting Technolog[M].Changchun: Jilin University Press. 2003.

[2] LIGang.The Principle Development and Application of Digital Signal Processing[M]. Tianjing University Press.2000:153—184.

[3] GUHai-jun,ZHAO Xiao-hui, WANG Hong-ge.Re-alization ofVirtual I2CMasterBased on HostPortInterfaces in DSP [J]Journal of JilinUni-versity(Information Science Edition)). 2004,22(1):13—17.

[4] ZHANG Run-zhou,CHENG De-fu.Design and Realization DataAcquisition System Based on DSP.[J]Journal of Jilin University(Information ScienceEdition. 2003,21(1):13—17.

[5] ZHANG Xiong-wei, CHENG Liang, XU Guang-hui.The Integrated Developmentand Practical Example ofDSP.Electron Industry Press.2002:42 -55.

[6] LING Zhen-bao,WANG Jun,ZHANG Tai-qing.Tap water pipeline leak location detection system realization of data processing[J].Pipeline technology and equipment.2015.12:17-28.

Nuclear magnetic resonance (NMR) high-pass filter design of advanced detection

Liang Shixuan; Wang Hailei; Li Pan

（Jilin university instrument science and engineering institute,Changchun,130021）

***Abstract*--In nuclear magnetic resonance (NMR) to find water meter to MRS signal is very weak, signal-to-noise ratio is very low, in order to enlarge the signal amplifier saturation, at the same time avoid low frequency interference before active filter design of the high-order passive high-pass filter, improve the industrial frequency harmonic interference suppression, to achieve the effect of industrial frequency harmonic filter. Test results can be seen that filter for trough at 1000 Hz, attenuation of 62.90 dB, between 1000 Hz - 2600Hz is monotonically, 1000 Hz attenuation between 51.16 dB and 62.9 dB, attenuation of 51.16 dB at 50 Hz, 100 Hz attenuation is 53.32 dB.**

***Key words*--LC high-pass filter Industrial frequency interference Nuclear magnetic resonance (NMR) water meter**

I. INTRODUCTION

IN nuclear magnetic resonance (NMR) to find water meter industrial frequency of odd harmonics (power system is composed of bidirectional symmetrical components, these components of voltage and current with half-wave symmetric properties, even order harmonic is offset [1]) cause serious interference to the extraction of nuclear magnetic resonance (NMR) signal, affect the accuracy of the signal, results in the decrease of measurement result credibility, and easy to make larger low power frequency harmonic active filter saturation, the inconvenience for groundwater exploration work. So you need to make low harmonic suppression, avoid saturated filter before the level. Design a good choice and bandwidth and performance can meet the requirements of the filter cutoff frequency is particularly important. MRS signal frequency range of 1.278 2.556 kHz, determines the LC high-pass filter pass band should be in 1-3 kHz range inner band width should be as flat as possible access to the stop-band attenuation gradient is as large as possible, especially in the factory and the second harmonic frequency and the attenuation of high frequency electromagnetic wave to quickly as possible (capacitance and inductance in series with the structure of passive filter for the main odd (3, 5, 7, 19) harmonic constitute a high impedance of the bypass, which for the most significant inhibition effect of fundamental frequency) to restrain the interference in the largest extent, prevent the front-end amplifier saturation, and obtain high signal-to-noise ratio of the nuclear magnetic resonance (NMR) signal.

II. THE DESIGN AND COMPARISON OF SCHEME

A. The Selection Of Filter Order

Using MATLAB software design filter order, the results as shown in figure 1.

Wp=1000*2*pi;%Wp-elliptic filter pass band cut-off frequency

Ws=900*2*pi;%Ws-elliptic filter stop band frequency

Rp=1;%Rp-pass band ripple（dB）

Rs=70;%Rs-minimum stop band attenuation(dB)

[N,Wn]=ellipord(Wp,Ws,Rp,Rs,'s'); %N is elliptic filter minimum order，Wn is filter bandwidth.

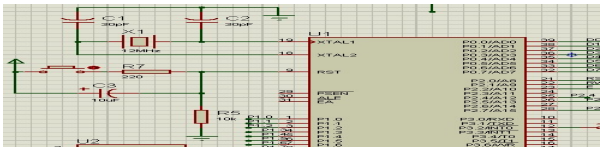

Fig. 1. The setting results of filter order

The high pass filter can be determined to be at least 9 order.

Using the Filter Solutions, software, the Filter parameters design: Filter the Attributes set in the Filter order number is 9, cutoff frequency is 1000 Hz, pass-band ripple is 1 db, stop-band attenuation to 70 db.

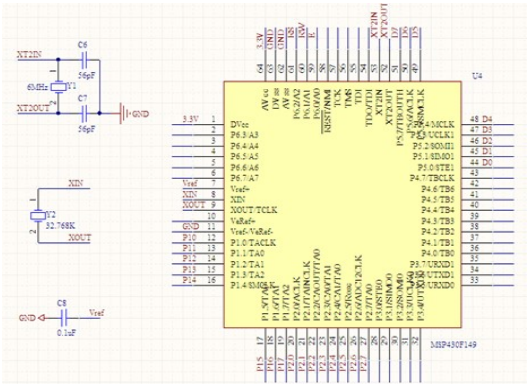

Fig. 2. The design of filter parameters

With the increase of elliptic filter order number, the closer the stop band frequency 1000 HZ, when the order is the order of 14, stop band frequency of 995.8 HZ, order, to increase the number of stop band increased frequency effect is not obvious, so make sure to choose 14 order elliptic high-pass filter function.

B. The selection of filter circuit

Analog filter is one of the most important part of electronic equipment. Commonly used filter has butter-worth, chebyshev and elliptic filter, butter-worth filter and cut than snow, filter network for all pole, only in stop-band attenuation with infinite to infinity, and the elliptic function filter on the limited frequency there are both zero and pole. Zero and pole, produced within the pass-band ripple, limited transmission within the stop-band zero reduced the transition zone, is extremely steep attenuation curve can be obtained. That is to say, for a given order and corrugated requirements, elliptic filter can obtain the transition of narrower bandwidth than other filters.

http://fanyi.youdao.com/Elliptic filter than chebyshev filter is further at the same time with the pass-band and stop-band ups and downs for transition zone at the expense of the more steep features. Compared with other types of filters, elliptic filter under the condition of the same order with the smallest pass-band and stop-band fluctuations, this distinction in pass-band and stop-band are flat butter-worth filter, and flat pass-band and stop-band corrugated or flat, pass-band and stop-band ripple chebyshev filter. So, choose the elliptic filter design.

III.THE OVERALL SYSTEM DESIGN

Overall system structure diagram as shown in figure 3, when the nuclear magnetic resonance (NMR) groundwater detectors work NMR signals were collected through the passive filter, active filter, and then transmitted to the PC through subsequent amplification and signal detection.

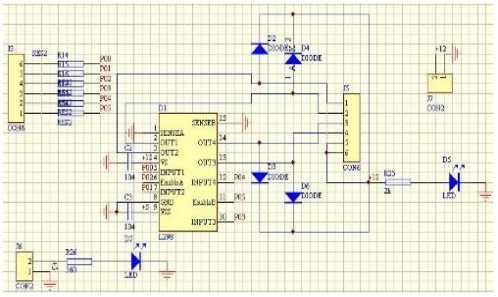

Fig. 3. the overall structure of the system

A. The Design Of Test Circuit Board

Schematic diagram is shown in figure 4. Drawing on Multisim11.0 software circuit principle diagram and simulation by adjusting the size of the component values after gradually explore all component values for the effects of the whole filter circuit to find the simulation effect is the best began after preliminary build hardware circuit circuit parameters.[3][4]Elliptic filter more strict with element parameters, so the adopt the method of parallel of the original circuit to achieve the value of the original device.

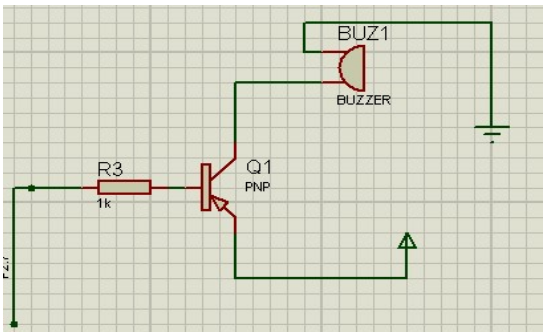

Fig.4. The schematic diagram of circuit

Test circuit board is to use an electrolytic capacitor with conventional inductor in ordinary welding plate structures, the hardware circuit. By the simulation values for each element according to the market the calibration value split and combination, series inductance capacitance in parallel way after preliminary estimate the required capacitance inductance, to electronic market with bulk purchase, and then in the laboratory on the actual values of capacitance inductance measurement calibration (market value and the actual value error in 20%), and marked according to the actual value after different inductance capacitance matching, one by one to match the actual circuit of capacitance inductance values for welding and then complete the hardware circuit.

The effect of the actual circuit and simulation circuit is a big gap, then in input voltage follower to adjust the input and output impedance effect test.

B. The Design Of PCB

During testing, we found that the series inductor has a great influence on the way the measured value of the inductor, the connection will be the size of the angle between the two series inductors string at the interface

between the two inductors and inductance values are such that the actual 5% ~ 10% of the variation in test results for the high-pass effect we decided to replace the ordinary shielded inductor to reduce the impact of external factors on the inductance value, instead of aluminum electrolytic tantalum capacitor capacitance experiments, and characterization PCB circuit board construction and welding, lifting the overall filter filtering effect. Fig.5 after welding template.

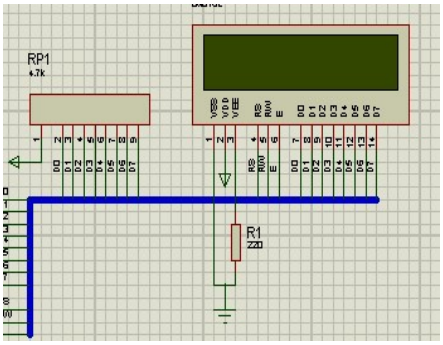

Fig.5. The PCB board of filter

IV.TEST PROGROMS AND RESULTS

A. Test Conditions And Instrumentation

The analog filter is placed in the shielding case, the input and output leads, respectively, the access model MS4630B network analyzer.

B. Test Methods

Setting the starting frequency network analyzer measurement, and measurement after the cut-off frequency, number keys to select, press the enter key input. Scan time can be set 10s, set impedance setting power to make it consistent with the gain of the current measurement system, select the default output B is 1M ohm, exit calibration settings. The probe input (inputs TA) output (outputs B) short, the right side of the screen displays the default after the second column into a measuring changes created, complete the calibration.

The output is connected to the system measuring probe measuring system to the input, the input connected to the probe measurement system to output, at this time can be obtained amplitude-frequency characteristics of the system.Key marker, or use the knob to adjust the knob on the right below the arrow keys, which can be read at different frequencies to the gain value.Key format, press the function key to see the Vice characteristics and system latency curve.Button scale, then select autoscale can automatically adjust the curve on the screen display range, It is in the appropriate display interface（Each adjustment parameters, the network analyzer should be recalibrated, if not calibration, measurement error will result, first reading at different frequencies according to a gain value marker or other key).

C. Test Results

Network analyzer display interface for different frequencies corresponding magnitude recorded. Wherein 50Hz to 3000Hz every 50Hz taken a point (because the data is too large, it will not listed) and draw a line Fig.6.

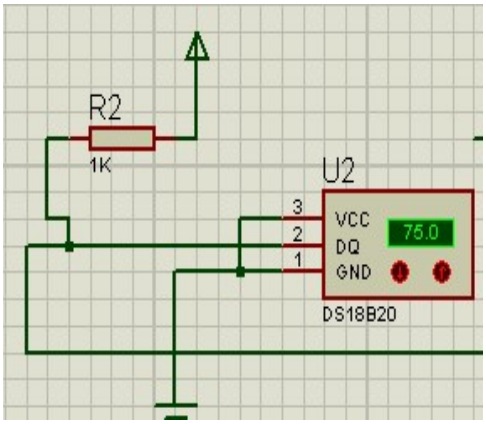

Fig.6.The line graph of test results

Test results analysis: as the inductor, the mutual inductance between the inductor's inductance value and the error of the calibration value, tantalum capacitor of capacitance values and the error of the calibration value, the influence of such factors lead to the gap between the measured results and simulation results, so the next step of work is the first measure inductance and capacitance, the element parameters using the method of series parallel configuration accurately, so as to make the test result is shown in figure 1 and close to.

V THE SUMMARY

The passive high-pass filter elliptic filter as a model by the shield inductance and capacitance of the tantalum. Achieved a significant attenuation of the signal frequency interference, frequency range MRS signal 1.278-2.556kHz of a weak attenuation, to achieve a high SNR gain of function in the case of the front end of the amplifier to prevent saturation of the NMR signals , part of the requirements to complete the subject.

References

[1] (A)Ramasamy Natarajan.Power Capacitors [M]．Machinery Industry Press，2007．

[2] Wangjian Peng. NMR detector analog tracking filter groundwater research [D].Changchun：Jilin Univertity ，

2012.

[3] Arthur·B·Williams.Electronic Filter Design Handbook【M】. Yuchun Xuan，Interpret．Beijing：Electronic Industry Press．2007．

[4] Bixiang Yang,Zhu LingDesign and simulation of Passive Filter [J]. Power Capacitor & Reactive Power Compensation，2008,29（5）：12-14.

[5] Pengxie Hua ,Zhangdai Run ,Zhudai Xiang .A new method of passive filter design [J]．Power electronics technology，2004，38(4)：29—31.

Design of smart home robot system controller based on Freescale K60

Long Yun; Fan Hua; Dong Kaiyan; Liang Jinfu
(College of instrumentation and Electrical Engineering, Jilin University, Changchun 130022)

***Abstract*--In recent years, by the pace of life for family environment clean laborious situation, we design a smart home robot system based on Free-scale K60 micro-controller. Robot uses ultrasonic sensors for automatic obstacle avoidance function, to avoid unnecessary collisions motion, real-time acquisition by the camera image processing to identify and calculate the angle and distance of the object from the robot; Hallmark filter algorithm in acceleration makes the dynamic case accurate output current posture, the angle of rotation for precise control of the robot. Robot uses two degrees of freedom robotic arm to achieve the object handling. Robot system saves time and effort to clean up debris, and its small body, high efficiency, practical, has a broad market prospect.**

***Keywords*--Freescale K60; image acquisition and processing; mechanical arm**

0. INTRODUCTION

AN environmental cleaning robot as an intelligent mobile robot practical development pioneer whose research began in the 1980s, so far, has produced some of the concepts and product prototypes. Development of home cleaning robot, led to the development of home service robot industry. Hitachi in May 29, 2003 should be cloth, the successful development of household cleaning robots. Early in the 1980s, the started company SANYO research and development work autonomy household cleaning robot. October 1, 2002, the Swedish Lax electronics company Toshiba to jointly develop and cleaning robot "Fallibly special" sale. " Talibly special" mainly consists of cleaning machines and ultrasonic sensors at work can be placed indoors to avoid all kinds of furniture products[1]

In recent years, intelligent cleaning robot products have been rapidly developed. From the market performance, intelligent cleaning robots to more than 50% per annul growth and its rate are rapidly growing. Its market share of sales also improved rapidly from 1% to 20% [2].A few years of rapid development, intelligent cleaning robot vacuum cleaner will occupy half of the market. According to the authoritative institutions predict that by 2015, smart home robot market demand at least $ 80 billion market, the market will grow to $ 250 billion. Ring cleaning robot as a service robot, has a huge market potential and broad prospects, and it will bring great convenience.

1. HARDWARE DESIGN

By the body modules, power modules, SCM control module, motor module, sensor module and camera module consist intelligent robots furniture hardware systems [3]. The overall system architecture shows in Figure 1.

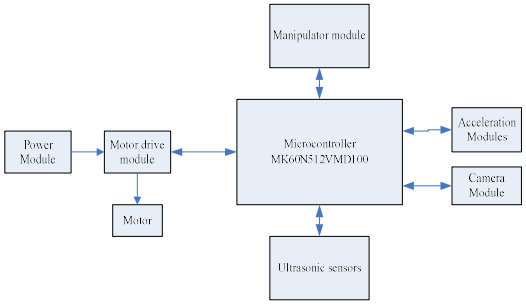

Figure.1. the structure diagram of baby sleep monitoring system

The system uses Freescale MK60N512MD0 controller chip as the core, the use of ultrasonic sensors detect obstacles and distance detection, thus achieving automatic obstacle avoidance.use MPU-6050 acceleration module precise angle measurement trolley current, real-time feedback, to achieve precision car control corner; the robot is equipped with CMOS video sensor for image acquisition, processing[4], identify the target object; manipulator controlled by the controller handling the pickup target object, the robot returns the final

destination in accordance with a redetermined route[4].

A. Module Body

Body made of aluminum mobile robot platform, which is all aluminum 4-wheel drive mobile robot platforms. This platform can carry a variety of controllers, drives, sensors, and wireless RF module. Platform body with a hard aluminum alloy materials, which has a light weight, high strength, non-deformation characteristics. Platform power output type four-wheel drive, a variety of ad hoc common DC gear motor fixing holes can be based on personal preferences and tires replace the motor, the robot easily obstacle, climbing and other high-performance test[5]. Platform made of high quality elastic rubber tires, shock absorption, abrasion resistance, strong grip, etc., can adapt to slippery roads and rough road.

B.Power Module

Taking into account the need to give the process of running the robot microcontroller, cameras, motors, sensors, power supply and other modules, so use 12 V/1300 mA high capacity Ni-MH rechargeable battery pack to provide strong support for the entire power system.

C.Motor Drive Module

Using dual H-bridge motor drive control module. The module uses SMT technology and high quality aluminum electrolytic capacitors, high stability [6], when the battery voltage is gradually decreased, still able to provide a stable voltage output, self-heat consumption, and high efficiency. Module input voltage is 5~12 V, own regulator chips that can provide a stable power supply for the 5 V DC, external micro-controller or other modules. L298 N driver chip micro-controller receives a control signal, the motor reversing, stop operation.

L298N module can drive two 5~30V DC, VDD module L298 N module, GND ports are connected to the battery positive and negative; OUT1 output port module, OUT2 connection left motor positive and negative, OUT3, OUT4 connecting the right motor positive and negative; the corresponding module IN1, IN2, IN3, IN4 port respectively micro-controller IO port is connected to the control terminal.

D.Servo Module

Steering is by a DC motor; reduction gear set the sensor and control circuit of an automatic control system [7]. There are three standard servo wires are: power lines, ground control line. In general, it has a maximum steering angle of rotation, with the difference that the ordinary DC motor, DC motor rotating a circle, but only within a certain steering angle of rotation, rotation is not a circle. Unable to ordinary DC motor feedback rotation angle information and the servo can. Servo voltage is typically between 4 ~ 6V, and generally 5V. Input control line is a width adjustable periodic square wave pulse signal cycle square wave pulse signal is 20ms. When the square wave pulse width changing, steering shaft angle changes, and changes the angle varies in proportion to the pulse width [8]. Their uses are different, ordinary DC motor typically powered by full circle of rotation; servo control is an object with a certain angle of rotation (for example, joint robot).

E.Single-chip Module

Intelligent robot system uses Freescale's 32-bit controllers' kinetis-k60 micro-controller as the core control processor[9], kinetics low power mixed signal micro-controllers based on ARM CortexTM-M4 core with superior scalability, with real-time high and other characteristics.

F.Motor Module

Using the superior performance of two DC gear motor 130 as a rear-wheel drive. DC gear motor control method is relatively simple, just two control lines to the motor with the appropriate voltage to the motor turn up, the higher the voltage, the higher the motor speed. For DC motor speed control can be used to change the voltage method can also be used PWM speed control method [10]. DC geared motor with high reliability, high torque, low power consumption, small vibration and so on.

G.Camera Module

To detect black objects, intelligent robots installed on the camera. Black and white and color camera division two, where the selection OV7620 digital color camera[11], since the object to find extract just the gray screen, without having to extract the color information, and thus only need to read the black and white signal. With appropriate external to the micro-controller chip, this chip should be able to extract their own camera signal line sync pulse, vertical sync pulse and blanking pulse to the micro-controller for control purposes.

H.Arm Module

Using two servos to achieve requirements. Servo control circuit board receives a control signal from the signal line, the control motor rotation, motor drives a series of gears transfer group, the reduction transmission to output the helm, steering gear and the output shaft position feedback potentiometer is connected to the rudder disk rotation at the same time, to drive the position feedback potentiometer[12], the potentiometer will output a voltage signal to the control circuit board, feedback, and the control circuit board to determine the rotation direction based on the position and speed of the motor to achieve the target stop. Gripping robot before and after the two servos fit to achieve, in front of the steering gear turning left at an angle, thereby controlling the opening clip closed in order to achieve the purpose of the gripping articles. Mechanical arm lift is transferred back through a certain angle servo counterclockwise to achieve.

2 SOFTWARE SYSTEM DESIGN

A.Software Development Tools

Select IAR integrated development tools. IAR is a Window-based development platform is ideal for embedded systems development.

B.Design of the main Program

Intelligent Robot smoothly and quickly with high efficiency and stability requirements of a corresponding program, this intelligent robot uses a CMOS camera sensor to find objects, image acquisition and processing has become the core of the entire software, is the second steering and speed control, the speed control is used robustness good classic PID control algorithm, using look-up table servo control mode, with theoretical calculations and practical way to use the compensation parameters, so look for things in the intelligent robots achieve steady and rapid results[13].

Software structure of the system is divided into: system initialization module, CMOS image data acquisition and processing module, the main motor speed control module, servo steering control module, path identification module. Figure 2 is a block diagram showing the overall structure of the system software.

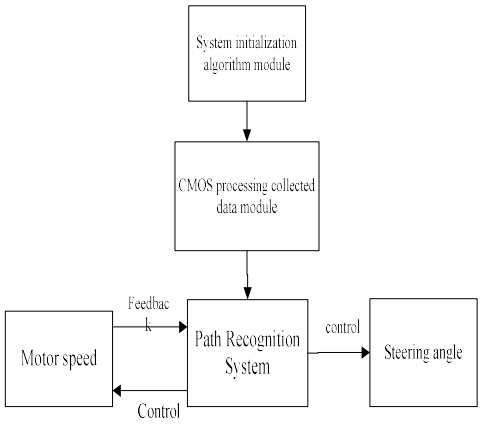

Fig.2. Block diagram of the overall system software

From the above chart we can see the beginning of the program runs through the initialization settings so that the system is running in accordance with pre idea; then, CMOS sensors collect data through image processing, information obtained when the object[14]; at the same time, the measured motor speed module model car current speed, feedback to the system; and finally, the current path path identification system utilization information and current velocity values make the appropriate treatment, servo motor control and in an appropriate manner. Program flow chart shown in Figure 3.

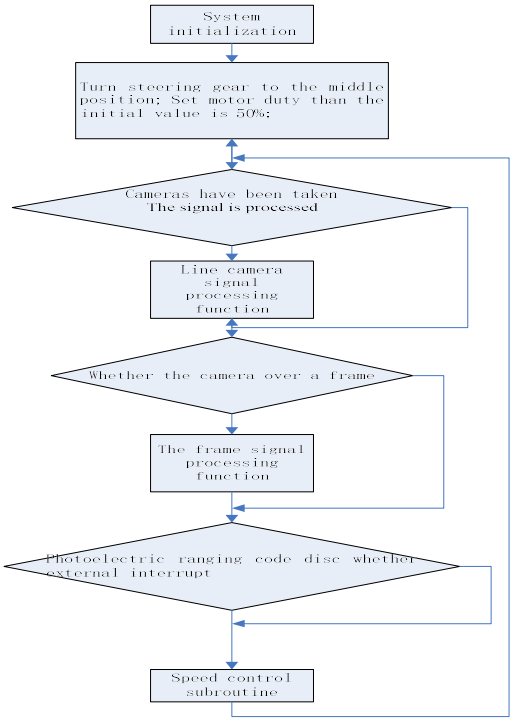

Figure.3. program flow chart

3 EXPERIMENTAL DATA

Selection 2m square KT whiteboard, set up barriers

on the whiteboard, the sample will be placed on the board, to be able to find within the camera range, the robot will return to the black object identification and recovery of specific items after the pickup area. Select the ambient light intensity of natural light in general.

Ultrasonic sensors detect the road. Sensor in the center front of the vehicle body, the sensor wills the left and right, the first three obstacle detection directions is determined routes. When the camera to identify the object, the body will rotate 180 degrees and the mechanical arm down to grip the object.

Table.1.the test data sheet

Testing times	Avoidance times	Find objects times	Objects pickup times	Recovery times
1	carry out	carry out	carry out	carry out
2	carry out	carry out	carry out	carry out
3	carry out	carry out	carry out	carry out
4	carry out	carry out	Error	Error
5	carry out	carry out	carry out	carry out

4 SUMMARY LANGUAGE

In the design of smart home system hardware options on each system module selection is reasonable, economical and practical, high-level language-based control software developed feasible and efficient, excellent overall performance of the robot, the successful implementation of the automatic obstacle avoidance and object recognition capabilities. This innovative project for college students to establish a kind of robot development platform, while changing the learning mode, to stimulate student interest in learning, improve the students' practical ability, thinking ability, and comprehensive application ability of scientific knowledge, but also to verify student learning a powerful tool effect.

References

[1] Gao Shan PROCEEDINGS comprehensive terrestrial mobile cleaning robot [J], Mechanical Engineering, 2008,44 (3): 228-233

[2] Xiao Hairong, Fu Wen Jun, Zhang Xiaojun, based on mobile robot navigation and other multi-sensor data fusion [J]. Systems Engineering and Electronics, 2001,23 (7): 66-69

[3] Ma Ping, Lu Feng, and other multi-sensor data fusion Duhailian basic principle and application [J] Control Engineering, 2006,13 (1): 48-51

[4] Cai Zixing, Xu Guang. Artificial intelligence and its application [M]. Tsinghua University Press. 1996.5.

[5] design Cai Xiong Hua, money thinking, Xiong Youlun, a new intelligent cleaning robot and Control System [J], machinery and electronics, 2007, (8): 46-49

[6] Huang Jiansheng The path planning of mobile robot research [D]. Zhejiang University, 2008

[7] Wang Lei, Yang Jie motion path analysis and autonomous household cleaning robot planning [J], mechatronics, 2007, (2): 70-73

[8] Luo Cheng studied household cleaning robot path detection and path planning [D]. Wuhan University 2008

[9] Yang Yuqin automatic cleaning robot [J] Technique and Applications, 1997, (3): 27-29

[10] Chen Song, Song Xiaolin smart car to follow the path DSP-based system design [J] Engineering Design 2012.19 (4): 312-317.

[11] Li Bo, Yang Wei, Zhang Wendong, etc. An intelligent autonomous car searching / tracking system [J]. Computer Measurement & Control, 2012.20 (10): 2798-2801.

[12] Zhu Simin Design and implementation of intelligent trolley self-tracking control system [D]. Hangzhou: Zhejiang University, 2013.

[13] Yi Lai Chi machine vision-based obstacle avoidance Intelligent Vehicle System [D] Changsha: Central South Humanity, 2012.

[14] 14. Xie Min MC9S12XS128 based Intelligent Vehicle Control System and Application [D] Nanchang: Nanchang aviation human science, 2012.

The matched filtering based on Curvelet transform

LiShengwei; LiHaoyang; LiuJiwei

（*College of Instrumentation & Electrical Engineering,Jilin University,Changchun 130026*）

***Abstract*--Along with the progress of the modern compression perception technology, the means of solving the sparse inversion under the restriction of rapid development.Curvelet transform is in recent years the development of a highly sparse transform method, can use signal transformation after the sparse feature, with less data to reconstruct the complete signal, so the Curvelet transform is more and more widely used in seismic data processing.First of all, in this paper, the noiseless and seismic data of containing gaussian white noise, using the algorithm of FISTA Curvelet domain fine scales of seismic data matching, higher waveform consistency, and the noise is suppressed.Secondly, based on sparse constraint inversion principle, will be matched filtering, lack of seismic data interpolation and gaussian random noise suppression problem together, calculated by iterative algorithm to solve the above problems, the matched filtering result of high SNR, and greatly improve the computational efficiency.Finally, the article of this new method is verified by practical data, obtained the satisfactory results.**

***Keywords*--Curvelet transform;Matched filtering;Seismic data processing;sparse**

I. INTRODUCTION

IN seismic exploration, the seismic data of different source limited by matched filtering method, the seismic data after the matched filtering is still many differences in low resolution and low signal to noise ratio[1];Or matching processing hierarchical fuzzy appears after the old and new seismic data, seismic attribute parameter extraction is difficult.Affected by external factors such as construction condition, field seismic exploration, the effect of different seismic data splicing, increased the difficulty of the seismic data matching processing.Signal to noise ratio of seismic data processing, the resolution has been restricted by these problems, in order to solve this problem is proposed in this paper a new method for seismic data processing matched filtering[2].

To solve the above problems, Wiener (1949) put forward the method of least square matching filter gives the effect of the seismic data processing must be improved.Berkhout (1977) proposed the least squares filter and wavelet deconvolution matched filtering processing.Random spread of mathematics application and development of computer technology, Rick Wallace (1992) put forward the issue of filtering and achieve high resolution.Wiener filtering method based on minimum error energy, jin-xing cheng (2004) put forward such as matched filtering method of wavelet domain fine scales, at the same time when applied to move the earthquake (jinlong, etc., 2005)[3].In recent years, might (2008200) proposed the Curvelet matched filtering and matched filtering method is used to separate Groundroll wave.Long (2013) proposed the wavelet domain optimal norm matched filtering, improving the precision of the matched filtering and suppress random noise[4].

In this paper, based on Curvelet transform seismic data of Curvelet domain matched filtering is proposed.Because the seismic data is all kinds of interference, low signal-to-noise ratio, the earthquake loss way, and the problem of insufficient samples which restricts the matched filtering precision.First, this paper has no noise and noise data on the matched filtering method based on Curvelet domain of FISTA algorithm, match after seismic data to achieve the high precision waveform, amplitude, phase consistency[5].Secondly, application of Curvelet transform, filtering, lack of interpolation and the random noise suppression problem into account, by FITSA algorithm deals with the influence of three aspects at the same time, in improving the signal-to-noise ratio at the same time greatly improve the efficiency of the seismic data processing[6].In the end, this new method are verified by practical data, achieved satisfactory results.

II. FUNDAMENTAL

A. Discrete Curvelet transform principle

Based on Curvelet transform, Candes (2006) proposed the more popular a new generation of Curvelet transform algorithm[7].For sparse discrete Curvelet transform, defining window function: radial and point of view, among them, $r \in \left(1/2, 2\right)$, $t \in [-1,1]$。 $W(r)$ 和 $V(t)$ meet the permissible conditions as follows:

$$\sum_{j=-\infty}^{\infty} W^2\left(2^j r\right)=1, r\in(3/4,3/2) \quad \text{……（1）}$$

$$\sum_{j=-\infty}^{\infty} V^2(t-l)=1, t\in(-1/2,1/2) \quad \text{……（2）}$$

For each frequency in the frequency domain definition window is as follows:

$$U_j(r,\theta)=2^{-3j/4}W\left(2^j r\right)V\left(\frac{2^{[j/2]}\theta}{2\pi}\right) \quad \text{……（3）}$$

The integer part. W And V support of the limit support interval, get the feature of wedge conforms to the scale of the anisotropy.Assuming that atomic frequency expressions for $\phi_j(\omega)=U_j(\omega)$, if known scales ϕ_j, then through the rotation and translation, can get the Curvelet other 2^{-j} scales.Set interval sequence of rotation Angle $\theta_l=2\pi\cdot 2^{-[j/2]}\cdot l$, l is a positive integer or zero, $0\le\theta\le 2\pi$;translation parameters $k=(k_1,k_2)\in Z^2$ [8].

Above all, define the direction θ_l, scale 2^{-j} and translation parameters (k_1,k_2) of Curvelet is:

$$\phi_{j,l,k}(x)=\phi_j\left(R_{\theta_l}\left(x-x_k^{(j,k)}\right)\right) \quad \text{……（4）}$$

Among $x_k^{(j,l)}=R_{\theta l}^{-1}\left(k_1\cdot 2^{-j},k_2\cdot 2^{-j/2}\right)$, Rotation for R_θ and θ_l。Curvelet transform can be represented as:

$$c(j,l,k)=\left\langle f,\phi_{j,l,k}\right\rangle=\int_{R^2} f(x)\overline{\phi_{j,l,k}(x)}dx \quad \text{……（5）}$$

Through the cartesian coordinates $f[t_1,t_2],0\le t_1,t_2<n$ for signal input，The discrete form of the Curvelet transform is a:

$$c[j,l,k]=\sum_{0\le t_1,t_2<n} f[t_1,t_2]\overline{\phi_{j,l,k}[t_1,t_2]} \quad \text{……（6）}$$

Among them $\phi_{j,l,k}[t_1,t_2]$ is Discrete Curvelet transform，Because of the Curvelet transform is implemented in frequency domain, so no specific expression.

B. Curvelet domain matched filtering and the interpolation principle

Through the t - x matching problem in the process of spatial data reconstruction:

$$\mathrm{A}x=\mathrm{b}+\mathrm{n} \quad \text{……（7）}$$

A is inverse matching operator and can approximate is known; x is model, usually to match data; b Is the observed data, which is to match the data, it can be divided into signal and random noise effectively.In the treatment of the random noise of period of time, A as the operator matrix, x is without noise data, b along with the noise generated by the observation record;In dealing with missing under the condition of the interpolation, x expressed as is lack of the seismic data gathers operator, b is the complete set of data, for the missing set observation records..In the above situation, n is expressed as the unknown noise data.Collect A and b physical significance in table 1.

Table 1 Equation (7) the physical meaning of A and b

Matched filtering	To suppress random noise	Missing the interpolation
Matched filtering operator matrix	Contain ingrand om noise matrix	The missing factor matrix
Refer to the seismic data	Data contain in random noise	Missing gathers the data

Normally affected by noise and exploration conditions of linear problem solving diverse solution will exist, can reduce the multiple solution applied regularization method.The optimal matching processing on the point of view of information theory is a matter of underdetermined equations, Chen (2001) proved that in theory, reconstruction of sparse modeling effect is optimal[9].With the development of compressed sensing technology, sparse constraint inversion method (Malioutov, 2005; Berk, 2009) has been developing rapidly.In this paper can be used to convert the data to the Curvelet domain into a sparse data, equation (7) can be converted to type, just put the minimum objective function J , the solution can be obtained:

$$J=\|Dm-b\|_2^2+\lambda\|m\|_1 \quad \text{……（8）}$$

m as the formula (6) in the Curvelet domain in sparse coefficient, $D=AR$ and R is x 'sCurvelet inverse transformation, namely, $x=Rm$. λ as L1 control constraint and L2 error term weight between regularization parameter.Equation (7) is the curvelet domain for solving sparse coefficient[10] t.As a result of the equation (7)'s D can be used by AR , said can list:

$$J=\|ARm-b\|_2^2+\lambda\|m\|_1 \quad \text{……（9）}$$

This article FISTA method (Berk, 2009) to solve the equation (8).As a kind of effective algorithm to solve the problem of linear inversion, FISTA has fast convergence rate, the advantages of fewer iteration times, greatly improve the computational efficiency.FISTA solving process is as follows:

Step 1: $b_1=x_0$ and $t_1=0$

Step k ：

$$\begin{aligned} x_k &= soft\left(x_{k-1}+\frac{1}{\alpha}A^{\mathrm{H}}(b-Ax_{k-1}),\frac{1}{\alpha}\right),\\ t_{k+1} &= \frac{1+\sqrt{1+4t_k^2}}{2}, \\ b_{k+1} &= x_k+\frac{t_{k-1}}{t_{k+1}}(x_k-x_{k-1}). \end{aligned} \quad \text{……(10)}$$

$soft(x,t)$ is defined as a soft threshold, when the input x is plural, make $x = ze^{i\omega}$ .Soft threshold can be represented as:

$$soft(x,t) = \begin{cases} (z-t)e^{i\omega}, & \text{if } z > t \\ 0, & \text{if } z \le t \end{cases} \quad \cdots\cdots\cdots\cdots(11)$$

FISTA algorithm has fast convergence rate and easy to implement, and the plural operation is also included, extended the scope of use.

C.Synthetic seismic data

Different wavelet convolution model represents the s or different source seismic data.Sub wavelength is inversely proportional to the time resolution, and its ability to distinguish thin layers are different[11].In this paper, we used two types of wavelet for synthesis of convolution model.In order to prove the effectiveness of this method, the selection of seismic data containing thin layer.With a low resolution of time, the minimum phase wavelet as the matching, high temporal resolution for reference.

Model thickness is 400 ms, a total of 45, two types of wavelet length is 140 ms, thin layer thickness for 140 ms.Multi-scale decomposition of the model, because the model in this paper is small, thus only break down the three dimensions of Curvelet transform.Figure 1 (a) are the convolution model of minimum phase synthesis.Figure 1 and figure 1 (b) (c) is the convolution model for the spectral analysis of amplitude spectrum and phase spectrum, it is about 10-80 hz frequency range.Effecting factors of wave type, the convolution model of the ability of distinguish between wedge and thin layer is reduced greatly, brought inconvenience to the subsequent processing and interpretation, therefore will receive minimum phase wavelet convolution model for matching.

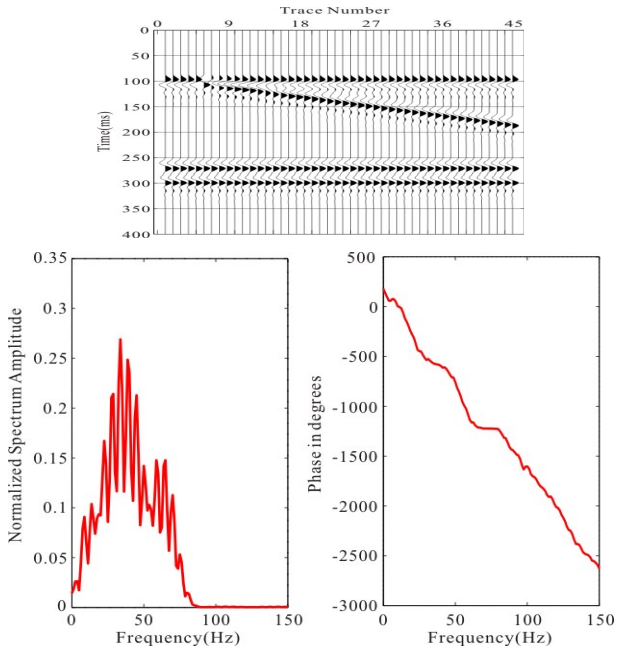

Fig.1 Minimum phase Seismic section(a) Amplitude spectrum(b) Phase spectrum(c）

By zero phase wavelet convolution with the data of 1 of the same reflection coefficient, with 45 zero-phase seismic data records, as shown in figure 2 (a).Amplitude spectrum for spectrum analysis of the data 2 in figure 2 (b) and the phase spectrum figure 2 (c).The figure shows that seismic wave in 10-80 hz frequency range, figure 2 (c) phase and figure 1 (c) differ from that of the phase, is nonlinear spectral lines.Because of high temporal resolution of data 2, as a reference for seismic observation data, provides the follow-up observation data processing and interpretation of convenience[12].

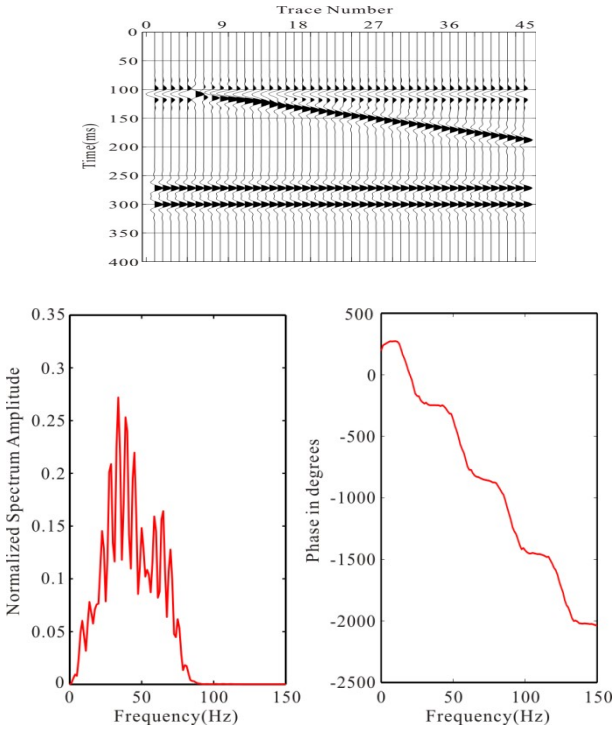

Fig.2 Zero phase Seismic section(a) Amplitude spectrum(b) Phase spectrum(c）

Figure 3 (a) is the Curvelet domain after FISTA calculating matching seismic section;And phase spectrum amplitude spectrum figure 3 (b) in figure 3 (c) is the result of spectrum analysis matched filtering.Compared with 2 reference seismic observation data analysis, we can get FISTA calculated seismic observation data of amplitude, waveform and phase of high consistency[13].So prove sparse constraint matching norm has the very good effect.

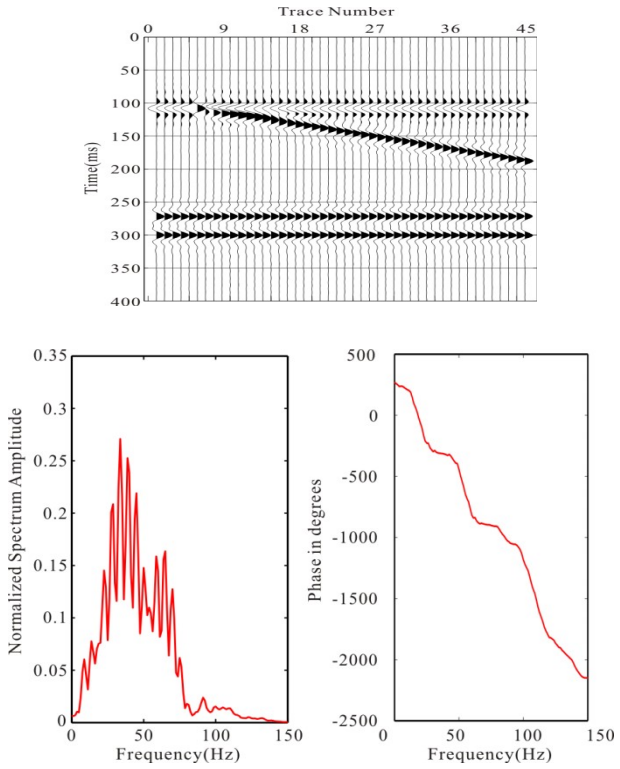

Fig.3 After the match Curvelet domain Seismic section(a) Amplitude spectrum(b) Phase spectrum(c）

In seismic data of practical exploration, there are often some noise.Data 1 and 2 on the gaussian white noise, so as to better simulate the actual situation.Figure 4 (a) after adding noise data 1 waveform figure, called the simulated data 3, PSNR is 7.45 dB.And phase spectrum amplitude spectrum figure 4 (b) in figure 4 (c) is 3 spectrum analysis of simulation data generated.

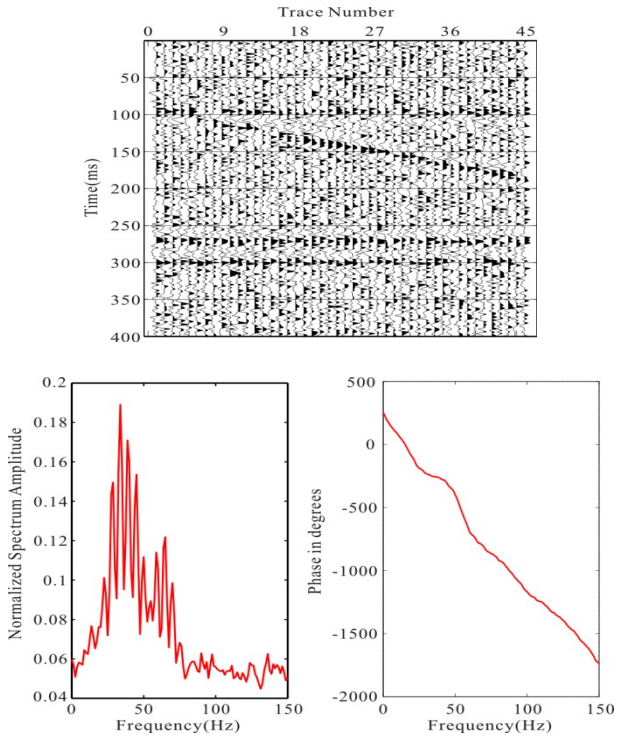

Fig.4 Simulated data 1 additive noise Seismic section(a) Amplitude spectrum(b) Phase spectrum(c）

Figure 5 (a) is after joining noise data waveform in figure 2, PSNR of 1.09 dB, referred to as the simulated data 4.And phase spectrum amplitude spectrum figure 5 (b) in figure 5 (c) is to join the noise spectrum analysis of the data generated.Due to the data of 4 types of zero phase wavelet and high signal noise ratio (SNR), as a reference for seismic observation data, so to have a better ability to distinguish between wedge and thin layer

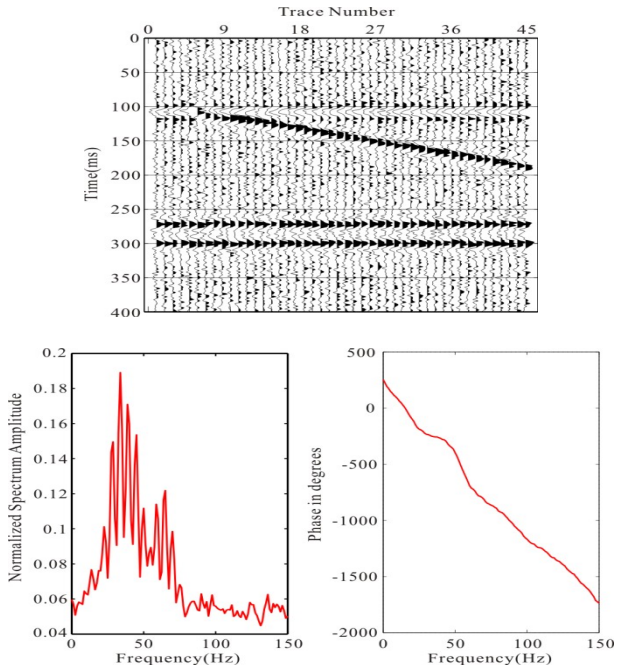

Fig.5 Simulated data 2 additive noise Seismic section(a) Amplitude spectrum(b) Phase spectrum(c）

Figure 6 (a) is to add noise simulation data of 3 Curvelet transform is matched filtering results, through the spectrum analysis to get amplitude spectrum and phase spectrum (b) (c).Compared with simulated data 4, waveform of high similarity, PSNR to 26 db.Comparing the amplitude spectrum and phase spectrum, they also have very high consistency[14].

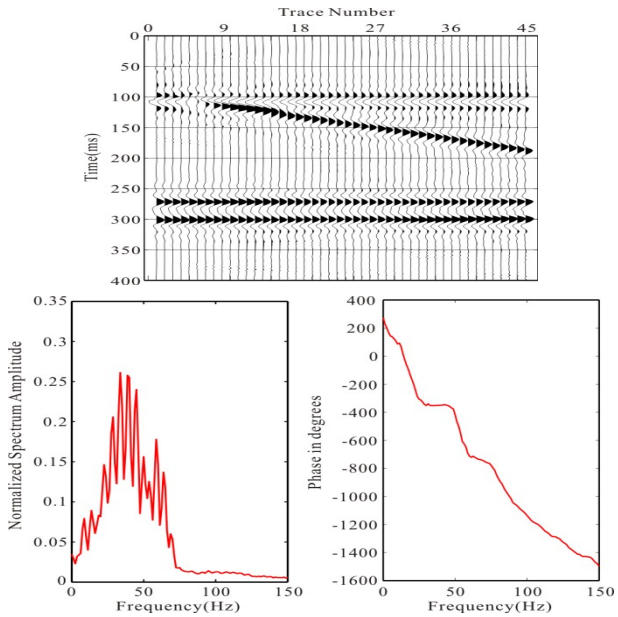

Fig.6 After Curvelet match Seismic section(a) Amplitude spectrum(b) Phase spectrum(c）

Missing data is 5 to 3 random data 40%, so as to better simulate the actual situation, as shown in figure 7 (a), the signal-to-noise ratio of 5.75 dB.Amplitude spectrum 7 (b) and the phase spectrum 7 (c) is the results of spectrum analysis of the data of 5.

C. Real seismic data processing

This article selects a particular area of seismic data from the same place, the observation data of 70, select a depth of 500 ms to 1000 ms, sampling time is 2 ms, spacing is 12.5 meters.The 1995 earthquake data as shown in figure 7 (a), it can be seen that the seismic data exist a lot of noise, increased the difficulty of the matching process;The 2007 earthquake data as shown in figure 8 (a), seismic event can be seen from the diagram is still relatively continuous, convenience is provided for subsequent processing and interpretation of data[15].

In order to verify the Curvelet domain interpolation and matching, the effect of different s in the two groups of the same place matching processing of seismic data[16], interpolation and matching results more clearly.Through the test, select four layers Curvelet decomposition, select 16 scale can get good results.Matching with the interpolation results are shown in figure 11 (a) below, with 10 (b) the difference between the profile as shown in figure 11 (b).Through 11 figure we can get the Curvelet domain interpolation and matching can obtain satisfactory results in practical data processing.

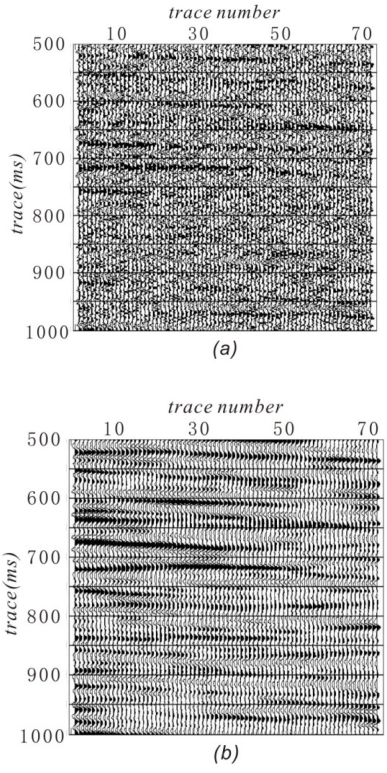

Fig.10(a) A regional seismic data in 1995
Fig.10(b) A regional seismic data in 2007

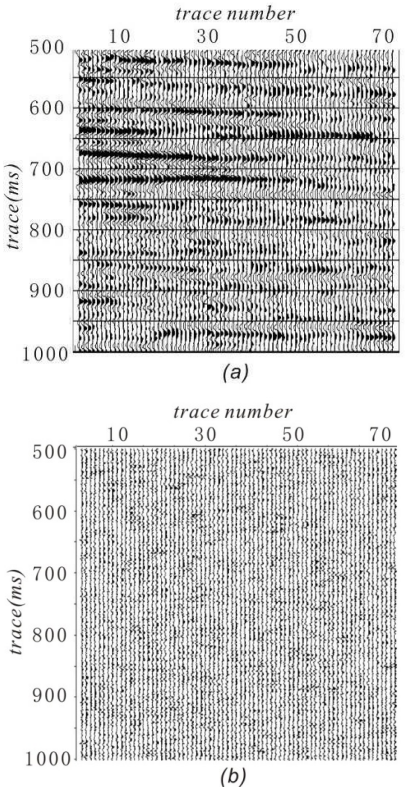

Fig.11(a) The results of seismic data matching and interpolation
Fig.11(b) Seismic data's differential profiles

References

[1] Brotzr, R., Maschall, R., and Knecht [M] .1987, Signal adjustment of vibroseis and impulsive source data: Geophysical Prospecting, 35(7), 739-766

[2] He Qiao, 2005, the seismic wave theory [M]. Jilin university publishing house, changchun

[3] ZhongBoJun xing-yao Yin, 2008, the complex region consistency in 3 d seismic data splicing processing technology [J]. Journal of petroleum exploration, 47 (4), 393-397.

[4] Chen Qiansheng. [3]., 1993, the mathematical principle of digital signal processing [M]. Beijing: petroleum industry press

[5] Wiener, N., Extrapolation, 1949, Interpolation, and Smoothing of Stationary Time Series, with Engineering Applications [M] . Cambridge: Technology Press of the Massachusetts Institute of Technology.

[6] Jin-xing cheng, an chang-chun Yang, Mr James tien pei-chun, 2004, based on the wavelet transform method of three-dimensional seismic data splicing [J]. Journal of petroleum geophysical prospecting, 39 (4), 406-408

[7] Jinlong, xiao-hong Chen, jing-ye li, 2005, based on the error criterion and loop iteration time shift earthquake matched filtering method [J]. Journal of geophysics, 48 (3), 698-703

[8] Berkhout, A.J., 1977, Least-squares inverse filtering and wavelet deconvolution [J] .Geophysics, 42, 1369-1383

[9] Herrmann, F.J., 2008, Curvelet-domain matched filtering [C] .78th SEG meeting Las Vegas: 3643-3649

[10] Yarham, C., Herrmann, F.J., 2009, Groundroll prediction by interferometry and separation by curvelet-domain matched filtering [C] .78th SEG meeting Las Vegas, 2576-2580

[11] Cand´es, E. J., Demanet L., and Donoho D. L., 2006, Fast discrete curvelet transforms [J] .SI-AM Multiscale Modeling and Simulation, 5, 861–899.

[12] Dianne P., 1990, Robust regression computation using iteratively reweighted least squares [J] .SIAM Journal on Matrix Analysis and Applications. 11(3), 466-480

[13] EWOUT V.D.B., M.P. Friedlander, 2008, Probing the pareto frontier for basis pursuit solutions [J] .SIAM J. on Scientific Computing, 31(2), 890-912

[14] Darche G, 1990, Spatial interpolation using a fast parabolic transform [C] .60th SEG meeting San Francisco, 1647~1650

[15] Herrmann, F.J., Hennenfent, G., 2008,Non-parametric seismic data recovery with curvelet frames [J] .Geophysical Journal International, 173(1), 233-248

[16] Hennenfent, G, Herrmann, F.J., 2008, Wavefield reconstruction via jittered undersampling [J] .Geophysics, 73(3), V19-V28

Design of double layer PID control four rotor aircraft based on PID algorithm

Chen Yuwei; Yang Fengming; Ren Yiping

(College of Instrumentation and Electrical Engineering, Jilin University, Changchun 130022)

***Abstract*— In order to improve the shortage of our domestic civil aircrafts which have huge ground base stations, operate difficultly and have a single use, aerial four rotor aircraft are designed which can use the APM software as the core, position navigation point based on GPS (Global Positioning System) and realise real-time image transmission. The core of flight control applys double PID control. The output of aircraft pitch Angle, roll Angle and gas are realised through the first stage PID system. The speed of control motor in the second stage PID system control the flight direction. At the same time, determination of course is realised through the application of GPS system. Then these input to the second stage PID system and the translational displacement x, y, z are corrected. Onboard cameras in four rotor directly input ground station via wireless connection. Test results show that the aircraft fly smoothly between destinations set by mobile phone. The distance of aerial images and data transmission is 200 m and mobile phone can be used to carry on the flight mode switch as a ground station.**

***key words*—Four rotor aircraft PID adjust parameter GPS system**

I. INTRODUCTION

THE four rotor is a kind of unmanned aerial vehicle with special structure. Compared with the fixed wing aircraft, it is small in size, can be vertically take off and land, strong mobility and load capacity, and also can quickly and flexibly maneuver in all directions. Therefore, it is particularly suitable to carry out monitoring and investigation in the indoor, urban and forest areas, and it has good prospects for military and civil applications[1].

The design of autonomous flight control algorithm has been one of the most concerned problems for many researchers in the field of control. The classical control strategy is that system model is usually linearized at a particular point in the aircraft system, and then the classical control theory is applied to the analysis and control of the system. This control precision and control ability is weak[2].

Four rotor aircraft is still in the initial stage of development in China, but in foreign countries has become a hot spot of research in various universities. As early as January 1921, the United States Army Air Corps, George de Bothezat and Jerome Ivan signed a contract to jointly build vertical aircraft[3]. A team from the Swiss Federal Institute of technology studies the angular velocity and altitude control of the four rotor aircraft. In the aircraft system dynamics simulation, they chose the LQ control method, and the final result is not very ideal. One possible reason for the poor representation of the LQ controller is that dynamic characteristics of drive design is not considered the transfer function of the system[4]. Today four rotor aircraft has been put into commercial and military fields, and achieved remarkable results[5]. At present, a foreign representative research: the MIT, Stanford University, University of technology of Compiegne, Japan Chiba University[12].

In fact, the PID control is more effective when there are errors in the model[6]. So we use double-layer PID control where the overall control is divided into inner ring (attitude) control and outer ring (flight position) control to make the aircraft fly to a fixed position and remain stable. Then the smooth transmission of aerial images and flight parameters are needed to enter the mobile phone ground station.

II. THE STRUCTURE AND FUNCTION OF FOUR ROTOR HELICOPTER

A. Architecture of the four rotor aircraft system

The main structure of the aircraft is a "X" type. The primary flight control system, GPS positioning system, a wireless control radio, image transmission system and flight dynamic system were added on the basis of a balance of physical.

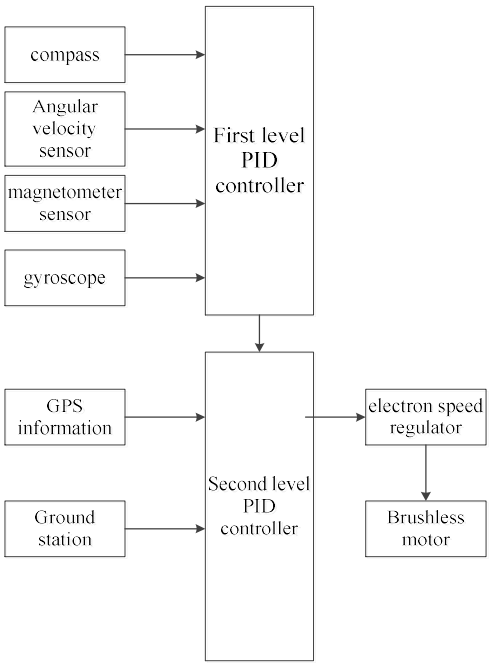

Fig.1. The system architecture of aircraft

B. Hardware of Four Rotor Aircraft

Flight control board of main control chip Atmega1280/2560, the chip can control all working group of the flight control panel software. When selection mode will be setted, the PPM decoding chip will be used, namely Atmega168/328. The chip can monitor mode channel PWM signal, and then we can switch between the manual mode and other modes (such as cruise landing mode) and improve the system security. The functions of other chips including air pressure gauge BMP085 and AD ADS7844 chip are respectively to measure pressure to convert to the specific height, to convert the analog voltage provided by measuring device into digital quantity for subsequent calculations.

In order to make the aircraft flying smoothly, we need an inertial measurement unit. The unit includes two-axis gyro, single axis of gyroscope and three-axis accelerometer. These a few parts can measure the three-axis angular velocity and triaxial acceleration, and cooperate with the direction data measured by the triaxial magnetometers or GPS to correct, realize the direction cosine algorithm and calculate the aircraft attitude.

Lea - 5 h signal of GPS module will be used for GPS orientation correction. This module can measure plane information such as current longitude and latitude, altitude, direction of track and the speed. In addition, three axis magnetometer module can measure the aircraft's current heading

Fig.2.The hardware structure of aircraft

C. Physical Model of Four Rotor Aircraft

The body structure of the four rotor aircraft are four motors, so there are 4 kinds of input forces. There are six kinds of state of single output, so it is a kind of vertical elevator with six degrees of freedom. In the process of aircraft flight, some external force will form the interference. In symmetrical motor rotation, the spiral effect and aerodynamic torque effect were offset and aircraft can fly smoothly. When the rotor through the axis of rotation by the engine drive to rotate, rotor give applied moment (or torque) to the air, creating a opposite torque. Its size is associated with the rotational speed of motor. Only when the speeds of four motors are not completely equivalent at the same time, the opposite torque will make the aircraft rotation. In order to overcome the opposite torque, just we should make sure that each rotation direction of rotor on the diagonal is the same and one group forward, other group reverse[10].

The basic viewpoint of modeling is that the aircraft will be regarded as a rigid body, and then we can build Newton - euler equation about three translational displacement of a rigid body x, y, z and three rotational displacement ϕ,θ,ψ . By x, y, z and φ as a set of control output, we can calculate the other two values when the system is in zero Angle stability[6].

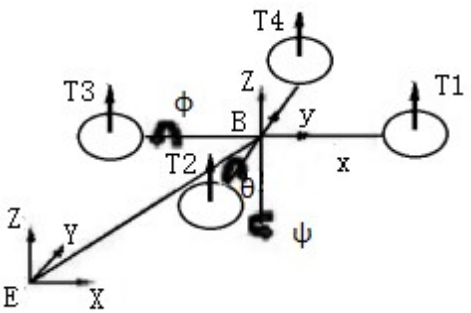

Fig.3. The principle of the four rotor aircraft flight

III. Flight Control of Four Rotor Aircraft

A. The PID Control Algorithm

According to the dynamics analysis, four rotor

aircraft system itself is unstable[11]. Therefore, the control algorithm is particularly critical.

PID control is a very common way of automation control. PID represents the proportion, integral and differential respectively. In APM flight control system, we use the sensor to collect the flight information as input of the system. Then, we calculate the output according to a specific formula and control the system.

In the process of discretization PID, T is as the sampling period , k as the sampling sequence number, discrete time k x T is used for standing for the continuous time T, summation form replace integral form of continuous time

and the incremental form replaces the differential form of continuous time[12].

$$t \approx kT$$

$$\int_0^t e(t)\,dt \approx T\sum_{j=0}^{k} e(jT) = T\sum_{j=0}^{k} e_j$$

$$\frac{de(t)}{dt} \approx \frac{e(KT)-e[(k-1)T]}{T} = \frac{e_k - e_{k-1}}{T}$$

Typing into the time domain equations of PID controller, we can get the discrete PID expression.

$$U_k = K_p[e_k + \frac{T}{T_1}\sum_{j=0}^{k} e_j + \frac{T_D}{T}(e_k - e_{k-1})] + U_0$$

Among them, Ki=KpT/Ti is integral coefficient. Kd = KpTd/T is the differential coefficient. T is the sampling time. PID control principle block diagram is shown in figure 3[10].

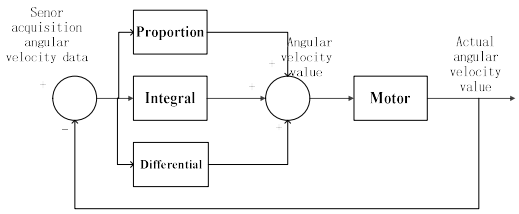

Fig. 4. PID control principle

B. The Realization of The Flight Control

Four rotor aircraft will be controlled by the onboard computer and ground computing system processing data transmited by sensors and cameras[10].

The double-layer PID control system is set in primary flight control system. The first level is mainly used for navigation, the second level is mainly used to control. According to the external rotation displacement ϕ, θ,ψ, the program of the first level PID system can calculate pitching Angle, roll Angle and the throttle needed by the flight. The data output to the second level PID system. It outputs a translational displacement x, y, z used to control motor speed, in turn, control the flight direction to ensure a smooth flight.

Four rotor aircraft landing is as a example. Before landing four rotor aircraft will hover in the position of the distance from the ground about 1 m and then apply a certain velocity to land. This the real-time speed through sensor is the value of P. The more P value, the greater the aircraft land more quickly, but more risky in landing; and if P value is smaller, the landing distance control will be more accurate, but down time is longer. This kind of contradiction will be solved by setting the D value. The function of D is to "brake" the landing of the four rotor. At the time of gradually close to the ground, D will affect the rate of aircraft landing. If the speed and distance will be used to create a coordinates, only under the influence of p is a straight line. While under the influence of D, will be a curve. For the four rotor aircraft landing, the introduction of D will make the speed of plane close to the ground is very slow. I is used to eliminate the error. Also for land, if the landing is off the 5°, then I will record this change, in the next land would be ahead of the recent land of 5°. For the flight, I coefficient is of great significance for the aircraft's smooth flight. If not I, is likely to be out of control in the process of aircraft flying in the side.

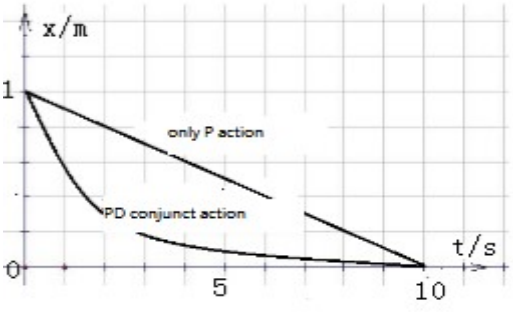

Fig. 5. PD landing control

In terms of effect, PID, respectively, represents the sensitivity, accuracy and smooth degree.

C.GPS Application in Flight

Set the plane flying target, this is the GPS system in a flight control chip. GPS system can provide the local latitude and longitude of the plane and target destinations of latitude and longitude. After system calculation to the point of view of target navigation target_bearing for vehicle navigation. When the aircraft flying according to target_bearing will have error on the route. This is drift away from production. When drift distance, the system will automatically calculate the drift correction. Finally, the target course Angle and yaw correction of navigation course Angle nav_bearing, provide second-level PID system.

In addition, the GPS system is also one of the four rotor aircraft insurance system. Only when the vehicle GPS and ground station GPS positioning, the plane is allowed to unlock.

IV. Measurements and Results Analysis

A. Flight Control Mode Selection

In practice, there are two kinds of APM control flight mode, one is based on the speed control, one is based on the height of the flight control.

When based on speed control, such as the plane did not climb to the due height. Fhe first step of flight control board will be to increase on the gas control. The speed of aircraft increased. After then flight control system drag the elevator, leading to elevation in hight. When rise to a predetermined height, due to higher space velocity, elevator has continued to lift, at the same time, the gas reduced. Until airspeed below reservation, the elevator will be boosted, the plane hight will be down. The condition of landing in contrast. This mode is with safe flight. When the engine is affected, it will land according to the speed control.

Based on the height control, for example, aircraft do not climb to the due level. According to the calculation of PID system, their own height and target height, flight control board will calculate a pitching Angle. The plane flew to the target height. Due to the change about the height of aircraft, space velocity would inevitably have change. So the throttle control makes the plane's airspeed close to its target airspeed. Reduce throttle when faster, step on the gas whens lower. This mode, the plane control more flexible, control of the height is more accurate.

In practice, because the height control lead to multiple occurrences of machine down. We finally adopt speed control mode. In speed control mode, the aircraft's flight lag behind compared with the instruction of ground station, but the flight is smooth, easy to operate.

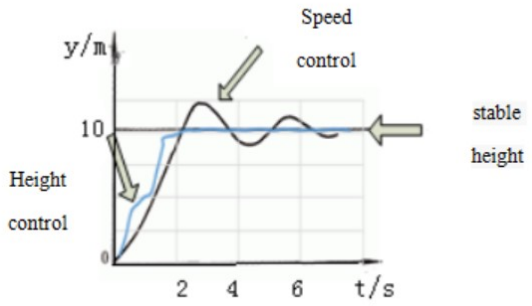

Fig.6.Speed control and height control

B. The Choice of Operating Mode

In terms of the operating system, flight control has three kinds of control modes, namely, manual control, electric balancing and autopilot operation. Manual control, signal is made by remote control. Aircraft will be controlled by hand; Autopilot is operation automatically by system , the operation of the station can only make disturbance effect on the plane. For the sake of safety, manual control with the highest priority, self-driving with lowest priority.

In practice, we priority automated driving. After the setting of waypoint in mobile phones, aircraft will fly automatically and at the same time process aerial, images and data transmission. At the same time, we select manual mode with higher priority as backup protection. In order to reduce the difficulties about manual mode of operation, including the control of the gas, elevator and aileron. These are firstly corrected by the first stage of PID system and prevent the occurrence of a cartwheel aircraft, stop runaway conditions.

C. Aircraft Digital Receiver

The four rotor flight vehicle adopts 3 drobotics radio and then make aircraft connect with the ground terminal (mobile phone). Among them there are USB interfaces on the phone radio, through the transformation in FTDI transmitter, machines can be controlled.

In practice, controlled aircraft will be connected to the phone, we can directly observate the system status and flight parameters of aircraft through mobile phone.

TABLE 1

SYSTEM STATE OF AIRCRAFT

Speed, current output and actual current

Speed（r/min）	Current output	Actual current
3042	31	2.11
3522	36	2.89
4063	95	5.43
4375	122	6.02

When the speed reaches to 4000r, aircraft will fly smoothly and began to hover. According to the attitude Angle in stable hover we can try to change the PID parameters to adjust its stability and eliminate the overshoot.

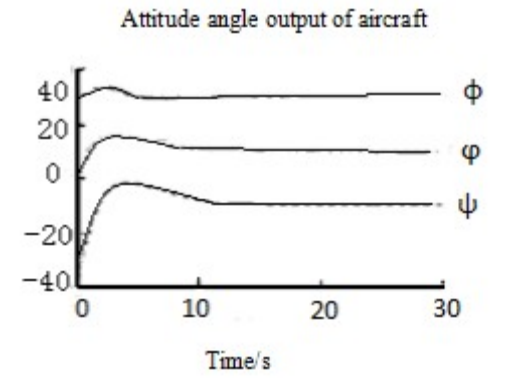

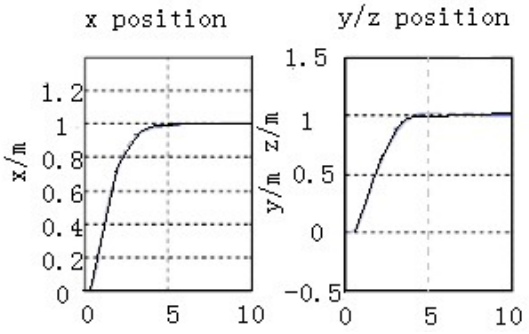

Fig.7. The six state variable output curve of vehicle

In the end, the overshoot of craft will be eliminated. The rise time is 2.45s, stability time is 1.94s and the error is less than 0.01 s. Aircraft can quickly stable at zero point. It is crucial for aircraft to perform a task. When four rotor aircraft close to target objects to collect data, it can effectively prevent from contacting with the target object. Short rise time and stable time is important basis of four rotor aircraft tracking control.

D.The image receiving aircraft

Using a dedicated video acquisition, image compression and wireless transmission system. System is mainly divided into model aircraft systems (airborne) and ground (ground receiver) two parts, model aircraft system requirements acquisition device installed on the aircraft model aircraft fuselage, complete the video acquisition, image compression, digital transmission ways in the form of PZP complete the wireless image transmission. Ground system on the ground using screen as the main body, with wireless data receiving device to complete video accept, decompression, preservation and display of work.

Measured in the aerial effect as shown in figure 8, more clearly shows the actual image, achieve the result of a default.

Fig.8.the fly effect in screen

V. CONCLUSION

The design of double-layer PID control four rotor aircraft based on PID algorithm realise that aircraft can automatically output the position information and parameters srates of systems in according to the data imported by sensor. And data connection is stable and reliable. Because of application of small ground station,aircraft fly automaticly and stably, real-time aerial monitoring can be realized. Through the mobile radio, the setting of free navigation point and colloction vehicle location data in real-time GPS module can be realised. So functions of small four rotor aircraft is more comprehensive. The setting of free navigation point in the four rotor aircraft do a very effective supplement for existing large ground station and further expand the application range of small aircraft.

References

[1] Yue Jilong，Zhang Qingxiang，Zhu Huayong．The research progress and key technology analysis in small four uav rotorcraft［J］． Electronics Optics & Control，2010，17(10) : 46-52．

[2] Wang Ao,Small unmanned helicopter flight control system research, Shanghai transportation university，2007

[3] SebastianO.H.Madgwick,AndrewJ.L.Harrison,RaviVaidya nathan.Estimation of IMU and MARG orientation using a gradient descent algorithm[J].IEEE International Conference on Rehabilitation Robotics .2011 .1:1-7.

[4] Nie Bowen. The research present situation and the key technology of small four rotor aircraft [J]．Electronics Optics & Control，2007，14 (6)：113—117．

[5] Voos Holger． Nonlinear state-dependent Riccati equation control of a quadrotor UAV［C］//Proceedings of the 2006 IEEE Inter-national Conference on Control Applicatioins． Munich: IEEE，2006: 2547 － 2552

[6] TAYEDI A，MCGILVRAY S．Attitude Stabilization of a

Four—Rotor Aerial Robot[C] //43rd IEEE Conference on Decision and Control December. Atlantis，Paradise Island，Bahamas：[S. n.]，2004：14—17.

[7]]ALTUG E，OSTROWSKI J P，MAHONY R.Control of a Quadrotor Helicopter using Visual Feedback[c]//Proceedings of the 2002 IEEE International Conference on Robotics and Automation. Pennsylvania Univ，Philadelphia，PA： [S. n.]， 2002， 1：72-77.

[8] Ming Chen, Mihai Huzmezan, A Combined MBPC/2 DOF H∞ Controller for a Quad Rotor UAV, 2003 AIAA Guidance, Navigation, and Control Conference

[9] Hassan K Khallil, Nonlinear Systems(3 edition), Prentice Hall, 2003

[10] Liu Jinkun . Advanced PID control and MATLAB simulation [M]. BeiJing：Electronic industry press，2004.

[11] Huang Yourui,Qu Liguo. PID control parameters setting and implementation［M］BeiJing: Science press，2010.

[12] E. Altuğ, J. P. Ostrowski, R. Mahony, Control of a Quadrotor Helicopter using Visual Feedback, Proceedings of the 2002 IEEE International Conference on Robotics and Automation, Washington, D.C, May 2012, pp 72-77

The LCR tester based on LabVIEW software system design

LiWendi; LiPengfei; ZouWenqiang

(College of Instrumentation & Electrical Engineering ， Jilin University ,Changchun 130021,China)

***Abstract*--Based on virtual instrument technology, we design a kind of hardware circuit based on LabVIEW software of virtual instrument LCR.Classical method of measuring the LCR impedance tester uses free axis method, realize the measurement of the parameters to be measured.This paper focuses on the design and implementation of software design of each module and the host computer program[1].We use graphics to realize the data processing and interface design of virtual instrument software development platform LabVIEW, and CLF by calling dynamic link library node, communication between the upper interface with the hardware.The design of its hardware system of making a useful exploration for the test method based on virtual LCR VIETS instrument, and achieved good results.Through the actual test results show that the actual test results show that the system has the advantages of simple operation, strong practicability, high precision, and can be widely used in teaching and industrial areas, and has a certain application value and promotion value, suitable for laboratory and other fields.**

***Key words*--virtual instrument technology Freedom axis method LabVIEW LCR tester**

0 PREFACE

AIMING at the front of the virtual instrument and automation, this paper designs a set of LCR testing system, which includes signal generation, data acquisition and analysis, which is applied in the field of experiment teaching and so on. Software platform using graphical virtual instrument software LabVIEW development[2]. The software is intuitive, convenient and flexible, and it can keep pace with the development of computer technology. To achieve in the work convenient and fast for the required passive basic components, resistance (R), capacitance (C) and inductance (L) for accurate and high-speed measurement.

1 THE OVERALL DESIGN OF LCR SOFTWARE SYSTEM

Figure 1 is the overall structure of the virtual LCR tester. Virtual LCR meter using parameter free axis method of measuring resistance, inductance, capacitance and so on, also can be in different frequency excitation signal measuring resistor, inductor, capacitor series parallel combination of impedance, admittance, dissipation factor D physical quantities[3]. The design of LCR tester can be divided into three units, which are signal generating unit, data acquisition unit and bus interface communication unit. The functional block diagram of the LCR tester is shown in Figure 1.

Application program using LabVIEW graphical software development, LCR meter driver and USB controller drivers with VC6.0 development, and hardware operation command package function, to dynamic connection library supplies use the program to call[4]. The software design of LCR testing instrument mainly includes two parts, the front panel and the back panel program block diagram of LabVIEW. Front panel that is the user interface, the definition of a variety of controls, set the instrument parameters and display the measured data. The program block diagram is used to control the data flow, and the data is processed [5].

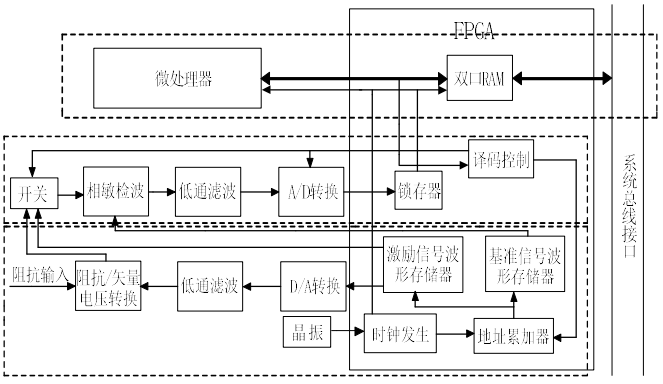

Fig. 1 the overall structure of LCR tester

1.1The test principle of free axis method

The free axis method uses the microprocessor to carry on the vector operation directly. The principle block diagram of free axis method is shown in Figure 2. Figure 3 is the vector diagram.

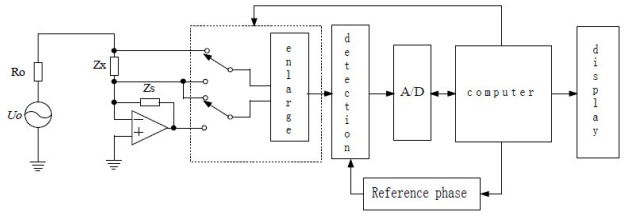

Fig. 2 principle block diagram of free axis method

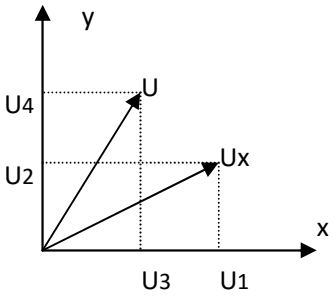

Fig. 3 vector graph of free axis method

The coordinate direction of free axis method can be chosen arbitrarily, that is, the phase reference of phase sensitive detector can be chosen arbitrarily. Through the multi-channel switch to select and, by the phase detector to detect and in the X, Y axis of each projection component.In order to get the vector voltage corresponding to the component of the orthogonal coordinate axes, the accurate phase difference is needed for each or two measurements. It is required that the phase generator can generate the waveform control signal which is strictly different from each other as the reference voltage signal of the phase sensitive detector. By the front-end circuit of 2-4 analysis:

$$Z_x = -\frac{U_x}{U_s} \cdot R_s \quad (1)$$

$$U_x = U_1 + i \cdot U_2 = a(N_1 + i \cdot N_2) \quad (2)$$

$$U_s = U_3 + i \cdot U_4 = a(N_3 + i \cdot N_4) \quad (3)$$

Type, respectively, in and the direction of voltage component, corresponding to the digital quantity, respectively in and the direction of voltage component, corresponding to the digital quantity; calibration coefficient for the A / D converter, namely each number represents the voltage values.

By formula (1) ~ (2) available:

$$\frac{U_x}{U_s} = \frac{U_1 + i \cdot U_2}{U_3 + i \cdot U_4} = \frac{N_1 + i \cdot N_2}{N_3 + i \cdot N_4} = \frac{(N_1 N_3 + N_2 N_4)}{N_3^2 + N_4^2} + i \cdot \frac{(N_2 N_3 - N_1 N_4)}{N_3^2 + N_4^2}$$

Therefore, directly through the calculation of the N_1、N_2、N_3、N_4 these numbers can complete the vector division operation, and the measured impedance.

1.2. LCR software system algorithm based on free axis method

In 1.1, through the hardware circuit to get the four component A, these numbers can complete the vector division operation, and the measured impedance. It can be extended to find out the value of the main parameters and the auxiliary parameter values. As follows:

Table 1 capacitance, inductance and resistance of each equivalent circuit formula.

	Main parameter	Secondary parameter
parallel connection(C)	$Cx = \frac{1}{\omega Rs} \times \frac{N_2N_3 - N_1N_4}{N_1^2 + N_2^2}$	$Dx = \frac{N_1N_3 + N_2N_4}{N_1N_4 - N_2N_3}$
series connection(C)	$Cs = \frac{1}{\omega Rs} \times \frac{N_3^2 + N_4^2}{N_2N_3 - N_1N_4}$	
parallel connection(L)	$Lp = \frac{Rs}{\omega} \times \frac{N_1^2 + N_2^2}{N_1N_4 - N_2N_3}$	$Qx = \frac{N_2N_3 - N_1N_4}{N_1N_3 + N_2N_4}$
series connection(L)	$Ls = \frac{Rs}{\omega} \times \frac{N_1N_4 - N_2N_3}{N_3^2 + N_4^2}$	
parallel connection(R)	$Rp = -Rs \times \frac{N_1^2 + N_2^2}{N_1N_3 + N_2N_4}$	$Qx = \frac{N_2N_3 - N_1N_4}{N_1N_3 + N_2N_4}$
series connection(R)	$R's = -Rs \times \frac{N_1N_3 + N_2N_4}{N_3^2 + N_4^2}$	

2 LABVIEW SOFTWARE FRONT PANEL DESIGN

The soft panel of LCR tester is realized by graphical programming software LabVIEW, and the user interface is friendly. The data transmission of the system is realized through the serial communication. Workflow software: in the VI program, first choose a name for the visa, set the baud rate, set the data bits and the serial port initialization operation, and then start the equipment. According to their own needs to send the test status command[6]. Hardware system receives commands to complete the corresponding action, and the collected data through the serial port to the computer, the application software for data processing, analysis and display and other functions[7]. The software interface of the LCR tester is composed of two parts: the instrument test setup and the test result, as shown in Figure 4.

2.1 Instrument setting test interface display

Mainly contains the instrument test start button, the instrument status, equipment slot number, the excitation signal frequency, the excitation signal amplitude, the bias.

2.2The test results of the instrument display part

LCR instrument test data display part, including inductance quality factor Q, capacitance loss factor D, reactance x, electric nano B, conductance g, the impedance, Z, value, conductance values, y, and impedance phase angle alpha, admittance phase angle beta, parallel equivalent inductance LP, series equivalent inductance ls and parallel efficiency

capacitance CP and series equivalent capacitance CS, equivalent parallel resistance RP and series equivalent resistance (RS).

Figure 4 LCR test interface front panel

3 DESIGN OF INTERNAL PROCEDURES

3.1 Progress design

First, because the data is transmitted through the U port, the test is relatively slow, add the progress bar to display. As shown in figure 5:

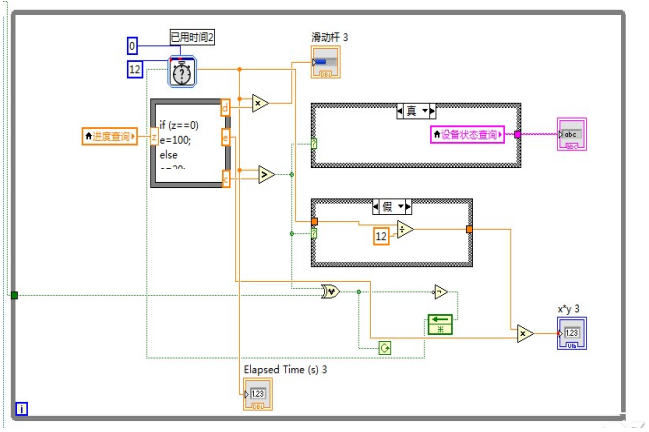

Figure 5 progress bar program

When the main interface point began, the progress bar began to record time, at the same time the progress bar to start reading, when the measurement error occurs, showing a variety of errors.

3.2 Measuring element judgment module

When the measuring element LCR tester to choose the wrong time, will automatically select which one should use the measuring element. For example, when the resistance is selected as the capacitance measurement, will determine the components for resistance. The program is shown in figure 6:

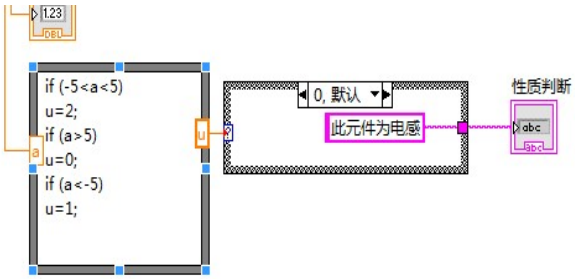

Figure 6 measuring element discrimination program

3.3Interface resistance, capacitance, inductance value display program

We will be based on the universal LCR testing instrument, identified only two mouth, showing the measurement of parallel equivalent, series equivalent data. The program frame is shown below in figure 7:

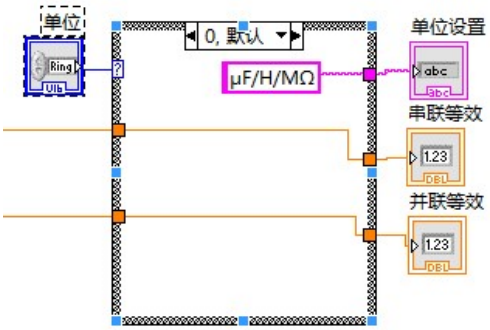

Fig. 7 LCR measurement results and unit program

3.4Test data to save a key

The LCR test value, easy to analyze and deal with the test data, we set up a test data storage function. I saved automatically to the d:\ document \LCR\LCR.xls document. Save the time to test the data, and test data for the various results and units. The program is shown in figure 8:

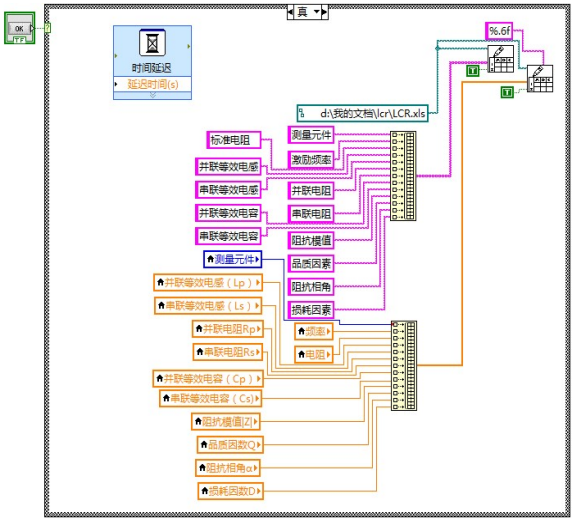

Figure 8 test data save

3.5Automatic selection of standard resistance function.

Due to the selection of standard resistance, for measurement will cause unnecessary trouble, selection error will cause deviation of the measured values, this design improved resistance standard, according to the

test procedure, automatic selection of the most appropriate standard resistor in the internal procedures. The measurement results more accurate. The program is shown in figure 9:

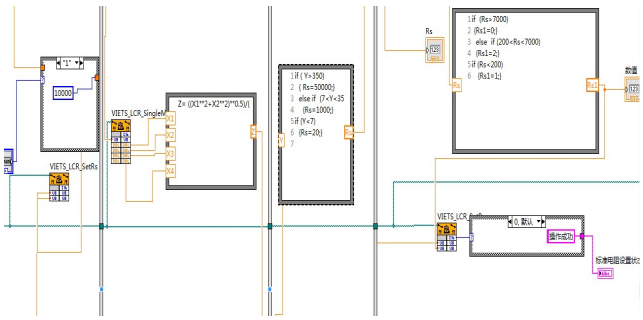

Figure 9 Automatic selection of standard resistance procedures

4 CALCULATION RESULTS AND COMPARISON

In order to test the reliability and practicability of the program, the L, C and R values are measured, and the results are as follows:

Table 1 Results of inductance, capacitance and resistance

	Nominal value	This instrument test result	Measurement deviation
inductance(L)	10uH	10.3741	0.3741
	100uH	102.513	0.2513
	10mH	10.5665	0.5665
capacitance(C)	10pF	10.5617	0.5617
	100pF	98.4377	1.5623
	1nF	0.99416	0.01584
	10nF	9.78757	0.21343
	10uF	9.83623	0.16377
	100uF	98.5699	1.4301
resistance(R)	1Ω	1.01014	0.01014
	10Ω	10.0508	0.0508
	100Ω	102.119	2.119
	1KΩ	1.00819	0.00819
	10KΩ	10.0619	0.0619
	100KΩ	99.5795	0.4205
	1MΩ	1.00945	0.00945

And the experimental results can be used to measure the parameters of the system:

1 inductance (L) is 10 uH ~ 100 mH;

2 capacitance (C) is 10 pF ~ 1000uF;

3 resistance (R) is 1 Ω ~ 10MΩ.

The measuring error of the instrument is less than 0.50%, so the measurement precision of the instrument can reach 0.50%.

5 CONCLUSION

The LCR tester with the program can improve the reliability, save the cost, shorten the development cycle, and can quickly and accurately detect the resistance, inductance, capacitance and the associated parameters. The hardware circuit of the signal analysis and display of the traditional instrument is enhanced, and the operation of the instrument is enhanced, and the user defined function is added. Compared with the traditional instrument, its price is low, reusable and configurable, and it has a certain practical value and promotion value. Its advantages make the virtual instrument gradually replace the traditional instrument to become the development of the test field. There are still some shortcomings in the method of the design, and the precision of the precision resistance of the hardware circuit will affect the measurement accuracy of the tester, and it needs further improvement.

Reference

[1] Lin Jun, Xie Xuansong. Virtual instrument principle and application [M]. Beijing: Science Press, 2006

[2] Wei Jianrong. The reconfigurable monitoring system research and design of [J]. master's degree thesis of Jilin University, 2006.10, 1-67.

[3] Zhang Chongxiong. Virtual instrument technology analysis and design [M]. Beijing: Electronic Industry Press, 2007

[4] Li Weibo. Research and design of graduation thesis of Undergraduates of Jilin University [J]. virtual LCR meter (Design), 2009

[5] Chen Shangsong, Fabregas, Guo Qing. Electronic measurement and instrument [M]. Beijing: Electronic Industry Press, 2005

[6] Where the bridge section of Ching Ming, Qiu Chunling. Principle and application of single chip microcomputer [M]. Beijing: China Railway Press, 2004

[7] Deng Yan, Wang Lei et al. Application of LabVIEW7.1 testing technology and instrument [M]. Beijing: Mechanical Industry Press, 2004

[8] Zhang Jing. Talk about L, C, R parameter measurement and LCR bridge table [J]. electronic quality testing technology, 2005, 7 (12).

Based on parallel sampling VIIS - EM data acquisition technology

Zhang Bo-yu; Kong Xiang-zhi; Zhang Ren-jie

(College of Instrument Science and Electrical Engineering, Jilin University, Changchun 130022, China)

***Abstract*—With the continuous development of testing technology, the virtual instrument technology has been paid more and more attention and applied in more and more designs for its high performance, scalability, less development time and seamless integration advantages. The oscilloscope is the core instrument of the electronic measuring, which has been widely used in various fields. Compared with the analog and digital oscilloscopes we use now, virtual oscilloscope with a more cost-effective and user-friendly operator interface, has a broader application prospects and space of development.This design is mainly to complete the design of the virtual oscilloscope data acquisition card. Including signal conditioning, A/D conversion, the bus communication and parallel data processing module, in which the parallel data processing module is the core content of the design. By using parallel sampling technique to improve system sampling rate, eventually we can achieve a measurement of less than 50V analog signal, the maximum sampling rate is 100 MSPS.**

***Key words:* Virtual Instrument Technology; Virtual Oscilloscope; FPGA; Parallel Sampling Technique**

I INTRODUCTION

THIS topic is Jilin University virtual electronic measuring instrument integration a very important part in the system. Through this topic research, design, to expand the input voltage range of original data collection system and improve the sampling rate, improve the existing virtual electronic measuring instrument performance, make the instrument to better serve basic courses teaching experiment and production practice teaching. The design of the main content of virtual storage oscillograph data acquisition card, including signal conditioning, A/D conversion, bus communication, parallel data processing four modules. Of signal disposal using differential circuit, effectively restrain common mode interference. A/D conversion part through the use of parallel sampling technology, the sampling data of the two channels is united into FPGA FIFO, implement two times the AD sampling frequency sampling rate. Use AT89S52 single chip microcomputer bus communication part, complete instructions transmitted and initialization configuration. The FPGA EP2C5Q208C8 chosen as the main control chip, implement sampling rate control and number according to the processing, and other functions.

II THE OVERALL PLAN

The oscilloscope card USES FPGA + 51 single chip microcomputer as the overall control, including the FPGA with Altera company Cyclone II series EP2C5Q208C8 as core controller, complete large-scale data storage, and exchange control unit circuit, 51 microcontroller and the use of Atmel company AT89S52, mainly to complete the bus communication system initialization and configuration.

According to the modular instrument design idea, the oscilloscope card system is divided into four modules: signal conditioning module, A/D conversion module, bus interface communication module, the parallel data processing module. The overall structure of the system block diagram is shown in figure 1[1].

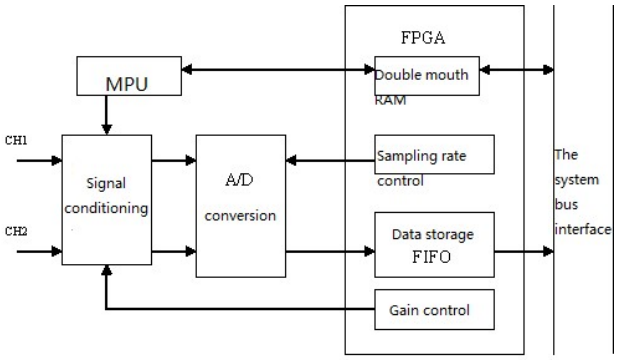

Fig 1 Block diagram of the overall plan

III METHODS

A The signal conditioning module

The input analog signal conditioning to the scope of the ADC can identify the large signal attenuation, small signal pass-through. Including high resistance attenuation, impedance transformation and difference transformation three parts. The parts through micro controller and FPGA to realize real-time control. The signal conditioning module circuit diagram as shown in figure 2-1.

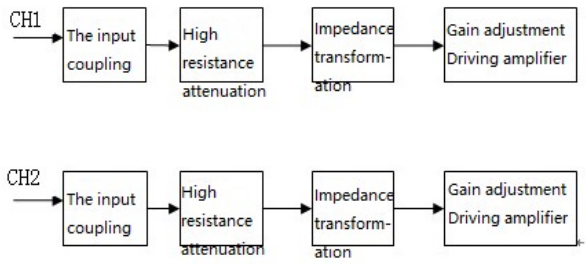

Fig 2-1 Signal conditioning module

1) Attenuation circuit

Oscilloscope for voltage range of the input signal to A certain extent, this design oscilloscope card requires 50 VPP input voltage range, and A/D conversion circuit using AD9288 chips for 1 VPP input voltage range, so need attenuation circuit. When the large signal input, attenuation, small signal input straight through[2].

Direct resistance partial pressure is suitable for low frequency circuits, high frequency, the resistance of stray capacitance will have great impact on the circuit performance, lead to actual pressure coefficient and the theoretical results of difference. When choosing compensating voltage divider can weaken the high frequency parasitic capacitance effect the performance of the circuit. But with the increase of frequency, the influence of parasitic capacitance on the circuit will be more and more obvious. This design USES the normal bleeder circuit working frequency of 1 Hz ~ 10 MHZ, meet the system requirements[3-4].

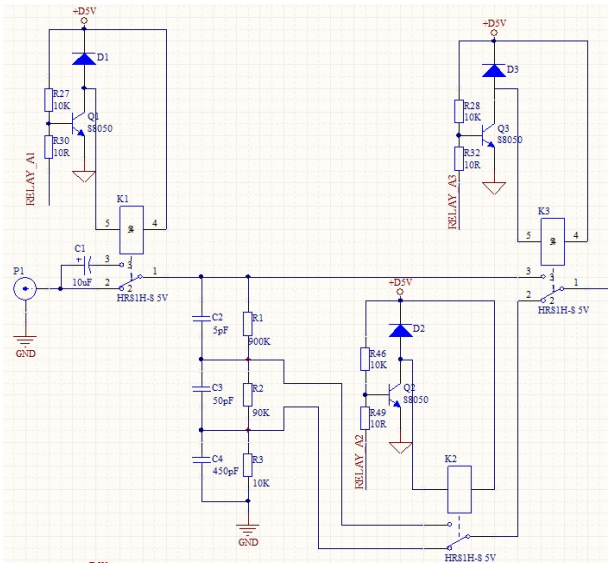

Fig 2-2 high resistance attenuation principle diagram

2) Impedance transformation circuit

Impedance converting circuit with TI company broadband high-speed amplifier TL071 implementation. Low noise operational amplifier jfets jfets input input in TL07x series similar TL08x series operational amplifier with low input, bias and offset current and fast conversion rate. Low harmonic distortion and low noise make ideal TL07x series is suitable for high-fidelity audio applications of preamplifier. The characteristics of each amplifier jfets input (high input impedance), plus a bipolar output on a single chip integration stage. Follow through TL071 voltage, increasing the system input impedance, to meet the requirements of the system to the input impedance. As shown in figure 2-3.

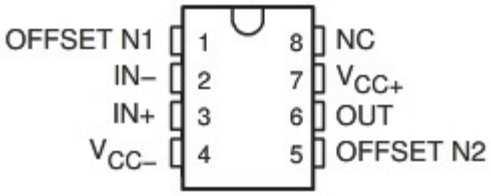

Fig 2-3 TL071

3) The differential transform circuit

The oscilloscope card adopts differential signal as input signal of the AD. Difference signals and the commonly used single ended, compared to common mode interference and electromagnetic interference, has the very good inhibitory ability can increase the system stability and accuracy. Differential transform select low distortion of ADI company differential AD8138ARZ ADC driver amplifier. G = + 1, 3 db bandwidth of 320 MHZ, which can realize single-ended input signal, double-end differential signal output[5].

Differential transform circuit principle diagram is reference AD9288 official evaluation board circuit diagram connection, as shown in figure 2-4, after the actual test through selection. Single-ended signals from AMPINA input, output from AMPOUTA and AMPOUTAB difference signal, the common-mode voltage VOCM by partial pressure resistance can meet the common-mode voltage of AD9288 as 1V.

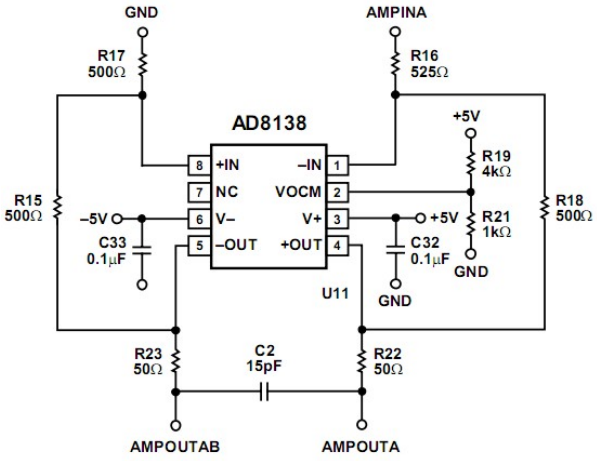

Fig 2-4 Difference transformation principle diagram

B A/D conversion module

A/D transformation is the core part of data acquisition. Chooses the AD converter type, determines the precision of the whole system can achieve performance in the end. The design of A/D

conversion part will use the parallel sampling technology, the realization of parallel sampling, dual channel to achieve the purpose of double sampling rate[6].

1) Principle of parallel sampling technology

Parallel sampling technology is to use two channel or multiple channels to the same signal sampling at the same time, each channel sampling clock has a certain phase difference, the sampling data unified storage can get higher equivalent sampling rate. Two pieces of AD sampling at the same time, for example, as shown in diagram 2-5:

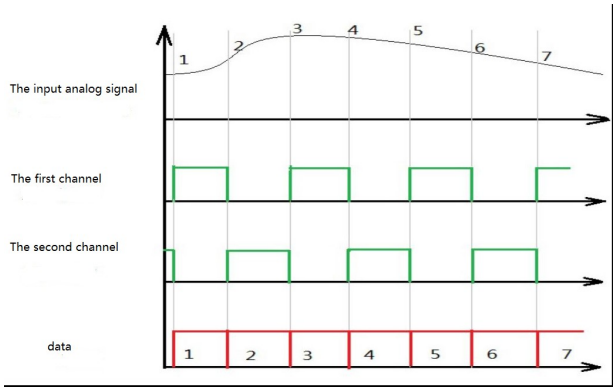

Fig 2-5 Dual channel parallel sampling schematic diagram

The first channel and a second sampling clock phase difference of 180 degrees, AD in rise along the sampling clock. The first channel to point 1, 3, 5, 7 of the analog signal voltage value, the second channel to point 2, 4, 6, the analog signal voltage value, then two channel data storage, can get 1-7 analog signal voltage value of each point sampling rate equal to 2 times a channel sampling rate, achieve the goal of improve the sampling rate.

2)A/D conversion circuit hardware

This design chooses the ADI company AD9288BST - 100 as the core of this card conversion chip. AD9288BST - 100 is a 8 bits, single channel sampling rate highest 100 installed base, dual-channel high-speed AD converter. IC integrates sampling keeping and reference voltage circuit. Each channel analog bandwidth of 475 MHZ, single channel 3 v power supply, the biggest 1 VPP input analog voltage range, output data queue. They can be used for handheld instrument and low-power digital oscilloscope. Specific AD9288 hardware connection as shown in figure 2-6:

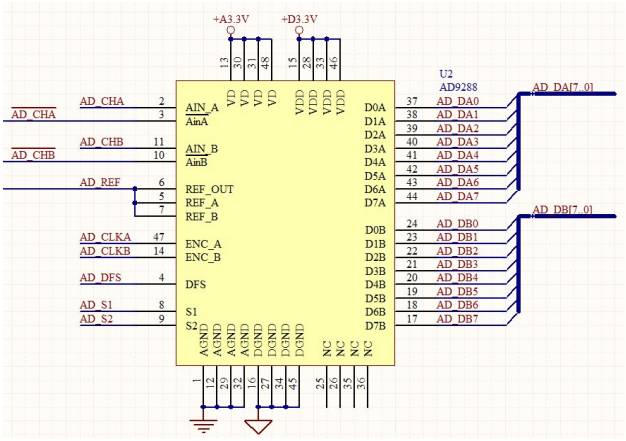

Fig 2-6 AD9288 wiring diagram

C Bus communication

Bus communication module is a PC with modular hardware instrument important interface card by the exchange of information. For the purpose of this oscilloscope card, mainly and USB control card exchange of information, including transfer analysis and initialization. Part by MCU and FPGA internal two partial implementation.

1) Single chip microcomputer part

Selection of Atmel company communication MCU AT89S52 single chip microcomputer as the system. Major transfer of a complete instruction parsing and initial state configuration, as well as for ac/dc coupling relay control, performed by RELAY_A1 and RELAY_B1. Specific hardware connection as shown in figure 2-7:

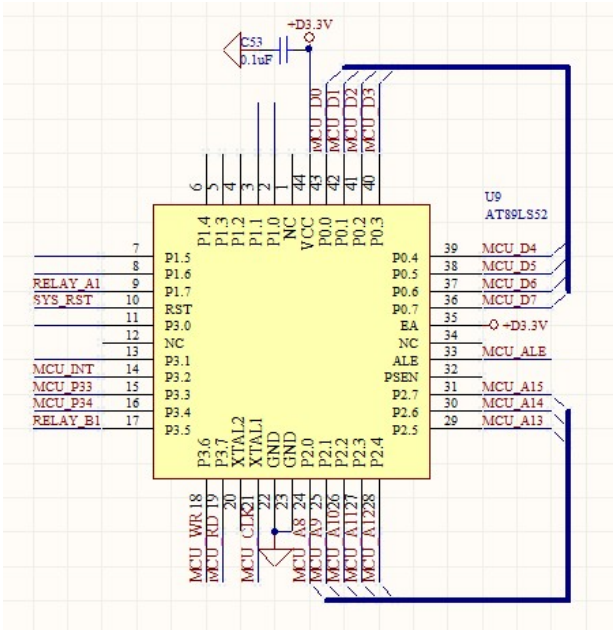

Fig 2-7 AT89S52 single chip microcomputer wiring principle diagram

2) The FPGA parts

FPGA part of the communication function mainly IDT7130 and MCU decoder two parts content. IDT7130 FPGA and MCU communication, instructions and information; MCU decoder to decode

and execute the command information and real-time control of each unit circuit.

MCU decoder is the interface of MCU and FPGA. MCU instruction code sent via the address bus and data bus to the FPGA, and through the MCU decoder, translate instructions for FPGA can identify command, to control the relevant work unit circuit[7-8].

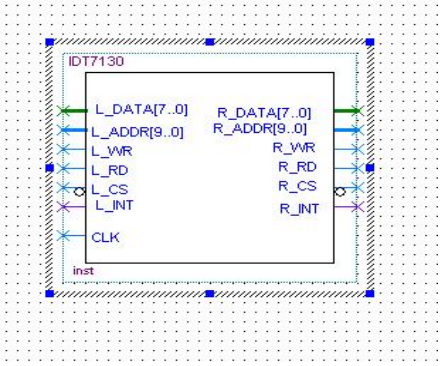

Fig 2-8 After IDT7130 instantiated model

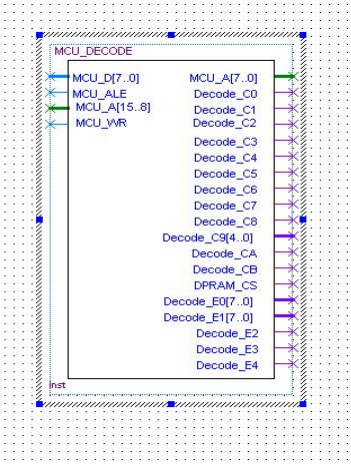

Fig 2-9 MCU decoder model after instantiated

B Parallel data processing module

Parallel data processing module is the core of the design content. Including the design and implementation of the FIFO, the design of the data selector and the realization of smoothing filter three parts content.

1) Design and implementation of the FIFO

FIFO is a relatively simple data cache first-in, first-out type, generally used for the data transfer between different clock domains, multi-purpose FIFO as data in the data acquisition system is data storage.

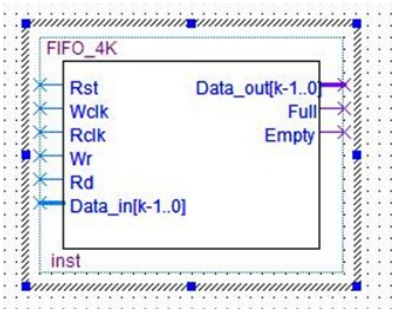

Fig 2-10 For 4k FIFO storage depth after the case of the model

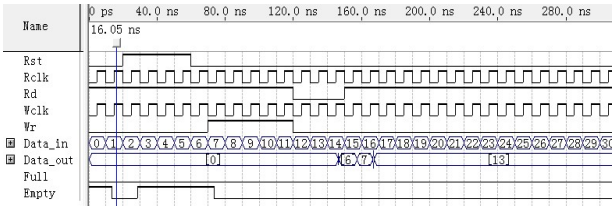

Fig 2-11 FIFO_4K timing simulation results

2) The design of the data selector

Adopts parallel sampling technology, the unit of time that the data mining is twice that of single channel when data to be unified into the FIFO, and design the following data selector, clock frequency twice of the sampling clock frequency, to count clock frequency rising along the odd when storing A channel data, even when the store B channel data, so as to realize the unification of data storage[9-10].

Two channel data unification in FIFO, due to the data transformation prone to intermediate state, which will produce competitive adventure. If directly into FIFO will have quite a number of error data[11]. When deposited in the FIFO, the add a synchronous clock, the clock up along the unified storage, to reduce the error rate.

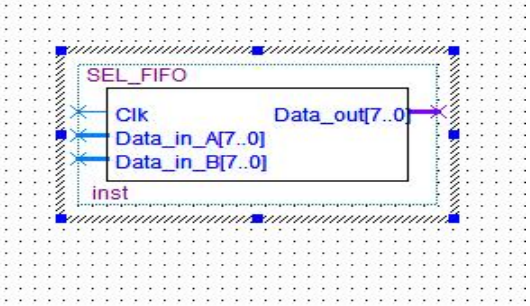

Fig 2-12 Model diagram after data selector is instantiated

Timing simulation results:

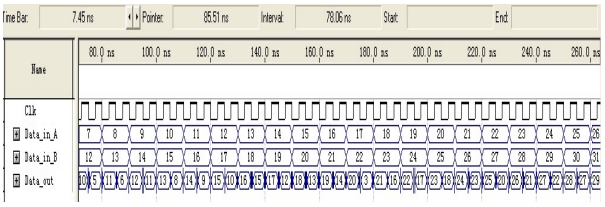

Fig 2-13 Simulation scheduling results

3) The realization of smoothing filter

Due to data transmission may occur in the process of storage and wrong words if gibberish, at the same time reduce the influence of the system noise, and need to the necessary filtering system data, in order to make the final waveform can be more smooth. Thus to design the following FILTER.The two median filter, the filter is to transfer in the four groups of data after the sum, average output as the final data output. So that we can reduce the influence of abnormal data on the results, making waveform effect of more smoothing[12].

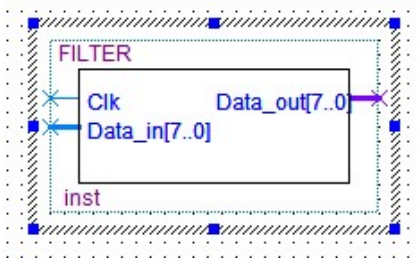

Fig 2-14 FILTER after the model

IV TEST RESULTS AND ANALYSIS

A A/D conversion circuit results and analysis

A/D conversion part of the output of digital signal and the FPGA directly connected, if you want to separate measurement needs in the signal output and DA are linked together, to test the result of the A/D conversion part separately. Due to the finished PCB board design is fixed, cannot lead wire connected to the DA, so only with the aid of the FPGA and the LabVIEW complete test.

The following from direct input signal before AD9288 test results:

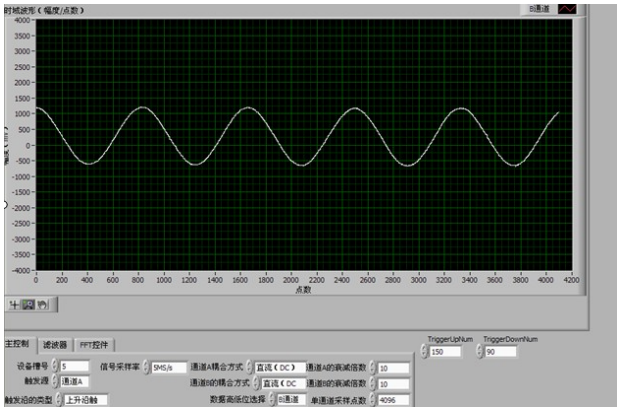

Fig 3-1 Input sine signal, the frequency of f = 1 KHZ, Vpp = 0.8 V, the sampling rate is 5

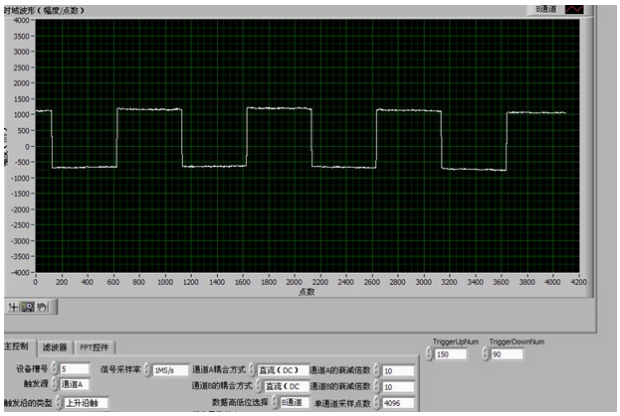

Fig 3-2 Input square wave signals, frequency of f = 1 KHZ, Vpp = 0.8 V, the sampling rate is 1

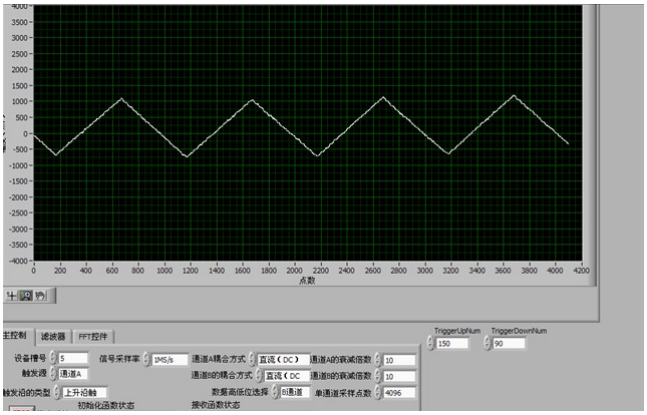

Fig 3-3 Input triangular wave signal, the frequency of f = 1 KHZ, Vpp = 0.8 V, sampling rate is 1

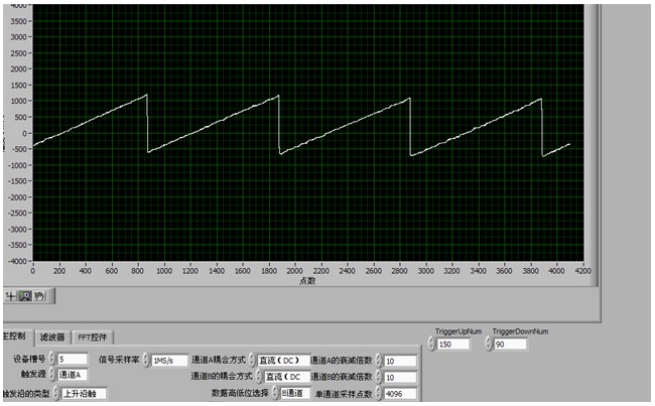

Fig 3-4 Input sawtooth wave signal, the frequency of f = 1 KHZ, Vpp = 0.8 V, the sampling rate is 1

B The whole plate test results and analysis

By a factor that signal attenuation 1 through testing the whole plate, test results are as follows:

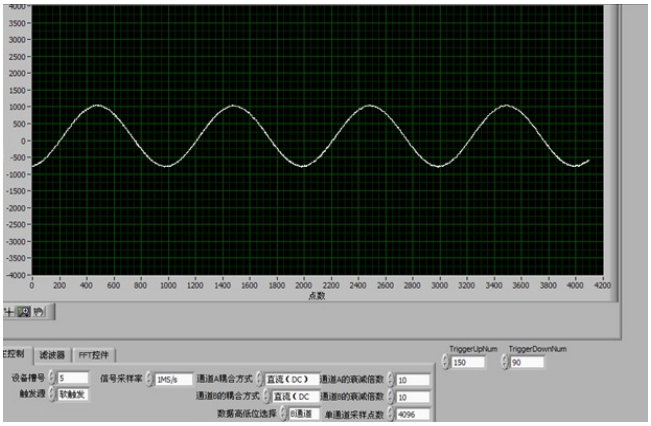

Fig 3-5 Input sine signals, frequency of f = 1 KHZ, Vpp = 0.8 V, sampling rate is 1

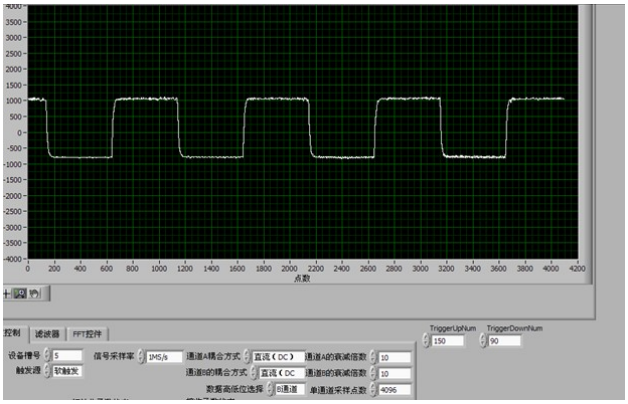

Fig 3-6 Input square wave signals, frequency of f = 1 KHZ, Vpp = 0.8 V, the sampling rate is 1

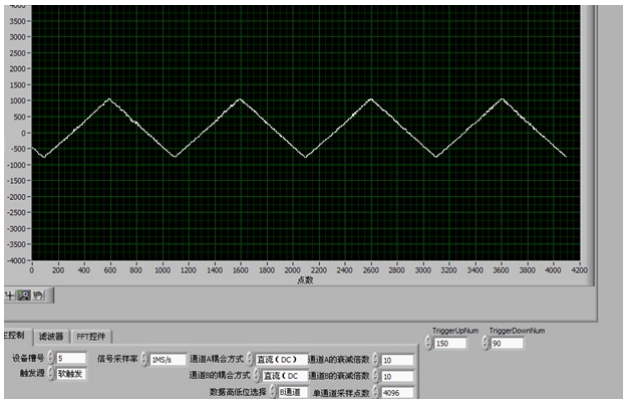

Fig 3-7 Input triangular wave signal, the frequency f = 1 KHZ, Vpp = 0.8 V, sampling rate is 1

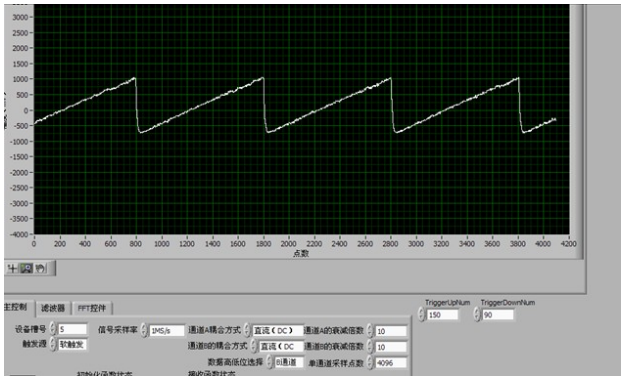

Fig 3-8 Input sawtooth wave signal, the frequency f = 1 KHZ, Vpp = 0.8 V, sampling rate is 1

Carefully observe the above test results can be found that the overall waveform is relatively smooth, beautiful and easy, satisfies the requirement of system design.

V CONCLUSION

This design is mainly to complete the virtual digital storage oscillograph of the design of data acquisition card. Including signal conditioning, A/D conversion, bus communication, and parallel data processing of four parts, including the parallel data processing module is the core content of this design. Signal conditioning part through high resistance attenuation, impedance transformation and difference transformation, meet the needs of the AD converter differential signal. A/D conversion module of the input differential analog signal is converted into digital signal, through parallel sampling technology to achieve two times the AD clock sampling rate, sampling data parallel output. Parallel data processing part after classifying sampling data filtering, unified in the FIFO, for the system call. PC and modular instrument bus communication module card by the exchange of information and control. Finally can realize the peak - peak value is less than 50 v analog signal measurement, the highest sampling rate can reach 100.

References

[1] WEI Jian-rong. The Research and Design of Reconfigurable Monitoring System[D]. Master Dissertation of Jilin University. 2006

[2] HONG Meng, GENG Xiang-ming. The Research of High Speed Parallel Sampling Technology Based on FPGA[J]. Modern Electronic Technology. Mar.1.2011. Volume thirty-fourth issue fifth

[3] XING Yi-nan. The Research of Key Technologies in High Speed Parallel Sampling System[D]. Electronic Science and Technology University Master Thesis. 2006

[4] TANG Zheng-hu. The Design of Digital System for 100MHz Digital Storage Oscilloscope[D]. Electronic Science and Technology University Master Thesis. 2004

[5] HUANG Rong-hua. The Design of Virtual Digital Oscilloscope[D]. Master Dissertation of Jilin University. 2006

[6] KANG Hua-guang. Basic Electronic Technology (Digital)[M]. Beijing: Higher Education Press. 2006

[7] HE Qiao, DUAN Qing-ming, QIU Chun-ling. Microcontroller Theory and Applications[M]. Beijing: China Railway Publishing House. 2005

[8] YAN Xiao-ming. The Design of Digital Storage Oscilloscope[D]. Master Dissertation of Jilin University. 2007

[9] Penzkofer A, Simmel M, Riedl D. Room temperature phosphorescence lifetime and quantum yield of erythrosine B and rose bengal in aerobic alkaline aqueous solution[J]. Journal of Luminescence, 2012, 132(4): 1055-1062.MLA

[10] Pérez-Patricio M, Aguilar-González A, Arias-Estrada M, et al. An FPGA stereo matching unit based on fuzzy logic[J]. Microprocessors and Microsystems, 2016.

[11] Franc M, Hace A. A study on the FPGA implementation of the bilateral control algorithm towards haptic teleoperation[J]. Automatika–Journal for Control, Measurement, Electronics, Computing and Communications, 2013, 54(1).

[12] Gorgoń M. Parallel performance of the fine-grain pipeline FPGA image processing system[J]. Opto-Electronics Review, 2012, 20(2): 153-158.

Design of indoor air quality monitoring system based on GSM network

WANG Jie; YANG Chen; DENG Xin-xin

（jilin university instrument science and engineering institute,changchun,130021）

***Abstract*--At present, with the development of the industry, the environment is becoming worse and worse, the PM2.5 levels indoor increase sharply because of the haze weather, the formaldehyde from materials also seriously affect the indoor air quality, which result in the incidence of respiratory diseases greatly increased. Therefore ,problems related to indoor air quality has become the focus of widespread attention. This design uses gas sensors for testing PM2.5 and formaldehyde content in indoor air, through the microprocessor for processing and analysis ,using the LCD screen for displaying the data, and according to the setting threshold for alarm, use the GSM wireless network for remote communication, remote real-time monitoring of indoor air quality.**

***Key words*--indoor air quality;PM2.5; formaldehyde; GSM network**

1 INTRODUCTION

INDOOR environment refers to the house people live in and work at and other relatively closed places, etc .According to statistics, people take more than an average of 80% to 90% of the time every day to stay indoors, so the indoor air quality has far higher influence to people healthy than outdoor air quality. [1] With the development of industry, people's living environment is becoming worse and worse, which result in the incidence of all kinds of respiratory disease increased significantly. Therefore it is quite necessary to create a real-time monitoring of indoor air quality. At present, the main pollutants affecting the quality of indoor air include formaldehyde、PM2.5,etc.

However, most of the traditional detection systems only detect one kind of air quality parameters, and their price are expensive, operations are complex, therefore, they can not be used commonly. Designing a kind of system which can detect a variety of air quality parameters, and use the GSM network for remote monitoring has a practical significance. [2-4]

2 THE OVERALL STRUCTURE DESIGN OF SYSTEM

Indoor air quality monitoring system based on GSM network, include the central processing module, the sensor detection module (PM2.5 detection module, the formaldehyde content detection module), the keyboard control module, display module, the threshold alarm module, the GSM communication module, power supply module [5-8]. The diagram of overall system design is shown in figure 1.

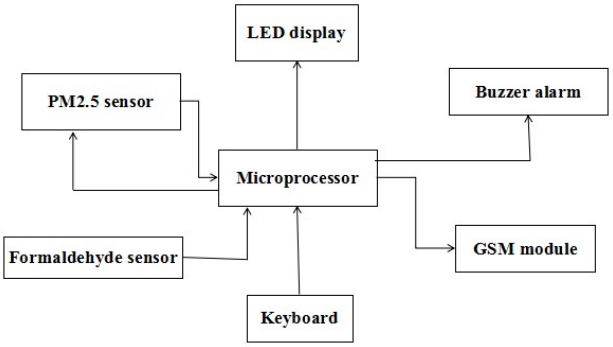

Fig1 Diagram of the system design

As shown in the above, the system uses sensors to collect information, processed by microprocessor, displaying data on the LED, when the concentration of the data value is greater than the setting threshold, alarm module would sound and light alarm, and send alarm messages to the mobile terminal by the GSM network, realizing remote monitoring.

3 HARDWARE DESIGN OF THE SYSTEM

3.1 PM2.5 detection module

The sensor for detecting PM2.5 is called GP2Y1010AU0F produced by sharp. It is a optical density detection sensor, on its internal diagonally, distributes the phototransistor and infrared light-emitting diodes. The sensor uses the theory of photosensitive to detect tiny particles in the air, by the light attenuation formula, $I = I_o e^{-pd}$ which converts the current attenuation difference into voltage pulse, according to the height of the output pulse to determine the concentration of PM2.5. Characteristics of sensor has small size, light weight, easy to install, the maximum current value up to 20mA.When the sensor uses current way, the dc voltage can up to 7v,

and output the 0 ~ 5v analog voltage signal, which is proportional to the dust concentration.

3.2 Formaldehyde detection module

Formaldehyde module uses formaldehyde ZE08 - CH2O electrochemical sensor, which applying the electrochemical method to detect formaldehyde in air, by the formula

$$E = E_0 - \frac{RT}{nF} \ln \frac{a_C^c a_D^d}{a_A^a a_B^b}$$

(type E_0 as the standard electrode potential, R for gas constant, T for absolute temperature , n to participate in the number of electrons in an electrode reaction, F for Faraday constant, a for participate in a chemical reaction matter concentration.) Calculate the potential difference of electrochemical reaction, the internal conversion data transmitted to the microprocessor. It has a good stability and selectivity. It possesses a internal temperature sensor for temperature compensation, at the same time it has advantages of high sensitivity, high resolution, low power consumption.

3.3 GSM network module

GSM module uses SIM900A produced by SIMCom as main control chip. SIM900A is a compact, high reliability of the wireless module , which adopts the STM encapsulation dual-band GSM/GPRS module solution. It has a powerful processor ARM9216EJ -s kernel, can satisfy the requirement of the development of low cost and compact size. It also has a standard of the AT command interface, can provide a short message, GSM and many other business. Microcontroller through serial ports to send the AT command to the GSM module , can control the SIM900A. The flow chart of the module is shown in figure 2.

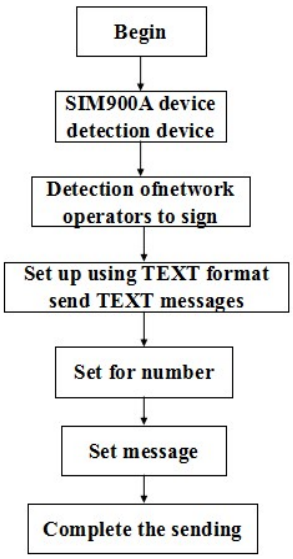

Fig2 The flow chart of the GSM network

4 SOFTWARE DESIGN OF THE SYSTEM

Monitoring system mainly controls STC12C5A60S to process data from sensors in a certain period, and then display data on the LCD screen, and write different AT commands to the SIM900A module to accomplish corresponding communication tasks [9-12]. The flow chart of system software is shown in figure 3.

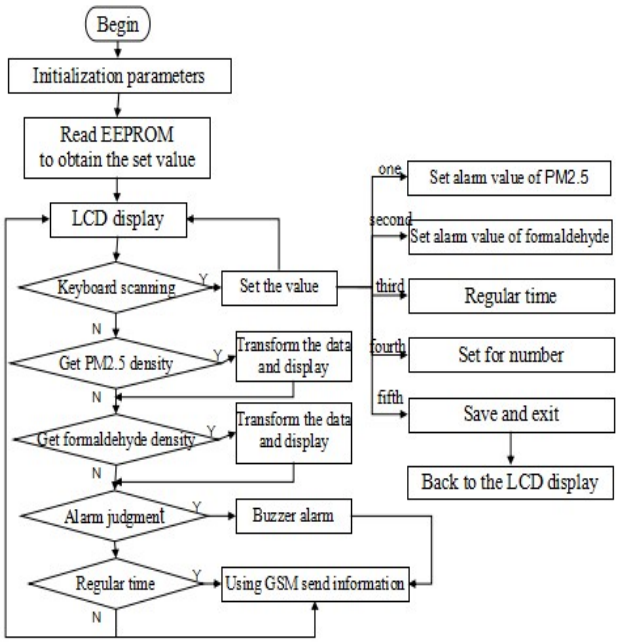

Fig3 The software flow chart of the system

5 THE EXPERIMENTAL RESULTS AND ANALYSIS

5.1Test the system's performance for detecting PM2.5

5.1.1 Collect data about PM2.5

Applying the method of diffusion of smoke to test the detection ability for PM2.5 of system. Lit a cigarette, put it near PM2.5 sensor, slowly increase the concentration of the smoke, read the 11 density roughly equal interval data, respectively measure the output voltage of the sensor under consequent concentration. With dust concentration (mg/m³) for the horizontal axis, the output voltage (V) as the longitudinal axis, draw the sensor characteristic curve under actual circumstances , which is shown in figure 4.

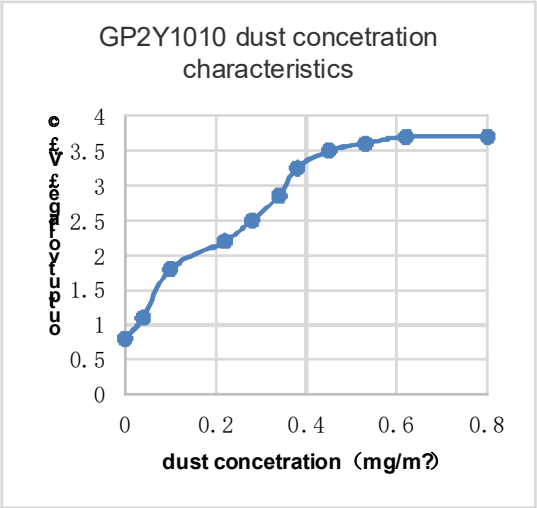

Fig4 The measured dust concentration characteristic curve

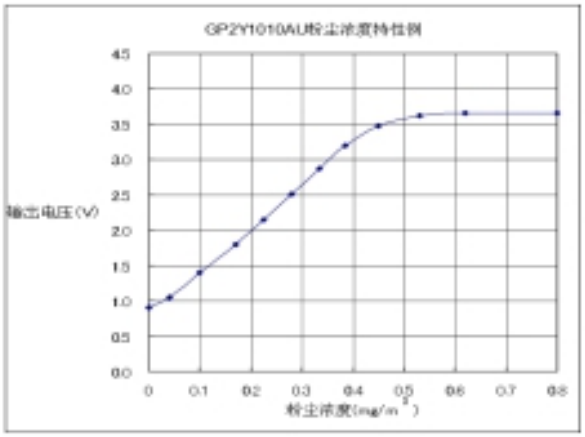

Fig5 The theory of dust concentration characteristic curve

By comparing the measured curve and the theoretical curve, contour is similar.

5.1.2 PM2.5 data processing and analysis

The sensor adopts the serial communication method that improves the accuracy of measurement, a serial port configuration requirements for: (1) the baud rate: 2400 bit/s, (2) every 10 ms send 1 byte, seven bytes, a parity bit:

$$Parity = V_{out}(H) + V_{out}(L) + V_{ref}(H) + V_{ref}(L)$$

Will receive the voltage value of the data according to the formula:

$$V_o = \frac{V_{OUT}(H) \times 256 + V_{OUT}(L)}{1024} \times 5$$

Calculate to get the value of the Vo, dust concentration for K x Vo, K for mass concentration conversion coefficient.

According to the measured data to calculate the range of output voltage :

$$V = V_{OH} - V_{OL} = (3.75 - 0.83)V = 2.92V$$

Then calculate the range of dust concentration:

$$C = C_{OH} - C_{OL} = (0.625 - 0.000)mg/m^3 = 0.625mg/m^3$$

Then calculate the detection sensitivity:

$$K = \frac{V}{C} = \frac{2.92}{0.625} = 4.67\text{V}/(mg/m^3)$$

.

According to the data above ,we can draw a conclusion that the system detection in the measurement of PM2.5 has good linearity and high sensitivity.

5.2 Test the system's performance for detecting formaldehyde

5.2.1 Collect data about formaldehyde

After the system is powered on, preheating of three minutes, then collect formaldehyde concentrations every 10 seconds, the measured data are shown in table 1:

Tab1 The measurement of formaldehyde concentration and output voltage

output voltage（Y/V）	formaldehydeconcentration（mg/m³）
0.21	0.449
0.53	1.117
0.80	1.786
1.22	2.679
1.63	3.572
1.84	3.681
2.12	4.688
2.45	5.357
2.66	5.804
2.73	6.093
2.82	6.321

5.2.2 Formaldehyde data processing and analysis

Formaldehyde module adopts serial interface communication mode, the following criteria: 1 stop bit, eight data bits, parity, baud rate to 9600. The module via a serial port to send digital signal by default , send density at intervals of 1 second, the default units is PPM, need to use formula:

$$mg/m^3 = \frac{M}{22.4} ppm \frac{273}{273+T} \frac{Ba}{101325}$$

(M for the molar mass, Ba for the pressure, T for the gas temperature) to convert unit, after simplified,

Testing data multiply 1.25 mg/m³.

Using the least squares fitting to calculate the sensitivity and linearity . A fitting equation of the straight line : $y = kx + b$, one of them

$$k = \frac{n\sum x_i y_i - \sum x_i \sum y_i}{n\sum x_i^2 - (\sum x_i)^2}$$

$$b = \frac{\sum x_i^2 \sum y_i - \sum x_i \sum x_i y_i}{n\sum x_i^2 - (\sum x_i)^2}$$

Number n for the actual measurement data, x for formaldehyde concentration, y is the output voltage, by calculation: $K = 0.4488v/(mg/m^3)$, $b = 0.03298$. By the formal: $\Delta_i = y_i - (kx_i + b)$ calculate the biggest nonlinear error $\Delta L_{\max} = 0.05v$. Fitting curves and residual map are obtained by the above data, as shown in figure 6, shown in figure 7.

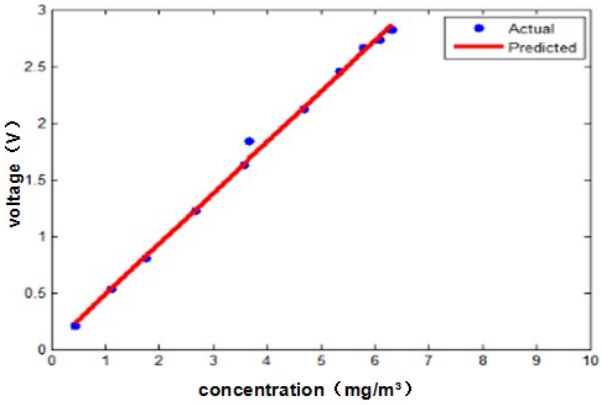

Fig6 the fitting curve

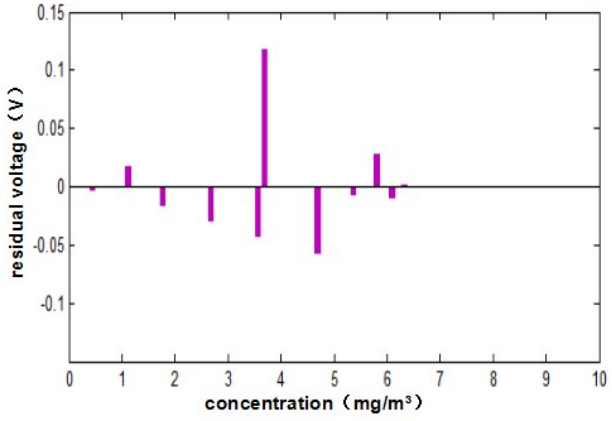

Fig7 the residuals of measured data and the fitting curve

According to the figure above, we can draw a conclusion that System for detecting formaldehyde has good linearity and high sensitivity.

5.3 The experimental contrast

Make monitor system compare with P - 5 l2c type dust meter and JC - 7 high precision formaldehyde monitor. Through the contrast test, results are shown in table 2.

Tab2 the data of contrast test

Serial number	x_1 (mg/m³)	x_2 (mg/m³)	δ_1 (mg/m³)	Y_1 (mg/m³)	Y_2 (mg/m³)	δ_2 (mg/m³)
1	0.021	0.018	0.003	0.449	0.437	0.012
2	0.036	0.032	0.004	1.123	1.109	0.014
3	0.137	0.139	-0.002	2.376	2.389	-0.013
4	0.156	0.157	0.001	3.546	3.530	0.016
5	0.238	0.241	-0.003	4.667	4.652	0.015
6	0.327	0.332	0.005	4.918	4.932	-0.014
7	0.359	0.361	-0.002	5.362	5.349	0.013
8	0.397	0.394	0.003	5.427	5.442	-0.015
9	0.425	0.429	-0.004	5.638	5.629	0.009
10	0.527	0.528	-0.001	5.936	5.921	0.015
δ			0.0028			0.0136
σ			0.0099			0.013

X1, Y1for the system measured PM2.5 and formaldehyde concentration; X 2,Y 2 for P-5L2C dust instrument detection PM2.5 concentrations and JC- 7 for formaldehyde concentration. Known from the analysis of experimental results, and compare with performance of existing PM2.5 monitor and formaldehyde detector on market , the system of PM2.5 and formaldehyde detection accuracy can be±0.3% and±1.3%, detection range is big, can assess the air quality in the current by content, good, light pollution and moderate pollution, severe pollution. And this system is easy to operate, small volume, low cost, suitable for household air quality detection.

6 CONCLUSION

This paper presents a portable design ,which can realize to monitor the indoor air quality remotely.The design uses STC12C5A60S2 micro controller combined with sharp GP2Y1010AU0F dust sensors and ZE08 - CH2O formaldehyde module to detect PM2.5 and formaldehyde in the air, and uses the keyboard to preset threshold, assesses the air quality standards, sets excessive warnings, and uses the GSM network technology to realize real-time monitoring of the indoor air quality, by remote alarm to remind people to take measures to improve indoor air quality and prevent the air pollution pose a threat to health.

References

[1] li ping. The ARM of the indoor air quality monitoring system design [D]. Chengdu: southwest jiaotong university, 2010

[2] Peng Jun. Sensors and monitoring technology [M]. Xi 'an: xi 'an university of electronic science and technology press, 2003.74 95.

[3] zhang qi, Du Qun expensive. Single chip microcomputer application system design technology [M]. Electronic industry press, 2004.117 128.

[4] Deng Guichang. Indoor research and design of intelligent monitor air quality [D]. Jilin: jilin university, 2009

[5] Liu Yujing. Remote monitoring system based on GSM data transmission [J]. Science, technology and engineering, 2007, 7 (9) : 2082-2084209-1.

[6] Liu Song Zhao Zhong, Sun Xuelei. Remote family intelligent monitor control system based on GSM design [J]. Journal of electronic measurement technology, 2009, (1) : 88-91.

[7] Huang Pei li-hong xu, Wang Leda, etc. Room temperature environment based on GSM/GPRS remote monitoring system design [J]. Micro computer and application, 2013, 31 (18) : 45-47.

[8] YuXiaoQing Zhang Zenglin. STC82C5A and GSM based remote monitoring system of irrigation [J]. Water saving irrigation, 2011, (4) : 55 to 57.

[9] He Jinzhi hai-yan MAO, Zhou Guoyun. GSM remote temperature controller design based on single chip microcomputer [J]. Journal of manufacturing automation, 2012 (21) : 138-131.

[10] Jiang Dingguo, bao-guo xu, ming-sheng wang. Based on the GPRS remote monitoring greenhouse control system design [J]. Journal of guangdong agricultural science, 2011, 38 (13) : 160-162.

[11] Zhong Qingyun, support, Qin Huabiao. Wireless pressure sensor water level measurement system based on GSM network design [J]. China instrumentation, 2013, (10) : 19-23.

[12] Chang Chao Hu Ying, etc. Based on the indoor environment monitoring and early warning of WSNs and GSM system design [J]. Journal of sensors and micro systems, 2011, 30 (6) : 141-144.

Research on microwave radiation features of Bullialdus crater area

Xiaoxiao Qiang[1]; Jianghua Li[2]; Nannan Lu[3]; Ying Guo[2]

（1.College of Instrumentation and Electrical Engineering, Jilin University,Changchun 130022,China；2.College of Chemistry Jilin University,Changchun 130022, China, 3.College of Geoexploration Science and Technology,Jilin University,Changchun 130022, China）

***Abstract*--Bullialdus crater as the most representative of the moon crater, the microwave radiation features for analysis rather than the same period in the study of a large crater has important reference value. Based on the Chang 'E 2 microwave radiometer (CELMS) data and Clementine satellite UV-VIS, LOLA LRO satellite data, the system analyzes the space-time distribution characteristic of microwave radiation Bullialdus area. The results show that Bullialdus crater area of lunar surface temperature is the decisive factor of microwave radiation, the region (FeO+TiO2) content, and the correlation of lunar surface slope, roughness and bright temperature**.

***Key words*--Bullialdus crater, microwave radiation, CELMS data**

I. INTRODUCTION

BULLIALDUS crater is located in a lunar crater in the west of Mare Nubium and its higher outer edge is rounded.

Microwave radiometer is one of the important load of Chinese Chang-E series of satellites, CELMS data gets multiple coverage of the surface of the Moon is the lunar soil with microwave radiation features of the most effective tools [1]. Radicals such as CHAN Chang-E CELMS, first satellite data, preliminary analysis of microwave radiation features of the full Moon. Therefore, this research base CELMS, Chang-E 2's data, analysis of the Bullialdus crater and its sputtering carpet area microwave spatio-temporal change features of thermal radiation combined with the surface composition and terrain data, microwave radiation causes exception on the region were discussed.

II. DATA ANALYSIS AND PROCESSING

A. CELMS Data

Chang-E 2 CELMS detection frequency of 3.0GHz, 7.8GHz and 19.35GHz and 37.0GHz, observation Angle 0°, resolution 0.5K [2], observed from October 2010 to May 2011. The brightness temperature data after system calibration and geometric correction, the PDS(Planetary Data System) standard format for storage, separate 2 C-level data and a header file consists of a set of observations, observations including observations, four-channel temperature value, Sun elevation angle, azimuth angle of the Sun, longitude, latitude, altitude and the quality of data [3].

B.LOLA's LRO satellite data

Based on LOLA data, roughness calculation method by Smith [4] and Rosenburg gradient calculation methods [5] calculated CELMS data with high accuracy wavelength scale of surface gradient and roughness information.

In the study, the use of data download at http://pds-geosciences.wustl.edu/missions/lro/lola.htm. Taking into account the spatial resolution of 0.25°×0.25° CELMS data. And there is plenty of surface roughness and slope data to a range of CELMS data. Here, CELMS is using data only within the scope of the average surface roughness and slope data.

C. Clementine's UV-VIS satellite data

(FeO+TiO2) content is one of the important factors lunar regolith microwave radiation. Based on 750 nm UV-VIS Clementine satellite data, we made Bullialdus crater region image (Fig 2 (a)).Based on UV-VIS data and Lucey model and improved Lucey model [6], we made Bullialdus crater region (FeO+TiO2) content distribution (Fig 2 (b)).Figure 2 shows, Bullialdus crater (FeO+TiO2) content differentiation significantly. Northeast area (FeO+TiO2) content is generally higher (S20.5°, W19.5°) the highest, the lower southwest area (FeO+TiO2) content.

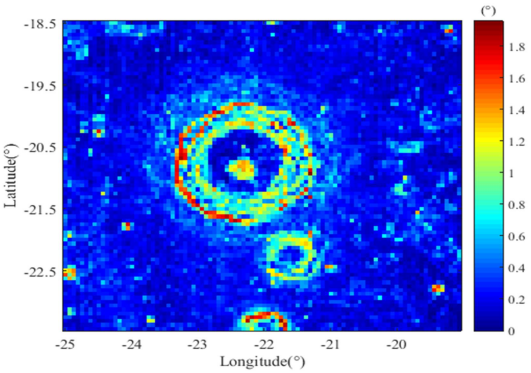

(a)

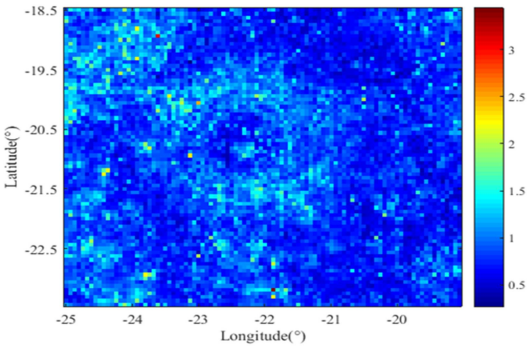

(b)

Fig.1 Surface slope (a) and roughness (b) distribution of Bullialdus area

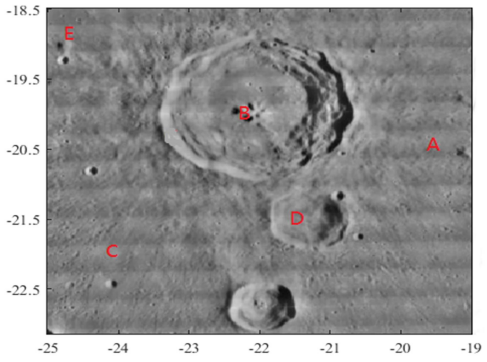

(a)

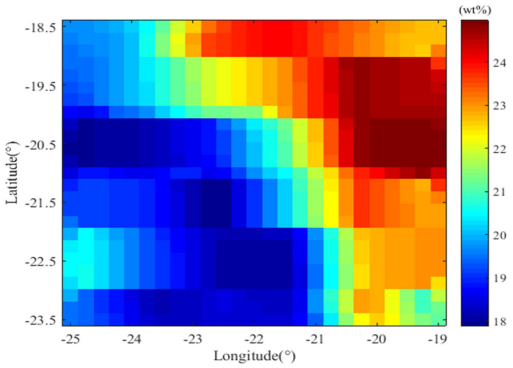

(b)

Fig.2 Remote sensing image (a) and (FeO+TiO2) distribution of Bullialdus area (b)

Combining Bullialdus region of image and terrain, (FeO+TiO2) content data, we selected four typical areas (A-E) for studying the microwave radiation features of the region. Among them, in the eastern crater, a maximum (FeO+TiO2) content, slope surface roughness is small. B is located in the central crater. (FeO+TiO2) content and surface roughness is small, large slope C is located in the southwest of crater direction. D is located in the south of smaller crater central hole, (FeO+TiO2) content, surface roughness and the slope is small. E, northwest of the crater (FeO+TiO2) content, surface roughness and the slope is small. C and A similar slope and roughness, to analyze the impact (FeO+TiO2) content on the brightness temperature. Area B and D (FeO+TiO2) content, roughness, to analysis the influence of the temperature gradient of light. E and C (FeO+TiO2) content and slope are similar, to analyze the influence of roughness of bright temperature.

III. MICROWAVE RADIATION FEATURE

A. The space distribution features

Here, we use a noon (Fig. 3) and mid-night (Fig. 4) of the brightness temperature distribution in the study area. Noon is the highest surface temperature of the day, the greatest moment of solar irradiance, the corresponding microwave bright temperature reflects the soil heat absorption and microwave radiation ability. Mid-night is the lowest surface temperature of the day, microwave brightness temperature corresponding reflected microwave radiation features of lunar soil inside.

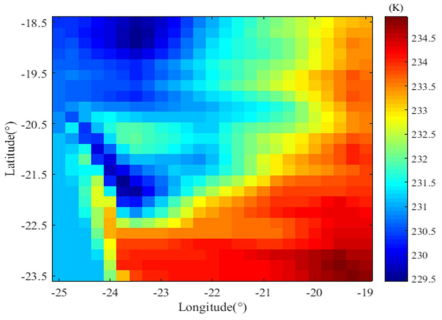

(a) 3.0GHz

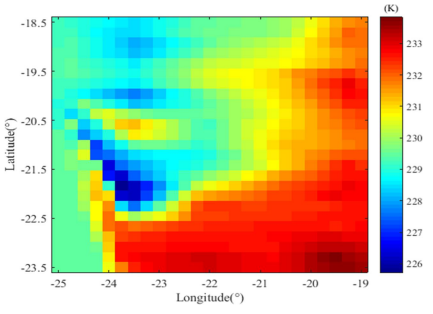

(b)7.8GHz

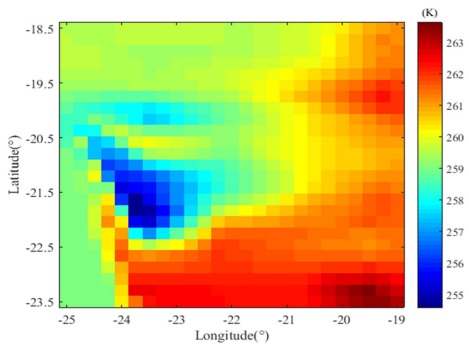

(c)19.35GHz

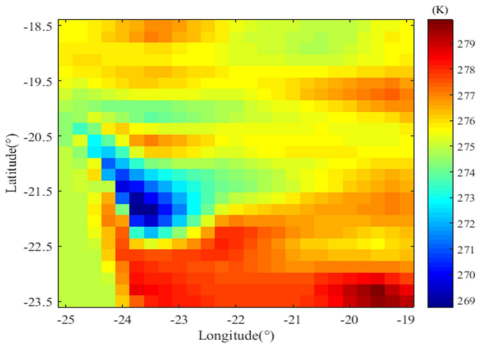

(d)37.0GHz

Fig.3 Brightness temperature distribution of Bullialdus area at noon

Figure 3 is a brightness temperature distribution in noon Bullialdus. Figure 2 shows that Bullialdus area of brightness temperature clearly divided into three parts. South-eastern and southern regions (including A), high brightness temperature. And the low temperature region northwest of crater (including E).And the crater and its low temperature zone in the southwest region (including B, C, and D). With increasing frequency, low temperature northwest region (including E) of the brightness temperature increases, impact craters low brightness temperature region (including B) brightness temperature increases, the Southeast and Northeast regions (including A) highlighted temperature region in the area of reduced. A comparison of C and it seems that we can draw (FeO+TiO2) content is positively correlated with the brightness temperature. But this, paradoxically, with the central and southern terrain A similar impact craters are showing temperature highlight. With increasing frequency, B in brightness temperature increases, but other steep slope areas, but did not show an increasing trend brightness temperature. At low frequencies, brightness temperatures of C and E are similar, but with increasing frequency, E's brightness temperature increased, the brightness temperature of C did not change significantly, indicating that as the frequency increases, the effects of surface roughness on the brightness temperature increasing.

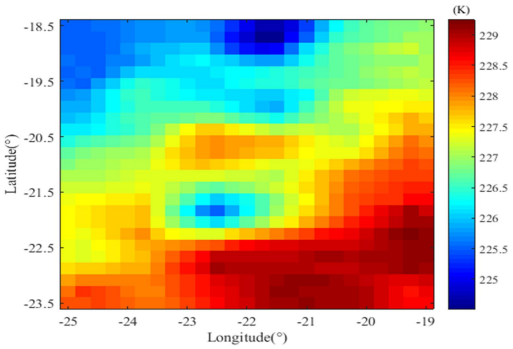

(a)3.0GHz

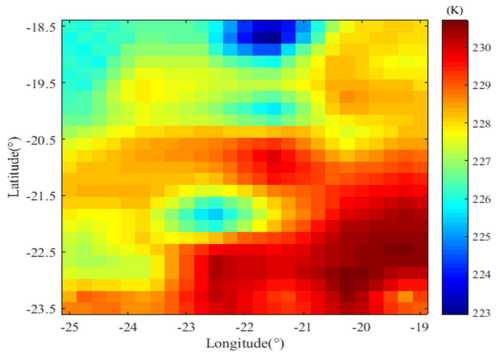

(b)7.8GHz

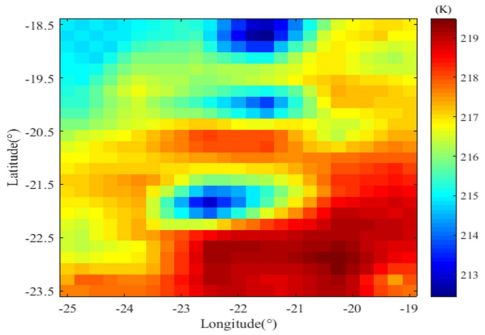

(c)19.35GHz

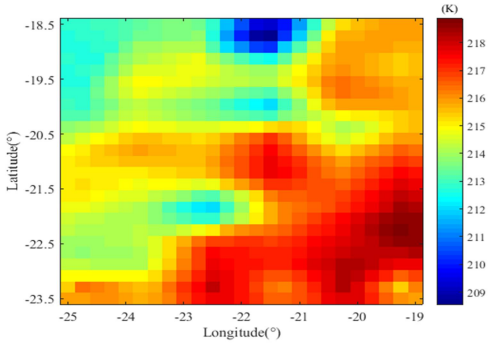

(d)37.0GHz

Fig.4 Brightness temperature distribution of Bullialdus area at dawn

Figure 4 is brightness temperature distribution of Bullialdus region at midnight moment. Figure 4 shows the distribution of brightness temperature midnight Bullialdus region of space. There are significant differences with the noon time, indicating that the zone of the solar radiation brightness temperature distribution of a greater impact. At low frequencies, most of the southern region is presented to highlight

the temperature, the maximum brightness temperature still appears in the southwest corner. An area is still the highlight zone. B, D and E area is still low brightness temperature zone. C area becomes high brightness temperature zone. As the frequency increases, crater north of brightness temperature increased, the southwest (including C) decrease in brightness temperature. Low brightness temperature area of Area D is located in the reduced and the brightness temperature increase (S18.5°, W22.5°) area of low brightness temperature changed little.

Figures 3 and 4 show, an area belonging to the highlighted area temperature, noon and midnight brightness temperature are high. B, D, E area belongs to the low brightness temperature region, noon and mid-night brightness temperatures are relatively low, but with increasing frequency, brightness temperature area in brightness temperature decreases or increases. Area C apparent brightness temperature anomaly distribution, noon and midnight brightness temperature characterization inconsistent, and midnight brightness temperature values greater frequency correlation.

B. The same frequency brightness temperature changes of different time

Regolith depth below a certain temperature is constant, the surface temperature of the lunar soil by solar radiation, greatly affected lunar soil composition. Therefore, the temperature difference between day and night light conditions at the same frequency value is within a certain depth range of lunar soil temperature and composition direct performance features [11].

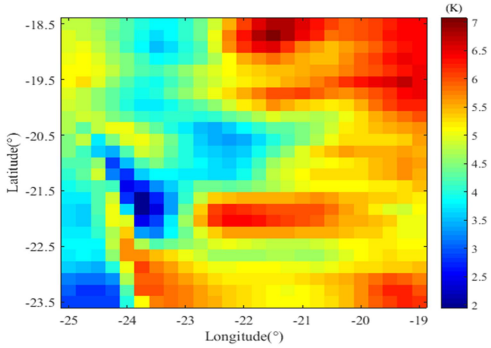

(a) 3.0GHz

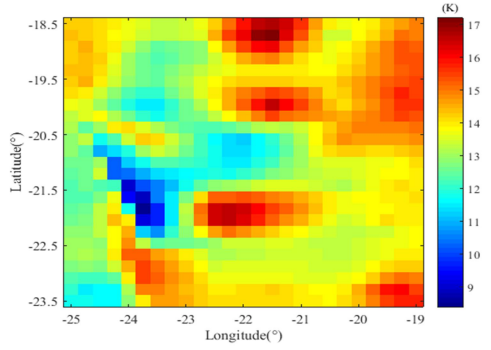

(b)7.8GHz

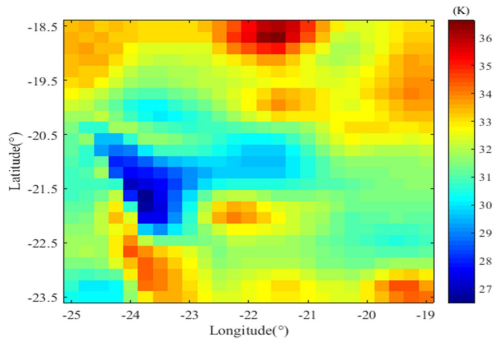

(c)19.35GHz

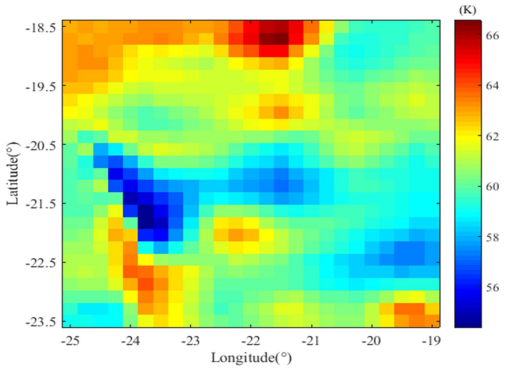

(d)37.0GHz

Fig.5 Distribution of brightness temperature difference between noon and dawn at Bullialdus area

Figure 5 is a region at different frequencies Bullialdus noon and midnight moments of brightness temperature difference value distribution. Figure 5 shows brightness temperature varies greatly with the frequency dependency. In general, with increasing frequency, brightness temperature difference inside and outside the crater uneven distribution in increased brightness temperature difference increases rapidly in value. For example, area A, 3 GHz when the brightness temperature difference of about 5.5 K, brightness temperature difference increases with increasing frequency, in the 37GHz brightness temperature difference of 61 K to dump. Diurnal variation of brightness temperature is very large, indicating that the crater area at noon by the strong solar radiation, brightness temperature contribution mainly from solar radiation, temperature difference between day and night light large, and the higher the frequency, the more obvious by the effects of solar radiation, the temperature difference between light The larger. Diurnal variation of brightness temperature area C is very small, indicating that the area affected by the brightness temperature distribution of solar irradiance is very small, and the brightness temperature at different frequencies similar distribution area C, a combination of different frequency of the microwave signal in the lunar regolith penetration, indicating that the structure of the lunar soil of the region in the vertical direction is not changed.

C. At the same time different frequencies of light temperature changes

Different frequency microwave signal penetration depth in the lunar soil. With the increase in penetration depth, brightness temperature under the influence of solar radiation, the terrain decreases, increasing under the influence of composition and other factors. Therefore, the observed brightness temperatures of the different frequency same time difference reflects the lunar body part most affected by solar radiation temperature and microwave radiation.

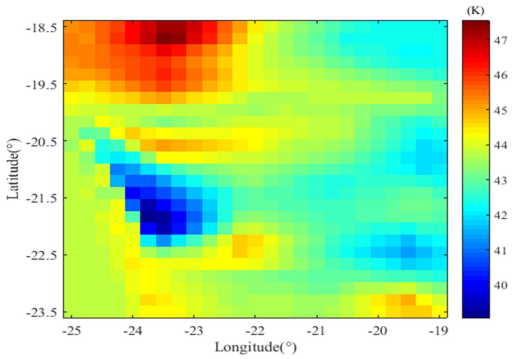

(a)

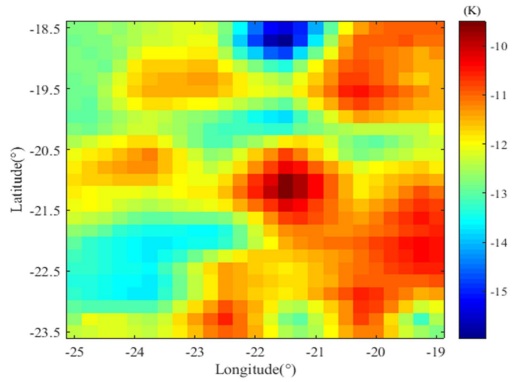

(b)

Fig.6 Distribution of brightness temperature difference between 3GHz and 37GHz at Bullialdus area: (a) noon, (b) dawn

Figure 6 is the same time Bullialdus area 3 GHz and 37 GHz brightness temperature difference distribution. Figure 6 shows that, at noon time brightness temperature difference of 40K, much higher than in the morning time; combined radiative transfer simulation [7], indicating that the temperature difference between the noon time lunar soil surface and deep than in the morning time. In Bullialdus region, wherein a noon time zone brightness temperature difference is 44k, midnight time brightness temperature difference values -10k; B, noon and midnight time brightness temperature values of 43k and -13k. C District noon and midnight brightness temperature values were 40k and -13.5k. D area were 42k and -11k. E region respectively 45K and -12K. Noon and midnight moment in time the regional brightness temperature differences at different frequencies are large and the difference is very small, indicating that the region noon time lunar soil surface and deep large temperature difference, and the difference in temperature in the morning time of lunar soil surface and deep is small, the study regional lunar regolith microwave radiation that is great lunar temperature.

Ⅳ THE IMPACT ANALYSIS

A. (FeO+TiO2) content

The main elements of the abundance of the lunar surface, especially the abundance and distribution of iron-titanium and other elements for the analysis of the radiation characteristics of the lunar surface, divide the lunar surface rock types, geological interpretation of the area has an important role in evolution [8].

Figure 2 shows that, (FeO+TiO2) content distribution specific of area Bullialdus obvious that the northeast high, southwest low. Comparative results Figures 2, 3 and 4 results show that Bullialdus brightness temperature in the area of distribution (FeO+TiO2) independent of the distribution of content. North of the study area (FeO+TiO2) of regions with higher levels without corresponding highlight temperature distribution. Southern high noon, evening brightness temperature of the place, (FeO+TiO2) content is very low. This shows that, (FeO+TiO2) content in the distribution of brightness temperature zone is very small.

B. Terrain factors

At present, the slope and terrain roughness for representatives of more and more attention to the effects of microwave radiation [7, 8]. Slope and its shadow will directly influence the form of the physical distribution of temperature, thereby affecting its microwave brightness temperatures [12]. Roughness is directly changed the microwave emissivity of lunar soil [9].

Figure 1 (a) shows that Bullialdus crater Central and the size of the edge of the pit slope maximum, and the variation. In addition, hit the slope changes little in other areas in the study area, flat. Comparative results show that B D impact on the brightness temperature gradient is very small.

Figures 3 and 4 show, E and B areas noon and midnight time brightness temperature and the surrounding area has no significant difference, indicating that the effect of surface roughness on the brightness temperature is small, but the contrast E and C showed that with increasing frequency impact of roughness on the brightness temperature increases.

Ⅴ CONCLUSION

The results show that, Bullialdus crater area, noon and midnight brightness temperature distribution significantly different, and the brightness temperature difference values at different times of the same frequency and the same time the temperature difference between different frequencies of light are large, indicating that microwave radiation characteristic of the region affected by the lunar surface temperature greatly influence the surface temperature (or solar irradiance) is in the area of microwave radiation, the decisive factor. Overall, (FeO+TiO2) content of the lunar surface slope, roughness and brightness temperature less relevant, not enough to significantly affect the distribution of brightness temperature, as the frequency increases, the impact of roughness on the increase in brightness temperature.

Meanwhile, the study found little change in brightness temperature interdiurnal area C, indicating that the area affected by the brightness temperature distribution of solar irradiance is very small, and at different frequencies zones C brightness temperature distribution is similar to a combination of different microwave frequencies signal in the lunar soil penetration, indicating that the structure of the lunar soil of the region in the vertical direction is not changed.

References

[1]. Jin Yaqiu, Yan Fenghua, Liang Zichang. Simulation for remote sensing of the lunar soil and rock by using multi-channels microwave radiometers. [J] Chinese Journal of Radio Science, 2003, 18(5): 477-486.

[2]. Zheng Y C, Tsang K T, Chan K L, et al. First microwave map of the Moon with Chang'E-1 data: The role of local time in global imaging.[J] Icarus, 2012, 219:194-210

[3]. Jiang Jingshan , Wang Zhenzhan , Zhang Xiaohui, etc. China Probe CE -1 Unveils World First Moon -globe Microwave Emission Map — The Microwave Moon Some Exploration Results of Chang'E -1 Microwave Sounder. [J] Remote Sensing Technology and Application., 2009

[4]. Smith D, Zuber M, Jackson G, et al. The Lunar Orbiter Laser Altimeter investigation on the Lunar Reconnaissance Orbiter mission. [J] Space Sic Rev, 2010, 150(1): 209-241

[5]. Rosenburg M A, Aharonson O, Head J W, et al. Global surface slopes and roughness of the moon from the Lunar Orbiter Laser Altimeter. [J] Geophys Res, 2011, 116(E2): E02001.18

[6]. Lucey P G, Blewett D T. Lunar iron and titanium abundance algorithms based on final processing of Clementine ultraviolet-visible images. [J] Geophys Res, 2000, 105(E8): 20297-20305

[7]. Meng Zhiguo, Ping Jinsong, Alexander GUSEV, etc. Research on Microwave Emission Features of Mare Orientale Using CELMS Data.[J] Journal of Deep Space Exploration, 2014, 3(1)

[8]. Meng Z G, Chen S B, Lu P, et al. Research on the Distribution and Content of Water Ice in Lunar Pole Regions Using Clementine UV-VIS Data. [J] Earth Sic, 2011, 22(5):595-600

[9]. Vasavada A R, Paige D A, Wood S E. Near-surface temperature on Mercury and the Moon and the stability of polar ice deposits. Icarus, 1999, 141:179-193

[10]. Li Xiongyao, Wang Shijie, Cheng Anyun. A Review of Lunar-surface Temperature Model [J] Advances in Earth Science. 2007, 22(5)

[11]. Fa Wenzhe, Jin Yaqiu. Inversion of lunar regolith layer thickness using microwave radiance simulation of three layer model and clementine UV-VIS data. Chin. [J]. Space Sci., 2007,27(1): 55-65

[12]. Florinsky I V, Kulagina T B, Meshalkina J L. Influence of topography on landscape radiation temperature distribution. Int [J] Remote Sens, 1994, 15(16): 3147-3153

Driverless car auto parking system design

Yang Botao

(1College of Instrument Science and Electrical Engineering, Jilin University, Changchun 130022)

***Abstract*--Automatic parking system is a kind of system which use the detected information about the surroundings of the vehicle to find a suitable parking spaces, by control the steering and speed, the system can lead the vehicle into parking automatically. Compared with frequent bruise artificial parking and the heavily driver relied common reversing radar, automatic parking system don't need the driver to operate ,avoid miss moves ,can improve the safety of the vehicle when parking, effectively reduce the difficulty parking vehicles for the drivers. Designed system in this paper realize the tracking, obstacle avoidance, automatic parking function by get traffic information from the sensors such as CCD camera, ultrasonic probe, infrared tube, and using microprocessor system build by freescale K60 to control the speed and direction of the motor.**

***Keywords*--Automatic parking automatic control K60 ov7620 camera**

I. INTRODUCTION

IN daily life, the reasons of vehicles damage for the most part, is not traffic accidents, but scratches when parking. Transportation research institute at the university of Michigan's Paul Green's research shows that according to the statistics from traffic accident database and insurance company, 44% of the accidents were happened when parking, among that about 1/2 to 3/4 of the parking collision is caused by failure of reverse[1]. Through the research of the automatic parking technology, the process of parking will be controlled automatically, may solve the parking problem in densely populated urban area to some extent. In the process of the automatic parking , there is no need for driver's operation, which will effectively make the novice drivers easier for parking and reduce property damage brought by misoperation.

II. RESEARCH STATUS

Automatic parking system has been regarded as a popular product using on the next generation of cars.

In 2003, Toyota began to provide intelligent parking assist system as a custom function on their product, Prius hybrids. This function only need the driver to move his car to the front of the location and slam on his brake when parking, electric control system will automatically work according to the designated parking location, guide the vehicle to the parking position.

In the spring of 2007, Citroen C4 Picasso equipped with Bosch parking measurement system. When the driver need for parking, just press the control button on center console, parking measurement system will open. The system can timely notify the driver if the length of parking Spaces is appropriate for the vehicle and will alarm when there are obstacles.

III.THE HARDWARE DESIGN

The hardware design mainly includes the power module, motor module, CCD sensor module, control system[2], infrared tube module and ultrasonic ranging module.

The design of the overall block diagram is shown in Fig 1:

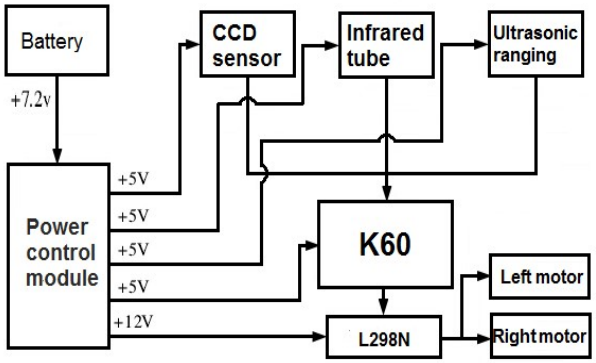

Fig.1 The overall block diagram module design

A. Power Control Module

This project use 7.2 v2000mAh nickel-cadmium battery, through the power control module to form the required voltage. Power module 5 v / 3.3 v part are shown in Fig 2 below:

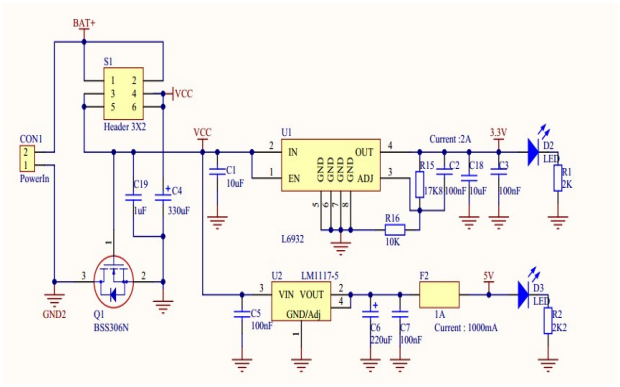

Fig.2 5v/3v voltage stabilizing circuit diagram

Power module 12v part are shown in Fig 3 below:

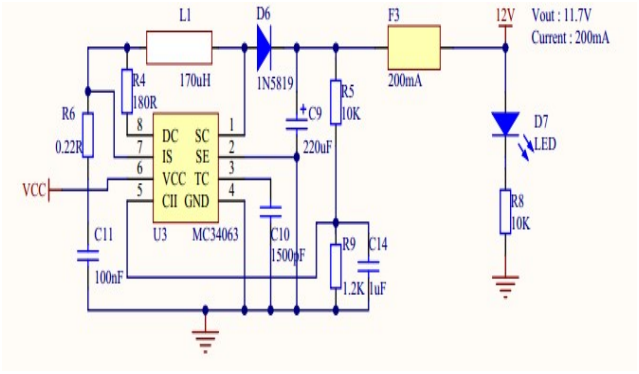

Fig.3 12v voltage stabilizing circuit diagram

The voltage specification required and functions for each device are showm in table 1.

TABLE 1

each device voltage required and its function

Device	Voltage	Function
CCD sensor	5V	Get black line information
Infrared tube	5V	Get obstacles information
Ultrasonic ranging	5V	Get rear distance information
K60	5V	Information processing and control
L298N	12V，5V	Motor control

B. Motor Module

The L298N driver module can drive two dc motor, the ENA. ENB will be effective when high level of voltage input. The two motor are controlled respectively, when there is a speed difference, the car steering.

Driver module circuit diagram are shown in Fig 4 below:

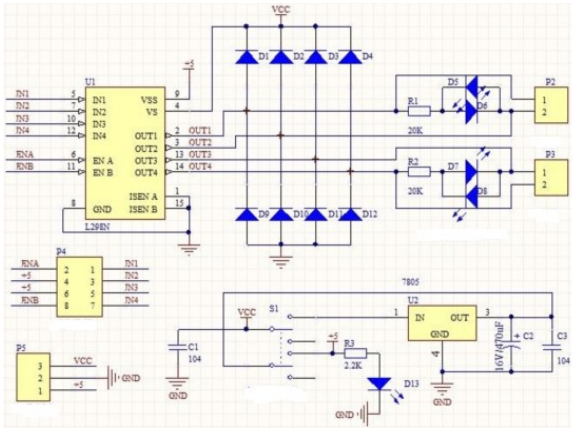

Fig.4 L298 motor driver circuit diagram

C.CCD Sensor Module

CCD sensor module is mainly composed of CCD sensor and LM1881 video decoding chip. It is the signal acquisition unit of the smart car control system.

OV7620 is a highly integrated high resolution (640x480) Interlaced / Progressive Scan CMOS digital color / black & white video camera chip. The digital video port supports 60Hz YCrCb 4:2:2 16Bit / 8 Bit format, ZV Port output format, RGB raw data 16Bit/8Bit output format and CCIR601/CCIR656 format. The built-in SCCB (Serial Camera Control Bus) interface provides an easy way of controlling the built-in camera functions[7].

The LM1881 Video sync separator extracts timing information including composite and vertical sync, burst/back porch timing, and odd/even field information from standard negative going sync NTSC, PAL and SECAM video signals with amplitude from 0.5V to 2V p-p. The integrated circuit is also capable of providing sync separation for non-standard, faster horizontal rate video signals[8].

The vertical output is produced on the rising edge of the first serration in the vertical sync period. A default vertical output is produced after a time delay if the rising edge mentioned above does not occur within the externally set delay period, such as might be the case for a non-standard video signal.

Manually adjust the focal distance, direction and pitching angle of OV7620 camera to determine the scope of the whole image capture. After the image captured by the camera and converted by the AD converter inside, the data was transmitted to LM1881 decoding chip to decode, deliver to K60

microcontroller in final.

D. The Infrared Tube

The sensor has a pair of infrared transmitting and receiving tube, the tube launch infrared in a certain frequency, when meet with obstacles or reflecting surface in the detecting direction, the reflected infrared will be receive by receiving tube, after the comparator circuit processing, signal output interface and output a low level signal. The detection distance can be adjusted through the potentiometer knob, effective distance range 2 ~ 30 cm, detection of 35 ° Angle.

For obstacle avoidance, infrared tube first send the signal, with the transmitting distance increase the signal gradually decay, if there are any obstacles, the infrared reflection will be form. When the reflected signal is weak, the photodiode L2 receives the weak infrared, voltage comparator LM393 3 feet higher than 2 feet voltage, receiving test pins output high level; When the reflected signal is strong, receiving test pins output low level.

Infrared tube circuit diagram is shown in Fig 5 as follows:

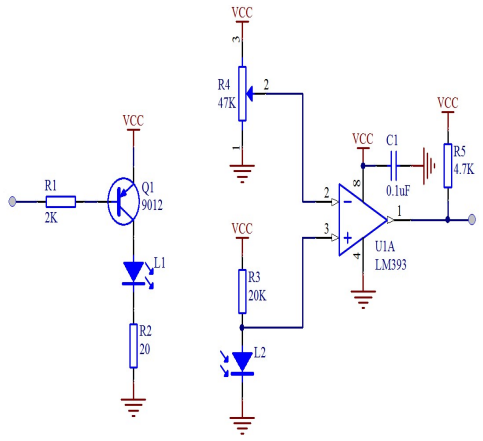

Fig.5 infrared tube circuit diagram

E. The Ultrasonic Ranging Module

HC - SR04 ultrasonic ranging module can provide 2 cm - 400 cm non-contact distance measurement function, ranging accuracy can be up to 3 mm.The module includes ultrasonic transmitter, receiver and control circuit.

Ultrasonic ranging basic principle: Using IO port TRIG ranging trigger, give 10 us high level signal; Module automatically sent eight 40 KHZ square wave, automatically detect whether there is signal return; When a return signal received, through IO mouth ECHO output a high level.

IV. Software Module Design

CONTROL system software structure is mainly divided into: system initialization module, a CCD data acquisition processing module, ultrasonic distance measurement control module, the infrared obstacle avoidance control module and path identification module and motor control module[3~6].

Software system diagram as shown below:

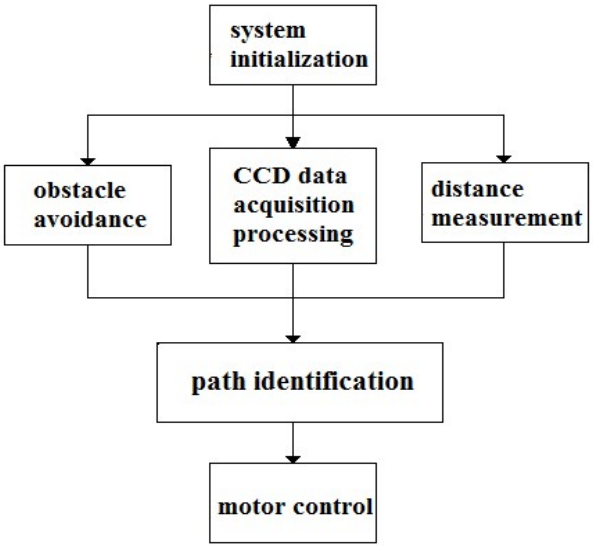

Fig.6 software block diagram

The main function of the main program is MCU initialization, image filtering algorithm, black line extraction algorithm and motor driver control algorithm.

Initialization algorithm mainly includes initialization, PWM signal timing interrupt initialization, AD conversion module initialization and initialization of an external interrupt.

A. The CCD Data Acquisition Processing Module

Images get by CCD camera will be sent into K60 microcontroller after AD conversion, LM1881 chip decoding. The image will be used for black line recognition after binarization. The first step of the process is the selection of appropriate threshold, with the threshold image segmentation into two parts, the pixel value greater than or equal to threshold set as gray = 255, pixel value less than the threshold set as gray = 0, the resulting image is a black and white images, the images can be clearly displayed.

Black line recognition program is used to extract the right side of the image after binarization for

tracking based on camera capture range. Calculate number of pixel gray value buy 255 in selected range , when the car parallel to the black line, the number of pixels gray = 255 set as balance value. When the car is running, proceed calculation and compare the results with threshold, if the ratio is less than 1, means car body is closing the black line, the ratio is greater than 1,the car body is getting away from the black line. According to the black line recognition program to control the car.

B. The Infrared Obstacle Avoidance Control Module

According to the signal from the infrared tube in front of the infrared tube On the right side of the car, infrared obstacle avoidance control module j udge the Obstacles bearing and give a traffic condition judgment.

Obstacle avoidance schemes as shown in table 2:

Table 2

Obstacle avoidance scheme

Front input	Right input	Control
Low	Low	tracking
Low	High	Slow down and Go straight
High	Low	Slow down and turn left
High	High	Slow down and turn left

C. The Ultrasonic Ranging Control Module

Ultrasonic ranging control program based on ultrasonic sensor outputs high level time, according to the formula (1) to calculate the distance from backward, according to the designed distance(10 cm to 20 cm)to guide the parked.

$$L = 1/2\ c * T \qquad (1)$$

Type: L for the distance; C for ultrasonic velocity; T time for high level.

D. The Motor Control Module

Motor control module through the PWM signal to control the motor drive, the initialization mainly includes: ban PWM, PWM channel using, use the crystal frequency, choose the polarity, select alignment mode, programming on duty ratio and the sampling period.

By adjusting the duty cycle of PWM output signal to adjust the motor speed.

$$\text{Actual power} = \text{duty cycle} * \text{total power.} \qquad (2)$$

Motor control module control method and dc motor status are shown in table 3 below:

Table 3

The control method and motor status

ENA	IN1	IN2	Motor
0	X	X	stop
1	0	0	brake
1	0	1	forward
1	1	0	backward
1	1	1	brake

V. THE RESULTS

A. Tracking

The car move along the black line on the right side of the simulated road ,rely on the CCD data acquisition module for keeping distance with black line and tracking.

Tracking results are shown in Fig 7.

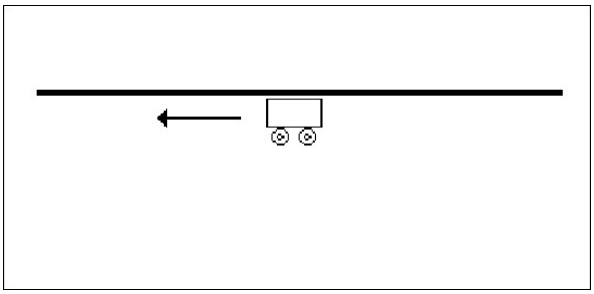

Fig.7 tracking

B. Obstacle Avoidance

When the car is nearing the obstacle in front of it, the infrared tube in front will output high level, inform the obstacle avoidance module to control the car to slow down and turn left;

When the left turn at a certain angle, the front infrared tube output low level, the right infrared tube output high level, the car go straight at low speed. When the front infrared tube and the right infrared tube both output low level at same times, according to tracking program, the car will move to the right.

If the car is already over the obstacles, the infrared tube's output will not change, the car get into the tracking mode.

If the car is not yet over the obstacles, according to the obstacle avoidance process, the tracking process will not start until the car is over the barrier.

Obstacle avoidance effect is shown in Fig 9.

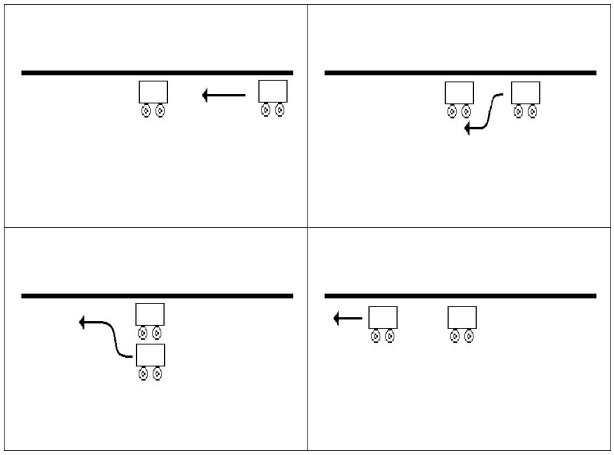

Fig.8 obstacle avoidance

C. Automatic Parking

The car move along the black line by tracking, when get close to the vehicle ahead the parking process start, the ultrasonic module get into operation. The obstacle avoidance module control the car to slow down and turn left to pass. According to the obstacle avoidance process ,the car won't stop moving until completely pass.

By tracking process, the car make it's direction to the right side of the road ,get close to the black line approximately . The ultrasonic detection module measures the distance and guide the car to park, the car stopped when distance at a specified range.

Automatic parking effect is shown in Fig 10.

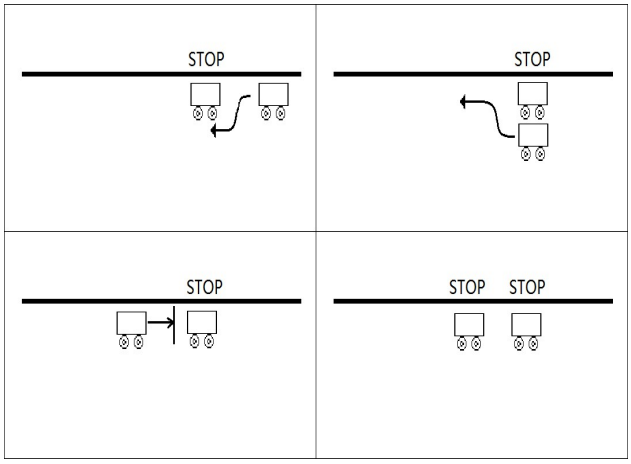

Fig.9 auto parking

VI. CONCLUSION

In the design of automatic t car parking system, it's hardware design use CCD camera to get road image, LMl881 chip to separate video signal, K60 chip as the control core. On the software ,adopts the black line processing algorithms to extract the path information.

Through simulation test of the car model, the system can realize automatic parking function, has a certain practical value.

References

[1] Paul Green. Parking Crashes and Parking Assistance System Design：Evidence from Crash Databases，the Literature and Insurance Agent Interviews． SAE World Congress，2006，1：1 685～1 700

[2] Ke Qiyan, Que Dashun, Yang Jintao, LU Wei. Design of an Intelligent Vehicle Tracking System Based on the Edge Detection Algorithm [J]. Electrical Automation, 2014,(3):48-50.DOI:10.3969/j.issn.1000-3886.2014.03.017.

[3] Li Xingze, Wang Fuping. Microcontroller-based control system of automatic tracking parking [J]. Microcomputer & its Applications, 2013,32(15):96-97,101.DOI:10.3969/j.issn.1674-7720.2013.15.031.

[4] Liu Jian-gang, Cheng Lei, Huang Jian, Zhang Zheng. Design of Smartcar's HCS12 MCU Control System Based on CCD Image Recognition [J]. Electro-Optic Technology Application,2007,22(6):52-55,59. DOI:10.3969/j.issn.1673-1255.2007.06.014.

[5] Hua Wen, Yu Bin, Weng Hua. Discrimirate Blackline Algorithm Based on CCD Camera [J]. Electronic Engineering & Product World,2009,16(1):103-105. DOI:10.3969/j.issn.1005-5517.2009.01.043.

[6] Lei Jun, Li Fengbo. Design of Autotracking Smart Car Control System Based on Camera [J]. Journal Of Suzhou University(Engineering Science Edition), 2010,30(2):49-52.DOI:10.3969/j.issn.1673-047X.2010.02.012.

[7] Quan Xiaofei, Li Weiguo, Wang Lili. The image acquisition system based on OV7620 research [J]. wuxian hulian keji,2015,(13):142-144. DOI:10.3969/j.issn.1672-6944.2015.13.068.

[8] Ge Yaming, Liu Tao, Wang Zongyi. Video sync

separator LM1881 and its application [J]. Applied Science And Technology,2004,31(9):20-22. DOI:10.3969/j.issn.1009-671X.2004.09.009.

Program design of material sorting system based on PLC and touch screen

Wang Qian

College of Instrument Science and electrical engineering, Jilin University,Changchun 130000,China)

***Abstract*--Automatic sorting system is a key factor to improve the efficiency of logistics distribution, and it has become an indispensable part of the large and medium-sized logistics center in developed countries. The thesis bases on the Tianhuang THJDME-1 light mechanical and electrical integration training device and designs three kinds of material sorting system software and a touch screen interface, gives the design of ladder diagram and state transition diagram, realize the automatic and manual control. After running the test, the design of the program can make the training device to achieve the correct sorting, verify the correctness of the program design.**

***Key words*--PLC material sorting , touch screen**

I. INTRODUCTION

WITH the development of society, market compete increasingly fierce , therefore, the production enterprises urgently need to improve the backward production technology, to improve the efficiency. In the United States, Japan, Germany and other developed countries, it shows the characteristics of increasingly high degree of automation in the application of sorting system.The sorting machine of the application is quite common in cosmetics manufacturing industry,Chain commercial industry automatic and medical industry.

In our country, the research of material sorting system is relatively late, and many of them are artificial sorting, which lead to low production efficiency, high cost and poor competition ability of enterprises. Nowadays, all kinds of enterprises, the degree of automation is getting higher and higher, the automatic sorting of materials has become a necessary choice for enterprises.[1-2]

As a new computer input device, touch screen is also a favorite of mechanical automation production. It is the most simple, convenient, natural way of man-machine interaction and a multimedia message or control a face lift equipment, greatly optimized the use of computers. From the industrial production, the touch screen is a great place to automatically work, and accurately realize the human-computer interaction, to bring convenience to the industry.[3-5]

Based on the design of THJDME-1 type Tianhuang company electromechanical integration training device has three types of material automatic sorting system. The material sorting system is divided into a warning lamp mechanism, a feeding mechanism, a mechanical mobile phone structure and a sorting mechanism, and a touch screen. The three phase motor drives the material conveyor belt, and the frequency converter controls the frequency of the conveyor belt. For three kinds of materials - metal materials, white nylon material, black nylon material sorting, material handling and sorting to three materials warehouse.

II.CONTROL REQUIREMENTS AND DESIGN PLAN

A.Control requirements

Stand by status, the warning lights are red lights. Press the start button, the red light goes out, the green light is on, the system has already begun to work. If the entrance do not detected material after three seconds ,the yellow light shining. if there is material ,the yellow light go out.

Feed mechanism sensor detects the material after a second, cylinder control metal rod to launch material, pause one second after retraction.

The manipulator detected material in the reference point , the material is transported to the conveyor belt .The manipulator returned to the original place, waiting for the next material in place, repeat the above action.

A conveyor belt detected to have a material, the material is traveling to the library 1 and detected, the metal material into the library. When other materials pass by the library 2, is detected color.White material is Imported into library2 by guide cylinder and black is into library3.

B.Design plan

Using the MITSUBISHI FX2N series PLC, through the developer GX from the warning light system, feeding system, manipulator system, sorting system to design program.

Using OMRON NP5MQ001B touch screen in the NP-Designer software design touch screen interface, connected to the system.

The system can be used to realize the control of the system operation, but also through the touch screen to control and monitor the working state of the system.

III. HARDWARE EQUIPMENT

Fig.1 Schematic diagram of equipment

A.Feeding and Warning Light System

Main functions: warning lamp can display equipment is in working state, have material or not; material can be introduced, so that the manipulator to pick up and delivery.

Main configuration: photoelectric sensor, single-phase electric control valve of pushing cylinder, warning lights, well type workpiece Library.

B.Manipulator System

Main function: grab materials from the storage table and transported to the sorting machine by the cylinder and stepper motor activities.

Main configuration: bi directional control valve control valve, pneumatic valve control rod cylinder, inductive sensor, magnetic sensor, stepper motor and driver.

C.Sorting System

Main functions:sort the white nylon, black nylon, gray metal material.

Main configuration: electric sensor: inductive sensor, optical fiber sensor, material library, one way electric control valve to control the feed and feed cylinder to the corresponding bit, conveyor belt, three-phase asynchronous motor, SIEMENS inverter.[6-7]

D.Other Equipment

PC,Mute pump

E.Touch Screen

This project uses the OMRON NP5MQ001B to cooperate with MITSUBISHI FX2N series PLC to realize the control function. The schematic diagram of the touch screen is shown in Figure 2.

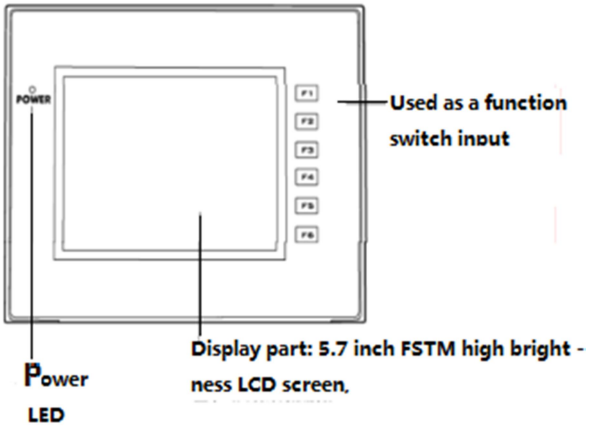

Fig.2 NP5MQ001B touch screen host

Installation of the touch screen: embed the main body of the NP operating disk installation, installate metal parts from the back of the panel. Power supply input terminal to access DC24V.

Start of touch screen: the first time to confirm the back of the sliding switch SW1 is located on the right side (OFF). The main power switch on the NP, positive LED lighting, NP main start. The display part displays the name, date and time series. Confirm the date and time is correct. Set the date and time of the system menu. Start the system menu, please turn off the power, will be on the back of the sliding switch SW1 on the left side (ON), and then switched on again.

When the picture data is downloaded to the NP main body:the confirm the back slide switch SW1 is located on the right side (OFF).The main power switch on the NP, positive LED lighting, NP main start. The display section shows the initial picture of the picture data downloaded to the NP main body.

When starting the system menu:SW1 on the back of the sliding switch placed on the left (ON),open power of the NP body, the front LED lights, NP starting body. Display system menu.

Touch screen and computer screen transmission:The USB flash mode is adopted to transfer the picture, and the USB port on the computer side and the USB main body of the NP are connected with the connector from the station.[8]

IV. SOFTWARE DESIGN

A.Set I/O address

Table 1 Enter the address of X

Serial number	PLC address	Name and function description
1	X0	Start button
2	X1	Stop button
3	X2	Reset button
4	X3	Material detection photoelectric sensor
5	X4	Material launch detection photoelectric sensor
6	X5	Pushing out limit sensor
7	X6	Pushing back limit sensor
8	X7	Arm extended limit sensor
9	X10	Arm retraction limit sensor
10	X11	Hand down limit sensor
11	X12	Hand up limit sensor
12	X13	Hand clamping claw limit sensor
13	X14	Mechanical hand reference sensor
14	X15	Push 1 extend limit sensor
15	X16	Push 1 retraction limit sensor
16	X17	Guide material transfer limit sensor
17	X20	Guide in situ limit sensor
18	X21	Incoming material detection photoelectric sensor
19	X22	Material library 1 detection sensor
20	X23	Material library 2 detection sensor

Table 2 Enter the address of Y

Serial number	PLC address	Name and function description
1	Y0	Stepper motor driver PUL-
2	Y1	Stepper motor driver DIR-
3	Y2	Stepper motor driver ENA-
4	Y3	Material launch
5	Y4	Arm reach
6	Y5	Arm down
7	Y6	Clamping claw
8	Y7	Gripper release
9	Y10	Push cylinder
10	Y11	Guide cylinder
11	Y12	Warning red light
12	Y13	Warning green light
13	Y14	Warning yellow light
14	Y20	Frequency converter STF

B.PLC program analysis and its main program:

Warning lamp : when it is at the non working state, M0 turns off, the red light Y12 lights up, the green light Y13 lights out. M0 turns on what means working,.The green light Y13 lights up, the red light Y14 lights out. If it detects the feeding port without material, X3 turns off delay 3S,yellow light Y14 lights up and means the missing material, Using relay M8013 to provide the pulse and make it light.

Start, stop and reset: the start and stop part of the self locking relay M0, when the M0 turns off, press the button to control the X2 button to reset.Reset is the program of all relays and state reset.

Feeding material: under the condition of M0, testing whether there is material X3.If it have material and is controlled by the air cylinder rods retracted, delays 1s after the launch of the cylinder. After the launch of the 1s delay, the cylinder is retracted.If you do not set the delay it will cause the material due to inertia bounce and result inaccurate positioning of material manipulator.

Manipulator: manipulator arm detect to the material in the reference point and forward. Cylinder of arm delays 0.5s and declines after detects in place; Hand of arm delays 0.5s to grip material after detects in place;If hand detects to the clamping signal,arm rise and

detection in place after 0.5s of time delay; Arm delays 0.5s and retracts; arm turn right anfer detects in place. If it rotates in place, arm is forward and declines as before. Hand grips release the material placed on a conveyor belt, and then the arm turn right to waiting for the next material in place, repeat the above action. Procedures need to pulse number n, From the previous set of parameters, stepper motor rotates 10000 steps as a circle,so the rotation angle is 63 °, the formula:

Pulse number N=10000*63 ° /360 ° =1750

The data required for the program is K1750.

In order to control step steering of stepper motor better , stepper motor set relay M4 as the initial state, to determine the benchmark X14 at the start of the manipulator operation procedures.

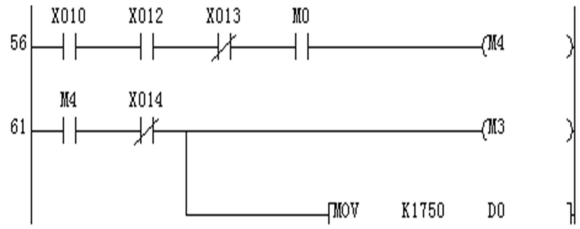

Fig.3 Initial state of Manipulator ladder diagram

The function of M8029 in the program is to start the next instruction with M8029 after the completion of an instruction execution and carry out the necessary data operations. M1, M2, M3 relay and PLSY continuous pulse instructions are used to control the running direction of the stepper motor relay.

Fig.4 Stepper Motor Control of Manipulator ladder diagram

Sorting:If it in the work state and the material entrance detects the material, X21 is switched on, inverter Y20 starts. When the pushing cylinder retra -ct x16 draw back and detectes metal material X22, cylinder Y10 pops up. In the detection of white nylon material X20 and guide cylinder at the origin, the cylinder extends and Y11 sets to 1, then setting the cylinder delays T20 for 1.5s to retract.

Key analysis: set a delay to prevent that material is not in storage, the guide rod returns9]

The state transition diagram of the main control process is shown in Figure 5.

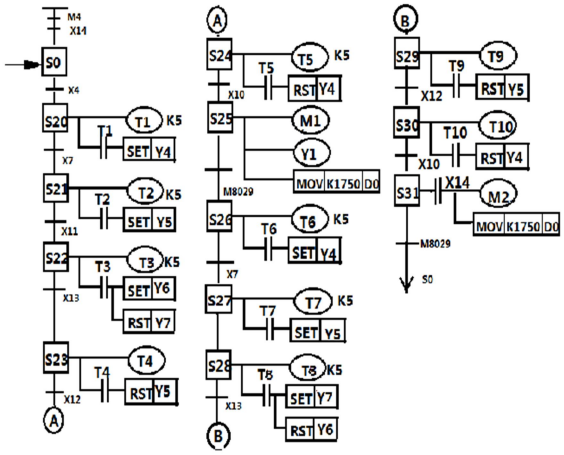

Fig.5 Manipulator SFC diagram

C.Touch screen editor

Using NP-Designer software to design the program and the screen through the USB downloads to the OMRON touch screen.

Touch screen interface design:The screen is divided into five sections, Above the screen there are three parts: feeding system, manipulator system, and sorting system. They are labeled with text and uses ectangular graphics object to represent the state.The below part is divided into the part of warn -ing lights and buttons.Warning lights use light object to represent the state and buttons use button object. The rectangular object variable to a dark gray said is set to 1, light gray is set to 0; button press said set to 1, otherwise set to 0; light object display gray set to 1, blank are set to 0, deep gray for that red light, shallow Gray said green, most shallow and flashing said yellow.

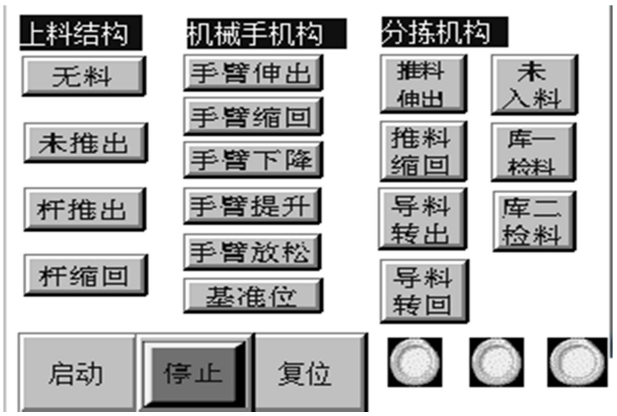

Fig.6 The touch screen

The touch screen action settings: The rectangular object: according to the reading numerical address ,

change the color is deep or shallow rectangular. The button object: set three button:start, stop, reset the start button for function set (Set address (Bit) to ON, even loosen or press the button again, it is always in the state of ON set address. When there is touch ON macro, it will be executed at the same time). Stop button; set reset function (set address (Bit) set to OFF. Even when the button is loosened or once again, the address is set.Is always in the OFF state. When there is touch OFF macro, it will be at the same time Execution. Reset button is set to function alternately (each time the button is pressed, when the OFF is changed to ON, the ON Touch macro will be executed; if it changes from ON to OFF, executes the Touch OFF macro).The light object: set of three lights means a warning lamp, the style is round,Reading the address value to change color.

Touch screen settings:Set the writing address or reading address to the touch screen.

Table 3 The address of PLC corresponding to the touch Screen

PLC Address	Touch screen address
X0 X1	M0
X2	M5
X3	M6
X4	M7
X5	M8
X6	M9
X7	M10
X10	M11
X11	M12
X12	M13
X13	M14
X14	M15
X15	M16
X16	M17
X17	M18
X20	M19
X21	M20
X22	M21
X23	M22
Y12	M23
Y13	M24
Y14	M25

V.CONCLUSION

The thesis bases on the material sorting apparatus to design Mitsubishi FX-2N series PLC control program and the Omron NP5MQ001B control with touch screen interface. The practice has proved that the design of programs to realize the correct material sorting and achieve the design goals.

References

[1] Wan Lixiang,Ding Baohua.The application of PLC in manipulator control[D].Jiangsu:Chinese Mining Uni -versity, 2010.08.

[2] Lv Jingquan. Installation and adjustment of automatic production line [M]. Beijing: Chinese railway press, 2009.

[3] Jin Yong. A test instrument for touch screen system design [M]. Beijing: automation information press, 2010.

[4] Ying Chaolong.Touch screen and controller design [M]. Shandong: Naval Aeronautical Engineering Institute press, 2010.

[5] Xue Yingcheng.PLC and touch screen control technology[M]. Beijing: Chinese power press, 2014

[6] Wu Yingchun, Xu Lianzhang, Zhang Jiahua. Touch screen and PLC in the sorting system [J]. The machinery manufacturing and automation 2012,41 (2): 171-173.

[7] Guang Shiyan, Wu Hongying. Electromechanical Integrated training guide book [M].Jiangsu: Huaian Information and Technology Career Academy.2012.

[8] OMRON.OMRON NP Series Guide Manual [M].

[9] Yan Yingfu Touch screen and PLC introduction [M]. Beijing: People's Posts and Telecommunications Press, 2006.

Design of adjustable DC regulated power supply based on single chip microcomputer

Xuxiaoshun; Panjinsheng; Wuqi

（School of Instrument Science and electrical engineering, Jilin University, Changchun, Jilin 130026）

***Abstract*--This paper is focus on the design of adjustable and stable DC source. And its maximum output current is 1A.The 430 single-chip serves as the master control core of the DC source, which controlled by a keyboard to decide different voltage. LCD1602 display the exporting voltage of the DC source.And the source is made up of rectifier, voltage regulator and so on. The DC source can export a adjustable voltage ranging from 0～12V and its circuit has the advantages of high precision, lower of cost,easy regulation , and it is durable in use, etc.**

***Keywords*--Stabilized voltage power supply adjustable 430 single chip microcomputer LCD1602**

INTRODUCTION

POWER supply technology, especially electronic technology is a very practical technology, services in all walks of life. Electronic power supply compared to traditional power supply circuit, easy to operate, high voltage stability characteristics. Currently, electronic DC power supply is one of the commonly used electronic equipment technology, widely used we live, work, and research fields. This article describes an adjustable DC power supply. It requires an output voltage range of 0 ~ 12V continuously adjustable output current ≦ 1A, output voltage display LCD1602.

I. CIRCUIT DESIGN

There are many design method of the power source, there are three relatively simple.

1.1 DC transistor series regulator circuit

Circuit block diagram shown in Figure 1, the circuit, the output voltage UO obtained by sampling circuit after sampling voltage sampling, the sampling voltage is compared with a reference voltage to obtain the error voltage, the error voltage to the work of the state regulator to be adjusted so that the output voltage changes, the changes due to the changes caused by the supply voltage change in output voltage UI just the opposite occurred, in order to ensure that the output voltage UO is a constant value (voltage value). Due to the output voltage from 0V since the requirements to achieve continuously adjustable, so to design an auxiliary supply at the reference voltage for controlling the output voltage can be adjusted from 0V.Simple series DC power supply circuit is very simple, but adds auxiliary power, the circuit is more complex, since the discrete components are used, it is difficult to ensure the reliability of the circuit.[1]

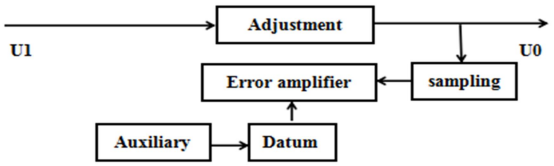

Fig.1. Tandem power supply circuit diagram

1.2 Three-terminal integrated voltage regulator circuit

The circuit diagram shown in Figure 2, which uses an adjustable output voltage and the internal overload protection of three-terminal integrated voltage regulator, the output voltage adjustment range is wide, designed to achieve a voltage compensation circuit output voltage is continuously adjustable from 0V onwards , because the circuit requires a strong load capacity, a soft-start circuitry shall be designed to accommodate the load carried by the start-up performance. The circuit with fewer devices, low cost and ease of assembly, high reliability.[2]

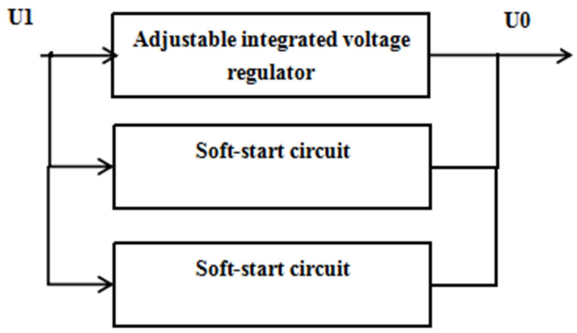

Fig.2 .Integrated voltage regulator power supply circuit diagram

1.3 MCU production of adjustable DC power supply

The entire circuit microcontroller as the core, by the filter module, A / D converter, LCD display and key components. System block diagram shown in Figure 3. MCU comes with PWM output function of adjustable duty cycle resolution PWM wave, the PWM signal LC Filter module, re-use TDA2030A power amplifier module DC signal amplification desired DC power supply. DC signal output after sliding rheostat partial pressure feedback input channel AD SCM, SCM and then read and compared by controlling the PWM duty cycle to regulate the output voltage, while the collected actual voltage output value is displayed in LCD1602.[3]

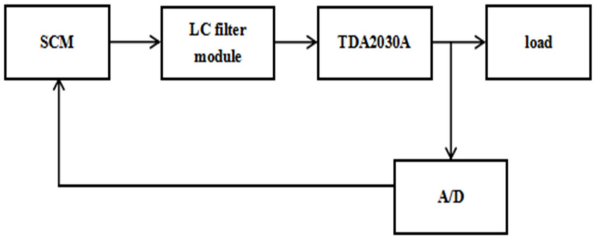

Fig.3. System block diagram

Traditional DC power supply output voltage through coarse and fine-tune band switch potentiometers to adjust, and by voltmeter indicate the size of the voltage value. This DC power supply is not intuitive readings exist, the potential for easy to wear, regulation accuracy is not high, easy alignment, circuit complexity, size and other shortcomings, based on microprocessor controlled DC power supply can solve the the above problem. The hardware circuit includes rectifier filter circuit, microcontroller, keyboard and display several components. Voltage and current sampling circuit controlled by a microcontroller real-time voltage and current sampled current to correct output voltage. The supply good stability, high accuracy, and can output adjustable DC voltage within the range of 0V ~ 12V, and its performance is better than traditional adjustable DC power supply. Therefore, this design uses a microcontroller-based production of adjustable DC power supply scheme.[4]

II ACTUAL CIRCUIT DESIGN

2.1 Hardware circuit

2.1.1 LC filter module

Based on the normalized LPF design parameters, in accordance with the steps shown in Fig. 2, obtained by a simple calculation. First, by changing the normalized original parameters of the LPF, to get a ring from the normalized frequency cut-off frequency 1 / (2pi) Hz filter design of the filter to be changed; and then by changing the component values transitional filters , the normalized characteristic impedance of the filter design to be converted into the desired characteristic impedance, which obtained the most demanded design filters.[7]

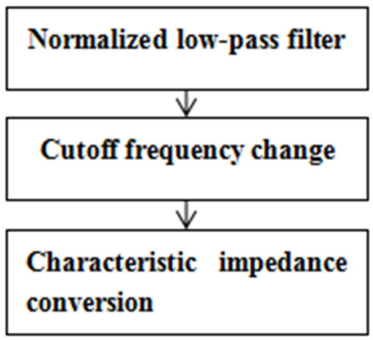

Fig.4. Parameter calculation step schematic

After designing the circuit configuration can be calculated as follows and component parameters.

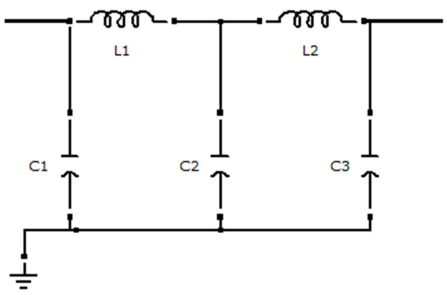

Fig. 5. a circuit diagram of the filter module

The actual parameters are as follows:

L1=6.4mH L2=6.4mH

C1=0.98uH C2=3.18uH

C3=0.98uH

2.1.2 TDA2030A power amplifier module

TDA2030A pin diagram is shown below

1 pin is the positive input

2 pin is the inverting input

3 pin is a negative power supply input

4 pin is the power output terminal

5 pin is a positive power supply input

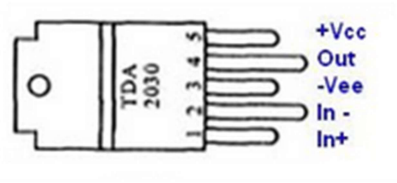

Fig.6. TDA2030APin Figure

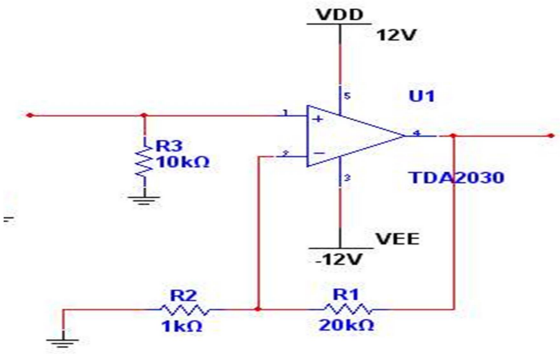

Fig.7. TDA2030AAmplifier circuit diagram

Circuit characteristics:

[1]. Very few external components.

[2] The output power, Po = 18W (RL = 4Ω).

[3] ultra small package (TO-220), the packing density can be increased.

[4] The power-minimal impact.

[5] contains various protection circuit, safe and reliable. The main protection circuit: short circuit protection, thermal protection, accidental open ground, reverse polarity (Vsmax = 12V) and load discharge voltage recoil.

[6] .TDA2030A to work at the lowest maximum ± 22V ± 6V voltage is ± 19V, 16W at 8Ω output impedance capable of effective power, THD≤0.1%[5][6]

2.1.3 A / D converter module

DC signal output by 50K sliding rheostat partial pressure feedback input microcontroller AD channel.

III. SYSTEM SOFTWARE DESIGN

3.1 PWM control

MSP430F413 maximum operating frequency is 8MHz, PWM counter by 200 to calculate the frequency PWM wave is 40kHz, this happens to be within the current frequency switching power supplies and common frequency range, relatively easy to buy switch components. The output voltage between 2-15V. Therefore, the duty cycle is taken as 10 / 200-190 / 200, at 18V input voltage, output DC voltage of the theory 0.9-17.1V, meet the design requirements. MSP430F413 actual operating frequency is 32768Hz, the use of the multiplier 240 to obtain the actual operating frequency of 7.86432MHz. Software design, call PWM, ADC and timer A after initialization functions, PWM wave output from the pin CPU will, when just power, the duty cycle can be selected 5/200, to output a low voltage value. In the main loop will continue to compare the preset voltage and A / D measured actual output voltage value, and constantly adjust. Function also initializes PWM timer interrupt, for adjusting the PWM duty cycle-by-cycle Pod, it has been the best response time.

3.2 A / D converter

Key A / D conversion section is 1 bit of timing to be accurate. Otherwise, bits 1 and 0 bits duration instability, the effect of low-pass filtering out the DC voltage value, the final value of the A / D conversion is not accurate. Therefore, there must be a bit timers highest processing priority. The method uses a timer to automatically trigger, you can achieve the most accurate timing, but taking into account that would increase the cost of hardware, and software optimization process, you can achieve the accuracy required for this application. Software processing is to determine the Timer 1 bit time, every time the timer counter is full, immediate detection comparator output if the comparator output is 1, indicating that the number of 1-bit data stream more, then the order a bit output 0; on the contrary, if the comparator output 0, indicating the number of 1-bit data stream less, then let the next 1-bit data stream output. A / D converter consists of bit timer interrupt subroutine is completed, each bit timer interrupts statistics m value, and the value of N plus 1, after the expiration of the value of N 1800, m value is the measured value, the program flow chart shown Figure 5 In order to measure the value of stability and reduce fluctuations in the data, the software uses a low-pass filtering process. In the design process does not use a dedicated A / D chip, using only one pair of op amp with a single-chip

software to make way Σ-Δ A / D conversion, simplifying the design, reducing costs.[8][10][11]

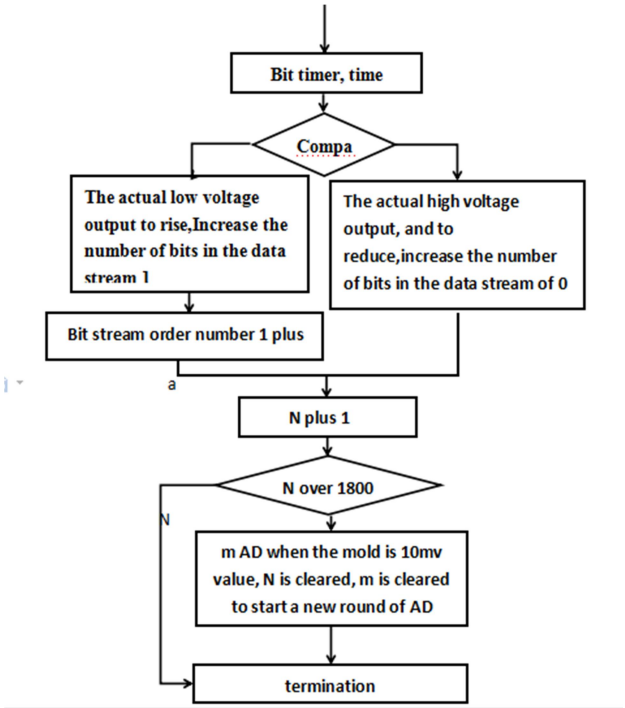

Fig.8. A / D conversion flowchart

3.3 Key Processing

Start self-inspection system and displays the initial state (2) function key "OK" press to preset voltage value, then you want a manual keyboard input voltage amplitude obtained in (3) determine whether the judge pressed again, if press again to the regulator, the actual value of real-time acquisition until close until the preset voltage value (4) error is less than 0.01V, and liquid crystal display the actual voltage value. (5) inquiry judge to cancel the function key is pressed, if you press it again under a new preset desired voltage value obtained, so that you can achieve the desired button control voltage obtained achieve adjustable. (6) increase the "backspace" function key, typing errors can backspace lose weight.[9]

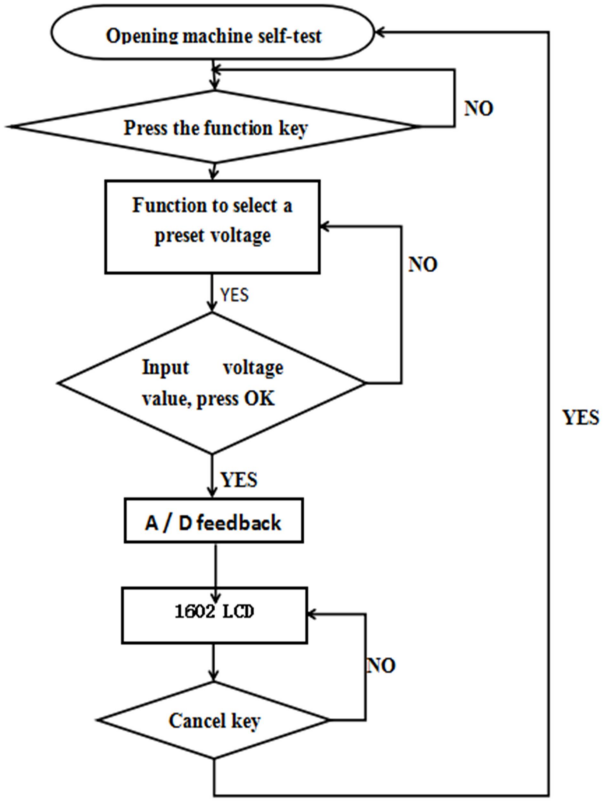

Fig.9. Key processing flow chart

IV. TEST RESULTS

Real made adjustable power supply as shown in Figure 10, the main test results are: power output accuracy, test results obtained are shown in Table 1.

TABLE.1. Test Results

Keyboard input value（V）	5.9	8.8	9.5	3.7	7.2
A / D sampling value（V)	5.8	8.8	9.4	3.7	7.1
Meter Found（V)	5.86	8.88	9.34	3.66	7.17

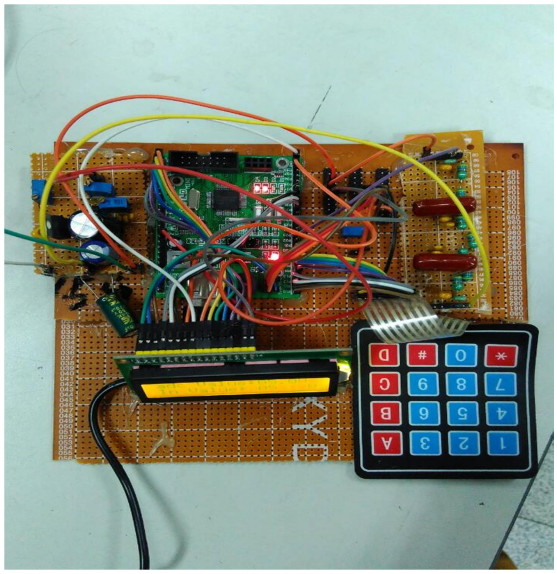

Fig,10.Adjustable power supply physical map

Keyboard input is 8.8, the measured results shown in Figure 10 the actual circuit

Fig.11 .Found Results

Keyboard input is 8.8, the measured results shown in Figure 11 the actual circuit

By table1, we can see that the adjustable regulated power supply preset value and the actual output gap, completely within the allowed error range.In order to reduce the error, we not only in the aspect of software through A/D acquisition in real time to adjust PWM wave duty ratios increased system stability, also add A few auxiliary in terms of hardware chip to reduce the ripple of reduce error.Through these two improvements, just had our regulated power supply is so precise output.

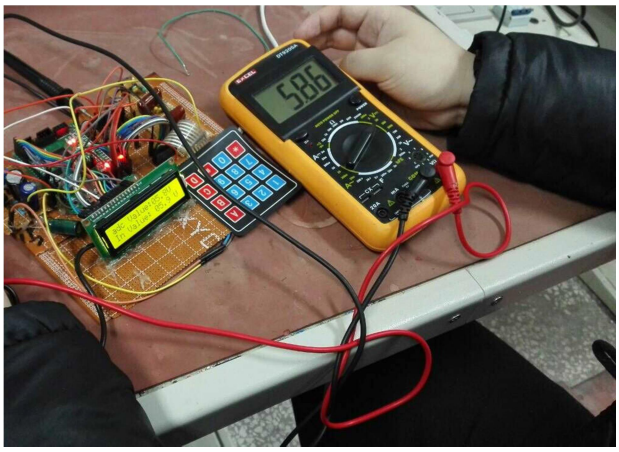

Fig.12. Found Results

V. EPILOGUE

In this paper, the adjustable power supply 430 microcontroller-based digital design ideas, the main hardware circuits are analyzed, and the software flow, a good combination of theory and practice. Test evaluation results showed that: 430 microcontroller based DC power supply is good stability, high accuracy, low cost, and its performance is better than traditional adjustable DC power supply, which greatly improves the performance of traditional regulated power supply, easy to use, low cost. After testing, the output voltage range of the circuit up to 0 ~ 12V.

References

[1] Zhao Xinmin design of intelligent instruments Harbin: Harbin Institute of Technology Press, 1999.7

[2] Zhou Zhimin power electronic devices and electrical and space. Modern power technology, 2004,8

[3] Liu Zhong election, Yang tied Branch Power Technology Practical Manual - Modular Power Volume Shenyang: Liaoning Science and Technology Press, 1999

[4] Jizong Nan microcontroller peripheral devices Practical Handbook - Volume input channel devices Beijing: Beijing Aerospace University Press, 2003.3

[5] Wang Shunqi power supply design Beijing: National Defense Industry Press, 1983.10

[6] Zhao Xuequan, Beijing Guohua Power circuit: Electronic Industry Press, 1995.3

[7] Li Zhaoqing, SCM principles and interface technology Beijing: Beijing Aerospace University Press, 1998.11

[8] Zhou Hangci MCU application design technology. Beijing: Beijing Aerospace University Press, 1991.8

[9] Yang Zhenjiang .A / D, D / A converter interface technology Xi'an: Xi'an University of Electronic Science and Technology Press, 1996

[10] . Mazhong Mei, Liu Bin microcontroller C programming language Windows environment Collection Beijing: Beijing Aerospace University Press, 2003.6

[11] Ma Zhongmei, nationality liking SCMC language application design Beijing: Beijing Aerospace University Press, 1998.10